Geological Survey of Finland

Bulletin 395

Geology and ore petrology of the Akanvaara and Koitelainen mafic layered intrusions and the Keivitsa-Satovaara layered complex, northern Finland

by Tapani Mutanen

Geological Survey of Finland
Espoo 1997

Geological Survey of Finland, Bulletin 395

GEOLOGY AND ORE PETROLOGY OF THE AKANVAARA AND KOITELAINEN MAFIC LAYERED INTRUSIONS AND THE KEIVITSA-SATOVAARA LAYERED COMPLEX, NORTHERN FINLAND

by

TAPANI MUTANEN

with 233 pages, 88 figures, 11 tables in the text and 5 appended maps

ACADEMIC DISSERTATION

in Geology and Mineralogy

To be presented, with permission of the Faculty of Science, University of Helsinki, for public criticism in Lecture Room 1 of the Department of Geology, on May 23rd, 1997, at 12 noon

GEOLOGIAN TUTKIMUSKESKUS
ESPOO 1997

Mutanen, Tapani., 1997. Geology and ore petrology of the Akanvaara and Koitelainen mafic layered intrusions and the Keivitsa-Satovaara layered complex, northern Finland. *Geological Survey of Finland, Bulletin 395*, – pages, 88 figures, 11 tables and 5 appended maps.

The Akanvaara and Koitelainen intrusions, ca 2440 Ma old, represent a group of cratonic mafic layered intrusions (aged from 2500 to 2440 Ma) of the Fennoscandian (Baltic) Shield. These intrusions, which show all the standard types of igneous layering, host deposits of chromite, vanadium, titanium, platinum-group elements (PGE) and gold.

The cumulate stratigraphy in Akanvaara and Koitelainen reflects both normal tholeiitic fractionation and superimposed intermittent selective and wholesale contamination by anatectic salic melt (now granophyre) from the floor and the roof, and by refractory residual phases after anatexis of the roof rocks. Cumulus phases separated mainly in a hybrid melt between the mafic main magma and the overlying buoyant acid melt. The contaminants are found in cumulates as fossil melt and magma inclusions in olivine, chromite, orthopyroxene and plagioclase, and as "granitic" intercumulus material. The composition of the intercumulus material in the most heavily contaminated cumulates deviates strongly from what one would expect of the mafic main magma. Unusual minerals (loveringite, chlorapatite. zircon, zirconolite, baddeleyite, thorite, allanite, galena, perrierite, a Ti-Th-REE-P silicate) are common in the intercumulus of the ultramafic cumulates; ilmenite, chlorapatite and zirconolite occur as daughter and occluded minerals in melt and magma inclusions in olivines and orthopyroxene. Chlorapatite, ilmenite and loveringite are the most common Doppelgänger phases (Mutanen, 1992), of which only the apatite phase (as a fluorapatite) appears as a late cumulus mineral.

The melting occurred both early and late in the crystallization history, corresponding to the water-saturated and dry melting of the granitic constituents of the surrounding crustal rocks. There is no evidence for, nor need of, multiple magma pulses; the reversals can readily be explained by contaminants transmitted by two-phase convection. Contamination of the magma by crustal material shifted the liquidus phase boundaries, resulting in excessive separation first of olivine and, subsequently of orthopyroxene. Refractory aluminous phases after partial melting of pelitic roof rocks were responsible for the anorthositic cumulates.

Chromitite layers occur from near the base of the intrusions to the 86 PCS level. Almost all the chromitites have elevated concentrations of PGE. The gangue is generally rich in biotite-phlogopite. All chromites are very low in MgO (from 0.0% to 1.2%). These features imply that chromite crystallized and was equilibrated in a melt poor in magnesium and rich in potassium. It is suggested that the chromium of the uppermost chromitites (UC layers) was exotic: it was liberated from melted high-aluminous schists averaging 500 ppm Cr. Exotic chromium may well have contributed to the genesis of some other anorthosite-associated chromitites, too (e.g., Fiskenaesset, Sittampundi, Soutpansberg, Bushveld, Stillwater).

In the Akanvaara and Koitelainen intrusions the PGE show little respect for sulphides, and are typically associated with oxides (chromite, ilmenomagnetite, ilmenite). Evidently the PGM phases crystallized from the silicate liquid direct.

The Keivitsa intrusion (age 2057 Ma) is located south of the Koitelainen intrusion. Isotopic (Sm-Nd, S-isotopes, Re-Os), geochemical (Ni/Co, Ni/S, PGE/S, S/Se, S/Te, Re/PGE, among others) and mineralogical data all point to significant exotic contamination by surrounding carbonaceous, sulphide-rich sediments and by solid refractory debris from disaggregated komatiitic rocks. The addition of exotic sulphur (as anatectic immiscible sulphide melt) and olivine debris was decisive for the genesis of the low-grade Keivitsansarvi Cu-Ni-PGE-Au deposit, which is located far above the basal contact of the intrusion. Other contaminants acquired from surrounding rocks were water, reduced carbonaceous material and chlorine, all of which affected the crystallization of the magma. Mineralogical evidence from Keivitsa and from other PGE-bearing magmatic sulphide deposits together with our experimental work (Mutanen et al., 1996) suggest strongly that immiscible sulphide melt either acted as a phase boundary collector for platinum-group mineral (PGM) particles already crystallized from melt or that the supersaturated PGM nucleated on sulphide droplets.

Key words (GeoRef Thesaurus, AGI): layered intrusions, contamination, degassing, petrology, chlorapatite, Cl, ultramafics, chromitite, gabbros, geochemistry, copper ores, vanadium ores, nickel ores, platinum ores, gold ores, Proterozoic, Finland, Lappi Province, Savukoski, Akanvaara, Sodankylä, Koitelainen, Keivitsa, Keivitsansarvi, Satovaara

Tapani Mutanen
Geological Survey of Finland
P.O. Box 77
FIN-96101 ROVANIEMI, FINLAND

ISBN 951-690-652-4
ISSN 0367-522X

Vammalan Kirjapaino Oy 1997

ABBREVIATIONS AND DEFINITIONS

ab	–	albite
an	–	anorthite
APB	–	Archaean-Proterozoic boundary
bi	–	biotite
CC model	–	convection-contamination model
CN	–	chondrite-normalized
cp	–	chalcopyrite
cpx	–	clinopyroxene (augite, diopside, hedenbergite)
crt	–	chromite
CuEQ	–	copper equivalent, wt% (includes Cu, Ni and part of Pd and Au)
cumulus crystal	–	settled (or floated) crystal
DDH	–	diamond (core) drill hole
D-value	–	simple ratio; distribution coefficient of an element between phases
Doppelgänger (doubleganger)	–	a premature magmatic phase, opposite to reversed phase (in phase reversal; (see Mutanen, 1992, p. 26)
economic	–	pertaining to the production, distribution, and use of income, wealth, and commodities — pertaining to an economy, or system of organization or operation, esp. of the process of production — pertaining to one's personal resources of money (Webster's Encyclopedic Unabridged Dictionary of the English Language. Portland House, New York, 1989). 'Economic' is misleadingly used in Finland as a synonym with 'profitable'.
false ore	–	Ore type in Keivitsa. Analogous to false money: rock with massive or rich disseminated sulphides but low in Ni. Metal analysis (as with false coins) is needed to distinguish false from genuine (viable) ore. No economic connotation!
Fe(tot)	–	Total iron calculated as FeO
GSF	–	Geological Survey of Finland
hb	–	hornblende
ilm	–	ilmenite
ilmenomagnetite	–	magnetite with exsolved ilmenite
KEI	–	type intrusion – Keivitsa-type intrusion
KOI	–	type intrusion – Koitelainen-type intrusion
KSC	–	Keivitsa-Satovaara Complex
LC	–	Lower Chromitite
LIB	–	Lapland Intrusion Belt
LLC	–	Lowermost Lower Chromitite
LZ	–	Lower Zone
mg#	–	atomic Mg/Mg+Fe ratio
MZ	–	Main Zone
Ni(100S), Ni(S)	–	Ni concentration (in wt%) in calculated 100% sulphides
ol	–	olivine
opx	–	orthopyroxene (Ca-poor pyroxene)
P(fl)	–	fluid pressure
P(lit)	–	lithostatic pressure
PCS	–	per cent solidified
PGE	–	platinum-group elements
PGE(100S), PGE(S)	–	PGE concentration (in ppb or ppm) in 100% sulphides (similarly, Pd(S), Au(S) etc.)
PGM	–	platinum-group minerals
phl	–	phlogopite
pl	–	plagioclase
pn	–	pentlandite
po	–	pyrrhotite
px	–	pyroxene
py	–	pyrite
q	–	quartz
RONF	–	Regional Office for Northern Finland
SHMB	–	siliceous high-Mg basalt
SLI	–	silicate liquid immiscibility
sp	–	spinel (denotes the spinel group, unless stated otherwise)
titanomagnetite	–	homogeneous (high-T) titaniferous magnetite
UC	–	Upper Chromitite
ULC	–	Uppermost Lower Chromitite
UZ	–	Upper Zone
VTT	–	Valtion Teknillinen Tutkimuskeskus (Technical Research Centre of Finland)
wr	–	whole-rock
%	–	weight per cent (unless stated otherwise)

A1: View east of Koitelainen hill. Photo by TM.

A2: View south of Lakijänkä towards Koitelainen fell

B1: Frosty bog, western part of Koitelainen

B2: Bog, north of Koitelainen fell

C1: Spruce swamp with Russki head tussocks, Koitelainen

C2: Piiku, field assistant in Koitelainen, 1985

CONTENTS

INTRODUCTION

General location and physiography of the study areas

The contiguous mapping area of Koitelainen and Keivitsa-Satovaara (map sheets 3714, 3723, 3732 and 3741) lies ca 150 km north-northeast of Rovaniemi in a wilderness between the rivers Kitinen and Luiro. The Akanvaara area (map sheets 3644 and 3733–4711) is located 75 km southeast of Koitelainen. The terrain is the type area of the aapa mire complex, consisting of interconnected bogs of this type (see Cajander, 1913). Geomorphologically the area is part of an ancient peneplain, with a general southern slope. The least fractured and chemically most resistant rocks stand up from the flats as smoothed ridges and asymmetric mesa-like hills (e.g., Koitelainen, Keivitsa). The mean height of the peneplain in the northern part of the Koitelainen area is 260 m a.s.l., and in the southern part of the Keivitsa-Satovaara area 220 m a.s.l. The highest point is the summit of the Koitelainen tunturi (fell), 408 m a.s.l. Keivitsa hill rises 80–90 m above the surrounding lakes and boggy flats. At Akanvaara most of the intrusion area is flat peneplain, with some low hills and ridges with a base level 180–190 m a.s.l. The Akanvaara hill (actually a row of hills), which is composed of the acid volcanic rocks of the roof of the intrusion, reaches a height of 440 m. Dry moraines are covered with spruce forests; pine grows on craggy ground and in reforested clear-cut areas in the west of the Koitelainen and Keivitsa-Satovaara areas. The old spruce forests of the southern part of Satovaara hill (eastern part of the Keivitsa-Satovaara complex) was strip-clear-cut in the early 1990s. Most of the area of the Koitelainen intrusion and the northern part of Satovaara lie within the planned Koitelaiskaira Wilderness Preserve area. The forests of the Akanvaara were clear-cut in 1970s; only the high-altitude old-growth forests (above ca 300 m) were spared.

The Koitelainen and Akanvaara intrusions and the Keivitsa-Satovaara complex are named after the dominant hills in the respective areas. Of the many other forms of the name Keivitsa (Keivitsainen, Kevitsa, Keevitsa, Keevitsä), we in the GSF have used Keivitsa, which is probably the original Sámi form (Samuli Aikio, pers. comm., 1993).

Preglacial weathering, glacial geology and bedrock exposure

During much of Phanerozoic time topographic, geotectonic and climatic conditions favoured intense chemical weathering and the formation of thick weathered regolith profiles (Afanasev, 1968, 1971, 1977). Scattered, mostly rather shallow, kaolinite and montmorillonite-saponite deposits occur throughout Central Lapland; Afanasev (1977) attributes them to warm, humid periods from the Mesozoic to Palaeogene. The most widespread type of formation of “rapakallio” – weathered bedrock – in Finnish Lapland and the Kola Penin-

sula is what Afanasev (1968) calls hydromica weathering. I have used the perhaps more universal term grussification (Mutanen, 1979b, and references therein), a process involving alteration of micas (hydration, removal of potassium and oxidation of iron) resulting in the formation of a soft, spadable rock. In grussified layered sedimentary rocks poor in mica, the sulphides and carbonates have been dissolved, leaving a hardy residue of macadam-like chips. Grussified rocks have developed and are typically preserved on gentle slopes, and the weathering profile roughly conforms to the present surface (Afanasev, 1968). Afanasev (1971, 1977) ascribed – quite credibly – this type of weathering to temperate, humid climate during late Tertiary time (Miocene to Pliocene), before the ice-sheet spread over northern Europe. More subtle changes in grussification weathering are found deep in hard rocks, for instance, maghemitization of magnetite and the formation of solid, primary-looking secondary sulphides (violarite-siegenite, marcasite and pyrite).

The thickness of grussification gives a good measure of the depth to which preglacial weathering extends. At Koitelainen it is mostly ca 14 m, about the same as in the Kola Peninsula (5–20 m, Afanasev, 1977). In micaceous, fractured rocks of the Bonanza, a copper prospect at Koitelainen, grussification extends to a depth of at least 60 m. In the Kejv area, central Kola Peninsula, sulphides are lacking in the uppermost 10–12 m of the bedrock; from there downwards supergene pyrite is found to a depth of 50–80 m, where it is superseded by primary pyrrhotite (Belkov, 1963). At Bonanza maghemitization reaches to a depth of 120 m (along DDH), more than the max. 70 m found in Bushveld (van Rensburg, 1965). A phenomenon noticed in the V-rich magnetite of the Koitelainen intrusion is what I have called "hematite inoculation effect". Where magnetite had suffered, no matter how slightly, from metamorphic oxidation into hematite ("martite"), it did not "catch" maghemitization. The same phenomenon has been noted in Bushveld, too (van Rensburg, 1965).

Grussification had considerable – and not entirely pleasant – effects on bedrock exposure. Rocks with even small amounts of mica are deeply grussified and exposed only by accident, as in the periglacial landslide gorge at Bonanza. Unfortunately, such rocks include chromitites and layers and stratigraphic intervals associated with ore layers (pyroxenites, anorthosites). During diamond drilling grussified rocks leave the hole with the flushing water. On the other hand, they provide welcome bedrock samples in large bog areas, as they can easily be sampled with percussion ("Cobra") drilling.

During the Pleistocene glaciations, Central Lapland was the area of ice accumulation, with very little basal ice movement and, hence, glacial erosion (Penttilä, 1961). In certain leading zones (e.g., in the western part of the Koitelainen intrusion, on the eastern slope of Koitelainen hill and through the eastern part of the Keivitsa-Satovaara area) erosion and transport were surprisingly powerful, as indicated by the long transport distances of indicator erratics and the existence of roches moutonnées, grooves, striations and crescentic fractures. Ice advance was strongest from north-northwest, the dominant direction of effective transport in the Koitelainen area.

Although glacial erosion seems to have been stronger and more uniform at Akanvaara, grussified regoliths have been preserved on steep northwestern (proximal) slopes, where movement at the base of the ice sheet stagnated. Hirvas and Tynni (1976) have described what may be an allochtonous Tertiary deposit from the southern part of the intrusion.

Due to preglacial weathering and glacial erosion the bedrock of the study areas, particularly at Akanvaara, is unevenly, selectively and, on the whole, poorly exposed. Apart from solid, glacially polished outcrops alongside streams, the exposures are frost-shattered outcrops and boulder fields, most often only groups of solitary, frost-heaved boulders.

Throughout postglacial time the area has been supra-aquatic, but only nominally so at Akanvaara, where vestiges of the big Salla glacial lake (Peter Johansson, oral comm., 1994) are seen as boulder banks, cobble reefs and reworked shores across the whole southern flank of Akanvaara hill. A washed gully in the southwestern corner of the intrusion served as an overflow outlet for the glacial lake.

Previous work and work in progress

The Exploration Department of the Geological Survey of Finland (GSF) started geological mapping and exploration of the mafic layered intrusions of Finnish Lapland in 1969. Work on the first target, near the western border of the large Koitelainen intrusion, was soon discontinued. The present mapping and exploration phase began in 1973 in the Koitelainen area and continued at a leisurely pace until about 1992, when events at Keivitsa and Akanvaara gave the justification for and a boost to a comprehensive exploration programme on the layered intrusions. The Regional Office for Northern Finland (RONF) of the GSF currently has four projects under way on some dozen mafic intrusions.

The Koitelainen intrusion has been known since the general geological mapping of the 1920s and 1930s by Erkki Mikkola, who also made keen observations on the ultramafic rocks of the Keivitsa intrusion (Mikkola, 1937, 1941). Geological mapping of sheet 3714 was completed in the early 1980s (Tyrväinen, 1980, 1983). More detailed information on the geological mapping of the Koitelainen area is provided elsewhere (Mutanen, 1979a, 1989a,b). I have cannibalized chunks of text from the last-mentioned publication for the description of the Koitelainen intrusion.

The results of the exploration work in the Koitelainen and Keivitsa-Satovaara areas have been presented in numerous technical open-file reports that are available at the GSF. Those of Mutanen (1979a) and Mutanen (1989a) are compilation reports of the Koitelainen area. Publications on the Koitelainen area deal with komatiites (Mutanen, 1976a), the Upper Chromitite layer (Mutanen, 1981), chlorapatite and dashkesanite (Mutanen et al., 1987, 1988) and loveringite (Tarkian & Mutanen, 1987). The Koitelainen intrusion and the Keivitsa-Satovaara complex were described in the excursion guidebook of the 5th International Platinum Symposium (Mutanen, 1989b). In my licentiate's thesis (Mutanen, 1992) I summarized my petrological ideas about the Koitelainen intrusion.

The latest comprehensive reports on the geology, exploration and mineral processing tests of the Keivitsa intrusion have not yet been released, but some geophysical, geochemical and geological data have been published as abstracts or extended abstracts (Jokinen et al., 1994; Mutanen, 1995a,b; Vanhala & Soininen, 1994; Soininen et al., 1995; Huhma et al., 1995b, 1996; Manninen et al., 1995; Hanski et al., 1996). Results of a comprehensive geological mapping project and other surveys (Quaternary deposits, geophysics, surface and ground water, and environmental geology) of the areas surrounding Keivitsa were reported by Tuomo Manninen and his team (Manninen et al., 1996).

The northern part of the Akanvaara intrusion is only vaguely outlined on the general geological map of Mikkola (1937). More recent work has produced more detailed maps (Manninen, 1981; Räsänen, 1983; Juopperi, 1986).

At an early stage it became apparent that the Koitelainen intrusion exhibits perplexing geological, mineralogical and geochemical features, that were not anticipated, still less ac-

cepted, in petrology books. The intrusion had no recognizable precedents, although we learned later that the Akanvaara intrusion is a good successor. Keivitsa is a petrological maverick of a different and more difficult kind. In this book I shall describe the intrusions to the extent necessary and in sufficient detail, I hope, to set some limits on petrological speculation. This book is, however, still a piece of raw fruit. The scrutiny of polished thin sections and the digestion of chemical analytical data call for more work. Supplementary chemical and isotopic analyses (S, Sm-Nd, Re-Os) are being made on old samples and fresh drill core material. The exploration diamond drilling currently under way and the preparatory work at many new or reactivated targets in Lapland will add to our knowledge, both regional and general, of the mafic layered intrusions.

Materials and methods

This work is based on protracted and somewhat arduous mapping in the wilderness and conventional microscopic petrographic studies. Many exciting finds were made with the electron microscope-microprobe by or together with my colleagues mentioned in the acknowledgements. The "production figures" are reported in the chronological order of investigations.

At Koitelainen and Keivitsa-Satovaara I mapped an area of 770 km^2; at Akanvaara I revised ca 40 km^2. In areas of poor exposure the geological maps of the Koitelainen (Appendix 3) and Keivitsa-Satovaara areas (Appendix 4) are based to a large extent on scrutiny of samples and analyses of percussion drilling samples (14 991 of till, 3785 of weathered bedrock). Many of the samples were studied under the binocular microscope, in addition to which 96 polished thin sections, 89 covered thin sections and 10 polished sections were made and examined. The geological mapping was supported by geophysical surveys. All areas are covered by both high-altitude and low-altitude (39 m) aerogeophysical line flights. Ground-geophysical surveys (mainly magnetic, routine electromagnetic and gravity) cover 187.75 km^2 at Koitelainen, 90 km^2 at Keivitsa-Satovaara and 102.5 km^2 at Akanvaara.

Diamond-core drilling has been indispensable in these poorly exposed areas. During 1973–1982, 99 holes with a total length of 12 007.25 m were drilled at Koitelainen, and 403 holes (43 139 m) at Keivitsa-Satovaara. The latter figures do not include the 175 shallow DDHs (total 5121.85 m) drilled as part of "The geology of the Keivitsa area" project (Manninen et al., 1996). Drilling continues at Akanvaara, and by 31st March, 1997, 84 holes totalling 13 563.60 m had been completed. The average depth (as measured along DDH) of loose deposits (till, peat, weathered bedrock) has been 3.56 m at Koitelainen, 5.56 m at Keivitsa-Satovaara and 8.99 m at Akanvaara.

The total count of polished thin sections studied is 4698, 1768 from Koitelainen, 2446 from Keivitsa-Satovaara and 362 from Akanvaara, 96 from percussion drilling samples and 26 from mineral processing test products). Ordinary (covered) thin sections from 89 percussion drilling samples and 383 thin sections from Koitelainen samples were also studied, as were 326 polished sections from Koitelainen, 3 from Keivitsa and 10 from percussion drilling samples. All these add up to 5509 sections.

Most of the chemical analyses are partial, made for practical exploration purposes. Unless stated otherwise, all analyses were made at the Otaniemi and Rovaniemi laboratories of the GSF. The analytical methods chosen depend on the practical needs and reflect the availability of facilities and development of

analytical equipment and automation techniques during the long span of the investigations. Some whole-rock compositions from Koitelainen were determined by wet-chemical techniques by Risto Saikkonen (GSF) but other rocks and ores were analysed by XRF on powders or powder briquettes; the chromitite analyses for Koitelainen were made on flux-fused samples.

Se and Te were determined by graphite furnace AAS after preconcentration by reductive coprecipitation from aqua regia digestion (see Niskavaara & Kontas, 1990). ICP-MS were used to analyse selected samples from Keivitsa for Ag, Ba, Bi, Cd, Hg, Mo, Rb, Se, Sr, Th, Tl, U and V. All drill core samples from Keivitsa-Satovaara and Akanvaara were analysed for Au and Pd by graphite furnace AAS (Kontas et al., 1990) and selected samples from all intrusions also for Os, Ir, Ru, Rh, Pt, Pd, Au and Re by nickel sulphide-ICP-MS (Juvonen et al., 1993, 1994); a smaller number of samples from Keivitsa were analysed for Pt, Pd and Au by Pb fire assay (Juvonen et al., 1994). The CN values for PGE and Au were calculated based on the following C1 chondrite values: Os 761 ppb (Tredoux et al., 1989), Ir 710 ppb, Ru 1071 ppb, Pt 1430 ppb, Pd 836 ppb (Taylor & McLennan, 1985) and Au 152 ppb (Krähenbühl et al., 1973). In earlier years the acid-soluble metals were determined with various dissolution (HCl, aqua regia) and analytical techniques (OES, AAS); for Keivitsa the base metals (Ni, Cu, Co, Zn, Pb) were determined first by AAS, later (from 1992 on) by ICP-AES.

Pedogeochemical till and weathered bedrock samples taken by the Geochemistry Department were analysed for Si, Al, Fe, Mg, Ca, Na, K, Ti, V, Cr, Mn, Co, Ni, Cu, Zn, Pb and Ag by OES ("quantometer") as described by Gustavsson et al. (1979); those collected by the Exploration Department were analysed for base metals (Cu, Ni, Co, Zn, Pb) by AAS. Keivitsa was one of the first prospects from which all till samples were analysed for Pd and Au by graphite furnace AAS (Kontas et al., 1990). H_2O, C and S were determined by LECO.

The following gives the number of analyses from each study area.

Koitelainen: 91 wr analyses (XRF and wet-chemical); 913 Pd-Au analyses; 890 Pb fire assays (Pt, Pd, Au); 33 nickel sulphide fire assays for PGE-Au-Re (of which 7 analyses by the Canadian companies NAS and XRAL); 84 ICP; 2840 partial silicate and ore analyses (AAS, XRF, OES); 82 XRF analyses of chromitites; 90 analyses of Cr of high-aluminous schists; 1559 metal analyses of the products of mineral processing tests of V-rich magnetite gabbro.

Keivitsa-Satovaara: 1824 whole-rock XRF analyses; 409 Se-Te-Sb-Bi, 2263 Te, 44 trace-element ICP-MS, 15 366 Pd-Au; 4627 PGE-Au-Re (of which 233 by the companies NAS and XRAL); 16 151 ICP; 2800 AAS base metals; 682 S (by LECO); 79 H_2O(tot) and 696 C.

Akanvaara: 1465 whole-rock XRF analyses; 3325 Au-Pd; 261 PGE-Au-Re; 371 ICP; and 261 XRF, ICP and PGE-Au-Re analyses of products of mineral processing tests.

Until the late 1970s electron microprobe analyses were made by Tuula Hautala (née Paasivirta), GSF, mainly on chromites and magnetite, using Microscan Cambridge equipment under ordinary operating conditions (accelerating voltage 15 kV, probe current 20 nA). Natural chromite from the Kemi deposits, magnetite (for V) and sphalerite (for Zn) were used as standards. The results were corrected with the Bence-Albee program. The next microprobe, a Jeol JXA, served until September 1993. It was used mainly for qualitative mineral analyses and analyses of olivine melt inclusions. Raw data were corrected with ZAF procedure. Most of the analyses presented here were made on a fully automated Cameca SX 50 probe, with four WD spectrometers. The data were processed with the Cameca PAP program (Pouchou & Pichoir, 1984). A PGT EDS instrument was used for mineral identification. In most cases natural minerals, but for

a few elements, pure metals, were used as calibration standards. The operating conditions (accelerating voltage, probe current and electron beam diameter) were as follows: 15 kV, 25 nA and defocused 10 mu beam for feldspars, micas and amphiboles; 15 kV, 30 nA and focused beam for olivines, pyroxenes and oxides; 20 kV, 30 nA and focused beam for sulphides and arsenides.

Electron microprobe analyses of Koitelainen rocks were made on olivines and pyroxenes (67 analyses), plagioclase (13, plus several partial analyses), garnet (7), magnetite and ilmenite (119), chromite (152), apatite and chlorapatite (14), loveringite (17), zircon (4), allanite (5), Ti-Th-P silicate and Ti-REE silicate (4), biotite-phlogopite and amphibole (5), chlorhornblende (3), platinum-group minerals (PGM) 12, sulphides (EDS identifications, 72), and fossil melt inclusions in olivine (70).

From Keivitsa microprobe analyses were made of olivine (169), clinopyroxene (114), orthopyroxene (19), plagioclase (32), magnetite, ilmenomagnetite and chrommagnetite (90), chromite (17), spinel (1), ilmenite (6), rutile (2), chlorapatite (9), zircon (10), dashkesanite (13), primary hornblende and secondary amphiboles (84), biotite-phlogopite (46), chlorite (12), serpentine (2), sulphides and arsenides (723), tsumoite (7), PGM (8), and uraninite (4). In addition, there are 56 EDS identifications of various minerals; 123 PGM and 95 sulphide and arsenide analyses reported by Kojonen et al. (1996, 1997); 20 EDS analyses of sulphides and 40 of PGM made by VTT (privately reported by Tuula Saastamoinen, 1994); and 3 PGM determinations made by Boliden Mineral (privately reported by Juhani Nylander, 1995).

From Akanvaara the following microprobe analyses were made: secondary Fe-Mg silicates from chromitite layers (87), chromite (878), ilmenite and ilmenorutile (89), loveringite (11), chlorapatite and apatite (60), chromian clinozoisite (8), titanite (11), tourmaline (10) and laurite (3). VTT supplied 70 EDS analyses of silicates and ilmenite.

Innumerable BE and SE images and EDS peeks were made during the microprobe work.

Pentti Kouri (GSF, RONF) made dozens of XRD mineral identification runs using a Philips automatic X-ray powder diffractometer.

Samples from the Keivitsa-Satovaara area have been used for isotope studies of Sm-Nd (Huhma et al., 1995b, 1996); S and C isotopes have been determined from 67 samples by L.N. Grinenko (see Hanski et al., 1996). Juha Karhu (pers. comm.) has made preliminary C and O isotope determinations on carbonate rocks of the Keivitsa area.

Extensive mineral processing and metallurgical tests of the UC layer of the Koitelainen intrusion were made in the late 1970s by Outokumpu Co and of the V-rich magnetite gabbro of Koitelainen by Rautaruukki Co. Flotation tests of the graphite gabbro were undertaken by Rautaruukki Co in 1988. A series of mineral processing tests on various ore types of the Keivitsansarvi Cu-Ni-PGE-Au deposit and on serpentinite of the big xenolith in the lap of the Keivitsa intrusion was made by VTT in 1993–1994. VTT also conducted processing tests on the Akanvaara UC and ULC material in 1995, and from the Akanvaara V-rich magnetite gabbro in 1996. The results of the mineral processing and metallurgical research have not yet been released.

GEOLOGICAL SETTING

Archaean basement complex

The eastern part of the Fennoscandian Shield (Shield in the following; note that the name Baltic Shield is still used in Russia) is composed mainly of Archaean tonalitic gneisses (infrastructure) and greenstone-schist belts of late Archaean to early Proterozoic age (superestructure). As the mafic magmas that formed the numerous layered intrusions on the Shield are thought to have been intruded the sialic craton it may be appropriate to try to examine some of the geochemical properties of the old crust. If the magmas that fed the layered intrusions had any interaction with the crust (which seems inevitable in the light of the large surface to volume ratio), knowledge of the geochemistry and isotope geochemistry along the feeder walls, if accessible, is necessary in efforts to assess the geochemical characteristics and degree of crustal contamination and its effect on the intrusive magmas.

Most zircons of the basement rocks were formed or reformed (that is, were purified of Pb) between 2600 and 2800 Ma. That time, called the Saamian orogeny in Russian Karelia and the Kola Peninsula, was an intense crust-forming epoch in the Shield. Apparently of global extent, it is represented in the Canadian Shield by the Kenoran event (e.g., Kouvo, 1976). Here I denote this event as Kenoran. The crust was evidently reborn, rather than newborn, as suggested by the ever growing number of zircons, or cores of zircons, older than 2600–2800 Ma found in the Shield and other old cratons in northern Eurasia.

According to zircon data, the preceding turmoil occurred at about 3100 Ma ago (e.g., Shurkin et al., 1979; Kröner et al., 1981; Mints et al., 1982; Hyppönen, 1983; Lobach-Zhuchenko et al., 1986; Paavola, 1986; Bibikova et al., 1989; Sergeev et al., 1990). This event was evidently of relatively short duration and not very thorough as indicated by the abundance of whole zircons, and older zones and cores of inherited zircons aged 3150–3650 Ma (Bibikova et al., 1989; Sergeev et al., 1989, 1990; Kröner & Compston, 1990). The calculated Sm-Nd model ages T(CHUR) for rocks containing >3100 Ma zircon generally fall within this same range, between 3200 and 3800 Ma (Jahn et al., 1984; Huhma, 1995a). This old age (of crust?) is recorded in the Sm-Nd memory of contaminated layered intrusions (see Iljina, 1994). Occurrences of zircon >3100 Ma old in acid volcanic rocks (Shurkin et al., 1979; Kapusta et al., 1985) possibly indicate newborn crust. The ε_{Nd}(3100 Ma) value for the old basement of the Koitelainen area is –3.7±1.8 (Jahn et al., 1984), one of the lowest (most negative) for Archaean crustal rocks.

Zircon ages falling between the 3100 Ma event and the Kenoran event are interpreted as representing high grade metamorphism (e.g., the 2860 Ma zircon in the Vodlozero block, Sergeev et al., 1990); zircon from acid volcanic rocks of the Koikar structure, northwest of Lake Onega, has, however, been dated at 2935 Ma (Bibikova & Krylov, 1983).

Late Archaean to early Proterozoic volcanism

The late Archaean to early Proterozoic post-Kenoran greenstone belts were laid upon older sialic crust (Goodwin, 1977; Gorman et al., 1978; Kröner et al., 1981; Lazko et al., 1982; Lowe, 1987). A greater number of isotopic ages of volcanic rocks and mafic dykes of the northern and eastern Shield has become available in recent years. As a result, a more compre-

hensive – and complicated – picture of pre-Svecokarelian cratonic magmatism has emerged. Volcanic and intrusive activity lasted longer than previously thought, and although there were evidently times of high magmatic activity, there seem to have been no lulls of any major length (see Balashov, 1996; Huhma et al., 1996). Magmatism was also compositionally more variegated, consisting of simultaneous or sequential extrusion of contrasting magmas such as komatiitic and acid lavas, alkali granites, carbonatites and tholeiites (Mutanen, 1989b, 1996; Balashov, 1996). The cratonic magmatism of the Shield also seems to have temporally faded into the preceding Kenoran diastrophism and the succeeding Svecokarelian orogeny.

In general the "Kenoran crust" in the Shield bears no evidence of older zircons. Thick sequences of acid volcanic rocks and related orthogneisses (e.g., the Lebyazhinsk series, 2620–2780 Ma, Pushkarev et al., 1978; Mints et al., 1992; Kuhmo greenstone belt, 2798 Ma, Hyppönen, 1983; Kiviaapa basement gneiss, Koitelainen, 2765–2820 Ma, Mutanen, 1989b) of this age group suggest formation of new crust.

The 2440–2490 Ma intrusion event was preceded by bimodal mafic-felsic volcanism, in which komatiitic lavas, basalts and siliceous high-magnesian basalts (SHMB) represent the mafic, and rhyolites the felsic, member. Acid volcanic rocks of the Salla Formation (Manninen, 1991) form the present floor and roof of the Akanvaara intrusion, but occur in lesser amounts in the immediate roof of the Porttivaara intrusion (my own observations) and the Koitelainen intrusion (Mutanen, 1996). Acid volcanic rocks of the Seidorechka Suite occur in the roof of the Imandra intrusion (see e.g., Kozlov et al., 1967), although, drawing on published descriptions and radiometric ages (Mitrofanov et al., 1995b) I do not consider that the "imandrites" of the area are volcanics as purported but rather that they represent the granophyre cap of the underlying intrusion.

As the pre-intrusion magmatism straddles the established Archaean/Proterozoic boundary (2500 Ma), I call it here APB magmatism.

Acid igneous rocks (lavas, dykes and intrusions) of the APB event, which are not spatially associated with the layered intrusions, are widespread in the Shield. Examples, with radiometric ages using various methods, are as follows (omitting the error limits if not unduly wide): Kaunismännikkö acid metatuff (northwest of Koitelainen) 2453 Ma (GSF, 1983; Seppo Rossi, oral comm., 1997); Sumian acid metavolcanics in Karelia 2480 Ma (Shurkin et al., 1979) and 2550 Ma (Kratts et al., 1984), pre-Jatulian quartz porphyry in Russian Karelia 2453 Ma (Kratts et al., 1976), some granites in the Kola Peninsula 2420 (±160–180) Ma (Mints et al., 1982), alkali granites 2456 Ma (Balashov, 1996), quartz porphyries 2448 Ma (op. cit.), a granite porphyry dyke east of the Kuhmo greenstone belt 2435 Ma (Luukkonen, 1988), granodiorite in the western White Sea area 2454 Ma (Levchenko et al., 1996), Nuorunen granite 2590 Ma (Kratts et al., 1984), metavolcanics of the Imandra-Varzuga zone 2540–2548 Ma (Balashov, 1996) and 2423 Ma (Mitrofanov et al., 1991), charnockites of the Topozero area 2425–2450 Ma (Shemyakin, 1980), and the Sadinoja quartz porphyry breccia below the Koitelainen intrusion 2526±46 Ma (Pihlaja & Manninen, 1988). The latter, about 200 m from the contact of the 3100 Ma tonalite and with rather wide error limits, also serves as a caveat for inherited zircons in acid volcanic rocks.

No reliable ages have yet been obtained for the APB komatiites of Central Lapland. In the eastern part of the Shield the komatiitic metalavas of the Vetren Belt and ultramafic dykes give Sm-Nd model ages of 2500 Ma (Girnis et al., 1990) and mineral Sm-Nd ages of 2460–2450 Ma (Pukhtel et al., 1991). Ultramafic dykes of the Pechenga-Varzuga zone have yielded an age of 2457 Ma (Balashov, 1996). These are a trifle older than, or indistinguishable from, the ages of the Koitelainen and Akanvaara intrusions.

There is evidence in the Shield of mafic intrusive activity that clearly predates the 2440–2490 Ma event. In the Kola Peninsula there are gabbro-norites with a Sm-Nd age of 2555±65 Ma. Relics of a pre-Koitelainen intrusion have been found below the Koitelainen intrusion (Mutanen, 1989b).

Sediments of the Parandova Series in Karelia, Russia, have yielded common lead model ages of 2420–2550 Ma (Vinogradov et al., 1959).

The mafic layered intrusions represented the finale of the APB eruptive activity; no external ultramafic, mafic or felsic dykes are found cutting the freshly consolidated cumulates. The quartz monzonite diapirs in the Koitelainen Lower Zone, felsic dykes in the Koitelainen magnetite gabbro, and dioritic and felsitic dykes in Keivitsa are "inside" phenomena of the intrusive systems, as described and explained later. In Bushveld the Nebo granite cuts through the supposedly penecontemporaneous mafic cumulates (see Walraven & Hattingh, 1993). Whether this is the only exception to the rule outlined above will be learned only after the mafic rocks of the Bushveld Complex are satisfactorily dated (see Walraven et al., 1990).

APB volcanism and intrusive activity are known from many parts of the world (see Alapieti & Lahtinen, 1989; Alapieti, 1990, 1996). Of interest is that a 2460 Ma old granophyre gneiss and acid volcanic rocks have been dated among the Transvaal sediments in the Bushveld area (Coertze et al., 1978; Walraven et al., 1990). Moreover, bimodal (mafic/rhyolitic) volcanism in the Hamersley Basin, Australia, took place between 2470 Ma and 2449 Ma (Barley et al., 1997). Glikson (1996) has presented an exciting and inspiring vision linking global magmatic events to meteorite bombardment.

As reliable ages of metasediments and metavolcanics in Finnish Lapland are lacking, intrusion ages become handy in fixing the minimum age for the floor rocks and immediate roof rocks.

Refractory volcanic rocks are found as xenoliths among cumulates. Xenoliths of basalts, basaltic tuffs, komatiites and pre-intrusive gabbros occur in the Koitelainen intrusion, komatiite xenoliths in the Koillismaa Group intrusions (my interpretation of the case reported by Isohanni, 1976), and basaltic xenoliths in the Akanvaara intrusion. Keivitsa is conspicuous for the abundance and wide variety of xenoliths.

MAFIC LAYERED INTRUSIONS OF THE FENNOSCANDIAN SHIELD

Mafic layered intrusions occur throughout the Fennoscandian Shield. A very incomplete presentation of their areal distribution is shown in Fig. 1. The data shown on the map in Fig. 1 were collected from published regional reviews (Alapieti & Lahtinen, 1986; Alapieti, 1996; Mutanen, 1989a, 1996), descriptions of individual intrusions, new unpublished reports and published U-Pb zircon and baddeleyite ages and Sm-Nd mineral isochron ages, as follows (intrusion/source): Koitelainen/ (Mutanen, 1976b; 1979a, 1981, 1989a, b, 1996); Kouvo, 1977; Fedorova-Pana/Mitrofanov et al., 1991; Bayanova et al., 1994; Amelin et al., 1995; General (Luostari)/Mitrofanov et al., 1991; Amelin et al., 1995; Bayanova & Smolkin, 1996; Grokhovskaya et al., 1996; Monchegorsk (Moncha)/Vinogradov et al., 1959; Kozlov et al., 1967; Kozlov, 1973; Mitrofanov et al., 1991, 1995a; Amelin et al., 1995; Amelin & Neymark, 1995; Glavny Khrebet (Monche-Chuna-Volche-Losevykh Tundr, MVL)/ Koz-

lov et al., 1967; Mitrofanov et al., 1993; Imandra/Mitrofanov et al., 1991; Dokuchaeva et al., 1992; Amelin et al., 1995; Kolvitsa (Kolvitsa-Kandalaksha)/Mitrofanov et al., 1993; Frisch et al., 1995; Pyirshin/Mitrofanov et al., 1993; intrusions of the Kejv area/Sharkov & Sidorenko, 1980; Mints et al., 1992; Mitrofanov et al., 1993; Olanga group (Kivakka, Tsipringa, Lukkulaisvaara and Kundozero; intrusions of the Topozero area)/Lavrov, 1971, 1979; Sidorenko et al., 1974; Sidorenko & Shemyakin, 1974; Shemyakin, 1980; Stepanov, 1984; Mitrofanov et al., 1991; Amelin et al., 1995; Haikola/Gorbik, 1976; Burakovka/ Lavrov et al., 1976; Amelin & Semenov, 1996; dyke complexes/ Sidorenko & Shemyakin, 1974; Ein, 1984; Kolbantsev, 1994; Vuollo et al., 1996). It is possible that many of the present individual intrusions, e.g., the Koillismaa Group (Alapieti), 1982), Monchegorsk and MVL (Sokolova, 1976; Rundkvist & Sokolova, 1978) and Koitelainen and Akanvaara intrusions, were originally parts of a single intrusion.

The first "respectable" ages of the 2440–2490 Ma group of intrusions are the 2450–2460 Ma common lead model ages of the massive vein sulphides of the Monchegorsk intrusion (Vinogradov et al., 1959). The first conventional isotopic ages on zircon of the ultramafic pegmatoids were obtained in 1974 of the Koitelainen intrusion (Mutanen, 1976b, 1989b; see also the sections on ultramafic pegmatoids in this book). Since then a great number of intrusions have been dated by U-Pb zircon, baddleyite and (or) Sm-Nd methods.

A man-made problem that causes some confusion among the uninitiated concerns the names of the intrusions. There are various ways of transliterating Russian into English, usage differs among Russian geologists, some writers use former Finnish names, and others present Russian names and so on. It is not difficult to see that Tsipringa is the same as Tsypringa, and one might guess that Burakovka is the same intrusion as Burakovsky, Burakovo or Burakovka-Aganozero and that Lukkulaisvaara is the same as Lukkulaisenvaara, but how could one know that Pana is the same as Panski or Pansky and Olanga the same as Oulanka. And what about the names Monche, Moncha and Monchegorsk? It may be possible to conclude from textual hints that Monche (Moncha) is in fact the old Monchegorsk, and not part of the long Monche-Volche-Losevykh Tundr (MLV) intrusion west and northwest of Monchegorsk. I hope that this book will become, if nothing else, an authoritative text regarding the names of the intrusions!

The large mafic differentiated "plutons" in southern Finland (the Ylivieska, Parikkala and Hyvinkää intrusions shown in Fig. 1) are not generally recognized as layered intrusions, which they undoubtedly are. They present fine examples of layering in outcrops and strong crystal fractionation down to cumulus ilmenite, magnetite and apatite. Their parent magmas were richer in Ti and more oxidized than those of older intrusions in northern and eastern parts of the Shield. These intrusions and their feeder sections represent the geosynclinal magmatism (island arch magmatism (?) in current usage) of the Svecofennian orogeny (ca 1880–1892 Ma; Neuvonen et al, 1981; Patchett & Kouvo, 1986), whereas the older intrusions (> 2000 Ma) intruded the Archaean crust and were emplaced either at the basement contact or at different levels in the overlying cratonic sedimentary-volcanic pile.

The magmas of the 2440–2490 Ma intrusions were mainly emplaced along the unconformity contact between the basement and late Archaean or early Proterozoic metasediments and greenstones (e.g., Mutanen, 1981, 1989b; Dokuchaeva et al., 1992). The upper feeder section of Näränkävaara, the connecting dyke (see Alapieti, 1982) as well as the feeder dykes southeast of the Kemi and Penikat intrusion trend northwest (Mutanen, 1989b) a trend that is also seen in the overall distribution of the intrusions of the Lapland Intrusion Belt (LIB).

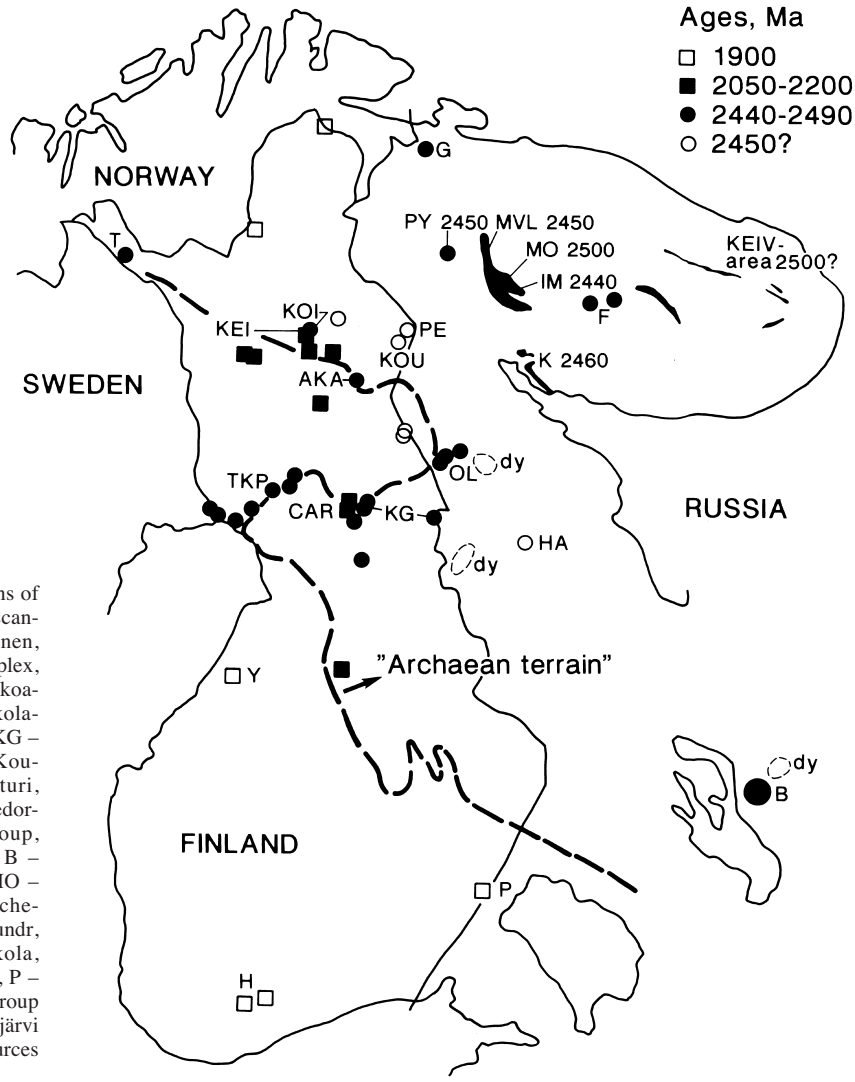

Fig. 1. Mafic layered intrusions of the central and eastern Fennoscandian Shield. KOI – Koitelainen, KEI – Keivitsa-Satovaara Complex, AKA –Akanvaara, T – Tsohkkoaivi-Kaamajoki, TKP – Kukkola-Tornio-Kemi-Penikat group, KG – Koillismaa group, KOU – Koulumaoiva, PE – Peuratunturi, G – General (Luostari), F – Fedorovo-Pana, OL – Olanga group, K – Kolvitsa-Kandalaksha, B – Burakovka, IM – Imandra, MO – Monchegorsk, MLV – Monche-(Chuna)-Volche-Losevykh Tundr, PY – Pyrshin, HA – Haikola, Y – Ylivieska, H – Hyvinkää, P – Parikkala, dy – 2450 Ma age group dyke complex. CAR = Kortejärvi and Laivajoki carbonatites. Sources in text.

The postulated feeders of the Kemi and the Penikat intrusions (the Loljunmaa dyke, see Alapieti et. al., 1990) were checked by gravity measurements and found to agree with the prediction (Elo, 1979). The Loljunmaa (Lolju) dyke is traceable as a string of gabbro outcrops for 7 km east of the base of the intrusion (see Perttunen, 1971).

Opinions vary as to the composition of the parent magmas of the 2440–2490 Ma intrusions. This is partly due to the lack of chilled rocks, which would be representative of the parent magma before fractionation and untainted by contamination or cumulus crystals (see e.g., Hoover, 1989) and partly because the bulk intrusion analyses were made on sections that do not represent the entire cumulate mass. Only the roots of many intrusions are exposed on the present erosion surface (Burakovka, Näränkävaara). The Tornio-Kemi-Penikat intrusions were tilted and beheaded by pre-Jatulian erosion and hence only remnants of the

granophyre caps have been preserved (Perttunen, 1991).

The most completely analysed of the best preserved intrusions is Akanvaara, which shows (Fig. 5) that the bulk composition of the intrusion corresponds to a fairly normal tholeiite, with ca 52% SiO_2, 6–8% MgO, 0.7% TiO_2, and low Cr and Ni. Thus, the magma was not particularly "primitive". It was rather similar in bulk composition to the Bushveld layered series (see von Gruenewaldt, 1979), and Bushveld magma at the Merensky Reef fractionating stage (Cawthorn, 1995, 1996).

From what we know of the fractionation of the Koitelainen and Akanvaara magmas (low H_2O) and the bulk intrusion compositions (MgO, Cr and SiO_2), it is clear that the magmas were not boninitic (see Crawford et al., 1989) as proposed by Alapieti (1996). The untainted chill compositions have a Cr content appropriate to tholeiitic basalts, low REE and a flat REE CN pattern (see Alapieti, 1982). SHMB-type volcanism (see Sun et al., 1989) preceded the Akanvaara intrusion, but the intrusion itself is not of the SHMB type.

The parent magmas of the 2440–2490 Ma intrusions were low in Ti and P, and the Fe^{3+}/Fe^{2+} ratio was low. Thus, ilmenite never crystallized as a "legal" cumulus mineral, cumulus apatite appeared only in the uppermost ferrodiorites, and cumulus magnetite (original titanomagnetite) entered late (at Koitelainen at about 94 PCS level).

The magmas were also heavily undersaturated in sulphur (sulphide liquid), and hence, aside from transient sulphide saturation due to contamination, terminal saturation of sulphide liquid (high Fe and Cu/Ni) occurred at or above the magnetite-in phase contact. In this respect the magmas were quite similar to that of other tholeiitic intrusions, e.g., the Bushveld Complex (Liebenberg, 1970) and Kiglapait intrusion (Morse, 1969a, 1979b).

The mafic layered intrusions in northern Finland and their counterparts in Russian Karelia and the Kola Peninsula host a variety of ore deposits. With their numerous known prospects of PGE (Razin, 1974; Mäkelä, 1975; Isohanni, 1976; Piirainen et al., 1977; Mutanen, 1979, 1989a,b, 1996; Vuorelainen et al., 1982; Piispanen & Tarkian, 1984; Lavrov & Pekki, 1987; Mutanen et al., 1987, 1988; Krivenko et al., 1989; Lazarenkov et al., 1989, 1991; Yakovlev et al., 1991; Barkov et al., 1991, 1994; Pchelintseva & Koptev-Dvornikov, 1993; Golubev & Filippov, 1995; Mitrofanov et al., 1995a,b; Nikitichev et al., 1995; Trofimov, 1995, Trofimov et al., 1995), of Ti and V (e.g., Proskuryakov, 1967; Juopperi, 1977, Mutanen, 1989b) and of chromite (Veltheim, 1962; Kujanpää, 1964; Kozlov et al., 1975; Barkanov, 1976; Mutanen, 1979, 1981, 1989a,b, 1996; Dokuchaeva et al., 1982a, b; Lavrov & Trofimov, 1986; Lavrov & Pekki, 1987; Alapieti et al., 1989; Smirnova et al., 1996), they are justifiable targets for the present exploration programmes in the Shield. Taken together, the chromitite layers of Koitelainen, Akanvaara, Monchegorsk, Imandra and Burakovka already constitute the largest known undeveloped resource of chromite in the world.

A belt of layered intrusions runs in a general southeasterly direction through Finnish Lapland and on into Russia (Fig. 1). The name Lapland Intrusion Belt (LIB) is used here for the belt. The LIB contains intrusions, sills and dykes with ages from 2490 Ma to 2000 Ma and younger. The intrusions of the 2440 Ma age group occur in the axial part, and throughout the length, of the LIB, from Tsohkkoaivi-Kaamajoki in the northwest to Kivakka, Tsipringa and Lukkulaisvaara (the Olanga group) in Russia. Small intrusions and dykes of the general magma type of 2440 Ma intrusions are met with southeast of Olanga (see Fig. 1); the belt may extend still farther southeastwards, to Burakovka in the Lake Onega region, Russia.

Relics of a pre-Koitelainen intrusion were intersected below the Koitelainen intrusion by two diamond drill holes, and its rocks occur as xenoliths near the base of the Koitelainen in-

trusion. The older intrusion is of an evolved (Ti-P-rich) magma type.

The Koitelainen event was preceded by extrusion of rhyolitic and komatiitic lavas and minor basalts (see Mutanen, 1989b). At Koitelainen, komatiites are more common, but at Akanvaara the intrusion was preceded mainly by rhyolitic and basaltic volcanism (SiO_2 52–53%, MgO 6.5%, TiO_2 0.85%). Komatiites and rare basalts occur in Koitelainen among mafic cumulates as xenoliths, in "horizons" marking the onset of anatexis of the roof rocks. Understandably, acid rocks immersed in hot mafic magma had little change of survival. In recent diamond drill holes remains of partially melted ("granophyrized") amygdaloidal acid lavas have, however, been found among granophyres in the southeastern part of the Koitelainen intrusion. Xenoliths of acid porphyries also occur in the Akanvaara granophyre.

Mafic dykes cut the rocks of the Koitelainen and Akanvaara intrusions. Their chilled contacts and general hypabyssal petrography suggest that they were channels for lavas that extruded not far above them. Because dykes like these have not been found cutting the Keivitsa-Satovaara complex, the post-Koitelainen dykes may represent pre-Keivitsa basaltic magmatism (see Huhma et al., 1996).

The intrusions were later metamorphosed, faulted and folded, sometimes into upright and even overturned positions. Faulting, folding and emplacement of younger granitoids dismembered the original intrusions. It seems that despite the superimposed folding, the LIB and associated cratonic supracrustal rocks are still in their original site, that is, the crustal rocks of Central Lapland were never hauled around as tectonic plates, eventually to be put together like a jigsaw puzzle along the healed seams of collided plates. My opinion is that the prime tectonic mover in Central Lapland was density inversion between the heavy superstructure (greenstones and mafic intrusions) and the underlying buoyant sialic crust. This caused diapiric rise of granitoids as brachyantiform structures.

The Keivitsa event, like that of Koitelainen, was preceded by bimodal and often explosive rhyolitic-komatiitic volcanism. Evidence of acid volcanism first appears among the pelitic sediments below the Keivitsa intrusion; acid volcanism was accompanied and followed by komatiitic lavas, agglomerates and tuffs, and by the intrusion of komatiitic sills. The U-Pb zircon age of 2048 Ma (Hannu Huhma, letter, 1992) for the Matarakoski quartz porphyry (metarhyolite), 10 km southwest of Keivitsa, is indistinguishable from the age of the Keivitsa intrusion, 2057 Ma (Huhma et al., 1995b; Huhma, 1997).

In Finland, magmatism roughly contemporaneous with Keivitsa produced the gabbro-anorthosite complex of Otanmäki (2060 Ma U-Pb zircon, Talvitie & Paarma, 1980); the acid and basic lavas of the Kuopio district (2060 Ma U-Pb zircon, by Olavi Kouvo; Heikki Lukkarinen, pers. comm.), acid porphyry of Ylitornio (2050 Ma U-Pb zircon, Vesa Perttunen, pers. comm.) and the basaltic metalava of the Jouttiaapa volcanics (Sm-Nd wr 2090±70 Ma, Huhma et al., 1990), the two last mentioned from the Peräpohja schist belt. At Rautuvaara, western Lapland, a differentiated dyke has been dated by U-Pb zircon at 2027±33 Ma (Hiltunen, 1982). The carbonatites of Laivajoki and Kortejärvi yield a U-Pb/zircon age of 2020 Ma (Vartiainen & Woolley, 1974). The U-Pb zircon age, 2060 Ma, of an alkali granite, Kola Peninsula (Pushkarev et al., 1978) Comes close to the Keivitsa age.

The peculiar mafic dykes that cut the solidified and cooled Keivitsa intrusion have no known compositional counterparts among the dyke rocks of the Shield. They may be contemporaneous with 1970 Ma tholeiitic dykes (Vuollo et al., 1992) and ophiolites (Kontinen, 1987) in eastern Finland. Considering the long magmatic history, these dykes represent the prelude to a restless future, the Svecokarelian orogeny.

PREVIEW OF THE CONVECTION-CONTAMINATION MODEL

I find it impossible to describe the cumulates of the layered intrusions in neutral terms, uninfluenced by the ideas to be presented later in this book. To help the reader follow the text I shall therefore, without arguments, look briefly at the convection-contamination (CC) model that runs like a leading thread (or perhaps to some, like a barbed wire) through the rest of this book.

The magma filled the chamber before any significant crystal accumulation occurred, and formed a chilled lining of microgabbro against the country rocks. The magma was convective due to heat loss through the roof (thermal convection) and spatial differences in bulk densities of the melt-crystal suspension (two-phase convection). There were intermittent accelerated bursts of convection and, possibly, convective overturns of the magma reservoir. The mingling-mixing zone between the mafic main magma and overlying buoyant anatectic melt was the prime setting of phase separation (crystallization of cumulus silicates and oxides, separation of immiscible sulphide liquid, degassing).

The crustal rocks were melted mainly due to the latent heat released by crystallizing cumulus minerals. The melting occurred in two stages, corresponding to fractional (water-saturated/dry) melting of the granitic constituents of the country rocks. Practically no melting took place during the interval between the two stages of fractional melting. At melting, chilled linings were detached and they foundered in the magma. New generations of temporary chills formed from the evolving magma against the walls and even against the salic roof melt.

The magma was contaminated by selective diffusion, wholesale mixing (hybridization) and refractory residual phases after partial melting of the country rocks. The added contaminants shifted the field boundaries of saturated and potential phases. The residual xenocryst phases equilibrated their compositions or, if not part of the set of phases separating from the mafic magma, reacted with it or were dissolved. Thus, the effects of contamination were mainly catalytic, visible only in trace element and isotope systems, and in the intercumulus. Contaminants were dragged along in crystal-laden density flows and trapped in the cumulus pile by settling crystals. The main magma that were not drawn into the density flows evolved independently towards iron enrichment.

The two stages of fractional melting are reflected in two main contamination stages in intrusions. Towards the end of fractionation, magma mixing became increasingly sluggish as the compositions of the mafic and salic silicate liquids approached the stable immiscibility solvus.

The character of contamination depends on the water content and chemical composition of the wall rocks, the size and surface/volume ratio of the magma chamber and on the type of melting (equilibrium/fractional). In KOI-type intrusions (Koitelainen, Akanvaara) the contamination was determined by fractional two-stage melting, and by salic and refractory aluminous residue materials, in KEI-type intrusions (Keivitsa-Satovaara) contamination was effected by selective contamination (H_2O, Cl, K), by water-saturated melting of sulphide-rich pelitic and carbonaceous sediments, and by refractory olivine xenocrysts from disaggregated komatiitic rocks.

Fig. 2. Akanvaara hill. The top consists of acid volcanic rocks. From the top downwards are granophyre, ferrogabbro and magnetite gabbro. The craggy banks are washed and reworked shores of the Salla glacial lake. A thick anorthositic sequence (with PGE) occupies the gully at the foot of the hill. Photo by TM.

THE AKANVAARA INTRUSION

General geology

The Akanvaara intrusion is located in the southeast of the LIB (Fig. 1), 80 km southeast of Koitelainen. Zircon from a crescumulate gabbro just above the Upper Chromitite layer gives a U-Pb age of 2430 Ma (Hannu Huhma, letter 1992; pers. comm. 1996).

Owing to the lack of outcrops the existence of the northern wing of the intrusion was not known at the time the Savukoski map sheet was printed (Juopperi, 1986; Heikki Juopperi oral comm., 1991). The geology of this wing is indeed still poorly known.

The new geological map (Appendix 1) is based on revised mapping of the area, low-altitude aeromagnetic maps, ground geophysical surveys (magnetic, gravity and electromagnetic), extensive diamond drilling, and new chemical analyses, thin sections and electron microprobe mineral analyses. Exploration by the RONF continues in the area.

The intrusion is a block-faulted monocline dipping southeast, with a surface area of 50–55 km^2. Its length from north to south is ca 15 km; its width in the southern part, along the strike of layering, is ca 7 km, and across the northern wing 2–3 km. In the east and west the intrusion is bounded by zones of steep NW-NNW faults. The eastern fault zone separates the intrusion from older acid volcanics. In the west, beyond the western fault zone, the terrigeneous psephitic and psammitic sediments of the Ritaselkä formation are considered younger than the Akanvaara intrusion (Jorma Räsänen, oral comm.). Thus, the southern part of the intrusion is an erosional section of a fault staircase descending to the west, the parts west of the boundary fault being buried beneath younger metasediments. This general structure of the intrusion is shown by the gravity field (increases westwards, towards the buried part of the intrusion and away from the lower-density acid rocks) and magnetic field (increases eastwards, towards the strongly magnetic acid volcanics).

The southern part of the intrusion consists of three large fault blocks and numerous sub-blocks. The general direction of these faults is between NW and NNW, the same as that of the boundary faults, and uncomfortably close to the ideal drilling direction.

The dip of igneous layering in the southern part varies from 25° in the westernmost block to 40° in the east, indicating relative rotation of blocks. Here the floor and roof contacts of the intrusion, where known, have been preserved, but in the northern wing long stretches of the western (floor) and eastern (roof) contacts have been faulted. The general strike of the magmatic layering in the northern wing seems to be northeasterly, the same as in the southern part of the intrusion.

Young faults (from post-metamorphic to postglacial) and other "zones of weakness" consist of crumbled material, and contribute to core loss. No displacement along young faults has been recognized.

Old healed faults and fault zones are formed before and (or) during regional metamorphism. They have been intersected by diamond drilling and are sometimes visible in outcrops. Apart from normal fracturing they are solid rocks. The broad fault zones are schistose blastomylonites, often with mineral veins (quartz, carbonate). Thin fault traces (width ≤ 0.5 m) are often filled with meta-pseudotachylytes (metamorphosed pseudotachylytes). In Tuorelehto a braided network of faults, shear zones and metapseudotachylytes is visible in the Upper Chromitite (UC) outcrop (Appendix 2). The pseudotachylytes formed through cataclastic comminution, frictional melting and post-frictional annealing (see Reitan, 1968; Sibson, 1975, 1977; Fleitout & Froidevaux, 1980). Pockets of coarse plagioclase (with minor chlorite) occur in meta-pseudotachylyte veins; they may represent segregated and slowly crystallized frictional neo-melt.

The chromitite layers of the Lower Zone frequently have contact faults, with displacement roughly parallel to layering. Such faults may already have formed during consolidation of the cumulate pile, between stiff chromitite layers and less competent host pyroxene cumulates (possibly still containing interstitial melt). Layer-contact faults may also have formed during metamorphic hydration as a result of dissimilar volume expansion of chromitite and pyroxenite. Similar contact faults are common in Bushveld (Lea, 1996).

The magma intruded supracrustal rocks among which acid volcanics were dominant. Basalt xenoliths occur in granophyre. The acid volcanics of the roof, well exposed on Akanvaara hill, typically contain large silicic amygdales. All the acid volcanites intersected by diamond drill holes below the intrusion are hornfelses (later altered to metahornfelses). Porphyric types are dominant here, but amygdaloidal rocks also occur. The hornfelses intersected and analysed so far are compositionally affected by the intrusion and hence resemble the ferrogranophyres of the roof (see Mutanen, 1996, p. 107). The hornfelses are more "primitive" (higher MgO and mg# and V, lower Mn, Pb and Zn).

Acid volcanic rocks heated by the crystallizing magma of the intrusion melted relatively easily, particularly if they contained glass. The nature and amount of the digested roof rocks are not known, but the presence of basaltic xenoliths indicates a lithology more variegated than that of the present roof. At Purkkivaara, 5 km south of the intrusion, high-aluminous pelitic schists and komatiites occur at about the level of the "missing" lithology of Akanvaara (Jorma Räsänen, 1983, and pers. comm.). They may correspond to the high-aluminous pelitic roof rocks of the Koitelainen intrusion.

Numerous mafic dykes with a general strike of NNW cut the Akanvaara intrusion and country rocks. The two dykes analysed represent two distinct magma types: a rather primitive one (MgO 11%, FeO(tot) 10%, TiO_2 0.85%, Cr 950 ppm, Ni 300 ppm, Cu 100 ppm, SiO_2 50.5%), and a more evolved one (MgO 7%, FeO(tot) 13%, TiO_2 1%, Cr 130 ppm, Ni

90 ppm, Cu 180 ppm, SiO_2 48%). Some newly intersected dykes are komatiitic in appearance.

The rocks of the intrusion, along with their envelope and dyke rocks, underwent amphibolite-facies regional metamorphism. The rocks of the intrusion suffered hydration but, apart from that, metamorphism appears to have been almost isochemical. The granophyre and gabbros down to the Main Zone are usually heavily recrystallized. The former cumulus pyroxenes have not been replaced by the usual, tidy uralite pseudomorphs but by a sheaf of long amphibole prisms that have grown far beyond the original grains. Plagioclase is whitish, having lost its characteristic dark pigment during recrystallization, and has altered into clinozoisite and a more albitic plagioclase, sometimes into scapolite. However, during alteration the plagioclase retained the pigment even when all the pyroxenes had been uralitized. With the general decrease in alteration downwards, the dark-pigmented plagioclase becomes more common, and in the lower Main Zone pyroxenes and olivine have survived in gabbro, troctolite and peridotite. Preserved pyroxene is common in the pyroxene cumulates of the Lower Zone. Unless stated otherwise, the terminology of the cumulates is based on the original magmatic minerals.

Igneous stratigraphy and petrography

There are very few outcrops in the Main and Lower Zones. However, overlapping drill cores provide a continuous profile from near the top of the granophyre down to the floor rocks. The cores were analysed gaplessly for Pd and Au, and XRF whole rock analyses were made on all cores or at regular intervals.

The total thickness of the cumulate succession plus granophyre as exposed on the present surface is ca 3100 m (Figs 3 and 5). The layered succession above the lower chilled margin is formally divided into zones.

The lower marginal chill is composed of fine-grained microgabbros and non-laminated (non-cumulate) gabbros, the latter often with dendritic plumose pseudomorphs of former pyroxene ("crescumulate microgabbro").

The Lower Zone (LZ) consists of a lower orthopyroxene cumulate unit and an upper gabbroic unit; there are several chromitite layers.

In orthopyroxene cumulates cumulus chromite is ubiquitous. The cumulates also contain, particularly when chromite is abundant, cumulus clinopyroxene as big, sparse cumulus crystals, more rarely as small euhedra. Interestingly, orthopyroxene has a reaction relationship with clinopyroxene, the latter finishing its crystallization with intercumulus quartz. Olivine (now altered) is a visiting cumulus mineral. It joins the pyroxene-chromite cumulus assemblage 1.4–3.1 m below each of the Lower Chromitite (LC) layers, occurs between closely-spaced chromitite layers and in one case continues for 2 m above the chromitite. Sometimes euhedral olivine occurs, without reaction, with euhedral orthopyroxene. As at Koitelainen and Keivitsa, I think that this does not really mean co-crystallization of olivine and orthopyroxene. The olivine abundance below the lowermost LC layer is very low. Olivine is not associated with the Lowermost Lower Chromitite (LLC) layers.

Plagioclase is the main intercumulus mineral in LZ. Brown primary hornblende also occurs in the intercumulus. The amount of postcumulus plagioclase, and also of quartz, is quite high (27–39 vol% pl+q) near the base, to the extent that some pyroxene cumulates are modally gabbros and quartz gabbros. Euhedral zoned crystal cores in plagioclase oikocrysts indicate that plagioclase began to grow as a

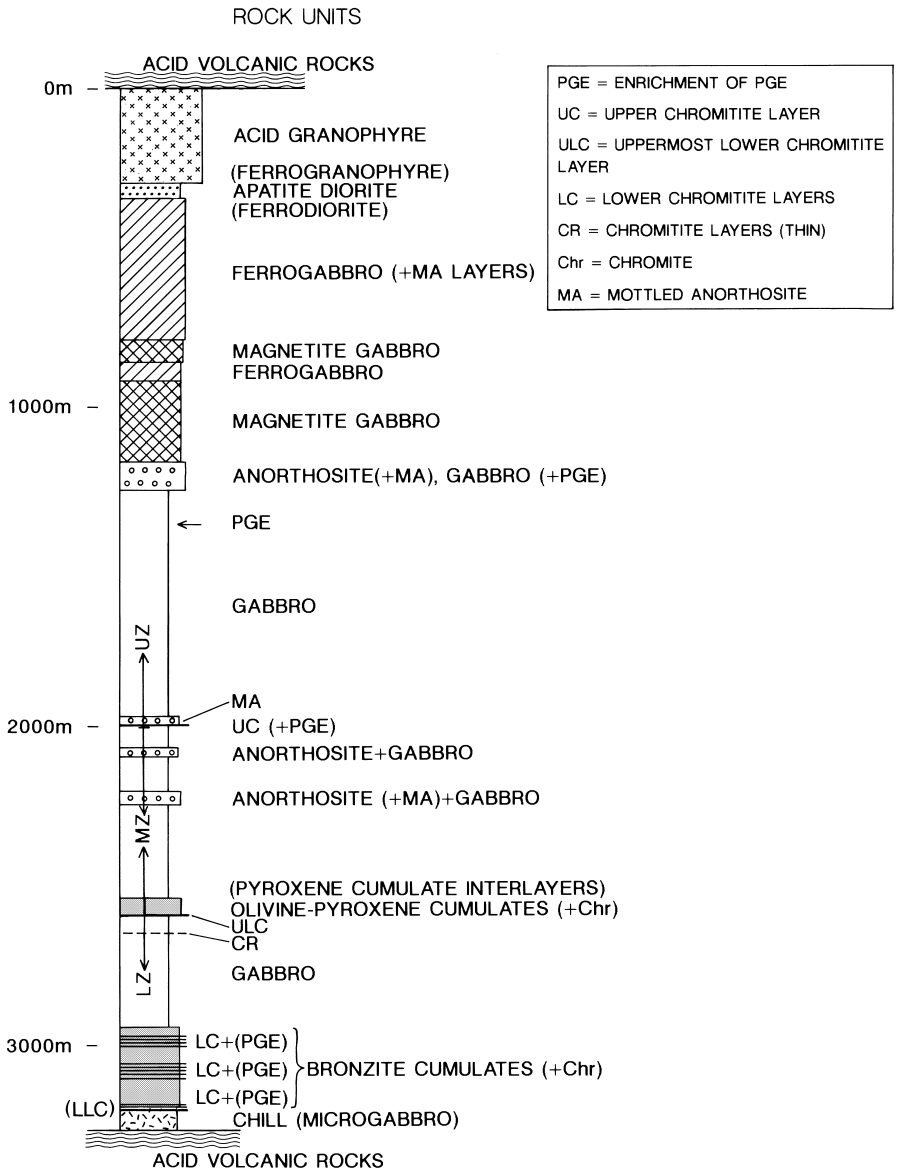

Fig. 3. Stratigraphy of the Akanvaara intrusion.

cumulus phase. Evidently these cumulates contain a considerable amount of acid contaminant magma from melted floor rocks. Layers of true gabbroic cumulates occur in the lower part of the unit. Fluorapatite and zircon are typical (but never abundant) accessory minerals. The amount of intercumulus plagioclase decreases upwards. Zircon is present, and loveringite is common (Fig. 4, Table 2). I have found crystals of loveringite as inclusions in orthopyroxene; thus, it is apparently a cumulus phase, as in the Koitelainen intrusion (Tarkian & Mutanen, 1987). Apatite is chlorapatite (Cl 5.03–6.84%, F 0.00–0.08%) in pyroxene cu-

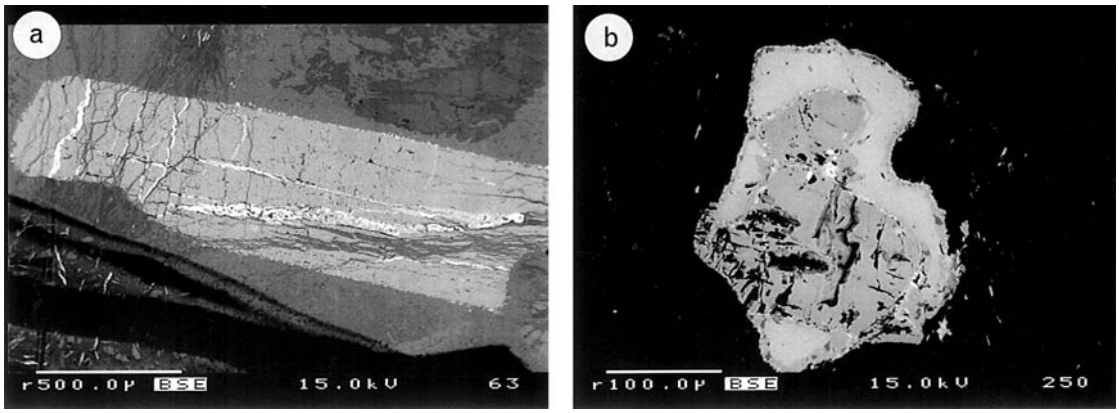

Fig. 4. Chlorapatite and loveringite from Akanvaara. BE images by Lassi Pakkanen. a – cumulus chlorapatite with veins of secondary magnetite. Olivine cumulate (peridotite) overlying ULC layer. DDH337/29.75 m; b – loveringite mantle around cumulus chromite in orthopyroxene-clinopyroxene cumulate. Loveringite has a thin ilmenite+rutile rim. In this thin section there are also laths of loveringite, zircon, primary phlogopite and quartz. DDH320/252.80 m.

mulates (Table 8), but in the heavily contaminated lowermost pyroxene cumulates and LLC layers the apatite is fluorapatite.

Interlayers of gabbro appear in the upper part of the unit.

The lowermost part of the gabbro unit contains pyroxenite interlayers. Otherwise the unit mainly consists of monotonous gabbroic cumulates. Discontinuous layers of pyroxene (-chromite) cumulates and a group of thin (≤ 5 cm) chromitite layers occur in the upper part.

Immediately below the base of the MZ is a 3 m-thick succession of alternating layers of pyroxenite, gabbro and mottled anorthosite.

The Main Zone (MZ) comprises cumulates from the base of the Uppermost Lower Chromitite (ULC) up to the base of the Upper Chromitite (UC) succession.

An olivine-pyroxene cumulate unit about 25 m thick overlies the ULC layer. This unit shows up well on the magnetic map. Disseminated cumulus chromite is always present; in the lower part of the unit chromite occurs as thin bands and as concentrated pockets between orthopyroxene cumulus crystals. Black oikocrysts of amphibolized clinopyroxene, enclosing olivine, give the rock its characteristic mottled look. Oikocrysts of orthopyroxene are preserved in unaltered rocks. Chlorapatite occurs as big cumulus crystals (Fig. 4, Table 8).

In the upper part of the unit there are interlayers of pyroxene cumulates (with chromite) and olivine-plagioclase-chromite cumulates (troctolites, with poikilitic pyroxenes). These are overlain by a succession, ca 35 m thick, of alternating layers of gabbro and pyroxenite. Most of the MZ rocks are cotectic plagioclase-pyroxene cumulates. In the lower gabbros, orthopyroxene typically occurs as small (≤ 1–2 cm) oikocrysts.

Solitary layers rich in cumulus plagioclase (anorthosite gabbros) and two thick successions of alternating layers of gabbro, anorthosite gabbro, gabbro-anorthosite and mottled anorthosite occur in the upper part of the MZ.

The coarse gabbros on top of the MZ contain plagioclase in excess to its due cotectic proportion. These rocks are also rich in intercumulus quartz and contain big fluorapatite crystals.

The Upper Zone (UZ) is set to begin from the top of the homogeneous gabbros underlying the Upper Chromitite (UC) layer. It starts

with the UC sequence, which will be described later in connection with the UC layer (see Fig. 10).

Leucocratic layers become thinner and more sparse upwards from 10 – 15 m above the UC, vanishing altogether about 40 m above it. The interval between the UC succession and magnetite gabbro consists mainly of cotectic pyroxene-plagioclase cumulates that are macroscopically monotonous except for size layering. In this innocuous gabbro a 14-m-thick interval enriched in PGE was revealed by systematic Pd assays. The overlying cumulates up to the magnetite gabbro are variably anomalous in PGE.

Near the top of the UZ is a 100-m-thick sequence of plagioclase-rich cumulates (mottled anorthosites, gabbro-anorthosites and anorthosite gabbro), with gabbro interlayers. Ilmenite may have crystallized as a cumulus mineral, possibly due to silicic-aluminous contamination. The sequence contains a 40-m-thick bipartite PGE-enriched interval.

The sudden arrival of cumulus titanomagnetite marks the sharp basal contact of the magnetite gabbro. At this phase contact there are marked anomalies of P_2O_5 (up to 0.3%), Zr (210 ppm), Cr (376 ppm), La (45 ppm) and Ce (76 ppm), which suggest that the arrival of magnetite was promoted by convective overturn and associated contamination of the magma. The high Cr reflects the high $D_{Cr}^{sp/liq}$, but the source of Cr may be Cr-enriched refractory residue matter of melted crustal rocks. Geochemical anomalies of Zr, P and REE seem to be characteristic of reversals analysed in detail (see Lambert & Simmons, 1984; Halkoaho, 1994) and I take the liberty to interpret them with the CC model.

The magnetite-gabbro unit consists of two magnetite-rich layers (with V > 0.1%) separated by a layer poor in magnetite. The lowermost 6 m consists of plagioclase-magnetite cumulate with a V content of 0.4%. Magnetite has partly altered into silicates (hornblende, biotite) in metamorphic reactions.

Titanomagnetite was evidently the sole cumulus Fe-Ti oxide in magnetite gabbro. With decreasing temperature ilmenite exsolved from titanomagnetite first by granule oxidation-exsolution, later by lamellar exsolution (ilmenomagnetite). Titanomagnetite crystallized as a cumulus phase up to the end with plagioclase and pyroxenes. These were probably later joined by fayalite. Apatite joins the cumulus assemblage at about 150–200 m below the granophyre.

Thin (1–4 cm) anorthosite layers occur in the lower part of the unit. In the magnetite-poor upper part there are seven layers of plagioclase-rich cumulates (mottled anorthosite, anorthosite gabbro), from 1 m to 7.5 m thick, and more than ten ultramafic layers (now hornblendite) 0.2 – 1.7 m thick. In these rocks there is a positive correlation between plagioclase content and P-Zr-Ce-La.

The uppermost mafic cumulates are ferrogabbros (SiO_2 < 55%, FeO(tot) 17–25%, CaO/Na_2O < 2), apatite-ferrogabbros (apatite 2–5%) and apatite-ferrodiorite.

Granophyre is the uppermost magmatic unit of the intrusion. The basal 20 m is ferrogranophyre (FeO 11 – 12.5%, SiO_2 60 – 65%), which grades into underlying ferrodiorite and overlying acid granophyre (SiO_2 70 – 75%). The total thickness of the granophyre is > 260 m. Plagioclase was the first major silicate to crystallize from the melt. The contact relations with the older acid volcanites of the roof are not known.

Microgabbros are encountered from the base of the intrusion up to the UZ. They include rocks of the lower chilled margin, layers (?) and autoliths in the basal LZ, and discontinuous layers and autoliths in the upper MZ and in the UC succession. Microgabbros in the cumulate succession are almost always associated with anorthositic cumulates. In the UC sequence microgabbros occur as irregular layers below, in and immediately above the UC layer, and as autoliths above the UC (see Appendix 2). There are two main types, a fine-grained

and a medium-grained microgabbro, both commonly present in one sample (see Fig. 7). The fine-grained microgabbro seems to have been consolidated earlier and is often embedded (as autoliths) in medium-grained microgabbro. Both are non-cumulate rocks, which I interpret as representing mafic magma frozen at contact with colder country rocks, an acid anatectic roof melt or a "cold" density flow. Hybrid microgabbro may have formed by mixing of acid-hybrid magma and mafic magma. Microgabbros, which I interpret as having been formed by internal chill phenomena, are found in Bushveld (Cameron, 1982), Ylivieska intrusion (my own observations, 1965–1974), in Stillwater intrusion (Page, 1979) and in the Duluth Complex.

Chemistry and fractionation

The general course of crystal fractionation is seen in cumulate compositions (Fig. 5). Analyses of some rocks are presented in Mutanen, 1996. As exploration is going on in Akanvaara and the material is not yet public, I cannot quarantee that I am able to send wanted analyses by request.

The undisturbed route from the parent magma (of the basal chill composition) would have been: pyroxene(s) + plagioclase (+chromite?) -> pyroxenes + plagioclase -> pyroxenes + plagioclase + magnetite -> pyroxene + plagioclase + fayalite(?) + magnetite -> pyroxene + plagioclase + fayalite + magnetite + apatite, and for the most part the magma did indeed evolve along this cotectic line. The basal part of the LZ shows the reverse fractionation from chilled and other non-cumulate rocks to orthopyroxene(-chromite) cumulates. The reverse fractionation continues up to the lowermost LC layers, as seen in the mg# curve (Fig. 15), and is quite similar to the reverse fractionation of the Basal zone of the Stillwater intrusion (Page, 1979).

Crystal fractionation produced rocks with decreasing Cr, Ni, Mg, and mg#. The build-up of incompatible elements (Cu, S, V, Ti) and iron in residual liquid is clearly visible in silicate cumulates only above the magnetite phase contact. The crystallization of magnetite effectively depleted the vanadium in the residual liquid. Towards the top of the magma chamber there is a dramatic rise in Cu, Cl, P, Zr and S (Fig. 5).

The last Fe-rich liquid was probably immiscible with any salic liquid, formed either by anatectic melting of the roof rocks or by spontaneous splitting of the residual liquid.

The most remarkable reversals and phase boundaries are:

1) chromite (in) / plagioclase (out), above the lower marginal chill;
2) orthopyroxene (out), each LC chromitite layer in the LZ;
3) chromite (in) / plagioclase (out), pyroxene-chromite cumulates, upper LZ gabbro;
4) olivine (in/out), before and after each LC layer;
5) pyroxene (out), anorthosite layers in the upper LZ;
6) chromite (in)/ pyroxene-plagioclase (out), chromitite layers in the LZ gabbros;
7) chromite (in)/ pyroxene-plagioclase (out), ULC chromitite at the base of the MZ;
8) olivine (in), olivine-pyroxene-chromite cumulate at the base of the MZ;
9) plagioclase (out), pyroxenite layers in the lower MZ;
10) pyroxene (out), anorthosite layers in the upper MZ;
11) chromite (in)/ plagioclase and pyroxene (out), UC chromitite;
12) pyroxene (out), anorthosite layers of the UZ;

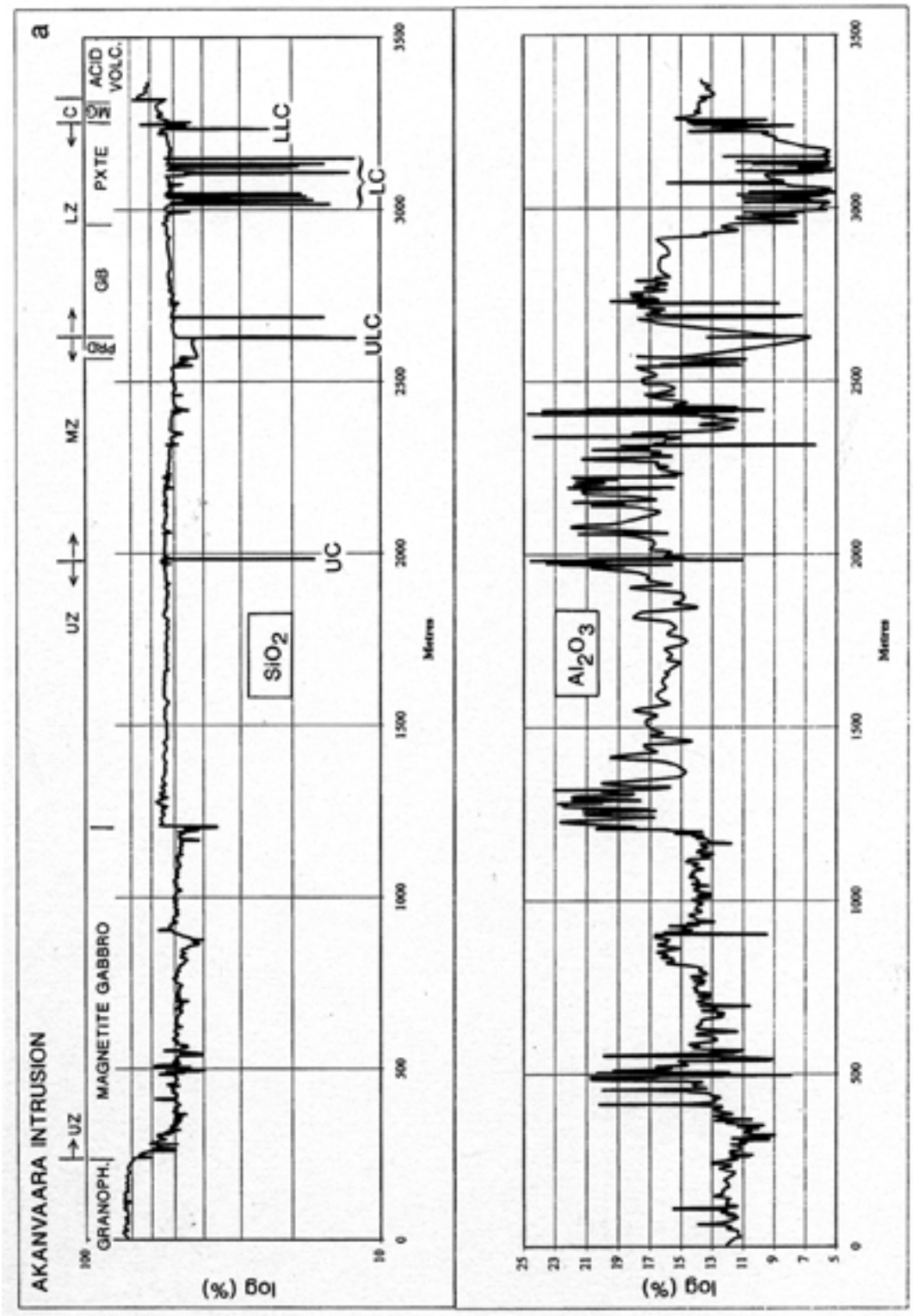

Fig. 5. Profiles of some major, minor and trace elements through the Akanvaara intrusion. Data combined and matched from several diamond drill holes. 5a – SiO_2 and Al_2O_3, 5b – FeO(tot) and MgO, 5c – mg# and Ni, 5d – Cr and P_2O_5, 3e – S and Cl, f – Zr and Cu, g – TiO_2 and V, h – DDH322 intersection, lower part of LZ (Cr, Ni, TiO_2, mg#, K_2O); C – chill, LZ – Lower Zone, MZ – Main Zone, UZ Upper Zone, MG – microgabbro, PXTE – pyroxenite, GB – gabbro, PRD – peridotite, GRANOPH – granophyre, ACID VOLC. – acid volcanic metahornfelses (following pages.)

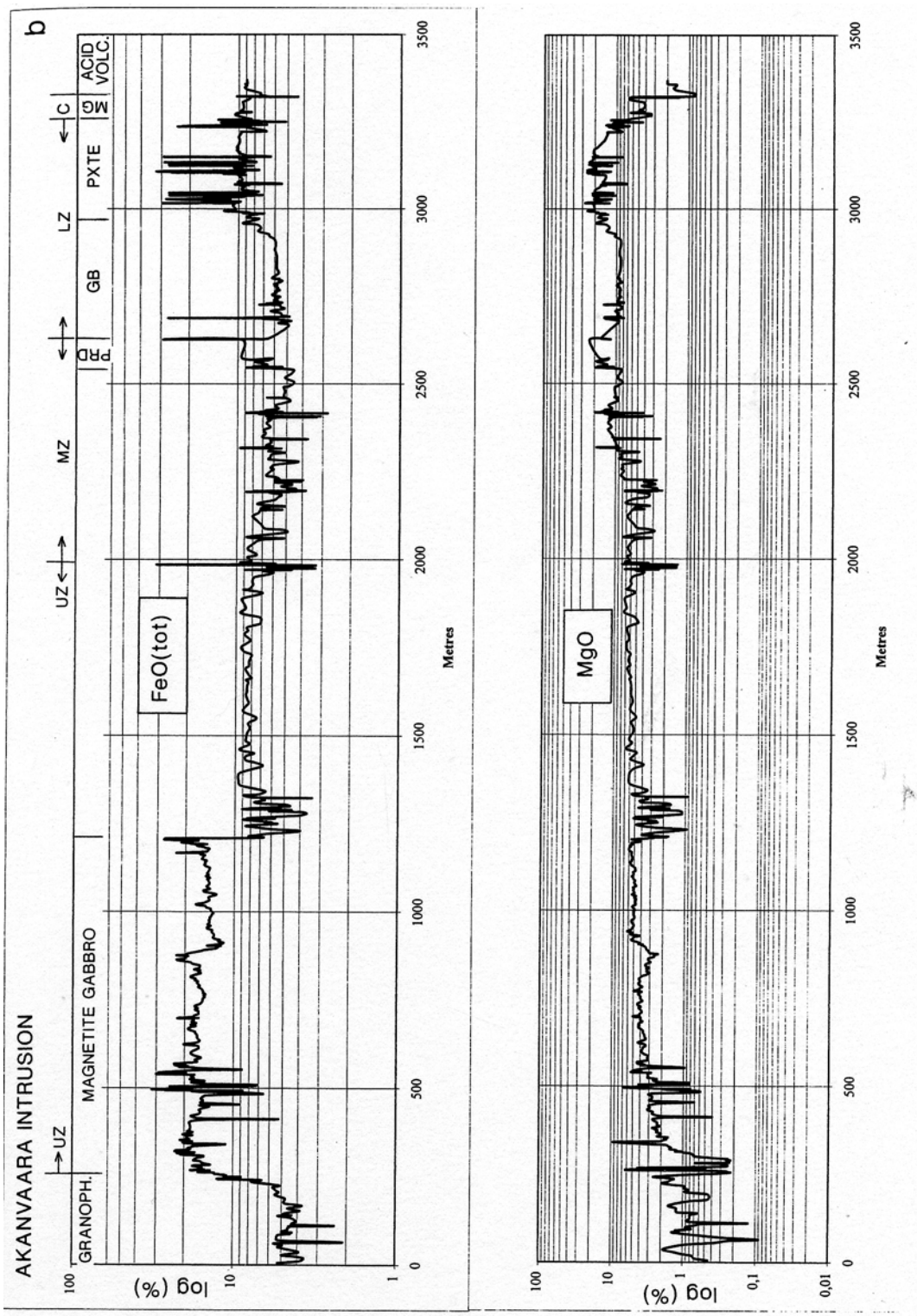
b
AKANVAARA INTRUSION
GRANOPH.
UZ
MAGNETITE GABBRO
UZ
MZ
PRD
GB
LZ
PXTE
C
MG
ACID VOLC.
FeO(tot)
log (%)
100
10
1
0
500
1000
1500
2000
2500
3000
3500
Metres
MgO
log (%)
100
10
1
0,1
0,01
0
500
1000
1500
2000
2500
3000
3500
Metres

Fig. 5b.

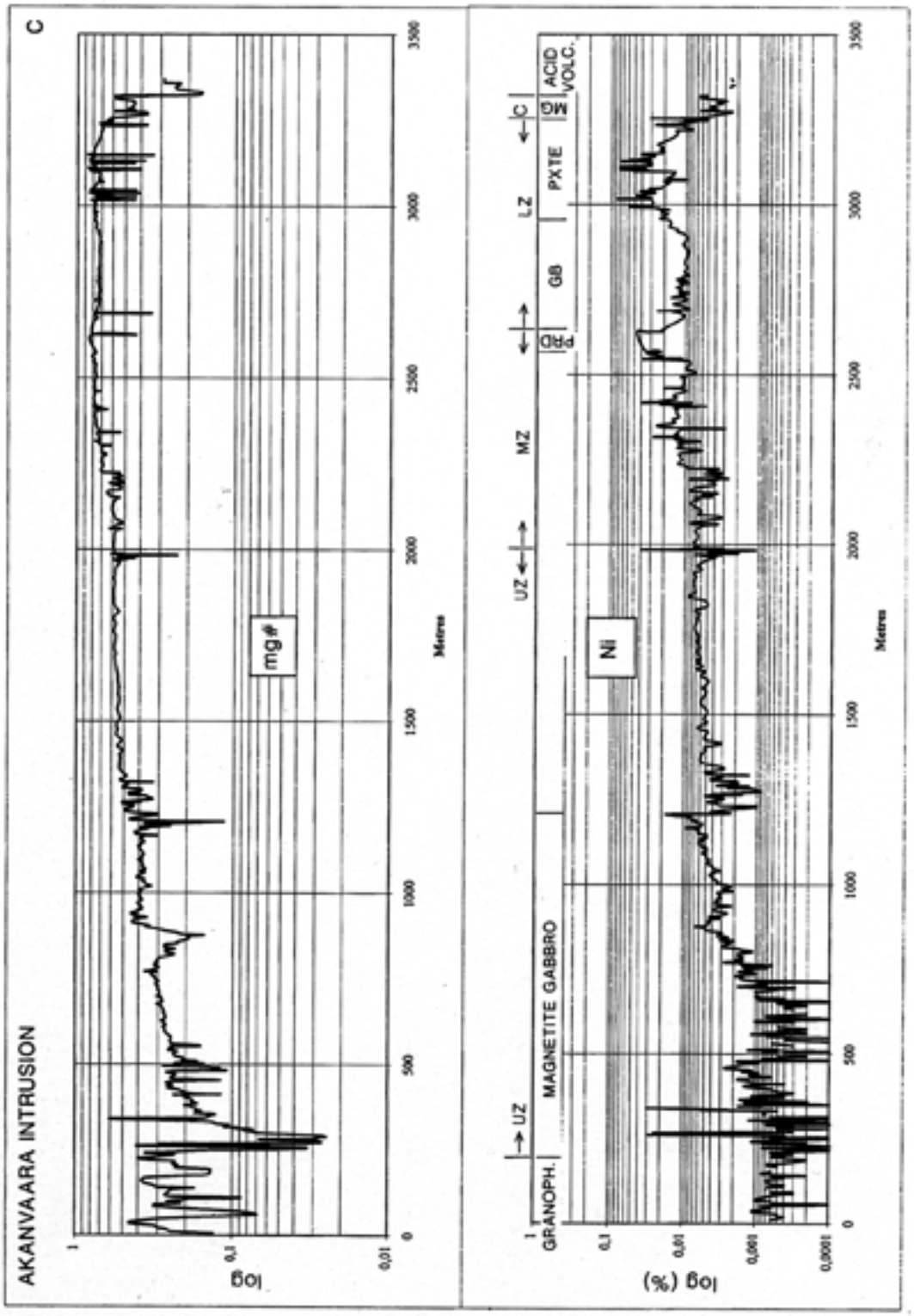
C
AKANVAARA INTRUSION
log
mg#
Metres
UZ
MAGNETITE GABBRO
GRANOPH.
UZ
MZ
LZ
C
PXTE
GB
MG
ACID VOLC.
Ni
log (%)

Fig. 5c.

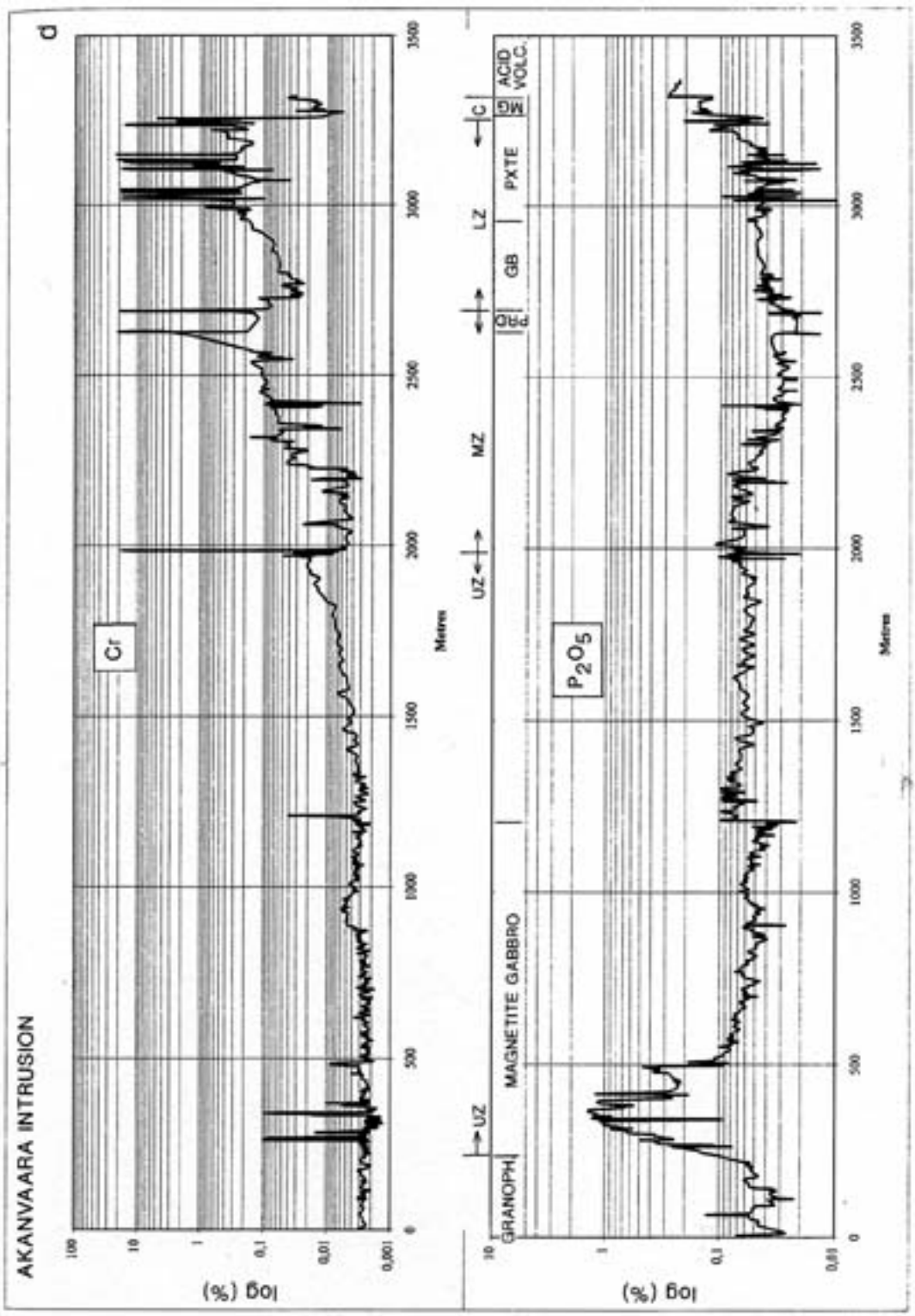
d
AKANVAARA INTRUSION
Cr
log (%)
Metres
UZ
MZ
LZ
C
GRANOPH
MAGNETITE GABBRO
GB
PXTE
ACID VOLC.
P_2O_5

Fig. 5d.

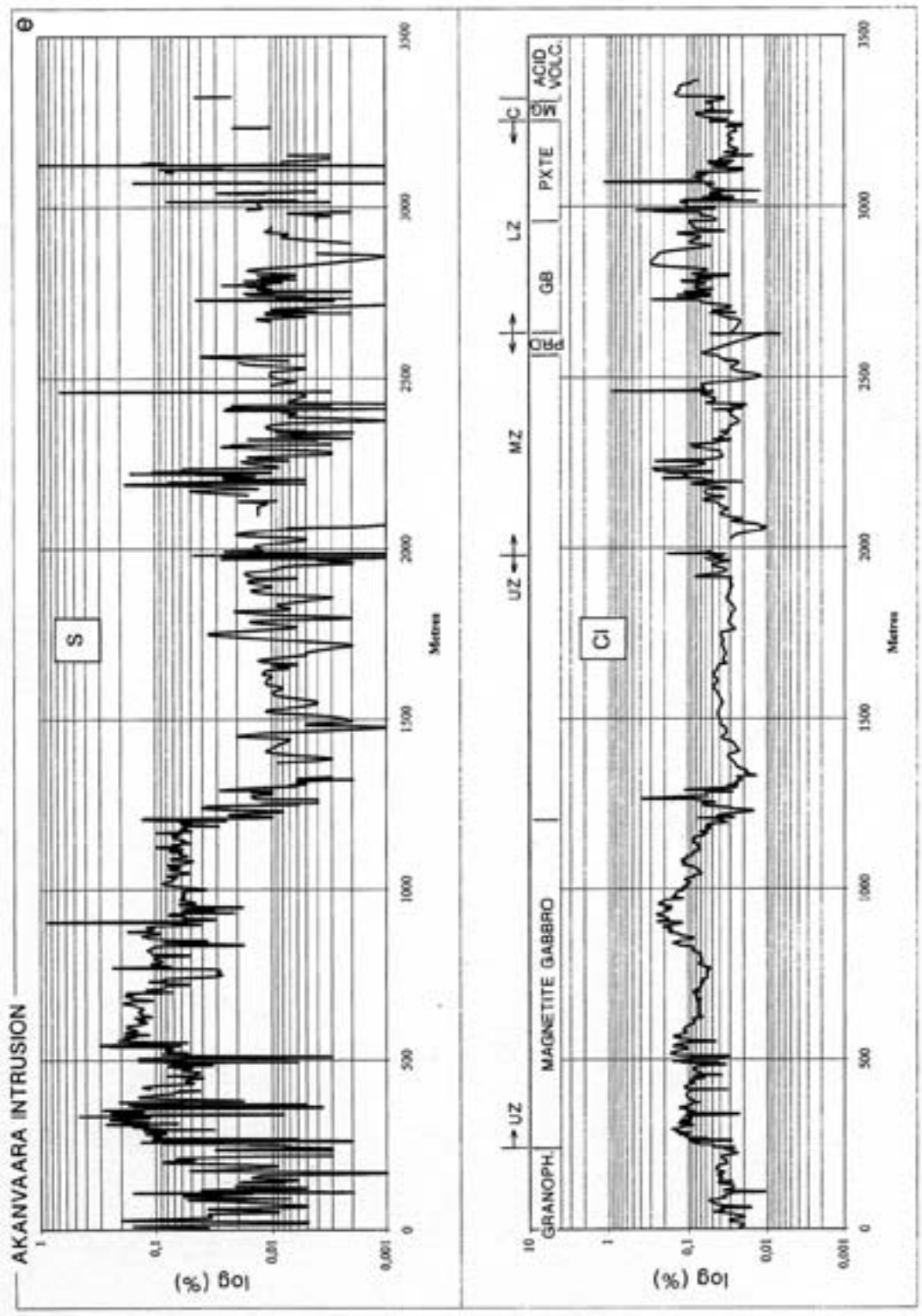
AKANVAARA INTRUSION
S
Cl
log (%)
Metres
UZ
MZ
LZ
GRANOPH.
MAGNETITE GABBRO
GB
PXTE
ACID VOLC.

Fig. 5e.

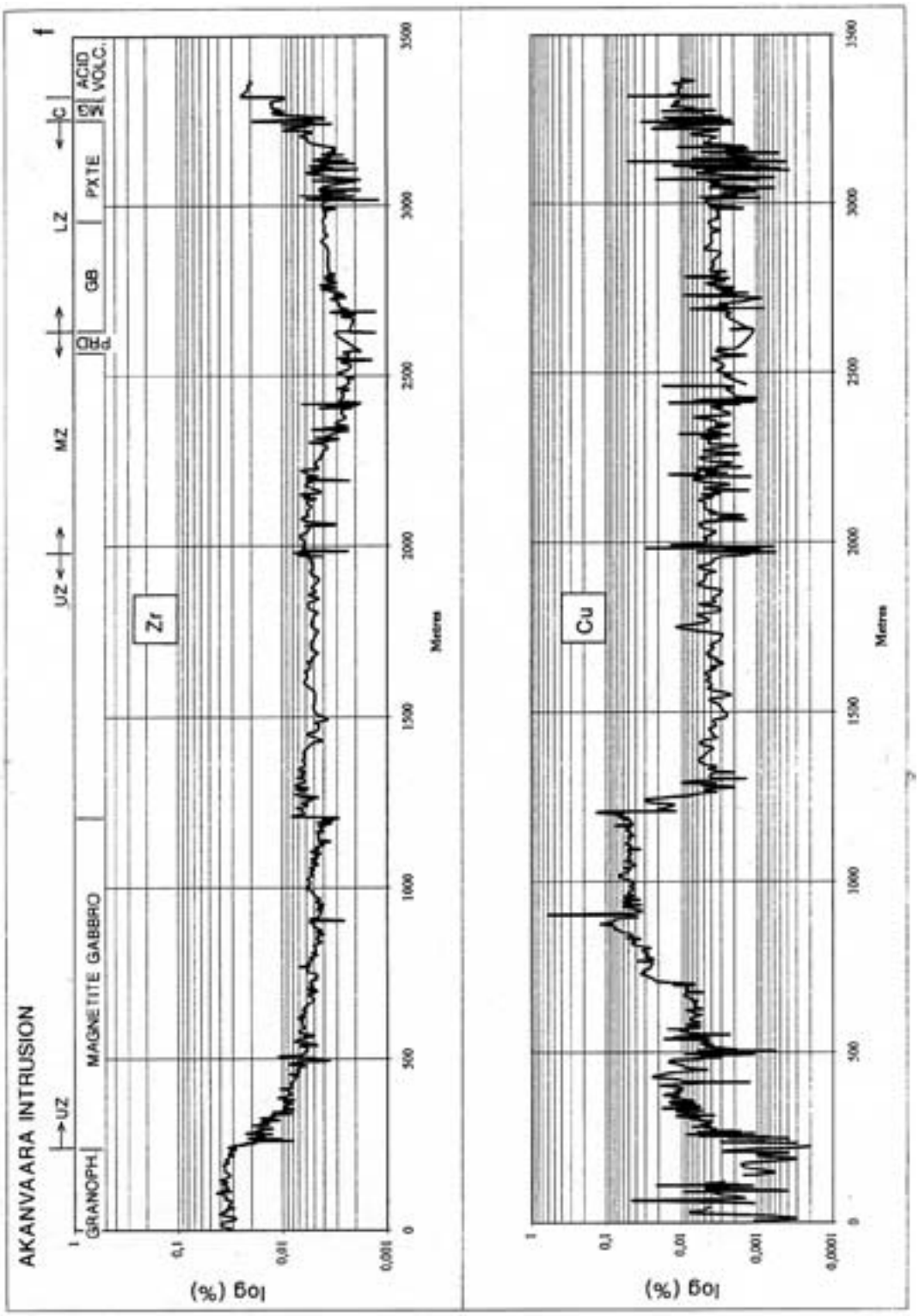
AKANVAARA INTRUSION
UZ
GRANOPH.
MAGNETITE GABBRO
UZ
MZ
PRO
GB
LZ
PXTE
C
ACID VOLC.
Zr
Cu
log (%)
Metres

Fig. 5f.

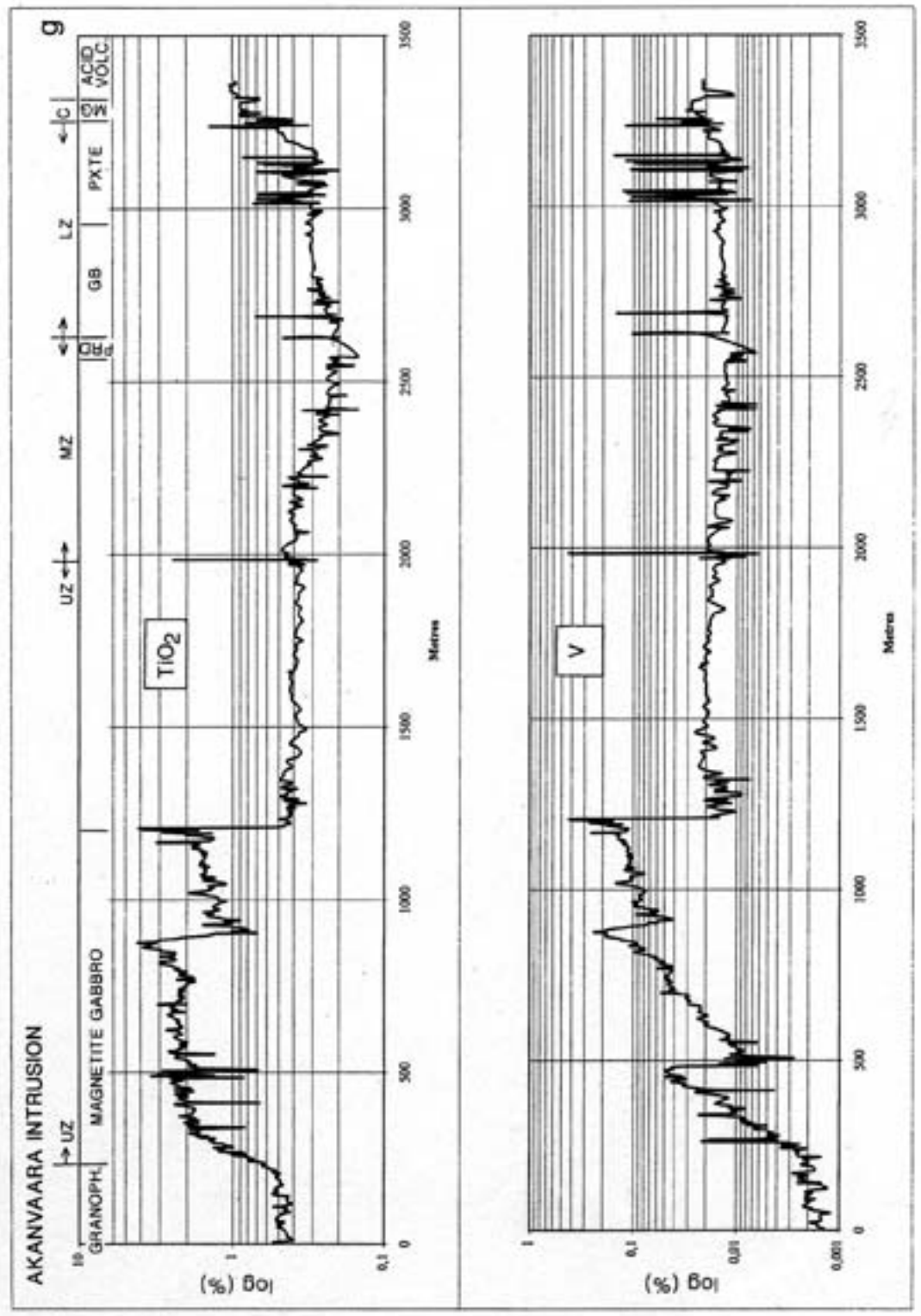
g
AKANVAARA INTRUSION
UZ
GRANOPH.
MAGNETITE GABBRO
UZ
MZ
GB
LZ
PXTE
C
ACID VOLC
TiO_2
V
log (%)
Metres
0
500
1000
1500
2000
2500
3000
3500

Fig. 5g.

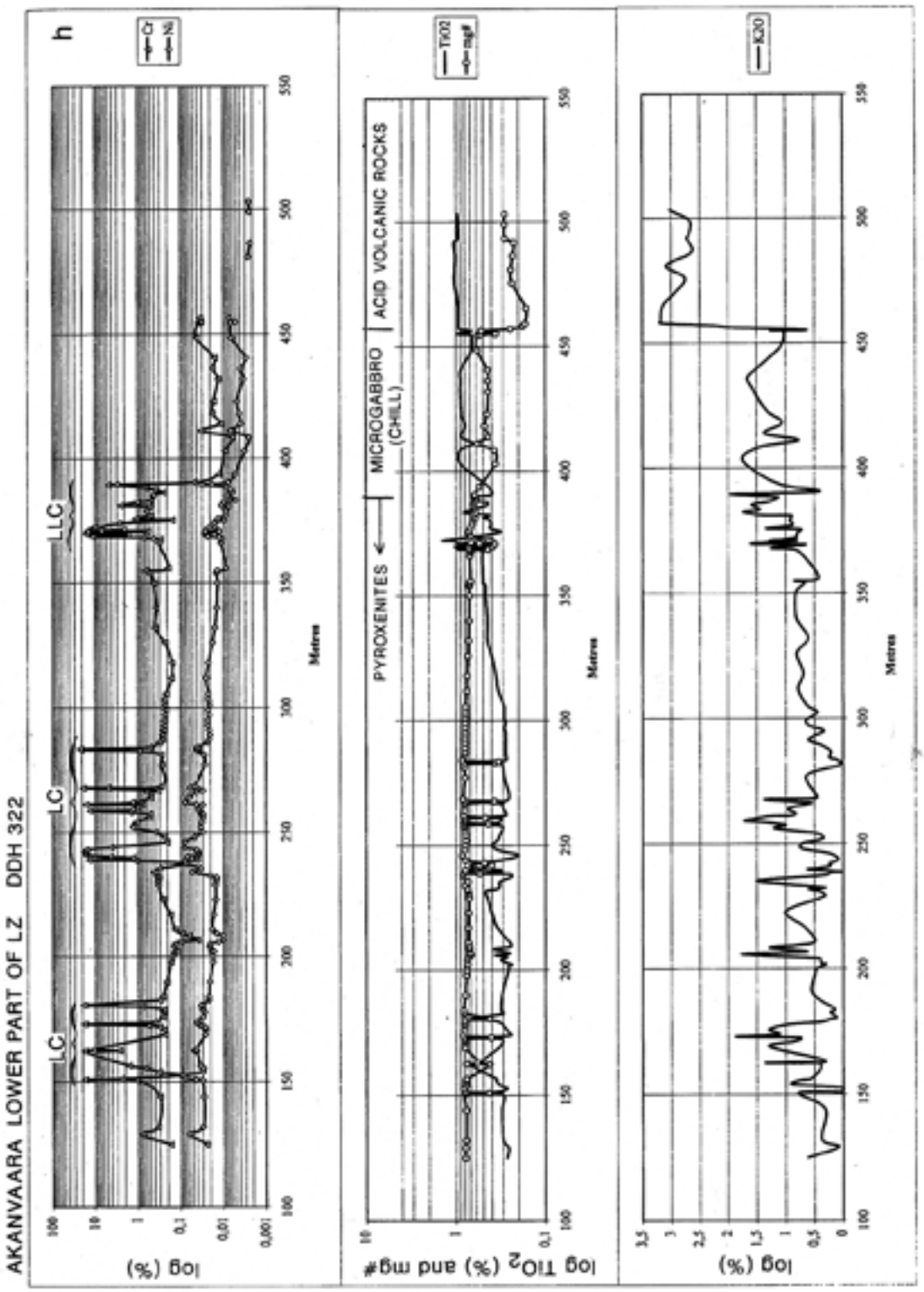
AKANVAARA LOWER PART OF LZ DDH 322
h
Cr
Ni
LC
LC
LLC
log (%)
Metres
PYROXENITES
MICROGABBRO (CHILL)
ACID VOLCANIC ROCKS
TiO2
mg#
log TiO2 (%) and mg#
K2O
log (%)

Fig. 5h.

13) pyroxene (out), base of magnetite gabbro;
14) Cr peak, basal contact of the magnetite gabbro;
15) pyroxene and magnetite(?) (out), anorthosite layers in magnetite gabbro;
16) plagioclase (out), ultramafic layers in magnetite gabbro

The reversals, which are associated with non-cotectic cumulus assemblages, imply that the composition of magma (melt) went astray from cotectic lines. I suggest that the cause of the reversals was the addition of exotic material from heated and melted country rocks. This addition changed the composition and structure of the melt, and shifted the liquidus phase boundaries. As at Koitelainen, there is no evidence of, nor need for, new magma pulses of any kind to explain the evolution of the magma system.

Chromitite layers

To date, 23 chromitite layers have been counted in the Akanvaara intrusion (Fig. 6): the Lowermost Lower Chromitite (LLC) group at the base of the layered sequence, the Lower Chromitite (LC) layers among LZ pyroxene cumulates, the Uppermost Lower Chromitite (ULC) at the base of the MZ and the Upper Chromitite (UC) at the base of the UZ. In the total count, closely-spaced layers are counted as one. In addition, there are numerous chromitite bands of uncertain continuity, particularly in LZ pyroxene cumulates and in the olivine cumulate layer above the ULC layer.

In the following I shall describe some general features of the chromitite layers and look at the UC layer in more detail.

Chromitites occur from the base of the LZ to the base of the UZ. Chromitite autoliths are met with in the lower chill rocks (Fig. 7). This implies that chromite had accumulated and consolidated into solid cumulate somewhere, and had then been detached, before the last chill rocks had crystallized. On the other hand, there are microgabbro autoliths in chromitite. Obviously, chill-formation was a process of alternate formation and peeling-off of temporary chilled linings.

The lowermost LC chromitites are associated with gabbroic and pyroxenitic cumulates, rich in quartz, feldspar and biotite-phlogopite. The other LC layers occur in pyroxene (-chromite) cumulates, underlain, intercalated and sometimes overlain by olivine-pyroxene-chromite cumulates. Thin chromitites between the LC and ULC are associated with thin plagioclase-rich layers and discontinuous layers of mottled anorthosite and pyroxenite. The ULC layer is underlain by alternating layers of gabbro, mottled anorthosite and pyroxenite, and overlain by olivine-pyroxene (-chromite) cumulates.

The UC is the most regular and tectonically least disturbed of the chromitite layers. The stratigraphic positions of the LC layers seem to be regular; however, because individual layers pinch and swell, and are often badly disturbed by faults, their connections between drill holes cannot always be established. In this respect, the Akanvaara chromitites are similar to the UC layer and LC layers of the Koitelainen intrusion. Load cast structures were found in a DDH at the base contact of a LC layer, where a lightweight feldspathic layer is overlain by a massive chromitite. Identified load casts seem to be rare among layered intrusions but they are reported below the Steelport Seam chromitite (Cameron, 1980) and below magnetite gabbro in Bushveld (Willemse 1969b).

As a rule, the chromitites are distinct monocumulate layers of small (0.1 – 0.5 mm), euhedral chromite crystals embedded in sili-

cate matrix. Fossil melt inclusions and embayments (re-entrant inclusions) are common; coarse chromite often has skeletal outlines (Fig. 8a). The base contacts are usually sharp, even under the microscope. The chromite crystals tend to coarsen towards the base of layers (Fig. 8a).

The LC layers typically grade upwards, and sometimes downwards, through a thin chromite-orthopyroxene cumulate to the ordinary orthopyroxene (-chromite) cumulate. The pyroxene cumulates and microgabbros associated with the UC layer contain a variable amount of chromite as dissemination, concentrated bands and schlieren.

The LC layers occasionally contain spots of talc(-tremolite), pseudomorphs after scattered cumulus crystals of orthopyroxene(?). Oikocrysts of hornblende (former pyroxene) are common in UC and LC layers; plagioclase oikocrysts occur in the salic intercumulus matrix of the lowermost LC layers. The oikocrysts have grown around scattered cumulus cores. The mutual modal proportions of secondary intercumulus minerals – biotite-phlogopite, talc, chlorite, amphibole and carbonate – vary in different layers. Ilmenite, which is ubiquitous as exsolved rods in chromite and as poikilitic grains enclosing chromite, has commonly altered to rutile and "ilmenorutile" (Fig. 9a; Table 2). The euhedral ilmenite occurs as a daughter mineral in fossil melt inclusions in chromites. Euhedral cumulus crystals of Mn-rich ilmenite (Fig. 9b; Table 2) imply that chromite and ilmenite saturated together, but this could not have happened in the main magma body. Apatite and tourmaline have been observed. Tourmaline (Cr_2O_3 1.35–3.65%) is found as poikilitic, oikocryst-like grains and oikocrystic bands reminiscent of layers (Fig. 8b). Light-brown oikocryst-like tourmaline occurs in a LZ troctolite. It is possible that boron was a primary contaminant from melted sediments, and the poikilitic tourmaline grains grew as true postcumulus oikocrysts from boron-enriched intercumulus melt.

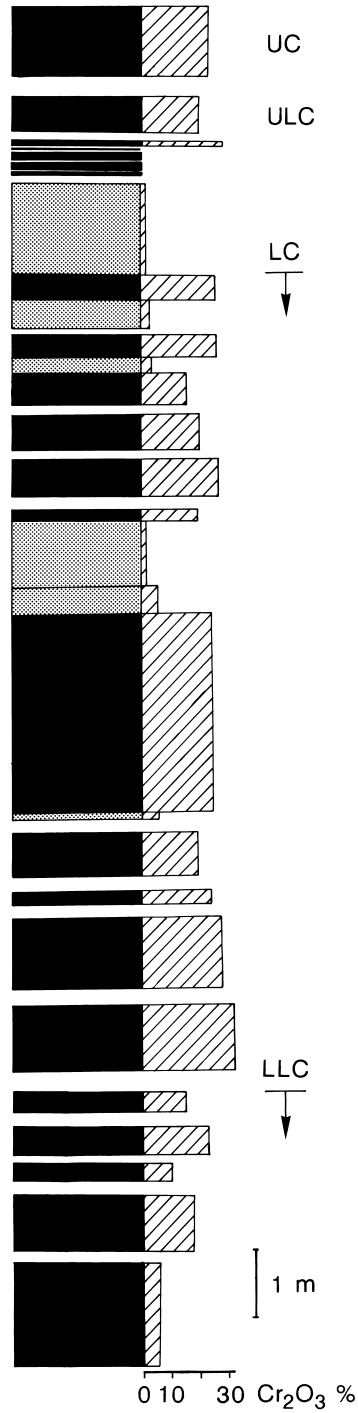

Fig. 6. Thicknesses and grades of Akanvaara chromitite layers. UC – Upper Chromitite, ULC – Uppermost Lower Chromitite, LC – Lower Chromitite Layers, LLC – Lowermost Lower Chromitite layers.

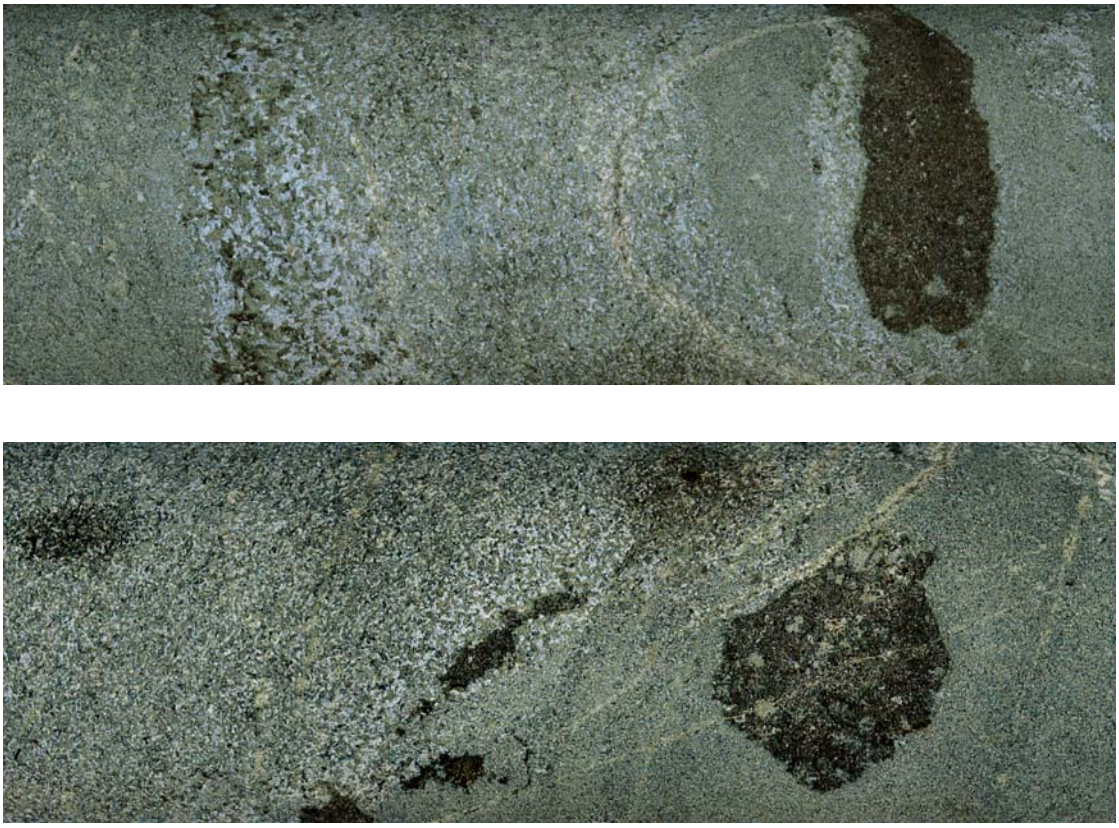

Fig. 7. Chromitite autoliths in heterogeneous non-cumulate microgabbro (including fine-grained chilled microgabbro), near the base of the Akanvaara intrusion. DDH340/138.24-138.30. Bar = 2 cm. Photo by Reijo Lampela.

Fluorapatite and zircon occur in pegmatoid rock immediately underlying a LC chromitite layer. Big zoned zircon crystals were found in a coarse footwall layer of the ULC chromitite.

Some chromitites are rich in interstitial sulphides (pyrite with relics of pyrrhotite, pentlandite and chalcopyrite, sometimes molybdenite), but they show no extra enrichment in PGE.

A few tiny (≤ 5 mu) PGM grains have been found; according to electron microprobe EDS determinations (by Bo Johanson and Lassi Pakkanen, GSF) the grains are composed of laurite, sperrylite and their intergrowths (Bo Johanson & Lassi Pakkanen, letter 1996).

The majority of the chromitites are rich in biotite-phlogopite, which occurs as oikocrysts, secondary filling of intercumulus space and in fossil melt inclusions. However, the ULC and the uppermost LC layer are extremely poor in K_2O.

Interestingly, biotite-phlogopite is always present, even in abundance in chromitites of various types (Sampson, 1932; Jackson, 1961, 1963; Bichan, 1969; Ferguson, 1969; Windley et al., 1973; Ghisler, 1976; Ivanov, 1977; Suwa & Suzuki, 1977; Genkin et al., 1979; Marakushev, 1980). Windley and co-workers (1973) suggest that the high potassium in the chromitites of the Fiskenaesset intrusion is a

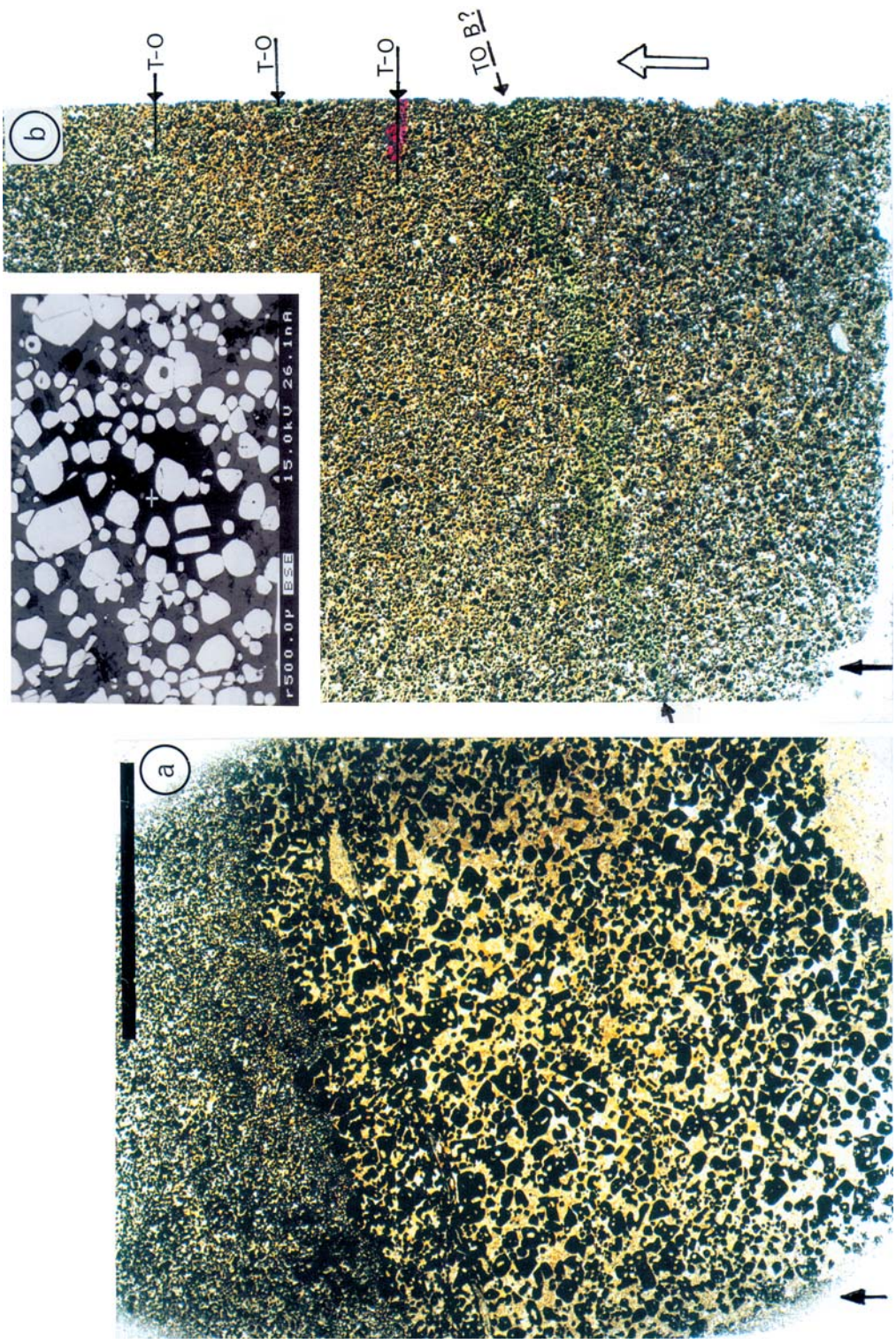

Fig. 8. Akanvaara LC chromitites. Diascanner photos of thin sections, by Reijo Lampela. a – a layer of fine-grained chromite and coarse, skeletal chromite with melt inclusions and embayments at the base of the LC layer. DDH340/69.90 m. Bar = 1 cm; b – tourmaline band ? (TO B?) and abundant tourmaline oikocrysts (some marked by T-O); inset in b – BE image of a tourmaline oikocrysts (black) enclosing euhedral chromite. DDH341/81.03 m. Bar = 1 cm.

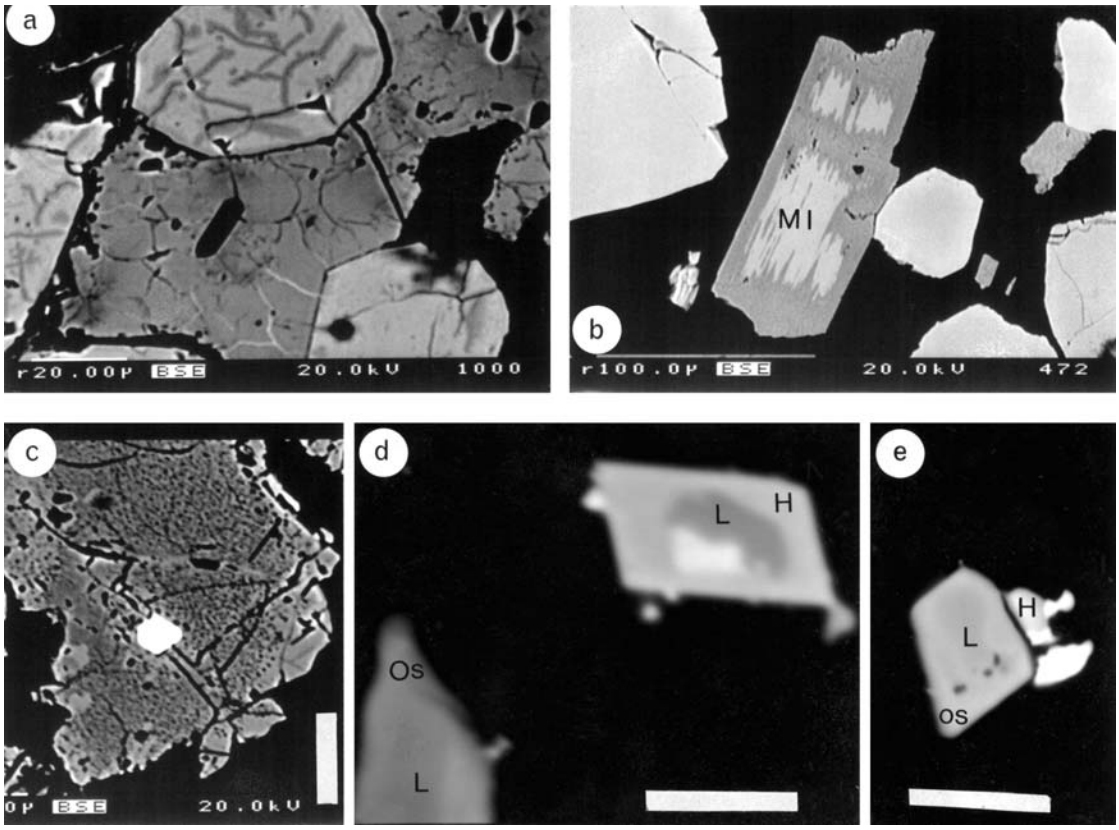

Fig. 9. BE images of Akanvaara chromitites. a – euhedral chromite and poikilitic "ilmenorutile". LC, DDH320/283.10 m. Bar = 20 mu; b – euhedral chromite and Mn-rich ilmenite (MnO 9.53%), the latter altered to "ilmenorutile". LC, DDH320/271.05 m. Bar = 100 mu; c – laurite crystal in chromite (laurite contains Ru 47.1%, Pd 1.8%, Os 6.5%, Ir 5.5%, Rh 0.36% and As 2.1%). UC, DDH363/131.19 m. Bar = 20 mu; d – laurite (L), hollingworthite (H) and sperrylite (white), lower left, a zoned laurite crystal with an Os-rich rim (erlichmanite). UC, sample TM-91-15.10. Bar = 2 mu; e – a zoned laurite crystal (L), hollingworthite (H) and sperrylite (white). UC, sample TM-91-15.3. Bar = 5 mu. Photos by Lassi Pakkanen (a–c) and Bo Johanson (d–e).

primary constituent. The chromitite layers of the Koitelainen intrusion are enriched in K_2O, particularly the UC layer (Mutanen, 1979, 1981, 1989b). A chromitite layer situated below the main chromite ore of the Kemi intrusion contains 3% K_2O (Alapieti et al., 1989). Here the chromite is low in MgO and the Ce-La of the chromitite are high (op.cit.). Similar features have been described from Entire anorthosite gneiss, where P, Zr and Nb are strongly concentrated in chromitite (see Sivell et al., 1985). In the CC model these features demonstrate the presence of crustal contaminant melt in chromite-charged density flow.

Cumulate petrography shows that the chromitite layers were formed by the sudden disappearance of cumulus silicates and the accumulation of chromite as a sole cumulus mineral; equally suddenly, the re-entry of orthopyroxene (in LC layers) and of pyroxene and plagioclase (at the UC) terminated the process. Banded contacts, internal banding and other signatures of co-cumulation of significant amounts of silicates along with chromite are

rare; they do occur, however, in the very lowermost chromite-rich layer 9 m above the top of the lower chilled margin. The layer, which occurs in cumulate gabbros, is 0.51 m thick and consists of alternating chromite-rich and pyroxene-rich layers. Quartz, plagioclase and biotite are abundant in the intercumulus, which also contains loveringite(?), zircon and fluorapatite. Near the base of this layer is an autolith of fine-grained microgabbro.

The compositions of chromite from the chromitite layers are listed in Table 1. There are no systematic upward trends in the LC layers, although there are clear differences (e.g., in Al, Mn, Fe, Cr and Mg) between the layers, intra-layer variation (Mg, Fe, Al, Cr) and even slight but distinct variation between grains in one sample. There is no correlation between Fe and Mn, Fe and V, but a positive one between Cr and V. There is a general, but not tight, negative correlation between Al and Fe, indicating Al^{3+}/Fe^{3+} substitution. In LLC layers the substitution is between Cr^{3+} and Fe^{3+}. The composition of the chromite from a pyroxene-chromite cumulate between two chromitite layers differs from that of the chromitites (Table 1).

Upwards from the LC to the ULC there is a slight decrease in Mg and an increase in Zn and Mn, but chromites with similar Mn values occur in the lowermost LC layers. The UC is distinct from the ULC and LC. Its chromite has an even lower Mg and higher Ti, V and Zn content; Mn is high, being about the same as in ULC chromite.

Post-cumulus re-equilibration was probably not very effective. Analyses of LC chromite on one sample (DDH322/258.27 m) in which chromite is enclosed by three different poikilitic matrix minerals – sulphide, plagioclase and carbonate – showed that the compositional differences between these chromites are negligible. Chromite in plagioclase is slightly higher in Al, whereas chromite in sulphide is higher in Fe and Ti and lower in Mg, Cr and Al.

Other evidence for the lack of significant post-cumulus changes come from the UC layer, where the mg# in bulk silicates is even lower than that in underlying and overlying silicate cumulates (Fig. 17). This indicates that the low Mg in UC chromite is an original feature and was not markedly lowered by postcumulus (magmatic plus metamorphic) re-equilibration.

As the $D_{Mg}^{chr/liq}$ in all imaginable magma compositions is > 1 (see Maurel & Maurel, 1982b, 1984), the low Mg in chromite implies that the chromites of all chromitite layers crystallized in an environment very poor in Mg.

The UC layer (see Appendix 2) is similar to the UC layer of the Koitelainen intrusion. It was found in an outcrop in 1991 and was later traced (1995–1996) by diamond drilling in the southern part of the intrusion. Between the eastern and western fault borders it is continuous over a strike length of 8 km. From east to west the relative stratigraphic elevation of UC succession decreases several hundred metres in relation to the base of the magnetite gabbro, whereas the combined thickness of the MZ and UZ remains approximately constant.

Figure 10 shows the general stratigraphy of the UC succession, and details of UC DDH intersections. The homogeneous MZ gabbro has a sharp boundary with the overlying UZ. This begins with a 0.5–4.6-m-thick unit of alternating layers of mottled anorthosite, gabbro-anorthosite, anorthosite gabbro and medium-grained non-cumulate gabbro and microgabbro. The layers are irregular and do not always persist laterally. Below the UC the mottled anorthosite is from 0.2 to 1.2 m thick, but in five DDH intersections it is lacking altogether. The irregularity of the sub-UC unit is ascribed, as at Koitelainen, to strong magmatic erosion.

Closely associated with the UC are microgabbro, medium-grained non-cumulate gabbro, pyroxenite, pyroxene pegmatoid and pyroxene-plagioclase pegmatoid, all of which contain chromite as dissemination, schlieren and thin layers. The UC is overlain by layers of mottled anorthosite and other plagioclase-rich cumulates, gabbro and layers/autoliths of non-

Table 1. Compositions of chromite from Akanvaara chromite layers. Electron microprobe analyses by Bo Johanson and Lassi Pakkanen (GSF, Espoo).

	UC	ULC	1	2	3a	3b	4	5a	5b	5c	5d	5e
	n = 30	n = 19	n = 15	n = 45	n = 15	n = 15	n = 15	n = 15	n = 19	n = 18	n = 18	n = 18
TiO_2	1.11	0.61	0.88	0.77	0.49	0.53	0.30	0.32	0.41	0.40	0.40	0.33
Al_2O_3	10.89	12.71	5.48	10.27	12.18	11.37	9.23	8.80	8.52	10.01	8.38	8.43
Cr_2O_3	37.70	42.95	44.20	43.86	43.25	44.37	42.44	42.56	41.33	41.39	40.91	42.39
V_2O_3	1.27	0.26	0.45	0.35	0.36	0.36	0.29	0.30	0.32	0.29	0.33	0.29
FeO(tot)	43.22	38.96	45.40	41.05	40.06	39.49	43.91	44.46	46.05	44.40	46.54	44.99
MnO	1.21	1.27	0.91	0.77	0.79	0.80	0.70	0.71	0.69	0.70	0.72	0.75
MgO	0.13	0.60	0.53	1.00	1.03	0.98	0.74	0.76	0.71	0.82	0.69	0.74
CaO	n d	n d	0.02	0.01	0.01	0.00	0.00	0.01	0.01	0.01	0.01	0.01
NiO	0.04	0.03	0.04	0.03	0.03	0.02	0.03	0.03	0.04	0.02	0.03	0.04
CoO												
ZnO	0.82	0.87	0.21	0.30	0.32	0.31	0.29	0.25	0.25	0.29	0.24	0.26
Total	96.39	98.26	98.12	98.39	98.51	98.25	97.94	98.18	98.32	98.33	98.23	98.22
Cr/Fe	0.77	0.97	0.86	0.94	0.95	0.99	0.85	0.84	0.79	0.82	0.77	0.83

	5f	6a	6b	6c1	6c2	6c3	6d	7a1	7a2	7a3	8a	8b
	n = 15	n = 19	n = 15	n = 14	n = 15	n = 15	n = 15	n = 12	n = 4	n = 4	n = 15	n = 19
TiO_2	0.35	0.34	0.29	0.54	0.33	0.36	0.27	0.34	0.31	0.64	0.33	0.59
Al_2O_3	8.72	8.30	9.39	6.04	8.03	7.32	8.71	11.57	9.28	12.16	11.02	10.78
Cr_2O_3	42.41	41.43	42.73	40.72	42.07	42.21	43.23	43.10	43.89	43.09	44.31	44.05
FeO(tot)	0.30	0.31	0.32	0.30	0.29	0.31	0.29	0.29	0.29	0.30	0.37	0.33
V_2O_3	44.59	45.42	43.22	47.97	45.29	45.67	43.80	40.95	42.77	40.50	40.71	40.81
MnO	0.78	0.94	0.96	0.93	0.96	0.96	0.89	0.85	0.84	0.83	0.88	0.88
MgO	0.75	0.69	0.98	0.63	0.70	0.83	0.79	0.96	0.86	1.08	0.93	0.89
CaO	0.01	0.01	0.02	0.01	0.01	0.08	0.01	0.01	0.00	0.00	0.00	0.01
NiO	0.02	0.04	0.03	0.02	0.02	0.01	0.04	0.04	0.02	0.03	0.03	0.03
CoO												
ZnO	0.25	0.23	0.29	0.22	0.27	0.26	0.28	0.30	0.24	0.30	0.33	0.32
Total	98.18	97.70	98.24	97.38	97.97	98.00	98.31	98.41	98.51	98.93	98.91	98.70
Cr/Fe	0.84	0.88	0.87	0.75	0.81	0.81	0.87	0.93	0.90	0.94	0.96	0.95

	8c	8d	8e	9a	9b	9c1	9c2	9d	9e	10a	10b
	n = 19	n = 19	n = 18	n = 19	n = 19	n = 8	n = 11	n = 19	n = 23	n = 6	n = 8
TiO_2	0.66	0.46	0.39	0.59	1.22	1.89	0.41	0.86	0.48	1.32	3.20
Al_2O_3	10.63	10.13	9.96	13.41	12.29	12.32	12.45	11.77	11.40	9.76	9.11
Cr_2O_3	44.53	44.50	44.59	43.75	44.66	44.49	44.55	45.72	44.89	44.07	46.54
V_2O_3	0.33	0.32	0.31	0.39	0.39	0.39	0.35	0.39	0.38	0.50	0.56
FeO(tot)	40.68	40.44	40.26	36.79	37.07	36.62	38.09	37.21	38.78	40.12	36.40
MnO	0.91	0.54	0.53	0.73	1.09	1.10	1.12	1.13	1.16	0.91	0.94
MgO	0.90	0.94	0.90	1.05	0.97	0.98	0.97	0.97	0.95	0.49	0.50
CaO	0.01	0.01	0.01	0.01	0.01	0.01	0.01	0.01	0.00	0.01	0.01
NiO	0.02	0.03	0.02	0.03	0.03	0.03	0.02	0.02	0.02	0.02	0.02
CoO										0.08	0.07
ZnO	0.32	0.33	0.32	0.40	0.37	0.36	0.37	0.34	0.36	0.36	0.39
Total	98.98	97.71	97.29	97.15	98.12	98.19	98.34	98.44	98.41	97.64	97.74
Cr/Fe	0.96	0.97	0.98	1.05	1.06	1.07	1.03	1.08	1.02	0.97	1.13

Table 1. (Continued)

	11a	11b	12	13a	13b	14a1	14a2	14a3	14a4	14a5	15
	n = 5	n = 6	n = 6	n = 4	n = 5	n = 6	n = 4	n = 5	n = 5	n = 5	n = 3
TiO_2	1.49	0.98	1.82	0.96	2.19	1.31	0.90	1.78	1.20	2.04	1.72
Al_2O_3	9.60	7.60	7.03	9.79	8.64	7.92	9.12	6.49	8.43	7.45	13.59
Cr_2O_3	46.72	46.41	45.75	47.46	49.13	44.07	46.66	44.26	44.82	46.86	37.26
V_2O_3	0.46	0.50	0.62	0.49	0.49	0.45	0.38	0.43	0.42	0.42	1.04
FeO(tot)	37.44	40.36	41.48	38.14	37.35	41.56	39.03	42.85	41.10	37.81	42.64
MnO	0.88	0.93	0.93	1.00	0.99	1.12	1.09	1.12	1.12	1.09	0.79
MgO	0.53	0.51	0.42	0.55	0.53	0.33	0.39	0.32	0.36	0.36	0.36
CaO	0.01	0.01	0.02	0.01	0.01	0.02	0.02	0.03	0.03	0.02	0.19
NiO	0.02	0.03	0.01	0.02	0.02	0.02	0.02	0.02	0.02	0.01	0.02
CoO	0.08	0.06	0.06	0.07	0.07	0.05	0.06	0.06	0.06	0.05	0.09
ZnO	0.49	0.39	0.43	0.46	0.46	0.31	0.36	0.29	0.34	0.33	0.64
Total	97.72	97.78	98.57	98.95	99.88	97.16	98.03	97.65	97.90	96.44	98.35
Cr/Fe	1.10	1.01	0.97	1.10	1.16	0.93	1.05	0.91	0.96	1.09	0.77

LC samples: 1 - accessory chromite between chromitite layers. Samples 2 to 9 are from chromitite layers, in descending order: 3 a/b - upper/lower part of a layer; 5 a - f, samples across a layer; 6c1 - chromite in sulphide matrix, 6c2 - chromite in plagioclase matrix, 6c3 - chromite in carbonate matrix; 7a1 - 7a3 - compositionally heterogeneous chromites in one sample; 8a-e - samples across a layer; 9a-e - samples across a layer, where 9c1 and 9c2 are from compositionally heterogeneous chromites in one sample; Samples 10 to 15 are from LLC chromitites, in descending order; 10 a/b - upper/lower part of a layer; 11a/b - upper/lower part of a layer; 12 - middle part of a layer; 13 a/b - upper/middle part of a layer; 14 - one thin section: a1 - in plagioclase matrix, a2 and a3 - in uralite-plagioclase matrix, a4 - in uralite-biotite matrix, a5 - in quartz or granophyre matrix; 15 - chromite autolith in microgabbro (Fig. 7). Analyses of this sample contain silicate impurities.

cumulate gabbro and microgabbro. The layer of mottled anorthosite overlying the UC is generally from 1.9 to 2.6 m thick, but is lacking in some DDH intersections.

Dendritic (crescumulate) plagioclase occurs in a coarse leucocratic gabbro a few metres above the UC. This rocks contains zircon (it is the "age sample" of Akanvaara). The layer seems to be laterally irregular. The plagioclase evidently crystallized from a supercooled aluminous magma (see Poldervaart & Taubeneck, 1959; Taubeneck & Poldervaart, 1960; Mutanen, 1974).

A persistent marker layer of mottled anorthosite, from 1 to 2 m thick, occurs 10–15 m above the UC.

The thickness of the UC layer, which has been intersected in 30 drill holes, ranges from 0.64 to 1.79 m (average 1.14 m). The massive chromitite contains on average: 23% Cr_2O_3, 2.4% TiO_2, 5% MgO, 1.5% K_2O, 4000 ppm V, 320 ppm Ni and ca 1 ppm PGE. Most of the PGMs (laurite, Os-rich laurite, hollingworthite, sperrylite) occur as inclusions in chromite (see Fig. 9).

The euhedral chromite (0.1–0.2 mm) is the sole cumulus mineral. It is rich in Fe, Ti, V, Mn and Zn and poor in Mg (Table 1). Fossil melt inclusions are common in chromite, and skeletal chromites have been found. The Ti in chromite resides in exsolved ilmenite rods; occasionally the exsolved ilmenite occurs as bigger euhedral laths. The matrix is very rich in biotite (with 1.44–1.50% Cr_2O_3) and in K_2O; the silicate tailings of a big sample from the ore outcrop, used for mineral extraction tests,

Table 2. Compositions of loveringite and ilmenite, Akanvaara and Koitelainen intrusions. Electron microprobe analyses by Lassi Pakkanen, GSF. Anal. No. 5 by Tarkian & Mutanen (1987).

	1	2	3	4	5	6	7
TiO_2	55.84	56.38	57.18	56.96	60.4	50.61	48.80
$FeO_{(tot)}$	16.49	17.10	16.40	18.04	17.9	39.46	37.50
Cr_2O_3	7.61	7.50	7.84	6.21	7.6	0.70	0.33
SiO_2	0.02	0.02	0.05	0.14	0.10	0.15	0.03
Al_2O_3	1.29	1.01	1.19	0.85	1.0	0.18	0.03
MgO	0.68	0.67	0.59	0.67	1.2	0.17	0.30
MnO	0.23	0.11	0.15	0.16	0.15	5.09	9.68
CaO	1.44	1.35	1.89	1.43	2.6	0.18	
SrO	0.34	0.44	0.39	0.32		0.00	
BaO	0.62	0.61	0.58	0.66		0.61	
PbO	1.73	0.00	0.00	1.46		0.00	
Na_2O	0.00	0.03	0.06	0.03		0.00	
K_2O	0.06	0.05	0.04	0.03		0.01	
ZrO_2	3.81	3.68	4.15	3.87	3.8	0.09	
HfO_2	0.00	0.14	0.05	0.15	0.22	0.00	
ThO_2	0.13	0.06	0.35	0.06		0.07	
UO_2	0.27	0.41	0.16	0.37		0.00	
V_2O_3					0.67		
Y_2O_3	0.18	0.18	0.19	0.25		0.05	
La_2O_3	2.03	1.96	0.88	2.16	0.96	0.00	
Ce_2O_3					1.6		
Na_2O_3	0.46	0.57	0.42	0.37		0.11	
Total	93.23	92.27	92.55	94.09	98.20	97.49	96.67

Analyses 1 - 5 loveringites, 6 - 7 ilmenites
1 - 4 - Akanvaara DDH320/252.80 m (3 grains)
5 - Koitelainen DDH363/339.45 m
6 - Mn-ilmenite, associated with loveringite Akanvaara DDH320/252.80 m
7 - Mn-ilmenite, enhedral in LC chromite Akanvaara DDH320/271.05 m (contains 0.47% Zn)

contained 7.5% K_2O. Biotite is abundant in fossil melt inclusions of chromite. The UC rock is high in Cl (average 1800 ppm Cl).

The other main intercumulus minerals are green chromian hornblende (with 0.77–2.04% Cr_2O_3) and light-green actinolite. Sodic plagioclase comprises a small portion of the intercumulus matrix. The amounts of intercumulus ilmenite and secondary titanite and rutile are relatively high. Protoclastic fractures in chromite were filled with postcumulus ilmenite and pyroxene (now amphibole). Ilmenite often occurs as large oikocrysts with euhedral outlines ("idiocrysts") enclosing chromite. Ilmenite oikocrysts seem to be lacking from the lower part of the UC.

Chlorite, quartz, chromian clinozoisite ("tawmawite", with up to 3.47% Cr_2O_3), fluorapatite and sulphides (pyrrhotite, pentlandite, pyrite, violarite, millerite, marcasite, bornite and chalcocite) occur in small to very small amounts. Like ilmenite, fluorapatite sometimes occurs as big oikocrysts enclosing chromite.

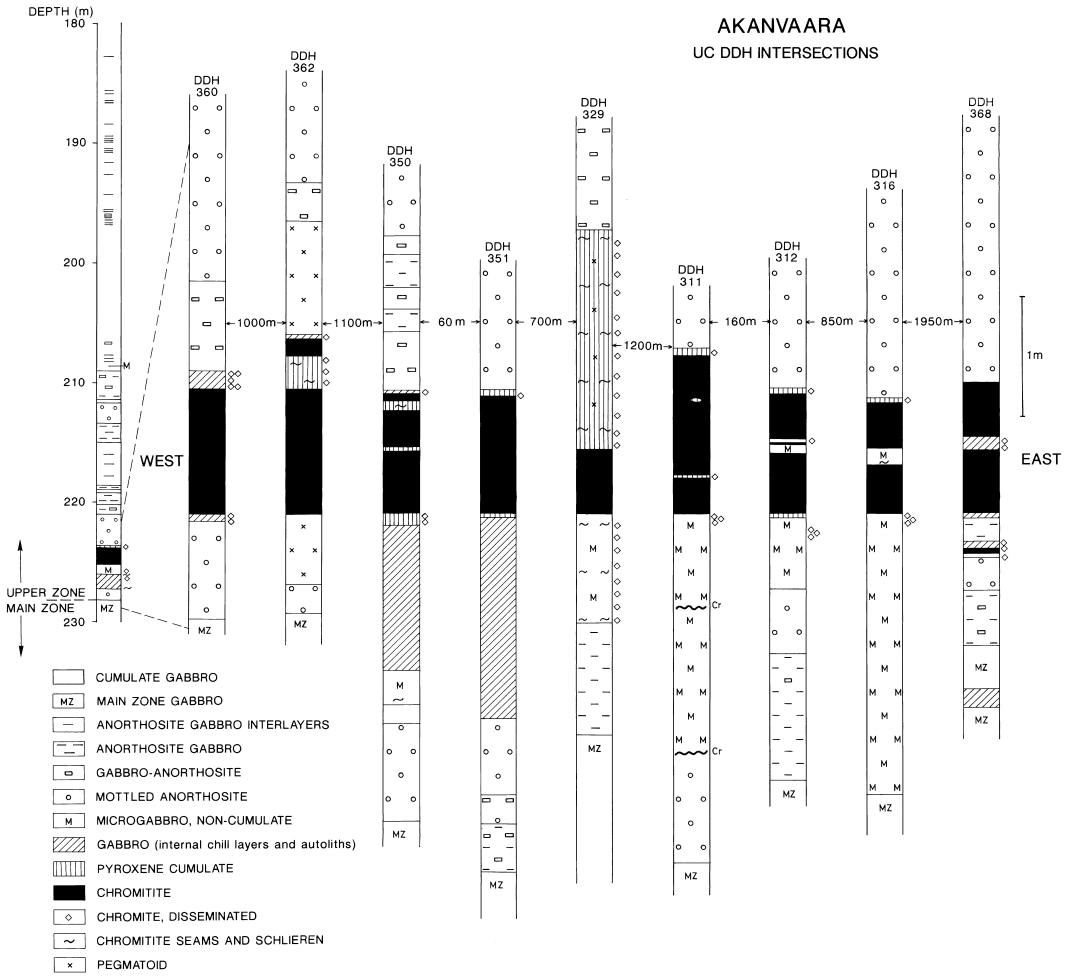

Fig. 10. The general layered sequence of the UC layer, and selected details of DDH intersections. Distance between intersections shown between columns.

Behaviour of PGE

Anomalous PGE values occur from the base of the intrusion up to the lowermost part of the magnetite gabbro, mostly in chromitites, but also in other rocks without any visual clues. Geochemically the most important PGE enrichment is in gabbros and anorthosites in the upper part of the intrusion.

There are no sulphide-associated concentrations of PGE. Terminal saturation of sulphide liquid took place with the arrival of cumulus magnetite (see Fig. 5). The sulphide liquid, quite naturally, was rich in Cu. Below that, in anorthosite 40 m below the magnetite phase contact, the Cu concentration jumps from low background values (ca 40 ppm) to 130–250 ppm, and at the same time S rises from very low values (generally below 100 ppm, the detection limit of the XRF method) to 100–400 ppm. A strong Au anomaly (1.5 ppm/1m) coincides with this Cu-S inflection, with a tail (20–

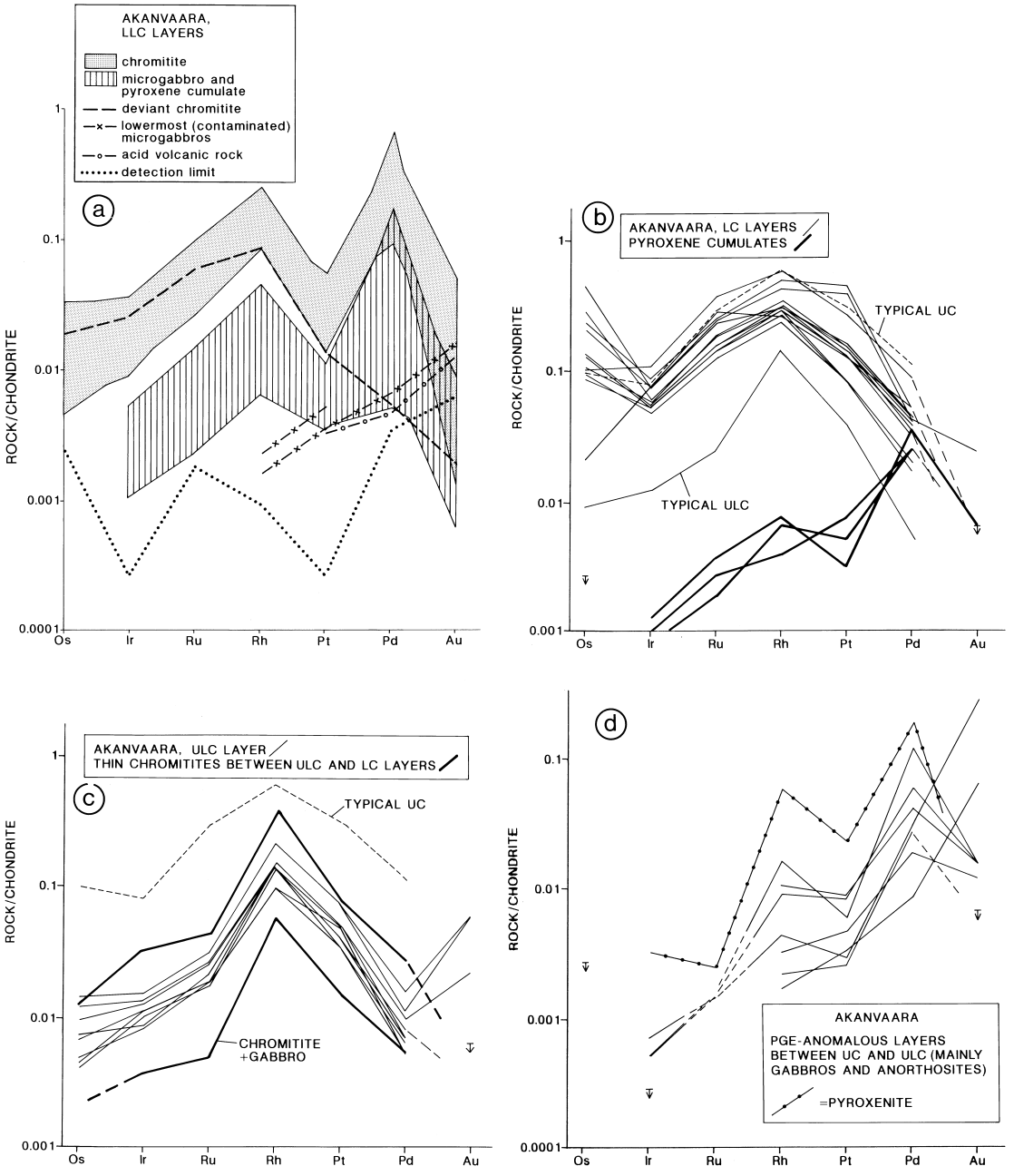

Fig. 11. Diagrams of chondrite-normalized values of PGE and Au from Akanvaara chromitite layers and associated rocks. Arrow top lines = analytical detection limits. a – LLC chromitites and associated rocks, b – LC and associated orthopyroxene-chromite cumulates; c – ULC layer and thin chromitite layers between LC and ULC; d – PGE-anomalous layers between ULC and UC; e – UC layer; f – UC ore, chromite concentrate and silicate tailings; g – silicate rocks (with or without accessory chromite) associated with the UC layer; h – Koitelainen and Akanvaara chromitites.

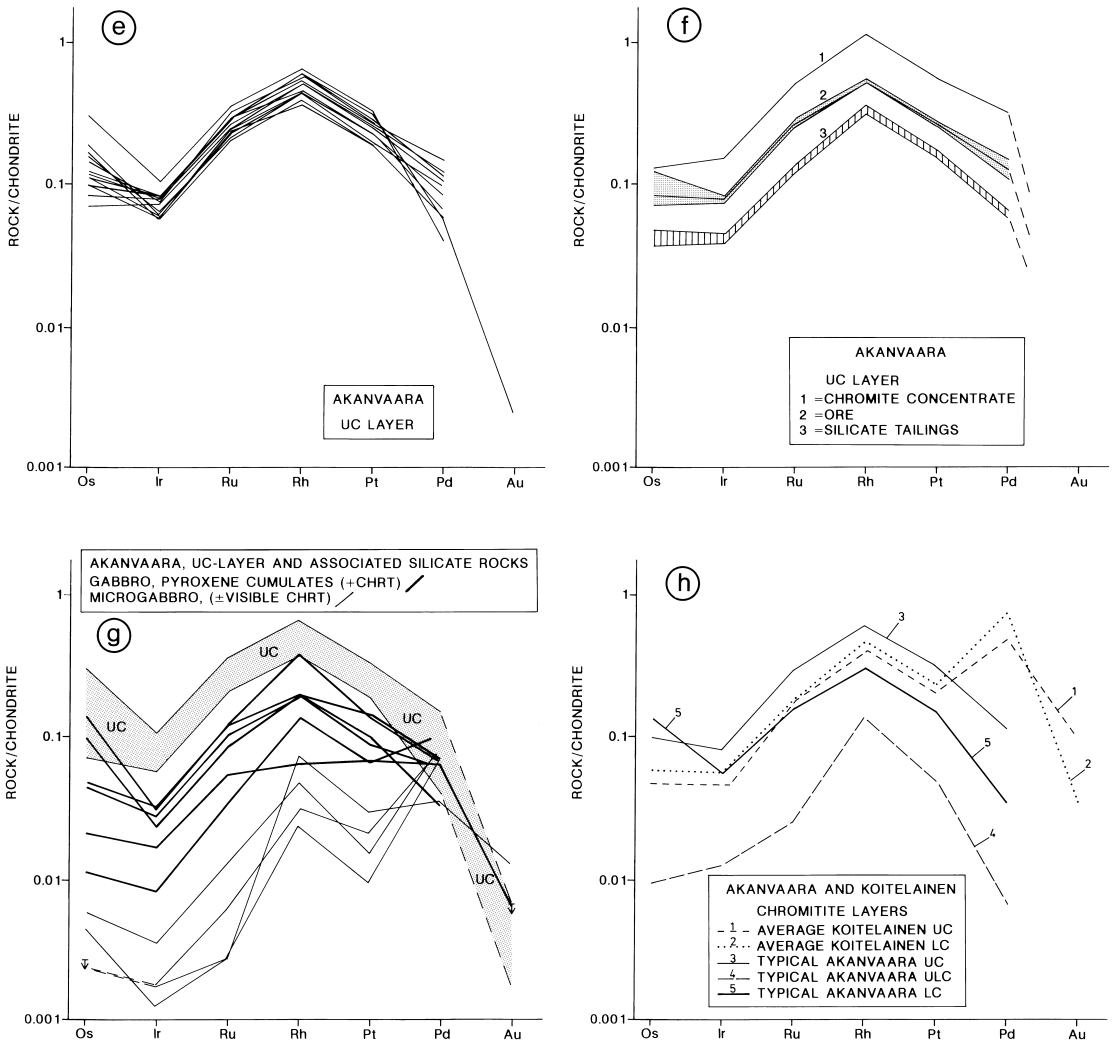

Fig. 11. (cont.)

50 ppb) extending for 15–20 m upwards. There is no associated increase in PGE. The Cu-S-enriched basal part of the magnetite gabbro is slightly enriched in Au (25–45 ppb) and Pt (10–40 ppb), but Pd is below the detection limit of 3 ppb (see Fig. 13).

Chondrite-normalized (CN) diagrams of PGE-Au for chromitites are presented in Figs 11a-h and for silicate-associated PGE-anomalies in Figs 13a-h. The Cr-PGE relationships are illustrated in Figs 12a-d. The LLC (Fig. 11a) layers differ from other chromitites in having an M-shaped CN profile, with peaks at Rh and Pd; the shape of the profile resembles those of the PGE-anomalous silicate rocks of the MZ and of the UC association (Figs 11d and 11g), the footwall rocks of the PGE-anomalous anorthosite in the UZ (Fig. 13c), and the chromitites of the Koitelainen intrusion (Fig. 11h). Other chromitite layers have a domed shape, sloping from Rh towards Au and Ir. Os(CN) is higher than Ir(CN), the only excep-

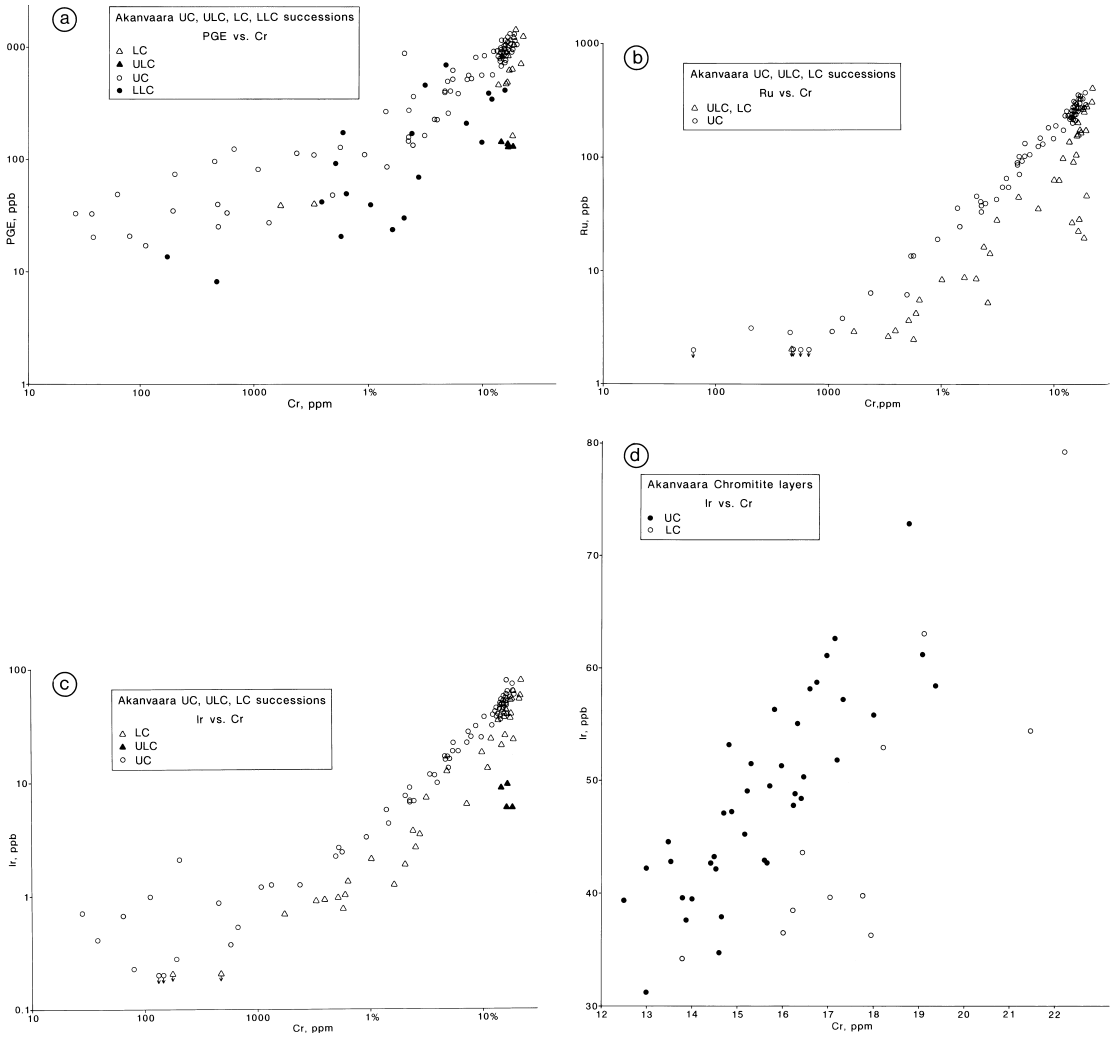

Fig. 12. PGE vs Cr, Akanvaara chromitites and associated rocks. a – PGE vs Cr; b – Ru vs Cr; c – Ir vs Cr; d – Ir vs Cr in UC and LC chromitites.

tion being the ULC layer. Silicate cumulates, whether separated from or associated with chromitites, show M-shaped CN profiles, with peaks at Rh and Pd. Au(CN) is always low. From UC upwards, Os, Ir and Ru are low, as if depleted by accumulated chromite. In the PGE-enriched anorthosites and gabbros below the magnetite gabbro (see Fig. 2), the PGE element ratios vary over a wide range and often very rapidly (Figs 13a–g). Here the CN diagrams have many shapes: M (peaks at Rh and Pd, Rh(CN) < or > Pd(CN)); flat domes, with a Pt-Pd top; peaked with varying slopes (peaks at Rh, Pt or Pd). Upwards from the anorthosites the diagram is M-shaped, but now the peaks are at Pt and Au.

There is a general but very weak positive correlation between the of Cr and PGE concentrations (Fig. 12a). Below about 1% Cr (corresponding to a chromite content of 3–4%) the total PGE is indifferent to Cr. In chromitites and in rocks with Cr concentrations down to ca

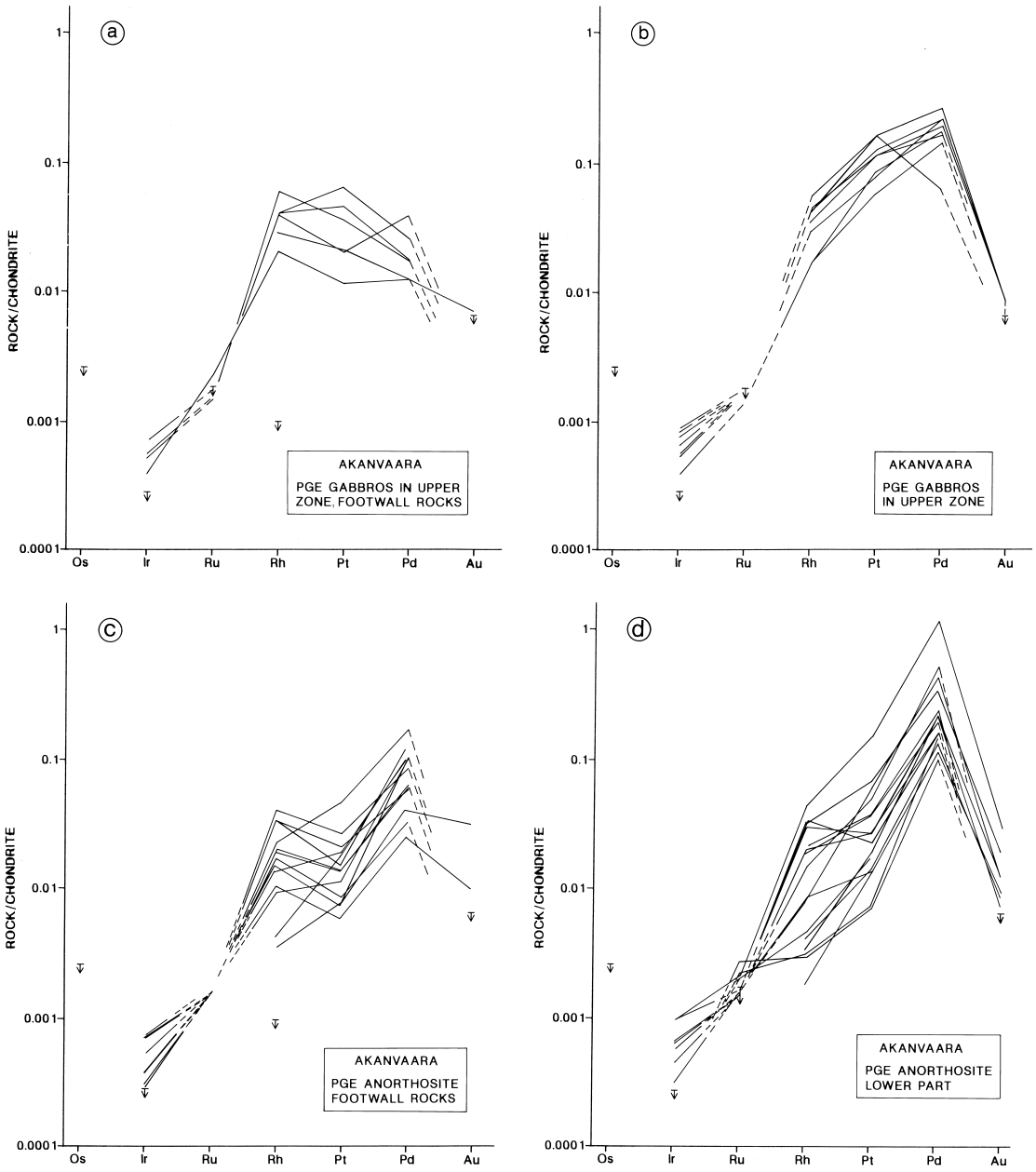

Fig. 13. Diagrams of chondrite-normalized values of PGE and Au from Akanvaara Upper Zone PGE-enriched anorthosites and gabbros. a – PGE-anomalous gabbro cumulates between UC and magnetite gabbro, footwall rocks; b – PGE-anomalous zone; c – g are for PGE-anomalous anorthosite sequence below magnetite gabbro: c – footwall rocks; d – lower part of the PGE sequence; e – low-PGE middle part of the sequence; f – upper part of the sequence; g – immediate hanging wall rocks; h – basal part of the magnetite gabbro.

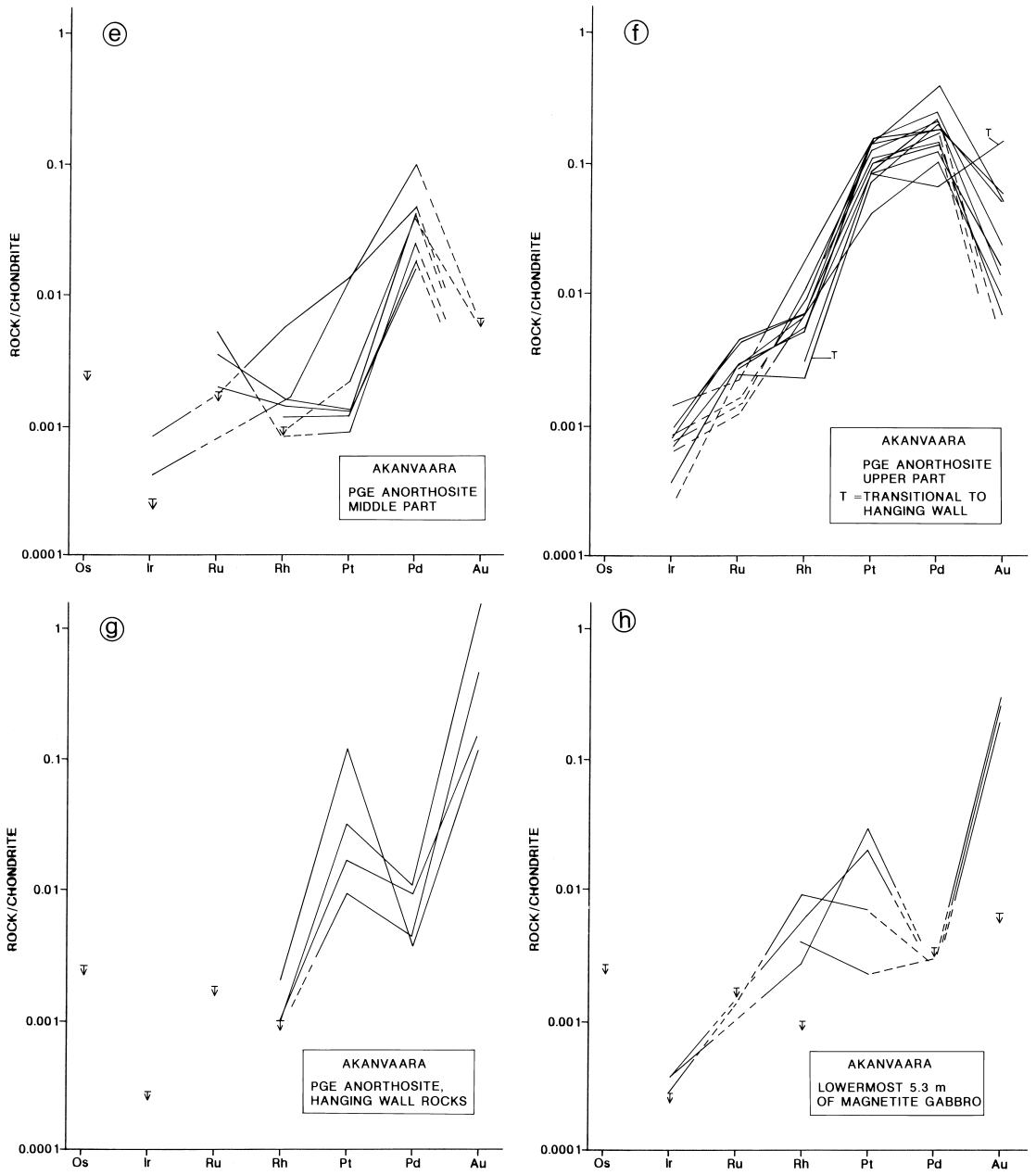

Fig. 13. (cont.)

1000 ppm, Ir and Ru correlate well with Cr (Fig. 12b–d). The diagrams suggest that chromite is the main collector of Ir and Ru (and, presumably, for Os). While Pt, Rh and Pd are clearly enriched in chromitites, there are other collectors and collection mechanisms for these elements. Sulphide liquid took no part in concentrating PGE in the Akanvaara magma sys-

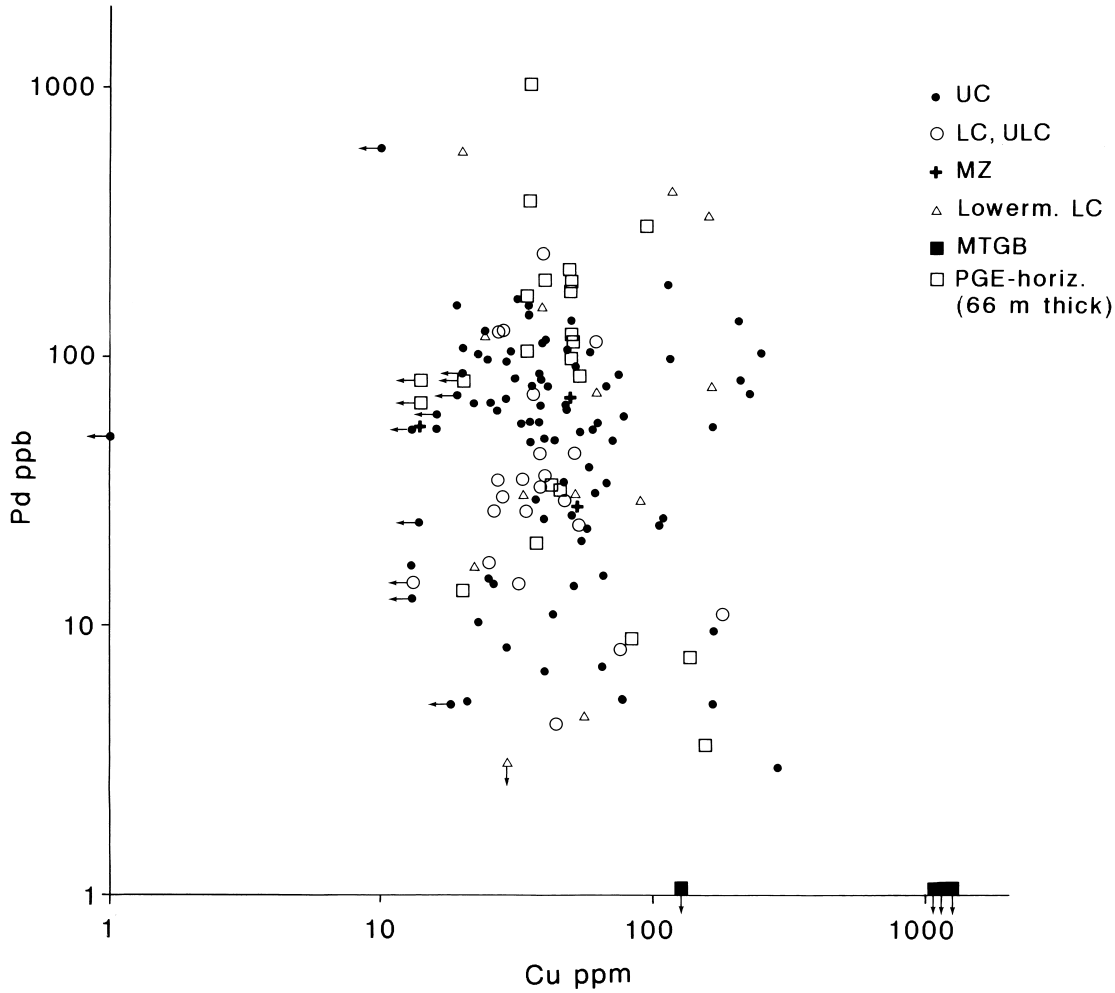

Fig. 14. Pd vs Cu in Akanvaara chromitites, associated rocks, and PGE-anomalous rocks.

tem because at the time of terminal sulphide saturation the residual liquid was extremely depleted in PGE by other collectors. Cu and Pd, which are generally regarded as chalcophile elements, show no mutual correlation in Akanvaara cumulates (Fig. 14).

The general order of depletion (i.e., of decreasing compatibility) in the evolution of the Akanvaara magma system seems to be: Ir > Os > Ru > Rh > Pd > Pt > Au. This order may hold in general for S-undersaturated magmas, with recurrent deposition of chromite monocumulates. As regards the end triplet, it is somewhat at variance with the order presented by Barnes and others (1985).

Some petrological aspects

Most of what I have conjectured about the Koitelainen intrusion (Mutanen, 1989b, 1992) applies to Akanvaara as well. The parent magma was a silica-saturated low-Ti basalt, low in P_2O_5 and sulphur. The magma was dry. Consequently, primary hornblende never crystallized as a stable phase from the fractionating main magma. At the beginning and throughout most of the crystallization the magma held on or aspired to the cotectic of augite, low-Ca pyroxene and plagioclase. Iron became enriched in the residual liquid, along with Ti, V, Zn, Na, and the truly incompatible elements. Fractional crystallization of pyroxenes rapidly depleted the liquid in Cr and Ni. The magma was in convective motion, driven by thermal and two-phase convection (see Morse, 1988). Extreme cases of two-phase convection were the sudden downdraft surges of chromite-laden density flows.

The cotectic routine was interrupted by episodic melting of country rocks. The roof portion of the magma chamber was stirred by sinking xenoliths and heavy residue minerals from partial fractional melting of pelites. The mixing of the mafic melt and the anatectic roof melt increased crystallization and accelerated two-phase convection.

The contamination was by:

- selective diffusion between mafic magma and solid or molten country rocks (floor, roof and immersed xenoliths), and across melt boundaries in the acid/mafic emulsion in the mixing zone of mafic magma and anatectic roof magma (see Watson, 1982);
- direct mixing of mafic magma and acid contaminant magma;
- refractory or otherwise insoluble phases (e.g., sulphide liquid) after partial melting of country rocks.

Mineralogical and geochemical indicators of contamination are the common occurrence of loveringite (Table 2), zircon and chlorapatite, fluorapatite (in the Lower Zone), the abundance of intercumulus quartz, potassium feldspar and biotite-phlogopite, and the presence of "granitic" intercumulus material and "granitic", Cl-rich melt inclusions in cumulus olivine and chromite.

Owing to contamination by salic alkalic material orthopyroxene crystallized in the basal part as the sole cumulus silicate, and olivine appeared at the MZ boundary. Plagioclase cumulates, without mafic counterlayers, are thought to represent the excess alumina left behind after partial melting of pelitic schists (Bowen, 1928; Wyllie & Tuttle, 1961; see later).

The case of the UC chromitite is discussed in greater detail later. Here I only present some facts and ideas concerning the Akanvaara UC layer.

The stratigraphic position of the UC high in the layered sequence, the composition of the chromite, and the petrography and geochemistry of the intercumulus and melt inclusions are all features not easily accommodated to standard petrogenetic models. Customarily, new primitive magma pulses (rich in Mg and Cr) are invoked to explain even lesser problems in layered intrusions. New magma pulses, regardless of their composition, seem to offer an explanation for mineralogical and geochemical reversals, regardless of their character (see e.g., Eales et al., 1990). The models based on new magma pulses rely on circumstantial evidence; transgressions of new magma through settled cumulates are hardly ever visible, even in well exposed mafic intrusions. At Akanvaara the UC layer is well exposed in trenches and has been intersected in 30 drill holes, but there is nothing in the field or in rock and mineral analyses to suggest the entry of new magma in any amount, or of any density or composition.

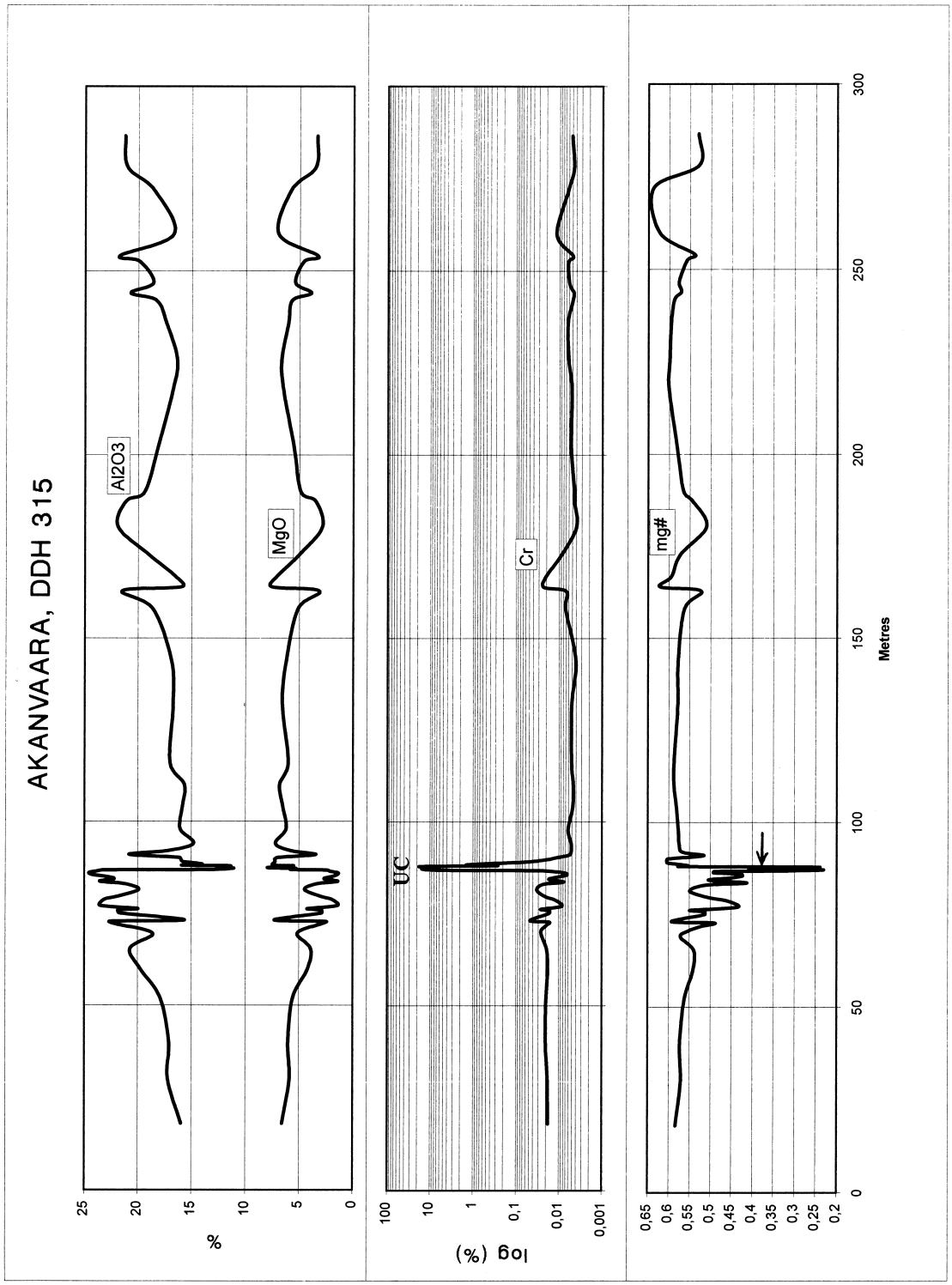

Fig. 15. Profiles of mg#, Al_2O_3, MgO and Cr through the UC sequence, Akanvaara intrusion. DDH315. The mg# of the UC silicate tailings shown by arrow.

The addition of primitive magma should have left its signature in the mineralogy and chemistry of the cumulate pile overlying the UC. But, as shown by Figs 5 and 15, the magma reassumed its former fractionation trend after the UC event. As seen in Fig. 15, there is no increase in mg# below, at or above the UC. In fact, there is a marked *decrease* in mg# at and above the UC (in chromitite the ratio is 0.233, in bulk UC silicates 0.438). The very low mg# in UC and plagioclasic cumulates is, of course, partly due to the trapped liquid shift effect, as recognized by Barnes (1986) and convincingly applied by Cawthorn (1995, 1996).

It is seen in Fig. 15 that the MgO, mg# and Cr curves each represent a mirror image of the Al_2O_3 curve. The latter reflects the amount of cumulus plagioclase. Thus, when plagioclase crystallized (or settled) in excess of the cotectic pl/px ratio, the MgO, mg# and Cr of the cumulate decreased. In the long run plagioclase would not have been able to crystallize in noncotectic proportion without having enriched the residual magma in MgO and, as a result, restarting pyroxene crystallization. As there are no counterlayers compensating for the excessive plagioclase separation, it must be concluded that alumina was added to the magma system, most probably as an aluminous residual phase from melted sedimentary rocks. I remind the reader of the fact that assimilation of aluminous sediments augments the crystallization of more anorthitic plagioclase and of Ca-poor pyroxene at the expense of Ca-rich pyroxene (see e.g., Bowen, 1928; Kuno, 1950; Gribble & O'Hara, 1967; Willemse & Viljoen, 1970). Suppression of the crystallization of the Ca-rich pyroxene and its removal from the cumulus assemblage results in a radical decrease of Cr in cumulate. Accordingly, assimilation of aluminous sediments would result in the compositional profiles seen in Fig. 15.

Let us then consider the possibility that the chromium was derived from the main magma. The uppermost Main Zone gabbro, a few metres below the UC layer, contains 50 ppm Cr. With a px/pl ratio of 1, the original "bulk" pyroxene would have had 100 ppm Cr; further, using $D_{Cr}^{px/liq}$ values from 10 to 20 (a reasonable range for terrestrial basalts, see e.g. Huebner, 1976; Duke, 1976; Grove & Bence, 1977; Henderson, 1979; Allègre et al., 1977), we get a concentration of 5–10 ppm Cr for the last MZ melt. Obviously, then, it was not possible to make the UC from the lean, old magma.

The low Mg in chromite and the potassic composition of the melt inclusions and of the intercumulus material suggest that the chromite crystallized in an environment poor in Mg and rich in K (and Cl). Thus, it seems that for the UC event to happen the only "primitive" additive was Cr.

The PGE do not keep company with sulphide concentrations. Apparently, PGE behaved as incompatible elements throughout most of the crystallization. However, at times (and sites) of contamination, the PGM crystallized as tiny free crystals, remaining in suspension or nucleating on chromite. The PGE-enriched intervals in the Upper Zone may represent true saturation of PGM phases in residual liquid. PGM nucleated homogeneously or heterogeneously on any substrate suitable and available, such as cumulus silicates and (or) ilmenite. The PGM paragenesis has still to be studied. Au seems to be the only truly chalcophile noble metal. Its first (and only) marked enrichment occurred when the first tiny premature fraction of sulphide liquid separated from residual liquid slightly below the magnetite phase contact.

THE KOITELAINEN INTRUSION

General geology

The intrusion is a flat, oval-shaped brachyanticline structure, 26 km x 29 km in size (see geological map, Appendix 3). The interior is made up of footwall rocks of the intrusion – Archaean granitoid gneisses, overlying late Archaean to early Proterozoic ("Lapponian") supracrustal rocks, pre-Koitelainen gabbroic intrusions and ultramafic dykes. The Archaean gneisses form two domes. The smaller one, immediately west of the peridotitic basal cumulates of the Koitelainen intrusion, consists of tonalites, trondhjemites and granodiorites (Peltonen, 1986), yielding a U-Pb zircon age of 3100 Ma (Kröner et al., 1981); however, Sm-Nd isotopic ratios suggest a prior crustal residence of about 250–500 Ma (Jahn et al., 1984). The few outcrops of the much larger easterly Kiviaapa dome (U-Pb zircon ages 2765–2821 Ma, Mutanen, 1989b) are located near the base contact of the Koitelainen intrusion. The eastern contact of the Kiviaapa dome gneisses with the Koitelainen intrusion has been intersected by two DDHs. These rocks were thermally affected by the intrusion.

A deep gravity low in the core of the Kiviaapa dome, with distict gradient boundaries against surrounding gneisses, suggest the presence of a granite mass with a great depth extent here.

The pre-Koitelainen supracrustal rocks around the Archaean gneisses beneath the intrusion include regionally metamorphosed subarkoses, various acid and intermediate volcaniclastic rocks, volcanic breccias (U-Pb zircon age 2526±42 Ma, Peltonen, 1986; Pihlaja & Manninen, 1988), diamictites, tuffs and tuffites, and basaltic lavas and tuffs. The most common, but rarely exposed (as a result of grussification), rock type is a biotite-plagioclase mica gneiss that contains various amounts of felsic volcanic material.

The Koitelainen intrusion is overlain by a thick succession of metamorphosed volcanic and sedimentary rocks. In the roof, within reach of the thermal effects of the intrusion, high-aluminous schists (for composition, see anal. 1, Table 3) and komatiitic volcanic rocks (Mutanen, 1976a), accompanied by smaller amounts of basaltic effusives and tuffs and subarkosic quartzites, predominate. Higher up, there must be a change from the pre-Koitelainen to post-Koitelainen, pre-Keivitsa supracrustal formations. The boundary has not yet been located; tentatively I would place it just above the level of calcareous rocks, micaceous arkosic rocks and low-Ti basalts between the Koitelainen and Keivitsa intrusions (see Appendix 4).

Emplaced among the volcanic-sedimentary rocks are several small mafic intrusions and extensive komatiitic layered sills. Some of these are older than, and probably unrelated to, the Koitelainen intrusion; these include "komatiite gabbros" and ultramafic intrusions of the komatiite kin, and a differentiated, "evolved" mafic sill found by diamond drilling immediately beneath the Koitelainen intrusion, at the eastern boundary of the Kiviaapa dome.

I conceive the two layered komatiitic sills between the Koitelainen and Keivitsa intrusions (see geological map, Appendix 4) as roughly consanguineous with the former. These sills occur all around the western perimeter of the Koitelainen intrusion. When close to the upper contact of the Koitelainen intrusion, the lower part of the lowermost sill regularly contains spots of augite (now mostly altered to amphibole), enclosing clusters of olivine crystals (for composition, see anal. 2, Table 3). I interpret the spots as having formed through the thermal effect of the Koitelainen intrusion.

Table 3. Chemical composition of some rock types of the Koitelainen area.

wt%	1	2	3	4	5	6	7	8	9	10	11
SiO_2	53.00	44.17	53.84	51.03	61.73	59.41	58.79	54.95	54.43	52.76	52.29
TiO_2	0.94	0.34	0.47	0.19	1.16	1.30	1.57	1.75	1.82	1.45	1.44
Al_2O_3	25.04	5.93	15.10	17.67	12.91	12.88	14.17	12.35	13.37	14.37	13.63
Fe_2O_3	6.06										
FeO	4.27										
$FeO_{(tot)}$		11.07	9.12	7.46	10.39	11.66	11.32	13.79	12.76	13.00	13.33
MnO	0.08	0.16	0.16	0.12	0.06	0.16	0.16	0.20	0.18	0.14	0.13
MgO	1.68	24.35	6.22	7.36	1.49	1.92	1.60	2.17	1.99	4.17	3.92
CaO	1.29	5.43	9.96	10.99	3.96	4.89	5.11	4.68	5.06	6.66	5.68
Na_2O	1.62	0.42	3.22	3.08	4.80	3.71	4.60	4.77	4.66	4.48	3.98
K_2O	2.00	0.00	0.68	0.80	1.19	2.43	2.19	1.94	1.90	1.42	1.25
P_2O_5	0.25	0.03	0.08	0.00	0.26	0.22	0.38	0.34	0.32	0.24	0.27
CO_2	0.00										
H_2O+	3.50										
H_2O-	0.04										
S	0.04									1.37	
S=O	-0.02										
Total	99.79	92.94	98.85	98.70	97.94	98.58	99.89	96.95	96.49	100.06	95.92
ppm											
Cr	400	2600	nd	nd	<15	<100	<100	<15	<15	<20	19
Ni	150	620	nd	nd	<20			<20	<20	59	80
Cu	78	13			380			480	640	340	590
Co	37	55								44	
V	190	110			140			190	240	180	200
Zn	130										
Zr	140		60	30	170	170	130	370	140		100
Ba	900		300	400	200	900	1300	1000	1000		800
Rb			nd	nd	<100	110	80	<100	<100		<100
Sr	160		390	320	130	300	320	460	520		710
Pb	23										

Samples:
1: High-aluminous schist, Rovakumpu, east of Koitelainen intrusion (sample TM-78-133)
2: Spotted komatiite (flow or lower part of sill), at the western contact of the Koitelainen intrusion (sample: R311/57.7 - 58.2 m)
3 - 4: Microgabbro autoliths from the Upper Zone of the Koitelainen intrusion; anal. 3 - R304/81.8-82.10 m, anal. 4 - R302/233.65-233.80 m (the latter contains plagioclase primocrysts).
5 - 11: Samples are from quartz monzonite diapirs, intruding the lowermost cumulates of the Koitelainen intrusion. Anal. 5 - TM-80-158.1 "monzonite", anal. 6 - R307/42.95-43.15 m, "monzonite", anal. 7 - R307/59.45-59.65 m dark "monzonite" autolith; anal. 8 - TM-80-160.1 "spinifex" monzonite (branching crystals of amphibolized fayalite(?); anal. 9 - TM-80-160.2 "spinifex" monzonite, branching crystals of fayalite pseudomorphs and plagioclase; anal. 10 - TM-80-159.11 microgabbro (monzogabbro), with disseminated sulphides; anal. 11 - TM-80-143.3 microgabbro (monzogabbro), with sulphides.

Analytical methods:
1 - wet chemical, by Christer Ahlsved, trace elements: OES by Ringa Danielsson
2 - XRF, Ni, Cu, Co: AAS; Cr, V: OES, by Väinö Hoffrén
3 - 4 - XRF, by Väinö Hoffrén
5 - 11- XRF (Cr, Ni, Cu, V OES), by Väinö Hoffrén

Countless diabase dykes (only the thickest are shown on the map, Appendix 3) cut the basement, the intrusions and the supracrustal rocks. No komatiitic dykes are seen to cut the Koitelainen intrusion. The northeasterly trending dyke in the western part of the Kiviaapa

dome (see Appendix 3) has yielded percussion drilling samples with rather high Ni and Cr; it may represent a feeder either to pre-Koitelainen komatiitic magmas or to post-Koitelainen (Ludian) komatiitic effusives. Thick (up to 90 m) dykes of diabases with a rather evolved geochemical signature (high Fe, Ti) are well exposed in the Koitelainen fell area. These dykes have chilled contacts against cooled Koitelainen rocks, and may represent pre-Keivitsa volcanism (2200–2100 Ma?). However, volcanism corresponding to these diabase magmas is all but unknown in the pre-Keivitsa sequence. During recent checking of thin sections from the eastern Kiviaapa and Iso Vaiskonselkä areas diabase dykes similar to the east-northeasterly olivine gabbro-diabase dykes of the Keivitsa intrusion (see later) were found.

During the Svecokarelian folding (ca 1900 Ma ago) the Koitelainen intrusion behaved mainly as a competent, brittle body and was fragmented into fault blocks along northeasterly and northerly faults. Plastic deformation styles are evident in blastomylonites in broad fault zones, in the foliated to schistose outermost granophyres and throughout the tectonically thinned western limb of the intrusion. A fault zone is well exposed at Lakijänkä, Koitelainen (see Mutanen, 1989b, p. 45). There, coarse pegmatoids have been deformed into banded hornblende-ilmenite-magnetite rock. A folded scapolite dyke indicates repeated movements in the fault zone. Younger northwesterly and north-northwesterly fault and fracture zones also occur.

The intrusion and the diabase dykes alike were regionally metamorphosed to varying degrees, most heavily long fault zones and near the upper contact. The alteration of primary non-hydrous minerals in gabbros and other competent rocks (into uralitic hornblende, tremolite, clinozoisite, scapolite, talc, serpentine minerals, chlorite, carbonate, biotite-phlogopite) typically advanced along an orthogonal system of narrow fractures (Fig. 17, upper left).

Original magmatic minerals have never been preserved in granophyres and only rarely in magnetite gabbros. The metamorphic grade of the area corresponds to that of lower and middle amphibolite facies.

Emplacement and fractionation

The U-Pb ages of zircons from ultramafic pegmatoids (see Fig. 18f) and from a porphyritic granophyre are 2435 Ma (Mutanen, 1976b, Kröner et al., 1981; Mutanen, 1989b). The estimated maximum thickness of the intrusion is around 3200 m.

The magma intruded through an old Archaean crust and was emplaced beneath the high-aluminous pelitic rocks. The situation is analogous to that of the Kejv area, central Kola Peninsula, where mafic layered intrusions occur between Lebyazhinsk gneisses (very similar to the gneisses beneath the Koitelainen intrusion) and high-aluminous gneisses, similar to the pelitic roof rocks of the Koitelainen intrusion (see Sharkov & Sidorenko, 1980; Kratts et al., 1984). The Akanvaara and Imandra intrusions are in a similar stratigraphic position, the latter between the Archaean gneisses and overlying superstructure of terrigenous metasediments, andesitic and basaltic metalavas and acid metavolcanics (Dokuchaeva et al., 1992).

The upper contact of the intrusion is roughly conformable. Nowhere is the intrusion seen to have breached the high-aluminous schists. These schists evidently halted the ascent and controlled the lateral spreading of the magma as a permeable, fissile layer and as a vapour barrier (see Mudge, 1968; Williams & McBirney, 1979).

The lower contact is transgressive, climbing the stratigraphy away from the feeder, which I assume was in the western part of the intrusion beneath the deep basin filled with thick olivine cumulates (see map, Appendix 3). A gabbro dyke projecting northwest from this basin may be an extension of the feeder.

The original contact hornfelses of the intrusion are hardly distinguishable because of superimposed retrograde (in relation to contact metamorphic facies) regional metamorphism. Hornfelsic sedimentary xenoliths have been found in the lower part of the intrusion, and relict contact metamorphic garnet occurs at the top of the granophyre. The magma melted and swallowed immediate roof rocks (high-aluminous pelitic schists and arkosic quartzites) for several hundreds of metres. Signs of incipient melting are seen in the granitic clasts of an older conglomerate immediately beneath the intrusion in the western Kiviaapa area. As will be discussed later, floor melting, rarely noted in layered intrusions, was intense among the salic floor rocks below the deep cumulate basin in the western part of the intrusion.

Shallow holes drilled recently (1995) in the granophyre cap area, in the southeastern part of the intrusion have intersected partially digested acid volcanic rocks in which quartz amygdales are often preserved (factually, as an insoluble refractory residue) in a matrix with the mineralogy and chemistry of granophyres (SiO_2 54.35 – 65.78%, CaO 3.04 – 7.24%, MgO 0.88 – 4.79%). Refractory roof rocks (basalts, basaltic tuffs, various komatiites) occur as xenoliths, typically at or above the major stratigraphic breaks and reversals.

There is no evidence of multiple magma pulses at Koitelainen, nor does the petrological explanation of the intrusion need them. As evidence of fresh pulses I value only cases in which magma is factually and unambiguously seen to have intruded from beneath and to have torn through cumulates. Considering the eroding power of density currents sweeping along the cumulate surface (see later) I attach little significance to cumulate autoliths as evidence of entry of fresh magma into the chamber. In my opinion the intrusion formed essentially as a single cast, before deposition of any significant amount of cumulates. I consider the reversals, often used as The Evidence for multiple magma pulses, a problem to be solved, not a solution to be satisfied with.

In analogy with the Akanvaara intrusion, the parent magma (the magma that entered the intrusion chamber) was silica-saturated or just-saturated, low-Ti tholeiitic in composition.

Fine-grained **chilled microgabbros** were formed against the walls. Field evidence from Koitelainen, Akanvaara and elsewhere suggests that this lining did not last for long but, loosened by the melting of the support rocks, was peeled of and fragmented and left to founder in magma (e.g., Hess, 1960; Morse, 1969a; Wadsworth, 1988; Wiebe, 1990). Before their true nature was revealed (Batashev et al., 1976; Lavrov et al., 1976), such detached, stoped chill slabs, often very extensive (and, naturally with at least one sharp contact), were earlier perceived as dykes.

New chilled rocks promptly formed in place of the peeled-off margins. Stepwise chill renewal from continuously fractionating magma may give a deceptive impression of successive magma pulses (Mutanen, 1989b, Hoatson et al., 1992). Later, we shall see how reversals in the layered igneous sequences, which are generally (and too casually) ascribed to new magma pulses, might be explained by contamination.

In principle, a succession of temporary chills would give a good measure of the evolution of magma. However, chilled rocks are well known to be porphyritic, i.e., they contain primocrysts (of olivine, pyroxene, plagioclase; see e.g., Page, 1977; Hoover, 1989). Still worse, chilled rocks are often mixed with contaminants (op. cit., and the following).

In the Koitelainen intrusion, autoliths of chilled rocks are common in the Upper Zone (UZ; analyses 3–4, Table 3). Most of them are

equigranular microgabbros and coarser noncumulate gabbros, some containing plagioclase primocrysts. There are also contaminated microgabbro autoliths in hybrid, quartz-rich matrix, suggesting that mafic magma chilled against salic anatectic melt (see Gibson & Walker, 1964; Blake et al., 1965; Eichelberger & Gooley, 1977; Wiebe, 1984, 1990; Furman & Spera, 1985).

The contacts of the autoliths are generally sharp, but the contaminated autoliths show rapid gradations to cumulates. In the southern part, a succession of autoliths was intersected by DDHs. The uppermost autoliths are aphyric, more or less contaminated microgabbros underlain by plagioclase-phyric microgabbros; lowermost are plagioclase-phyric microgabbros with amygdale-like granophyre pockets. This series of autoliths represents an interesting record of roof melting, contamination and chilling. In one of the DDHs, salic melt (now granophyre) was found trapped beneath a foundered autolith.

Thus, there are no satisfactory, representative chilled rocks untainted by cumulus crystals or contamination, approximating the composition of the parent magma of the Koitelainen intrusion. The examples cited above suggest that such virgin chills are all but impossible to come by anywhere. This is certainly one of the reasons why the actual cumulus successions in layered intrusions deviate from the liquidus phase relations determined experimentally for chill compositions (see Biggar, 1974, and compare with Hoover, 1989). The main reason in many intrusions, however, was the addition of exotic contaminants, and their effects on the cumulus paths (see Kushiro, 1973; Irvine, 1975a; Mutanen, 1989b, 1992). At Koitelainen the apparent reverse fractionation from lower chill rocks to thick early olivine(-chromite) cumulates, as well as later reversals are ascribed to the various effects of contamination.

Even if we never manage to learn the exact compositions of parent intrusive magmas, many of their characteristics can be deduced from what compositional data are available on the lower marginal gabbros and on the general course of fractional crystallization as seen in the cumulate sequence. The magma was, and remained, rather dry to the very end. Thus no primary hydrous silicates crystallized from the main magma as cumulus or intercumulus phases. Primary biotite-phlogopite and magmatic hornblende occur only as daughter minerals in melt inclusions in olivine and chromite, and in intercumulus of contaminated cumulate layers. The last liquid fraction shows an increase in Cl. The parent magma was low in P_2O_5. Fluorapatite, an intercumulus mineral in contaminated Lower Zone cumulates, was soon superseded by chlorapatite (see Table 8). The latter is common in intercumulus and as a daughter mineral in melt inclusions in the Lower Zone. In the mixed-rock peridotite unit in the Main Zone chlorapatite visits as big cumulus crystals (see Mutanen, 1989b). Apatite reached the terminal cumulus status (as fluorapatite) only just below the granophyre.

Cumulus magnetite appears at about the 95 PCS level, suggesting that the oxidation state of the magma was low, and hence crystallization of magnetite was suppressed. As the magma was also low in Ti, ilmenite never crystallized as a proper cumulus mineral; it does occur, though, as daughter crystals in melt inclusions in olivine and as big Doppelgänger cumulus crystals in the felsic part of the mixed rock peridotite (see Mutanen, 1989b). The Ti content remained relatively low until late stages of fractionation. The first cumulus titanomagnetite depleted the melt in Ti, and no ilmenite crystallized from magma.

The magma was low in sulphur and, apart from transient sulphide saturation associated with contamination, the terminal saturation of sulphide liquid was attained only 40 m above the magnetite phase contact, well above the 95 PCS level.

For most of the crystallization history pyroxenes and plagioclase precipitated cotectically. The residual liquid was gradually en-

riched in Fe to the point where pigeonite crystallized in the upper Main Zone. Eventually magnetite and, finally, fluorapatite joined plagioclase and pyroxenes.

The massive accumulation of olivine cumulates in the basal part of the intrusion seems to be at variance with the assumption of a just-saturated magma. Although it is well known that olivine can crystallize from a silica-oversaturated liquid, the amount of olivine accumulation as found at Koitelainen seems incredible. The composition of early olivine (ca Fo_{80}, see later) is typical of a tholeiitic magma rather than the ultramafic magma often invoked as a promoter of reversals. I will return to the olivine problem later when discussing the effects of contamination.

Igneous stratigraphy and petrography

First, I repeat my advice that the reader should consider (but not necessarily subscribe to) the CC model previewed before, though only to better understand the description that follows. The petrographic description deals only with primary magmatic and post-magmatic minerals, which are amply available throughout most of the cumulate succession; secondary minerals are mentioned when necessary. Also, I will drop petrological explanations en route, as I do not think it is fair to swamp the confused reader with petrological data and arguments at the end of the book.

The general division and cumulus stratigraphy of the intrusion is presented in Fig. 16. The intrusion is divided into an ultramafic Lower Zone (LZ), a gabbroic Main Zone (MZ) and a gabbroic Upper Zone (UZ; with anorthosites and magnetite gabbro). Granophyre forms a continuous cap above the mafic succession. In the text, individual rock units, distinguishable sequences and isomodal layers (e.g., mixed rock peridotite, pigeonite gabbro, magnetite gabbro) are informally called units.

Xenoliths of intrusive gabbros and extrusive komatiites, and chill-autoliths occur near the base contact of the intrusion. Neither autoliths nor xenoliths have been found in the MZ, but in the UZ and granophyre they are common once again, particularly at or near the base of the anorthosite unit of the Upper Chromitite (UC) sequence, and of the magnetite gabbro unit. The xenoliths and autoliths are concentrated at levels corresponding to episodes of fractional melting of the roof and a concomitant increase in two-phase convection.

Phenomena that might be characterized as magmatic-diagenetic were associated with the consolidation of the cumulus pile. They include diapirs of anatectic floor melt (Fig. 21), ultramafic pegmatoid pipes and veins in the MZ (see Figs 28–29, 34), and acid dykes and veins (Fig. 17, middle right). The pegmatoids represent accumulations of intercumulus liquid, the acid dykes "back-intrusion" either of the first anatectic melt from the wall rocks or of the last minimum-melting liquids from granophyre magma.

Load cast structures occur in cumulates at sites of density inversion (Fig. 17, middle left), but no large-scale upward seepage of intercumulus liquid caused by compaction of the growing cumulus pile (as suggested by Cameron, 1969 and Irvine, 1978b) has been noted at Koitelainen. At Koitelainen there is no unambiguous evidence of significant vertical movement of the intercumulus liquid, in agreement with McCarthy and co-workers (1984), Barnes (1986) and Cawthorn (1995), or even of compaction (Morse, 1986, 1988). If compaction were effective in driving the intercumulus liquid, the initial porosity should decrease, and the proportion of adcumulates increase, downwards, but this is not generally

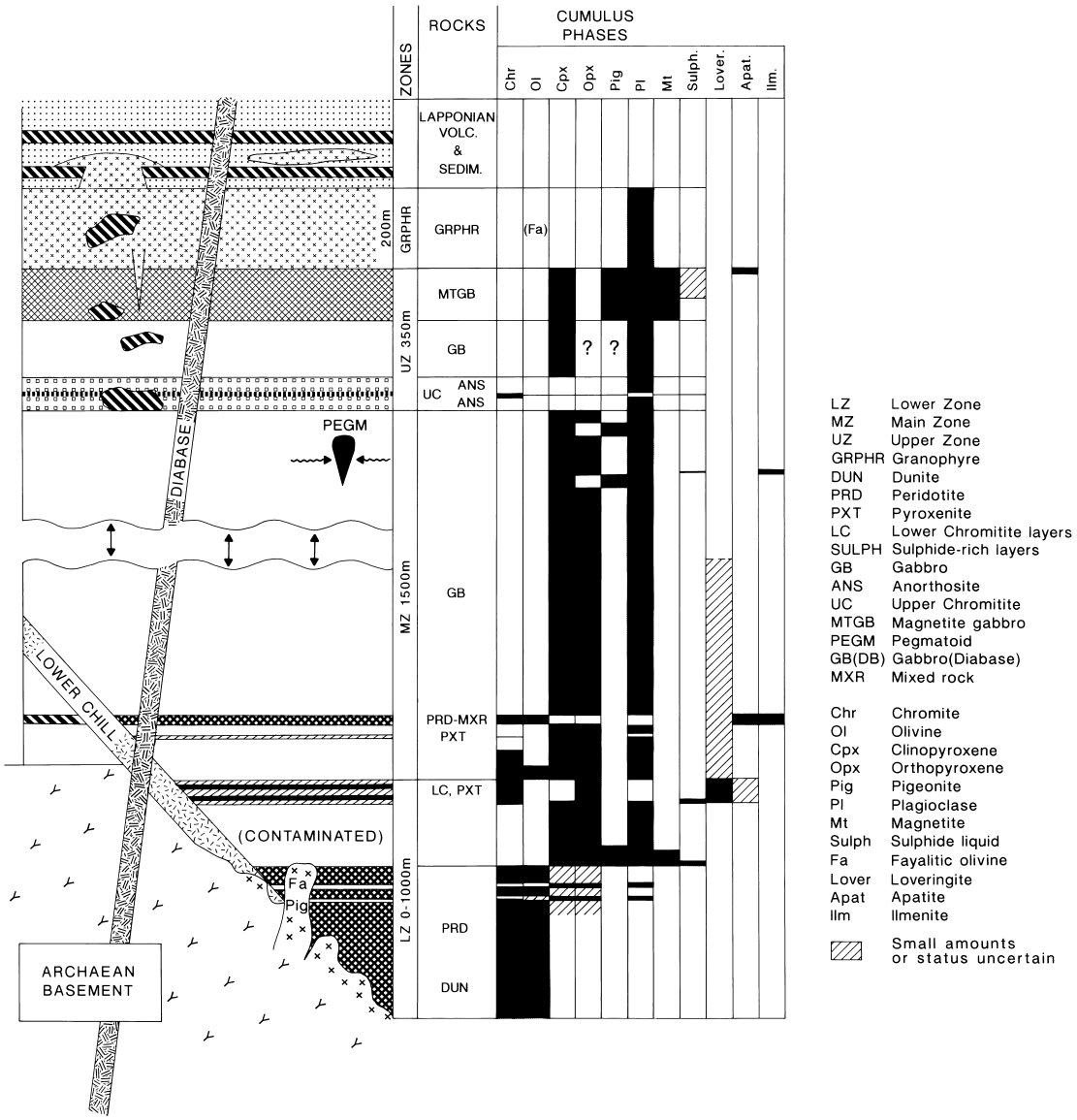

Fig. 16. Rock units and cumulate stratigraphy of the Koitelainen intrusion.

the case (e.g., Jackson, 1961; see also Wager & Brown, 1968). At Koitelainen the opposite is true: orthocumulates are more common in the lower part of the intrusion. Still more significant is that the intercumulus liquids of the ultramafic cumulates were of the low-density, low-temperature type, conceivably with a long liquid life and sensitive to compositional convection.

At a first, perfunctory glance the Koitelainen intrusion is a textbook example of a layered intrusion. In a single relatively thin layered se-

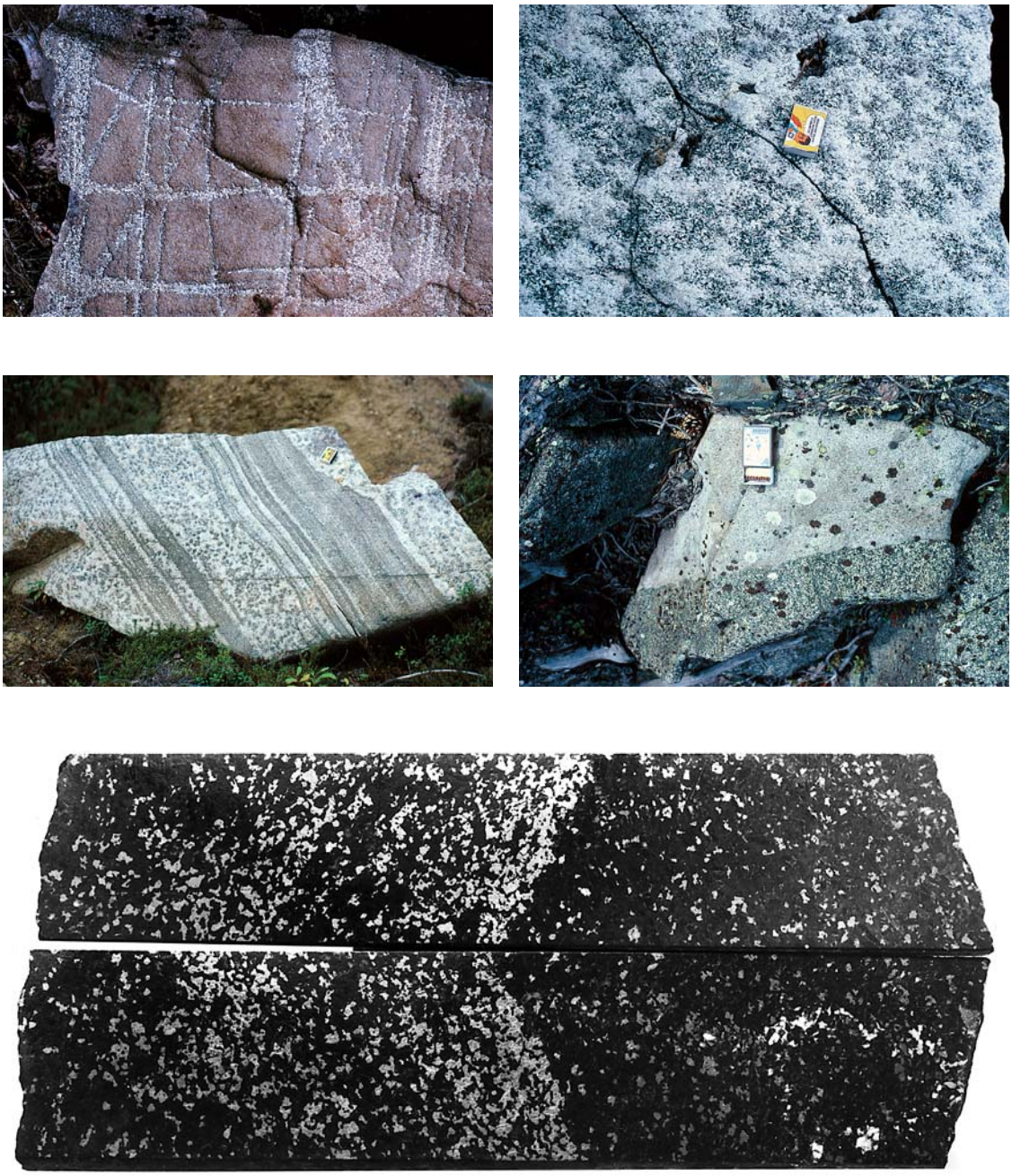

Fig. 17. Rocks of the Koitelainen intrusion. Upper left – Main Zone pyroxene-plagioclase cumulate, uralitized along fissures; upper right – mottled anorthosite of the UC sequence, Koitelaisenvosat; middle left – fine layering in mottled anorthosite, a few metres above the UC layer. Layers truncated by anorthosite pothole edge (right). The wavy upper surface of the mottled anorthosite layer in the middle suggests load cast bulging. Glacial boulder; middle right – contact between a vein of granophyre (light-coloured) and magnetite gabbro. The granophyre intrudes downwards into magnetite gabbro, and the vein can be traced for hundreds of metres, Iso Vaiskonselkä, southern part of the intrusion; lowermost – reverse grading in magnetite gabbro (stratigraphic top to the right, magnetite appears white). Koitelaisenvosat, DDH320/63.90 m. Drill core diameter 3 cm. The last photo by Erkki Halme, others by TM.

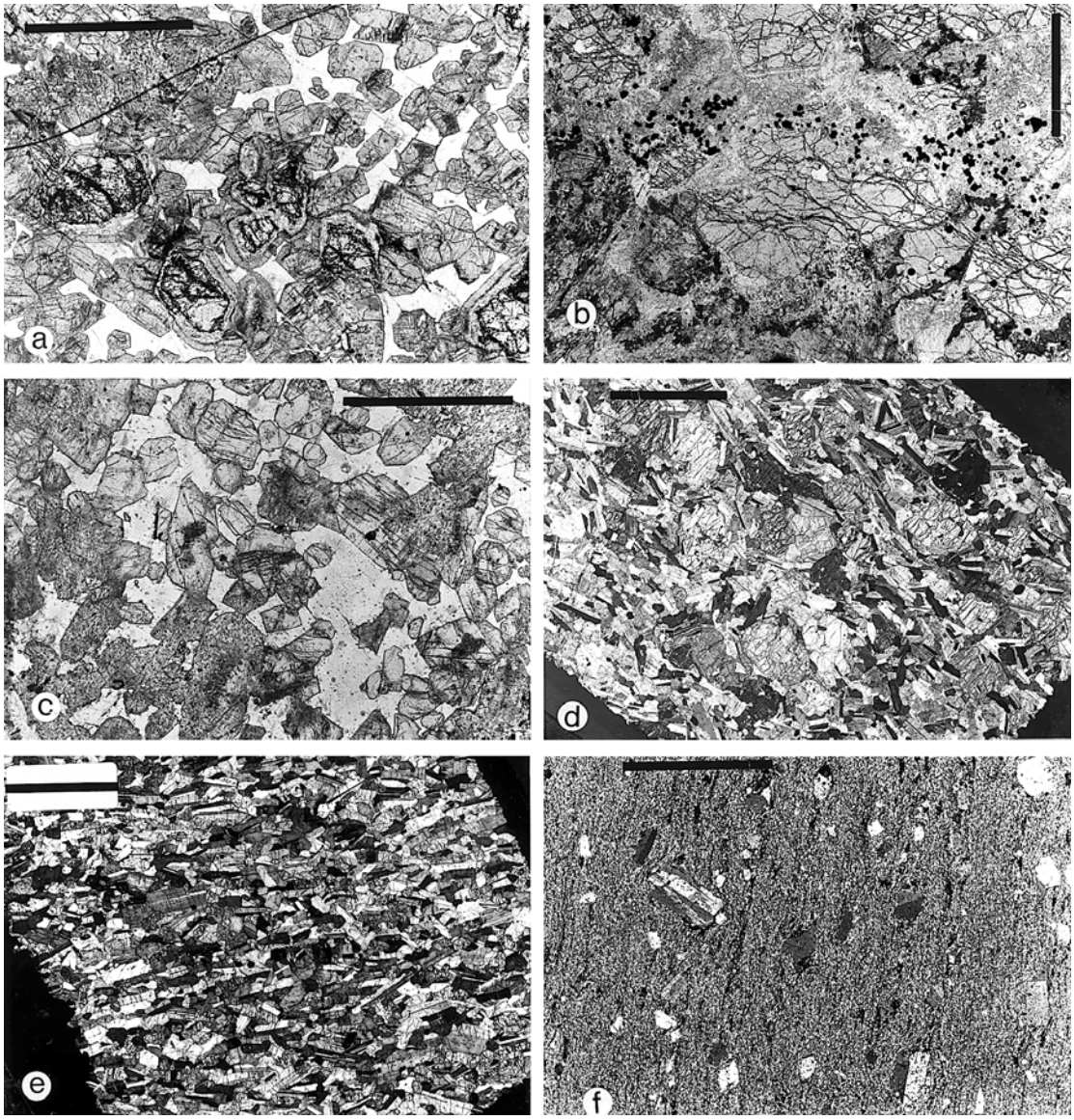

Fig. 18. Cumulates of the Koitelainen intrusion: Lower Zone cumulates from a to c, Main Zone cumulates d and e; f is granophyre. All photos by Erkki Halme. a – olivine-clinopyroxene cumulate, intercumulus oikocrysts of plagioclase. Parallel nicols. DDH302/12.25 m. Bar 2 mm; b – band of cumulus chromite in slightly altered olivine-pyroxene cumulate. Parallel nicols. DDH302/28.30 m. Bar = 1 mm; c – feldspathic pyroxene cumulate, with cumulus clinopyroxene and intercumulus oikocrysts of plagioclase. Parallel nicols. DDH302/7.95 m. Bar = 2 mm; d – plagioclase-clinopyroxene-orthopyroxene cumulate, plagioclase laths draped over orthopyroxene. Crossed nicols. Sample TM-74-27. Bar = 1 cm; e – planar lamination in plagioclase-pyroxene (clinopyroxene and inverted pigeonite) cumulate. Crossed nicols. Sample TM-74-29A. Bar = 5 mm; f – porphyritic granophyre, with primocrysts of plagioclase. Crossed nicols. Sample TM-78-51C. Bar = 5 mm.

quence phenomena familiar from other, well-known intrusions are to be seen: the gross features of layering, crystal fractionation, reversals and the selection of ore layers. It is important, however, to read the fine print, the petrologically revealing and often surprising de-

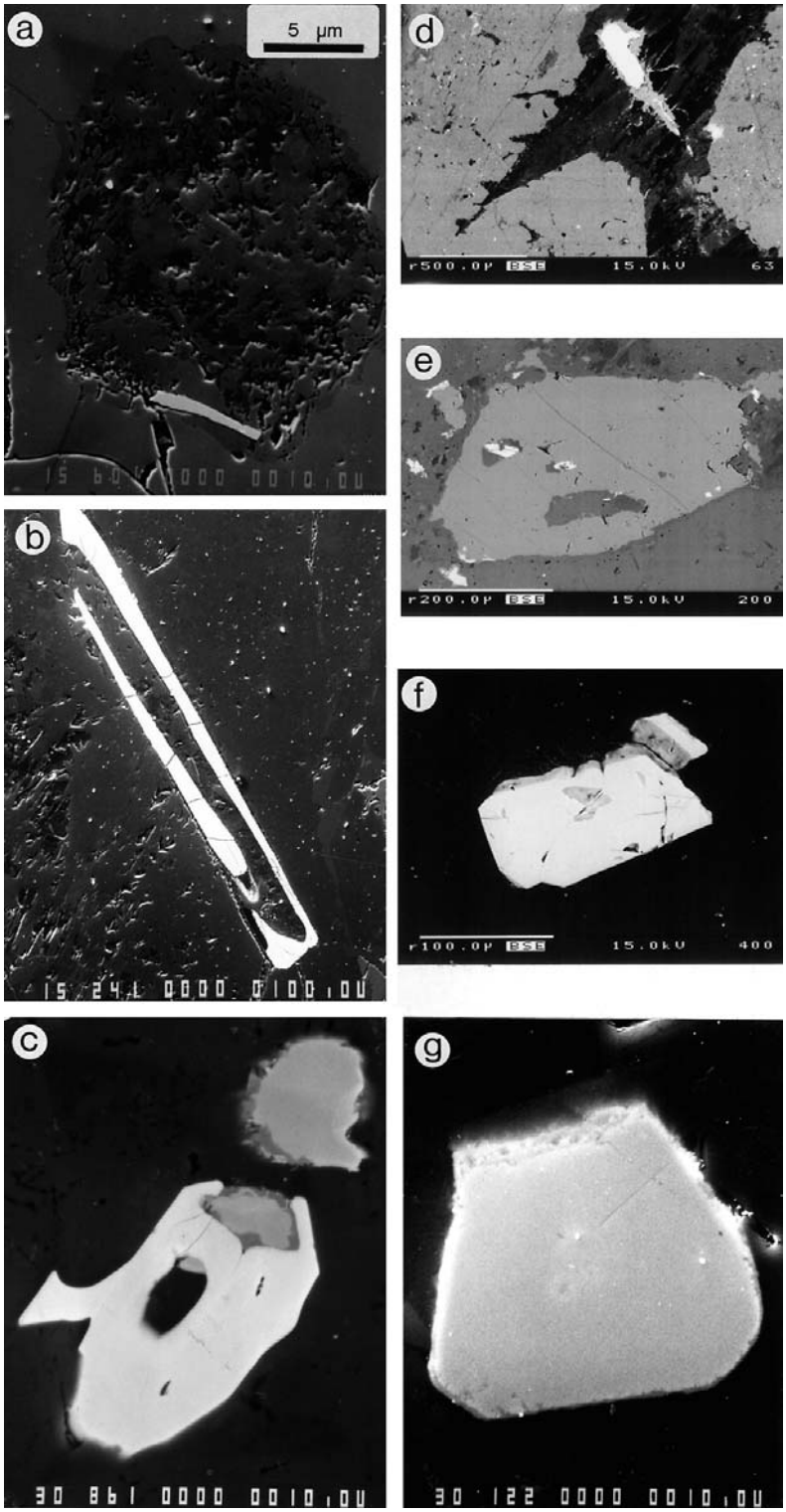

Fig. 19. SE and BE images of fossil melt inclusions and accessory minerals of the Koitelainen intrusion. Photos by Bo Johanson (a), Ragnar Törnroos (b,c,g) and Lassi Pakkanen (d–f).

a – SE image of a fine-grained (devitrified glass?) melt inclusion in olivine, with an ilmenite daughter crystal. Lower Zone olivine cumulate, DDH310/82.50 m; b – SE image of a skeletal zircon crystal, length ca 0.4 mm, mixed rock peridotite layer, Main Zone of the Koitelainen intrusion, DDH365/181.05 m); c – BE image of a zircon crystal (length 40 mu?) pinching a loveringite grain; another loveringite in top right corner; d – BE image of part of a large orthoclase perthite oikocryst (dark) in olivine-clinopyroxene cumulate. Grey – euhedral cumulus clinopyroxene, white – ilmenite. Lower Zone, DDH308/28.00 m; e – BE image of a big cumulus crystal of chlor-fluorapatite, with allanite inclusions, the same sample as in d; f – BE image of zircon crystals in mixed rock peridotite layer, Main Zone of the Koitelainen intrusion, DDH365/190.55 m; g – SE image of a baddeleyite crystal (50 mu?), with a thin zircon rim, in mixed rock peridotite, DDH365/191.00 m.

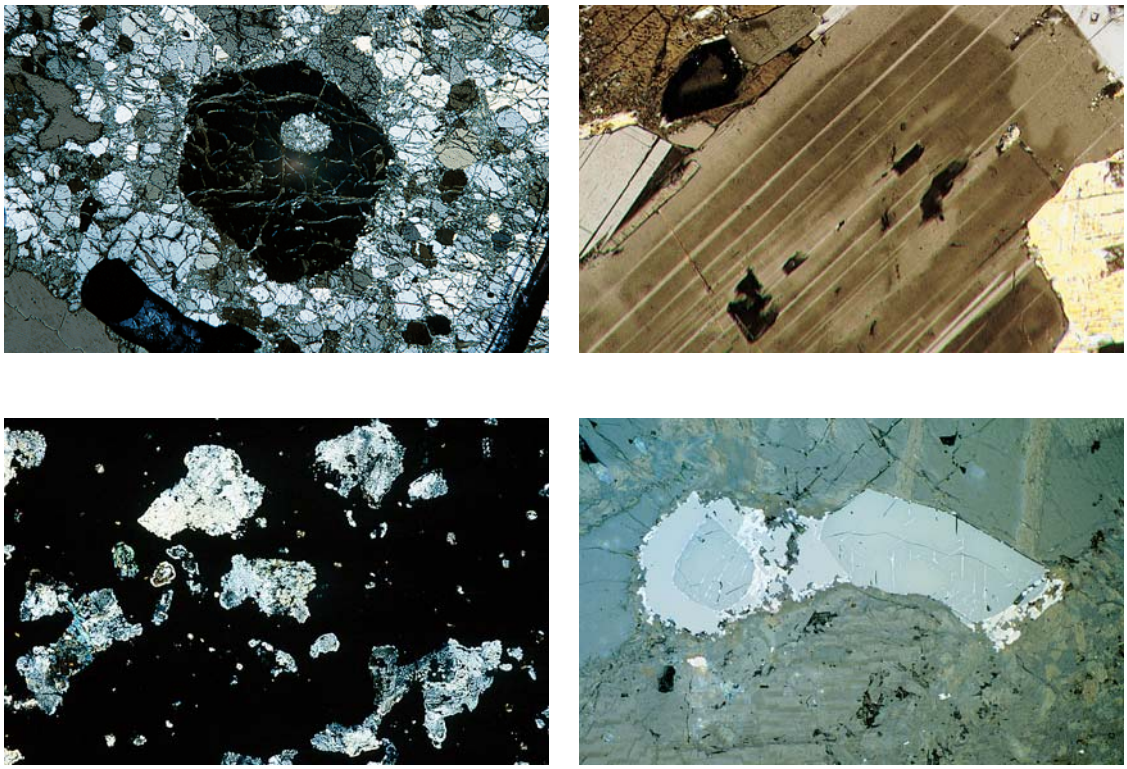

Fig. 20. Microphotographs of contaminant inclusions and loveringite from the Koitelainen intrusion. Photos by Jari Väätäinen. Upper left – olivine crystal (diameter 3 mm) with a fossil melt inclusion. Olivine(-chromite) cumulate, Lower Zone, DDH309/258.05 m. Crossed nicols; upper right – angular inclusions of potassium feldspar (black) in the core of a cumulus plagioclase crystal. Darker shades in plagioclase are relatively rich in anorthite, lighter shades (core and marginal zone) are more albitic. From a plagioclase-pyroxene(-olivine) interlayer in the Lower Zone, DDH310/19.55 m. Crossed nicols. Width of photo 0.8 mm; lower left – salic granophyre inclusions (melt droplets) in massive sulphides. The layer of massive sulphides is overlain by disseminated sulphides in pyroxene cumulate. Upper part of the Lower Zone, DDH360/139.03 m. Crossed nicols. Width of photo 1.6 cm; lower right – cumulus chromite crystals partially mantled by loveringite. The ilmenite rim of loveringite is altered to rutile. Feldspathic pyroxene cumulate (cumulus orthopyroxene and clinopyroxene), with primary phlogopite and intercumulus potassium feldspar. DDH363/329.87 m. Reflected light. Width of photo 0.8 mm.

tails. I have found many of these, such as fossil melt inclusions in olivine, in the Keivitsa and Kemi intrusions (Mutanen, 1989b). Without doubt they are common in other intrusions, too, if only looked for.

All standard types of layering and corresponding layer contacts occur, e.g., phase layering, isomodal layering, ratio layering, size layering, cryptic layering, igneous lamination (planar lamination) and mineral graded layers (for terminology, see e.g., Jackson, 1967, 1970; Wadsworth, 1973). Small-scale layering has been noted in anorthosites (Fig. 17), chromitites and magnetite gabbro, possibly caused by seismic longitudinal waves traversing a stagnant, supersaturated liquid (see Hoffer, 1966). Inverse grading occurs in magnetite gabbro (Fig. 17). Igneous lamination is present in all gabbros of the MZ and UZ, but it has not been observed in gabbroic interlayers of the LZ.

Formally the gabbroic rocks are mesocumulates (gabbroic rocks) and orthocumulates. Only those rocks whose intercumulus compo-

sition deviates conspicuously from the mafic residual magma (pyroxene cumulates, chromitites) show orthocumulate textures. Typical adcumulates have never been found.

The lower part of **the Lower Zone** (LZ) consists of peridotites, with two pyroxenite-gabbro interlayers in the upper part. The peridotites are olivine-chromite cumulates with varying amounts of the following primary minerals: orthopyroxene, clinopyroxene and intercumulus plagioclase, potassium feldspar (orthoclase perthite) and minor sulphides, primary phlogopite, brown primary hornblende, chlorhornblende, chlorapatite and fluorapatite, ilmenite, zircon, allanite, graphite, zirconolite(?), perrierite(?) and an unknown Ti-Th-Fe(-REE-P) silicate.

The lowermost LZ cumulates are either orthocumulates or mesocumulates. In general the pyroxenes seem to be true postcumulus phases (intercumulus phases or formed by reaction between olivine and intercumulus liquid). Upwards, the grain sizes and the amount of pyroxenes increase to the degree that they can be thought to have partly formed by reaction before settling, and should thus be regarded as cumulus phases. Many orders of crystallization and peritectic reactions are observed. The ubiquitous occurrence of smooth, roundish inclusions of clinopyroxene in olivine suggests that the former started to crystallize before the latter, perhaps together with chromite. In general, the lowermost rocks are ol-crt cumulates (possibly with cpx as a transient early phase), followed by postcumulus reaction-opx, intercumulus cpx and pl; higher up, the general evolution of cumulus orders and assemblages is crt-ol-opx-cpx (Fig. 18a–c).

I have not undertaken a systematic study of the composition of cumulus minerals. One microprobe determination on the basal peridotite unit gave an olivine composition of $Fo_{80.6}$. Olivines analysed from one DDH through 70 m of the topmost peridotite layers vary (upwards; corresponding mg# values for coexisting opx and cpx are in parentheses): $Fo_{80.6}$ –> $Fo_{81.4}$ (cpx 91.4) –> $Fo_{82.3}$ (opx 82.0, cpx 81.1) –> $Fo_{82.8}$ (cpx 84.9) –> $Fo_{71.8}$ (opx 75.0–77.1, cpx 82.2).

Intercumulus ilmenite is surprisingly common in peridotitic cumulates, much more so than in the MZ gabbros. Several zircon crystals in orthopyroxene oikocrysts have been observed.

Both chlorapatite and fluorapatite occur in intercumulus spaces (for compositions, see anal. 4–5, Table 8), even existing together in one and the same thin section. The fluorapatites (atomic Cl/Cl+F ratio 0.28–0.38) have high Ce-La and contain allanite inclusions (Fig. 19e). The chlorhornblende (see Table 9) is rather rich in Mg, not like the dashkesanite (potassian hastingsite) of the Keivitsa intrusion.

Orthoclase (checked in several cases by microprobe EDS) is a common intercumulus mineral, even in the lowermost olivine-rich cumulates, and mostly altered to secondary phlogopite. In the uppermost peridotites orthoclase-perthite occurs as large (>2 cm^2) oikocrysts enclosing euhedral clinopyroxene (Fig. 19d). I suspect that this phenomenon is in fact not so exceptional after all, as orthoclase is too easily misidentified as plagioclase. The Merensky Reef contains locally up to 10.6% orthoclase (Vermaak & Hendriks, 1976).

There are gabbroic cumulate interlayers (see Fig. 16) in the upper part of the peridotite unit that grade downwards via pyroxene cumulates to peridotites. Sometimes olivine occurs as a cumulus phase in gabbro. The passing precipitation of cumulus plagioclase in ultramafic cumulates is uncommon, yet probably more common than reported. Even in Bushveld, contrary to general belief, cumulus plagioclase occurs deep in the Lower Zone (Cameron & Desborough, 1969; Cameron, 1978).

Two peculiar features deserve mention. First, graphite occurs as tiny spherical aggregates; second, the cumulus plagioclase crystals are inversely zoned, with relatively sodic cores containing angular inclusions of potassium

feldspar (Fig. 20). Similar potassium feldspar inclusions in plagioclase have been described from the Stillwater intrusion, where the potassium enrichment in magma is ascribed to adjacent crustal xenoliths (Barker, 1975). Overgrowth of more calcic plagioclase on sodic, often embayed, corroded or patchy-zoned cores, has been described from intrusions and extrusive rocks (e.g., Fenner, 1926; Homma, 1932; Kuno, 1950; Lebedev, 1962b; Maaløe, 1976; Eichelberger & Gooley, 1977; Dungan & Rhodes, 1978; Hibbard, 1981; Nickel, 1981; Nielsen & Dungan, 1985). Most of the above authors ascribe the phenomenon to magma mixing. The sodic cores grew in a relatively acid, alkali-rich magma before being brought into a mafic magma; that the cores were not entirely dissolved is attributed, first, to the sluggish dissolution kinetics and second, to the fact that the sodic feldspar had originally crystallized from a Supercooled melt (Wager, 1959; Morse, 1988). I agree with these explanations: the plagioclase cores grew in an environment very rich in alkalies, not from the overlying resident magma. I will return to this subject soon.

Both fossil melt inclusions and magma inclusions occur in olivine and orthopyroxene. Melt inclusions are ubiquitous in olivine (see Fig. 19a, Fig. 20, upper left). Sometimes several inclusions occur in one crystal ("Swiss cheese" olivine). The smallest inclusions (ca < 20 mu) are very fine-grained; they most probably remained glassy until regional metamorphism (see Roedder & Weiblen, 1971) but bigger inclusions (up to 200 mu or more) crystallized from the walls inwards, in due order (see Fig. 46). Ilmenite is an easily identifiable daughter mineral (Fig. 19a). Chlorapatite is common as a daughter phase in olivine melt inclusions at Koitelainen, Keivitsa and Kemi intrusions (Mutanen, 1989b).

Magma inclusions in olivine contain sulphide beads. Sometimes the inclusions are crowded with chromite crystals. This indicates crystallization of olivine in dense chromite suspension and hints at the possibility of early chromite accumulation at the base of the olivine cumulate basin. Magma inclusions in orthopyroxene contain zirconolite, carbonate and big occluded crystals of chlorapatite.

The composition of the inclusions in olivine is quite strange (Table 5), but only if one imagines that the olivine grew from, and trapped samples of, the overlying resident main magma. Because of a possible reaction between the trapped liquid and host olivine (see Fig. 46a) and the growth of small amounts of olivine on inclusion walls (Roedder, 1984) the present composition of the inclusion is not exactly that of a trapped liquid, but is enriched in components rejected by olivine. It is, however, a well known and much utilized fact that glass inclusions in olivine and other phenocrysts in lavas approximate the melt composition surprisingly well (e.g., Roedder, 1979) and, when analysed in a series along fractionation, yield a well defined liquid line of descent. Observations (Lu et al., 1995) do not support significant boundary layer buil-up of rejected components, like K_2O. The melt inclusions in the Koitelainen olivine, with end members of a potassic-calcic (potassic in the following) melt and siliceous-sodic (sodic in the following) melt, represent trapped liquids of a heterogeneous, hybrid melt of a mingling-mixing zone between an anatectic salic crustal melt and a mafic melt, most probably at the roof. The potassic melt represents the mafic magma which gained K_2O from the salic melt by selective diffusion (Watson, 1982); the sodic melt represents the salic melt which lost potassium to, and gained sodium from, the mafic magma (op. cit.). The breeding magma was also rich in Cl, as shown by the high Cl in the potassic inclusions (Table 5) and by the occurrence of chlorapatite daughter crystals.

Inclusions too alkali-rich (most commonly potassic) or otherwise not on a par with the conceived breeding magma are known from olivines (Predovskii & Zhangurov, 1968; Glazunov et al., 1973: Ludden, 1978; Fenogenov &

Emelyanenko, 1980; Lorand & Ceuleneer, 1989) and from ilmenite (Weiblen, cited by Roedder, 1979). Alkalic inclusions are known to occur in chromite both in tholeiitic intrusions (McDonald, 1965; Irvine, 1974; Alapieti. 1982; Alapieti et al., 1989) and in ophiolitic chromites (e.g., Talkington et al., 1984). The chromites and chromitites of Akanvaara and Koitelainen represent an extreme case of alkali enrichment: both the melt inclusions and the matrix are very potassic. The subject is discussed in more detail later.

Ascending the stratigraphy we find right above the peridotites a peculiar and seemingly incompatible association of olivine pyroxenites, sulphide-disseminated pyroxene cumulates and pyroxenites rich in quartz, potassium feldspar, biotite and fluorapatite. An unknown Ti-Th-Fe(-REE-P) silicate with inclusions of perrierite(?) occurs in the intercumulus of a sulphide-disseminated pyroxene cumulate. The sulphides are very low in Ni and show only slightly elevated PGE-Au concentrations (see Fig. 27c); in fact, they are quite similar to the false ore sulphides of Keivitsa. The pyroxene cumulates are closely associated with, and grade into, alkali-rich quartz gabbros containing inverted pigeonite, cumulus magnetite and, interestingly, solitary chromite euhedra. The latter rocks are often fine-grained, resembling chilled microgabbros.

Here we find the unholy cohabitation of magnesian olivine and intercumulus quartz (0.1 mm apart at the closest), encountered later again above the Lower Chromitite layers and also in the Merensky Reef, Bushveld (Mutanen, 1989b), and recently at Keivitsa, too. This disequilibrium assemblage, which was brought about by magma currents from different parts of the chamber, was incompletely mingled before settling. Disequilibrium phenocryst assemblages of quartz and olivine are known from mixed lavas (Sakuyama, 1981). A peculiar feature found in mixed lavas is the reverse peritectic resoption of orthopyroxene to olivine and augite (Kuno, 1950). Similar resorption of orthopyroxene (to clinopyroxene) is common in pyroxene cumulates in the upper LZ.

Olivine and orthopyroxene often occur in these rocks as separate crystals, apparently without a reaction relationship, suggesting coprecipitation of the minerals. But the pressure needed, 5.4 kb, (Boyd et al., 1964), corresponding to a depth of ca 18 km, is certainly too high for the basal part of the Koitelainen intrusion, and also for the Keivitsa intrusion, where olivine and orthopyroxene co-exist similarly. I think that this is another case of bastard cumulate assemblage, of minerals bred separately but later mingled together (see also Jackson, 1961).

The unexpectedly early appearance of inverted pigeonite may be due to chilling (Wager & Brown, 1968), but here it suggest contamination by exotic iron, such as has been noted or suspected elsewhere, for instance, in Dore Lake Complex (Allard, 1986), Stillwater (Barker, 1975; Page, 1979; Raedeke & McCallum, 1984), Duluth Complex (Tyson & Chang, 1978) and Platreef area, Bushveld (Buchanan & Rouse, 1984). The occurrence of cumulus magnetite indicates that the contaminant increased the oxidation state of the local system.

This local system is spatially intimately associated with the quartz monzonite diapirs (see Fig. 21). The quartz monzonite magma stocks (diapirs) intruding the LZ cumulates are manifestations of large-scale early melting of the floor rocks (labelled monzonite diapirs on the geological map, Appendix 3; for quartz monzonite compositions, see anal. 5–11, Table 3). Their U-Pb zircon age, 2434 Ma (Olavi Kouvo, letter, May 19th, 1994), is the same as the age of the intrusion. The quartz monzonite contains finer-grained autoliths of about the same composition. Dendritic growth of plagioclase and olivine(?) suggests superheating and subsequent supercooling of the quartz monzonite magma. Against the overlying cumulates the stocks have a blanket of chilled rocks (internal chill) with abundant sulphides

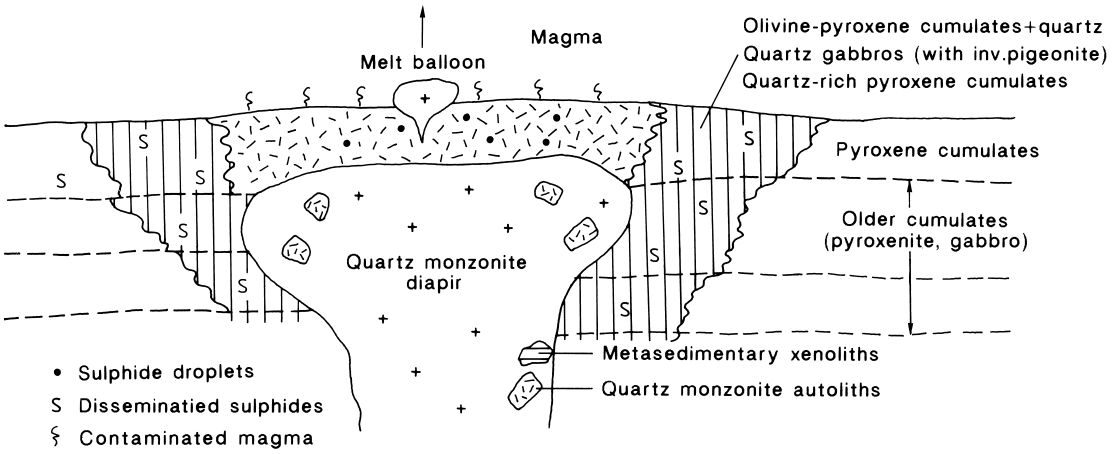

Fig. 21. Schematic cross-section of the quartz-monzonite diapirs, lower part of the Koitelainen intrusion. See text.

as round droplets and dissemination. Closely associated with the stocks, at about the level of their tops, are pyroxene cumulates, olivine-pyroxene cumulates and pigeonite gabbros, all with disseminated sulphides and intercumulus quartz. The acid magma withstood superheating by exchanging components with the intercumulus liquid and the main magma, thus acquiring its present quartz monzonitic composition. All observations indicate that the magma rose through hot cumulates and reached the main magma. Mixing of the magmas resulted in rapid crystallization and the introduction of salic contaminants into the main magma. Portions of acid magma possibly escaped to the roof as "melt balloons".

Similar "rheomorphic" igneous bodies occur in the lower parts of the Stillwater and Bushveld intrusions (see Page, 1977; Willemse & Viljoen, 1970). The composition of the quartz monzonites of the Koitelainen intrusion are very similar to those of the granofelses and intrusive palingenetic quartz monzonites of Bushveld (see Willemse & Viljoen, 1970). At Stillwater the quartz monzonite bodies intruding the lowermost cumulates are of the same age as the intrusion (see Lambert et al., 1985). Veins, segregations and roundish bodies of anatectic magma occur at the lower contact of the Insizwa complex (Lightfoot et al., 1984). In a trip to the Penikat intrusion led by Vesa Perttunen (GSF) in 1981 I was shown a salic spherical body (ca 50 cm across) near the base of the intrusion. I interpret this as having been a buoyant megadroplet of floor melt which was frozen in the ultramafic cumulate during its ascent. The U-Pb zircon age of the rock, ca 2440 Ma (Olavi Kouvo, private comm.), indicates that there is no inherited basement zircon, and the zircon crystallized from the anatectic melt (see Mezger & Krogstad, 1997).

Stratigraphically, the contaminated cumulates are located at about the level where the tops of the diapirs touch the magma chamber. The situation strongly suggests that the diapirs were feeding the contaminants to the overlying magma, which mixed rapidly with the convecting resident magma. The outcome was the formation of miscellaneous, variously contaminated cumulates and the occasional chilling of the mafic magma.

It is here that we encounter the first tenuous bands of disseminated chromite (Fig. 18b). I suggested back in 1973 that the magma system was prone to incursion into the chromite phase field. True chromitite layers appear higher up,

among the orthopyroxene cumulate unit (see Fig. 16).

A unit of heavily contaminated gabbros with apparent reverse fractionation lies between the peridotite unit and the overlying uppermost LZ unit, the pyroxenite. In the eastern Kiviaapa area the contaminated gabbros (with pigeonite and cumulus magnetite) grade upwards with decreasing contamination into pyroxene gabbros and low-Ti microgabbros; in the latter, the plagioclase laths exhibit igneous lamination. Relics of a pre-Koitelainen intrusion have been intersected by drilling below laminated microgabbros (see Fig. 5, Mutanen, 1989b). Immediately below the pyroxenite unit olivine visits as a cumulus mineral.

The pyroxenite unit hosts the Lower Chromitite (LC) layers. The pyroxenites consist of opx-crt cumulates, with intercumulus plagioclase, clinopyroxene, primary phlogopite (less often primary hornblende), potassium feldspar and quartz. Clinopyroxene mantles orthopyroxene, suggesting a reverse peritectic (?) reaction. Both pyroxenes contain inclusions of primary phlogopite and hornblende, particularly when the intercumulus is rich in quartz and potassium feldspar.

Ubiquitous accessory minerals are chlorapatite and fluorapatite (sometimes as composite chlorapatite-fluorapatite grains), and zircon. Loveringite is also ubiquitous, often occurring as fair-sized, roundish cumulus crystals (Fig. 20, compositions in Table 2; see also Tarkian & Mutanen, 1987). Loveringite is usually mantled by Mn-ilmenite, which contains chromite inclusions. The customary Mn-ilmenite mantle of loveringite crystals has a thin, almost continuous rim of zircon. Bigger zircon crystals embrace loveringite (Fig. 20). Tarkian and Mutanen (op. cit.) suggested that loveringite, like armalcolite in lunar basalts, reacted with the FeO + MnO in residual liquid, producing Mn-ilmenite, zircon and chromite (see also: Lindsley et al., 1974).

The LC layers are treated later in more detail. The chromitites lack sulphides, but these sometimes occur close to chromitite layers. A case of special interest is in DDH360, where sulphide-disseminated rock grades rapidly (in about 1 metre) downwards into a layer of massive pyrrhotite. The pyrrhotite contains acid blebs with beautiful granophyric textures (Fig. 20). As the main magma was still far from true (terminal) sulphide saturation, this must be a choice example of transient sulphide saturation. The sulphide liquid droplets had separated from a contaminated magma portion and were escorted along their trajectories by salic liquid dragged along in the density flow. The salic liquid, now preserved as blebs in the layer of massive sulphides, protected the sulphide droplets from re-solution. I consider this one of the key observations of Doppelgänger phase saturation (premature phase separation, see Mutanen, 1992, p. 26).

In general there are no ol-opx cumulates, with ol and opx mixed in all proportions, nor similarly mixed ol-crt cumulates as at Stillwater (Jackson, 1961); instead, at Koitelainen chromite and orthopyroxene form density-graded cumulates. Such grading (Fig. 23) which clearly does not represent hydraulic grading, seems to be a characteristic feature of both the Akanvaara and Koitelainen intrusions. Differences in the ultramafic cumulus assemblages suggest some fundamental features (e.g., silica activity, extent and timing of early selective contamination) of the early magma system.

The Main Zone (MZ) consists chiefly of gabbroic cumulates (pl+opx+cpx; Figs 17, 18d). In the lowermost part there are interlayers of feldspathic pyroxene cumulates. As in the lower MZ of the Akanvaara intrusion, there are some rare places where olivine and plagioclase crystallized as cumulus minerals (troctolites). Cumulus olivine is found together with intercumulus quartz and big crystals of apatite and loveringite. Chromite and loveringite continued to crystallize high into the gabbros, but in decreasing amounts. In the analogous Bird River intrusion, the chromite extended its crystallization for tens of metres into the gabbroic cumulates above the chromi-

tites (Bateman, 1943). At Koitelainen loveringite has been found high in the MZ. When in intercumulus quartz it lacks the ilmenite mantle, suggesting that the quartz inhibited the exchange of components between loveringite and intercumulus liquid.

In the lower part of the MZ two prominent reversals interrupt the cumulate succession. About 250 m above the base of the zone there is a 2.5-m-thick layer of feldspathic pyroxenite (opx-cpx cumulate), with a 5-cm-thick chromitite layer at the base. The chromite is rather aluminous and, curiously, the most Mg-rich among the Koitelainen chromitites (Table 4). Just below the chromitite the cumulus plagioclase is calcic (An_{78}), the mg# of the clinopyroxene is 0.87. In the pyroxenite overlying the chromitite the mg# for orthopyroxene is 0.78, for clinopyroxene 0.83.

About 60 m above this pyroxenite, there is a 13-m-thick layer of peridotite with patches of coarse feldspathic material. Called the mixed rock peridotite (mixed rock in the following), it is underlain by 4 m of pyroxene cumulates. The salic patches contain large euhedral crystals of ilmenite and skeletal crystals of chlorapatite; the ultramafic rock has cumulus olivine, chromite and chlorapatite. Chromites and chlorapatites contain potassic melt inclusions. The basal pyroxenitic layer and the alternating cumulate layers (px, px-pl, pl) below it are anomalous in Pt and Pd (Fig. 22). This mixed rock sequence is a relation (although a poor one) of the Stillwater mixed rock and the associated PGE-rich J-M reef (Bow et al., 1982).

That contamination contributed to the mixed rock reversal is clearly attested to by the range of accessory minerals: chlorapatite (in crystals up to 6 mm in length), zircon (Fig. 19b, f), baddeleyite (Fig. 19g), loveringite, thorite(?) and galena. Such minerals would hardly be expected were the peridotite the result of a new pulse of primitive magma. The peridotite is enriched in both Zn and Pb compared with the background values in gabbroic cumulates (Fig. 22). There are no primary sulphides to explain the Zn-Pb anomaly. I interpret the layer as having formed through the combined effects of selective alkali contamination and salic contamination. The crystals formed in the contaminated environment (e.g., olivine, chromite, ilmenite, baddeleyite, zircon, chlorapatite) deposited from a density flow. The sodic (feldspathic) portions represent the salic contaminant melt, modified by selective diffusion of alkalies in the emulsion (Watson, 1982; this topic will be discussed later in this book). As in melt inclusions and in contaminated PGE-anomalous rocks higher up in the MZ (see later), ilmenite was a liquidus phase in the salic, sodic liquid (see Green & Pearson, 1986). Potassic matter in melt and matrix represent samples of the K_2O-enriched magma which bred the olivine.

Thin layers of feldspathic pyroxene cumulates occur about 13 m above the mixed rock sequence; precipitation of minor chromite and olivine continued in gabbroic cumulates above the mixed rock, that of olivine for ca 30 m. A plagioclase cumulate layer (0.3 m) occurs 24 m above the mixed rock.

From the mixed rock sequence up to the first reversal above the first pigeonite gabbro unit (see Appendix 3) the MZ cumulates are well preserved and well exposed in the Koitelainen fell area. As there are no direct observations of the dip of layering, the thickness of the MZ as indicated in Fig. 16 is only an educated guess.

The gabbros are very monotonous, laminated pl-cpx-opx cumulates (Fig. 18d, e). The adcumulus growth of cpx is poikilitic; in opx oikocrystic enlargements enclose small plagioclase laths. Upwards, approaching the pigeonite gabbro ("ferrogabbro"), there are pl-opx cumulates with intercumulus or poikilitic cpx (poikilitic norites). Regular intercumulus minerals in MZ gabbros are quartz, potassium feldspar, primary biotite and minor amounts of ilmenite and fluorapatite. Intercumulus magnetite occurs in the uppermost MZ gabbros. Up to the lower pigeonite gabbro unit small grains of loveringite are present in most of the thin

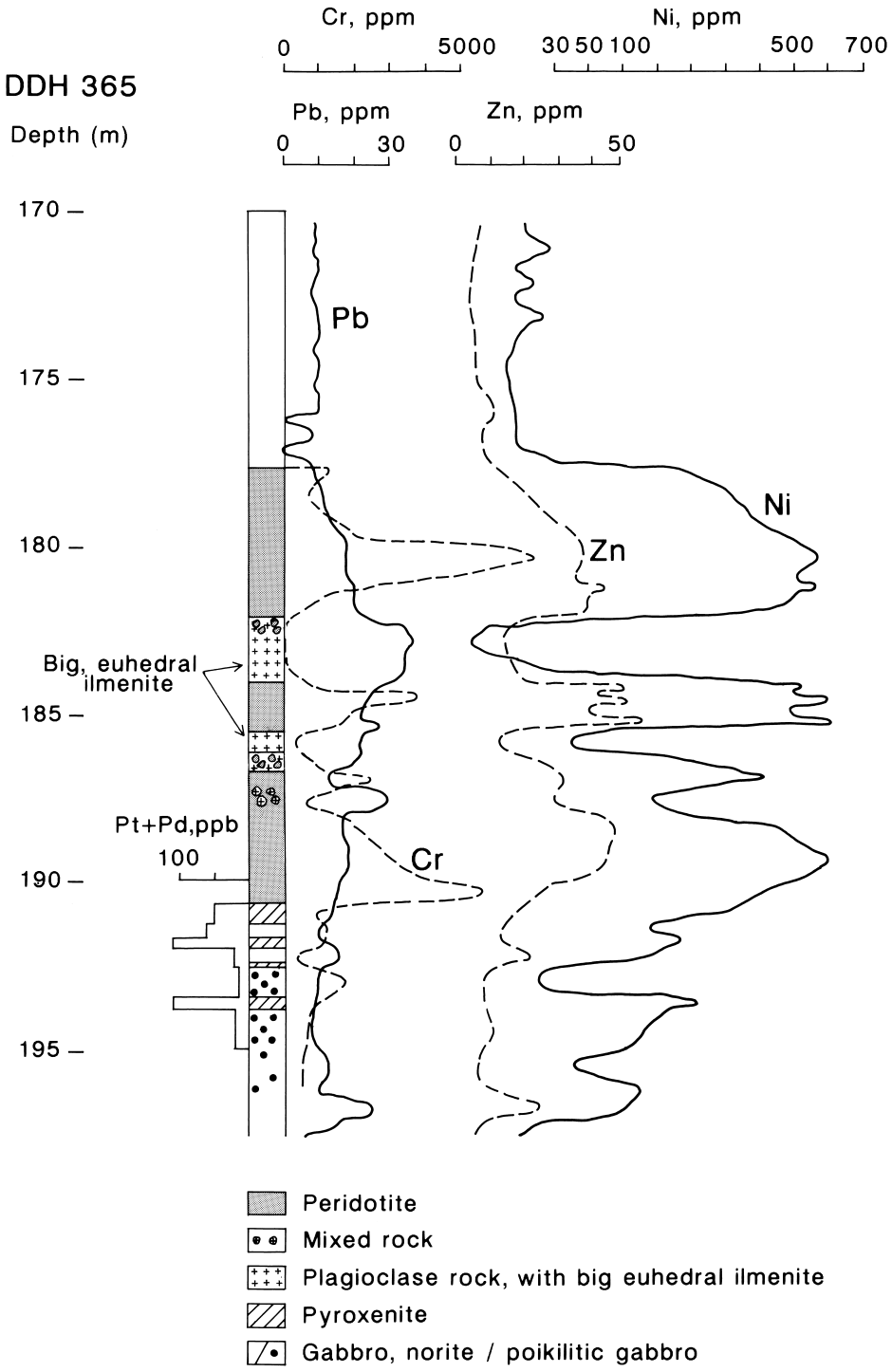

Fig. 22. Columnar section of the mixed rock peridotite layer (DDH365), showing variations in Pt+Pd, Cr, Ni, Pb and Zn. Note that the scale for Ni is not linear. Koitelainen.

sections studied. The MZ cumulates are very similar to those of the Main Zone of the Bushveld Complex, where the intercumulus is rich in quartz (up to 6 vol%) and granophyre (Groeneveld, 1970).

Formally, the MZ gabbros are mesocumulates. Any adcumulus growth seen can be attributed to simple extension growth of pyroxenes from trapped mafic liquid (Cameron, 1969), not the delicate (and all too slow) process of diffusion of components from overlying magma.

The cores of the opx oikocrysts probably represent original primocrysts (see Cameron, 1969), but it is even possible that the oikocrysts settled as glomerophyric aggregates of opx and pl (e.g., Hess, 1960; Jackson, 1961; Wager & Brown, 1968; Olmsted, 1979).

In the upper MZ the Ca-poor pyroxene is inverted pigeonite (Fig. 18e), with one or possibly two reversals back to opx (see map, Appendix 3). Unlike other MZ gabbros these do not contain salic intercumulus material. In Bushveld, too, the salic intercumulus disappears in the Upper Zone (Groeneveld, 1970). The pigeonite crystallized as a cumulus mineral together with pl and cpx. The cumulus crystals were later (probably at or after inversion) recrystallized (annealed ?) into big, optically continuous crystal networks.

In Bushveld inverted pigeonite appears soon above the Merensky Unit (Willemse, 1969a, von Gruenewaldt, 1973; Coertze, 1974; Mitchell, 1990). Likewise, in the Keivitsa intrusion pigeonite began crystallizing shortly above ultramafic cumulates. The relative level of appearance of pigeonite (at about En_{30}) is a good measure of fractionation of residual liquid, but the differences – early in Bushveld and Keivitsa intrusions, late in the Koitelainen intrusion in relation to uppermost ultramafic cumulates – craves explanation. Pyroxene fractionation is the most effective means to increase the mg# in residual liquid; accordingly, in intrusions with vast separation of pyroxenes (Bushveld, Keivitsa) the decrease in mg# needed for pigeonite crystallization is attained earlier than when olivine is a major fractionating phase, as in the Stillwater (Hess, 1960) and Koitelainen intrusions.

The pigeonite gabbro unit is topped by a reversal back to "normal" pyroxene. The reversal itself is not exposed; the nearest outcrop above consists of contaminated orthopyroxene gabbro (cumulus pl+opx, intercumulus cpx). The rocks contain spots of quartz and biotite and coarse salic and ultramafic pockets. Very small amounts of stringer and disseminated copper-rich sulphides are encountered in this outcrop. The rock exhibits anomalous to high PGE-Au (Fig. 25c), but these have no direct relation to sulphides (for more details, see Mutanen, 1989b). These rocks contain independent, cumulus-like ilmenite, a further indication of salic contamination (Green & Pearson, 1986). Further north, at about the level of this reversal, thin layers of anorthosite (pl cumulate) with poikilitic cpx have been found.

From the pigeonite reversal to the Upper Zone (UZ) the rocks are poorly exposed. Drill cores show that from the second pigeonite gabbro unit upwards the normal pl-cpx-opx cumulates grade, with increasing amounts of poikilitic opx, into pl-cpx cumulates with big "snowball" oikocrysts of opx enclosing small pl laths. Higher up, small primocryst cores become visible in opx oikocrysts.

I have not yet any systematic data of the composition of the cumulus minerals of the MZ. I have made, however, 16 accurate optical determinations of plagioclase compositions (symmetric sections normal to (010) cleavage). These show that in all pl-cpx-opx cumulates of the MZ, plagioclase has a sodic core, a more calcic middle zone and again a more sodic rim, but in pigeonite gabbros the zoning is normal. The compositions from core to rim in lower and middle MZ are (in An mol%): (60–63) –> (70–68) –> (63–60) –> 58 –> 53; in poikilitic norite: 62 –> (68–70) –> 65 –> 61 –> (58–54); in gabbro below the lower pigeonite gabbro unit: (66–63) –> (59–57) –> (55–56); in pi-

geonite gabbro: 55 –> 47; and in MZ gabbro above the lower pigeonite unit: 61 –> 68 –> 61. Thus, inverse zoning occurs in rocks with salic intercumulus but normal zoning in rocks without it. From this I conclude that the sodic cores crystallized near the roof in a slightly contaminated magma, the calcic middle zone on them from the relatively uncontaminated main magma, and the rim from fractionated intercumulus liquid. The plagioclases in pigeonite gabbros were bred in the uncontaminated main magma and evolved by the book.

Electron microprobe analyses on samples from five MZ rocks show relatively little variation of the mg# in pyroxenes and mol% An in plagioclase in a traverse from the lower MZ to upper MZ. The lowermost gabbro (possibly from below the first chromitite-pyroxenite reversal) has mg# in opx 0.765, in cpx 0.797, An in pl 71.7 mol%; in the next sample from above the mixed rock mg# in opx is 0.726–0.701, in cpx 0.786, An in pl 75.5–61.5 mol%; in a pigeonite gabbro mg# in opx is 0.717, in cpx 0.746 and An in pl 67 mol%. In the uppermost cumulate from above the lower pigeonite gabbro unit the mg# in opx is 0.708–0.701, in cpx 0.737, An in pl 67.7–65.2 mol% (one spot: An 89 mol%). In a pyroxenitic pegmatoid from the lower part of the lower pigeonite gabbro unit the opx had a mg# of 0.713–0.699, cpx 0.731–0.719 and the interstitial pl An 60.5 mol%.

The apparent lack of signatures of fractionation in cumulus plagioclase, even a reverse evolution towards more calcic composition, is not unheard of in layered intrusions (e.g., Ferguson & Wright, 1970; Mathison & Hamlyn, 1987). All the cumulus plagioclases are more calcic than the intercumulus pl in the LZ. This is a common phenomenon (e.g., Cameron & Desborough, 1969), but not easily explained in the (many) cases without any possibility of Ca-Al fractionation in intercumulus liquid, especially if it is presupposed that the intercumulus liquid represents the mafic main liquid of the magma chamber. The intercumulus compositions of ultramafic LZ cumulates (olivine cumulates, orthopyroxene cumulates, chromitites) are very salic, even granitic (quartz, sodic plagioclase, orthoclase, phlogopite, apatite).

Besides the KOI-type intrusions described here, quartz-rich intercumulus seems to be a general feature in layered intrusions; e.g., Page (1977) reports up to 6% of intercumulus quartz from Stillwater orthopyroxene cumulates; Merensky Reef contains locally abundant quartz (Vermaak & Hendriks, 1976). Although salic intercumulus is a regular feature, it seems that only Sharkov (1980, p. 138–139) has paid any attention to this glaring discrepancy, although he does not interpret it as I do here: as samples of contaminant magma carried in the density flow.

The Upper Zone (UZ) begins with a 40-m-thick succession of anorthosites. The Upper Chromitite (UC) layer, to be described later in this book, is located in the middle of this unit. The anorthosites are overlain by gabbros and anorthosites, the amount of anorthositic material decreasing upwards. The UZ gabbros are pl-px cumulates; the pyroxenes are completely uralitized.

The uppermost unit of the UZ is magnetite gabbro. The entry of magnetite at ca 95 PCS is about the same as estimated by Morse for the Kiglapait intrusion (88.6 PCS; Morse, 1969a; 93.5 PCS, Morse, 1979b). The late entry of magnetite suggests that the oxidation state of the magma was, and remained, low.

The magnetite gabbro is underlain by a unit of spotted anorthosite, with interlayers of pure anorthosite and ultramafic cumulates (for more detail, see Mutanen, 1989a, b). The pl cumulates contain granophyre pods and are in general rich in intercumulus granophyre material. Fluorapatite is common; skeletal apatite crystals up to 5 mm long have been found.

The magnetite gabbros (Figs 17 and 26) have been intersected by the holes of DDH profiles at Koitelaisenvosat, in the eastern part of the Koitelainen intrusion (see Fig. 12, Mutanen, 1989b). The magnetite gabbros form a

tripartite unit with a sharp contact against the underlying spotted anorthosites. The lower subunit consists of pl-cpx(-pig)-mt and px(-ol?)-mt cumulates and is 40 m thick, with ca 0.2% V. The 20-m-thick middle part (0.03–0.07% V) consists of plagioclase-rich cumulates with small amounts of cumulus magnetite. The upper subunit (35 m thick) is similar to the lower one (0.2–0.3% V). Terminal saturation of sulphide liquid was attained near the top of the lower subunit, where the Cu jumps from a background value of 40 ppm to 1000–1500 ppm (Fig. 26). Near the top of the lower unit there is a 0.2–0.9 m-thick plagioclase-rich layer. Small-scale layering (pl/mt ratio layering) is most common near the top of the lower subunit and in the upper unit.

Cumulus ilmenomagnetite grains, 0.5–2 mm in size, have interstitial adcumulus enlargements. In the southern part of the intrusion, magnetite (9.4–10.9 vol%) occurs as roundish (subhedral?) cumulus grains. I have estimated at Koitelaisenvosat that the content of ilmenomagnetite was 10–15 wt%. These figures are within the observed range (9–12.7 vol%) for magnetites of pl-px-mt cumulates in layered intrusions (see Lebedev, 1962a; Irvine & Smith, 1969; Molyneux, 1974; Bogatikov, 1979; Morse, 1979b). The magnetite percentage probably represents the cotectic ratio (Bogatikov, 1979). When the liquid is still richer in Fe, and Fe-rich olivine enters the cumulus assemblage, the cotectic proportion of magnetite increases to 15–20 vol% (op. cit.).

For magnetite to become overenriched (to supercotectic amounts) the residual liquid must have stayed in the magnetite phase field. With the increase in polymerization of the melt (due to contamination or silica enrichment during mt(-ol)-px fractionation) the cotectic proportion of magnetite decreases; e.g., in the Bushveld magnetite gabbro the proportion of magnetite decreases upwards in the series (wt%): 12.7 –> 7.4 –> 6.4 –> 5.4 –> 3.3 (see Molyneux, 1974). In the magnetite gabbro of the Koitelainen intrusion the original magnetite content of the middle (pl-rich) subunit was 3–7 wt%, which I interpret as representing the cotectic magnetite/silicate ratio in a contaminated magma.

Ilmenite occurs as coarse granule exsolution grains in association with magnetite, and as exsolution lamellae and late-stage lace-like ilmenite (Fig. 14 in Mutanen, 1989b). The Ti concentration of the residual liquid before the magnetite phase contact, and the oxidation state of the magma were both so low that, discounting the Doppelgänger ilmenite in melt inclusions, the mixed rock and other contaminated cumulates, the ilmenite did not crystallize as a proper cumulus mineral and the first titanomagnetite was not saturated with Ti. The proportion of granule-exsolved ilmenite was dependent on the concentration of V in the original titanomagnetite (Mutanen, 1979a). The vertical distribution of V in magnetite reveals cryptic variations (op. cit.). The V in magnetite varies between 0.9 and 2.4%, and in ilmenite between 0.17 and 0.7%. There are, however, very high-grade magnetite concentrates with up to 2.84% V in magnetite and up to 0.94% in ilmenite.

In the main part of the magnetite gabbro unit, Cr in magnetite concentrates is very low (<50 ppm), but at the very base of the unit magnetite is very rich in Cr, with up to 3.8–6.1% Cr_2O_3. As proposed for the Upper Chromitite, this Cr may be of exotic origin, not "innate", as proposed by McCarthy and Cawthorn (1983) for a similar phenomenon in the Bushveld intrusion.

Apatite and tourmaline are typical accessories. Sulphides (chalcopyrite, bornite, chalcocite, pyrrhotite and pyrite) occur in the upper part of the unit. The amount of interstitial apatite seems to increase upwards, and hence it most probably attained cumulus status above the section intersected by drilling.

The original (premetamorphic) ilmenomagnetite was altered to secondary biotite and hornblende, while ilmenite was mostly preserved. The alteration, called silication of

magnetite during the exploration stage, is very uneven and irregular and proceeded mostly along thin subvertical joints, as uralitization did in gabbros (Fig. 17, upper left). The boundary between completely silicated and preserved magnetite gabbros is generally sharp. Of the many possible reactions, silication in the Koitelainen intrusion was due to the reaction of magnetite with intercumulus feldspars (potassium feldspar, plagioclase) with the active participation of a water-rich fluid (Eugster, 1957; Wones & Eugster, 1965) during regional metamorphism. The $D_V^{sv/bi}$ for the metamorphic assemblage is ca 1.7.

The relations between the magnetite gabbro unit and the overlying **granophyre** are not quite clear. In some parts of the intrusion the magnetite gabbro seems to grade into granophyre with the decrease in magnetite and increase in interstitial granophyric material. In the southwestern part an anorthosite layer separates the magnetite gabbros from the granophyre. The thickness of the granophyre cap in the least tectonized parts is 200–400 m. Plagioclase (≤ 4 mm) was the first mineral to crystallize from the granophyre magma. The euhedral to subhedral plagioclase crystals are now completely altered to albite + epidote. The mafic minerals – dark hornblende and biotite – are secondary (metamorphic), formed from original pyroxenes, magnetite and possibly fayalitic olivine. Residual garnet from melted schists is found in a DDH in the western limb and in the northwestern part of the intrusion (Fig. 33). Aggregates and individual grains of residual quartz also occur (Mutanen, 1996, p. 36).

The lowermost granophyres are medium- to coarse-grained, but upwards the grain size decreases. Some of the granophyres in the southern part of the intrusion resemble plagioclase-phyric lavas (Fig. 18f); lava-like granophyres are known to form at the incipient melting of country rocks (Smith, 1969, and they are typical of the upper part of the Sudbury granophyre ("micropegmatite"; Stevenson & Colgrove, 1968).

In the main part of the granophyre the Cr concentration is below the detection limit of 50 ppm, but at Kaitaselkä, in the northeast of the intrusion, a percussion drilling sample taken from near the roof of the granophyre (with residual garnet from melted high-aluminous schist) was very high in Cr (Cr_2O_3 1800 ppm in rock, 1.7-3.8% Cr in magnetite).

Granophyres also occur as pockets trapped beneath autoliths and xenoliths, as frozen droplets in massive sulphides (Fig. 20), patches in anorthosites, pockets in pegmatoids (Fig. 29) and also as dykes in UZ rocks. At Iso Vaiskonselkä a dyke of acid granophyre projecting from the ferrogranophyre cap can be traced for a couple of hundred of metres down into magnetite gabbro (Fig. 17). Most probably this represents the last residual (eutectic) liquid of the granophyre magma, which seeped into a contraction crevice.

Chromitite layers

The pessimistic prediction of Thayer (1973) concerning the limited scope of potential ground for chromite ores became outdated in 1977, when the extensive UC layer was intersected in DDH329 in Koitelainen. "Impossible" by any grounds – stratigraphic position, and the composition of both the chromite and the intercumulus – the discovery of the UC was followed by that of the LC layers at Koitelainen in 1981, and in 1991–96 by the equally paradoxical chromitites of Akanvaara.

The chromitites of Finnish Lapland are not completely without relations. With regard to the stratigraphic position near the level of the

plagioclase phase contact, the ore grade and the Mg-poor chromite composition, the LC layers of Koitelainen are similar to the chromitites of Penikat (Kujanpää, 1964) and Bird River (Bateman, 1943, 1945; Davies, 1958) and the lower chromitites of Fiskenaesset (see Ghisler, 1976).

The stratigraphic position of the UC is comparable to that of the upper chromitite layers of Fiskenaesset (Windley & Smith, 1974; Myers, 1975; Ghisler, 1976) and the anorthosite-associated chromitites of Sittampundi (Janardhanan & Leake, 1975), Soutpansberg (van Zyl, 1950), Entire (Sivell et al., 1950) and possibly some of the Imandra chromitites (see Kozlov et al., 1975; Dokuchaeva et al., 1982b; Zhangurov et al., 1994). The peculiar, alkali-enriched concentrations of Ti-rich chromite in the uppermost part of the Norilsk sill (Genkin et al., 1979) have a certain kinship with the UC of Koitelainen. The most complete analogy of the Koitelainen intrusion is the Fiskenaesset intrusions, with chromitites and magnetite gabbro in comparable positions (see Bridgewater et al., 1978).

In the Koitelainen intrusion the lowermost LZ cumulates represent crystallization along the olivine-chromite boundary. The presence of chromite-rich magma inclusions in olivine suggest that chromitite accumulations may occur in the depths of the olivine cumulate basin in the western part of the intrusion (see Appendix 3).

The Lower Chromitite (LC) layers have been intersected by drilling in the Porkkausaapa area, east of the Kiviaapa dome and more recently in the Rookkiaapa area, southwest of the dome (see the geological map, Appendix 3). According to the results of diamond and percussion drilling the LC layers are continuous over a distance of about 20 km. In the Kiviaapa area the dip of the chromitites and of the lower contact of the intrusion is ca 10° SE.

The LC layers occur in the pyroxene cumulate unit in the uppermost part of the LZ within a vertical span of 37–59 m. The uppermost chromitites are 30–55 m below the base of the MZ. There seem to be four to six layers over 0.3 m thick, with Cr_2O_3 from 10.6 to 32.2%. The thickest DDH intersection of chromitite was 2.9 m. The basal contacts are generally sharp; the hanging wall contact is gradational from massive chromitite to net-textured ore to chromite-disseminated pyroxenite (Fig. 23).

Besides the counted layers there are numerous thinner, possibly discontinuous, bands, net-textured schlieren and chromite-disseminated layers.

The chromite octahedra (0.1–1 mm) occur in a matrix of secondary phlogopite, colourless or slightly greenish secondary amphibole, and plagioclase, with variable but usually smaller amounts of scapolite, talc, chlorite and carbonate. Fossil melt inclusions are common in chromite (Fig. 25L).

Electron microprobe analyses of typical LC chromites are presented in Table 4. The chromites are of the Akanvaara LC type, with similar low MgO and a substitution relation between Al and Cr.

The PGE assays are generally high in the LC layers. Weighed total PGE values for individu-

Table 4. Average compositions of chromite from the UC layer, a thin chromitite in MZ (DDH365/527.46 m) and four LC layers, Koitelainen intrusion. Electron microprobe analyses by Tuula Hautala and Jaakko Siivola (GSF).

	1	2	3	4	5	6
TiO_2	3.8	0.79	0.32	0.52	0.42	0.19
Al_2O_3	9.4	14.09	11.8	8.4	12.5	13.8
Cr_2O_3	42.33	42.84	44.7	46.0	42.8	41.3
V_2O_3	0.87	0.44	0.32	0.36	0.33	0.35
FeO(tot)	39.4	35.93	43.9	43.0	42.8	43.6
MnO	0.8	0.90	0.84	0.88	0.90	0.90
MgO	0.5	3.07	1.1	1.0	1.7	1.3
ZnO	0.3	0.13	0.39	0.14	0.18	0.28

1 - UC (n = 33)
2 - MC (n = 9)
3 - LC1 (n = 10)
4 - LC2 (n = 10)
5 - LC3 (n = 10)
6 - LC4 (n = 10)

al layers vary between 0.1 and 3.41 ppm (weighed average 1.4 ppm). The mean of individual analyses of Pt/Pd is 0.87, weighed mean 0.34. Au is very low. The CN pattern is M-shaped, with peaks at Rh and Pd (Fig. 27a). Suspect PGM have been found but not yet checked by electron microprobe. The chromitites do not contain any primary sulphides.

The position of the LC far above the floor of the intrusion and after voluminous pyroxene and chromite accumulation makes the occurrence of chromitites at the stratigraphic level where they were in fact found rather unlikely. The paradox of massive pyroxene and chromite prior to chromitite accumulation is shared by most of the Bushveld chromitites (see Cameron, 1978, p. 446 and p. 459), that is, by around 90% of the world's chromite reserves. Another paradox is that most of the chromite deposits are associated with tholeiitic, relatively Cr-poor (around 300 ppm) magmas, but chromite deposits are not known associated with komatiitic magmas, with ca 2000–3000 ppm Cr!

In the lower MZ, a 5 cm-thick layer of chromitite occurs at the base of a feldspathic cpx-opx cumulate layer. This **middle chromitite** (MC) was intersected by two DDHs and has not been traced laterally. The chromite (Anal. 2, Table 4) is the most magnesian (MgO ca 3.1%) and most aluminous of all Koitelainen chromitites. With regard to V, the best indicator of fractionation, the MC chromite comes between the LC and UC chromite.

The Upper Chromitite (UC) layer is located at the base of the UZ, at about 86 PCS level, only ca 170 m below the magnetite gabbro (Mutanen, 1981).

The UC is a distinct layer, 0.75–2.18 m thick (mean DDH intersection thickness 1.35 m, true thickness ca 1.2 m), containing 21% Cr_2O_3, 0.4% V and 1.1 ppm PGE. For an ultramafic rock in general, and for a chromitite in particular, the Ag (2–6 ppm) is very high. As a whole, the UC is continuous, and compositionally and mineralogically homogeneous. It also has a constant, predictable stratigraphic position.

The UC layer has been encountered in all corners of the intrusion (see Appendix 3). The mottled anorthosite is always accompanied by the UC and vice versa. In the southern part (shown on the map as a gap) irregular dissemination, pockets and schlieren of chromite occur in a mess of contaminated gabbroic cumulates and microgabbro autoliths several tens of metres thick.

Mottled anorthosites are dominant in the UC sequence (Figs 17, 24). The contact with the underlying homogeneous MZ gabbros is sharp. A xenolith of amydgaloidal basalt has been found at the base of the UC succession (Mutanen, 1989b, p. 44–45). The UC usually rests directly on mottled anorthosite, but in some drill holes a layered succession, up to 11 m thick, of alternating gabbroic and anorthositic rocks occurs between the UC and the footwall anorthosite. This succession includes microgabbros (homogeneous, with pl primocrysts, sometimes with minor chromite), pegmatoid gabbros and a discontinuous layer (≤ 0.8 m) of spotted anorthosite, containing cumulus plagioclase, minor chromite and interstitial quartz. This footwall succession evidently represents relics of layers that were beheaded in most places by magmatic erosion. They stand like buttes in the desert.

Thus, strong convection and concomitant magmatic erosion preceded, but also accompanied and succeeded, the accumulation of the UC.

The maximum thickness of the preserved succession (11 m) gives a measure of the thickness of the unconsolidated cumulus mush in the Koitelainen intrusion. It is of the range estimated from other intrusion: 1–3 m in Bushveld cumulates, 26 m in potholes (Ferguson & Botha, 1963), 14 m from potholes (Viljoen et al., 1986a), 2–3 m in the Skaergaard intrusion (estimated from cumulate slumping, Wager & Brown, 1968); 1–5 m in the Kiglapait intrusion (Morse, 1969a); max. 15–20 m in various in-

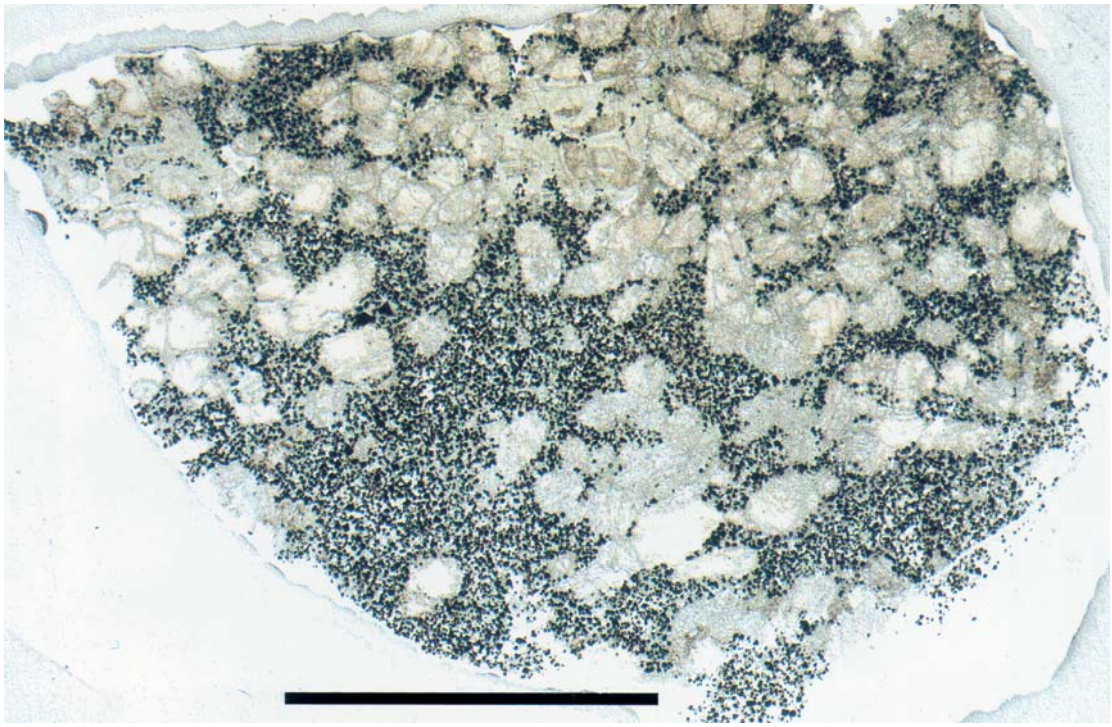

Fig. 23. Spotted chromitite (chromite-orthopyroxene cumulate) grades into net-textured orthopyroxene-chromite cumulate. Koitelainen LC layer, DDH359/31.25 m. Bar = 1 cm. Diascanner photo by Reijo Lampela.

trusions (Roobol, 1974); ca 1 m at Skaergaard (McBirney & Noyes, 1979); 1.8 m below a chromitite layer at Stillwater (Sampson, 1969), and 18–20 m in the Ilimaussaq alkaline intrusion (Sørensen & Larsen, 1987).

Intercumulus quartz is always abundant in the mottled anorthosite; other intercumulus minerals are ilmenite and fluorapatite.

The basal contact of the UC is invariably sharp. In one DDH there are disseminated chromite and thin chromite bands immediately below the UC. As in the Akanvaara intrusion, contact faults are common in the base contact. The fault blastomylonites are sheared, silicified, albitized and carbonatized rocks containing biotite and very fine-grained euhedral tourmaline (3.1% Cr_2O_3 by electron microprobe). Layer-parallel veins (1 mm) of sodic plagioclase are common in massive UC ore.

The top of the UC normally consists of a 5–8 cm-thick zone of two or three bands of massive or disseminated chromite in gabbro matrix. In places the banded part is missing, and a thin anorthosite layer separates the UC from the hanging-wall gabbro. In this anorthosite, small chromitite fragments, eroded from the upper massive UC (Fig. 25b), indicate scouring by magma currents. Strong erosion occurs on the upper surfaces of Bushveld chromitites (Ireland, 1986). The case of UC is also a strong indicator that adcumulus growth began soon after settling (Cameron, 1969) and the chromitite hardened immediately into an adcumulate hardground (see Wager & Brown, 1968; Sparks et al., 1985). The lack of overenrichment by resolution and annealing (Cameron & Emerson, 1959; Cameron, 1969; see also Vogt, 1924) at Koitelainen, at both LC

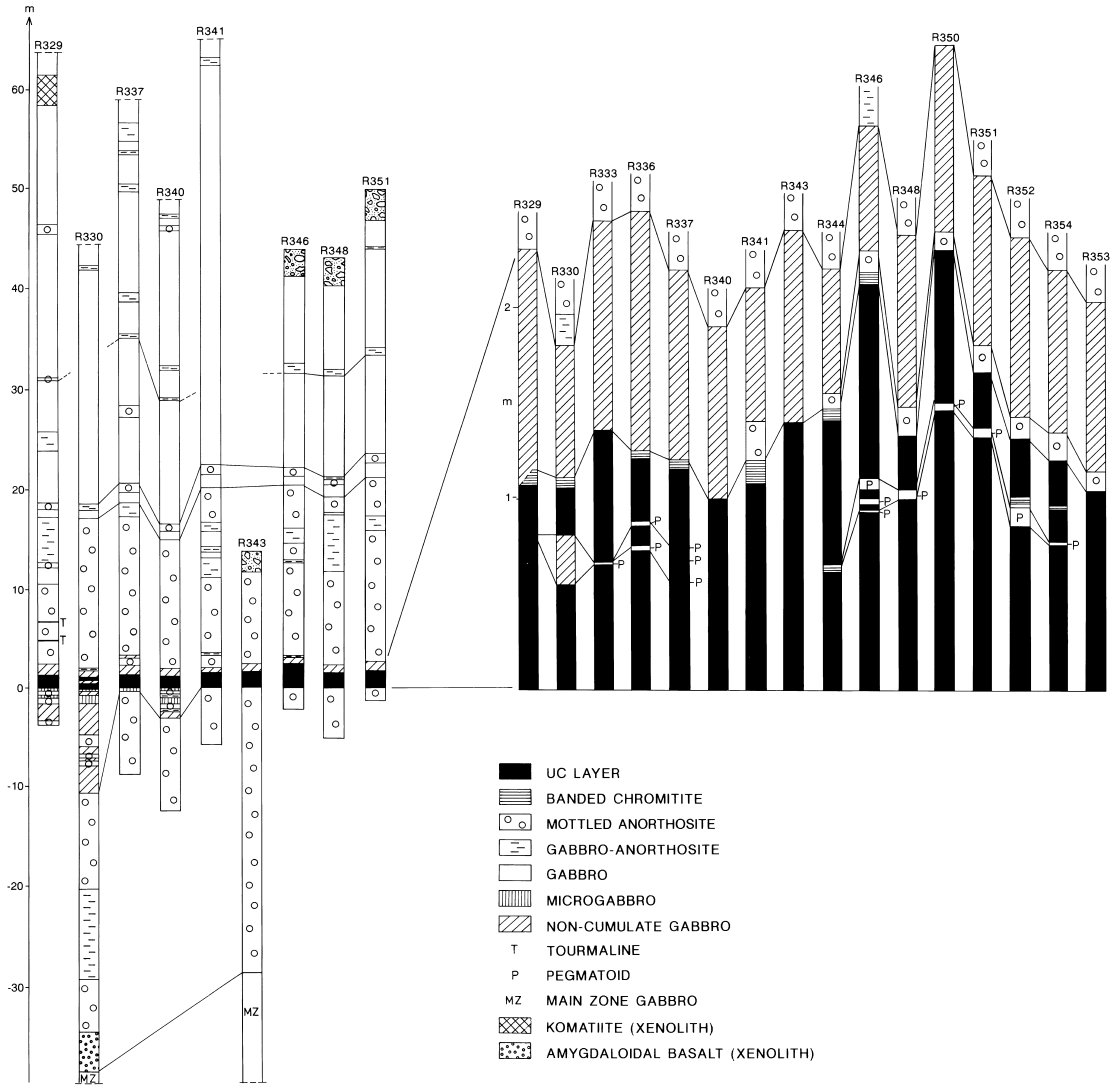

Fig. 24. DDH intersection through the UC sequence and details of some UC intersections. Koitelainen intrusion.

Fig. 25. "The mother of all reversals", the UC layer of the Koitelainen intrusion. Photo l by Jari Väätäinen, all others by Erkki Halme. a – cumulus pyroxene (now uralitized) in chromitite. Cumulus crystals of pyroxene and plagioclase are rare in UC. DDH337/105.20 m. Parallel nicols. Bar = 1 mm; b – fragment of chromitite in the anorthosite immediately above the UC layer. DDH346/41.51 m. Parallel nicols. Bar = 5 mm; c – base contact of the upper part of the UC layer against a gabbro interlayer. DDH330/214.15 m. Parallel nicols. Bar = 3 mm; d – ilmenite exsolution bodies partly replaced by secondary titanite and biotite. Bar = 0.2 mm; e – exsolved ilmenite grains in chromite. DDH333/225.25 m. Reflected light. Bar = 100 mu; f – detail of the secondary silicate inclusions (biotite, titanite). Reflected light. Sample not on record. Bar = 100 mu; g – skeletal chromite crystal, width 0.8 mm. DDH330/214.50 m; h – a big inclusion in chromite (chromite diameter 0.4 mm), possibly an embayment. DDH341/276.05 m; i – "Swiss cheese" chromite, 0.5 mm in size, with several fossil melt inclusions. DDH333/225.25 m. The inclusions mainly consist of biotite, hornblende and plagioclase; j – an ilmenite-rich graded chromitite layer, at top right. The composition varies from that of an original Cr-rich ulvite (graphic ilmenite-chromite symplectite in the massive bottom) to that of Ti-rich chromite (from lamellar to ordinary isolated ilmenite lamellae, with increasing idiomorphism of the host chromite) towards the top. DDH346/42.74 m. Bar = 5 mm; k – Pt(-Pd-Bi)Te (moncheite?) and Rh sulphide (cannot be distinguished from the former). Length of chromite grain is 0.13 mm; l – "Swiss cheese" chromite (0.5 mm) from LC layer. DDH359/59.60 m. (Next page).

and UC, is a strong indicator of the very low solubility of chromium in the breeder and carrier melt.

The plagioclase cumulates overlying the UC are mottled anorthosites and minor spotted anorthosites. From 2.4 to 6.0 m upwards above the UC there are groups of finely layered rocks (Fig. 17, middle left), the "warning layers" (during drilling, the depth to UC could be predicted approximately from these bands). A warning about these layers is in place here, however: they seem to overlie a discordance

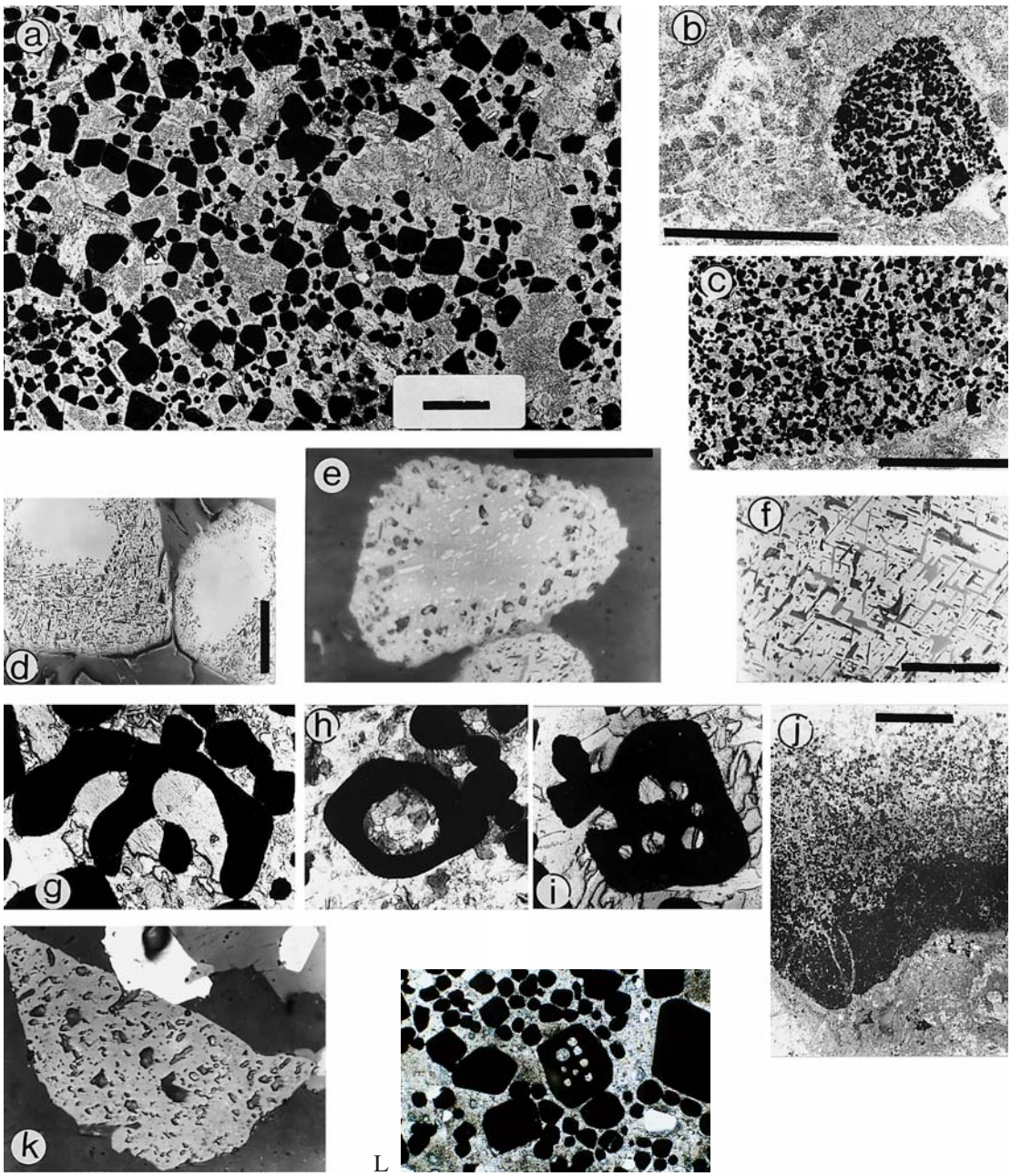

and hence, the depth to the UC varies over a short distance.

There are also two layers of tourmaline in mottled anorthosite above the UC, and one of them mocks a graded cumulate layer. Higher up, gabbroic interlayers appear, and from 20 m above the UC upwards, gabbros dominate anorthosites.

In the UC the chromite shows size layering (graded bedding) and ratio layering (downwards-increasing chromite/silicate ratio), with a reversal to coarser size in the middle of the layer. The grain size of chromite in the lower parts of the size-graded layers is up to 1 mm (sometimes up to 1.5 mm), in the upper parts, 0.2–0.3 mm. As in the Akanvaara intrusion, a layer of fine-grained chromitite occurs in coarser chromitite (see Fig. 8a). Thus, it seems that there are two grain-size populations, both of which are easily seen in thin section. Either we have here a mingled population of various grain sizes, or an unmingled one, with two stages of chromite nucleation. The two size classes also occur in the Kemi chromite deposit (Veltheim, 1962).

The UC is always separated from the hanging wall anorthosites by a layer of medium-grained, homogeneous non-cumulate gabbro 0.7–1.0 m thick. Sometimes the gabbro layer "splits" the UC layer (seam splitting; Wadsworth, 1973) at the level of the size reversal. When the middle gabbro thins down, its place is taken by coarse pegmatoid gabbros. In two DDHs there is a 1–3-cm-thick pl-crt layer on top of the pegmatoid interlayer. In this position a massive to disseminated, compositionally graded layer was noticed and analysed (Fig. 25j). The combined thickness of the split layer is the same as the thickness of the undivided layer (see also Ferguson & Botha, 1963).

In DDH346 there is a big (several cm in diameter) pocket of granophyre in an anorthositic part of the interlayer. The contacts of the gabbroic interlayer against massive chromitites are always sharp (Fig. 25c).

Euhedral, unchained chromite octahedra constitute 39–47 (aver. 43) vol% of the ore, corresponding to an initial porosity of 61–53 vol%. In a cumulate with practically no postcumulus growth of chromite, this percentage equals the volume proportion of apparent initial porosity. The original figures would have been somewhat lower (ca 54 vol%) because of the later volume increase due to metamorphic hydration. Still, it is higher than generally observed in, and estimated for, natural magma suspensions (from 20 to 50 vol%,; see Jackson, 1961; Cameron, 1969; Kobayashi, 1972; Couturié, 1973; Hamlyn & Keays, 1979; Morse, 1988), which suggests that either the carrier liquid was very viscous or that, besides the obvious "holes" of cumulus silicates (Fig. 25a), there was always a small amount (10–20 vol%) of cumulus phases other than chromite. Irvine's (1978b) estimate for the initial porosity was 60%. Thus, the interesting possibility arises that my calculated value (average 57%) is the true one.

Large chained crystals of chromite were observed near the base of the layer. Potassic fossil melt inclusions (with secondary biotite, plagioclase, secondary amphibole) are common (Fig. 25g–i) in chromite. Ilmenite exsolved at lower temperatures from the original, high-T chromite (Fig. 25e); in metamorphism the ilmenite exsolution bodies were replaced, from crystal faces inwards, by secondary biotite and titanite (Fig. 25d, f).

The other original minerals are plagioclase, clinopyroxene, Ca-poor pyroxene (orthopyroxene or pigeonite), ilmenite, fluorapatite, allanite, sulphides and platinum-group minerals (PGM). I assume that potassium feldspar was a primary intercumulus phase. Primary intercumulus quartz occurs near the base of the UC, and it is common in the banded top. Occasionally postcumulus primary hornblende has been noticed; also some primary biotite may have been present. The primary oikocryst phases are plagioclase (particularly near the base), pyroxene, ilmenite and fluorapatite. The proportions of primary postcumulus phases are still reflect-

ed in the vertical distribution of secondary minerals: in graded layers biotite is most abundant in the upper part, hornblende in the middle and plagioclase in the lower part. In some cases the lowermost 10 cm consists mainly of poikilitic plagioclase and chromite.

Of the primary minerals cumulus pyroxene either crystallized or, more probably, settled, with chromite (Fig. 25a). Big (up to 1 cm) euhedral cumulus crystals of plagioclase are common at Jänessaari, southwestern Koitelainen (see Mutanen, 1989b, p. 44 and 49). Large crystals of fluorapatite, partly of cumulus status, occur in places; fluorapatite oikocrysts are seen to enclose chromite crystals. Ilmenite, too, sometimes occurs as cumulus crystals. Tourmaline (3.1% Cr_2O_3 by electron microprobe) is always present in small amounts; it may be a primary postcumulus mineral.

The intercumulus consists mostly of secondary silicates and other secondary minerals: biotite (1.4% Cr_2O_3 by electron microprobe), colourless amphibole, greenish amphibole, bright green amphibole (1.1–2.1% Cr_2O_3 by electron microprobe), titanite, rutile, two kinds of chlorite, epidote-clinozoisite, porphyroblastic scapolite, carbonate, hydrobiotite-vermiculite, zeolites, and the present paragenesis of sulphides (two generations of pyrite, chalcopyrite, pyrrhotite, pentlandite, covellite, millerite, violarite, galena and marcasite). In some strongly carbonatized places the margins of chromite crystals have been altered to a ferromagnetic spinel (Cr-magnetite ?).

Of the PGM, moncheite (Fig. 25k) and a Rh-S phase were found first, but ruarsite (RuAsS) is most common; it occurs as tiny (<10 mu) euhedra in both chromite and matrix. Laurite and sperrylite have also been encountered.

When the UC layer was found and preliminarily studied, it soon became apparent that the chromite has a unique and quite unexpected composition (anal. 1, Table 4). The high Ti is due to exsolved ilmenite rods. The Mg is very low, and even the modest MgO values in analyses are mainly due to secondary biotite inclusions. Narrow beam analyses give MgO 0.0% and TiO_2 0.2–0.4% for "pure" chromite. All chromites analysed are very poor in Mg and rich in Fe. The UC chromite is conspicuously rich in V.

The chromite as a whole, even in different parts of the intrusion and certainly re-equilibrated under different postcumulus conditions, is surprisingly homogeneous in composition. However, a strong vertical variation in V has been observed. In the case studied in detail, the V in chromite was high in the upper part (range 0.5–1.34% V) and lower part (range 1.34–1.46%) of the UC layer, but only 0.30–0.50% V in the middle.

The calculated normative oxide (spinel + ilmenite) compositions of the chromite are (in wt%): chromite 56–71%, ilmenite 0.7–15%, hercynite 12–18%, magnetite 7–12%, franklinite 0.6–1.8%, jacobsite 1–4% and coulsonite 1.0–3.2%. Evidently the original high-T spinel was above the solvus of the continuous ulvite-chromite solid solution system (see Arculus, 1974; Arculus & Osborn, 1975). The "pure", low-Ti matrix chromite represents a very low-T composition on the solvus, with the oxidation-exsolved ilmenite. Understandably, because of the necessary combination of "primitive" (Cr) and "evolved" (Ti, Fe, V, Zn) components, there were not many opportunities for the natural chromite ores to experiment with the system. However, the series is seen in association with accessory spinels in both lavas and intrusive rocks (Evans & Moore, 1968; Gunn et al., 1970; Evans & Wright, 1972; Thompson, 1973; Zolotukhin et al., 1975; Neradovskii & Smolkin, 1977; Rozova et al., 1979; Genkin et al., 1979; Muraveva et al., 1979; Eales, 1979; Eales & Snowden, 1979; El Goresy & Woerman, 1977; Smolkin & Pakhomovskii, 1985; Neradovskii, 1985; see also: Cameron & Glover, 1973).

According to experimental data given by Maurel & Maurel (1983, 1984), the liquid in equilibrium with the UC chromite contained Al_2O_3 11–12% and MgO << 0.5%.

All chromitite layers known from the Koitelainen intrusion accumulated after voluminous fractionation of pyroxenes and plagioclase. There is no evidence of the purported peritectic reaction between chromite and pyroxene (Irvine, 1967; Maurel & Maurel, 1982b), neither is there evidence of the alternative (op. cit.; Ridley, 1977), namely that the peritectic reaction produced a chromite different from the original composition (op. cit.; Ridley, 1977). Quite the contrary, chromite seems to have crystallized and survived even with a Ca-rich pyroxene (see Neradovskii, 1985). Experimental evidence of the existence and effect of the peritectic reaction is negative or ambiguous (Arculus, 1974; Arculus & Osborn, 1975; Maurel & Maurel, 1982b).

Occurrences of PGE and Au

Several occurrences of PGE-Au are known from the Koitelainen intrusion, but the grades are always too low to be economically interesting. In the layered sequence, enrichments of PGE-Au occur from the lowermost olivine-pyroxene cumulates up to the magnetite gabbro. The CN PGE-Au diagrams for the various PGE enrichments are presented in Fig. 27a–f.

Two PGE-anomalous DDH intersections were found in systematic Pd-Au assays in the LZ peridotites. These anomalies have no visible or analysed connection with sulphides. Their CN PGE-Au graphs (Fig. 27a) have the M-shape typical of Koitelainen chromitites and silicate rocks of both Koitelainen and Akanvaara (see Fig. 11, Fig. 27e).

At Rookkijärvi, pyroxene cumulates with weak sulphide dissemination contain traces of PGE (max. total PGE 1300 ppb, Pt/Pd 0.12–0.18). Au is very low (max. 36 ppb) and the CN graphs (Fig. 27c, graphs 1 and 2) have a steep positive slope. PGM have not been found. The host rocks are feldspathic pyroxenites (opx-cpx cumulate) with abundant intercumulus quartz, potassium feldspar and biotite. A quartz monzonite diapir occurs in close proximity to sulphide-disseminated rocks. Sulphide separation is thought to have been provoked by salic material fed by the felsic diapirs to the mafic magma.

The pyroxene cumulates associated with the LC layers have been systematically analysed for Pd and Au (each length ca 0.5 m). All assays were well below the treshold of economic interest. Au is slightly anomalous, but Pd exceeds 20 ppb only over a combined DDH length of 19 m. Disseminated and massive sulphides (Fig. 20, lower left) over a DDH core length of ca 1 m are associated with a pyroxenite-chromitite breccia. The disseminated rock, with 1.1% Cu and 0.08% Ni, contained 0.13 ppm Pt+Pd, the massive sulphides (with 0.3% Cu and 0.34% Ni) had a mere 100 ppb Pt+Pd. Pyroxene cumulates between individual LC layers contained a maximum of 0.23 ppm Pt+Pd.

The LC layers are enriched in PGE. The CN PGE graphs (Fig. 27b) cannot be distinguished from those of UC (Fig. 27e).

The slightly PGE-anomalous basal part of the peridotite mixed rock, described above in connection with MZ cumulates, has a maximum of 100 ppb Pt (Fig. 22).

The geology of the PGE occurrence at the reversal of the lower pigeonite unit was described in connection with the MZ cumulates. The CN PGE pattern (Fig. 27c, graphs 3 and 4) has the expected positive slope. The calculated PGE+Au(100S) values range from 56 to 1532 ppm. This reversal zone is now once again in the PGE exploration programme of the GSF RONF.

The occurrence of PGE in the UC layer was described in the context of the UC. The CN

PGE graphs are shown in Fig. 27e. Note that the graph for mottled anorthosite exhibits the same M shape but that the Pd/Ir is much higher than in the UC.

The PGE-Au enrichment in the magnetite gabbro unit is one of the most conspicuous features of the Koitelainen intrusion. Although not exactly a bonanza economically, the deposit presents a challenge to the established models of PGE ore genesis; also, it may well be a harbinger of similar (or, hopefully, better) deposits to be found one day.

Continuous assays of the cores from two holes (DDH318, 319) show the distribution of Pt, Pd, Au, Cu, V and Pt/Pd (Fig. 26). The grades are low in the V-poor subunit in the middle of the magnetite gabbro unit, and finally die out rapidly at about 75 m above the base of the unit. The weighed average Pt+Pd+Au grade of the lowermost 75 m of magnetite gabbro is 0.5 ppm. The peak total assays are 1.17 ppm/2.0 m and 1.21 ppm/2.35 m.

There is no correlation between PGE+Au and Cu, except for the highest value of Au, which coincides with the first Cu hike, i.e., with the first sulphide liquid separated from magma. The PGM (cooperite, Pt tellurides, Pt-Fe alloys) do not follow sulphides, not even in the Cu-rich part, but occur as separate grains, mostly in ilmenite and magnetite.

The PGE correlate very well with V, i.e., with the abundance of original cumulus magnetite (Fig. 26b). The Pt/Pd ratios fluctuate within wide limits, even in successive core samples. However, the vertical patterns of the ratio are similar (Fig. 26c) in the two cores assayed. The average Pt/Pd in the Cu-poor lower part is 0.32, and 0.51 in the upper, Cu-rich part. Thus, considering both Akanvaara and Koitelainen intrusions, Pt was more incompatible than Pd, sulphide liquid or not.

The CN graphs of the Cu-poor and Cu-rich parts (Fig. 27f) are similar to each other. Os, Ir and Ru are strongly depleted; curiously, however, the values of Ir, Ru and Rh are higher in the upper part of the unit than in the lower part. One explanation is that some exotic Ir, Ru and Rh were contributed by convective contamination at about the stage of the V-poor subunit.

The PGE+Au allotted to sulphides is 2234 ppm (max. 11626 ppm) in the Cu-poor lower part and 870 ppm (max. 4321 ppm) in the Cu-rich upper part.

The ultramafic pegmatoids will be described soon, and their genesis will be discussed later in this book. The pipes occur among the MZ rocks whose intercumulus was not unduly affected by salic contaminant melt. The pegmatoids themselves I interpret as representing the intercumulus liquid, or part of it, and thus their PGE concentrations would give an estimate of the PGE concentrations in evolved residual, uncontaminated liquid.

The main, magnetite-disseminated parts of the pipes have Pt grades of 0.1–0.2 ppm with Pt/Pd > 1. Pt is enriched in magnetic fraction; a magnetic concentrate contained 2.3 ppm Pt. Sulphides are practically lacking from the pipes, but some vein (that is, late) pegmatoids contain disseminated Fe-Cu sulphides; in such rocks Pd is dominant over Pt. The CN graphs of two magnetite-ilmenite-rich pegmatoid samples show a positive slope up to Pt, and a drop thereafter to Pd. Similar pipes in Bushveld also contain anomalous PGE values (van Rensburg, 1965).

For most of magmatic evolution PGE and Au behaved as incompatible elements and were enriched in residual liquid. In the sulphide-disseminated cumulates in the Lower Zone and upper Main Zone the PGE values are only modestly elevated, but even in those cases the correlation of PGE and sulphide contents is not straightforward. The lowermost PGE enrichments occur in the ultramafic basal cumulates, which carry no sulphides. The PGE are markedly concentrated in chromitite layers which are always very low in sulphur. Even when primary sulphides are associated with chromitite (in the pyroxenite chromitite breccia), the sulphides are not enriched in PGE. A

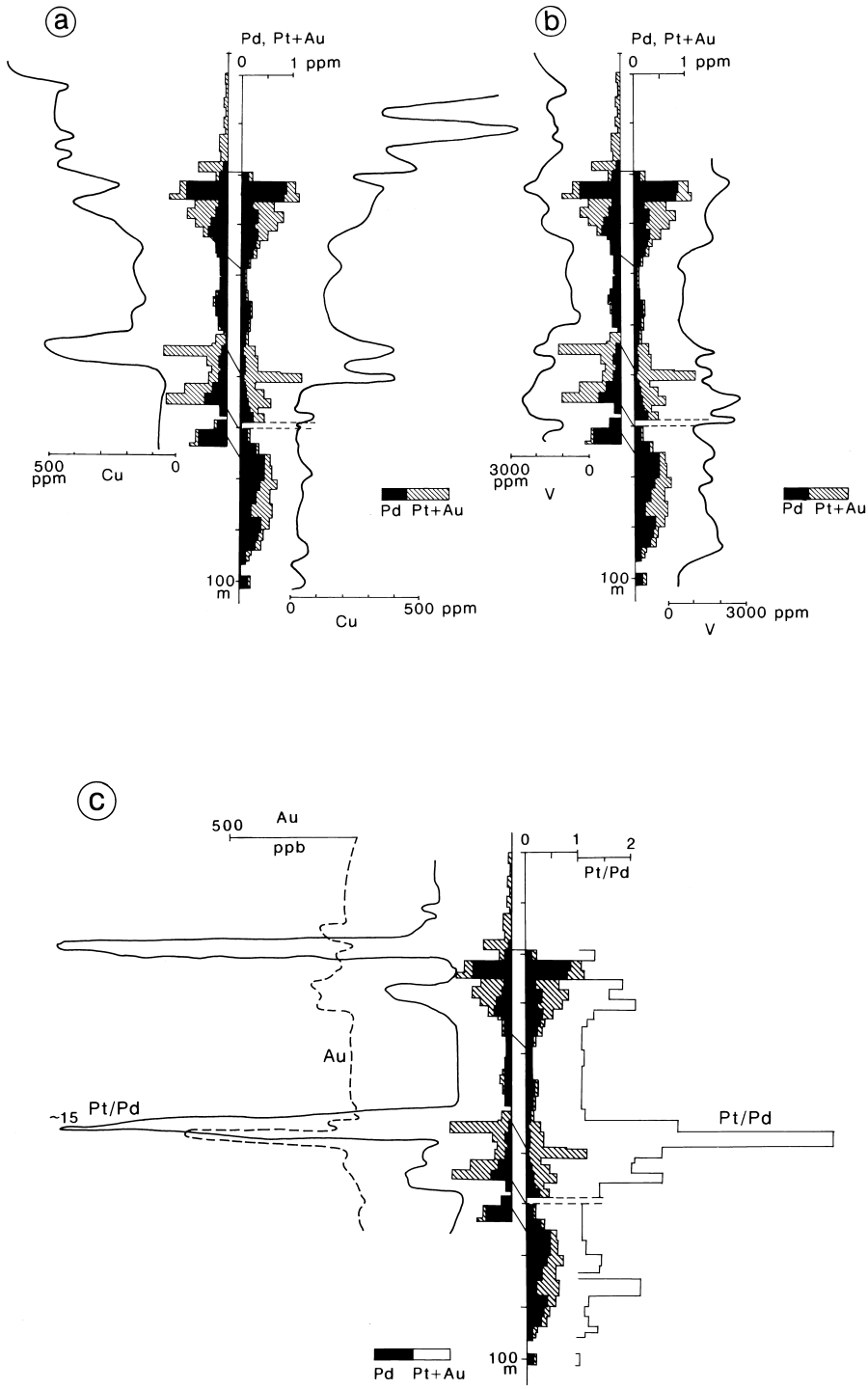

Fig. 26. Variation in PGE, Cu (a), V (b) and Au, Pt/Pd (c) values across the magnetite gabbro unit, Koitelaisenvosat, Koitelainen intrusion. The DDH318 (scale to left) failed to reach the base contact, which is indicated by the sudden increase in V in DDH319 (scale to the right). Thickness of magnetite gabbro unit ca 100 m.

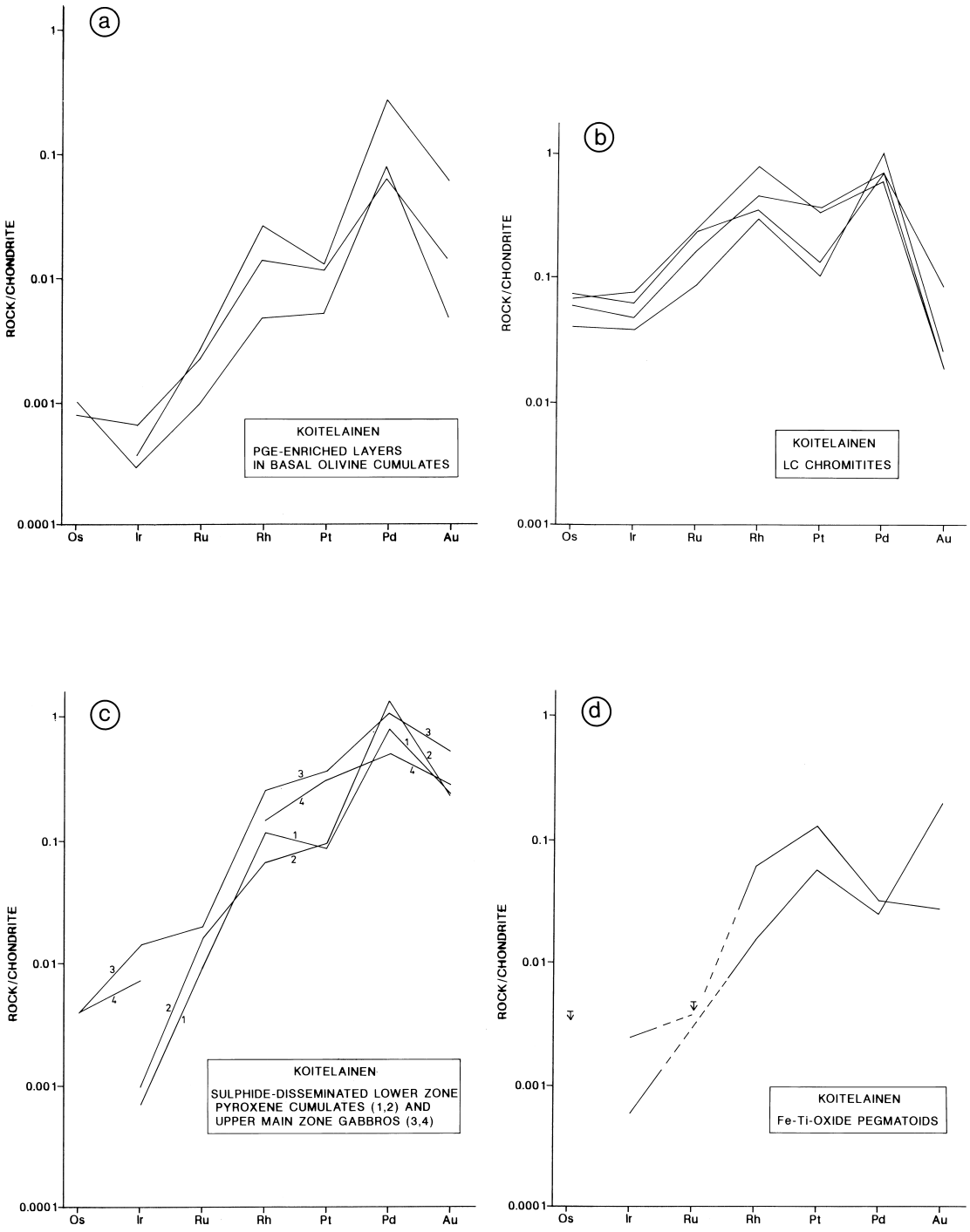

Fig. 27. Diagrams of chondrite-normalized values of PGE and Au, Koitelainen intrusion. a – PGE-anomalous intervals in basal olivine-rich cumulates; b – LC layers; c – layers with disseminated sulphides in Lower Zone and upper Main Zone; d – ultramafic pegmatoid pipes rich in ilmenite and magnetite, Main Zone; e – UC layer and underlying mottled anorthosite; f – magnetite gabbro.

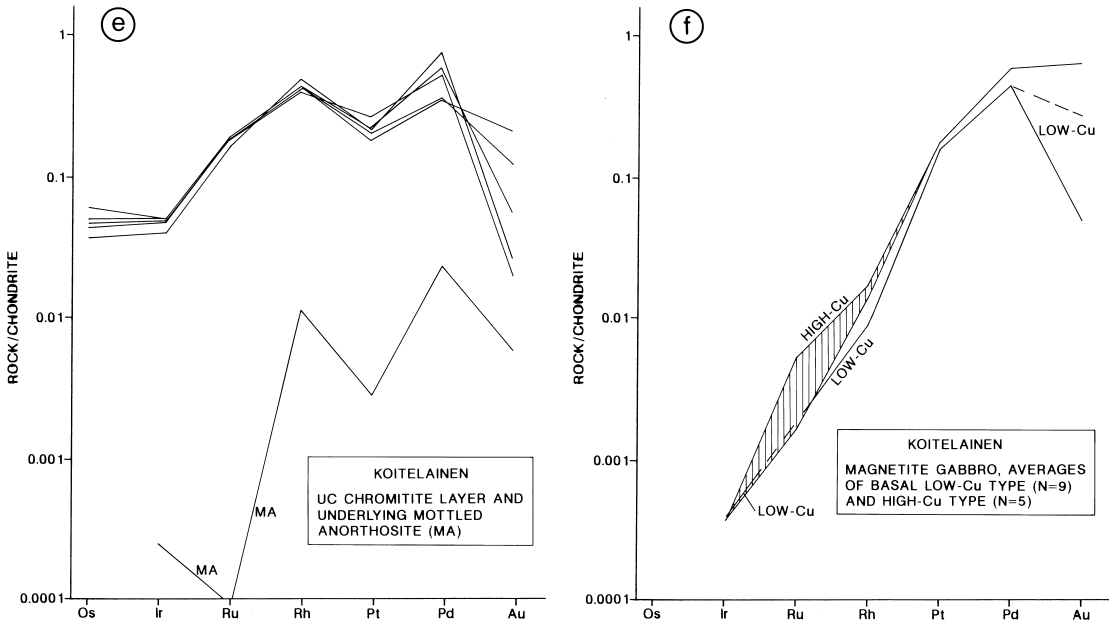

Fig. 27.

major part of the PGE-Au is incorporated in the magnetite gabbro unit.

In the Koitelainen intrusion the apparent order of decreasing compatibility of the PGE was: Ir – Pd – Pt – Au.

There must have been a special mechanism of fixation for PGE in chromitites, different from the mechanisms in cases where the PGE are associated with silicates and sulphides. The mineralogy of the PGM indicates that in chromitites and magnetite gabbro the PGM either crystallized as stable liquidus phases (alloys, sulphides, AsS phases) before chromite and magnetite or nucleated on spinels. The only truly chalcophile metal was Au, which shows a spectacular rise (2 ppm) just at the level of terminal saturation of (Cu-rich) sulphide liquid. But even in the sulphide-saturated regime of the upper magnetite gabbro the PGM occur separate from sulphides.

Enrichments of PGE in the upper part of the magma chamber are known from other intrusions, e.g., from Skaergaard (Nielsen, 1989), Bushveld (Harney & Merkle, 1990) and Norilsk (Tuganova & Malich, 1990).

Thus, as at Akanvaara (and Keivitsa), the relation between PGE (and, in detail, PGM) and sulphides is lukewarm, haphazard or nonexistent. The relationship between PGE and sulphide liquid may have been mechanical (i.e., it was between *PGM* and sulphide liquid) rather than chemical (Mutanen, 1992, Mutanen et al., 1996). In exploration at least, it is better not to count on the chalcophile character of the PGE!

Contrary to common belief the mantle source of the SHMB magmas, proposed as parents of large Precambrian layered intrusions (Bushveld, Stillwater), is not particularly enriched in PGE (Sun et al., 1989). Thus, as in the case of the Cr needed for chromitites discussed above, the initial PGE concentrations of magmas are of little consequence with regard to, or in favour of, the genesis of the PGE

ores. What is necessary is that the PGE should be concentrated in the residual liquid (and this the PGE themselves take care of), that there should be a good collector operating in magma, and that great volumes of magma should be stirred and mixed. At present it seems that cumulus spinel phases (magnetite, chromite) are as good collectors for PGM as any.

An ever growing list of cases shows that spinel phases really did act as PGE collectors. PGE deposits and anomalies are associated with magnetites (Ivanov & Lizunov, 1944; Latysh, 1959; Rozhkov et al., 1962; Fominykh & Khvostova, 1971; Razin, 1974; Perry, 1984; Golubev & Filippov, 1995), where the PGE often occur as independent PGM phases (e.g., Latysh, 1959; Fominykh & Khvostova; Razin, 1974); with ilmenite (Parry, 1984) or with chromite (Ivanov & Lizunov, 1944; Rozhkov et al., 1962; Razin & Khomenko, 1969; Razin, 1974; Parry, 1984; Lee & Parry, 1988; Scoates et al., 1988; Perring & Vogt, 1989; Lazarenkov et al., 1991). Despite the general perception, the PGE and (still less) the PGM in Merensky Reef are not in fact associated with sulphides but with chromite (e.g., Viljoen, Theron et al., 1986), down to a cm scale (Scoon & Teigler, 1994). With regard to PGE, in the Lower and Critical Zones of the Bushveld Complex it was not the case of an increase in S and PGE towards the climax at Merensky Reef, but an increase of PGE as incompatible metals in residual liquid and their increased fixation in chromitite layers until the UG2, the true climax located from tens to hundreds of metres below the Merensky Reef (Hatton, 1989).

It has been suggested, even quite recently, that PGE make use of diadochic substitution in spinels (Razin & Khomenko, 1969; Fominykh & Khvostova, 1971; Capobianco & Drake, 1990). It has been noted that, as with sulphides, the PGM phases in spinels are concentrated at grain boundaries (Parry, 1984); this suggests the possibility that cumulus spinels could serve as phase boundary collectors for PGM phases (Mutanen, 1992; Mutanen et al., 1996). I will return to the PGE problem after providing more facts about Keivitsa.

Ultramafic pegmatoid pipes

Various sections of ultramafic pegmatoid pipes are exposed in the Lakijänkä area in Koitelainen fell. Moving northeastwards, up the gentle dip of layering, we first encounter small (2–3 m in diameter) root parts of the pipes which are very rich in magnetite and ilmenite (up to 30–40 vol%). At a higher level, deep blue quartz appears and the amount of oxides decreases until, in the northernmost sections of the swarm, granitic (granophyre) pockets appear. Figure 28 presents the general form of the pipes, as interpreted by using outcrop mapping and DDH core data. Microphotos of some pegmatoid types are also presented in Fig. 29.

A big pegmatoid pipe, about 200 m in diameter, has been intersected by drilling at Mukkajärvenaapa, in the southwestern corner of the intrusion (see geological map, Appendix 3). The pipes of Koitelainen are similar to the magnetite-rich ultramafic pipes of Bushveld (e.g., Willemse, 1969b).

The pegmatoid rocks were originally clinopyroxenites rich in magnetite and ilmenite, but clinopyroxene is almost completely altered to hornblende. Besides clinopyroxene, magnetite, ilmenite, quartz and plagioclase, other primary minerals are apatite, zircon, allanite (?) and in one uncertain case, olivine.

The large Mukkajärvenaapa pipe regularly contains small amounts of sulphides: pyrrhotite, chalcopyrite, pentlandite, millerite, thiospinels of the linneite-siegenite series, and covellite.

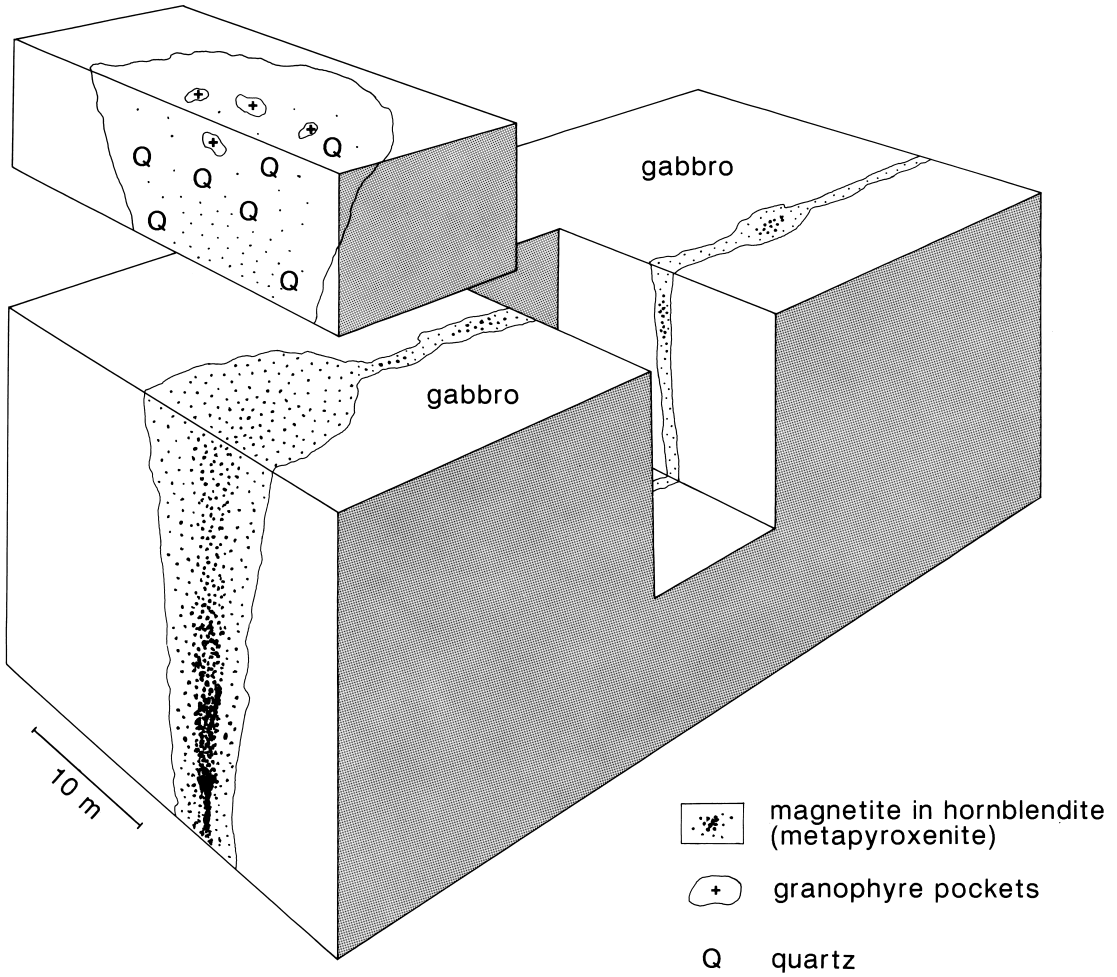

Fig. 28. Schematic picture of ultramafic pegmatoid pipes and veins in Koitelainen.

Secondary minerals of the pegmatoids are amphiboles, epidote-clinozoisite, scapolite, biotite, chlorite, tourmaline, titanite and rutile. The deep-blue, isometric and amoeboid quartz grains most probably represent primary liquidus crystals of a silica phase, possibly cristobalite, that crystallized cotectically along with cpx, pl and mt plus the accessory phases zircon and apatite.

Big zircon crystals (Fig. 29d) found in the pegmatoids in 1973 were used to get the first "honourable" age for the layered intrusions of the 2440 Ma age group (Mutanen, 1976b; Kouvo, 1977). Before that, Silver (1968) had used zircon from mafic pegmatoids of the Adirondack area for radiometric dating.

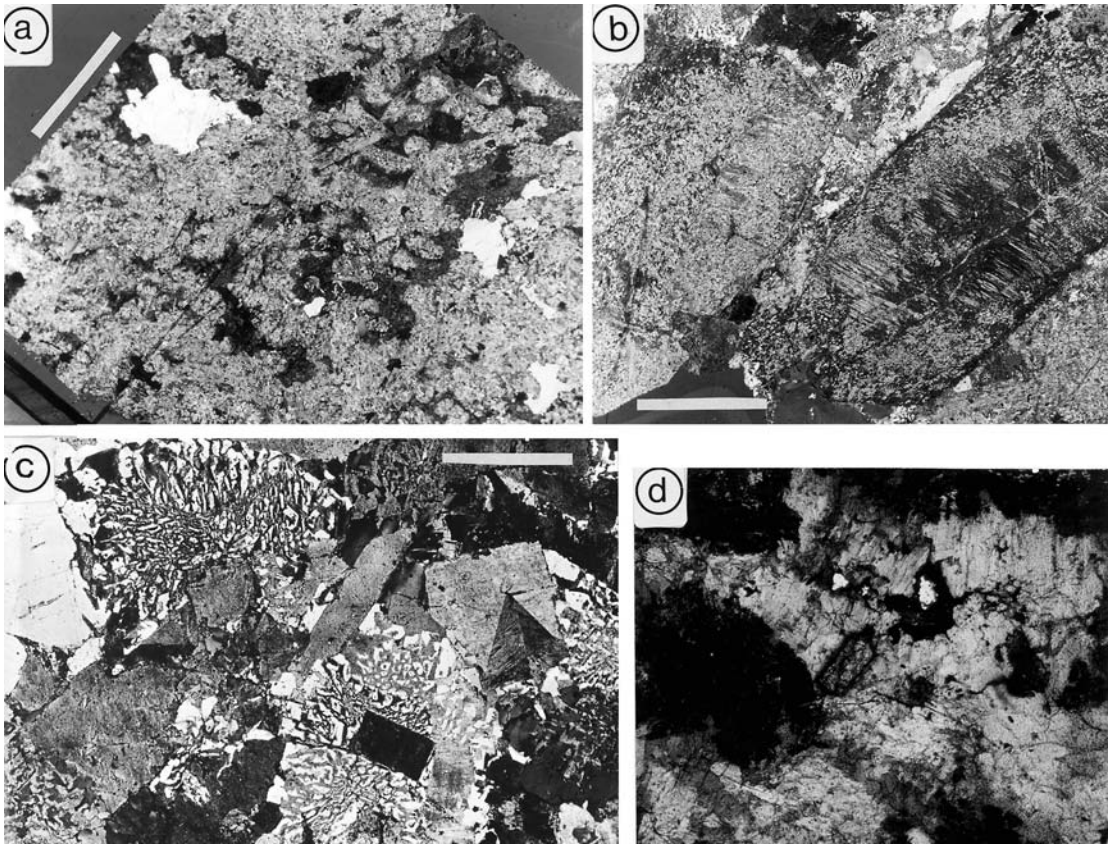

Fig. 29. Microphotographs of ultramafic pegmatoid rocks, Lakijänkä, Koitelainen. a – metapyroxenite, with amoeboid quartz grains (white). Parallel nicols. Sample TM-76-10F. Bar = 5 mm; b – Big, altered clinopyroxene crystals and interstitial granophyre. Crossed nicols. Sample TM-76-10Å. Bar = 5 mm; c – granophyre pocket from the upper part of the pipe. Note euhedral plagioclase cores. Crossed nicols. Sample TM-76-10Z. Bar = 2 mm; d – zircon crystal (length 0.15 mm) in metapyroxenite. All photos by Erkki Halme.

PETROLOGY OF THE KOITELAINEN INTRUSION

On reversals and multiple magma pulses (MMP)

Since the late 1970s, new doctrines have emerged or been reinvigorated to explain the genesis of mafic layered sequences and associated ore deposits.

Although hailed by many as a progressive new theory, the first of these concepts did not add much to our understanding of layered igneous sequences, and nothing to that of magmatic ores. It was nothing less than an attempt to abolish the cumulus theory, which states that the cumulus crystals had formed in a different part of the magma system and had accumulated where they are now. The new hypothesis suggests instead that the crystals had in fact formed practically in situ (Campbell, 1978; McBirney & Noyes, 1979). The large value of Reynold's number of silicate liquids was calculated to be too high to allow settling

of plagioclase, the most common mineral in mafic layered intrusions; on the other hand it was purported that the plagioclase crystals did not settle as cumulus crystals but grew from the bottom (see Campbell, 1978), as, indeed, they sometimes do.

The news of the death of the cumulus theory soon proved exaggerated, however, as geologists were reminded of the facts everyone already knew (see e.g., Morse, 1969a; Cox, 1985; Cox & Mitchell, 1988; Ghiorso & Carmichael, 1985; Marsh & Maxey, 1985; Martin & Nokes, 1988, 1989; Martin, 1989; Martin & Nokes 1989). Most geologists involved with the study of layered intrusions probably regarded the new dogma unworthy of a fight, and paid no heed to it. Of one of the many fallacies of the un-cumulus theory Morse stated, rightfully: "The notion that the [cumulus] theory deals only with crystal settling and molecular diffusion is a recent myth" (Morse, 1985).

The other fashion, also at variance with classical cumulus models, was the concept of double diffusive convection (DDC). This is essentially a single phase compositional convection model (McBirney & Noyes, 1979; Chen & Turner, 1980: Tait et al, 1984), relevant in low-viscosity fluids, such as water. Applied to intrusions, it needs a calm magma and does not tolerate overall convection (see e.g., Morse, 1985) and probably no stirring other than that caused by the DDC itself. The DDC denies the significance of crystal settling in magmas (McBirney & Noyes, 1979) and is, thus, another aspect of un-cumulus thinking.

The third trend in explaining the filling and crystallization of layered intrusion is what I call the MMP (for multiple magma pulses) hypothesis and its kin. Considering the huge volumes of many layered intrusions, the incremental intrusion of magma appeals to our common sense. Incredible as they may seem, single eruptions of basaltic magma with volumes of up to 6000 km^3 are known (McDougall, 1962; Feoktistov, 1976; Williams & McBirney, 1979).

Actually, MMP is not a recent fad; proposals of new magma surges can be traced back to Kuschke (1939). When one sees a radical change (a reversal or the appearance of a Doppelgänger phase) in the cumulate succession, it is only natural to invoke a new kind of magma. It is seldom thought that this new magma (mixture of liquid and crystals) might have been generated in the magma chamber itself, with no help from the mantle. Here I propagate the idea that the new magmas were products of "inside" events resulting from magma/wall rock interaction.

In many well-studied intrusions the possibility of MMP has been considered but rejected, and with good reason. In Stillwater, Hess (1960), Jackson (1961) and recently Loferski and co-authors (1990) concluded that the magma chamber was filled about to its final volume before significant crystal accumulation, and the "oscillations" (layering, reversals) were due to mechanisms operating inside the magma chamber (Hess, 1960). There is a continuous iron-enrichment trend through the famous J-M reef, from footwall to the hanging wall, with no evidence for a new magma pulse at that important reversal (Bow et al., 1981). A variant of the MMP hypothesis maintains that a new pulse of a heavy anorthositic magma was injected beneath a buoyant old magma evolved from an ultramafic magma (Irvine et al., 1982). The Pb isotope studies indicate very convincingly that the Stillwater magma chamber was filled to capacity before any essential cumulus sedimentation (Wooden et al., 1991).

At Bushveld the old ideas of MMP have been redesigned from time to time (e.g., von Gruenewaldt, 1979; Sharpe, 1981). How was it then that the old field geologists were not able to see the MMPs? Cameron and Emerson (1959) did not find MMP as satisfactory explanation for the innumerable reversals, nor did Cameron (1969, 1970) find signs of MMP in the Transition and Critical Zones, the favoured stratigraphic interval for MMP. Cameron and Desborough (1969) did not find any breaks in the px-pl compositional trends at ore intervals.

Neither did Ferguson (1969) find evidence for MMP in the Bushveld intrusion; besides, he had the early brilliant insight of the mock reversals which appear if cumulus phase compositions are not singled out from intercumulus compositions (op. cit.). Ferguson and Botha (1963) ascribed cumulate autoliths to internal processes (e.g., slumping), not to MMP.

The present situation at Bushveld is perplexing. There are UA advocates (ultramafic magma followed by an anorthositic magma), P people (for intermittent primitive magma pulses) and traditionalists (no MMPs). The various UA models invoke entry of an anorthositic or pl-saturated magma at the Merensky level, not a hotter, opx-saturated magma as postulated by some others (e.g., Hatton, 1989 and references therein); the P model denies new anorthositic magmas and support MMPs of primitive liquids in the upper Critical Zone (Eales et al., 1986, 1990 and references therein). The traditionalists cannot see any signs of the MMPs at postulated levels (Mitchell, 1990; Scoon & Teigler, 1994), and conclude that the Lower and Critical Zones formed from a single magma (McCarthy et al., 1984), with no evidence in favour of a new anorthositic magma pulse (op. cit.). Oxygen isotope studies have not furnished evidence of MMP, but rather indicate that cryptic and modal layering is produced by processes internal to the magma chamber (Schiffries & Rye, 1989).

In the Skaergaard intrusion the cumulates crystallized from a single, homogeneous parent magma (Hoover, 1989). There are no signs of a new magma pulse being in any way involved with the formation of the newly found PGE-Au-enriched sequence (Bird et al., 1991).

Acceptance of MMP requires some fundamental difficulties to be overcome. First, even in the well exposed and thoroughly studied intrusions (e.g., Muskox, Stillwater) the cumulus sequences are undisturbed, without definite manifestations of repeated magma influxes having broken through cumulates into the magma chamber (Jackson, 1961).

The other difficulty is that, provided that the base of the magma chamber was at or below the liquidus temperature (Jackson, 1961), the arrival of a new pulse would have caused massive, rapid crystallization (see Fig. 30, the curve with the positive slope). The common notion that the intersection of the adiabatic gradient and the liquidus gradient favours crystallization at the bottom of the magma chamber (see e.g., Jackson, 1961) implies that the uppermost part of the magma was a superheated liquid. Observations on mafic lavas show that they always contain phenocrysts, i.e., they are not superheated (Marsh & Maxey, 1985). Applied to intrusions, this would mean – remembering the relation between the liquidus and adiabatic gradients – that they should crystallize with the low temperature cotectic assemblages at the bottom and the first liquidus phase on top. This has never happened. However, taking supercooling (which may be hundreds of degrees in salic systems; see Lofgren, 1974a) into account, it follows (Fig. 30) that only the degree of supercooling increases downwards. Due to heat loss through the roof, the other part of the maximum degree of supercooling is located at the top of the magma chamber. The temperature is nearest that of the true liquidus is below the roof zone. Naturally, this scenario is worse still as regards the MMP models. Be that as it may, apart from temporary chill linings, most of the crystallization and other phase separation took place in the cool roof area.

In the mafic-salic mixing zone local and temporal superheating and supercooling are both possible, as discussed later.

As the MMP are mostly inferred from, and placed at, the reversals in layered sequences, it is only proper to point out what the old scholars noted: That the compositions of magmatic minerals depend on the amount of postcumulus growth (Ferguson, 1969; Cameron, 1970). More recently Barnes (1986) and Wadsworth (1986) warned against this fallacy; Barnes (op. cit.) called it trapped liquid (shift) effect,

while Wadsworth (op. cit., p. 594) formulated its practical consequences mercilessly: "Any attempt to interpret cryptic variations in terms of original cumulus mineral compositions are [sic] doomed to failure." The conclusions drawn by Barnes and co-workers (1990) cast serious doubt on the rationale of analysing cumulus minerals. In the case of Merensky Reef, Cawthorn (1995a, b; 1996) showed that when the trapped liquid shift effect is adjusted, the compositional reversal vanishes – and with it the need to appeal to MMP.

The fourth idea, promoted mainly by Elliott and co-workers (1982) and Boudreau and co-workers (Boudreau 1988, 1993; Boudreau & McCallum, 1986; Boudreau et al., 1986; Boudreau, 1988, 1993), concerns the evolution of the intercumulus liquid. Fluids, the reasoning goes, separated in the intercumulus space, ascend through the permeable cumulate pile and interact with the magma. Cl-rich fluids are thought to be important in transporting and concentrating the PGE (Boudreau et al., 1986; cf. Karpinskii, 1926). The preferred sites of gaseous intra-intrusive "fumaroles" are the potholes at about the level of Merensky Reef, but no conclusive evidence for their existence has ever been found (Cawthorn, 1995b).

I will deal with the Cl question in more detail when discussing the petrology of the Keivitsa intrusion. Summarizing the observations made at the Akanvaara, Koitelainen and Keivitsa intrusions, I can now state that even at modest pressures Cl does not degas but is fixed in cumulus and postcumulus minerals (apatite, amphibole, biotite-phlogopite). In fact, the basaltic and intermediate magmas are, and remain, strongly undersaturated in Cl and act as a sponge for the element. The occurrence of boron-rich intercumulus material, apparently of primary origin, in Akanvaara and Koitelainen intrusions (see, e.g., Fig. 8) implies that, even at very low pressure, degassing of a water-rich fluid was not possible (see Chorlton & Martin, 1978). Moreover, addition of boron can easily split the fractionated residual liquid or intercumulus liquid into two stably immiscible liquids (see Levin, 1970)

Melting of country rocks

Glassy, acid rocks are ideal for melting, as their melting needs only heating to the melting point (but no heat of melting for the glassy part!). In fact, their heating first induces crystallization, and, as a result, vast amounts of latent heat of crystallization are released. It would be still better if these rocks were preheated, as at Sudbury (Naldrett et al., 1986). Most of the material of the Sudbury granophyres (micropegmatite") derived from felsic glassy rocks (Stevenson & Colgrove, 1968; see also Faggart et al., 1985).

In the normal case of crystalline roof and floor rocks, melting occurred both early and to late in the crystallization history, corresponding to the early fluid-overpressure melting of the floor and water-saturated melting of the roof rocks, and late-stage dry melting of the granitic constituents of the roof. At the time of dry melting there was no melting in the floor rocks, because they were progressively insulated from the heat transferred from magma by the growing cumulus pile and intercumulus melt. The monotonous gabbroic cumulates of the Main Zone accumulated during the interval between the two melting episodes, with only slight signs of contamination.

In country rocks that were water-saturated at the time of the intrusion, the heating resulted in fluid overpressure, with P(fl) far exceeding P(lit). The build-up and sustenance of fluid overpressure, up to 3.5–4 kb (Williams & McBirney, 1979; Litvinovskii et al., 1990), was limited only by the tensile strength of the wall rocks (Smith, 1969) and their permeability to vapour transfer (Litvinovskii et al., 1990).

It is easy to imagine that water-saturated porous or fractured rocks that got trapped below the intrusion provided ideal conditions for the build-up of fluid pressures and, hence, early melting (see Fig. 30, the left hand curve). I ascribe the large-scale early melting of the floor rocks below the Koitelainen intrusion to fluid-overpressure melting of fractured, water-saturated, low-melting point granitoids. The effect was augmented by the rough architecture of the original base contact, providing a large contact surface favourable to melting and retention of pressurized fluid pockets. These fluid-enriched melt pockets were the autoclave-founts of the quartz monzonite diapirs (see geological map, Appendix 3).

The rough base contact of the Kemi intrusion (see Alapieti et al., 1989) may have resulted from hydraulic-exploside excavation of the floor rocks at the site of thick chromite accumulation (pinpointed by the proposed feeder, Mutanen, 1989b, Fig. 2; Elo, 1979), followed by their fluid-overpressurized melting and subsequent deportation by floating as loosened footwall blocks and anatectic melt through the main magma up to the roof. This created an ideal basin for early chromite accumulation, while the acid emulsion accumulating at the roof was an ideal habitat for chromite breeding (see Irvine, 1975a, b; cf. Alapieti et al., 1989). There is no need to invoke a primitive, new Cr-rich magma pulse at Kemi, as the composition of chromite (op. cit., Table 2) indicates crystallization from a magma with < 10% MgO (see Maurel & Maurel, 1984); if salic contamination was involved the MgO in magma was << 10% (op. cit.). The configuration of the base contact of the Konttijärvi intrusion, as depicted by Iljina (1994, Fig. 44) Could represent a Still of the break-up of the floor.

Apart from this kind of fluid-overpressurized anatexis, the melting of country rocks was fractional and took place in two stages separated by a wide temperature interval (Presnall, 1969).

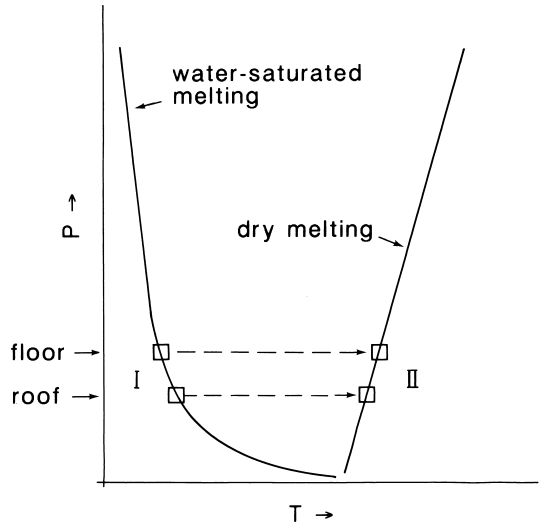

Fig. 30. Melting of country rocks above and below a layered intrusion. I – first melting, II – second melting. See text.

The first stage involved the breakdown of hydrous minerals (e.g., Wyllie & Tuttle, 1961; Patchett, 1980) and produced only a modest amount of liquid (see Vielzeuf & Holloway, 1988). An interesting property of the P-T melting curves (Fig. 30), when applied to layered intrusions, is that as the decrease in temperature away from the intrusion contacts roughly parallels the decrease in liquidus temperature during wet melting of the floor and dry melting of the roof rocks, thick zones of melt were produced almost instantaneously in the floor during the early melting phase, and likewise in the roof during the late, dry-melting phase (Mutanen, 1992). This has important corollaries as regards magma contamination. From the left-hand curve in Fig. 30 one can be deduce that the first breakdown of OH-minerals produced very little melt at the roof. Moreover, as the melting curve and rock temperature curve have opposite signs of slope, there was no instantaneous roof melting of greater thicknesses. However, as I will demonstrate later in the Keivitsa case (Fig. 49), mechanical disintegration of hydrated pelitic rocks played an important role at the early stage at Koitelainen, too.

The first high-aluminous schists in the roof to melt were boron-rich layers (see Mutanen, 1989b, p. 44). The addition of boron lowers the eutectic of the water-saturated granite composition by 125°C (Chorlton & Martin, 1978). Thus, depending on the vertical distribution of the lowest-melting point sediment compositions, incipient roof melting may have occurred simultaneously at many levels and the melt fraction at those levels may have been very large (Holtz & Johannes, 1991). Even before the experimental study of Chorlton and Martin (1978) the fluxing action of boron was noted in the field (e.g., Ashworth, 1976).

By its very nature, boron is concentrated in residual liquid; indeed, high boron concentrations have been noted in the granophyre of the Dillsburg sill (Hotz, 1953). The occurrence and effects of boron in mafic magmas deserve more studies (I have not found any). High boron concentrations (up to 1000 ppm) have been reported from the Varena Ti-Fe deposit (Kazimieras, 1996). Tourmaline, apparently as a primary constituent, abounds in many parts of the Koivusaarenneva Ti-Fe-V deposit, western Finland (my own observations, 1972).

I must remind my readers here that the melting in the roof advanced upwards, after the complete solidification of the mafic (but still hot) intrusion (Kadik, 1970). The melted, boron-rich layers high above the granophyre and also the Cr-enriched upper margin of the granophyre of the Koitelainen intrusion actually represent this belated melting.

Sandstones and shales generally contain excess silica and alumina in relation to a eutectic granite melt. The discussion that follows deals mainly with pelitic rocks, these being the most common metasediments associated with layered intrusions.

The refractory residue material after fractional melting is impoverished in silica and enriched in Al, Mg and Fe (Bowen, 1928; Wyllie & Tuttle, 1961; Smith, 1969); also, mg#, Cr, Ni, Co and V increase in the residue (Vielzeuf & Holloway, 1988; Evans, 1964). Thus the contamination of magma by residue phases may give rise to reversals that mimic the effect of new, primitive magma pulses. Moreover, the ferric-ferrous ratio increases in the residue (Vielzeuf & Holloway, 1988), which, when brought to mafic magma, would promote the crystallization of chromite and magnetite. The effect of melting and contamination by pelitic material adds Si, Al, Cr and increases the ferric-ferrous ratio of the magma, all of which are good for the crystallization of chromite (Irvine, 1977b).

The refractory phases were dense minerals, and eventually they got through the granophyre melt to the mafic main magma. Even plagioclase settled through granophyre magma (Roobol, 1974). Participation of refractory phases in the magma contamination is inevitable, and although solitary grains are doomed, by reaction, to annihilation, the results are obvious (Bowen, 1928). Pelites, containing typical refractory minerals of the fractional melting (sillimanite, mullite, cordierite, spinel, corundum, staurolite), have been found preserved as big xenoliths in most layered intrusions (e.g., Hall & Nel, 1926; van Zyl, 1950; Worst, 1960; Cameron & Desborough, 1969; Willemse & Viljoen, 1970; Kozlov, 1973; Molyneux, 1974; Hor et al., 1975; Myers, 1975 Page, 1977, 1979; Buchanan & Rouse, 1984; see also Sharkov & Sidorenko, 1980, Fig. 40).

In the Lukkulaisvaara intrusion rocks rich in staurolite and corundum are associated with crustal metals (Pb, Mo, Re, Ag, Sn) and PGE (see Barkov et al., 1996a); these I interpret as representing an aluminous refractory contaminant. Similarly, the peculiar Fe-rich, aluminous layer at an important reversal boundary in the Penikat intrusion (see Halkoaho et al., 1990) I interpret as representing a cumulate of undigested detritus of xenolithic pelitic material from the original roof. This conjecture is supported by the coincident P-Zr anomaly (see Halkoaho, 1994).

Although the occurrence of aluminous refractory xenolith material is sometimes accred-

ited to assimilated aluminous material, as at Fiskenaesset (Herd, 1973; Windley et al., 1973), it is surprising how little attention geologists have paid to the "fate of argillaceous material" (Willemse & Viljoen, 1970) since Bowen (1928) showed the possibility and consequences of aluminous contamination.

The granophyre of the Koitelainen intrusion represents about 70% melting of the schists, and the undigested residue consisted mainly of alumina. As the excess alumina is not found in the granophyre, it must have been carried down to the main magma. At Koitelainen this excess phase was garnet, which had already been formed as a high-temperature contact metamorphic mineral. The garnet is a "forbidden" (high-T) mixture of almandine and grossular (40–47 mol% grossular, anal. by Tuomo Alapieti). Interestingly, such garnets occur in the intercumulus of the Stillwater intrusion (grossular-pyrope, Jackson, 1961) and in plagioclase crystals in the Porttivaara intrusion, Koillismaa group (Mäkelä, 1975). The garnet seems to be a stable, high-T mineral in high-Ca, high-Al environments (Nemec, 1967; Firsova, 1980). At Koitelainen, in one granophyre outcrop garnet still occurs as resorbed cores of plagioclase crystals (Fig. 33; Mutanen, 1989b, p. 44).

Generally, when a component is added to a melt, the composition of the melt shifts into the field of the phase with the highest concentration of the added component. Thus, addition of alumina shifted the melt composition into the primary field of plagioclase. In fact, the plagioclase-to-garnet reaction is widely known from eruptive rocks (e.g., Edwards, 1936; Oliver, 1956; Davis, 1968; Gelman, 1980; Popov et al., 1981). A refractory garnet would explain many trace-element (REE, Zr) and Sm-Nd isotope anomalies in the cumulate successions (e.g., the REE-Zr anomaly at the J-M reef of Stillwater; Lambert et al., 1985).

Evidently, the garnet (and possibly other aluminous phases) that passed to the main mafic magma reacted similarly with melt to form plagioclase. The excess alumina from melted pelites thus incorporated in the mafic magma would shift its composition into the plagioclase phase field and give rise to anorthositic cumulates (Mutanen, 1989b, 1992). The contribution of alumina from pelites to anorthosites has been inferred or indicated elsewhere (see e.g., Hall & Nel, 1926; De Waard, 1968; Philpotts, 1968; Schwellnus, 1970; Willemse & Viljoen, 1970; Herd, 1973).

The addition of alumina provides a feasible solution to the anorthosite problem of the Stillwater intrusion. Compared with the noncumulate rocks (internal microgabbros and other non-cumulate rocks) reputed to represent the composition of fractionating magma (Page, 1977), the evolution of cumulate composition swerves towards Na-Al enrichment and, thus, the proportion of plagioclase cumulates increases (op. cit.). One of the biggest problems at Stillwater is the source of the plagioclase of the thick anorthosite layers, which have no mafic counterlayers (McCallum et al., 1980; see Lofgren, 1974b; Mutanen, 1974; McBirney & Noyes, 1979). The magma mixing model advanced by Irvine (1975d) does not apply to the Stillwater intrusion because of the exorbitant amounts of magma volumes needed (McCallum et al., 1980).

The sulphide liquid remaining after the sulphide-rich crustal rocks had melted was also an insoluble residual phase in the anatectic salic melt (see Barker, 1975). In the Keivitsa intrusion the false ore sulphides approach the sulphide composition of the pelitic wall rocks. If the mafic main magma was sulphide-undersaturated, the exotic sulphide liquid droplets would have re-dissolved if their trajectories brought them into the undersaturated main magma.

In siliceous sediments quartz may remain as a residual phase after partial melting of the rocks. In the granophyres of the Koitelainen intrusion occasional big quartz grains clearly represent the siliceous residue. In the southeast of the intrusion quartz amygdales occur in par-

tially melted ("granophyrized") acid lavas. In the Sudbury granophyre xenocrystic quartz grains occur in a position similar to that of the Koitelainen granophyre (Stevenson & Colgrove, 1968).

As well as melt-depleted pelitic hornfelses, refractory mafic and ultramafic xenoliths (komatiites, pre-Koitelainen gabbros, basalts, basaltic tuffs) are common. Naturally, they sank into the magma in their appropriate stratigraphic order and, thus, their relative position in the igneous sequence define their stratigraphic order in the melted supracrustal sequence. In principle at least, it is possible to map the refractory roof rocks that have existed above the present erosion surface.

As xenoliths were loosened during the melting of the roof, their concentration at certain levels (see Cameron & Desborough, 1969) designates the episodes of roof melting. In the Koitelainen intrusion xenoliths are concentrated at the base of the MZ and of the magnetite gabbro unit, but some komatiitic xenoliths have been intersected by DDHs between UC and magnetite gabbro. Large basaltic xenoliths occur in the south and northeast of the intrusion (see the geological map, Appendix 3). At times of roof melting the sinking xenoliths augmented the effects of contamination by stirring the salic roof melt, and pierced the salic/mafic melt boundary (DePaolo, 1985; Campbell & Turner, 1987). Sinking further down into the main magma, the xenoliths butted acid contaminant melt beneath and dragged it in tow.

Granophyre caps are generally thought to represent crustal rocks melted by underlying intrusions (e.g., Daly, 1914; Irvine, 1970a, b; Stevenson & Colgrove, 1968; Wager & Brown, 1968; Narldrett et al., 1972; Kuo & Crocket, 1979; McBirney, 1975; McBirney & Noyes, 1979).

Contrary to a perception common among non-specialists, it is not the heat of the magma but the latent heat of crystallization which causes the surrounding rocks to melt – with astonishing capability: granophyres may comprise up to one quarter or one third of the thickness of the whole intrusion (Vakar, 1967). Kadik (1970) calculated that a crystallizing magma layer 10 km thick (about the thickness of the Bushveld layered series) can melt up to 1.6 km of roof.

At Koitelainen the granophyre cap is regarded as representing the buoyant lumped pool of anatectic floor and roof melts, after removal (sinking) of residual phases.

The composition of the quartz monzonites bodies piercing the LZ cumulates (analyses 5–11, Table 3) is similar to that of the granofelses and quartz monzonite bodies near the base contact of the Bushveld intrusion (see Willemse & Viljoen, 1970). The composition of the anatectic melt was initially close to the minimum melting (granitic) composition of silicic crustal rocks. This, of course, was prone to superheating (McBirney, 1980; Sigurdsson & Sparks, 1981; Campbell & Turner, 1987), but, as in convection (to be discussed soon), feedback regimentation (according to the Le Châtelier principle) fought against superheating.

Smith (1969) and Presnall (1979) noticed that the compositions of granophyres, or even those of their salic part, do not correspond to the granitic ternary minimum, but lie closer to the feldspar join in the system Ab-Or-Q. I still adhere to my earlier proposition (Mutanen, 1989b, 1992) that the granophyre melt checked its superheating by digesting a portion of the residue phases from partially melted and mechanically disintegrated pelitic rocks and by giving silica to the orthopyroxene. This occurred in the only region where massive crystallization of a magnesian, silica-rich orthopyroxene was possible – in the mingling-mixing zone between the granophyre melt and the main magma.

In the crystallization of orthopyroxene the silica (from the ample salic stock) combined with the Mg (from the equally ample mafic magma). In terms of the ternary Ab-Or-Q sys-

tem both the reaction of residue phases (to plagioclase) and the crystallization of orthopyroxene drove the liquid composition from the ternary minimum towards the Ab-Or base. This also implies a simple solution to the syenite problem, namely, that there are igneous rocks whose composition hangs precariously on the high-T ridge in the larger ternary system, kalsilite-nepheline-silica (see Nolan, 1966; Morse, 1969a; MacKenzie, 1972). Thus, the association of syenites and trachytes with eruptive rocks of basaltic compositions (Daly, 1914; Glazunov, 1979; Morse, 1969b) becomes understandable. MacKenzie (1972) anticipated that "a mafic phase" must control syenitic rock composition.

As Na could enter plagioclase, the salic composition path gradually veered, after the entry of cumulus plagioclase, towards the orthoclase corner (see Morse, 1969b). In the potassic (K_2O 7–11%) syenitic granophyres of the Sierra Ancha (Smith & Silver, 1975) this evolution led the melt to its natural compositional destiny.

Whether the granophyre melt checked superheating by reacting with residual phases or by exchanging components with the underlying mafic magma, the compositions of the salic and mafic melts approached the solvus of truly immiscible silicate liquids from opposite sides (see Roedder, 1951; McBirney, 1975). At this stage, contamination was by residual phases only. Thus, while olivine cumulates (associated with selective contamination by H_2O, K_2O and Cl) and pyroxene cumulates (associated with regimentation of the superheating of the salic melt) characterize the early contamination episode(s), cumulates enriched in, or composed alamost entirely of residual phases of melting (anorthosites, chromitites) prevail in the upper part of the Koitelainen and Akanvaara intrusions.

Convection

Convection is by far the most effective mechanism for transferring the latent heat of crystallization to the roof (Jackson, 1961) and essential for its melting (Kadik, 1970; Irvine, 1970b). Convection also maintained the mixing of the mafic and salic melt, and convective flow was the "public transport system" for cumulus crystals. The mafic main magma kept the overlying salic melt in vigorous convection (Sigurdsson & Sparks, 1981). This resulted in thorough homogenization of the roof melt layer and increased its agressiveness by transferring latent heat from the crystallizing mafic magma to the still unmelted roof. Moreover, convection was both the cause and effect of crystallization in the upper part of the magma chamber.

Basically convection is not a thermal but a mechanical (hydrodynamic) phenomenon. Vertical convection in intrusions is caused by density differences in magma, and these in turn to local differences in either the composition, temperature or density (mass per unit volume) of suspension. An early array of **thermally driven convection** was formed above the feeder (the "stove action" by Morse, 1969a; 1985). This stove action caused strong melting above the feeder (Morse, 1988). As I see it, this dome of salic melt above the sinking centre (the sinking produces the funnel-shaped form typical of layered intrusions, as at Kiglapait, Great Dyke, Muskox and Skaergaard) was displaced sidewards by the weight of the roof and further upwards along the inclined beds. The end result would be exactly like that in the Muskox intrusion (see Irvine, 1975a, Fig. 2), where the granophyre is either thin or lacking in the centre, thickens sidewards and seems to be escaping from the intrusion in the flanges. Evidently, a simple kind of convection like this operated in the Keivitsa intrusion.

There is isotopic evidence for early, vigorous single-phase (thermally driven) convection homogenizing the magma volume very effectively (Stewart & DePaolo, 1989).

The most common type of convection in intrusions, however, was **two – phase convection** (Morse, 1969a, 1985, 1986, 1988), which often developed into a concentrated current, the density flow. In principle the two phases may consist of crystals and liquid, two immiscible liquids, etc.

In reality many density flows were complex multiphase suspension-emulsion systems consisting of crystals and mingled liquid emulsions. The case depicted lower left in Fig. 20, for instance, probably represents a suspension-emulsion that consisted of cumulus crystals, sulphide liquid and a salic silicate liquid mingled with mafic silicate liquid. Thus, the system was actually a quadri-phase system of two mingled silicate liquids, an immiscible sulphide liquid and crystals.

The concept of **density flows** in magmas may be dismissed as pure speculation, as we do not know the actual suspension particle densities (amounts of crystalline mass per unit volume of melt). What we do know is that magmas carried suspended crystals before to settling (Rice & Eales, 1995), and, depending on the density of cumulus phases, even small amounts of suspended crystals had a significant effect on the magma density (op. cit.). In fact, density flows are inevitable in crystallizing mafic magma chambers (Hess, 1960).

There is evidence from both cumulates and experiments that the suspension densities were so high and crystal settling so massive that even light-weight xenoliths were buried against their will in cumulates (acid gneiss xenoliths in the Skaergaard intrusion, Wager & Brown, 1968; quartz xenoliths in Duke Island ultramafic cumulates, Irvine, 1978a; experiments by Irvine, 1979). I have already described several cases from Koitelainen where pockets of salic granophyre melt were trapped in chromitites, anorthosites or even, once, in massive sulphide. In fact, the salic intercumulus of orthopyroxene cumulates and the potassic intercumulus of the chromitite layers of Akanvaara and Koitelainen intrusions represent lightweight carrier liquids of the density flows, buried along with heavy cumulus crystals.

Almost all cotectic crystal assemblages are heavier than melt (Morse, 1979a). The density flow originates and develops as a labile density inversion at the site of crystallization. When the supporting liquid loses its tenacity, density flows surge downwards (or upwards) as suspension plumes (Hess, 1960; Morse, 1969a; Brandeis & Jaupart, 1986).

The simplistic vision of crystals settling through magma has impeded realistic understanding and utilization of the original cumulus concepts (see Morse, 1985). It is important to realize that the settling velocities of individual cumulus crystals are far smaller than the velocities of density flows (Hess, 1960). It was early noticed that the crystals of various cumulus phases are not hydraulic equivivalents, and thus, instead of having been settled gravitationally through the magma, must have deposited from density flows (Jackson, 1961).

Wager and Brown (1968) proposed that cumulus crystals settled from a decelerating density flow. I think, however, that in many cases settling is aided by the fact that crystallization of cumulus minerals produces a lighter residual liquid (see McBirney & Noyes, 1979). This holds good especially in contaminated environments, where the density contrast between mafic cumulus silicates (say, olivine) and the residual liquid is great (see Irvine, 1975c).

Thus, paradoxically, in density flows the density of the carrier liquid is lower than that of the mafic magma. The flow moves only because of the mass of the suspended crystals. An extreme case of this phenomenon is the suspension of chromite in a salic liquid, a topic I will return to later. When the density flow sweeps along the bottom of the magma reservoir, heavy crystals are easily settled and so

separated from the carrier liquid. The latter, relieved of its load, ascends to the roof. I suggest that this is the dominant mechanismn for the formation of ultramafic monocumulates; fittingly, though paradoxically, the proportion of "granitic" trapped liquid is greatest in these cumulates.

It has been proposed that convection is continuous (Irvine, 1979). Usually, however, it is conceived as an intermittent (Brandeis & Jaupart, 1986; Francis, 1994), even periodic, process (Hess, 1960; Wager & Brown, 1968; Naslund, 1984). Jackson (1961) depicted the process as a **convective overturn** of the magma chamber. Several feasible models have been presented to explain intermittent or periodic self-damping convection (Jackson, 1961; Morse, 1979a; Brandeis & Jaupart, 1986). Koyaguchi and co-workers (1990) showed empirically that a suspension may experience spontaneous, periodic overturns even at very low suspension densities.

In the Koitelainen intrusion I envisioned the following self-regulating feedback mechanism (somewhat modified from Mutanen, 1992): With fractionation, concentrations of Fe and fluxes (H_2O, K_2O, P_2O_5, Cl, F, B, Ti, V) increased in the residual liquid. This resulted in a decrease in viscosity, whereas the fall in temperature (which tends to increase viscosity) along the cotectic px-pl plateau was negligible (Yoder & Tilley, 1962). The lowering of viscosity boosted convection, which increased heat loss through the roof and mingling-mixing between the buoyant roof melt and the convecting mafic magma. The mixing augmented crystallization. The thickening of suspension launched the density flow down to the floor, along with increased crystal settling from the hybridized, lower density carrier melt. The density flow forced an upward ebb of the displaced liquid (Morse, 1988). The density flow itself, rid of some of the load that had settled as cumulates, was buoyed back to the roof, and so on. The dampening began when the mingling at the salic-mafic magma contact and the separation of silica-poor crystals (relative to the breeding liquid) increased the silica content of the hybrid liquid and the proportion of suspended crystals, both of which increased the viscosity of the magma suspension. This led to the displacement of the path of the density flow downwards to a more mafic (and less viscous) magma with a smaller amount of suspended crystals (towards the Sargasso Sea of the toroid core; see below). The dampening was restrained by the inertia of the toroidal flow system; thus, there probably never was a simple, one-stage overturn of the innards of the magma chamber.

There are indications, that the density flow sweeping along the floor was channelled into concentrated, even turbulent, streams, resulting in **magmatic erosion** and formation of funnels (e.g., Jackson, 1961; McBirney & Noyes, 1979; Morse, 1979a; Page, 1979; Myers, 1985; Ireland, 1986). Schmidt (1952) explained the potholes of Merensky Reef, Bushveld, by turbulent magma currents. The magmatically eroded mesa topography of Merensky Reef (Viljoen et al., 1986a, b) and the sub-UC surface of the Koitelainen intrusion both bear strong evidence of differential magma current erosion.

Observations from the Akanvaara and Koitelainen intrusions, e.g., the almost ubiquitous occurrence of igneous lamination and the presence in MZ gabbros of souvenirs from the contaminated roof melt of the intrusion (loveringite, salic intercumulus compositions, sodic cores in cumulus plagioclase crystals and the very coexistence of the hydraulically disparate cumulus silicates) indicate that convection, although continuous, was punctuated by accelerated bursts of convection. The most remarkable revolutions coincide with episodes of melting and accompanied density surges.

Crescumulate growth (see e.g., the UC outcrop map, Appendix 2) can be fed by a supercooled convecting liquid (Irvine, 1979), even by a turbulent melt (Mutanen, 1974); thus, crescumulate growth does not necessarily im-

ply that the magma was stagnant. It only implies constitutional supercooling (supersaturation; e.g., op. cit.; Lofgren, 1974a), possibly with prior superheating associated with magma mixing which destroyed all potential crystal nuclei.

With a suitable magma chamber geometry the exciting possibility of **toroidal acceleration** and ensuing erosion (Morse, 1988) emerges. The Keivitsa intrusion looks like a good example of a toroidal convection system.

The general autonomous iron-enrichment fractionation trend of the rest magma suggests that the main magma reservoir of the Koitelainen and similar intrusions was not much involved in, nor affected by, two-phase convection and associated contamination. This was the region between the basal part (with the highest degree of supercooling) and the contaminated top, where crystallization was realized. It was also the hottest (relative to true liquidus) part of the chamber. This calm region inside the convection toroid(s) is what I call the **Sargasso Sea** of the crystallizing layered intrusions.

Contamination

Contamination is often used, and the process even understood, synonymously with assimilation. In fact, wholesale mixing of magmas so that the contaminant becomes "similar" to the magma hardly ever occurs, and any models using such a presumption are "inappropriate", as pointed out by Francis (1994) and formulated in the same vein by others. Particularly in the case of selective contamination (selective diffusion; see Watson, 1982), but also in the case of contaminant-magma mixing with subsequent separation of crystals and the hybrid magma, contamination is not apparent in the cumulus assemblages or their compositions. This is because there are no high temperature "salic" cumulus minerals and because the suspended crystals have been separated from the carrier liquid.

Thus, in the case of contamination by, say, sedimentary alumina, chromium, sulphur and iron, or by exotic olivine detritus (Keivitsa), the contaminants are camouflaged in magmatic attire. Early or unexpected, Doppelgänger-like iron enrichment in the layered series might be a sign of contamination by a sedimentary material with a relatively high FeO/MgO ratio (see Barker, 1975; Tyson & Chang, 1978; Raedeke & McCallum, 1984; Buchanan & Rouse, 1984; Allard, 1986). The occurrence of inverted pigeonite in the Merensky Unit (Cameron, 1982) is almost incomprehensible if viewed as a product of normal fractionation. The effect of Fe contamination depends on the fractionation stage of the magma in relation to the Fe/Mg ratio of the contaminant (Evans, 1964); thus, in a late fractionation stage the addition of sedimentary iron may induce a reversal.

The added contaminants shift the field boundaries of the established primary phases, and so their effect is only **catalytic**. Particularly in lavas, in the absence of discernable, revealing minerals the contamination is shown only by the trace element and isotope characteristics (e.g., Thompson et al., 1982). In intrusions, though, contaminants were trapped in cumulates, and there the mineralogical evidence of contamination is visible practically everywhere to the vigilant eye.

Except for natural wear the stock of catalysts is inexhaustible in principle. In intrusions, natural wear includes the contaminant melt lost in melt inclusions and in trapped intercumulus liquid. Also, catalysts lose their effectiveness if the magma is deprived of feed (e.g., of the Mg needed in the catalytic production of olivine; see later). Eventually, magmatic catalysts may turn into an inactive form, as,

for example, when K_2O is bound to a salic melt phase immiscible with the late-stage Fe-rich liquid (Roedder, 1951).

Cumulates often reflect the oxidation state of the contaminant. Thus, sedimentary contamination may be seen in the increased ferric-ferrous ratio of the cumulates (e.g., Cameron & Desborough, 1969) or in their oxygen isotope composition (e.g., Schiffries & Rye, 1989). An increased Fe^{3+}/Fe^{2+} of the contaminant may induce crystallization of Doppelgänger magnetite and (or) ilmenite. The Keivitsa intrusion provides good examples of the effects of reduced carbonaceous contaminants.

Igneous bodies with a large surface-to-volume ratio, such as dykes or sheet-like layered intrusions are more susceptible to contamination than isometric intrusions (Thompson et al., 1982), but only if their solidification lasts long enough for melting and contamination to take effect.

The crustal geochemical signature imitates that of the purported metasomatized mantle enriched in crustal-like elements. During their residence in the mantle their unstable isotopes produce radiogenic isotope signatures not unlike those of the crustal rocks. There seems to be an ever increasing tendency to ascribe the geochemical freaks so common in layered intrusions to the geochemical characteristics of some peculiar regions of the mantle (e.g., Hamilton, 1977; Lambert et al, 1985; 1989; Amelin & Semenov, 1996). Even then, the crustal components are plain in the mineralogy and petrography of the cumulates, as readers will soon be able to read.

Contamination of intrusions by wall rock materials was first reported over 80 years ago (Daly, 1914). It is usually referred to as "local contamination" (e.g., Morse, 1969a), implying that the contamination had no larger, intrusion-wide effects.

Irvine (1970a; 1975a, c), however, presented a hypothesis of how the effects of **salic contamination** would shift the primary phase fields of liquidus minerals so that the evolution of magma would veer from the predictable cotectic route to the salic contamination path(s) of cumulus assemblages. The hypothesis provided feasible explanations for many observed successions of cumulate assemblages, for the genesis of super-cotectic ore cumulates (chromitites, magnetitites) and for sulphide liquid separation. Characteristic of the silicate path is crystallization of the most siliceous cumulus mineral, orthopyroxene, before plagioclase. This is the normal case in KOI-type intrusions of the Shield, in Finland, Russian Karelia and the Kola Peninsula (see, e.g., Lavrov et al., 1976; Lavrov, 1979; Sharkov, 1980).

Irvine soon questioned his own hypothesis (see Irvine, 1977a, b). It is interesting to note that when rejecting the hypothesis he apparently did not remember the salic droplets found in chromite crystals (Irvine, 1975a), which constitute very strong evidence for salic contamination.

Petrographic signs of salic contamination observed at Koitelainen, and finally, the discovery of the UC layer in 1977 led to re-interpretation and **rehabilitation of the salic contamination hypothesis**. The points of the hypothesis Irvine (1977a) thought were vulnerable turn out to be its strengths when it is realized that contamination was effective only temporally and locally, i.e., during strong convection, in a vertically resctricted mingling-mixing zone between the mafic magma and the buoyant salic melt. However local, the products of contamination were spread far and wide by density currents.

The weaknesses of the original hypothesis, according to Irvine (1977a), were, first, the prohibitively high mixing ratio of salic to mafic liquid needed to accomplish the salic contamination cumulus path, from olivine via orthopyroxene to the plagioclase-pyroxene cotectic (Irvine, 1975a), and second, the iron enrichment trend the magmas should not show if contaminated. In the following I present a solution to these problems.

The essence of the argumentation is as fol-

lows: In thick intrusions, contamination is episodic because of the episodic nature of the fractional melting (Fig. 30) and because of cyclic, self-damping convection (e.g., Jackson, 1961, and discussion above). Contamination is effective only during strong convection and, even then, in a vertically restricted mingling-mixing zone between the buoyant, viscous salic roof melt and the underlying mafic magma. This floating of the roof melt (e.g., Stevenson & Colgrove, 1968; Irvine, 1970b) and the kinetic difficulty of mixing the contrasting magmas (e.g., Gibson & Walker, 1964; Blake et al., 1965; Yoder, 1971; McBirney, 1980; Furman & Spera, 1985) generally guaranteed the isolation of the melts and the autonomous evolution of the mafic melt towards iron-enrichment. In fact, as will be shown later, the effect of contamination was to increase the Fe(tot)/Mg ratio in the mafic residual melt.

Vigorous convection in the granophyre melt (e.g., Sigurdsson & Sparks, 1981) and across the interface between the melts helped the contrasting magmas to mix. Another important factor which lowered the viscosity contrast and eased diffusion between the melts was the greater solubility of water in the acid melt when the melts were at equal temperatures (see Kadik, 1970).

Due to its convective homogenization, the granophyre melt, with all its large mass, regulated the mg# of the crystallizing mafic cumulus phases. Therefore, even before the stable SLI was reached the granophyre melt was de facto in equilibrium with the hybrid magma in the mingling-mixing zone, and the same phases with the same compositions separated from both magmas. Thus, the cores of original plagioclase crystals of granophyre were highly calcic, as inferred from the abundance of secondary epidote there.

If the melts are really (stably) miscible, the mixing zone may evolve from an emulsion to a homogeneous hybrid melt. However, the very crystallization processes evoked by salic contamination tend to restore the salic character of the contaminant melt; only its silica content will be lowered. In the Koitelainen intrusion magma mixing strongly augmented crystallization (see Irvine, 1975a), and the mingling-mixing zone was the preferred site for crystallization of cumulus minerals.

Without considering contamination, many scholars favour the cooler roof part as the environment of cumulus crystallization (Sampson, 1932; Cameron & Desborough, 1969; Umeji, 1975; Morse, 1979a; Naslund, 1984). Morse (1979a) thought, however, that crystallization took place largely in the downdraft and on the bottom, when the liquidus gradient (of the liquid of the density flow carrier melt) intersected the pressure gradient (= adiabatic gradient).

As shown earlier, silica was consumed to form orthopyroxene, and, as a result, the granophyre melt composition crept away from the ternary minimum towards the Ab-Or join in the system Ab-Or-Q.

In general, phases crystallized (separated) in the mixing zone were not stable, either compositionally or as phases, when brought into the hot mafic magma. If not protected by overgrowth zones or reaction armour, they adjusted their composition, and reacted with or dissolved in the mafic melt (e.g., Vogt, 1924; Sampson, 1932; Jackson, 1961; Cameron & Desborough, 1969; McBirney & Noyes, 1979).

Phases which were unstable in the main magma often survived in the density flow thanks to a familiar escort magma. Thus sulphide concentrations in the LZ are always accompanied by acid intercumulus material (Fig. 20).

The intercumulus oikocrystic plagioclase in ultramafic cumulates is more sodic than the cumulus plagioclase in the overlying cumulates. Ghosts of growth zones are occasionally seen in plagioclase oikocrysts, suggesting that the plagioclase crystallized in an alkali-contaminated hybrid melt and was then carried in a density flow charged with salic contaminant melt. Apart from rare euhedral ghosts, the pla-

gioclase failed to adapt to the hotter environment and dissolved. After mafic cumulus silicates, the sodic plagioclase crystallized from the salic intercumulus melt as oikocrysts around sparse cores. The mafic oikocrysts (e.g., those in mottled anorthosite) could be explained in a similar way: the original pyroxene was too rich in Fe to survive in the main magma, and most of the pyroxene crystallized at postcumulus stage.

The following is a reiteration and summary of the **contamination mechanisms**.

The magma was contaminated by selective diffusion (of H_2O, K, Na, Cl), outright mixing of the anatectic acid melt and mafic magma, and by digestion of (or reaction with) residual phases after partial melting of country rocks. The cumulus phases crystallized in the hybrid mixing zone between the main magma and the buoyant anatectic acid roof melt (Mutanen, 1989b, 1992). The plagioclase crystals, with sodic to potassic cores, patchy zoning and resorption, are not unlike those found in mixed lavas (see e.g. Fenner, 1926; Kuo & Kirkpatrick, 1982; Tsuchiyama, 1985, and many others). The melt inclusions in olivine (Figs 19, 20) and chromite (Figs 8 and 20) are likewise samples from the contaminated melt: the environment of – and requirement for – their crystallization. Acid and hybrid melt was dragged along in strong, crystal-laden downdrafts and buried in rapidly depositing cumulates (see Irvine, 1978a). The chromitites and pyroxenites are striking examples of strong density flows. The potassic intercumulus of the chromitites represents a hybrid melt enriched in K_2O by selective diffusion from acid melt; the "granitic" intercumulus of the orthopyroxene cumulates represents the raw acid melt (for analyses, see Table 5). The unholy cohabitation of olivine and quartz in some feldspathic olivine pyroxenites (which I have found also in Merensky Reef and the Keivitsa intrusion) indicates that the density flow was compositionally heterogeneous, carrying an incongruous mixture of crystals and contaminant melt (see also Sakuyama, 1981). Evidently the incongruous phases in a cumulate were formed in different parts of the chamber (see e.g., Gamble, 1979; Jackson, 1961).

The first stage and mechanism of the entry of contaminants into magma was **selective diffusion** of components between the country rocks and magma, and between the salic and mafic magmas in emulsion (Watson, 1982). The most important peculiarity as regards contamination is that the mafic melt is enriched in K, but Na diffuses, even against the concentration gradient, into the salic melt (op. cit.). The exchange can be seen as a means for the magmas to strive for thermal-compositional equilibrium. The effects of selective contamination are seen at the contacts of the intrusions. Thus, the mafic contact rocks are often enriched in potassium (e.g., Page, 1979; Konnikov et al., 1981; Huhtelin et al., 1989; my own observations in the Ylivieska intrusion, 1965–1968).

Even before Watson's experiments, selective contamination had been observed and described as such in field studies (Barker, 1975; Compston et al., 1968; Morse, 1969a; Pankhurst, 1969; Willemse & Viljoen, 1970). The selective transfer of H_2O into mafic magma has been documented in many intrusions (e.g., Morse, 1969a).

I ascribe the sodic enrichment in granitoids ("albitites") underlying the Kemi, Penikat and Koillismaa intrusions (respectively: Veltheim, 1962; Kujanpää, 1964; Ohenoja, 1968) and the sodic composition of the Keivitsa granophyre, to the selective transfer of Na, as demonstrated by Watson (op. cit.).

In general, the selective transfer of components obeys the order of solubility of accessory minerals in mafic/salic magma pairs (see Ringwood, 1955) or between immiscible silicate liquids (e.g., Rutherford & Hess, 1974; Watson, 1976; see also MacDonald et al., 1987). Selective contamination may have important consequences for isotope ratios (see e.g., Pankhurst, 1969; Tegtmeyer & Farmer, 1990; Stewart & DePaolo, 1992). The REE are

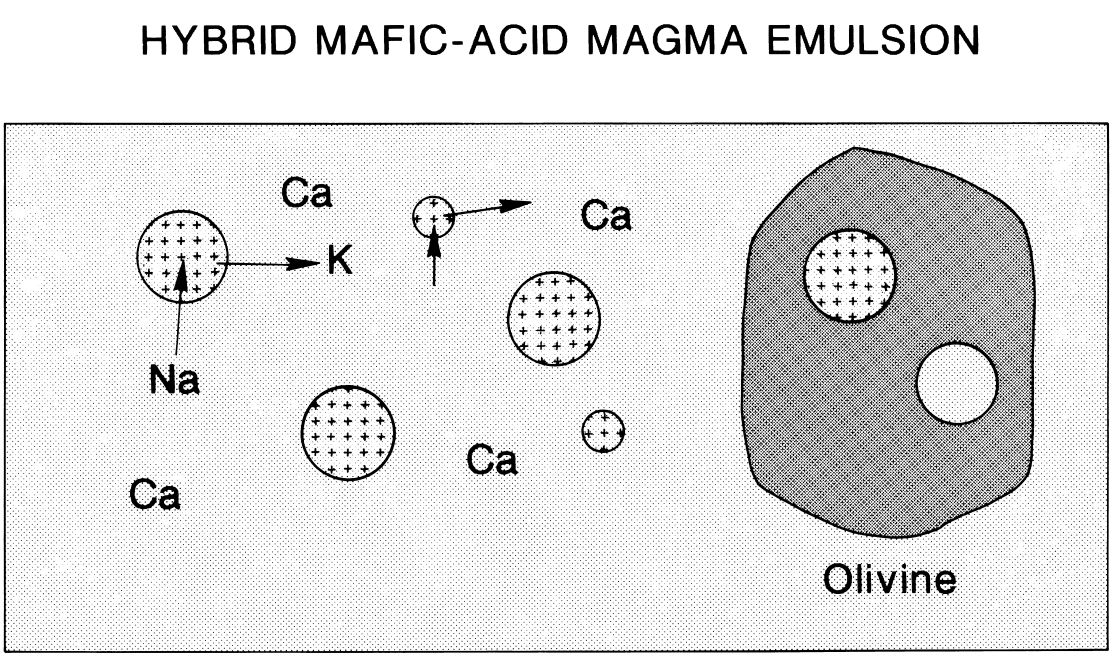

Fig. 31. Schematic presentation of the crystallization of olivine and trapping of melt inclusions in heterogeneous contaminated roof melt emulsion. Crosses – salic melt, grey matrix – basaltic melt.

enriched in the mafic melt (Rutherford & Hess, 1974; Watson, 1976) but the results of experimental studies to establish whether LREE are enriched in mafic or salic melt contradict observations made in nature (compare Gorbachev et al., 1994a and Vogel & Willband, 1978).

The early accumulation of thick olivine cumulates at the base of the Koitelainen intrusion, and also the recurrence of olivine in the peridotite – mixed rock, is ascribed to the effect of added alkalies, mainly K_2O (see Kushiro, 1973, 1974b). The addition of alkalies, which evidently took place by selective diffusion (Watson, 1982), shifted the melt composition into the olivine phase field. Thus, wholesale mixing is not necessary to drive the melt composition into the olivine phase field, as proposed by Irvine (1975a), and this alone removes the difficulty of the execution of the salic contamination cumulus path (Irvine, 1977a).

Melt inclusions, ubiquitous **in** cumulus **olivine**, are samples of the hybrid environment in which the olivines grew. The potassic-calcic inclusions and the sodic-silicic inclusions are the two end members of a trapped melt emulsion (for analyses of the inclusions, see Table 5). A schematic picture of the situation is shown in Fig. 31. The potassic melt is ubiquitous in chromite in the Koitelainen intrusion; the sodic inclusion analysed by Alapieti (1982; Alapieti et al., 1989) in chromite represent the sodic end member melt.

The Stillwater J-M reef contains abundant postcumulus biotite (Todd et al., 1982). Bow and co-workers (1981) suggested that the olivine reversal was due to a higher water concentration.

Besides phase reversals the alkalic addition may produce Mg/Fe compositional reversals in mafic cumulus minerals by increasing the ferric-ferrous ratio of the melt, the **alkalic – fer-**

Table 5. Electron microprobe analyses of olivine melt inclusions, wt%. Lower Zone dunite, Koitelainen. Analyst Bo Johanson.

	1	2
SiO_2	43.2	59.2
TiO_2	0.35	0.00
Al_2O_3	9.69	16.6
$FeO_{(tot)}$	7.09	1.90
MnO	0.05	0.03
MgO	27.10	11.1
CaO	3.34	1.16
Na_2O	0.7	8.83
K_2O	5.61	0.27
Cl_2O	0.45	0.11
Total	97.58	99.70

1 - K - Ca - type inclusion
2 - Na - Si - type inclusion

ric iron effect (Paul & Douglas, 1965; see also: Carmichael & Nicholls, 1967; Thompson, 1975; Pavlov & Dymkin, 1979; Luhr & Carmichael, 1980, Sack et al., 1980; Thornber et al., 1980). This is demonstrated by the case described by Maury & Bizouard (1974, p. 279), in which a pelitic xenolith in olivine basalt was surrounded by a hybrid melt. The hybrid glass and the basalt both contain olivine, but the olivine in the hybrid melt is more magnesian than that in the virgin basalt.

In an analogous manner the highly magnesian olivines in the Slieve Gullion intrusion were suspected to being xenocrysts (Gamble, 1979). The other details of that case (op. cit.) are revealing for the contamination idea advocated here: Rb and K concentrations are highest in the very same sample that has the high-Fo olivine; the Rb/Sr ratio is also extremely high (0.33) compared with that (generally < 0.027) in other high-magnesian cumuluates of the Slieve Gullion intrusion, and the Sr is very low (op. cit.): At the same time, the Cr and Ni values are higher than in any other samples. All this persuades me to think about the presence of trapped granitic material in the cumulate. Eales (1980) has described a similar anomaly (high K, P, Ti, Y, Zr, and anomalous low Sr) from an ultramafic cumulate in the Karroo complex, for which I propose the same solution as for the Slieve Gullion case.

The alkalic – ferric iron effect may be the cause of the unrealistically low apparent KD values of the Fe-Mg exchange distribution coefficients (liq/ol) obtained in some experiments (see e.g., Irvine, 1976, Fig. 61B), i.e., the mg# in liquid was increased due to alkali enrichment.

I ascribe the compositional reversals in the upper MZ, from pigeonite to orthopyroxene, to the alkalic – ferric iron effect in association with reinvigorated convections. Contamination is evident at the PGE-Au anomalous reef above the lowermost reversal.

Contamination is likely to change the D values of elements. Polymerization of melt structures increases the xl/liq distribution coefficients of transition metals (see e.g., Duke, 1976; Irvine & Kushiro, 1976; Irving, 1978; Campbell & al., 1979). Thus, as salic addition is prone to increase the $D_{Ni}^{ol/liq}$ value, contamination would produce Ni reversals coincident with phase reversals.

From all this it follows that salic contamination, possibly enhanced by a higher mg# derived from sediments (see Roeder & Emslie, 1970; Irvine, 1975a; Thompson, 1975: Morse, 1979b; Luhr & Carmichael, 1980), may be an important contributor to the compositional reversals commonly (if not always) present in layered intrusions. It is significant for the genesis of stratiform chromitites that such reversals are always associated with them (e.g., Bichan, 1969; Cameron, 1970; Jackson, 1970; Hamlyn & Keays, 1979). As shown by Cameron (1970) at Bushveld (see also Morse, 1979a), these reversals are not artificial (e.g., due to post-cumulus equilibration), but reflect real cumulus conditions.

I regard the evidence from inclusions as almost conclusive. Several other lines of evidence support the importance of contamination from wall rocks in layered intrusions. I have

already mentioned many of the macroscopic phenomena, such as xenoliths and trapped melt pockets. The most reliaable, unambiguous evidence comes from isotopic and trace element studies of layered intrusions in general, and Koitelainen and Keivitsa in particular (Huhma et al., 1996, b; Hanski et al., 1996), when combined with mineralogical and petrographical indicators.

Isotopic and trace-element studies of continental lavas usually show the presence of high amounts of crustal contaminant component(s) (e.g., Betton, 1979; Carlson et al., 1981; Palacz & Tait, 1985; Sun et al., 1989; Condie & Crow, 1990).

Even without isotope data, contamination in intrusions is revealed in the trace element geochemistry (e.g., Y, REE) of the intrusions (e.g., Hoatson et al., 1992). Isotopic (Sr, Nd, Os, Pb, S) studies of layered intrusions support either bulk contamination or, more commonly, selective contamination mechanisms (Al-Rawi & Carmichael, 1967; Barker & Long, 1969; Davies et al., 1970; Pankhurst, 1969; Moorbath & Welke, 1969). The proportion of radiogenic crustal matter seems to depend on the amount of trapped liquid (see Davies et al., 1970), in conformity with the petrography of the Koitelainen cumulates and the high Rb/Sr ratios of ultramafic cumulates in general (e.g., Hamilton, 1977; see also Lambert et al., 1985).

Nd isotope studies of the Shield show negative εNd(T) values for cumulates (Huhma et al., 1990; Amelin & Semenov, 1996; Mitrofanov et al., 1991). The ε-values in Burakovka intrusion show a clear negative trend upwards, as in the Kiglapait intrusion (DePaolo, 1985).

Note that all negative ε-values are from rocks compatible with the contamination cumulus path of Irvine (1975a); rocks with cumulus olivine and plagioclase, of the normal path, show higher, even positive, values (see Amelin & Semenov, 1996; Lambert et al., 1989). Note also that the lower microgabbros of Burakovka have posive (up to + 2.9) ε-values (op. cit.).

In general Nd, O, Pb, Sr and multi-isotope (Re-Os, Pb, Rb-Sr, O) studies show clear crustal signatures (Lambert et al., 1989; Schiffries & Rye, 1989; Harmer et al., 1995; Bichan, 1969), sometimes with a very high calculated portion of crustal isotopes (Dickin, 1981; Wooden, 1991; Chaumba & Wilson, 1997. In some cases the crustal contributions have been very high (e.g., Muskox, see Stewart & DePaolo, 1989). In Sudbury the amounts of crustally derived REE are so high that they make the mantle component, if there is any, practically invisible (see Faggart et al., 1985).

Even in intrusions where contamination is not particularly suspected, crustal contributions are revealed by isotopic studies, as in the Skaergaard intrusion (Leeman & Dasch, 1978).

As at Koitelainen, the geochemical signs of crustal contamination are more clearly visible in ultramafic than in mafic rocks (Francis, 1994). In a similar way, the chromitites of Stillwater have very high initial ε-values (Lambert et al., 1989); the contamination is also visible in the presence of radiogenic Os (Martin, 1989; Schiffries & Rye, 1989. The ε-values in the Stillwater intrusion, as in thick intrusions (e.g., Burakovka) in general are very variable (Tegtmeyer & Farmer, 1990). As a whole, the crustal signature is straightforward (McCallum et al., 1980; Schiffries & Rye, 1989; but cf Lambert et al., 1989)

The reversals are levels of “perestroika” of the isotope systems as well. Typical of Merensky Reef are rapid vertical changes across the Reef and lateral inhomogeneity of the initial Sr(i) values (Hamilton, 1977; Kruger & Marsh, 1982; Eales et al., 1993;

The ancient Sm-Nd model ages, T(DM), of the layered intrusions of the Fennoscandian Shield can be interpreted as a signature of an old crust (Iljina, 1994; Balashov & Torokhov, 1995; Balashov, 1996; Amelin & Semenov, 1996).

Apart from the geochemical and petrographic evidence for contamination already present-

ed and commented on from Koitelainen, the most assuring evidence comes from intercumulus mineral phases, daughter minerals of the melt inclusions and Doppelgänger cumulus phases. The daughter minerals usually presage the Doppelgänger phases. It often happens though that the true, "living" phase never actually materializes.

The common granitic and primary hydrous minerals and disequilibrium assemblages (olivine plus quartz) are most easily detected most frequently reported (e.g., Vermaak & Hendriks, 1976), but very rarely marvelled at. The list of accessory minerals found in intercumulus of ultramafic rocks compares with granitic pegmatites: apatite and monazite (Boudreau et al., 1986), chlorapatite, minerals of REE, Th and Sc-Y (Volborth et al., 1986), zircon and REE-rich titanite (Lambert & Simmons, 1983, 1988) in the Stillwater J-M reef, tourmaline and zircon in Merensky Reef (Vermaak & Hendriks, 1976), and baddeleyite and zirconolite in the Rhum intrusion (Williams, 1978).

The mineralogical marvels of Koitelainen, Akanvaara and Keivitsa to be discussed here have been described in earlier papers, too (Tarkian & Mutanen, 1987; Mutanen, 1989b). Chlorapatite, common to all three intrusions, will be treated later in Keivitsa section of this book. Now I shall look only at some aspects of loveringite.

Loveringite (see analyses, Table 2) is a collection of lithophile elements (Zr, Hf, REE, U, Th) and, in addition to optional Cr (Tarkian & Mutanen, 1987), is enriched in the transition metals (Ti, Fe, V) which in crystal fractionation are enriched in the tails. Loveringite, however, occurs as a cumulus mineral, mostly in orthopyroxene cumulates enriched in salic intercumulus, but also in gabbroic cumulates (Tarkian & Mutanen, 1987). This means that the "incompatibles" (Y, REE, Zr, Hf, U, Th) contained in the mineral behave like "compatibles" at the entry of the high-T loveringite. Crystallization of such minerals (apatite, zircon, baddeleyite) from magmas would strongly affect the crystal fractionation and trace-element fractionation models based upon it.

As crichtonite-group minerals seem to be stable under mantle conditions (Arculus & Powell, 1986), this type of phase may be a key to understanding the generation of low-Ti, low-REE (and low-LREE) basalts (Coish & Chursh, 1979; Weaver & Tarney, 1981; Thompson, 1982; Walker, 1984; W.E. Cameron, 1985; Arculus & Powell, 1986; Green & Pearson, 1986; Jolly, 1986; Duncan, 1987;

Loveringite reacts with the Fe and Mn of the intercumulus liquid to produce Mn-rich ilmenite (Lindsley et al., 1974; see Tarkian & Mutanen, 1987). REE-enriched ilmenite (op. cit.), Zr-enriched ilmenite (with up to 1400 ppm Zr in the Akanvaara intrusion) and Mn-rich ilmenites with exsolved chromite and baddeleyite (Mekhonoshin & Paradina, 1986; Naslund, 1987) may be relics of perished loveringite (see Tarkian & Mutanen).

Considering the slow diffusion of elements in magmas in general and in the salic intercumulus liquid in particular, it is highly unlikely that the combination and concentrations of compounds (Zr, REE) needed for the loveringite crystals, which are sometimes embraced by zircon (Fig. 19c), could form by diffusion in the sticky liquid in the narrow intercumulus passages.

The solubility of Ti-rich oxide minerals in silicate liquids is lowered by salic contamination (Green & Pearson, 1986). Oxides of Ti (ilmenite, loveringite) in Koitelainen and other intrusions are associated with cumulates contaminated by a salic melt (Tarkian & Mutanen, 1987). Loveringite seems to be a regular mineral in dry, low-Ti intrusions (op. cit. and references therein; Alapieti, 1982; Alapieti & Lahtinen, 1986; Huhtelin et al., 1989; Barkov et al., 1994b; Barkov et al., 1996b). Although the necessary elements seem to be available (Zr in zircon, REE in monazite), loveringite has not been found in the Keivitsa intrusion. This may be due to either a high H_2O concentration in the Keivitsa intercumulus, which

may render loveringite unstable, or the reduced state of the Keivitsa magma, which lowers the stability of Ti phases (Green and Pearson, 1986).

The parent magmas of the Ti-poor siliceous type intrusions (Bushveld, Stillwater, KOI-type intrusions of the 2440–2490 Ma group in the Shield) were strongly undersaturated in S (e.g., Liebenberg, 1970). Transient sulphide separation was possible only in an environment contaminated with salic material and preservation only when the sulphide droplets had a familiar, salic melt-escort. The sulphides being low in Ni, it is possible that sedimentary sulphur contributed to the Doppelgänger sulphide masses. In general, the exotic sulphur or sulphides associated with salic contamination are seen as important, even sine qua non, factors in the formation of magmatic Fe-Ni-Cu sulphide deposits (Lebedev, 1962a; Barker, 1975; Irvine, 1975a; Mutanen, 1975; Peredery & Naldrett, 1975; Tyson & Chang, 1978; Sasaki & Smith, 1979; Takahashi & Sasaki, 1983; Naldrett et al., 1986; Mutanen, 1996).

Accompanying elements (As, C, Liebenberg, 1970; As, C, Au, Se, Te, Mutanen, 1996) and even PGE (Mutanen, manuscript, 1981; Schiffries & Rye, 1989) may be, at least partly, of crustal origin. The high-aluminous schists in the Koitelainen area, with 4–14.3 ppb Pt, 3.6–8.6 ppb Pd and 0.18–0.45 ppb Ir (Mutanen, 1993, unpublished), must be seriously regarded as a potential source of PGE).

Sulphur isotope data provide good evidence for the exotic sulphur (e.g., Grinenko, 1967; Mainwaring & Naldrett, 1977; Ripley, 1978; Buchanan & Rouse, 1984).

It is of interest to note that sulphides seem to be associated with wholesale salic contamination, but chromite with selective potassium contamination. I consider that the early chromitites were formed at the mixing of K_2O-contamined magma (with olivine on liquidus) and the mafic main magma. This could have happened because the mixing of magmas with olivine, with a steep slope of the liquidus surface, and those magmas on the px-pl cotectic plateau (Yoder & Tilley, 1962) brings the melt composition into an apparently "empty", that is, superheated, space above the silicate primary phase volumes. As both alumina and alkalies lower the solubility of chromite, a phase space of chromite may be hidden in this "empty" regime. But the story of Upper Chromitites is different.

Genesis of the Upper Chromitite

"How, then?" I persisted.

"You will not apply my precept, " he said, shaking his head. "How often have I said to you that when you have eliminated the impossible, whatever remains, however improbable, must be the truth? We know that he did not come through the door, the window, or the chimney. We also know that he could not have been concealed in the room, as there is no concealment possible. Whence, then, did he come?"

"He came through the hole in the roof!" I cried.

"Of course he did. He must have done so. If you will have the kindness to hold the lamp for me, we shall now extend our researches to the room above – the secret room in which the treasure was found."

– Sir Arthur Conan Doyle, The Sign of Four.

.. "there is no concealment possible"

To the extent discernable through folding and metamorphism, the chromite deposit of Fiskenaesset is very similar to the UC layer (see Ghisler, 1976). The chromitites there are also situated in the upper part of the intrusion, where fractional crystallization had evidently emptied the old liquid of Cr. Trying to find a place of concealment in the room, Ghisler (op. cit.) suggests that the magma was rich in water which caused the Cr to became enriched in the residual liquid. It is known (Yoder, 965), however, that in basaltic systems water enlarges the diopside liquidus field at the expense of plagioclase. Thus early pyroxene would deplete the magma of Cr even more than in a dry magma. A high water content in magmas would also mean higher oxygen pressure, which promotes the crystallization of spinel, a further depleter of Cr. Moreover, the high Al ascribed to the Fiskenaesset magma (Ghisler, 1976) would have decreased the solubility of Cr (Schreiber & Haskin, 1976; Irvine, 1977b). Finally, if the oxygen pressure was high as stated (Windley & Smith, 1974), it would have augmented chromite crystallization (Roeder & Hill, 1974; Maurel & Maurel, 1982b). In general, even at high temperatures (1200 °C) the solubility of Cr in basaltic magmas is very low (380–300 ppm, depending on oxygen pressure; Shiraki, 1966; Hill & Roeder, 1974; Maurel & Maurel, 1982b)

At Koitelainen the uppermost Main Zone gabbro immediately below the UC succession contains < 20 ppm Cr. Calculation similar to that conducted in the Akanvaara case gives the residual liquid a Cr content of < 4 ppm, appropriate for late mafic liquids (see e.g. Wager & Mitchell, 1951). Probably no chromite would nucleate from a magma that lean but if, by magic, all its Cr were collected to the UC, a melt layer about 40 km thick would have been needed; however, only some 300 m were left.

Of course we could still speculate that Cr, somehow, became enriched in residual liquid. This means, first, that the $D_{Cr}^{px/liq}$ was originally < 1 and decreased continuously (because Cr decreases in the Main Zone pyroxene-plagioclase cumulates). If the amount of Cr needed for the UC really was collected from the residual liquid, then the $D_{Cr}^{px/liq}$ in this Cr-enriched liquid should have been < 0.01. This is highly unlikely. The D_{Cr} for clinopyroxene at the low-T end of the px-pl cotectic (corresponding to the UC event) probably exceeded 30 (see Duke, 1976) and for opx, 10 (Irving, 1978; Maure & Maurel, 1982b). Even for olivine the D value in terrestrial (relatively aluminous) basalts, is > 1 (Schreiber & Haskin, 1976; Maurel & Maurel, 1982b). There was no concealment possible for Cr.

".. he did not come through the door, the window, or the chimney."

The UC layer is the mother of all reversals. Naturally, the magic words "new magma pulse" have been uttered by visitors to Koitelainen; to no avail, though. Neither in the UC nor below or above it has anyone ever seen anything geological, mineralogical or geochemical suggesting that the chromium needed was introduced by a new, primitive magma pulse. The composition of chromite (low Mg, high Fe, V, Ti), as well as the potassic composition of the melt inclusions and of the intercumulus, indicate that the chromite crystallized in an environment poor in Mg (see Maurel & Maurel, 1984) and rich in K. The chromium did not come through the door.

Might it then be possible that the intrusion acted as a kind of passageway for basaltic magmas, erupted elsewhere, which conveyed the Cr found in the UC? Evidence for this kind of magmatic airing is lacking in the Koitelainen intrusion; in fact there are very few basalts of the appropriate age in the surrounding areas. The chromium did not come through the window either.

"..we shall now extend our researches to the room above.."

The granophyre was formed by partial melting of the surrounding rocks, mainly the high-

aluminous schists of the roof. The excess alumina ultimately went to anorthosites. From the thickness of the granophyre (ca 300 m) we can deduce that the the melted schist layer was about 400 m thick. The high Cr of these schists has been known for decades (Sahama, 1945). According to new analyses, the aluminous schists from around Koitelainen contain, on average, 370 ppm Cr (and up to 1200 ppm). In general, the Archaean and Palaeoproterozoic pelites are rich in Cr and Ni (see e.g., Danchin, 1967; Condie et al., 1970; Arutyunov, 1971; Collerson et al., 1976; Nagaitsev & Galibin, 1977; Naqvi, 1978; Fryer et al., 1979; Gibbs et al., 1986; Wronkiewicz & Condie, 1990), compared with Phanerozoic pelites and recent clays (Fröhlich, 1960; Shiraki, 1966; Lisitsyn, 1984).

At one time it was thought that the high Cr and Ni in old pelites derived from ultramafic source rocks (e.g., Danchin, 1967; Condie et al., 1970), but later it became apparent that at least part of Cr and Ni came from more felsic rocks (McLennan, 1983; Gibbs et al., 1986). The pelites of the ancient greenstone belts are commonly interpreted as products of normal or halmyrolytic weathering of felsic volcanic rocks (Viljoen & Viljoen, 1969, 1971; Golovenok, 1977; Fryer et al., 1979; Venkov et al., 1978). As to the Koitelainen area I have postulated that the high Cr of the high-aluminous schists in Central Lapland derived from felsic volcanites (Mutanen, 1976). The Cr in felsic volcanites in old greenstone belts is often high (see Jolly, 1975, Condie, 1976; Bridgewater et al., 1978; Kojonen, 1981), sometimes incredibly so (see Boyle, 1976, 1979).

Similar high-aluminous schists with high Cr, as shown by analyses or indicated by mineralogy, regularly occur near layered intrusions containing chromitite layers: Fiskenaesset (Worst, 1960; Windley et al., 1973; Friend, 1976; Ghisler, 1976; Bridgewater & al., 1978), Sittampundi (Janardhanan & Leake, 1975), Stillwater (Page, 1977), Saranovskoe (Ivanov, 1977), Campo Formoso (Hedlund et al., 1974), Soutpansberg (van Zyl, 1950; Hor et al., 1975), Imandra (see Gilyarova, 1974; Barkanov, 1976) and Bushveld (van Biljon, 1963).

A marked contribution to the intrusions by aluminous schists is sometimes indicated or suspected (Hall & Nel, 1926; Willemse & Viljoen, 1970; Herd, 1973). I have not noticed the restriction of chromitite layers solely to old Precambrian intrusions bothering anyone, but to my mind it is no coincidence that, with the dramatic decrease in Cr in pelitic rocks about 2200–2100 Ma ago (Gibbs et al., Wronkiewicz & Condie, 1987, 1990) to the low Phanerozoic (and present) level, the chromitite layers also vanish from layered intrusions. This is not to say that chromitite could not be made from ordinary pelites; the difficulty lies with the unrealistic amounts of rock that would have to be melted. Thus, making a layer of chromitite (with 20% Cr_2O_3) only 0.4 m thick would require extraction of all the Cr from a schist layer 800 m thick. The peculiar chromite enrichments in the roof part of the Norilsk intrusion (Ryabov et al., 1982) could represent a miserable attempt to make chromite ore by melting sediments.

" – the secret room in which the treasure was found."

The main mass of the Koitelainen granophyre is very poor in Cr (< 23 ppm), the content being comparable with that of the Ca-rich granites (Carr & Turekian, 1962), but in the upper contact Cr increases up to 1800 ppm (here Cr resides in magnetite and hornblende). In the Kannusvaara intrusion, southwest of Koitelainen (Fig. 32) the Cr is very low in magnetite gabbro, but increases towards the top of the granophyre to more than 200 ppm (the magnetite in the granophyre contains up to 4000 ppm Cr). The increase in Cr in the granophyre has been noted elsewhere, too (see e.g., Naldrett & Mason, 1968; Wager & Brown, 1968, p. 196).

Accordingly, the high Cr in the uppermost granophyre indicates that Cr was supplied to

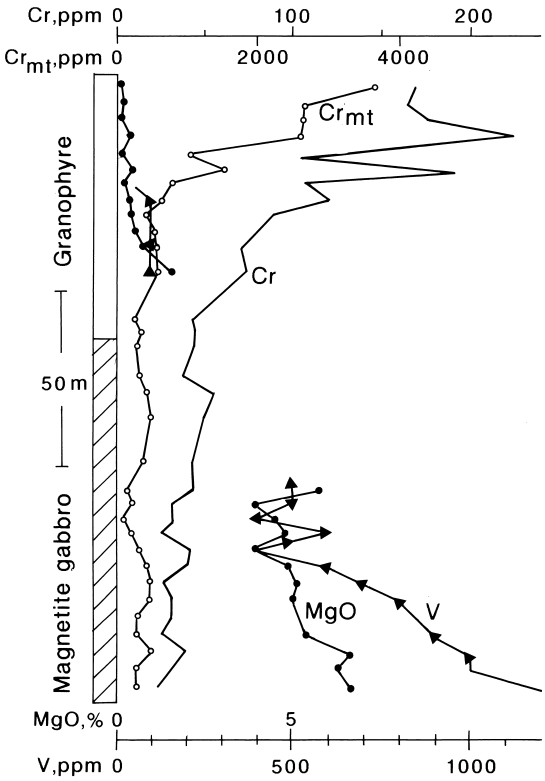

Fig. 32. Geochemical profile through the upper part of the Kannusvaara layered intrusion, Tanhua, Savukoski. Compiled from two diamond drill holes. Courtesy of Rautaruukki Co.

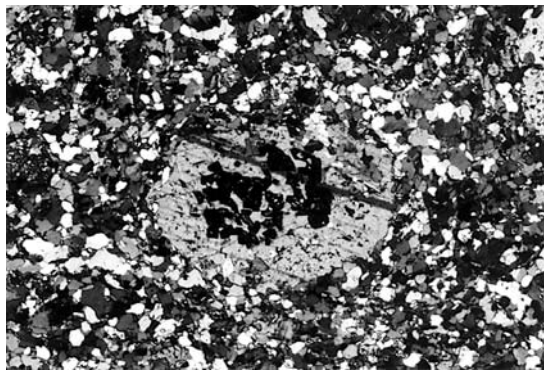

Fig. 33. Phenocryst-like plagioclase in granophyre, crystallized by reaction of magma with residual almandine-grossular garnet (CaO 15.9%, grossular 47 mol%, electron microprobe analysis by Tuomo Alapieti). Length of plagioclase crystal ca 1 mm. Northwest part of the Koitelainen intrusion, sample TM-79-18.

the first anatectic magma by melting pelites; on the other hand, the low Cr in the main part of the granophyre shows that the Cr did not remain there. I have suggested (1981, 1989b) that this unaccounted for Cr sank, incorporated in an insoluble mineral, through the acid melt down to the main magma, where it ultimately formed the UC chromitite.

The amount of Cr liberated from the partially melted roof (400 m thick, with 370 ppm Cr) corresponds to one metre of chromitite with 14.4% Cr (21% Cr_2O_3). This is surprisingly close to the Cr content actually found in the UC layer.

Evidently the Cr phase in acid melt was a spinel-type mineral. This nucleated easily, and in acid, viscous magma it formed very small crystals that remained in suspension behind the bigger aluminous residual phases (Fig. 33). The latter reached the mafic main magma relatively rapidly, reacted with it and formed a mat of plagioclase, floating on the mafic magma. Even if the aluminous phases reacted completely to form plagioclase, the latter was still able to settle in the granophyre magma (see Roobol, 1974).

The main part of the granophyre melt (magma) formed late in the crystallization history of the intrusion. The anatectic melt was originally of granitic minimum-melting composition. Due to heating from below, the salic melt was probably in a state of vigorous convection, which helped to transfer heat from the main magma to the roof. It also promoted the mixing of the salic melt and the underlying mafic magma, resulting in compositional modification ("syenitization", see above) of the granophyre melt. Both the heating and the compositional modification lowered the viscosity of the acid magma and checked its superheating.

As stated above, the small crystals of Cr-rich spinel lagged far behind the settling aluminous phases. Eventually they reached the bottom of the granophyre magma, only to be brought to a halt by the floating mat of plagioclase.

"He came through the hole in the roof"

The UC is a discrete, laterally continuous layer. It has sharp boundaries, and was neither preceded nor succeeded by disseminated cumulus chromite. At the mid-level size reversal there is often a thin layer of coarse pegmatoid gabbro; when thicker, this interlayer consists entirely of medium-grained non-cumulate gabbro, similar to the gabbro immediately above the UC layer. The combined thickness of the internal and overlying gabbro in each place is ca 0.7 m (see Fig. 24).

Deposition of chromite was preceded by strong magmatic erosion of the underlying unconsolidated cumulates, locally down to 11 m. Magmatic erosion continued, albeit somewhat subdued, after chromite deposition (Mutanen, 1989b). Strong magmatic erosion seems to be common in chromitites (Cameron & Emerson, 1959; Ferguson & Botha, 1963; Ireland, 1986).

The small grain size of the chromite, the almost complete lack of cumulus silicate crystals, the composition of the intercumulus, and the magmatic erosion associated with the UC imply that the chromite crystals did not sink through the magma but settled from density flows of contaminated magma, loaded with chromite crystals. At Bushveld, too, Cameron and Desborough (1969) consider that chromite, at least partly, crystallized in the upper part of the magma chamber and was settled from density currents.

The bipartite, often split, structure of the UC indicates that there were two different, almost simultaneous, density flow surges. The common occurrence of melt inclusions and skeletal chromite crystals indicates that the final growth of chromite took place rapidly.

The density surges originated from the thick chromite soup above the hanging anorthosite mat. Naturally a situation like this involves density inversion and is highly labile, not unlike that preceding an avalanche. Eventually the plagioclase mat was punctured as a result of convective thinning from below or (and) by refractory xenoliths foundering from the melting roof. Immediately, a powerful surge of dense chromite suspension rushed down the hole. The phenomenon can be demonstrated with toy water frames: a layer of heavy black sand above a mat of air bubbles and subsequent events convey a powerful sense of the scene imagined above.

Chromite had already crystallized before the onset of the density flow(s); moreover, the carrier silicate liquid had a low liquidus temperature. Thus, there was relatively little release of latent heat of crystallization. As the surges were launched from an environment cooler than the mafic magma, they caused chilling in the bottom melt. Accordingly, the non-cumulate gabbros associated with the UC formed from mafic magma chilled by density surges. The thicknesses of the separate gabbro layers correspond to the combined "coldness content" of each of the two density surges, and the thickness of the single (overlying) gabbro corresponds to the combined "coldness content" of two almost simultaneous surges. I think it is no mere coincidence that similar internal chill layers occur in intimate association with the Akanvaara UC layer.

The bipartite structure implies that there were at least two punctures and downdraft surges. As the stock of thick chromite suspension above the mat was emptied rather rapidly, the likelihood of multiple surges declined, because the holes in the mat sucked the suspension very rapidly and so reduced the hanging load. In this respect, the situation was an upside-down, accelerated version of the rise of salt diapirs.

The density surges lashed against the floor and spred laterally. The density inversion was eventually dissolved, and almost all the exotic Cr was effectively collected in the UC layer. A small amount of Cr spinel remained in suspension in the granophyre magma. I would attribute the Cr rise at the base of the magnetite gabbro (at Koitelainen and Akanvaara) to this kind of exotic addition. Like the UC layer, the deposition of magnetite gabbro was also pre-

ceded by accumulation of plagioclasic cumulates.

The above account is what remained after I had eliminated the impossible.

> Alice laughed. "There's no use trying, " she said: one ca'n't believe in impossible things." "
> I daresay you haven't had much practice," said the Queen.
>
> – Lewis Carroll, Through the Looking-glass

Genesis of pegmatoids

What have these magma-diagenetic bodies to do with contamination, the main theme of this book? According to the genetic model delineated in this section, pegmatoids provide samples of pore liquid, high in normative clinopyroxene, from the Sargasso Sea that was little affected by density flow-transmitted contaminants. As I will explain soon, cumulates of that stage, with a high overall content of normative pyroxenes, yield a large total volume decrease and are, hence, propitious to magma-diagenetic pegmatoid formation.

A well known fact, which can also be deduced from Fig. 30, is that while the total volume of vapour-saturated magmas (the sum of volumes of crystals, liquid and vapour) increases from the moment of vapour phase separation (see, e.g., Burnham, 1967), dry magmas will contract during crystallization.

The volume decrease (contraction in the following) is the sum of thermal contraction (of liquid, crystals and rocks), contraction due to crystallization, to inversion (polymorphic transformation), to crystallographic ordering and to adiabatic contraction (of liquid and vapour phases). To the genesis of pegmatoids the most important are the combined volume decrease of crystallization and inversions.

The contraction of crystallization depends on the degree of ordering of the melt just before crystallization (Shipulin, 1971) and on the melt composition. Of utmost importance to the genesis of pegmatoids is that melts rich in normative olivine and pyroxenes show the greatest amount of contraction, as can be seen from the following list.

Liquid/crystal contraction for diopside (liq/xl) has been calculated as 10.8%, measured – 15.1–18.0% (Yoder, 1952), glass/xl – 12.9%, melt/xl – 14.9% (both by Dane, 1941); for plagioclase (liq/low-pl) – 4.5% (Barth, 1969); for bytownite (glass/xl) – 3.7%, and bytownite (liq/xl) – 4.2% (Dane, 1941).

The following percentages of contraction have been estimated for liquids and respective rocks: olivinite – 16%, pyroxenite – 13%, gabbro – 8% (Orlov, 1963), diabase (glass/xl, at 20°C) – 6.5% (Dane, 1941), diabase (liq/xl, melting at 1250°C) – 8.6% (Dane, 1941), diabase (liq/xl, melting at 1200°C) – 8.6–9.9% (Skinner, 1966), Skaergaard magma – 10.6% (Osipov, 1982), Thingmuli basalt – 10.6% (Lange & Carmichael, 1990), anorthosite and norite – 8.9–9.7% (Martinogle, 1974), diorite – 7%, granite – 10% (both by Orlov, 1963), granite – 8.4% (Osipov, 1970), dry granite (crystallization 800 -> 600°C) – 8.2% (Lange & Carmichael, 1990).

Thermal contraction of crystals and rocks has been determined as: albite (600 -> 0°C, 1 kb) – 1.5% (Burnham & Davis, 1971), plagioclase, An_{67} (1050 -> 200°C) – 1.5% (Barth, 1969), calcic labradorite (1200 -> 0°C) – 2% (Stewart et al., 1966), anorthosite (1000 -> 0°C) – 1.8%, leuconorite (1000 -> 20°C) – 1.9%, ferrogabbro (1000 -> 20°C) – 2.7% (all by Martinogle, 1974), basalt (1200 -> 800°C) – 2.7% (Murase & McBirney, 1973).

Contraction percentages for inversions have been determined as follows: high-pl/low-pl – very small but detectable (Barth, 1969; Stewart et al., 1966), α/ß quartz – 2.5–3% (Yu-

supov, 1972) and 5.36% (Ermakov, 1972; the latter figure includes inversion and thermal contraction 600 -> 300°C; Ermakov, 1972). The reversible Ó/ß quartz inversion, being instantaneous, is very important in all quartz-bearing rocks (for corollaries, see Dolgov, 1963).

Deduced from mineral densities for pyroxenes of similar mg# figures, the pig/opx inversion involves ca 6% volume decrease. In mafic layered intrusions where the inversion often occurred in supersolvus temperatures (see Wager & Brown, 1968, p. 47), this inversion had important consequences to the mechanical failure behaviour of the consolidating cumulus pile. In the Koitelainen intrusion pegmatoid bodies are common in, or immediately beneath, the pigeonite gabbro unit. These are the rocks where it is reasonable to expect a large combined contraction of pyroxene crystallization and pig/opx inversion.

Evidently, a major part of contraction was consumed in the general decrease of the periphery of the intrusion, mostly in the sagging of the layered sequences (see Orlov, 1963; Dolgov, 1963; Osipov, 1967, 1982; Feigin, 1971; Mikhailov et al., 1966; Arnason et al., 1997). The sagging of the central part of the intrusion, where the layered sequence is thickest is, after all, a characteristic feature of layered intrusions. A smaller but important part of the contraction, however, resulted in openings – isometric voids, tubes and cracks – in the consolidating cumulus pile. In the following, all kinds of dilatational spaces formed in the cumulate mush are called voids. The voids were filled, in pace with the dilatation, with anything that flowed, most often silicate residual liquid (Bowen, 1920; Mead, 1925), in some cases even crystal-liquid suspension (Hibbard & Watters, 1985). The high-density fluid (liquid or melt in the following) crystallized to coarse-grained pegmatoid rocks (Fig. 34).

As pegmatoids occur both in noncumulate rocks (lavas, dykes) and cumulates, all kinds of interstitial, residual liquids are termed pore liquids in the following.

The proportion of contraction that resulted in voids depended, among other factors, on the depth, geometry of the intrusion, composition and consistency of the pore liquid, and the timing of maximum contraction in the consolidation history. In general, voids make less than 1 vol% of the consolidated rock mass. In the Kilauea Iki lava lake the amount of late coarse segregations is less than 1% of the thickness of the lava crust (Richter & Moore, 1966); the case described by Abovyan (1962) gives a figure of 0.3 vol%.

The early segregations in lavas formed at about 1065–1050°C, ca 100–50°C below the eruption temperature, but silicate liquid was still present at 970°C (Peck et al., 1966; Richter & Moore, 1966). Residual sulphide liquid, rich in Cu, remains to a much lower temperature (e.g., Likhachev & Kukoev, 1973).

Pegmatoids are found in intrusions, dykes and lavas. Generally they have been interpreted as representing segregations of late fractionated, "familiar" liquids (e.g., Bowen, 1920; Shannon, 1924; Lacroix, 1928; Osborne, 1928; Wagner, 1929; Walker, 1930, 1940, 1950; Zavaritskii et al., 1937; Emmons, 1940; Yagi, 1953; Lapham, 1968; Willemse, 1969b; Bunch & Keil, 1971; Makarov, 1972; Batiza, 1978, Butcher, 1985). They are stated or inferred to fill voids formed due to contraction of the solidifying magma (e.g., Hibbard & Watters, 1985). The filling process has been described in various terms: auto-intrusion, filter pressing, secretion and lateral secretion.

Grain sizes of up to 60 cm have been reported from mafic pegmatoids (Karpov, 1959). The term pegmatoid, however, does not necessarily denote a coarse grain size. Excepting coarse "pegmatoid" layers (e.g., Merensky Reef), the best criteria of true, late magmatic pegmatoids are that their composition is related to that of the residual liquid, their contacts are generally sharp, and that there are no retrograde alteration aureoles.

Discordant, pipe-like bodies of dunite, hortonolite dunite (Wagner, 1929) and other ultramafic rocks of Bushveld (e.g., Cameron & Desborough, 1964; Vermaak, 1976) loom as the most cited paragons of pegmatoids ascribed to metasomatic processes (Bowen & Tuttle, 1949). Less radical models invoke replacement and recrystallization (Zavaritskii, 1937; Karpov, 1959; Cameron, 1961; Lebedev, 1962b; Chelishchev, 1963; Shcheka, 1969; Makarov, 1972). Partial melting, combined with recrystallization, has been suggested for some pegmatoids of the Norilsk intrusion (Zolotukhin et al., 1975; Vasilev & Zolotukhin, 1975). Pegmatoids surrounded by alteration aureoles have evidently been formed by later fluids and associated recrystallization. Some "mafic pegmatoids" are actually desilicated granite pegmatites (e.g., Gordon, 1921; Gurulev & Sambuev, 1968; Matrosov, 1979).

One of the most authoritative, or most cited, of the hydrothermal models is that presented by Bowen & Tuttle (1949) for the genesis of the hortonolite dunite pipes of the Bushveld Complex. Actually, hortonolite dunites form the cores of composite, concentic pipe structures and comprise a tiny fraction of the overall volume of the pipes. The pipes are discrete, discordant bodies, which pierce through various cumulates of the Bushveld Complex, delicately leaving palimpsestic remains of chromitite layers in their former positions (Wagner, 1929; Cameron & Desborough, 1964), as if these had been "transparent" to the penetrating fluid (or magma). In the Basal Zone, too, layers of harzburgite can be traced through sulphide-rich pegmatoid pipes which cut the pyroxenitic cumulates of the Complex (Vermaak, 1976).

Bowen and Tuttle (op. cit.) interpreted the genesis of the dunite pipes by the action of high-T hydrous fluid which removed silica from pyroxenites along the route, thereby turning them into dunites, the present cores of the pipes. Many features of these pipes, as, for example, the source and destiny of fluids (Cameron & Desborough, 1963), the 30% volume loss required by the model (Cameron & Desborough, 1964; the volume loss was 12% according to Schiffries, 1982), the apparent dryness of the fluid (lack of metasomatic aureoles), and the presence of dunite pipes among gabbros (Söhnge, 1964) remain unaccounted for by the Bowen-Tuttle hypothesis. The submodel applied to the Driekop pipe by Schiffries (1982), which invokes a chloride fluid as the mover of material, leaves many problems unaccounted for or untreated, some of the foremost being the fate of the residual alumina of the noritic wall rocks, and the occurrence of both unaltered blocks of wall rocks and concentrically zoned, inward-grown pegmatoid bodies amongst the pipe rocks.

All the features of these pipes and other ultramafic pegmatoids can be explained by magmatic diagenetic processes operating in a closed system. Whether a small amount of vapour (fluid) separated late in the process of the pegmatoid crystallization is immaterial to the validity of the genetic model I will propose later in this section. In a concise form the model is as follows: True mafic/ultramafic pegmatoids were formed from adjacent pore liquid that filled contraction voids opened in a still partially molten crystal mush. The first stage pegmatoids, typically with more or less indistinct contacts, crystallized from pockets of a relatively early pore liquid, and represent pore melts separated from crystals (xl/liq separation). Later pegmatoids, with sharp contacts, represent a more evolved liquid that was separated from crystals or from crystals and other liquids by xl/liq or liq/liq ("chromatographic") separation processes.

Before introducing the model, however, I must furnish the ground by presenting some general features of mafic pegmatoids, as well as some details which I consider crucial for the understanding of the pegmatoids in general and the "pipe mystery" in particular.

Although pegmatoids occur at all levels of intrusions, a greater number (if not volume) of

them are concentrated in the upper parts of the intrusions and sills, where they usually have small dimensions (Walker, 1953; Andreeva, 1959; Eales, 1959; Baragar, 1967). The pegmatoid stockwork shown in Fig. 34 is located near the upper contact of the Ylivieska layered intrusion. The "vesicle cylinders" in lava flows (see e.g., Rose, 1996) are quite similar to the pipes shown in Fig. 34. The vesicle cylinders have aureoles similar to the melt-depleted aureoles seen in 34. Based on my own observations during a visit to Isle Royale, Lake Superior in 1996, I interpret the "vesicle cylinders" as contraction pipes filled by magmatic pore liquid.

True pegmatoid bodies are always "blind", with no feeder veins to or from the outside of the intrusion. Generally there are no apparent structural features to account for their location (e.g., Hoffman, 1931), but sometimes they are found concentrated in linear zones, suggesting some kind of prototectonic control; indeed, the pegmatoids in Fig. 34 fill prototectonic crevices. In the Bushveld Complex the pipes are sometimes seen to parallel the local fracturing (Schwellnus, 1935; Lombaard, 1956). Sometimes pegmatoids are concentrated within localities of pre-existing elastic contrasts, as in the vicinity of big xenoliths (Walker & Poldervaart, 1949), and in cumulate units with high initial porosities. The pegmatoids themselves often served elastically contrasted loci for later deformations and associated alterations (e.g., Ferguson & McCarthy, 1970; Makarov, 1972, Yusupov, 1972), which sometimes tend to confound original features with secondary effects.

The elastic inhomogenities in the consolidating cumulus pile around the first pegmatoid melt pockets also account for the relationship between pipe and vein pegmatoids (see Figs 28, 34). The first voids opened in a plastic regime. The voids, striving towards minimum surface energy, assumed roundish cross sections (Figs 28, 34). With the change over to the elastic regime the tension release was jerky; thus, rapid build-up of stress may lead to rupture even in a plastic crystal mush, as envisioned already by Bowen (1920). Magmas begin to behave as non-Newtonian liquids at relatively low suspension densities, and, with only 30% of suspended crystals show significant strength; with 40% of crystals they behave essentially as solid matter (Philpotts & Carroll, 1996). The corresponding early pegmatoid fillings have more gradual contacts than the late-stage, dyke-like pegmatoids. Later crevices tended to join the earlier voids, elastic "knot points", usually seamlessly (Fig. 34; Andreeva, 1959; Osipov, 1967; Kozlov, 1973).

The crevices opened perpendicularly to the maximum tension (the vertical stress being smaller in the upper crust). The crack propagated downwards, thereby creating new tensions of its own, and ultimately ended even beneath the niveau of the (original) tension (see e.g., Lachenbruch, 1962). Typically, as at Koitelainen, the pipes are downward-tapering "carrots" (see also, e.g., Wagner, 1929; Karpov, 1959).

The diameters of the pipes may be up to 1.5 km (Willemse, 1969b); the diameter of the upper part of the famous Mooihoek pipe is 250 m, but its (still more famous) hortonolite dunite core is only 15–20 m across (Wagner, 1929). The massive sulphide veins, an integral part of the pegmatoid system of the Monchegorsk intrusion, have an average thickness of

Fig. 34. Ultramafic pegmatoids in Ylivieska mafic layered intrusion, central Finland. Upper left – ultramafic pegmatoids (pyroxene, primary hornblende) filling prototectonic contraction cracks. The roundish pocket formed early in a plastic crystal mush. (cf. Fig. 1.24 in Rose, 1996). Dyke-like pegmatoids filled cracks that formed later, in an elastic regime. Note the light-coloured aureoles, depleted of the pegmatoid material. Note also that the prototectonic crack that failed to open (top) has no aureole; upper right – a rectangular network of filled/failed contraction cracks; lower photo – prototectonic extensional fault, filled with pyroxenitic intercumulus liquid. Note contractional warping and sagging of layers around the pegmatoid, and compare with Figs 2 and 3 in Schiffries, 1982. (Next page).

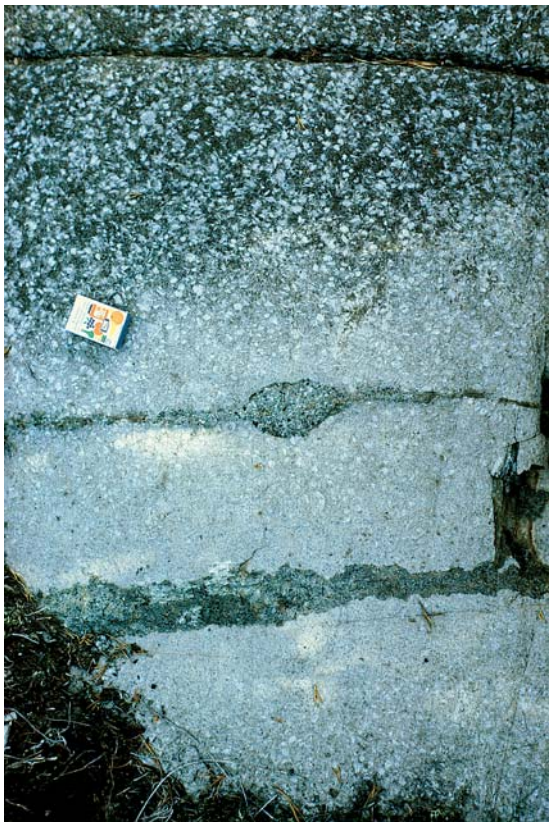

27 cm, vertical span up to 400 m and a length of up to 1.4 km (Karpov, 1959; Polferov, 1966; Kholmov & Sholokhnev, 1974; Orlov & Sokolova, 1982). The pipes and veins are typically oriented perpendicularly to the igneous layering.

The pegmatoids have no chilled contacts. Protoclastic deformation of minerals (bending, breaking) is commonly noted (e.g., Osborne. 1928; Baragar, 1962). In the Ylivieska intrusion sulphides (originally as a sulphide liquid) fill the interstices of broken orthopyroxene crystals. The bent lamellae of ilmenite in the coarse magnetite grains in the Lakijänkä pipes, Koitelainen, also point to magma movement inside pegmatoid chambers.

The filling of the pegmatoid pipes and veins was passive, the pore liquid seeping laterally into the voids. The process is explicitly seen in the outcrops of the Ylivieska intrusion (Fig. 34). In general, the composition of the pegmatoids reflects the composition of the adjacent fractionated pore liquid (see, e.g., Heckroodt, 1959; Liebenberg, 1970; Peck et al., 1966; Willemse, 1969b).

Thus, the dunite pipes do not break the chromitite layers in the Mooihoek pipe because magma was not flowing vertically. The chromitite, solidified to adcumulate hardground (see Wager & Brown, 1968; Sparks et al., 1985), did not contract at all, at least not with the pace of the retreating pipe walls. The chromitite layer remained in place as a shelf, dividing the pipe void. At contraction, differential shear occurred at the contacts between the chromitite "hardground" layer and mushy silicate cumulates. The contact-parallel faults so common in Bushveld (Lea, 1996), Koitelainen and Akanvaara, may be expressions of the late-magmatic volume adjustments between the unyielding chromitite hardground and the more pliant silicate mush.

Now this model of mine implies that when pore liquid was sucked from the surrounding cumulates, there should be sagging of layers around the pipes, and the dip of the sag should increase towards the pipe (= void), in the direction of increased liquid withdrawal. Detailed studies of the pegmatoid aureoles are almost lacking. However, the only case which I know of, the Driekop pipe, is surrounded by an aureole of sagging layers 300 m wide (see Figs 2, 3 in Schiffries, 1982). It is either an excellent partial proof of the model or an accidental fulfillment of my hopes.

The Bushveld chromitites are generally rich in PGE, but the best PGE assays in the pipe are from the level of the chromitite layers (Wagner, 1929). In the framework of the model presented here, the projecting chromitite shelf may have halted PGM particles that settled in the pipe liquid. The problem of the hortonolite rock composition is discussed later in this section.

Both lateral and vertical zoning is common in pegmatoids. The lateral zoning (e.g., in the zoned pipes of Bushveld; Wagner, 1929; see also Andreeva, 1959) and the occurrence of prismatic crystals that grew inwards from the walls suggest fractional crystallization into free core liquid (Mutanen, 1974; see, e.g., Fig. 5 in Schiffries, 1982). The build-up volatiles during fractionation ultimately led to the Crystallization of primary phlogopite and a brown, high-T hornblende (Cameron & Desborough, 1964; Schiffries, 1982).

The contraction continued in the crystallizing pegmatoid space, amounting ca 10–15 vol% of pyroxene-rich liquids (see above and Schiffries, 1982).

At the opening of the void the liquid (if not vapour-saturated) became superheated (again, see Fig. 30, right-hand curve; Dolgov, 1963), minus adiabatic cooling. The acicular habit of pegmatoid pyroxenes (see once more Fig. 5 in Schiffries, 1982) corroborates this reasoning (see e.g., Lofgren, 1974b), suggesting crystallization from supercooled liquid which had experienced prior superheating.

Crystal fractionation and gravitative accumulation of crystals continued in the hot, metal-rich liquid. As the viscosity of the liquid

was low and the size of cumulus crystals large, settling by Stokes' law could easily have taken place in the pegmatoid magma. In the Koitelainen intrusion the pegmatoid melt represents fractionated pore liquid from below the magnetite-in phase boundary, just as in the magnetite pipes of the Bushveld Complex (Willemse, 1969a). Evidently, at the time of void filling the pore liquid was just about reaching the magnetite phase boundary. Thus, in the magnetite pipes of Koitelainen the root parts are packed with cumulus oxides, while quartz and, finally, granitic droplets appear and increase in amount upwards. This upward enrichment of lightweight silica and salic melt droplets was probably due to their floating in the pipe magma.

Most of the time the evolution of the pipe melts of Koitelainen followed the cotectic boundary between clinopyroxene, magnetite and a silica phase (tridymite?), later joined by intercumulus plagioclase, zircon and apatite.

Lateral seepage of pore liquid resulted in negative primary aureoles of components withdrawn into pegmatoid voids. If two or more liquid phases were present, that (those) with the lowest viscosity (-ies) seeped faster and from a farther distance. The least viscous of the high-density fluids known is the sulphide liquid (with a viscosity of 1/3000 of that of the basaltic melts; Olshanskii, 1948). A negative aureole of S about 80 m wide occurs around a sulphide pyroxenite pegmatoid in the Ylivieska intrusion (Mutanen, unpublished), an indication of the sulphide liquid seepage. The lowest sulphur concentrations in the wall rocks occur immediately beyond the contact of the sulphide-rich pegmatoid. Wagner (1929) already noticed that S and Pt decrease in the Merensky Reef near sulphide-bearing pegmatoids. Sulphide pegmatoids similar to those of the Ylivieska intrusion are the Vlakfontein pipe in Bushveld (Vermaak, 1976), the pegmatoids hosting the Carr Boyd Ni deposits (Purvis et al., 1972), those described by Shcheka (1969), and the Monchegorsk pipes (e.g., Kozlov, 1973). Part of a negative sulphur aureole, similar to that of Ylivieska, is seen in Fig. 12 in Vermaak's (1976) paper.

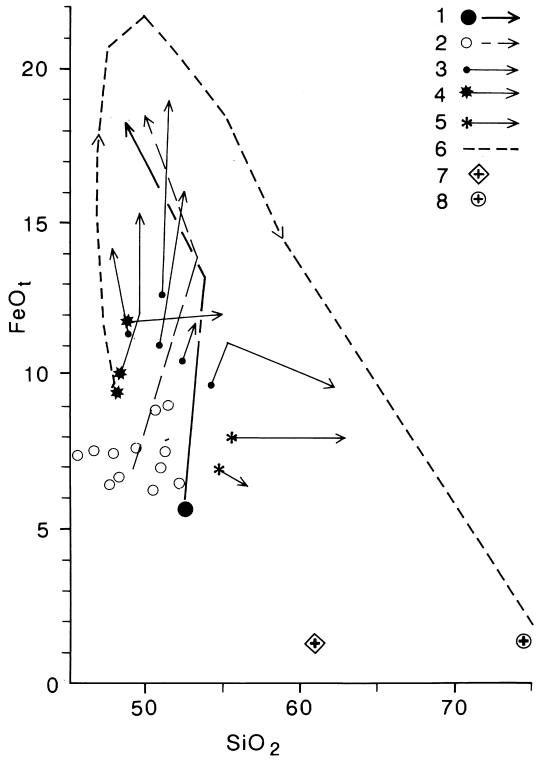

Fig. 35. FeO-SiO_2 diagram, showing compositions and the evolution of residual liquids in basalts (Kuno, 1965) and pegmatoid compositions of Ylivieska and Koitelainen layered intrusions. 1 – Koitelainen gabbro and pegmatoids; 2 – Ylivieska gabbros and pegmatoids; 3 – tholeiites and their magma (melt) evolution; 4 – high-alumina basalts and their magma (melt) evolution; 5 – calc-alkalic evolution; 6 – Skaergaard melt evolution; 7 – salic segregations in Ylivieska pegmatoids; 8 – granophyre pockets in Koitelainen pegmatoids.

At the time of withdrawal of the pore liquid into the voids it was separated from cumulus crystals. Accordingly, approaching the pegmatoid the cumulus silicates should show increasingly higher An% and mg# values. This indeed happens in the aureole of the Ylivieska sulphide pegmatoid, where An% of plagioclase increases rapidly towards the pegmatoid, in the

inner part of the negative S aureole. Mafic mineral compositions have not yet been studied. But it is gladdening to see that a prominent positive An% aureole surrounds the Driekop pipe (see Fig. 8, Schiffries, 1982).

A late sulphide liquid can travel along thin contractional passageways with considerable ease (see Kholmov & Sholokhnev, 1974; Rundkvist & Sokolova, 1978; Orlov & Sokolova, 1982. Neither was there any problems with the movement of silicate liquid in the pore space, driven by the pressure gradient (the suck of the void). The pore liquid formed an interconnected passageway-network when the liquid percentage was as low as 10% or even less (Lewis, 1964, 1973).

Thus, pegmatoids were formed by an effective process of crystal/liquid separation (or by liquation, the original term for the process). The reader, however, probably already noticed a serious inconsistency in this scenario: as the Koitelainen magma at time of void opening, and till the end, was saturated with plagioclase, this should occur as a cumulus phase in pegmatoid melt, but is does not. The same problem is well known from lavas, where the segregations are impoverished in Si, Al or both (Aoki, 1967; Wright & Okamura, 1977). In some cases the late segregations are either enriched or impoverished in Si (Aoki, 1967). Compositions of segregations and host lavas are depicted in Fig. 35, together with ultramafic pegmatoids and their host rocks from the Ylivieska and Koitelainen intrusions.

Fenner (1937) saw the bimodal compositional distribution of the lava segregations and proposed that they represent immiscible silicate liquids. He might have had it about right. At that time, however, experimental petrology did not give the slightest possibility for immiscible silicate liquids to occur in nature (see Roedder, 1951, p. 282). Or the possibility was as far as, well, the Moon. Indeed, in 1970 Roedder and Weiblen (1970, 1971) found silicate liquid immiscibility (SLI) in lunar basalts; later, De (1974) described it in Deccan basalts. Furthermore, McBirney and Nakamura (1974) showed that mafic intrusive magmas evolve toward SLI and probably attained it in the late fractionation stage of the Skaergaard intrusion, at about 1000°C (op. cit.).

Projected on Roedder's (1951) diagram the pyroxenitic rocks and the salic pockets of the Koitelainen and Ylivieska pegmatoids plot on the opposite ends of the SLI field (not shown here). Thus, spontaneous splitting of the pore liquid into immiscible acid (granitic) and mafic (pyroxenitic) liquids would provide a feasible solution to the plagioclase problem. Although plagioclase was (and must have been) stable with both liquids, its amount in the pyroxenitic liquid was small, hence the low Al in segregations (e.g., Aoki, 1967). Anyway, plagioclase should have had continued as a primary phase in both liquids. It does so in the acid pockets (Fig. 29 c) but is only an intercumulus phase in the mafic magma. As the normative plagioclase of the pore liquid in this late stage of fractionation was probably low (as reported earlier, cumulus plagioclase of the lowermost pigeonite gabbro unit had rim compositions of 47% An), the lack of cumulus plagioclase in pegmatoids may be simply due to the failure of nucleation of the acid plagioclase (see Wager, 1959).

The ultramafic liquid is less polymerized and far more fluid than its salic immiscible pair. Thus, at the opening of voids, the ultramafic liquid preferentially filled the voids (see Wiebe, 1979), while only a minuscule fraction of the sticky, salic liquid got that far. The granitic pods in the upper part of the Koitelainen pipes (Fig. 28, Fig. 29b, c) may represent salic liquid that separated either in the intercumulus space or in the pegmatoid chamber due to continuous separation with falling temperature (and broadening SLI volume) of a small fraction of immiscible, and increasingly salic liquid. The granophyre rock from the upper part of the pipe of Koitelainen (Fig. 29c) contains 74.92% SiO_2.

In general, the timing of the SLI depends on

how the fractionation proceeded towards Fe-enrichment and the intersection of the stable immiscibility volume by the liquidus. At the moment of SLI the MgO of the pyroxenitic liquid should be very low, below ca 3% (Roedder & Weiblen, 1970, 1972). In lunar basalts SLI occurred at 90–98 PCS (per cent solidified; Roedder & Weiblen, 1970, 1972), in Deccan basalts the PCS was 80 at the SLI stage (De, 1974).

So far, the SLI origin of the Koitelainen pegmatoids seems doing well. However, the diagram in Fig. 35 does not show a suspicious feature of the pegmatoids: their MgO is rather high, varying between 12.4–14.2%. Normally this would mean that the immiscibility volume was out of reach, well below the liquidus. There are several realistic possibilities to overcome that difficulty. First, the pressure release at the opening of voids may have lowered the liquidus temperature of the pore liquid more than the top temperature of the SLI volume; second, the pore liquid may have experienced supercooling to the metastable ("submerged") SLI volume (Wyllie, 1960; Seward, 1970) lying beneath the basalt plateau. Then, Ti and P, which were enriched in the residual liquid, may have bloated the SLI volume (Ryerson & Hess, 1978; Freestone, 1978). The combined effect of these and other fluxes (which naturally are progressively concentrated in the fractionating pore liquid) might have been enough for the stable SLI to occur. The presence of tourmaline in pegmatoids reminds of the powerful effect of boron. Generally unanalysed and mineralogically mostly "invisible", boron reduces viscosity, lowers solidus temperatures (Chorlton & Martin, 1978) and may suppress crystal nucleation (Wones, 1980); moreover, as discussed before, boron enlarges the SLI volume. All these effects, combined (or even alone, like the boron effect) may have helped to bring the pore liquid into either the metastable (submerged) SLI volume or into the stable SLI volume.

But even without the above contrivances the SLI, stable or metastable, was a real possibility. In lunar rocks mafic liquids in SLI relationship with acid liquids are sometimes high in MgO (6.32% MgO, Roedder & Weiblen, 1972; 7–9% MgO, Dungan et al., 1975). The maximum MgO reported from an immiscible ultramafic liquid (glass) is 15.5% (Roedder & Weiblen, 1972). In fact, when compared with the most magnesian immiscible lunar liquids the hortonolite dunites of the Bushveld pipes are not much different (compare: anal. 56, p. 257 by Roedder and Weiblen, 1972 and analyses of Table 1 by Viljoen & Scoon, 1985). It seems quite possible that the hortonolite dunites represent late fractionated Fe-rich liquids of the pipe melt. A final notice serves this point: olivine was a late-crystallizing mineral in the cumulates surrounding the hortonolite dunite pipes (Heckroodt, 1959).

The distribution of trace elements between immiscible liquids was different from that of crystal fractionation. As predicted by Ringwood (1955), Zr and P are enriched in the mafic liquid, but Y and REE, too (e.g., Roedder & Weiblen, 1970; Rutherford and Hess, 1974; Hess & Rutherford, 1974; Ryerson & Hess, 1978). No wonder, thus, that apatite and robust zircons occur (Fig. 29d) just in the ultramafic rocks. The philosophy of dating pegmatoid zircon was based on the model that the pegmatoids, although apparently discordant, are coeval with the pore liquid.

Very steep concentration gradients develop in liquid ahead of growing crystals (Anderson, 1967; Kushiro, 1974a, b; Lofgren, 1974b; Donaldson, 1975; Lofgren & Donaldson, 1975; see also: Rosenbusch, 1887; Hills, 1936); as a result, true SLI may occur in the diffusion gradient (e.g., Anderson & Gottfried, 1971). The compositional gradients translate into steep viscosity gradients. Hydrodynamically the different liquid portions behaved like immiscible liquids in pore spaces. Thus, efficient liquid/liquid separation in the Koitelainen intrusion was possible in pore liquid even without the SLI.

Fig. 36. View north of Keivitsa hill towards the Keivitsansarvi Cu-Ni-PGE-Au deposit. The distant blue hill is Koitelainen. Photo by TM.

Fig. 37. An aapa mire east of Satovaara. Typical central Lapland terrain. Photo by TM.

THE KEIVITSA – SATOVAARA COMPLEX

Location and exploration history

The Keivitsa – Satovaara complex (KSC) is situated 34 km north of Sodankylä, in the area of map sheets 3414 and 3732, just south of the Koitelainen intrusion (Fig. 38). Exploration has been concentrated in the western part of the complex, the Keivitsa intrusion. Of several prospects, the main target of recent work has been the Keivitsansarvi Cu-Ni-PGE-Au deposit.

Since the 1960s several mapping and exploration programmes have been conducted in the area. However, the massive and disseminated sulphides encountered were always very low in

Ni, of the type called "false ore" during the last exploration phase by GSF.

The present exploration was prompted by glacial erratics of sulphide-disseminated ultramafic rocks I found on the bank of the Luiro river (1973) and in Satovaara (1983), southeast of Keivitsa. These erratics contained petrological signs of and legitimate clues to the presence of viable Ni-Cu sulphides among intrusive rocks of the area. The first diamond drill holes (spring 1984) in Keivitsa intersected several metres of sulphides at the basal contact of the intrusion, but they proved to be false ores – and paltry at that.

A large area around Keivitsa and Satovaara was covered by systematic ground geophysical (magnetic, gravity, electromagnetic) surveys and pedogeochemical line sampling of basal till in 1984 – 1987. Percussion soil sampling at a good electric conductor yielded massive sulphides with 1% Ni, 2% Cu and 0.33% Co. This and other geochemical and geophysical indications were investigated by diamond core drilling in 1987. All the good electric conductors proved to be false ore sulphides. A peculiar PGE-Cr-V deposit in quartz-carbonate rocks ("chondritic" PGE mineralization; Mutanen, 1989b) was found, as a Pd anomaly, by percussion sampling. Two of the last drill holes of the programme – the twenty-third and twenty-fourth holes drilled in Keivitsa – intersected 22–24 m of disseminated sulphides with 0.36% Ni, 0.46% Cu and 1 – 1.4 ppm PGE+Au. Small trenches made in the vicinity indicated the continuity of the deposit between and beyond the discovery holes. (The trenches were visited in August 1989 by participants at the pre-symposium field trip of the 5th International Platinum Symposium.).

Subsequent drilling programmes in Keivitsa in 1990 and 1992–1995 delineated a large, low-grade Cu-Ni-PGE-Au deposit, the Keivitsansarvi deposit. The two discovery holes had probed a part of the deposit which was later known as the Upper Ore. Most of the drilling metres were used to the Keivitsansarvi deposit. More trenches and shallow pits were also dug in the ore subcrop area. Some more holes were drilled in the PGE-Cr-V deposit and other targets in the Keivitsa area.

In Satovaara a disseminated Ni-Cu-PGE-Au deposit, similar to the Upper Ore of Keivitsansarvi, was intersected in 1991. The results from the widely-spaced holes drilled in 1995 by GSF RONF were not encouraging.

The Keivitsansarvi deposit has features which make it difficult to discover by routine sampling and surveys. First, the percentage of sulphides is too low, and their grains are not sufficiently interconnected to give a perceptible response to the electromagnetic inductive method used in the routine regional surveys, before the discovery. Second, the subcrop failed to show up in pedogeochemical sampling. Detailed *post festum* till sampling of trench walls revealed that above the ore subcrop the secondary (glaciogenic) dispersion aureole is very thin, that it lies at the till-bedrock contact and that it is not traceable downstream. Also, the stony basal till is impenetrable to percussion sampling. Even with hindsight, only one sample on the distal side of the subcrop shows anomalous Cu, Ni, Pd and Au. And finally, the Keivitsansarvi deposit, located as it is several hundreds of metres above the basal contact of the intrusion, has an unpredictable stratigraphic position.

General geology

The KSC is situated in the northeastern part of a faulted brachysynclinal structure on the southern limb of the Koitelainen brachyanticline (Fig 38, Appendix 4). The Keivitsa intrusion (in the west) and the Satovaara intrusion (in the east) probably represent blocks of a single intrusion, separated by a zone of northeasterly faults (Satojärvi fault zone). The

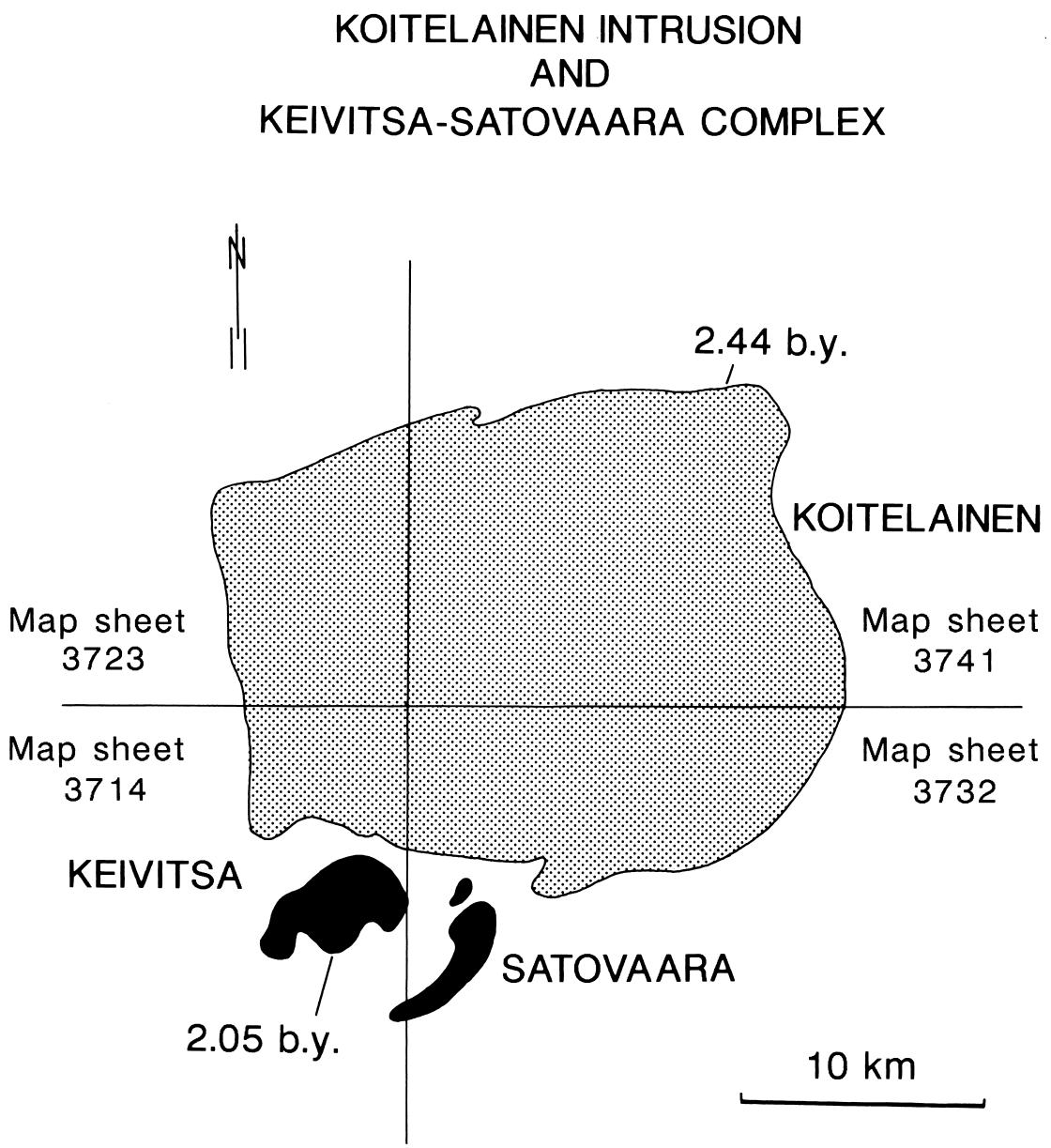

Fig. 38. The location of the Koitelainen intrusion and Keivitsa-Satovaara complex.

Satovaara block has been displaced downwards, perhaps 2–3 km, in relation to Keivitsa.

With the exception of the short description that follows I will not deal with the Satovaara here. The ultramafic cumulates in Satovaara have a higher MgO content (higher olivine/pyroxene ratio) and the proportion of gabbros is smaller than in the Keivitsa intrusion. Unlike Keivitsa, the Satovaara intrusion is concordant and intruded higher in the stratigraphy, well above the black schists. The hornfels aureole is considerably thinner than that around the Keivitsa intrusion. The thick basal olivine-rich cumulates are overlain, successively, by py-

Fig. 39. Pre-Keivitsa rocks. Left – layered metapelite, Allemaoja creek, northeast of Satovaara; right – komatiitic agglomerate, Annikanselkä ridge, south of Keivitsa. Photos by TM.

roxenite (10 m) and gabbro (100 m). On top are quartz gabbros and sodic granophyres, whose thickness ranges from a few metres to tens of metres. Near the top of the ultramafic zone (ca 100 m below the gabbro) is a discontinuous layer of disseminated Fe-Ni-Cu sulphides, with PGE and Au. In relation to the thick main mass of the Keivitsansarvi deposit, which is considered to represent the proximal (delta front) facies of a stationary downdraft of a convective toroid, the Satovaara sulphide reef represents the distal facies. The stratigraphic position of the Satovaara sulphide reef is comparable to the Upper Ore of the Keivitsansarvi deposit.

The shortest horizontal distance from the southern (upper) contact of the Koitelainen granophyre to the base of the Keivitsa intrusion is ca 800 m. Assuming that the top of the granophyre is parallel to the base of the Keivitsa intrusion, the true distance between the intrusions is 500–600 m. Immediately above the Koitelainen intrusion are (in ascending order) metasedimentary hornfelses, micaceous arkoses, calcareous rocks, low-Ti basaltic volcanics (now plagioclase-hornblende-chlorite rocks, possibly flows and tuffs), arkosic quartzites and a thick sequence of pelites. The pelites, with MgO from 3.0 to 4.5% and elevated Cr and Ni, are comparable to early Archaean high-Mg pelites (see e.g., Sheraton, 1980).

The lower pelites (anal. 20, Table 7) are very poor in sulphides and exhibit cm-scale graded bedding (Fig. 39). The pelites and carbonaceous metasediments below the Keivitsa intrusion typically contain titanite and porphyroblasts of ilmenite, very rarely porphyroblasts of magnetite. These pelites are Ti-rich (TiO_2 1.2–1.5%).

Upwards, beginning with the appearance of thin bands of chert and fine bands rich in sulphide and graphite, the general content of sulphides and graphite increases. There are thick carbonaceous beds – black schists – very rich in graphite. One drill hole intersection assayed 32% graphitic carbon across 14 m. The uppermost pelites are rich in sulphides (see anal. 21 in Table 7) but poor in graphite. These are also poorer in Ti (TiO_2 ca 0.8%, anal. 21, Table 7). Komatiitic volcanic rocks (flows, agglomerates, pillow lavas, tuffs; Fig. 39, 40b, c) occur above the black schists intercalated with sulphide-rich high-Mg pelites.

Provisionally I correlate the pelitic and carbonaceous rocks and associated bimodal volcanism with the post-Jatulian Ludian formations, which include the famous shungites, high-carbonaceous beds (Sokolov, 1980; Karhu, 1993; Karhu and Holland, 1996). The Ludian has been bracketed between 2113 Ma and 2062 Ma by Karhu and Holland (1996). The 2114±52 Ma age (Rb-Sr age; Kolosjoki volcanics in the Pechenga area) put by Balashov (1996) to Ludian is very imprecise

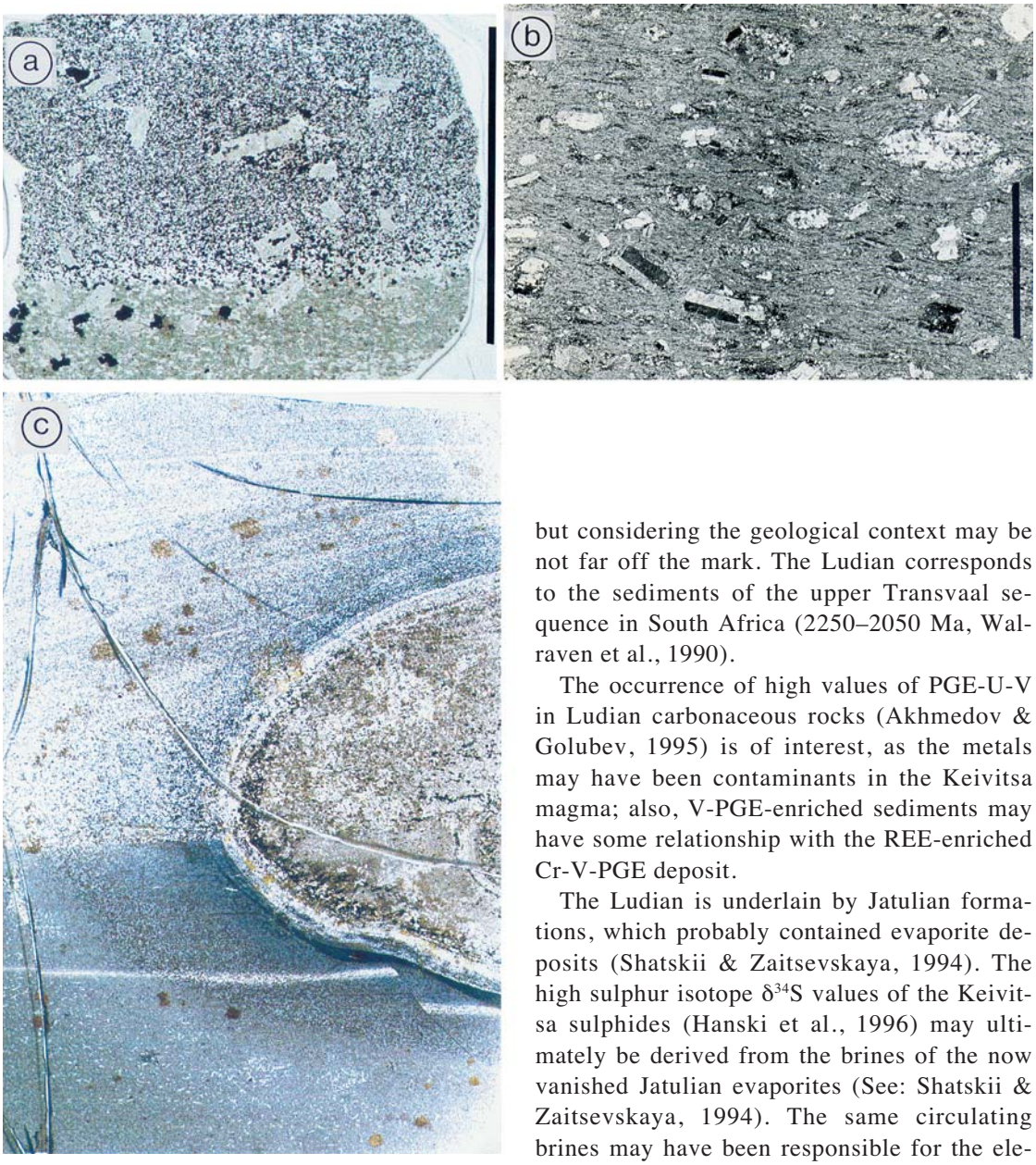

but considering the geological context may be not far off the mark. The Ludian corresponds to the sediments of the upper Transvaal sequence in South Africa (2250–2050 Ma, Walraven et al., 1990).

The occurrence of high values of PGE-U-V in Ludian carbonaceous rocks (Akhmedov & Golubev, 1995) is of interest, as the metals may have been contaminants in the Keivitsa magma; also, V-PGE-enriched sediments may have some relationship with the REE-enriched Cr-V-PGE deposit.

The Ludian is underlain by Jatulian formations, which probably contained evaporite deposits (Shatskii & Zaitsevskaya, 1994). The high sulphur isotope $\delta^{34}S$ values of the Keivitsa sulphides (Hanski et al., 1996) may ultimately be derived from the brines of the now vanished Jatulian evaporites (See: Shatskii & Zaitsevskaya, 1994). The same circulating brines may have been responsible for the ele-

Fig. 40. Acid volcanic rocks, Keivitsa area. a – magnetite keratophyre and hornblende keratophyre from near the Puilettilampi hydrothermal breccia stock. Percussion drill sample RP87/42243 070. Bar = 1 cm. Diascanner photo by Reijo Lampela; b – quartz porphyry from Matarakoski (Pb age on zircon: 2048 Ma). Crossed nicols. Bar = 5 mm. Photo by Erkki Halme; c – acid volcanic dropstone in hornfelsed pelitic sediment in floor rocks of the Keivitsa intrusion. The history of events is plainly visible: small curved faults formed in the bottom clay at the impact of the stone; tephra deposited later was draped smoothly over the stone; still later, oxygen imported by the pumiceous dropstone diffused, causing formation of magnetite dust in the reduced bottom sediments (dark halo around the dropstone). Width of thin section 2.5 cm. DDH308/77.95 m, Keivitsa. Diascanner photo by Reijo Lampela.

vated Cl in metasediments and serpentinite, with common occurrence of scapolite porphyroblasts in eruptive and metasedimentary rocks.

The increase in sulphides and graphite in pelites coincides with the appearance of acid volcanic dropstones (Fig. 40c). Evidently, from then on acid volcanism contributed material to the pelitic sediments.

Emplaced in the lower part of this succession are two thick differentiated komatiitic sills composed of thick olivine cumulates (+chromite) overlain by pyroxene cumulates and gabbro. At the top of the upper sill is a thin seam of granophyre, with dendritic hornblende (the "spider rock" of Jorma Isomaa). The peridotitic main part of the lowermost sill contains augite oikocrysts enclosing olivine crystals. These "spotted komatiites", which I formerly considered lavas, hug the roof contact of the Koitelainen intrusion round its western half. The komatiitic peridotites of the sills are lower in MgO than the dunitic to peridotitic komatiites which occur as xenoliths in the Keivitsa intrusion.

About 20 m below the base of the Keivitsa intrusion a 10 m-thick peridotite sill has been intersected by two diamond drill holes. Xenoliths of similar rocks occur in the deeper parts of the intrusion.

Evidently, there was a long time break in the supracrustal succession between the Koitelainen and Keivitsa intrusions. I tentatively consider the lower sediments and komatiitic sills older than the Koitelainen intrusion (2435 Ma); from the arkosic quartzites upwards the rocks are younger than Koitelainen but somewhat older than Keivitsa (2057 Ma).

Recumbent folds in hornfelsed pelite have been intersected by diamond drill holes at Keivitsa. The thermometamorphism postdates the folding. There is other evidence of pre-Keivitsa folding. The folds may have been formed by slumping of unconsolidated sediments due to crustal instability that was associated with volcanism and in anticipation of the Keivitsa event; also, like the tight folds below the basal contact of the Palisades Sill (Walker, 1969), they may have been formed in connection with, and by, the emplacement of the Keivitsa magma.

Several bodies of peculiar albite-rich breccias occur in a wide area west and northwest of the intrusion. The Puilettilampi hydrothermal breccia pipe west of Keivitsa (see Appendix 4) contains abundant carbonate, magnetite and pyrite. In the same area there are stocks of tonalite(-trondhjemite) which often have wide albitized aureoles and albitite contact breccias. The tonalites and breccias are massive, non-foliated rocks which have undergone regional metamorphism. The stocks and breccia bodies cut through high-aluminous schists, presumably of pre-Koitelainen age, but not the Keivitsa intrusion and the pelites immediately below the intrusion. Closely associated with the Puilettilampi hydrothermal pipe are porphyritic keratophyres (Fig. 40a) and gabbros. I interpret the breccia bodies and tonalite stocks as coeval with – and related to – the pre-Keivitsa acid volcanism. They may represent roots of volcanoes and volcanic hydrothermal vents.

Younger dyke rocks will be described and discussed later.

The grade of regional metamorphism reached the amphibolite facies, and embraced the rocks of the KSC and dyke rocks. Metamorphism obliterated almost all the magmatic minerals of small igneous bodies as well as the original hornfels minerals around the KSC and the komatiitic sills. Thermometamorphic minerals are locally preserved inside the Keivitsa intrusion. Large portions of the ultramafic rocks in Keivitsansarvi have undergone surprisingly little jointing and are mineralogically fresh. There are also unaltered parts in the gabbro cumulates, but the granophyres and uppermost gabbros are wholly altered.

During the subsequent folding the intrusions and their hardened hornfels aureoles behaved as competent blocks, and the deformation inside the intrusions was largely elastic. Fold

structures are large and the bedding in general dips at angles less than 45°. Subhorizontal bedding occurs in the western part of the map area (see Appendix 4).

The brachysyncline is sliced by northeasterly faults and fault zones. The fault zone separating the Keivitsa and Satovaara intrusion contains numerous blocks of ultramafic rocks similar to the olivine-pyroxene cumulates of the intrusions. On a ground magnetic map a northwesterly fracture system is visible, but no associated displacements have been detected in this area.

Preglacial weathered bedrock regoliths are ubiquitous in Central Lapland, but in the KSC area glacial erosion has been surprisingly strong. Kaolinite weathering occurs in the western part of the map area. Late Tertiary to early Quaternary grussification (see Mutanen, 1979b) was probably responsible for the weathering of the "pitted peridotites" (Fig.42) as well as the allochthonous vermiculite fillings in deep fissures, intersected in drill holes. Oxidation of sulphides in the subcrop is restricted to the aerated zone and it is generally slight or totally lacking. In one case pyrrhotite is completely altered to marcasite and pentlandite to violarite at 68.33 m (DDH depth). The surface oxidation is evidently postglacial. Freshly broken rock surfaces oxidate very rapidly (in a matter of days). The rapid oxidation is due to talnakhite and troilite in ore.

THE KEIVITSA INTRUSION

Age, form and internal structure

The U-Pb/zircon and pyroxene-plagioclase-whole rock Sm-Nd dating methods both give an age of about 2050 Ma (Sm-Nd 2052±25 Ma, U-Pb/zir 2050 Ma; Huhma et al, 1996). Recent "upgrading" of the zircon gives an age of 2057±5 Ma. The zircons used for dating are euhedral, zoned crystals in olivine pyroxenite evidently crystallized from magma. Primary pyroxenes from olivine pyroxenite and ferrogabbro, intercumulus plagioclase from olivine pyroxenite, and cumulus plagioclase from ferrogabbro were used for the Sm-Nd dating (op. cit.).

Zircon from a diorite dyke cutting ultramafic cumulates, interpreted to represent "back-intrusions" from the granophyre cap and to be coeval with the intrusion (Mutanen, 1996) give an age of 2054±7 Ma (Huhma, 1997).

The intrusion is of the same age as the Phalaborwa carbonatite and the Losberg intrusion in South Africa (2050 Ma, Walraven et al., 1990) and the Nebo granite, 2054 Ma, the latter giving the lower bracket for the age of the Bushveld Complex (Walraven & Hattingh, 1993).

The intrusion is funnel-shaped and dips soutwest (Appendix 4). The surface area is ca 16 km^2, of which ultramafic rocks make up 6.4 km^2, pelitic hornfels xenoliths 0.5 km^2 and the big peridotite-serpentinite xenolith 0.5 km^2; the remainder (8.6 km^2) are gabbros and granophyres. The separate gabbro bodies south and southwest of the intrusion may be apophyses from the main magma chamber.

Chemical analyses of the most common rock types of the Keivitsa area are presented in Table 7.

The contacts of the intrusion are discordant to the strata of the supracrustal rocks. The basal contact dips 45–50° south. Near the base contact, xenolithic rafts and tectonic slices of pelitic schists are interfingered with ultramafic

cumulates. The roof was intersected by one DDH, and there the contact between the granophyre and the pelite hornfels roof is sharp.

The igneous layering in the lower part is roughly conformable to the base contact, but upwards the dip of layering becomes more gentle, being 20–30° in the upper part of the ultramafic zone (see Appendix 5) and almost horizontal in the gabbro zone and the granophyre.

The intrusion is formally divided into zones:

The basal *marginal chill zone* is 0 – 8 m thick, and consists of microgabbro or contaminated quartz gabbros and quartz-rich pyroxenites. The contact rocks are massive but altered into uralite gabbros. The composition of the chilled margin (Table 6) was calculated from the analysed microgabbros least affected by contamination, added cumulus crystals or metamorphic alteration. The effect of contamination (S, Cl) is evident in the analytical data; it is plausible, though, that the composition has some bearing on the composition of the parent magma. A DDH core profile through the marginal microgabbro (Fig. 41) shows that with the increase in cumulus pyroxene and olivine, the gabbro rapidly grades into olivine pyroxenite.

Table 6. Chemical composition of Keivitsa chilled margin, recalculated to 100 per cent.

	%		ppm
SiO_2	52.14	Cr	194
TiO_2	0.89	Ni	113
Al_2O_3	11.92	Cu	261
$FeO_{(tot)}$	10.40	Sc	49
MgO	9.15	V	269
MnO	0.11	Zn	37
CaO	9.47	Sr	78
Na_2O	4.20	Zr	84
K_2O	0.32		
P_2O_5	0.09		
S	0.68		
Cl	0.25		

The *ultramafic zone* thins and tapers out to the west; in the southeast it runs against the wall rocks. The zone is thickest in the northeast of the intrusion, where the Keivitsansarvi deposit is also located. The maximum thickness is not known, but it may be as much as 2 km or more. The zone consists of olivine-clinopyroxene-(orthopyroxene)-magnetite cumulates (mesocumulates and poikilitic orthocumulates).

Modally the ultramafic cumulates are olivine websterites and olivine wehrlites, but in the field (and here) they are called olivine pyroxenites (for compositions, see anal. 1–9, Table 7). The name metaperidotite is used for altered (hydrated) olivine pyroxenite.

Among the olivine pyroxenites there are discontinuous layers (?) of pyroxenites and gabbros and sharply-defined masses (autoliths ?) of gabbros. Xenoliths of various komatiitic rocks abound, particularly in the host rocks of the Keivitsansarvi deposit (Fig. 48). Pelitic xenoliths are common near the base contact but rare in the main part of the zone (see below). Komatiite xenoliths are all but lacking in these rocks.

The rocks of the lower part of the zone, about 500 m thick, are petrographically indistinguishable from the overlying ore sequence. However, in the Ni/Co plot (Fig. 61) the rocks form a low-Ni group, separate from the rocks of the ore sequence. Moreover, the Au and Pd contents are always low, generally below the detection limit of 1 ppb.

In the upper ultramafic zone, immediately overlying the upper ore layer, is a peculiar olivine pyroxenite called “pitted peridotite” (Fig. 42). It is composed of two cumulate domains with relatively sharp boundaries. The weathered parts (pits), roundish or amoeboid in outline, consist of olivine websterite that is relatively rich in orthopyroxene and contains biotite-phlogopite and disseminated sulphides. The knobs are richer in clinopyroxene and carry neither sulphides nor mica. In a series of outcrops across the southwest of the intrusion the size of the pits decreases westwards (up in

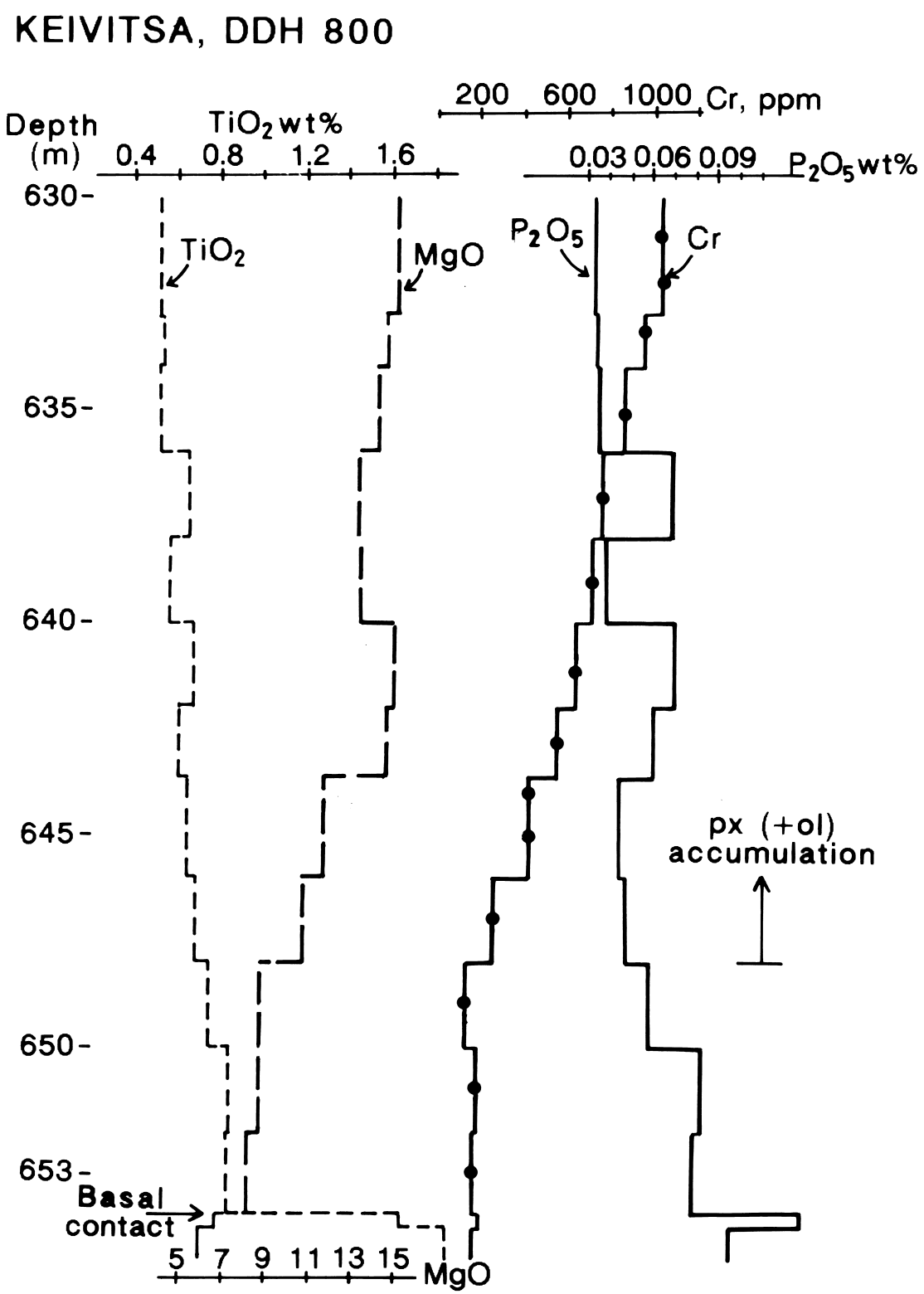

Fig. 41. Profile through the basal chilled contact rock and underlying pelitic metahornfelses, Keivitsa intrusion.

Table 7. Chemical compositions of rock types of the Keivitsa intrusion. Analyses recalculated to 100 per cent. Analyses made by XRF; some trace P and Sc by ICP.

	1	2	3	4	5	6	7	8	9	10	11	12	13
SiO_2	49.25	46.10	45.62	47.77	48.45	48.73	48.10	50.35	49.52	41.86	58.20	58.03	65.01
TiO_2	0.31	0.28	0.24	0.32	0.37	0.31	0.29	0.36	0.51	2.05	1.31	0.40	0.40
Al_2O_3	3.14	2.66	2.29	3.00	3.68	2.08	1.88	2.34	6.88	14.25	15.95	13.47	9.88
Cr_2O_3	0.403	0.411	0.318	0.0800	0.375	0.440	0.406	0.340	0.0676	0.0057	0.0008	0.0216	0.0775
V_2O_3	0.0223	0.0222	0.0209	0.0287	0.0217	0.0153	0.0140	0.0191	0.0340	0.1583	0.0230	0.0085	0.0121
FeO(tot)	9.62	12.02	14.20	12.43	6.65	6.67	7.33	7.281	13.66	19.58	8.38	6.18	4.86
MnO	0.20	0.19	0.18	0.17	0.11	0.11	0.12	0.10	0.14	0.11	0.03	0.145	0.09
MgO	21.90	22.56	22.15	17.10	22.76	25.57	24.98	23.13	14.03	6.84	2.27	4.71	8.93
BaO	0.0149	0.0098	0.0076	0.0071	0.0080	0.0055	0.0048	0.0052	0.0089	0.016	0.0027	0.0683	0.0066
CaO	14.05	12.65	11.79	16.10	15.65	15.16	14.65	15.01	11.43	11.01	2.09	9.15	5.28
SrO	0.0080	0.0049	0.0031	0.0033	0.0063	0.0024	0.0015	0.0015	0.0071	0.0259	0.0028	0.0131	0.0044
Na_2O	0.40	0.33	0.19	0.29	0.41	0.40	0.35	0.20	1.13	2.50	8.59	6.21	5.17
K_2O	0.21	0.16	0.10	0.098	0.13	0.13	0.10	0.07	1.31	0.50	0.12	1.27	0.13
Rb_2O	0.0002	0.0001	0.0001	0.0005	0.0008	0.0004	0.000	0.0008	0.0052	0.0012	0.0004	0.0020	0.0001
P_2O_5	0.015	0.015	0.011	0.0058	0.0048	0.009	0.010	0.008	0.020	0.001	0.176	0.066	0.028
C	na	na	na	na	na	na	na	na	na	na	na	na	na
Cl	0.1188	0.1122	0.0560	0.1036	0.1639	0.1660	0.1603	0.0835	0.1917	0.589	0.0547	0.2211	0.0455
Cu	0.0415	0.4879	0.1798	0.0413	0.1500	0.0018	0.0146	0.0059	0.0485	0.0151	0.0831	0.0082	0.0076
Ni	0.0680	0.3033	0.0742	0.0229	0.3606	0.1977	0.8667	0.3923	0.0106	0.0162	0.0030	0.0112	0.0205
S	0.212	1.672	2.58	2.41	0.695	0.074	0.721	0.279	0.990	0.459	2.72	0.01	0.039
Zn	0.0083	0.0083	0.0078	0.0055	0.0044	0.0035	0.0042	0.0030	0.0042	0.0034	0.0006	0.0035	0.0041
Sc, ppm	na	na	49	75	62	na	na	56	64	55	3	1	na
Zr, ppm	18	18	12	10	19	20	20	16	28	14	199	193	129

Analysed samples. R = Diamond drill hole

Anal. number	Sample	Rock type
1	R336/42.2 - 44.0 m	Olivine pyroxenite, hanging wall of the upper ore layer
2	R336/53 - 54 m	Olivine pyroxenite, upper ore layer
3	R364/14 - 16 m	Olivine pyroxenite, false ore
4	R802/76 - 78 m	Olivine pyroxenite, false ore
5	R725/30 - 32 m	Olivine pyroxenite, transitional ore type
6	R333/72 - 73 m	Olivine pyroxenite (Ni-PGE ore type)
7	R333/76.95 - 79 m	Olivine pyroxenite (Ni-PGE ore type)
8	R713/16 - 18 m	Olivine pyroxenite (Ni-PGE ore type)
9	R831/180 - 182 m	Olivine pyroxenite, upper part of Keivitsa intrusion
10	R831/104 - 106 m	Ferrogabbro
11	R728/56 - 57.5 m	Sodic granophyre
12	R695/238.15 - 240 m	Diorite (dyke)
13	R366/57.9 - 58.75 m	Diorite (margin of composite dyke)

stratigraphy) and the contrast between knobs and pits diminishes.

The *gabbro zone* consists mainly of pyroxene gabbro, ferrogabbro, with pigeonite and fayalite (anal. 10, Table 7), magnetite gabbro (with V-rich magnetite), and their uralitized equivalents. Graphite gabbro (with euhedral cumulus graphite, see Mutanen, 1989b) occurs

Table 7. (Continued)

	14	15	16	17	18	19	20	21	22	23	24	25	26
SiO_2	69.62	40.05	41.82	40.99	56.87	92.66	57.57	60.92	47.39	42.03	43.32	46.74	48.28
TiO_2	0.45	0.05	0.17	0.12	1.28	0.080	1.32	0.81	0.90	0.41	0.27	0.69	0.80
Al_2O_3	13.19	0.51	1.35	1.07	2.68	0.30	14.98	19.18	12.44	5.92	4.10	13.01	14.37
Cr_2O_3	0.0131	0.833	0.636	0.608	13.52	1.69	0.0261	0.0321	0.1572	0.4850	0.4827	0.0753	0.0472
V_2O_3	0.0056	0.0058	0.0120	0.0123	1.44	0.264	0.0392	0.0310	0.0449	0.0237	0.0182	0.0431	0.0506
FeO(tot)	2.55	10.27	12.69	13.32	21.37	4.64	12.40	7.13	11.73	10.30	11.19	11.47	11.15
MnO	0.05	0.14	0.18	0.198	0.19	0.040	0.070	0.020	0.22	0.17	0.14	0.23	0.195
MgO	3.20	47.59	37.04	36.19	0.82	0.17	6.52	3.53	13.42	28.81	34.08	10.87	8.59
BaO	0.0052	0.0030	0.0035	0.0041	0.0049	0.0021	0.0289	0.0399	0.0192	0.0042	0.0027	0.0237	0.0095
CaO	2.91	0.01	5.02	4.32	0.38	0.05	1.03	0.87	11.47	11.01	6.06	13.87	12.90
SrO	0.0041	0.0000	0.0006	0.0013	0.0021	0.0002	0.0071	0.0087	0.0115	0.0028	0.0012	0.0159	0.0100
Na_2O	7.56	0.00	0.13	0.00	1.06	0.02	3.27	2.45	1.48	0.43	0.00	1.77	2.44
K_2O	0.267	0.00	0.067	0.018	0.046	0.034	2.32	3.10	0.29	0.087	0.030	0.46	0.53
Rb_2O	0.0002	0.0000	0.0001	0.0003	0.0002	0.0000	0.0090	0.0077	0.0010	0.0002	0.0001	0.0009	0.0016
P_2O_5	0.07	0.0038	0.012	0.007	0.151	0.001	0.095	0.138	0.064	0.028	0.011	0.048	0.056
C	na	na	0.08	na	0.08	<0.01	na	na	na	na	na	na	na
Cl	0.0378	0.1863	0.2056	0.3357	0.043	0.0262	0.2641	0.3095	0.2015	0.0858	0.0446	0.5501	0.3893
Cu	0.0061	0.0000	0.0239	0.0559	0.0005	0.0002	0.0015	0.0121	0.0182	0.0020	0.0129	0.0308	0.0153
Ni	0.0084	0.2619	0.2209	0.1759	0.0560	0.0162	0.0106	0.0102	0.0422	0.1561	0.2134	0.0269	0.0185
S	0.043	0.096	0.32	0.240	0.001	0.000	0.04	1.41	0.08	0.04	0.36	0.05	0.10
Zn	0.003	0.0059	0.0086	0.0079	0.0592	0.0079	0.0025	0.0037	0.0104	0.0089	0.0044	0.0068	0.0065
Sc, ppm	na	na	22	na	6	na	22	10	40	35	27	44	45
Zr, ppm	246	1	10	2	59	0.0000	121	109	46	21	2	37	33

Analysed samples. R = Diamond drill hole

14	R366/54.6 - 56 m	Felsite (dyke)
15	R334/39 - 41 m	Serpentinite, big xenolith
16	R679/398 - 400 m	Dunite (xenolith intersection 386.1 - 407.45 m)
17	R360/112.16 - 112.38 m	Dunite (xenolith)
18	R347/7.50 - 9.00 m	Quartz rock, with Fe-Cr-Ti-V-oxides
19	R350/8 - 11.8 m	Quartz rock
20	R800/656.7 - 657.4 m	Mg-rich pelite metahornfels, sulphide-poor
21	R728/6 - 8 m	Mg-rich pelite metahornfels, sulphide-rich
22	R814/187.65 - 188.5 m	Olivine gabbro-diabase (dyke, marginal part)
23	R814/180 - 181 m	Olivine gabbro-diabase (dyke, central part)
24	R811/355.4 - 356.1 m	Olivine gabbro-diabase (dyke, central part)
25	R904/21.4 - 24.7 m	Diabase (dyke)
26	R372/114 - 116 m	Diabase (dyke)

in the southeastern part of the intrusion. Graphite is common in the small satellite gabbro soutwest of the intrusion.

Visible layering is rare; only indistinct ratio layering (plagioclase/pyroxene) has been seen in one outcrop.

High up in the gabbro zone there are discontinuous units of olivine-pyroxene cumulates, which, compared with those of the ultramafic zone, are rich in Fe and poor in Mg, Cr and Ni. In these rocks ilmenite is a cumulus phase. These rocks often host concentrated sulphides

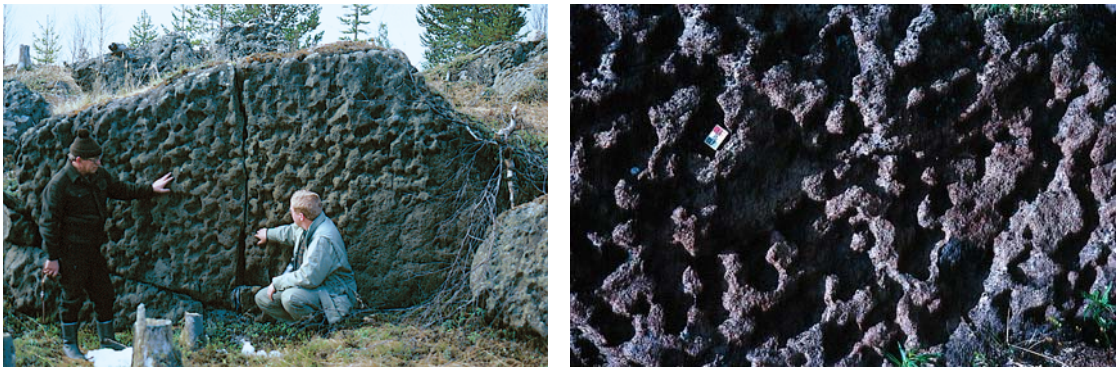

Fig. 42. "Pitted peridotite", a heterogeneous olivine-pyroxene cumulate. The mixed cumulate consists of clinopyroxene-rich olivine pyroxenite (knobs) and domains richer in orthopyroxene and biotite-phlogopite (pits, formed by grussification weathering). Both rock types contain intercumulus plagioclase. Photo by TM.

of the false ore type (for ore types, see a later chapter). Huge rafts of pelitic hornfelses and minor komatiites occur in the gabbro zone. Some of the hornfels rafts may actually be wedges projecting from the walls. Ultramafic cumulates seem to have been deposited upon the hornfels rafts, which thus acted as intermediate floors. The thickness of the gabbro zone is not known, but diamond drilling indicates that it is more than 500 m in the axial part of the intrusion.

Magnetite gabbro grades rapidly into the *granophyre* (anal. 11, Table 7), the uppermost magmatic unit of the intrusion. It is well displayed on the magnetic map due to its magnetite content. A vertical DDH drilled near the southeastern wall of the intrusion intersected 22 m of the granophyre, but the actual thickness is less. Shallow holes drilled in the southern part of the intrusion indicated that the granophyre is considerably thicker there. Small xenoliths of pelitic hornfels occur in the granophyre. In the overlying hornfelses there are salic pockets that evidently represent incipient melting. Granophyres are composed of sodic plagioclase, quartz and light-green secondary hornblende (dark green against feldspar). Magnetite, ilmenite, fluorapatite and sulphides (mainly pyrrhotite, plus minor chalcopyrite, cubanite and secondary pyrite) are abundant; biotite and stilpnomelane occur in lesser amounts. Accessory and secondary minerals are epidote-clinozoisite, carbonate, scapolite, titanite, rutile and chlorite.

The cores of subhedral plagioclase crystals are rich in epidote, suggesting that the original plagioclase was a calcic magmatic feldspar. The lower, plagioclase-rich part of the granophyre may actually be a flotation cumulate of plagioclase. Albitized pseudomorphs of interstitial microcline are common; thus, granophyre was originally more potassic; part of the potassium turned mobile is fixed in secondary biotite.

Superimposed on other structures are fractal structures, seen in the size distribution of xenoliths (from single olivine grains to huge xenoliths), in the concentrations of disseminated sulphides (from the size of a nail to homogeneous masses hundreds of metres across) and in the sulphide veins (from about 1 m down to 1 mu thick). The latter, called "chicken wire" structures (Fig. 79), which form largely invisible circuitries, are important in interpreting the electric conductivity and electromagnetic behaviour of disseminated sulphides.

Petrography of ultramafic cumulates

The basal microgabbro grades into a pyroxene cumulate and pyroxene-olivine cumulate rich in intercumulus plagioclase. This transitional zone, with MgO 10.8 – 17.0% and Al_2O_3 7.4 – 5.0%, is ca 40 m thick. Chlorapatite and euhedral zircon (with 1920 ppm U in zircon fraction, 2600–5300 ppm U in electron microprobe analysis of the skeletal zircon in Fig. 46f) occur in this rock. Sulphide-mantled euhedral orthopyroxene (Fig. 77) is common in the basal ultramafic zone.

The main part of the ultramafic zone consists of olivine-clinopyroxene-orthopyroxene-magnetite cumulates. Chromite occurs only in clinopyroxene, as tiny euhedral to subhedral inclusions.

The H_2O-rich intercumulus liquid crystallized largely to primary hornblende and biotite. Orthocumulate textures are best displayed where the intercumulus consists of sulphides and plagioclase. Because of the original "bastard" nature of the cumulates, and reflecting it, H_2O was inhomogeneously distributed in the intercumulus liquid. Thus, the degree of replacement of clinopyroxene by brown hornblende commonly varies in a single clinopyroxene grain, the part against plagioclase being fresh. In general, in samples and in parts of thin sections that are rich in intercumulus plagioclase clinopyroxene crystals are fresh, not spattered by inclusions of brown hornblende.

The amount of olivine generally varies in the range 15 – 25 vol%. Unless encased in sulphides, orthopyroxene occurs as anhedral to oikocrystic grains and contains resorbed olivine and clinopyroxene inclusions (Fig. 77). This indicates a reaction relation of olivine with orthopyroxene and calcic clinopyroxene. The outlines of orthopyroxene oikocrysts are sometimes euhedral, suggesting settling of composite olivine(-clinopyroxene)-orthopyroxene cumulus grains (e.g., Jackson, 1961). Stress-lamellae sometimes occur in olivine.

On the other hand, as in the peridotitic cumulates of Koitelainen intrusion, clinopyroxene commonly occurs as roundish inclusions in olivine, suggesting that the magma began crystallizing in the clinopyroxene field and turned, possibly due to added H_2O, into the olivine field. On the other hand, clinopyroxene contains olivine inclusions. All this can be translated into a cumulus path cpx -> ol -> kpx -> (peritectic reaction of ol, and apparent reaction of kpx) -> opx. Euhedral plagioclase inclusions are found in orthopyroxene oikocrysts, suggesting that it was an early cumulus phase. Of course, before the intervention of contamination, plagioclase and pyroxenes crystallized together from the original basaltic parent magma (Table 6).

Along the deepest DDH slight downward trends can be discerned: the proportion of clinopyroxene and its replacement by primary hornblende increase and the amounts of orthopyroxene and primary OH minerals decrease. Nevertheless, primary biotite-phlogopite is common in the Main Ore at the bottom of the westernmost DDH (Appendix 5).

The clinopyroxene/orthopyroxene ratio varies in ultramafic cumulates; false ores are normally richer in orthopyroxene, whereas in the Ni-PGE ore type the orthopyroxene content is very low. Chlorapatite often occurs as big grains, not unlike cumulus crystals.

Cumulus magnetite occurs as solitary euhedral crystals. The original magnetite was a mixed Fe-Al-Cr-Ti-Mg spinel, which exsolved into a complex fractal lattice-lace symplectite of spinel, ilmenite and magnetite. In spot analyses the Cr_2O_3 content varies between 2.45 and 21%, and that of Al_2O_3 between 0.75 and 8.35%. The exsolved "pure" spinel contains (wt%): 15.98 Al_2O_3, 6.70 MgO, 34.47 Cr_2O_3, 35.01 FeO(tot), 3.21 TiO_2, 0.49 MnO, 0.64 ZnO, 0.25 V_2O_3. The rocks that contain more primary OH minerals (hornblende, biotite-phlogopite) also contain more primary magnetite, while those rich in intercumulus plagiocla-

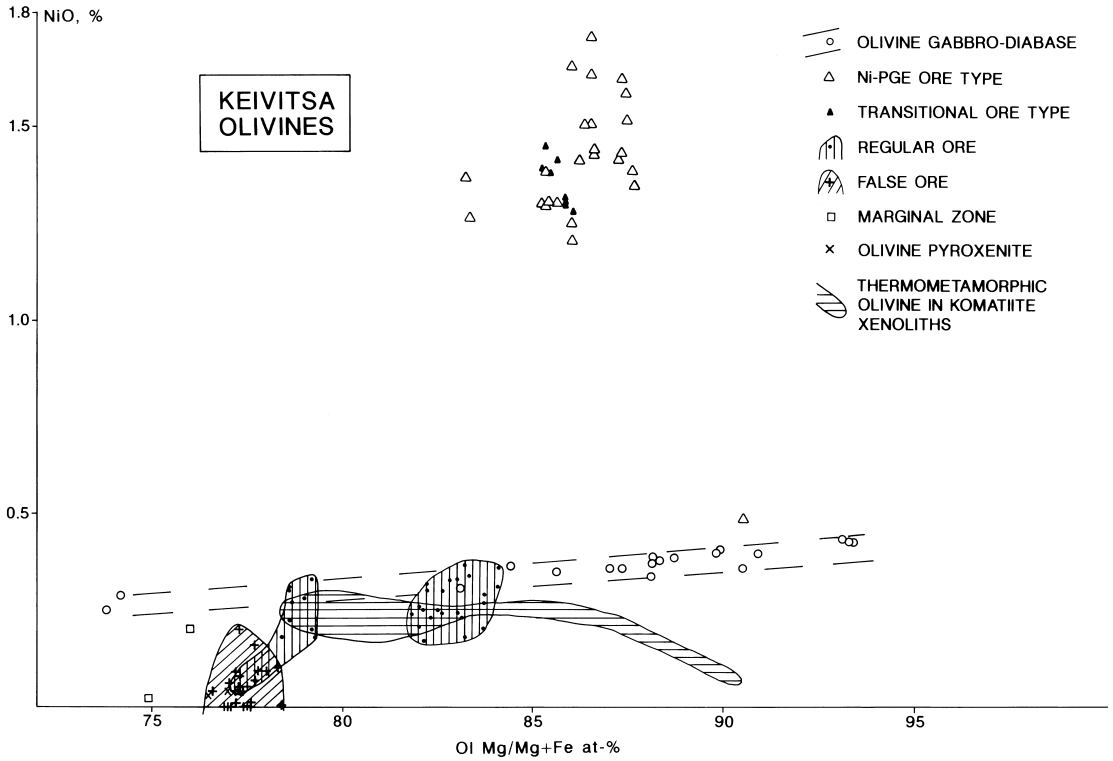

Fig. 43. Plot of NiO(wt%) vs Mg/Mg+Fe (at%) for olivines of the Keivitsa intrusion.

se are very poor in primary magnetite and chlorapatite. In the deeper parts of the Keivitsansarvi deposit (see Appendix 5) crystals of homogeneous chromite occur in olivine and clinopyroxene, and mixed spinels are lacking. Though distinctly more affected by pelitic contaminants, the false ores do not contain primary magnetite more than the other rocks and ore types, indicating a reduced nature of the contaminants.

Beyond reasonable doubt the fair-sized, euhedral Chrommagnetites are cumulus crystals. Their amount is so small, commonly 1–2 crystals per one thin section, that there is no point of counting their volume proportion, which is certainly << 1%. That low amount means a very small cotectic ratio, characteristic of a breeding magma that was either highly polymerized or rather reduced, or both. About equally strange is the fact (remembering the supposed reaction relationship between Ca-pyroxene and chromite; e.g., Irvine, 1967) that true chromite (the most "primitive" with 35–40% Cr_2O_3, 13.5% Al_2O_3 and 5.6% MgO) occurs, of all minerals, in clinopyroxene, sometimes in olivine. This feature and other lines of evidence suggest that chromite is a residual phase, inherited from disintegrated komatiitic material.

The compositions of olivine, pyroxenes and unaltered intercumulus plagioclase are presented in Figs 43 to 45. From the base upwards pyroxenes and olivine become more magnesian ("reverse fractionation") up to the level of the Ni-PGE ore; from there upwards data are lacking, but evidently fractionation followed the normal trend of decreasing Mg/Fe, as inverted pigeonite and fayalitic olivine occur in

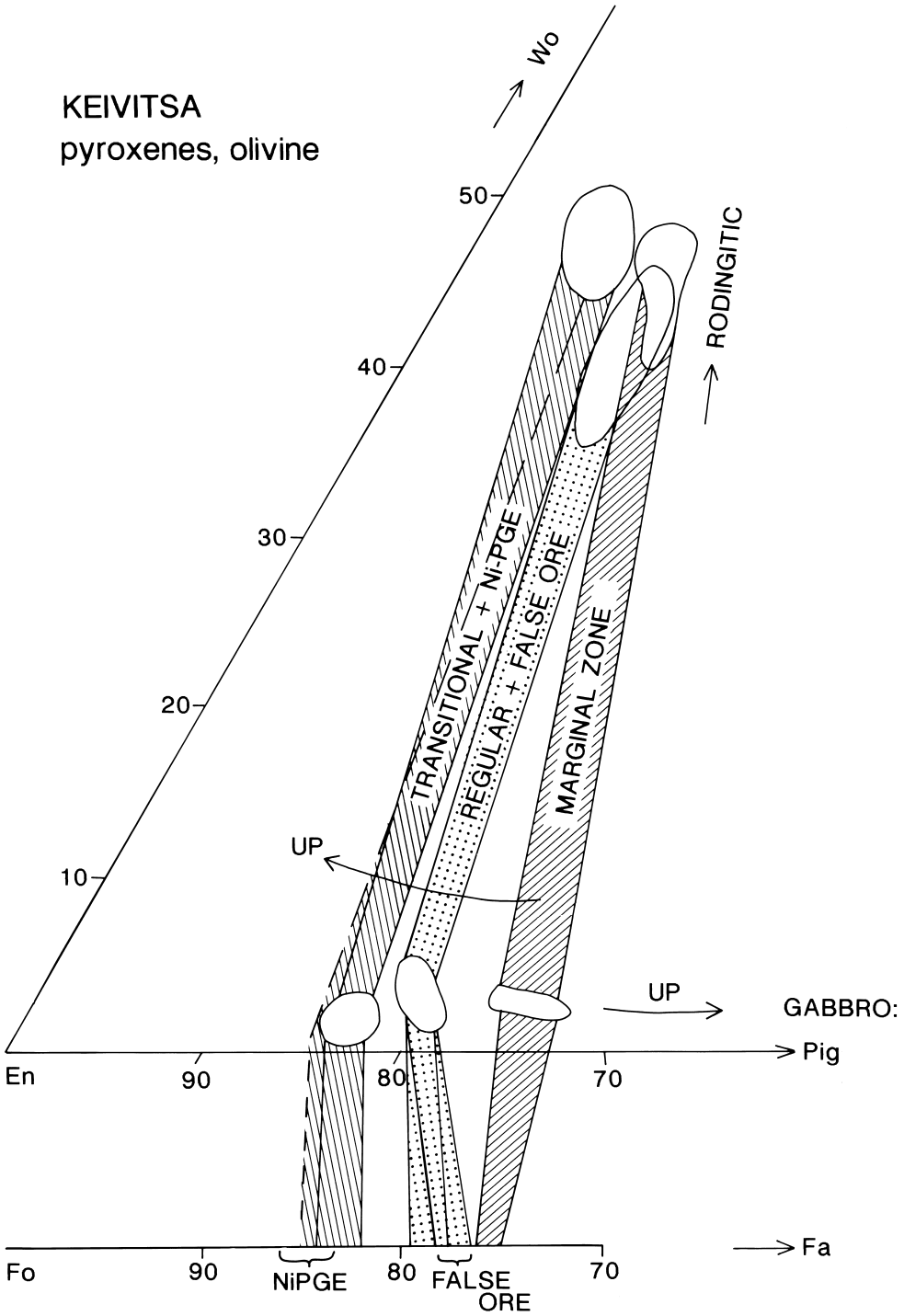

Fig. 44. Compositions of pyroxenes and olivines in various ore types and olivine lherzolite in marginal zone. Fayalitic olivine and inverted pigeonite occur in the gabbro overlying ultramafic cumulates. Rodingite alteration pulls the clinopyroxene fields towards the wollastonite apex.

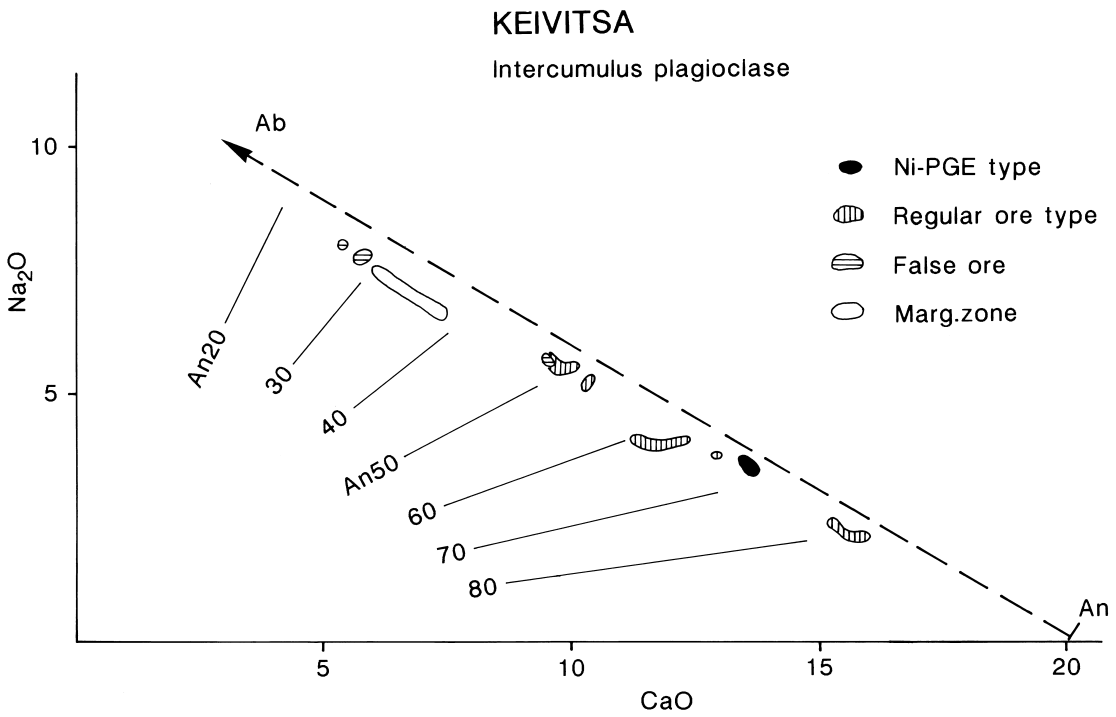

Fig. 45. Compositions of intercumulus plagioclase, Keivitsa intrusion.

gabbro not far above the big serpentinite-peridotite xenolith. Olivines of the Ni-PGE ore type are remarkably high in Ni. Olivines with similar high Ni contents have been found as inclusions in chromite (Talkington et al., 1984, and references therein), but there are no known magmas of ordinary or extraordinary composition and of a significant volume which, at about normal conditions, could produce such high-Ni olivines. The subject is discussed later.

Using the T-calibrated distribution of Ni between olivine and augite Häkli (1971) estimated model crystallization temperatures of 1150 – 1200°C for the ultramafic rocks of Keivitsa. A special feature of the ultramafic cumulates of Keivitsa is that the range of Ni in mafic silicates is large for small differences in model temperatures (op. cit.). This suggests that olivine and clinopyroxene crystallized in magma portions diluted by different amounts of wall rock contaminant material.

Primary intercumulus minerals are plagioclase, biotite-phlogopite, brown hornblende, dashkesanite, chlorapatite, monazite, graphite, ilmenite and sulphides (mainly pyrrhotite, chalcopyrite, pentlandite, cubanite and mackinawite). Sulphides and other ore minerals are described in association with ore types. The ore minerals identified are listed in Tables 10 and 11.

Intercumulus plagioclase contains anhedral inclusions of orthoclase.

In the Keivitsa intrusion dashkesanite is common in ultramafic cumulates; it also occurs in gabbroic interlayers in the upper part of the ultramafic zone and in pigeonite-fayalite gabbro. Dashkesanite is associated with biotite-phlogopite, and seems to be a product of reaction between primary hornblende, primary

Table 8. Compositions of chlorapatite of Akanvaara, Koitelainen and Keivitsa intrusions. Electron microprobe analyses by Ragnar Törnroos (6) and Bo Johansson (8–9) and Lassi Pakkanen (1–5,7).

	1	2	3	4	5	6	7	8	9
SiO_2						0.08		0.36	0.09
$FeO_{(tot)}$	0.06	0.01	0.13	0.05	0.11	0.02	0.16	0.25	0.18
MnO	0.07	0.03	0.05	0.04	0.05	0.03	0.05	0.10	0.01
MgO	0.00	0.00	0.00	0.00	0.00		0.00	0.24	0.03
CaO	53.71	53.23	52.72	52.40	52.50	52.8	53.17	54.2	53.5
SrO	0.22	0.19	0.88	0.37	0.22	1.65	0.07		
PbO	0.04	0.00	0.20	0.01	0.01	0.22	0.01		
Na_2O	0.00	0.00	0.00	0.00	0.03		0.00		
K_2O	0.00	0.00	0.01	0.00	0.02		0.00		
Th_2O	0.00	0.00	0.00	0.01	0.00		0.05		
UO_2	0.00	0.10	0.14	0.00	0.00		0.01		
La_2O	0.16	0.07	0.18	0.00	0.25		0.00		
Ce_2O	0.00	0.05	0.09	0.33	0.45		0.67		
P_2O_5	40.29	40.53	41.73	41.44	42.16	40.2	41.50	40.9	42.1
F	0.00	0.02	0.00	0.34	1.60	1.66	0.00	0.26	0.33
Cl	6.88	7.58	6.96	4.31	1.57	6.18	7.11	6.95	7.20
Br	0.00	0.00	0.07	0.00	0.00	0.00	0.03		
I	0.00	0.00	0.00	0.00	0.00		0.00		
	101.42	101.82	103.17	99.29	98.81	102.84	102.80	103.26	103.44
F,Cl,Br≡O	-1.55	-1.72	-1.57	-1.12	-1.05	-2.06	-1.60	-1.68	-1.76
Total	99.87	100.10	101.60	98.17	97.76	100.78	101.20	101.58	101.68

1 - 3 Akanvaara, 4 - 6 Koitelainen, 7 - 9 Keivitsa - Satovaara
1 - DDH320/277.50 m olivine pyroxenite, Lower Zone
2 - DDH320/272.80 m olivine pyroxenite, Lower Zone
3 - DDH337/29.75 m Main Zone olivine pyroxenite above ULC layer
4 - DDH308/28.00 m Lower Zone olivine pyroxenite (basal ultramafic cumulates)
5 - Fluor-chlorapatite DDH308/28.00 m
6 - Cumulus chlorapatite, mixed rock (plagioclase + peridotite), DDH365/180.0 m
7 - DDH307/92.50 m skeletal chlorapatite in feldspathic olivine pyroxenite near the base of the Keivitsa intrusion
8 - 9 - Cumulus chlorapatite, Satovaara (glacial erratic), sample TM-83-3.2

blank space - not analyzed

Note: Another grain of cumulus chlorapatite from mixed rock, Koitelainen, had 0.67 wt% Br.

biotite-phlogopite and high-density chloride fluid (Fig, 47). It always contains rods of (exsolved?) ilmenite (Fig. 46e). Dashkesanite analyses are presented in Table 9. Like other high-Cl hornblendes the Keivitsa dashkesanites are potassian hastingsites, but they are richer in MgO than are most of the analysed chloramphiboles (see e.g., Krutov, 1936; Krutov & Vinogradova, 1966; Pavlov, 1968; Jacobson, 1975; Dick & Robinson, 1979; Sharma, 1981; Kamineni et al., 1982; Vanko, 1986; Volfinger et al., 1985; Suwa et al., 1987). The ilmenite rods suggest that the original high-T dashkesanite was probably richer in Ti than the present hornblende matrix analysed by microprobe. Compared with other chloramphiboles (e.g., Krutov et al., 1970; Dick & Robinson, 1979; Gulyaeva et al., 1986) the intercumulus

Table 9. Compositions of dashkesanite and chlorine-bearing hornblende, Koitelainen and Keivitsa-Satovaara. Electron microprobe analyses by Lassi Pakkanen (1–3) and Bo Johanson (4–6).

	1	2	3	4	5	6
SiO_2	40.41	36.54	35.80	36.6	37.5	35.34
TiO_2	1.00	0.01	0.98	1.05	0.99	1.63
Al_2O_3	14.52	10.86	11.53	14.8	14.1	12.78
Cr_2O_3	0.85	0.03	0.31		0.29	
V_2O_3				0.08		
ZnO	0.00	0.03	0.11			
NiO	0.00	0.10	0.00			
FeO(tot)	12.29	26.99	26.33	18.1	17.2	22.08
MnO	0.04	0.15	0.29	0.15	0.15	0.29
MgO	12.46	3.95	3.82	8.68	9.32	6.57
CaO	11.66	10.82	11.02	11.6	11.2	10.49
SrO	0.14	0.02	0.03			
BaO	0.00	0.26	0.01	0.15	0.16	0.24
Na_2O	2.39	0.74	0.78	1.81	1.85	0.99
K_2O	0.79	3.76	3.66	1.88	1.62	2.68
Cs_2O	0.02	0.00	0.02			
F	0.32	0.22	0.25	0.00	0.17	0.58
Cl	2.59	6.08	5.80	4.50	4.42	3.66
I	0.00	0.00	0.06			
	99.46	100.58	100.79	99.32	98.68	97.70
F,Cl,I≡O	-0.72	-1.47	-1.42	-1.02	-1.07	-2.14
Total	98.74	99.11	99.37	98.30	97.62	95.56

1 - chlorine-bearing hornblende, in feldspathic olivine pyroxenite, Koitelainen DDH310/33.60 m.
2 - 6: dashkesanites from Keivitsa-Satovaara:
2 - 3 - in feldspathic olivine pyroxenite near the base of the Keivitsa intrusion, DDH307/92.50 m.
4 - 5 - in olivine pyroxenite, Satovaara (glacial erratic), sample TM-83-3.2
6 - in olivine pyroxenite, near the base of the Keivitsa intrusion, sample TM-93-6.1

chlorhornblendes of Koitelainen and Keivitsa are rather high in Ti (Table 9) and, considering the exsolved ilmenite, the original mineral was still richer in Ti. Evidently, the high-T hornblende is able to accommodate more Ti than the lattices of the lower-T skarn amphiboles. Then, high Ti would indicate high crystallization temperatures.

Chloramphiboles have been reported from the Lukkulaisvaara layered intrusion (Olanga Group, Fig. 1; Rudashevskii et al., 1991; Grokhovskaya et al., 1992). There, as in general, the minerals enriched in Cl are ascribed to later hydrothermal fluids, but the circumstances at Koitelainen and Keivitsa show that the extra, later hydrothermal fluids are incompatible with the results of our painstaking petrographic and electron microprobe work. The results also show that degassing of Cl from intercumulus liquid is highly improbable, or inconsequential. I will discuss this matter later.

The primary mica is mostly phlogopite, sometimes biotite. It contains up to 0.66% Cl, and is rich in TiO_2 (up to 4.18%) and Na_2O (up to 0.82%). The micas richest in Ti are also rich in V (up to 1.81% V_2O_3). Many electron microprobe spot analyses show high contents of Br

Table 10. Ore minerals of the Keivitsa intrusion. (W)=supergene mineral

Pyrrhotite, hexagonal	
Troilite	
Pentlandite	
Chalcopyrite	
Cubanite	
Cu-pentlandite (?)	
Talnakhite	
Millerite	
Pyrite	
Niccolite	
Magnetite	
Graphite	
Pyrrhotite, monoclinic	Bi_2Te_3(?)
Mackinawite	Altaite
Putoranite	Hessite
Chalcocite	Uraninite
Bornite	Melonite
Cr-magnetite	Arsenopyrite
Maucherite	Wehrlite (?)
Gersdorffite	Tsumoite
Co-gersdorffite	Frohbergite
Chromite	Violarite (W)
Ilmenite	Violarite-polydymite (W)
V-rich ilmenite	Marcasite (W)
Ni-rich magnetite	Covellite (W)
Ni-rich chromite	Maghemite (W)
Titanomagnetite	Gypsum (W)
"Ilmenomagnetite"	Fe(-Mn)-hydroxides (W)
Ti-Fe-Al-Cr-V-spinel	Malachite (W)
V-rich chromite	Azurite (W)
Valleriite (?)	$(Mg,Cu,Ni,Fe)SO_4 \cdot 7H_2O$ (W)
Tochilinite (?)	Copper (W ?)
Heazlewoodite	Baryte
Cobaltite	Monazite
Sphalerite	Zircon
Galena	
Cu-Zn-alloy	
Ni-rich chlorite	
Ni-rich olivine	
Ni-V-rich biotite	
Molybdenite	

(up to 3.67%) and I (up to 0.18%). The biotites of the Lukkulaisvaara PGE-Cl association contain about the same amounts of Cl (0.28–0.5%; Grokhovskaya et al., 1992).

Brown primary hornblende has growth extensions of green to colourless amphibole. These amphiboles are always low in Cl (≤ 0.27%), but occasionally high in Br (up to 2.5%) and I (up to 0.26%). The high Br contents analysed in biotite-phlogopite and amphiboles need to be checked.

After chlorapatite was found associated with the Stillwater J-M reef and in the Koitelainen intrusion (Volborth et al., 1986) it has been reported from many other PGE deposits and linked with the hydrothermal process that is said to have nourished PGE mineralizations (e.g., Boudreau et al., 1986; Barkov et al., 1993). Now, however, chlorapatite (and other Cl-rich minerals) must be discredited as, special signals from known or undiscovered PGE deposits. Without really trying hard, I have found it in every intrusion in northern Finland where I have looked for it (Koitelainen, Akanvaara, Keivitsa, Ahvenlampi, Koulumaoiva, Silmäsvaara, Kemi). Thus, it is only a signal of contaminated magma breeding the cumulus crystals, or of trapped contaminated liquid rich in Cl, but interesting as such.

In the Keivitsa intrusion, chlorapatite occurs from the base of the intrusion to the uppermost quartz gabbros. In the basal ultramafic zone chlorapatite occurs together with U-rich zircon (Fig. 46f). In the ultramafic zone chlorapatite is ubiquitous, and it occurs there as an early daughter mineral in salic melt inclusions (Fig. 46a-c) and as robust cumulus crystals, which crystallized before biotite-phlogopite. Euhedral chlorapatites are found in postcumulus plagioclase and orthopyroxene; thus, the latter silicates terminated before chlorapatite. In the gabbro zone chlorapatite continues upwards to quartz gabbros near the granophyre, where it is associated with potassium feldspar, quartz and the primary minerals biotite, hornblende, magnetite and ilmenite.

Electron microprobe analyses of chlorapatites from Koitelainen and Keivitsa intrusions are presented in Table 8.

Chlorapatite contains melt inclusions with euhedral daughter phlogopite, one in a matrix rich in Ba-Cl phlogopite (Fig. 46a-c). Such Ba-rich phlogopites have been found in the Coldwell alkaline complex, Ontario (Shaw & Penc-

Table 11. PGE(-Au) minerals, Keivitsa-Satovaara complex, with ideal formulas.

	Analysed/observed by		
Mineral	Bo Johanson/ Tapani Mutanen	Tuula Saastamoinen/VTT	Note
Arsenopalladinite $Pd_8(As,Sb)_3$		x	
Au	x		Ag-bearing
"Au_2Te"	x		
Bi-Pt-Ni-Au-telluride	x		
Braggite *(Pt,Pd,Ni)S*	x	x	
Cooperite *(Pt,Pd)S*	x	x	
Electrum *AuAg*	x		
Erlichmanite OsS_2	x		
Froodite $PdBi_2$	x		
Gersdorffite+Pt *(Ni,Co,Pt)AsS*	x		
Hollingworthite *(Rh,Pt,Pd)AsS*	x		
Irarsite *(Ir,Ru,Rh,Pt)AsS*	x		
"Irosarsite" *(Ir,Os)AsS*	x		IrOsAsS
Isoferroplatinum Pt_3Fe		x	
Kotulskite $Pd(Te,Bi)_{1-2}$	x		
Maslovite *PtBiTe*	x		
Maucherite+Pt $(Ni,Pt)_{11}As_8$	x		
Merenskyite $(Pd,Pt)(Te,Bi)_2$		x	
Michenerite *(Pd,Pt)BiTe*	x	x	
Moncheite $(Pt,Pd)(Te,Bi)_2$	x	x	
Ni-Ag-Bi-telluride		x	
Ni-Bi-Te-As		x	
Ni-Pd-Sb(-Bi)-Te	x		
Omeiite $OsAs_2$		x	
Os-Pt-Rh-As-S		x	
Pd-melonite (?) $(Ni,Pd)Te_2$	x		
Pd-Sb-S		Kojonen & al. (1996)	
(Pd,Sb) (Bi,Te)		-"-	
Pd-Bi-Sb-Te		-"-	
Pt-Bi-hessite $(Ag,Pd)_2(Te,Bi)$		x	
Pt-(Pd)-Fe-Ni	x		
Pt-Ni-Bi-Au-telluride	x		
Pt-Te	x		
Sperrylite $PtAs_2$	x		
Tellurobismuthite+Pd Bi_2Te_3		x	

zak, 1996), where they are interpreted to have crystallized from a Ba-rich intercumulus liquid. (Shaw & Penczak, 1996). Though apparently not noticed by the authors, the Coldwell phlogopites are exceptionally rich in Cl (up to 1.92%; see op. cit., Table 1).

Chlorapatite is rimmed by fluorapatite, and contains inclusions of monazite, galena and dashkesanite. Monazite occurs at the margins of chlorapatite grains, particularly in Ni-PGE-type rocks. Evidently, chlorapatite crystallized from magma with a high Cl content (see Taborszky, 1972, and Fig. 46). The crystallization of fluorapatite after chlorapatite is consistent with the decrease in Cl/F in apatites in layered intrusions (Nash, 1976, 1984; Boudreau & McCallum, 1988), in lava series (Metrich, 1990), even in single apatite crystals (Fig. 46a-c; Boudreau et al., 1986). Crystallization of early fluorapatite (in Stillwater, see Boudreau & McCallum, 1988; and in the Akanvaara and Koitelainen intrusions, see before) is associated with severe contamination by salic crustal rocks. Thus, the early fluorapa-

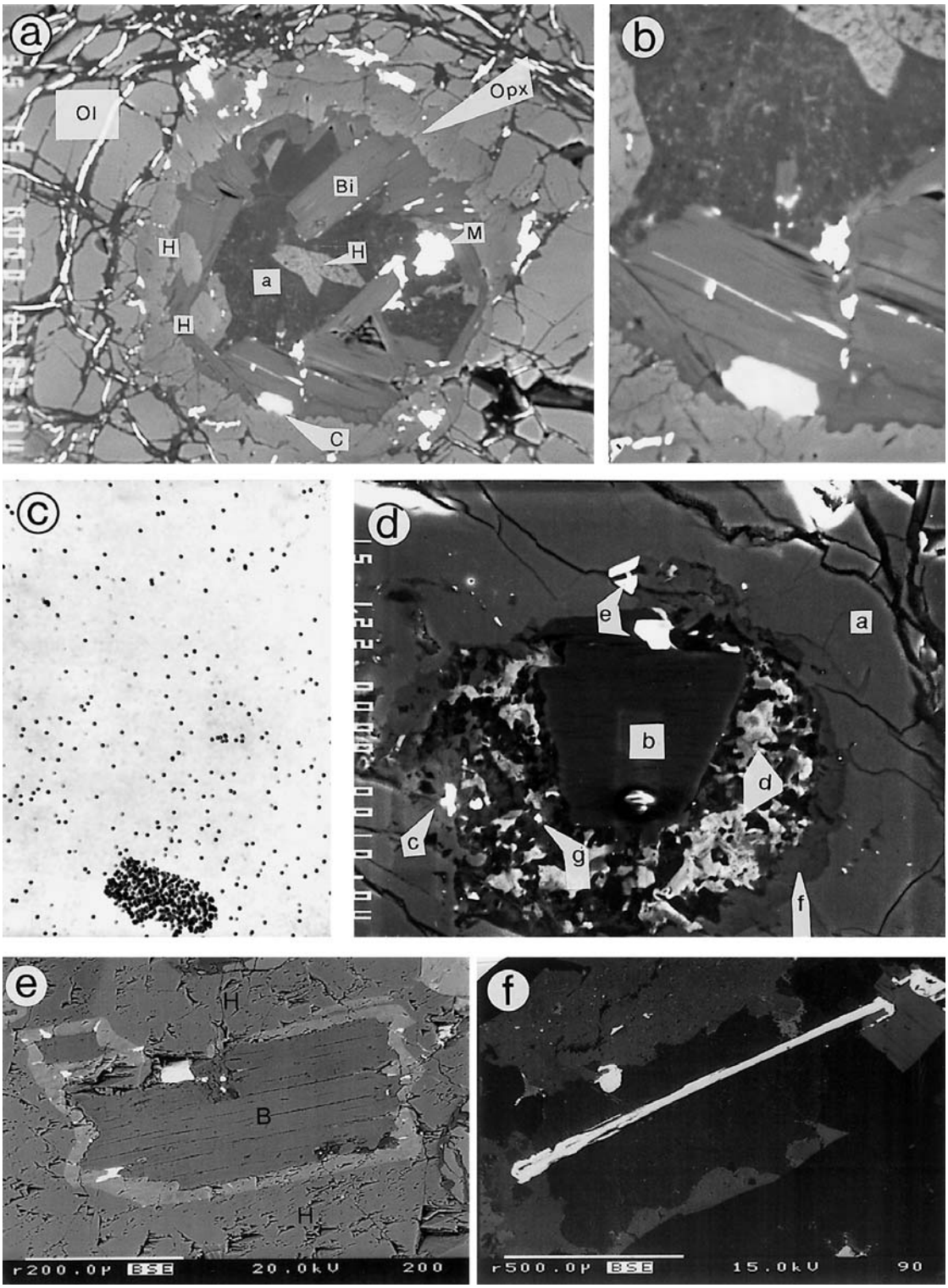
a
Ol
Opx
Bi
M
H
H
a
H
C
b
c
d
e
a
b
d
c
g
f
e
H
B
H
r200.0µ BSE 20.0kV 200
f
r500.0µ BSE 15.0kV 90

tite is a Doppelgänger; cumulus fluorapatite materialized only at a very high PCS level.

The local magma was also rich in REE. When the concentration of REE grew unbearably high in front of the growing apatite crystal, monazite crystallized and was occluded in apatite (see Baumer & al., 1983).

These observations show that the natural, F-free chlorapatite has, and crystallized with, a lattice different from that of ordinary apatite. It is not an end member of any Cl-F apatite series, but a monoclinic phase (Young et al., 1968; Hounslow & Chao, 1970). It did not allow the trace elements (Ce, Mn, U, Th) – and, evidently, fluor – so comfortable in ordinary apatite lattice (Baumer et al., 1983). Deduced from analyzed F-Cl apatites of Koitelainen, the fluorapatites can accommodate only up to 38 at% Cl (of the F+Cl sum), while F is practically lacking in chlorapatite proper (in terms of at% F+Cl; note, however, that many analysed chlorapatites are clandestinely hydrated (Taborszky, 1972); therefore, F+Cl do not add up to 100 at%). Thus, microanalyses (only a small part of which is presented in Table 8) of ordinary F(-Cl) apatites indicate that REE are in their proper crystal chemical site, increasing with increasing at% F, while chlorapatites have zero values and haphazard peaks for Ce and La. This is evidently due to tiny mineral particles of unaccepted compounds that crystallized in front of, and were ultimately included in, the growing chlorapatite crystal (see Baumer et al., 1983). Of the phases of unfit elements, monazite, galena and fluorapatite have been identified in chlorapatites of the Keivitsa intrusion (Fig. 46d).

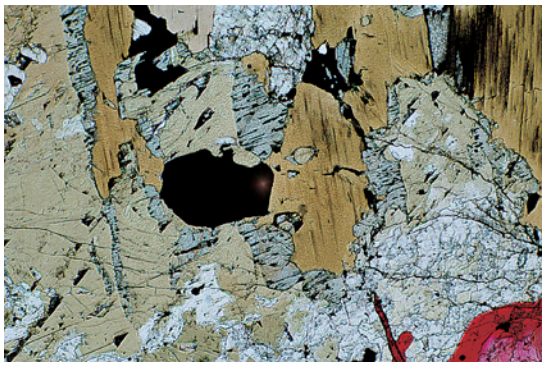

Fig. 47. Dashkesanite (light green) with ilmenite lamellae (black), between primary hornblende (brownish green) and biotite-phlogopite (brown); white – Ca-clinopyroxene. Microphotograph by Jari Väätäinen. Parallel nicols, width of photo 3 mm.

In metamorphic and retrograde processes primary mafic minerals were hydrated (into serpentine, amphiboles, talc, chlorite, secondary phlogopite) and plagioclase was altered into chlorite, clinozoisite-epidote, carbonate and scapolite. Analcime (XRD identification) is associated with scapolite. Orthopyroxene was the most susceptible to hydration, followed (in order of decreasing susceptibility) by olivine, plagioclase and clinopyroxene. The alteration generally proceeded along fractures, mineral veins and dyke contacts. The advancing alteration has a thin front of serpentinized olivine, but with completion of the process olivine was altered into tremolite. The complete-

Fig. 46. Evidence of contamination in feldspathic olivine pyroxenites, Keivitsa. BE images by Ragnar Törnroos and Bo Johanson (a–c), SE image (d) by Ragnar Törnroos and BE images by Lassi Pakkanen (e–f). a – a large, crystallized acid melt inclusion in olivine. False ore-type rock. Glacial erratic, Satovaara, sample TM-83-3; ol – host olivine, Opx – orthopyroxene reaction rim, Bt – biotite-phlogopite rim, a – albite, H – hornblende, M – magnetite, c – chlorapatite daughter crystal. Diameter of the inclusion ca 0.2 mm; b – close-up of the chlorapatite daughter crystal in Fig. 46a; c – distribution of Cl in area of Fig. 46b (a negative); d – melt inclusion (0.2 mm) in chlorapatite. a – host chlorapatite, f – La-rich fluorapatite rim, b – Mg-phlogopite crystal (low Cl and Ba), d – Ba-Cl-rich phlogopite (light-coloured matrix crystals), c – monazite, g – galena, e – chalcopyrite; e – rim of dashkesanite (medium grey) with ilmenite lamellae (white) around biotite-phlogopite (B) in brown hornblende (H). Sample TM-84-116.3; f – skeletal zircon crystals (cross-sections upper right and left of the long crystal). The zircon contains 2600–5300 ppm U. DDH307/92.50 m.

ly hydrated olivine pyroxenites (metaperidotites) always contain mineral veins (carbonate, amphibole, sulphides) and are more fractured than unaltered rocks. Partial hydration sometimes pervades the rock without connection to any visible fluid paths; a field name "pervasively amphibolized olivine pyroxenite" is applied to such rocks.

Rodingite alteration is highly characteristic of the ultramafic cumulates of Keivitsa. Rodingite (talc, hydrogrossular, diopside, carbonate) typically appears as small (1–2 mm) white spots. There are also coarse, vein-like bodies of rodingite (former pegmatoid pockets of intercumulus plagioclase ?), with big, zoned hydrogrossular crystals. Rodingite alteration occurs in all olivine pyroxenites, but is particularly common (or most visible) in the Ni-PGE ore type. The effect of rodingitization is seen in the stretching of Ca pyroxene compositions toward the diopside apex (Fig. 44). Evidently, rodingitization at Keivitsa did not involve true Ca metasomatism, but was essentially an autometasomatic alteration of calcic intercumulus plagioclase.

Emplacement, contact effects and xenoliths

The feeder dyke of the intrusion has not yet been located for sure. The most likely candidate is currently the dyke-like row of mafic and ultramafic rocks extending 20 km northeastwards from the faulted junction of the Keivitsa and Satovaara intrusions.

The intrusion chamber was filled as a single cast. No evidence of repetitive entries of magma has been found in the Keivitsa intrusion.

The Keivitsa magma intruded into the sedimentary pile at about the level where the amounts of sulphides and graphite increase. The intrusion is discordant to the surrounding rocks. Black schists are found both below and above the intrusion. The base contact of the intrusion is slightly discordant to the floor strata. Both flanks are discordant. The western flank is composed of interfingered gabbros and hornfelses; the eastern flank is also interfingered and cuts steeply across the strata.

The intrusion has a broad thermometamorphic hornfels aureole. Hornfelses were altered into metahornfelses in later regional metamorphism. The roof hornfelses still retain the original decussate textures; hornfelses of xenoliths are trim, granoblastic rocks. Of the original hornfels minerals, kyanite is preserved in pelitic rocks in both the floor and the roof rocks; Its presence indicates high fluid pressure in rapidly heated, wet sediments rather than high lithostatic pressure (Rutland, 1965; Smith, 1969; Atherton et al., 1975; Masaitis & Yudina, 1976; Litvinovskii et al., 1990). Likewise, garnet and hornblende near the base of the intrusion are probably relics of the contact metamorphic facies assemblage.

Wall rocks hydrated to any degree (pelites, serpentinites) underwent contraction by dehydration (14 vol% in Stillwater; Barker, 1975), which efficiently increased the surface area of the xenoliths swallowed by magma and thus accelerated their melting. Dissociation of graphite into CO and CO_2 had the same explosive effect, and comminution of graphitic xenoliths continued in magma. The comminution effect is described by Furlong and Myers (1985) as "thermal stress", by Ulff-Møller (1990) as "influence of the hot magma". As I have figured this out, the whole process would include alternating contraction, expansion and melting: early hydrous explosion (fluid overpressure, the only direction of yield in the roof being down towards magma), fluid-overpressure melting (see Fig. 30), fluid-saturated melting (with total volume contraction), dehydration contraction, instantaneous build-up of tension at α/ß quartz inversion, and continuous thermal expansion in fragments. In the

Keivitsa intrusion, selective melting of layers of low-melting-point compositions above the intrusion resulted in progressive cave-in of the roof. Dehydration contraction of the floor rocks ripped gashes, to be filled by sulphide liquid of the Cu-rich "offset" deposits (e.g., Godlevskii, 1968). All these processes resulted in effective demolition of the envelope of the intrusion, continuous comminution and, ultimately, melting and mechanical disintegration of xenolithic material.

The magma swallowed and digested significant quantities of country rocks. Pelitic rocks, now pyroxene-plagioclase hornfels, are found as large xenoliths and as half-digested (rotten) xenoliths. Komatiitic rocks occur as solid layered, banded and massive ultramafic xenoliths (Fig. 48) or as mechanically disintegrated rotten xenoliths. Composite komatiitic-pelitic xenoliths are also present.

Fresh komatiite xenoliths (komatiite hornfelses) are composed of olivine, chromite, clinopyroxene and orthopyroxene, the mineral proportions depending on the original chemistry of the rocks (Table 7). The original chromite is sometimes recrystallized into chrommagnetite, suggesting that inherited chromites served as seed crystals of cumulus chrommagnetite.

Komatiite xenoliths are often overlain by contaminated material rich in pyroxene and sulphides, presumably from the melted sedimentary part of the original composite xenoliths. It is often seen that the cumulus mush has intruded into the cracks of komatiite xenoliths. Olivine pyroxenites beneath many xenoliths contain abundant primary brown hornblende, which often has euhedral cores; euhedral hornblende crystals occur inside orthopyroxene oikocrysts.

The komatiite xenoliths contain fine-grained disseminated sulphides corresponding in bulk composition to the interstitial sulphides in the surrounding cumulate matrix. The xenoliths in barren olivine pyroxenites do not contain sulphides. Thus, it seems that sulphides infiltrated (as liquid) into the xenoliths from the surrounding magma.

On account of graphite dissociation and accompanying disintegration of xenoliths high-carbonaceous xenoliths are rare, but small graphitic xenoliths (ca 5–10 cm across), however, do occur – telltale signs of incorporated graphite-rich black schist material. Graphite-rich pelitic hornfels xenoliths are associated with false ore sulphides ca 2 km west of the Keivitsansarvi deposit (see map, Appendix 4).

Graphite is found in many intrusions and in many forms, often in clots suggesting half-digested xenoliths. Graphite is closely associated with PGE in Merensky Reef and Stillwater J-M reef PGE deposits, the Platreef deposit in the Bushveld Complex (Buchanan & Rouse, 1984) and it occurs in ultramafic pegmatoids below the Stillwater J-M reef (Volborth & Housley, 1984). Sedimentary origin of graphite is often indicated by field relationships and by the carbon isotope composition (Liebenberg, 1970; Buchanan & Rouse, 1984; Touysinthiphoexay et al., 1984; Fletcher, 1988). A primary igneous origin is sometimes suggested (e.g., Kornprobst et al., 1987). In the Keivitsa intrusion, graphite crystallized as beautiful euhedral cumulus crystals (Mutanen, 1989b) from a magma that had digested carbonaceous sediments.

Gaseous or solid carbonaceous contaminants will be dissolved in magma as carbon, or degassed, until equilibrium between C, CO and CO_2 is attained (Grinenko, 1967). This depends on the magma composition and, above all, on total pressure. At a P(tot) of only 400 bar (ca 1.5 km depth) graphite is stable in basaltic magmas without metallic iron, i.e., at oxygen pressures above the IW buffer line (Goodrich & Bird, 1985). The association of carbon and chlorine is established already in magmas (Hoefs, 1965); thus, their close association in Stillwater (Volborth et al., 1986) may well be a feature that reflects the composition of pore liquid (see also Slobodskoi, 1981).

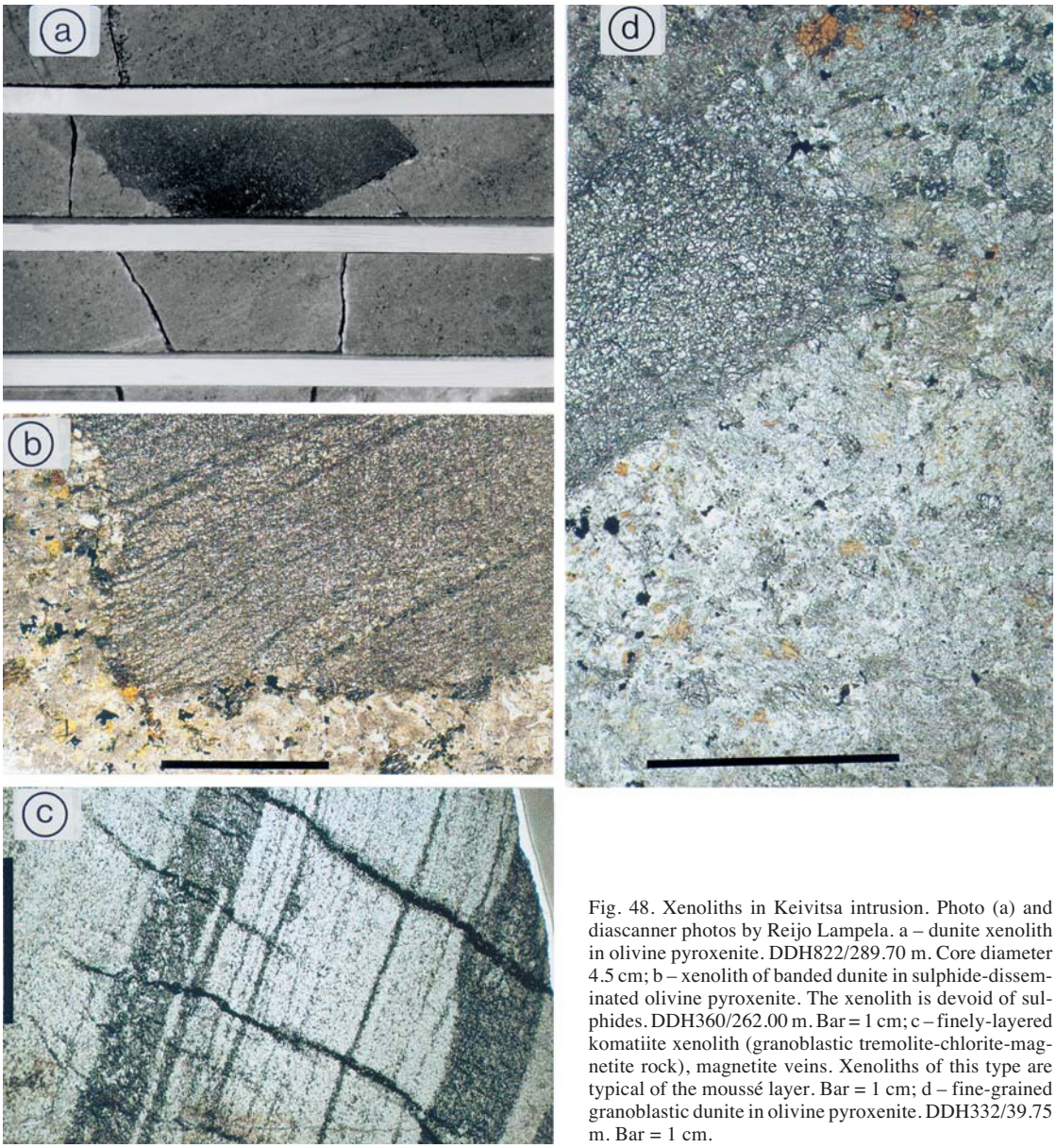

Fig. 48. Xenoliths in Keivitsa intrusion. Photo (a) and diascanner photos by Reijo Lampela. a – dunite xenolith in olivine pyroxenite. DDH822/289.70 m. Core diameter 4.5 cm; b – xenolith of banded dunite in sulphide-disseminated olivine pyroxenite. The xenolith is devoid of sulphides. DDH360/262.00 m. Bar = 1 cm; c – finely-layered komatiite xenolith (granoblastic tremolite-chlorite-magnetite rock), magnetite veins. Xenoliths of this type are typical of the moussé layer. Bar = 1 cm; d – fine-grained granoblastic dunite in olivine pyroxenite. DDH332/39.75 m. Bar = 1 cm.

For all of the so called volatile components (S, C, H_2O, Cl) the same principle applies as for carbon: with increasing P(tot) the equilibrium in a system crystal – silicate liquid – gas will shift away from the gas toward liquid solution and crystal; thus, an increase of P(tot) will check degassing and the volatiles "behave": they are increasingly bound to dense liquid and crystalline phases, such as sulphide liquid and the high-T Mss, graphite, magmatic hornblende, dashkesanite and graphite. At pressures prevailing in intrusions there is no need for degassing (cf., e.g., Boudreau & McCallum, 1984); as seen in Table 9, even in the

absence of H_2O, Cl will form the "dry" amphibole, dashkesanite.

Undoubtedly, the small pelitic xenoliths were readily melted. At the partial melting of bigger xenoliths alkalies and silica were lost to the main magma, leaving a residue enriched in pyroxene and sulphides. Sulphide liquid remained a residual phase after total melting of pelites; false ore sulphides closely correspond to this residual sulphide phase.

The Keivitsa magma was clearly not able to melt the komatiitic xenoliths. However, the 10–15% dehydration-contraction of the original komatiitic rocks (composed mainly of serpentine, tremolite and chlorite) resulted in mechanical disintegration of both roof and xenoliths (Fig. 49). When the roof was rapidly exposed to magma, dehydration began with the initial separation of a high-pressure fluid. This "fluid explosion" shattered the rock and prepared the ground for further comminution. Most of the fluid components (H_2O, Cl) were subsequently dissolved in magma. Melting of sedimentary interlayers promoted the demolition of komatiitic roof rocks and xenoliths.

Komatiitic xenoliths are characteristic of the Keivitsa intrusion (Fig. 48). Even more significantly, as regards the ore petrology, the xenoliths are most abundant within the Keivitsansarvi deposit. On the other hand, rotten pelitic xenoliths are always associated with false ore sulphides (see later). The komatiite xenoliths are of all sizes, from single olivine grains to the huge serpentinite-peridotite xenolith in the middle of the intrusion (see Appendix 4, for compositions, see anal. 15–17, Table 7). This mother xenolith has a low-density serpentinite core and a rim of peridotite. Its position on top of the ultramafic cumulate pile could be explained as follows: The smaller ultramafic fragments were dehydrated early and began to sink in magma after detachment. Dehydration of the innards of the big xenolith, however, was slow and, thus, sinking was delayed until the xenolith reached critical overall density; also, at the moment of sinking, the density of the magma decreased when plagioclase entered (and olivine finished) as a cumulus phase.

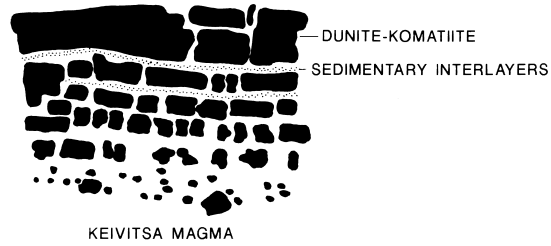

Fig. 49. Schematic presentation of the mechanical decomposition of dehydrating serpentinite roof rocks and xenoliths in Keivitsa magma (see text).

Near the top of the Main Ore is a layer of concentrated komatiite xenoliths, called the moussé layer. It is usually 4 – 10 m thick, and in diamond drill holes can be traced for 300 m from north to south. Typical of the moussé layer are big, thin-layered xenoliths of komatiitic tuff.

The komatiite xenoliths exchanged components with the surrounding magma, and solitary olivine xenocrysts reacted with, and adjusted their composition to, the melt. In this reequilibration the thermometamorphic komatiitic olivine became richer in Fe. But still more important was that it lost Ni to magma (see Fig. 43). This Ni addition markedly increased the Ni content of the sulphides of the Keivitsansarvi deposit.

A peculiar quartz-carbonate rock occurs at the base of the biggest serpentinite-peridotite xenolith (anal. 18–19, Table 7). Variable, but generally high, PGE, Cr and V concentrations are characteristic of the deposit; also, REE are sometimes very high (up to 1132 ppm Ce and 643 ppm La).

Besides quartz there are euhedral, zoned carbonate crystals, albite, magnetite, chromite, ilmenite and rutile in varying amounts. The rocks are massive or banded and hornfels-like. The colour ranges from white and grey to dark grey and black, depending on the abundance of Fe-Ti-Cr oxides. Structures reminiscent of

load-cast occur between ligh-coloured and dark, oxide-rich layers (Fig. 58). The weathered parts are cavernous due to dissolved carbonate. Associated with the quartz-carbonate rocks are carbonate rocks and albite-talc (± vermiculite) rocks.

Contamination and crystal fractionation

As at Akanvaara and Koitelainen, the Keivitsa magma received contaminants from various rocks and by various mechanisms. The contaminants from komatiites, black schists and pelites swayed the crystallization path and all but obliterated the geochemical colour of the parent magma. Contamination is seen in the occurrence of reduced carbon (graphite) and a high content of volatiles (H_2O, Cl) and of certain trace elements (PGE-Au, S, Se, Te, Se, Ni, Co, V, REE, U). Isotope data (Sm-Nd, S isotopes, Sm-Nd, Re-Os; see Huhma et al., 1995b; Hanski et al., 1996) also indicate heavy contamination by surrounding crustal rocks.

The principal contamination mechanisms were, first, selective diffusion of H_2O, Cl, K, P and REE from wall rocks, xenoliths, and salic anatectic melt; second, bulk assimilation of salic neo-melts; and, third, incorporation of residue phases of partially melted or mechanically disintegrated rocks (sulphide liquid from pelites, sulphide liquid and insoluble graphite from black schists, olivine and chromite from komatiites).

Most affected by contamination was the uppermost part of the magma chamber. Moreover, as discussed before, it was also the principal nursery of cumulus crystals, which were promptly transported downwards by density flows and deposited upon earlier cumulates. Contaminated liquid was dragged along in the density flow and eventually trapped between settled crystals. Study of the gabbro zone cumulates and comparison with intercumulus material of the ultramafic zone suggest that the main mafic magma was not stirred and homogenized (the Sargasso Sea phenomenon).

The ultimate reason for selective contamination was that the mafic magma was undersaturated in components (H_2O, Cl, K, P, REE) transferred from country rocks and neo-melts. As regards quantity, petrological implications and petrographic visibility, H_2O was undoubtedly the principal contaminant. The main effect of added H_2O and K (possibly augmented by Cl) was expansion of the olivine liquidus field. The H_2O that entered the roof of the magma chamber was not dispensed in the main magma, but was carried down, along with cumulus crystals, by density flow suspension and stored in the cumulus deposits that were rapidly piling up. Ultimately, at the prevailing total pressure, H_2O was fixed in high-T postcumulus OH minerals (hornblende, biotite-phlogopite). No degassing of H_2O from intercumulus space has been noted (or needed). The main magma body remained poor in H_2O and, as far up as can be seen, hornblende did not crystallize from magma.

As a case example of selective contamination I shall describe the behaviour of Cl, which has been studied rather little in magmas and their environs. The selective transfer of Cl from the serpentinite xenoliths and from pelites can be followed in several diamond drill holes (see Figs 51 to 53). The transfer ("transvaporization") of Cl into magma as opposite to degassing was associated with selective diffusion of H_2O and K. In fact, it seems that the diffusion of Cl and K was coupled. The serpentinite has a very high Cl content; the change from Cl-rich to Cl-depleted serpentinite is sharp. In pelites the Cl is enriched in argillic beds (Fig. 53); the Cl depletion goes smoothly towards magma. Note that Cl enrichment in the underlying magma is accompanied by enrichment of K_2O. Note also (Fig. 52) that the granophyre magma evidently had a low ca-

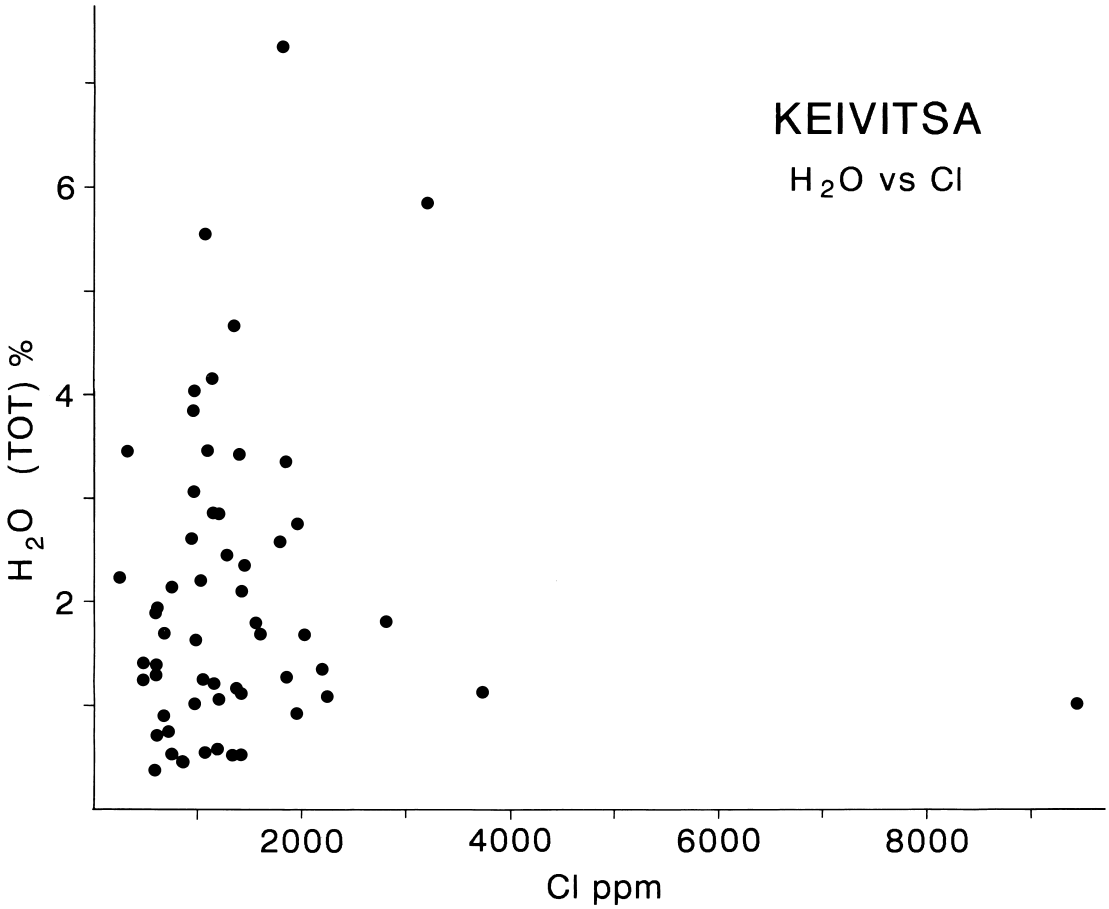

Fig. 50. H_2O vs Cl in Keivitsa ultramafic cumulates.

pacity to dissolve (or to keep) Cl. Besides the Cl fixed in minerals in wall rocks, an important source of Cl was presumably the brines in pores and cracks of the wall rocks. The source of the brines may have been the Jatulian evaporites (Shatskii & Zaitsevskaya, 1994) underlying the Ludian formations. Sea water and (or) brines are a source favoured by many for the Cl-enriched assemblages (e.g., Prichard & Cann, 1982; Vanko, 1986; Michael, 1988; Symonds et al., 1988, 1990; Michael & Schilling, 1989). The "evaporitic" elements (e.g., Li and perhaps Na in spilites, Cl in metasedimentary and igneous rocks) are among the few vestiges of the ancient evaporites that once existed (see Serdyuchenko, 1975, and references therein; Ramsay & Davidson, 1970; Appleyard, 1974).

The magma had a considerable capacity to dissolve Cl (see Carroll & Webster, 1994). Mantle magmas, being very poor in Cl (50–60 ppm Cl; e.g., Byers et al., 1984, 1986; or 10–40 ppm; Michael & Schilling, 1989), are undersaturated in Cl and, thus, acted as a sponge for Cl. Evidently, the Cl of Cl-rich magmas came from sediments. The Cl content in lavas can be very high, up to 1–1.62 wt% (e.g.,

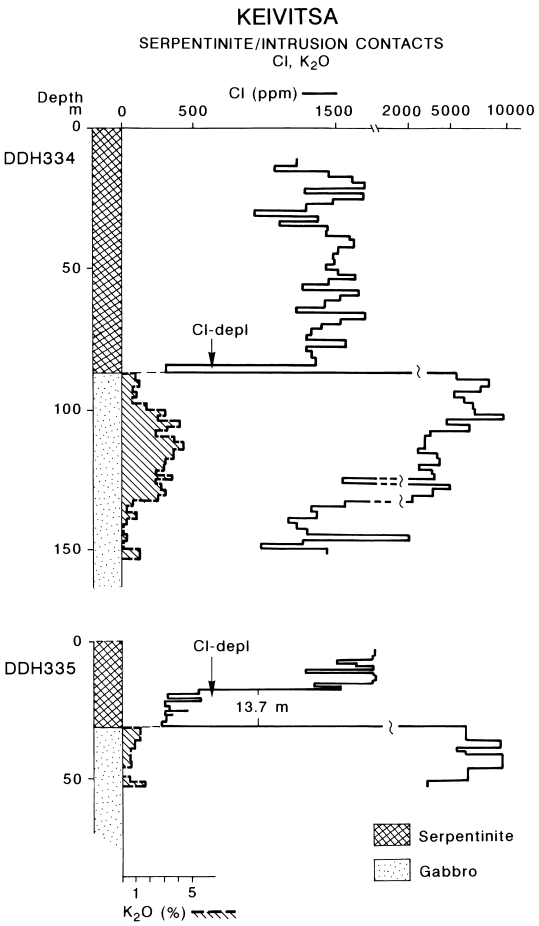

Fig. 51. Depletion of chlorine in the big serpentinite xenolith near the magma contact. Keivitsa, DDH334 and 335. The thinner Cl-depleted zone in DDH334 is against a magma apophyse, the broader Cl-depleted zone in DDH335 against the main magma chamber. Note the dramatic high in Cl (and K) in the underlying intrusion rocks.

Johnston, 1980; Metrich, 1990; Kovalenko et al., 1992; Naumov et al., 1996). In general, increase of Mg, Fe and Ca increases the solubility of Cl (Delbov et al., 1986). The highest solubilities, though, are attained in alkalic intermediate rocks (Kovalenko et al., 1992; Naumov et al., 1996), probably due to the right chemistry (coupling of Cl and K in melt structure ?) and relatively lower magma temperatures which increase the solubility of gases (e.g., Kadik et al., 1971). Selective contamination, as depicted above, is certainly a feasible process. At Keivitsa the Cl was hitched to magmatic and high-T postmagmatic minerals (chlorapatite, dashkesanite, biotite-phlogopite); thus, at the pressure conditions of layered intrusions Cl is not necessarily enriched proportionally to the amount of crystal fractionation as generally purported (Metrich, 1990). Also, as Cl can build high-T phases of its own, the question of Cl/F distribution between low-density fluid and silicate liquid (e.g., Boudreau et al., 1986) is not relevant at all, if we had the alternative equilibrium of a solid phase and silicate liquid. In the Koitelainen, Akanvaara and Keivitsa intrusions, at least, there is no evidence of degassing of Cl, the idea suggested and elaborated by Boudreau and co-workers (Boudreau et al., 1986; Boudreau & McCallum, 1988, 1988; Boudreau, 1988). Furthermore, as the solubility of PGE in fluid, in a fluid/silicate liquid system, is too low to be of any consequence in the genesis of PGE deposits (Gorbachev, 1989), and lacking any positive evidence from Keivitsa, I will not discuss further the idea of the transfer and deposition of PGE by fluids exsolved from intercumulus liquid (Boudreau, 1993).

Neither is there evidence for magmatic degassing of Cl from the intrusion. Only ca 50% of Cl was degassed from subaerial lavas (Kovalenko et al., 1992). Metrich (1990) estimates that degassing [evidently of "free" Cl dissolved in melt] occurs only at pressures below 4 MPA (40 bar).

The Cl content of ultramafic cumulates of Keivitsa varies but is generally high, commonly 1000–1500 ppm but occasionally up to, and more than, 3000 ppm. As the Cl content does not correlate with the total OH content (i.e., degree of metamorphic hydration; Fig. 50) of the rock, Cl was not introduced later by the the metamorphic fluid. There is local but no general correlation between Cl and S contents. Remarkably, an upward inflection in the Cl profile occurs at the upper ore layer (Fig. 54). A

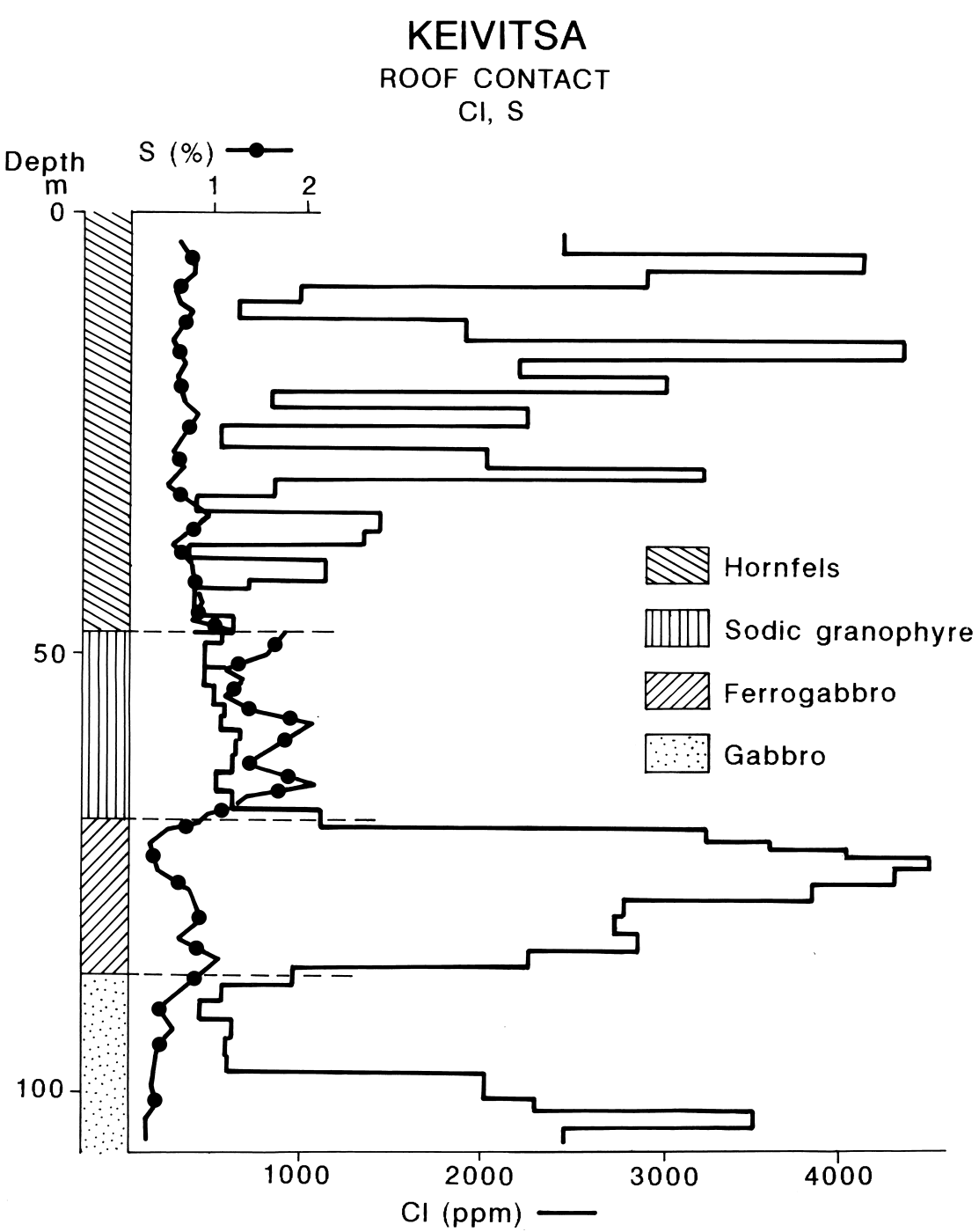

Fig. 52. Gradual downward depletion of Cl in pelitic metahornfelses, roof rocks of the Keivitsa intrusion. Note the low Cl and high S in the granophyre, and the lack of S depletion in roof rocks. Data from DDH728.

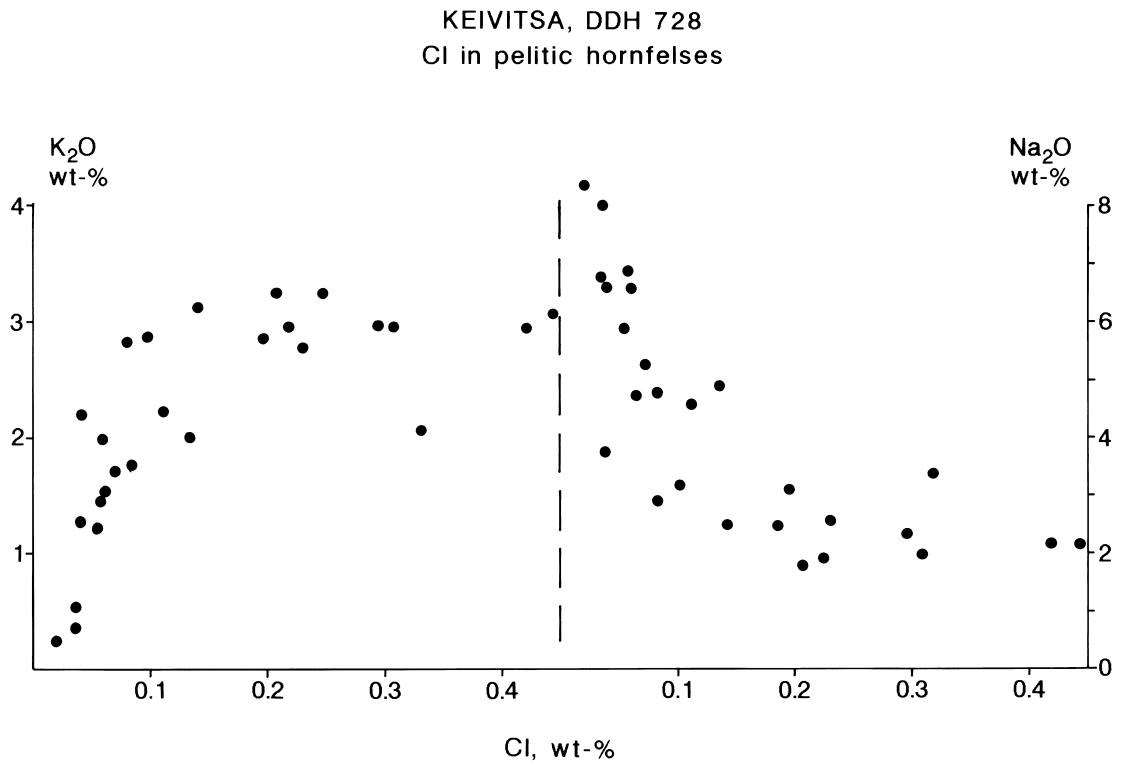

Fig. 53. Plots of Na_2O and K_2O vs Cl in pelitic metahornfelses overlying the Keivitsa intrusion. Data from DDH728.

similar marked increase in Cl occurs at the level of the Ni-PGE type ore in DDH 333 (not shown).

The contaminated magma immediately below the roof obviously had a very high Cl content (see Fig. 51). It is possible that the high Cl, either alone or, particularly, in combination with other contaminants, expanded the apatite liquidus field to the extent that chlorapatite crystallized from magma. Thus, the big chlorapatite crystals in ultramafic rocks would be true cumulus crystals, extended by postcumulus growth. Daughter crystals of chlorapatite in melt inclusions in olivine (Fig. 46a) indicate that chlorapatite crystallized early from this hybrid melt.

In conclusion I reiterate: all the evidence from KOI-type and KEI-type intrusions shows, unambiguously, that chlorapatites crystallized directly from magmas, either as true cumulus crystals (see e.g. Mutanen, 1989b, Fig. 24, Fig. 46a-c, in this book) or high-T postcumulus phases from the Cl-enriched pore liquids. Fluorapatite was a later, separate phase, which deposited on chlorapatite. Thus, chlorapatite did not attain its composition by re-equilibration with the intercumulus liquid as postulated by Cawthorn (1994), nor did it crystallize from a low-density fluid degassed from intercumulus spaces below, as suggested by Boudreau (1988, 1993; Boudreau et al., 1986; Boudreau & McCallum, 1986, 1988).

The studies of Watson (1982) show that in salic/mafic emulsion K is transferred from the anatectic salic melt to the mafic magma; contrariwise, Na is enriched in the acid melt. This

is what actually seems to have happened at Keivitsa. The granophyre is rich in Na and the Na/K is very high, whereas the melt inclusions and the intercumulus are rich in K. Like H_2O and Cl, the K was compatible by association: included in the contaminated mafic melt, it was retained in the intercumulus melt and eventually formed (by reaction with orthopyroxene) postcumulus biotite-phlogopite.

Comparison of REE distribution in the granophyre and sedimentary rocks (Figs 86 and 87) shows that the granophyre is depleted of the LREE in relation to sediments, which suggests that LREE were enriched in the contaminated melt, possibly transferred as Cl complexes. Concentrated carriers of REE are fluorapatite and monazite (Fig. 46). Chlorapatite contains concentrated particles of REE phases. It was noted at an early stage that the host rocks of the Ni-PGE ore type are rich in La and Ce (Fig. 73). The general high REE content reflects the high REE in contaminated magma.

As I shall discuss later, the Ni-PGE type reflects the geochemical characteristics of the komatiitic dunite and the associated quartz rock in many ways. High contents of REE (Ce up to 1130 ppm, La up to 640 ppm) in quartz rock suggest that it may have been an important source of REE contamination.

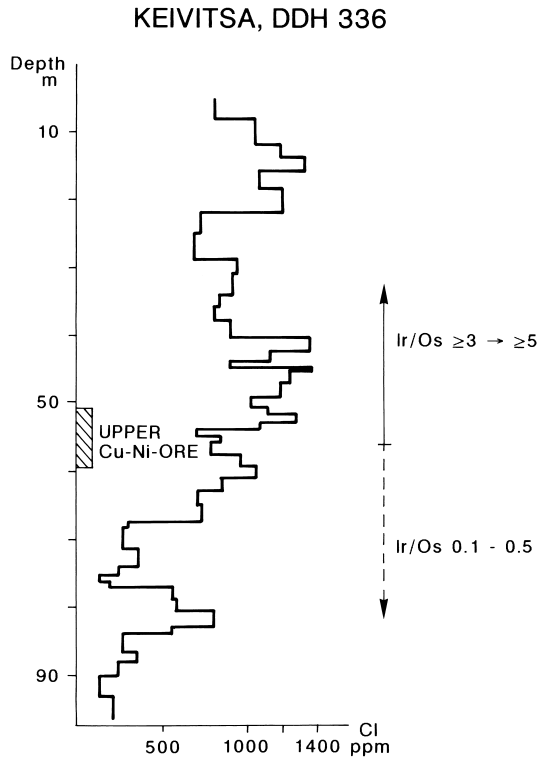

Fig. 54. Profile through the upper ore layer, Keivitsa (DDH336), showing a gradual increase in Cl and the sudden jump in the Ir/Os ratio in the middle of the ore layer.

The granophyre and most of the cumulates seem to have preserved the negative Eu(CN) anomaly inherited from sediments (Fig. 87). Only some late gabbros with cumulus plagioclase have a flat or positive Eu.

The relatively low REE and the drooping LREE end of the regular and low-Cr false ores (Fig. 87) reflect the salic melt depleted in REE by selective diffusion to the mafic magma, and the high proportion of orthopyroxene (see Schnetzler & Philpotts, 1970).

Strong convection caused local mixing of the anatectic acid melt and the mafic liquid, resulting in the formation of a hybrid melt. The apparent simultaneous crystallization of olivine and orthopyroxene can be understood if orthopyroxene crystallized in a hybrid melt richer in silica, and the two nursing environments were only incompletely mixed. The pitted peridotite (Fig. 42), with two domains of cumulus assemblages, would then represent this kind of heterogeneous cumulate (see Jackson, 1961). The low-Cr type of olivine pyroxenite, the host of some false ore sulphides, also indicates bulk mixing of salic and mafic magmas. The wide spread of the intercumulus plagioclase compositions (Fig. 45) implies a heterogeneous intercumulus liquid with variable amounts of salic contaminant melt. The hybrid melt is preserved as inclusions in olivine (Fig. 46).

Melting and assimilation of pelitic schists promoted the separation of sulphide liquid by the double effect of added sulphur and siliceous liquid. Understandably, assimilation of

ordinary pelites, as such, did not contribute anything of value to the ores; quite the contrary, it diluted the magma with Ni-poor material. However, the relatively high Au in sulphides, when compared with other Ni-Cu(-PGE) deposits (Fig. 76), may be explained by the addition of Au from assimilated rocks. In fact, in the southern part of the intrusion, several sulphide-bearing hornfels intersections have high Au values (270 ppb/0.7 m, 1510 ppb/1.4 m, 15–88 ppb/9.3 m). Thus, it may not be mere coincidence that false ore sulphides in this same area are noted for their relatively high Au and high Au/Pd.

Olivine xenocrysts from disintegrated komatiites were residue phases (see above). Insoluble as they were, they were not chemically inert, but reacted and exchanged components with the magma they arrived in. The dunite-serpentinite, with 0.2 – 0.4% Ni, is the rock richest in Ni in the complex, the Keivitsansarvi deposit included. On the other hand, the Ni content of the parent magma was only ca 100 ppm (Table 6) and, so, with the fractionation of olivine and pyroxenes, Ni was doomed to decline in the residual liquid. With no evidence of added primitive magma, the only possibility that remains is that a great part of the Ni in the Keivitsansarvi deposit was supplied by Ni-rich komatiite debris.

The melting of pelites left a residue of sulphide liquid, most of it not soluble in the hybrid magma, which was charged with cumulus crystals. Mixing and equilibration with the main magma and komatiitic olivine xenocrysts produced a beautiful mixing line between pelitic sulphides and komatiitic dunites (see Figs 62 and 65). The main magma was undersaturated in sulphide and acquired little of the added sulphur. It evidently reached terminal sulphide saturation only at the level of the uppermost ferrogabbros.

Note (Fig. 52) that depletion of S did not occur in the roof (if anything, there is an *increase* in S towards the magma). Thus, magma did not acquire S by selective diffusion or by trickling of anatectic sulphide melt down to magma (cf. Thompson & Naldrett, 1984).

Partial melting of black schists left a residue of graphite. Under the total pressure conditions of the intrusion, part of the graphite oxidized to CO_2 and part dissolved in melt as carbon (see Mathez & Delaney, 1981). That graphite can crystallize from magmas in layered intrusions has been realized since the early 1980s (e.g., Elliott et al., 1981; Ulmer, 1983).

At Keivitsa, graphite crystallized locally from carbon-saturated magma as euhedral crystals, and the local residual liquid remained saturated with graphite (Mutanen, 1989b). Intercumulus graphite is particularly common in the Ni-PGE ore type.

Assimilation of carbonaceous sediments caused reduction of magma. The low ferric/ferrous ratio is reflected in the suppression of magnetite crystallization, in the relatively low Mg/Fe of the equilibrated komatiitic olivine and in the early appearance of primary pigeonitic pyroxene and fayalitic olivine.

The presence of intercumulus graphite indicates that the graphite buffer had not been consumed but had survived to subsolidus temperatures. The sulphide paragenesis, with troilite, talnakhite and very rare secondary magnetite, reflects reducing subsolidus conditions.

Graphite and graphite-rich xenoliths, having a density lower that that of the magma, were able to float and stack at the roof. The trajectories of any crystalline phases, whether cumulus or residual, would have crossed this reducing float layer. The graphite gabbro may have crystallized from this kind of carbon-saturated, graphite-enriched melt. The absence of primary magnetite and the presence of inverted pigeonite in this rock are testimonies of the low oxidation state of Fe. In olivine pyroxenite immediately below the graphite gabbro, graphite occurs as roundish, radial-textured aggregates.

As in the contaminated KOI-type intrusions, olivine and plagioclase did not crystallize together cotectically. In the late stage of the evolution of the gabbroic main magma plagiocla-

se, pyroxenes and a fayalitic olivine crystallized together.

Naturally, the Al/Ti ratio, sometimes used to characterize the parent magma, is of no use in Keivitsa, where it varies in a complex way. In cumulates the ratio depends on Al/Ti of the parent magma, of the partially melted contaminants (with different Al/Ti ratios in low-Ti and high-Ti pelites), of disintegrated komatiitic material and on the amount of cumulus plagioclase. Cumulus plagioclase occurs as honest cumulus crystals in gabbroic interlayers in the ultramafic zone and in gabbros, and as euhedral inclusions in orthopyroxene in some "pitted peridotites". The most subtle form of cumulus plagioclase is the partially redissolved cumulus plagioclase camouflaged as an intercumulus mineral. In general, Al/Ti in crustal intrusions is an undecipherable figure that is a result of mixing of myriad contaminants and fractionated crystals, with highly variable Al/Ti (plagioclase, ilmenite, loveringite, chromite), with the magma, beginning from the mantle source.

The fractional crystallization soon began to deviate from the path predestined by the composition of the parent magma as a result of the contaminants acquired. The contaminants (H_2O, alkalies) leading to an increase in the olivine liquidus field, had effects similar to those at Koitelainen except that no olivine monocumulates were formed but that olivine and clinopyroxene (+Cr-magnetite) crystallized together in roughly fixed proportions.

Nowhere in the ultramafic zone are there discernible geochemical trends. At times, and in places, the increased role of acid contaminant melt is reflected in an increase in V, decrease in Cr and the change in the sulphide liquid toward sedimentary composition (low Ni/Co, Ni(100S), Se/S, Te/S, etc; see below).

In the upper part of the ultramafic zone in general, in the Cu-Ni-PGE-Au deposit in particular and above all in the host rocks of the Ni-PGE ore type, the residual olivine from disintegrated komatiitic dunites significantly contributed to the olivine content of the rocks.

The contamination by carbonaceous sedimentary material caused a general reduction of the magma (see above). During accumulation of the ultramafic zone the effect of carbon assimilation in decreasing the ferric-ferrous ratio of melt (and, thus, of crystallizing silicates) was countered by the alkalic-ferric iron effect (Paul & Douglas, 1965) associated with selective transfer of K and general assimilation of salic material.

Apart from general reduction, the main magma was only marginally affected by contaminants and thus evolved autonomously. Cumulus plagioclase appeared soon after the disappearance of magnesian olivine, to be joined later by pigeonite, and locally by graphite, fayalitic olivine and magnetite. Remarkably, the P content of the residual liquid remained very low, and so terminal apatite saturation failed by a wide margin in Keivitsa intrusion (the last ferrogabbros contain only 0.1% P_2O_5). It is possible that the crystallization of chlorapatite continuously skimmed P_2O_5 from the main magma. Chlorapatite occurs in gabbro interlayers in the upper part of the ultramafic zone and in the uppermost gabbros in the western part of the intrusion. In the uppermost quartz gabbros of the Satovaara block fluorapatite (1.4 vol%) crystallized as a cumulus mineral.

Dyke rocks and mineral veins

Several kinds of dykes cut the Keivitsa intrusion. The earliest generation of the veins are gabbroic veins, often porphyritic with microgabbro matrix (Fig. 55, top), with sharp contacts. The mineralogy of these veins (e.g., chlorapatite is abundant) is what would be expect-

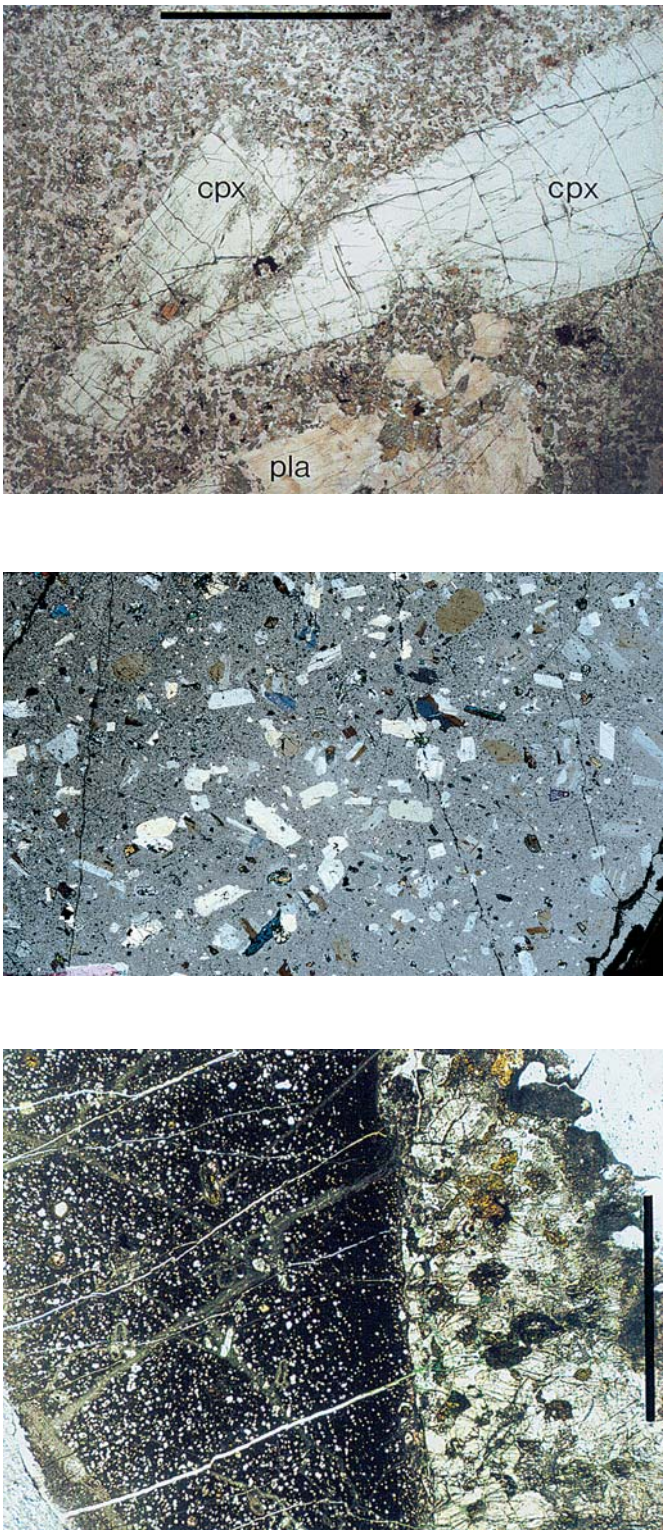

Fig. 55. Dyke rocks, Keivitsa. Top – olivine microgabbro, with megacrysts of Ca-clinopyroxene (cpx) and plagioclase (pla). Chlorapatite is very common in this rock. DDH696/405.75 m. Bar = 1 cm; middle – porphyritic felsic dyke rock, with euhedral phenocrysts of plagioclase, quartz and magmatic hornblende. Pyroxene phenocrysts also occur in these rocks. DDH397/30.15 m. Crossed nicols, width of photo 2.2 cm; bottom – chilled contact of olivine gabbro-diabase with olivine pyroxenite. Phenocrysts of partly altered olivine and Ca-clinopyroxene. DDH760/41.50 m. Bar = 1 cm. Diascanner photos (top and bottom) by Reijo Lampela, microphoto in the middle by Jari Väätäinen.

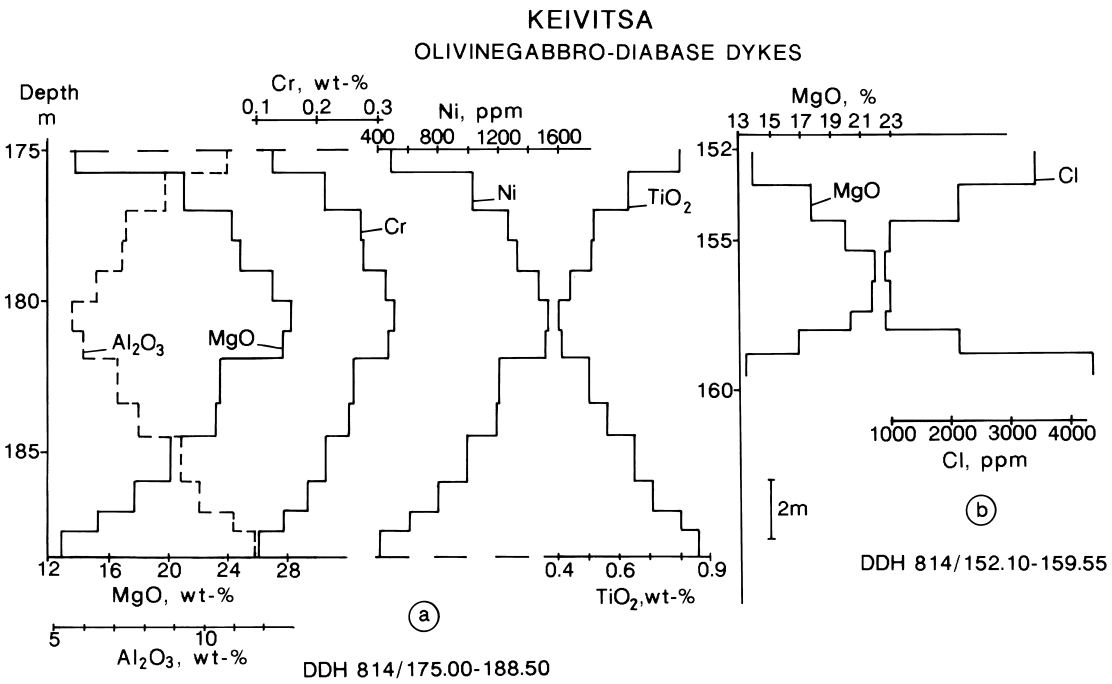

Fig. 56. Profiles across two olivine gabbro-diabase dykes, showing (a) strong effects of flow differentiation and (b) enrichment of Cl near dyke margins. Vertical scale in metres along DDH.

ed from intercumulus melt. Thus, I interpret these to represent local evolved intercumulus liquid, which seeped into late contraction cracks. Being enriched in H_20, the magma chilled at the continuous release of pressure (see Fig. 30). Small coarse-grained pockets, sometimes with sulphides, occur sparsely throughout the ultramafic cumulates; these I interpret to represent pegmatoids similar to those described earlie from Ylivieska and Koitelainen.

The *diorite*, *felsite* and *composite diorite-felsite* dykes (anal. 12–14, Table 7) have sharp, winding contacts, and contact effects are often surprisingly slight. Felsite dykes are rare; most often felsite occurs in the middle of the diorite dykes (composite dykes). These dykes are typically composed of coarse marginal zones containing big, zoned plagioclase crystals and a medium-grained inner part (with plagioclase, hornblende and quartz). Felsites are leucocratic, fine-grained rocks with occasional zoned phenocrysts of plagioclase. Some acid veins are composed of lava-like porphyritic rock,

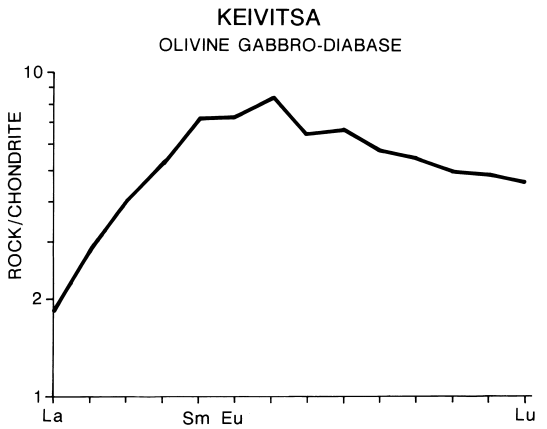

Fig. 57. Diagram of chondrite-normalized REE for olivine gabbro-diabase. Sample DDH332/31.95-32.15, marginal part of the dyke.

with phenocrysts of quartz, feldspar, clinopyroxene (hedenbergite ?) and magmatic brown hornblende in a fine-grained matrix (Fig. 55, middle). These dyke rocks invariably contain disseminated and (or) mobilized pyrrhotite and chalcopyrite. Both rock types have a high Na/K ratio. There is a paragenetic and compositional continuum between diorite and felsite. I suspect that the magmas formed by anatectic melting of the roof rocks and then intruded downwards into contraction cracks opened during late stages of consolidation of the intrusion (compare analyses 11 and 12, Table 7). The U-Pb/zircon age, 2054±7 Ma, corroborates this interpretation.

Some pink dykes near the eastern contact of the intrusion may represent anatectic melt that formed in floor rocks and intruded upwards into late contraction cracks.

The *diabase* and *olivine gabbro-diabase* (anal. 22–26) dykes have not been dated, but they are considerably younger than the Keivitsa intrusion. They have fine-grained, chilled contacts against the Keivitsa cumulates (Fig. 55, bottom), and their magmas were geochemically quite different from that of Keivitsa. The dykes strike ENE, with a vertical or steep dip to south. The diabase dykes are thicker (up to 10 m); the thickness of the olivine gabbro-diabase dykes varies from about 1 dm to 3–4 m. They represent a remarkable case of flow differentiation (Bhattacharji & Smith, 1964), with a heavy concentration of olivine crystals in the centre (Fig. 56). The marginal parts are enriched in Cl. The composition of the diabase dykes is similar to that of the margins of the gabbro-diabase. It, thus, seems that the respective magmas were genetically related.

The olivine gabbro-diabase has a few exceptional features. The thin (ca 3–5 cm) marginal selvage contains phenocrysts of olivine, clinopyroxene, plagioclase chromite and ilmenomagnetite; however, the narrow margin against the wall rocks lacks plagioclase, and ilmenomagnetite phenocryst. The order of crystallization in the chilled margin is chromite -> olivine -> clinopyroxene. The interior is composed of the same minerals, but brown interstitial hornblende and orthopyroxene (reaction mineral around olivine) are more easily distinguished. Olivine typically occurs as skeletal (hopper) crystals, up to 2 cm across. The large compositional spread from Fo_{73} to Fo_{94} (analysed on a single thin section) also indicates disequilibrium crystallization. On the other hand, the Fo-Ni relationship is surprisingly regular (Fig. 43). The magma had low REE and was strongly depleted in LREE (Fig. 57). The initial ε_{Nd} value of the rock is > +3.8 (Hannu Huhma, letter Febr. 22, 1995). The strangest feature is the apparent co-crystallization of chromite and titanomagnetite (now ilmenomagnetite). In one case only have I seen ilmenomagnetite partly moulded onto chromite. The inner parts of the dykes are coarse grained (olivine gabbro, by any measure), so similar to the olivine pyroxenite wall rocks that, unless one keeps an eye on the chilled contacts, the dykes easily go unnoticed in DDH cores.

Mineral veins (carbonate, albite and quartz, and combinations of the three) are usually accompanied by appropriate wall rock alteration. Crystals of uraninite occur in carbonate veins.

Massive sulphide veins are common but they account for an insignificant proportion of the total mass of sulphides. Geochemically they are of the false ore type. The contacts of sulphide veins are sharp and tidy, and contact effects are often very faint. Evidently, sulphide veins that poor in Ni cannot represent sulphides mechanically mobilized from surrounding disseminations at any reasonable temperatures. They may represent low-viscosity interstitial sulphide liquid of the false ore type sucked down into prototectonic contraction cracks from the overlying crystal mush containing false ore sulphide liquid.

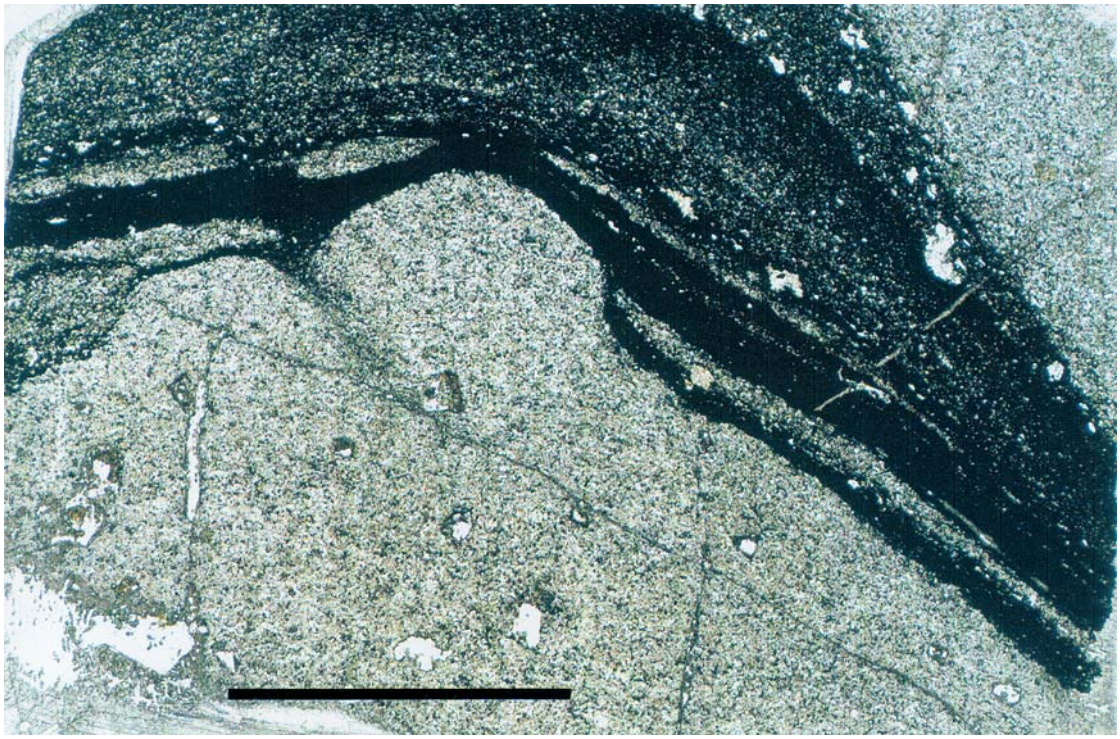

Fig. 58. Load-cast (?) structure in quartz-albite rock, pushing through magnetite-rich layers. Carbonate idioblasts in quartz-albite rock. The sample contains 4000 ppb PGE. Keivitsa, DDH323/10.70-13.60.1. Bar = 1 cm. Diascanner photo by Reijo Lampela.

Mineral deposits of the Keivitsa intrusion

Besides the Keivitsansarvi deposit, to be described in the following chapter, there are other metal and mineral occurrences, that would have deserved a longer presentation, but they are only listed as follows:

1) Basal contact sulphides. Semimassive, buckshot and disseminated sulphides. Very low Ni, Cu and noble metals.
2) Offset sulphide veins in footwall hornfelses. Rich in Cu (up to 20%), anomalous Au, low Pd.
3) False ore sulphides in ultramafic rocks, frequently associated with pelitic hornfelses. The sulphides have a bulk composition similar to that of false ores in and around the Keivitsansarvi deposit. Massive, breccia and disseminated sulphides. Sometimes with high Cu and anomalous Au, sulphides low in Ni(100S) and PGE.
4) Graphite in gabbro. A high-grade graphite concentrate was obtained in tests, but the percentage of recoverable graphite is low.
5) PGE-Cr-V deposit in quartz(-carbonate) rocks (for chemical compositions, see Table 7). A discontinuous deposit (up to 25–30 m thick) between the big serpentinite-peridotite xenolith and underlying cumulates of the Keivitsa intrusion (gabbro, feldspathic metapyroxenite). Black, fine-grained, massive or banded rocks with widely varying amounts of magnetite, chromite, rutile and ilmenite. Unevenly distributed carbonate rhombohedra, albite and coarse milky

quartz. Near the surface often vuggy (from dissolved carbonate). Variable, often high V and Cr (up to 0.97% V and 13% Cr_2O_3); low Ni (generally 200–500 ppm), low Mg; anomalous to high Ce and La (see above); anomalous PGE (up to 6 ppm). There is a slightly positive slope in the PGE(CN) diagram, similar to that in overlying serpentinite (see Fig. 65b). This peculiar rock may have been formed by hydrothermal (?) leaching of Mg and Ni from serpentinite (Mutanen, 1989b).

6) Serpentinite xenolith, Ni in magnetite. Occasionally brucite (?). Mineral processing tests.
7) Chrysotile asbestos. Veins in the horfelsed marginal part of the serpentinite-peridotite xenolith.
8) Vermiculite. Allochthonous filling in an open fissure.
9) Fresh olivine pyroxenite. A valuable building stone.

THE KEIVITSANSARVI Cu-Ni-PGE-Au DEPOSIT

General structure

The Keivitsansarvi deposit is a large, low-grade deposit (in the following, ore, ore deposit or deposit for short) of disseminated sulphides in olivine pyroxenites and their hydrated equivalents (metaperidotites). It consists of a few ore bodies containing several ore types (for their description, see the following section).

The subcrop of the deposit covers an area of ca 13 hectares. The combined area of false ore subcrops in the vicinity is ca 12 hectares. The thickness of the till cover is generally between 0.3 and 2.5 m. Along the northwest axis the length of the projected ore is > 1200 m, the width > 500 m, and the maximum vertical depth established so far is ca 800 m. The tonnage figure released is 263 million of metric tons calculated down to 630 m (Anonymous, 1995).

The thick, monotonous main orebody (Main Ore, for short) is overlain by a hanging deposit, the Upper Ore (the relatively thin layer, hanging above the Main Ore, see Appendix 5). All known Ni-PGE type ores are above the Main Ore. Ore types transitional between the regular and the Ni-PGE type (transitional type) occur above the Main Ore but also beneath it. The distance between the Main Ore and the upper ore increases downdip. The Main Ore grades upwards into barren rocks and eastward into false ores. The upper contact of the Main Ore dips southwest. The base of the deposit, in the north, is rather sharp; inferred from the common occurrence of "hot" mylonites the base contact is controlled by prototectonic faults. However, forerunner ores occur far beneath the base of the Main Ore north of it.

The eastern margin has a complicated structure, with fingers of false ores extending into the Main Ore. In fact, the structure is deeply fractal, but this is not easily conveyed in a picture. A big finger of false ore has a separate subcrop east of the Main Ore subcrop (see Appendices 4 and 5).

Lenses of false ore, with very low Ni(100S), occur high above the Upper Ore.

From east down to west, false ores grade rapidly into the regular ore type of the Main Ore. Even in the deceptively homogeneous Main Ore there are strong lateral variations

both across and along the long axis, e.g., in Pt/Rh and PGE(100S). I suggest that the west-sloping planes in Appendix 5 mark the direction of a stationary system of density flow downdraft, part of a central convectional toroid, with very strong magmatic erosion near the confluence of accelerating density currents downdip (Morse, 1988). The deposit represents a rapidly accumulated intra-intrusion delta of unknown distal extension. Movement was from northeast to soutwest (from east to west in the profile, Appendix 5). In the following, terms such as distal and proximal refer to this model. The Upper Ore, with its more lateral spread, may represent the waning deposition of ore on a shelf overlying the cumulate delta.

The deposit is cut by ENE dykes of diabase and olivine gabbro diabase, described before, and faults running in the same direction.

Ore types

The ore types are classified according to their Ni(100S) and Ni/Co (Figs 59–61 and 63–64). As a matter of fact, ore types arranged this way have distinguishing identities in other compositional diagrams. From false ores to Ni-PGE type ores PGE, PGE(100S), PGE/(Ni+Cu), Pt/Rh and Pt/Au increase, and S/Se, S/Te, Re and Re/PGE decrease (see Figs 65–72 and 76). Some of the ore types have a characteristic REE signature (Fig. 87) and S-isotope composition (see Hanski et al., 1996). In general, there is a good correlation between Cu and Au (Fig. 73).

Likewise, the various ore types have distinguishing mineralogical, paragenetical and textural features, as discussed below. Of course there are more transitional cases and some odd natural and sampling mixtures, but these do not significantly affect the picture as a whole. It should be stressed that the classification presented below is geochemical and geological; it cannot be used for technical purposes direct.

Without much exaggeration or oversimplification it can be stated that the ore types represent mixtures of komatiitic dunite and pelitic sulphide. As usual with PGE deposits in layered intrusions, the parent magma was low in PGE (Sun et al., 1989). A high PGE was not a prerequisite of PGE deposits to form. The roles of the Keivitsa intrusion and of the parent magma were hardly more (or less) than those of the pot and the cooking liquid in making a soup.

In the west-east profile of the deposit (Appendix 5) the regular ore type is divided into four quality classes according to their CuEQ, and the false ore type into two classes according to the Ni(100S); the transitional type and the Ni-PGE type presented in the profile are geochemical types without strict regard for CuEQ values.

Rocks of the *false ore type* have Ni(100S) < 4% and Ni/Co < 10 (typically ca 4–5) (Figs 59–64). False ores are rich in sulphides and generally look better than the regular ores. The Ni content in the rock is low, generally < 0.1%, the record low is 87 ppm. The meanest false ores, with Ni(100S) 0.3 – 0.5% and Ni/Co 1–2, are identical to pelitic sulphides, as are their S/Se and S/Te (Fig. 65). The total PGE-Au content in false ores is low, and directly proportional to Ni(100S) grade (Fig. 76). Gold and particularly Rh are enriched relative to other PGE (Figs 68, 71, 76). The Re content is distinctly higher than in other ore types, and the Re/PGE ratios are very high (see the Re/Ir plot, Fig. 69). The Re is attributable to sedimentary contribution; shales and sapropelites sometimes contain high amounts of Re (e.g., Kalinin et al., 1985; Hulbert et al., 1992). In places the false ores show slightly elevated Zn contents.

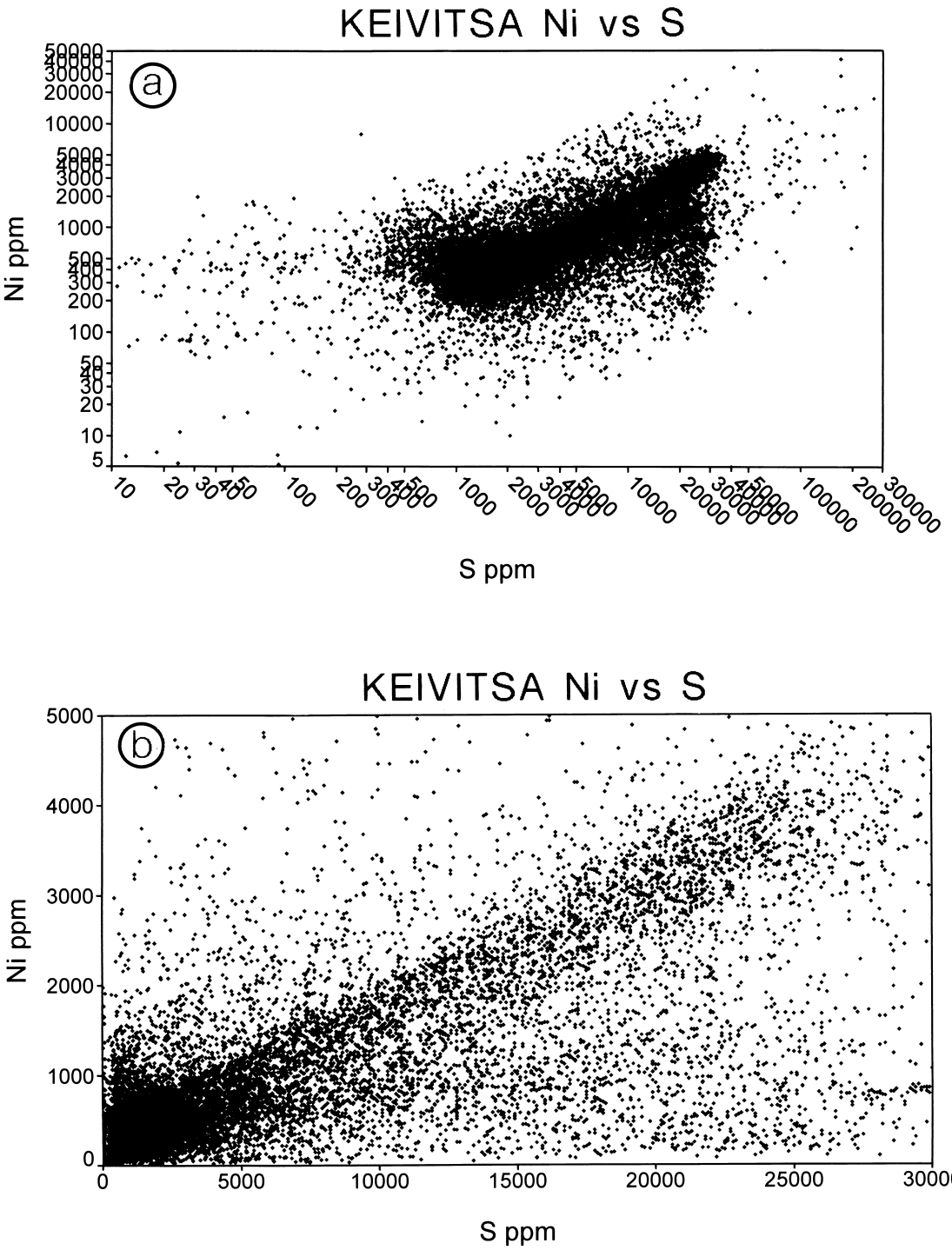

Fig. 59. Plots of Ni vs S, Keivitsa intrusion. a – all samples, b – samples with Ni < 0.5% and S < 3%.

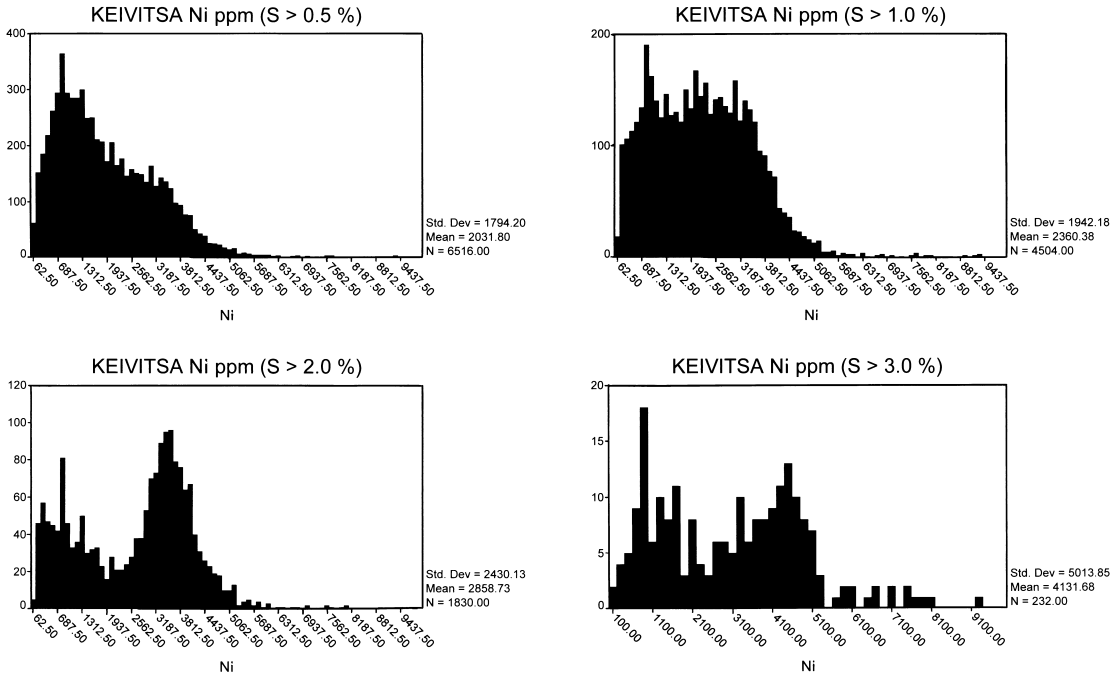

Fig. 60. Ni histograms for various classes of S concentrations, Keivitsa intrusion. Note the prominence of false ores in high-S samples.

It is significant that low-Cr false ores (400–700 ppm Cr in host olivine pyroxenite) are depleted of LREE relative to other ore types and sediments and enriched in HREE relative to other ore types (Fig. 86–87). This indicates that the acid contaminant was already depleted in REE in general and LREE in particular before it was incorporated in the magma. In low-Cr type the V is higher than in high-Cr false ores.

The occurrence of sulphide-mantled orthopyroxene crystals is diagnostic of false ores (Fig. 77). They are occasionally present in regular ore types with a low sulphide content.

The compositional mixing line is continuous between sediments and false ores, but there is a gap between false and regular ores (Fig. 63c). Spatially, too, the proximal false ores grade very rapidly into regular ores (Appendix 5). Evidently, the change from false to regular ore was caused by rapid and effective (turbulent?) mixing of "sedimentary" sulphide melt with magma enriched in Ni and PGE-Au. The silicate part of most of the false ores is compositionally and mineralogically similar to that of the host olivine pyroxenites of the regular ore; thus, mixing of silicate ingredients apparently preceded the mixing of the sulphide liquid and silicate magma.

Results of exploration drilling suggest that

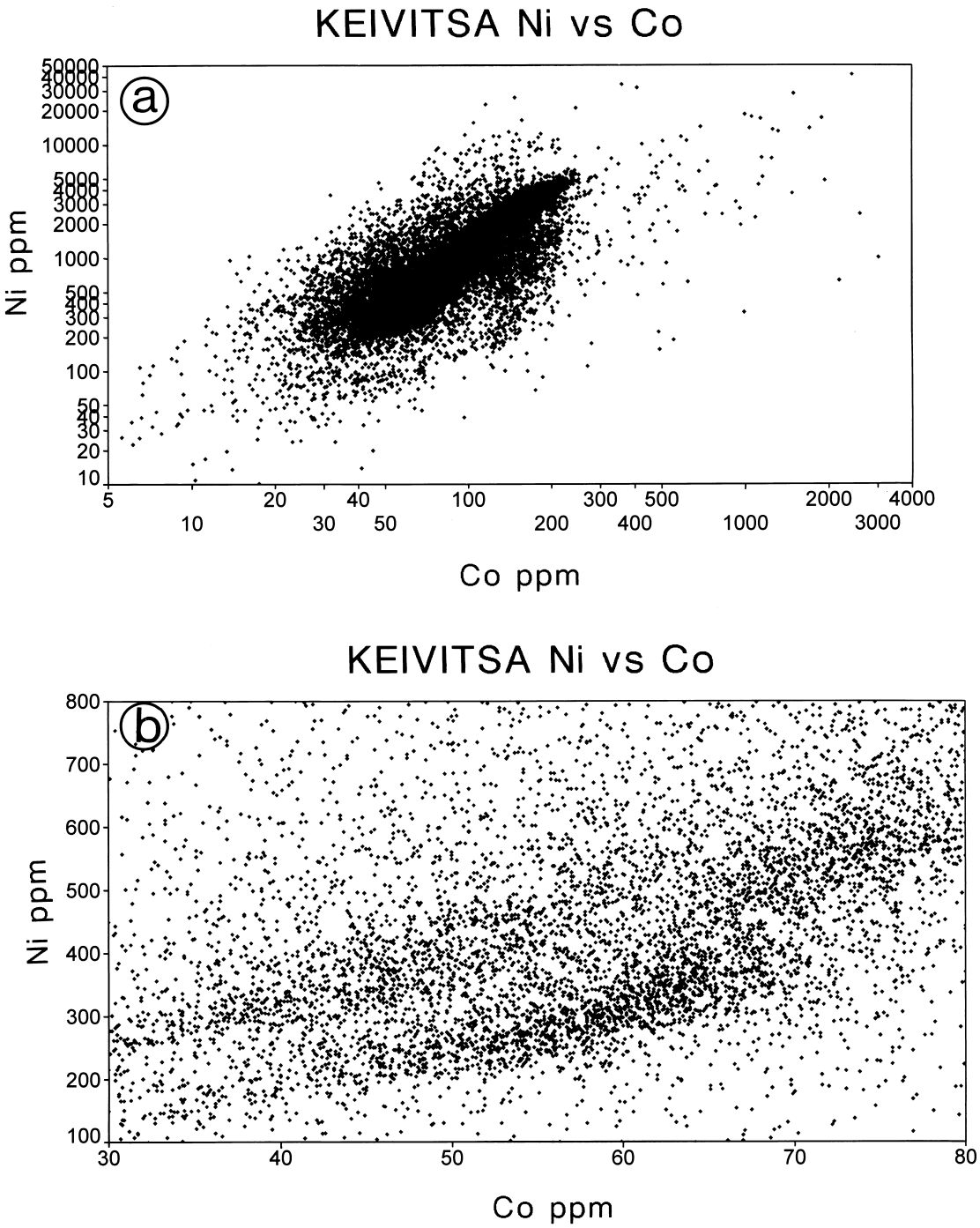

Fig. 61. Plot of Ni vs Co, Keivitsa rocks and ore types. a – all samples; b – zoomed on Ni 100–800 ppm and Co 30–80 ppm; note bimodal distribution of Ni for each band of Co concentrations. The Ni-poor cluster represents lower marginal part of the ultramafic zone, also characterized by very low PGE.

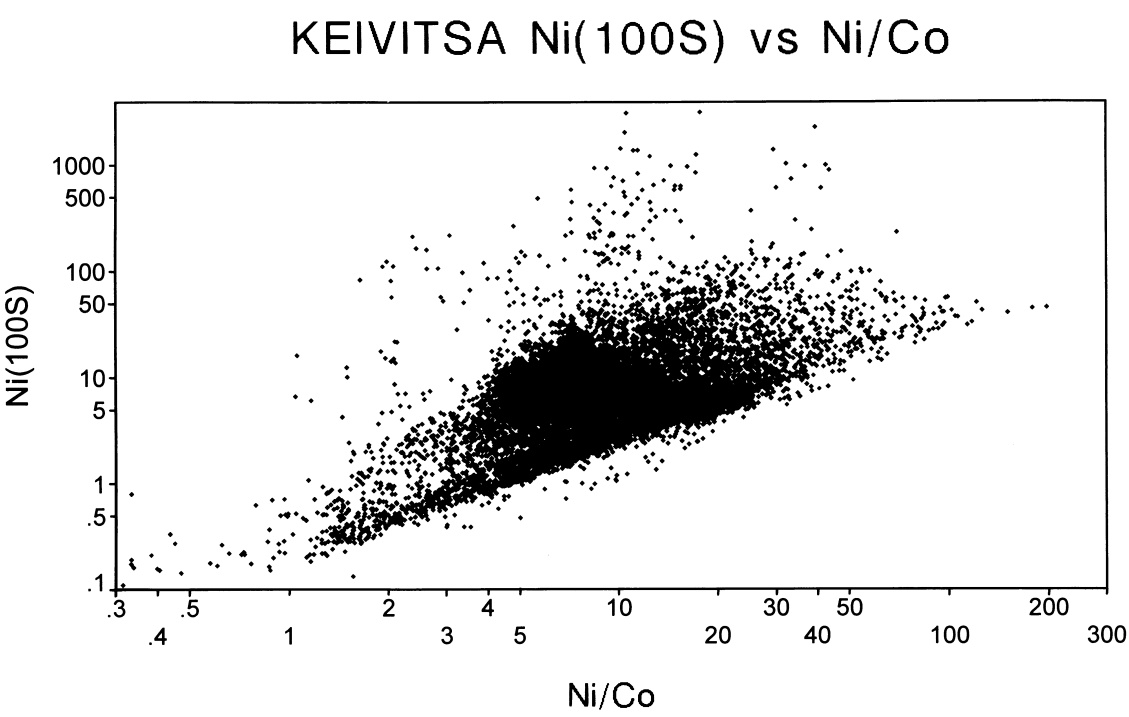

Fig. 62. Plot of Ni(100S) vs Ni/Co, all cases, Keivitsa intrusion. Note the sharp lower boundary of the plot cluster; this seems to represent the mixing line between pelitic and komatiitic sulphides. The halo extending into high Ni(100S) values represents sulphide-olivine mixtures.

sulphides of the false ore type make up the bulk of the total mass of sulphides in the intrusion.

The *regular ore type* forms the main mass of the Keivitsansarvi deposit. Its sulphide content is 2–6%, with Ni(100S) 4–7%, Ni/Co 15–25 (Fig. 63) and Ni/Cu 0.6–0.8. A typical fair ore contains 0.5–1 ppm PGE+Au. The ore mass consists of homogeneous dissemination over hundreds of metres, almost without a break. There are, however, invisible lateral trends in the Main Ore from the proximal to the distal part. For example, the Ni/Cu ratio has been found to change within a short distance from 1.5 to 0.4, while the Pt/Rh ratio decreases from 40 to 10.

In the regular ore type the PGE+Au sum generally correlates positively with Ni+Cu (Figs 70–71), but among successive drill core samples there are numerous aberrations normal to the linear trend (i.e., Ni+Cu decreases as PGE increases). This behaviour indicates admixtures of transitional and Ni-PGE-type material.

The *transitional ore type* occurs in the upper part of the deposit, between the regular ore and the Ni-PGE-type ore. Gradations into both are common. A thick transitional ore was intersected in a deep DDH below regular ore in the Main Ore (see Appendix 5). Rare pegmatoid pockets with massive to semimassive sulphides occur in this type. The gradual contacts, presence of euhedral olivine and clinopyroxene in massive sulphide matrix and high Ni(100S) contents indicate that the pegmatoids represent intercumulus sulphide-silicate emulsion, accumulated in contraction voids.

This type has a lower sulphide content,

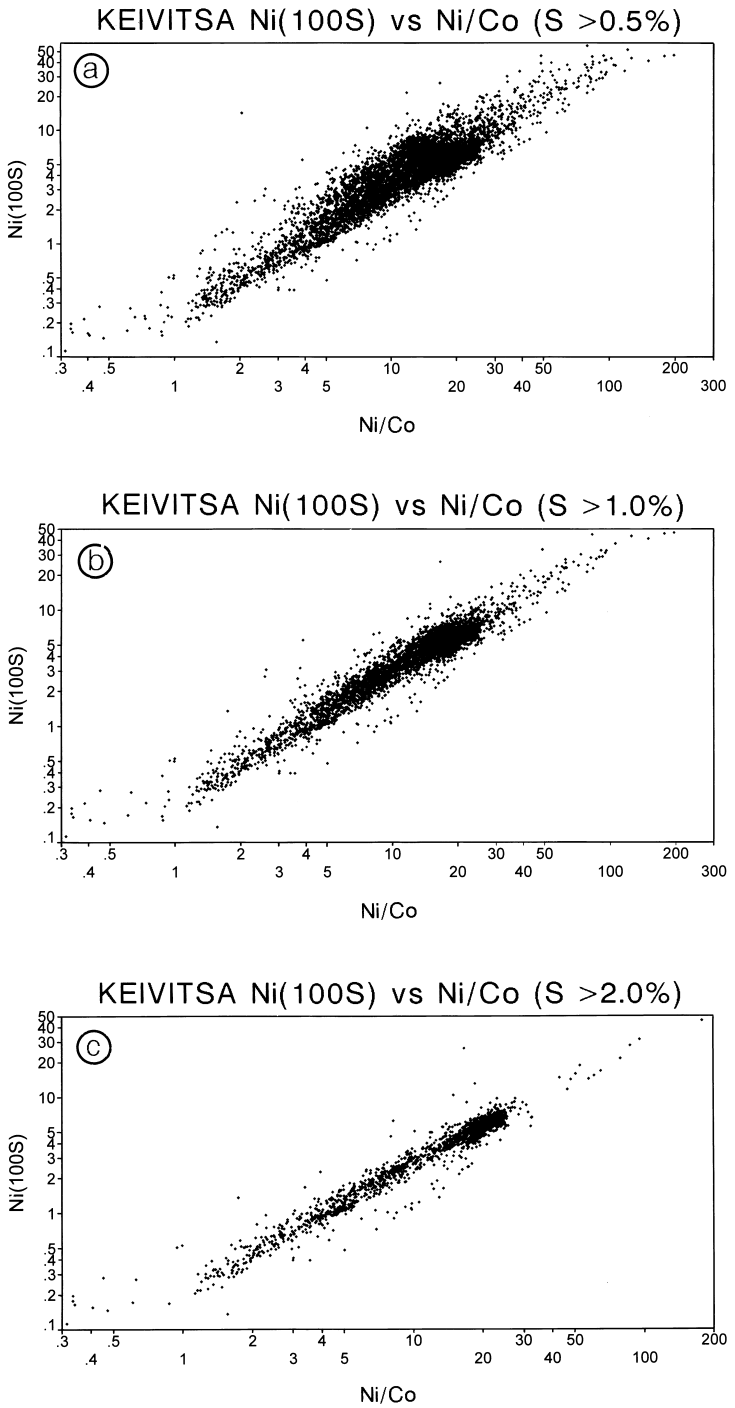

Fig. 63. Plots of Ni(100S) vs Ni/Co, Keivitsa intrusion. a – samples with S > 0.5%, b – S > 1%, c – S > 2%. Note the parting of the cluster into regular and false ore with the increase in sulphur.

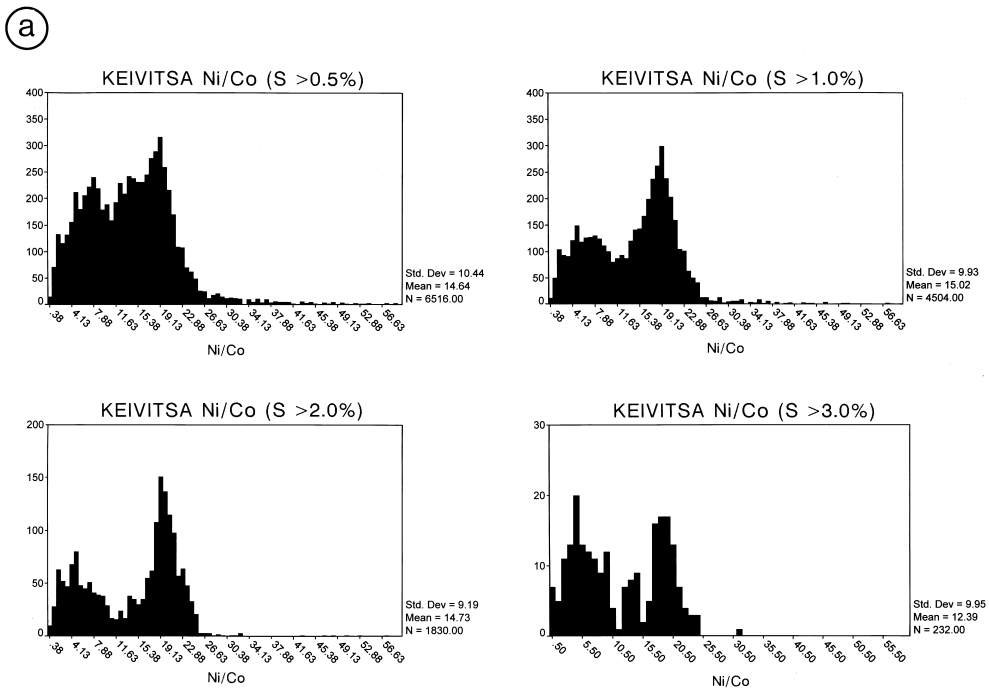

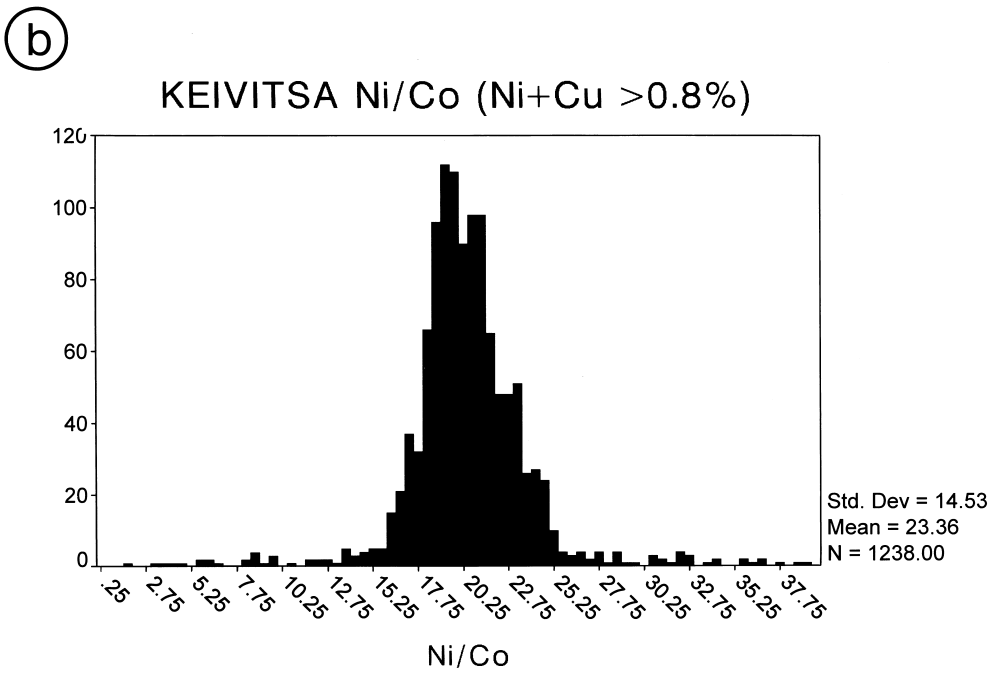

Fig. 64. Histograms of Ni/Co, Keivitsa. a – for various classes of S concentrations. Note the gradual parting of the histogram into regular and false ore with the increase in sulphur; b – samples with Ni+Cu > 0.8%. The peak around 21 represents the regular ore.

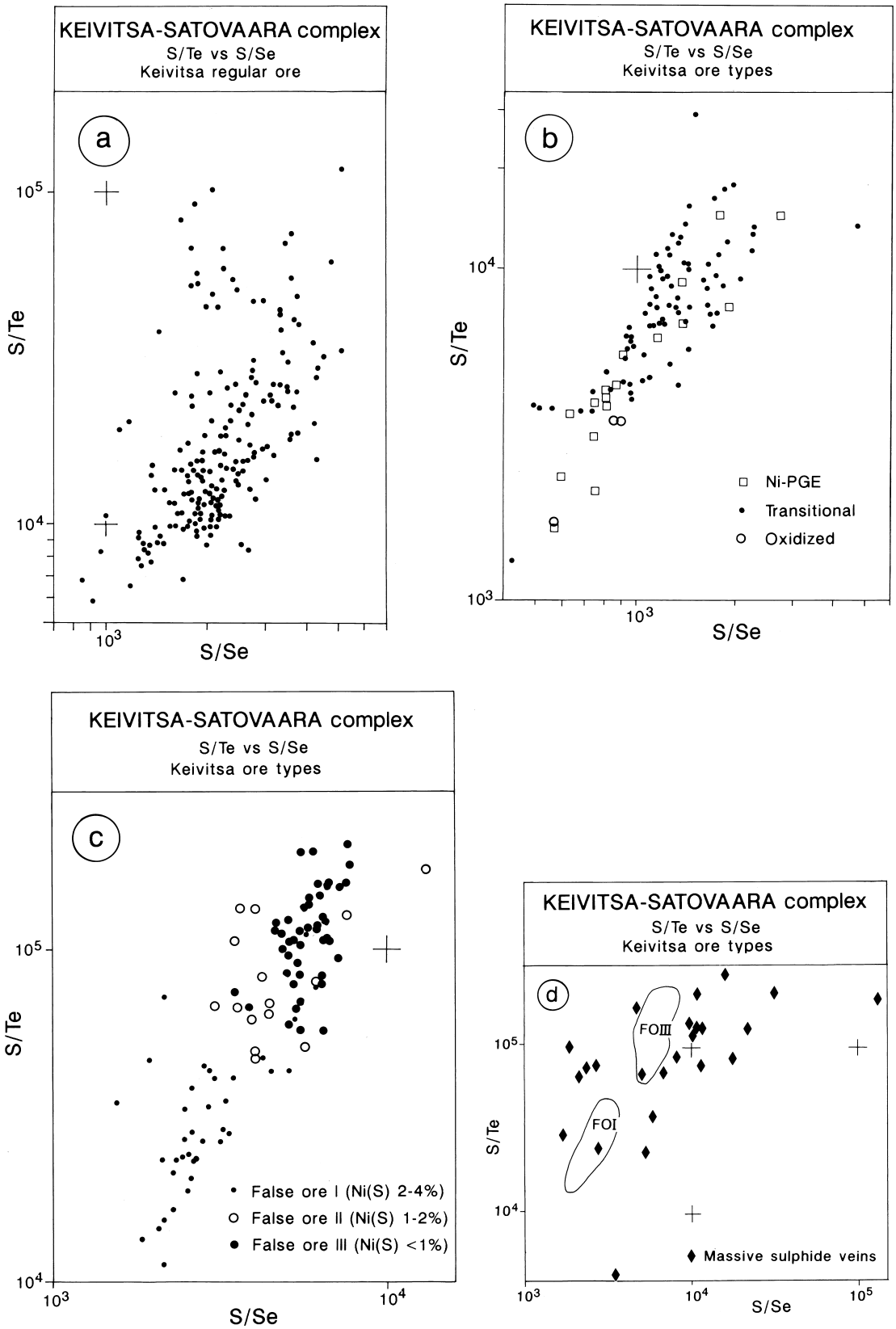
KEIVITSA-SATOVAARA complex
S/Te vs S/Se
Keivitsa regular ore
a
S/Te
S/Se
10^5
10^4
10^3
KEIVITSA-SATOVAARA complex
S/Te vs S/Se
Keivitsa ore types
b
Ni-PGE
Transitional
Oxidized
KEIVITSA-SATOVAARA complex
S/Te vs S/Se
Keivitsa ore types
c
False ore I (Ni(S) 2-4%)
False ore II (Ni(S) 1-2%)
False ore III (Ni(S) <1%)
KEIVITSA-SATOVAARA complex
S/Te vs S/Se
Keivitsa ore types
d
FOIII
FOI
Massive sulphide veins

Fig. 65 a–d.

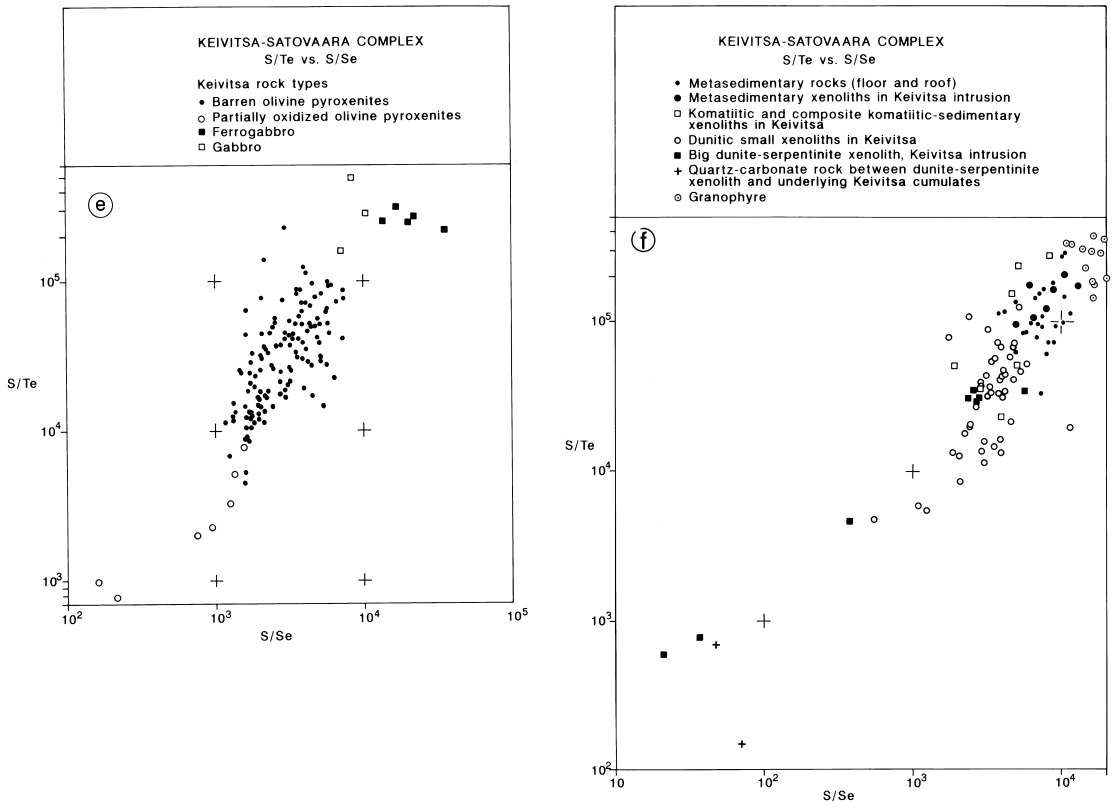

Fig. 65. Plots of S/Te vs S/Se, rocks and ore types of the Keivitsa-Satovaara complex. Ni(S), = Ni% in 100% sulphides. a – regular ore type, Keivitsa; b – Ni-PGE ore type and transitional (between regular and Ni-PGE type) ore type; c – false ore types; d – massive sulphide veins; e – barren olivine lherzolites and partially weathered (oxidized) olivine lherzolites, gabbros and ferrogabbros; f – metasedimentary floor and roof rocks, xenoliths in the Keivitsa intrusion (pelitic, komatiitic and mixed komatiitic-sedimentary xenoliths, komatiitic dunite xenoliths), quartz-carbonate rocks at the base of the big serpentinite-dunite xenolith, and granophyre; g (next page) – fields of various rocks classes, Keivitsa-Satovaara complex.

higher Ni/Cu (1.5–2.5 or more) and Ni(100S) (15–23%), higher total PGE and higher Pt/Au (6–10) than regular ore. In contrast to regular ore, there is no correlation whatsoever between PGE and S (see Fig. 72). Moreover, the Cu-S correlation is weak, particularly in samples poor in S (Fig. 74). Transitional ores in the lower part of the Main Ore differ from the upper transitional ores only in their higher Pt/Rh ratios.

This type differs from the Ni-PGE type in having a higher sulphide content, lower Ni/Cu and slightly higher S/Se and S/Te (Fig. 65). The Ni content in olivine is equal to or lower than in the Ni-PGE type. The REE(CN) distribution is similar to that of the Ni-PGE type (Fig. 87).

The volume of the *Ni-PGE type* ores is small. The ores occur in the upper part of the deposit, at about the level of the Upper Ore,

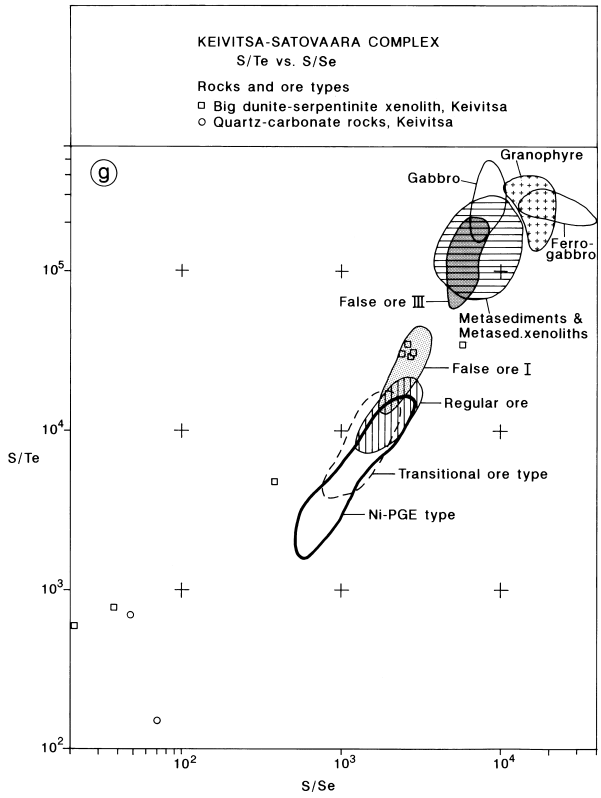

Fig. 65 g.

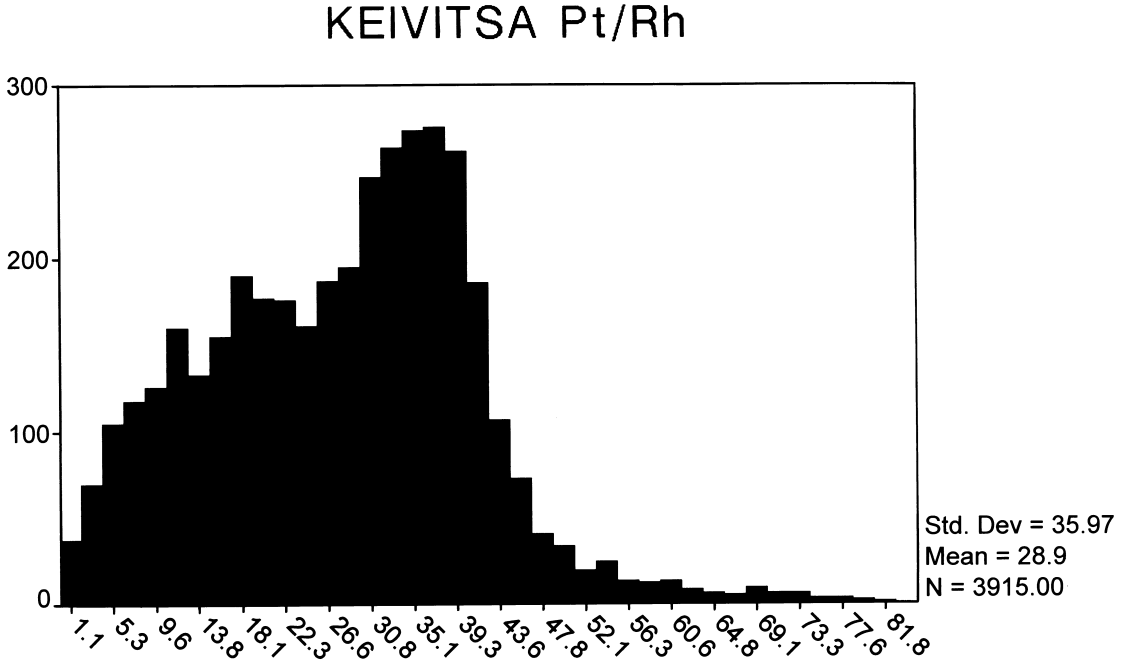

Fig. 66. Histogram of Pt/Rh ratios, Keivitsa intrusion.

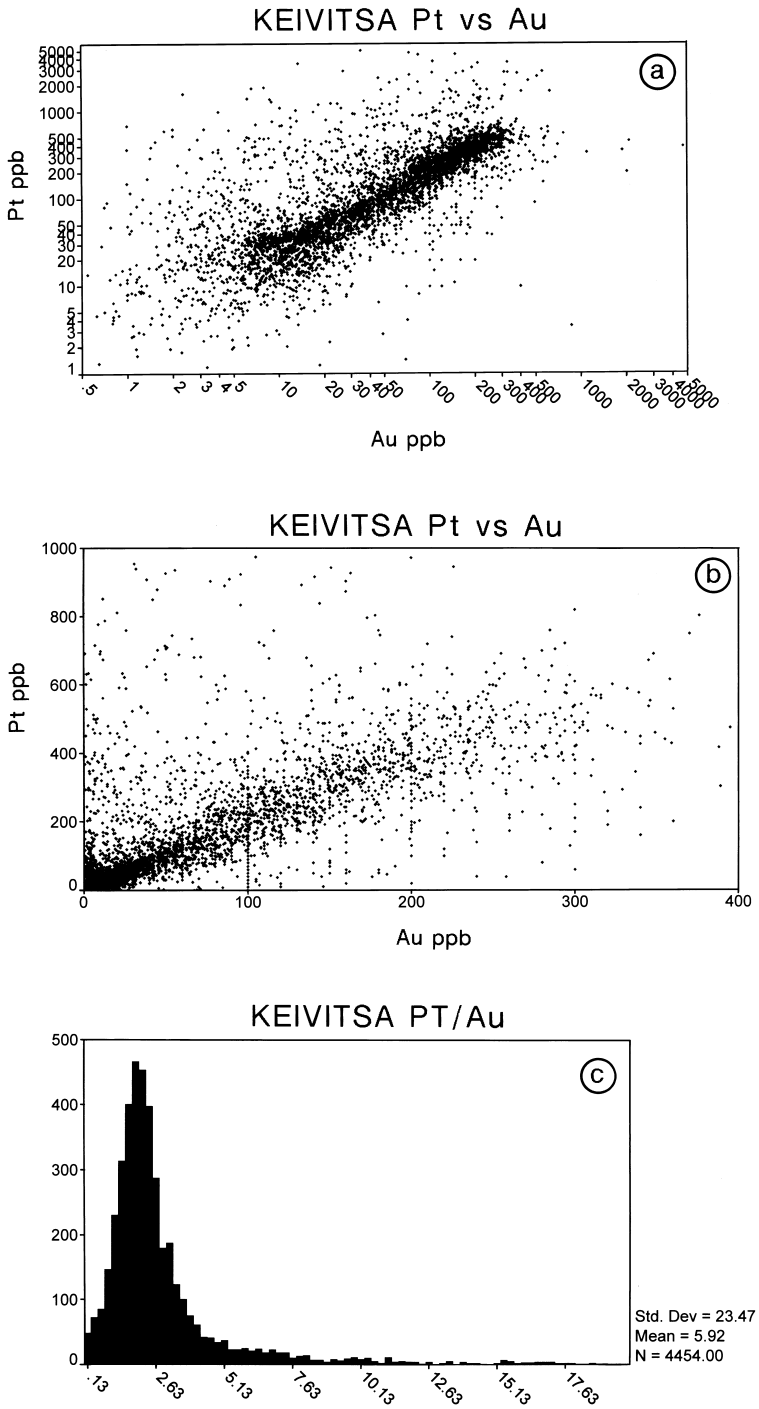

Fig. 67. Pt-Au relationships, Keivitsa intrusion. a – plot of Pt vs Au; b – plot of Pt vs Au for samples with Pt < 1000 ppb and Au < 400 ppb; c – histogram of Pt/Au ratios.

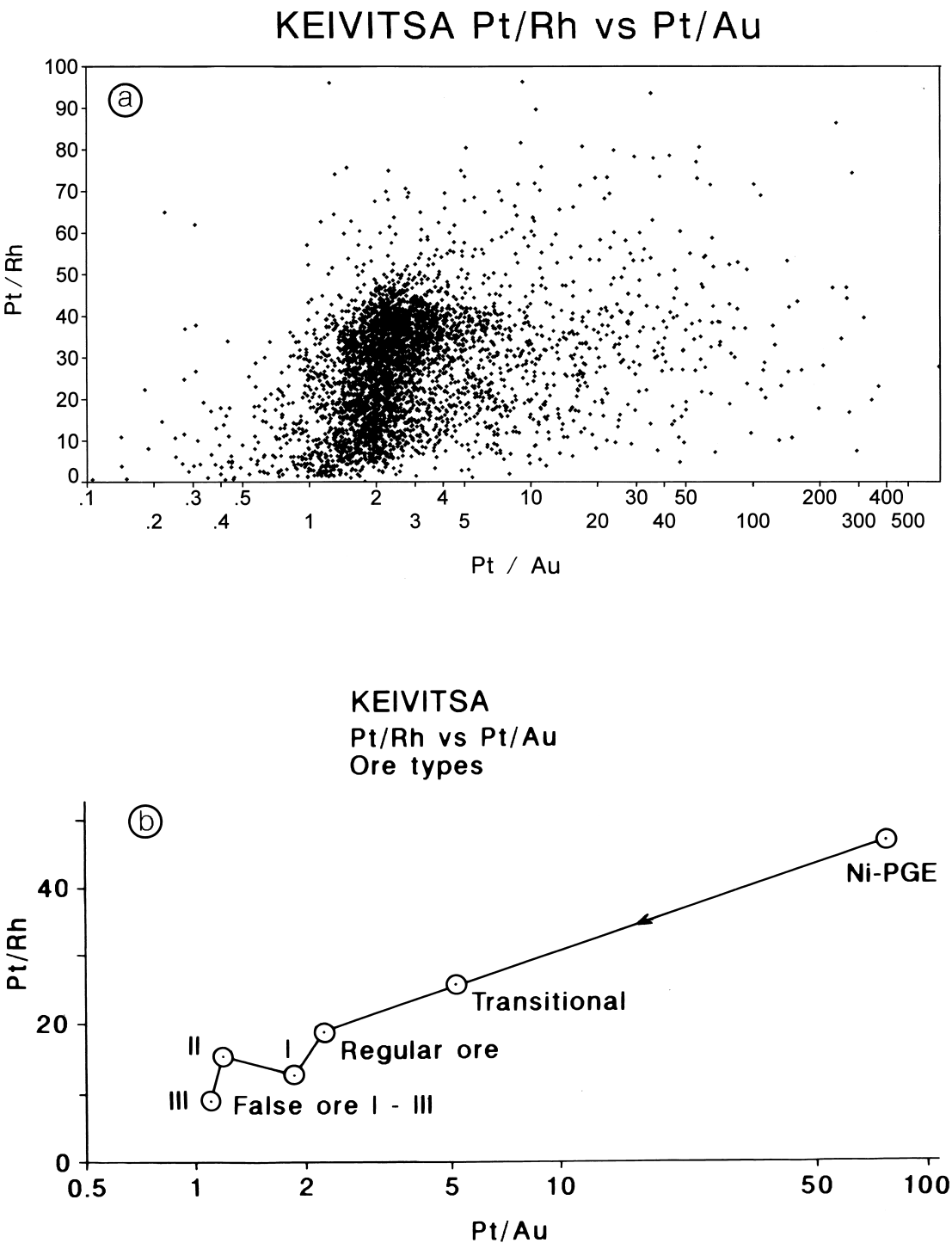

Fig. 68. Pt-Rh-Au relationships, Keivitsa rocks and ore types. a – plot of Pt/Rh vs Pt/Au; b – ore types in the Pt/Rh vs Pt/Au plot.

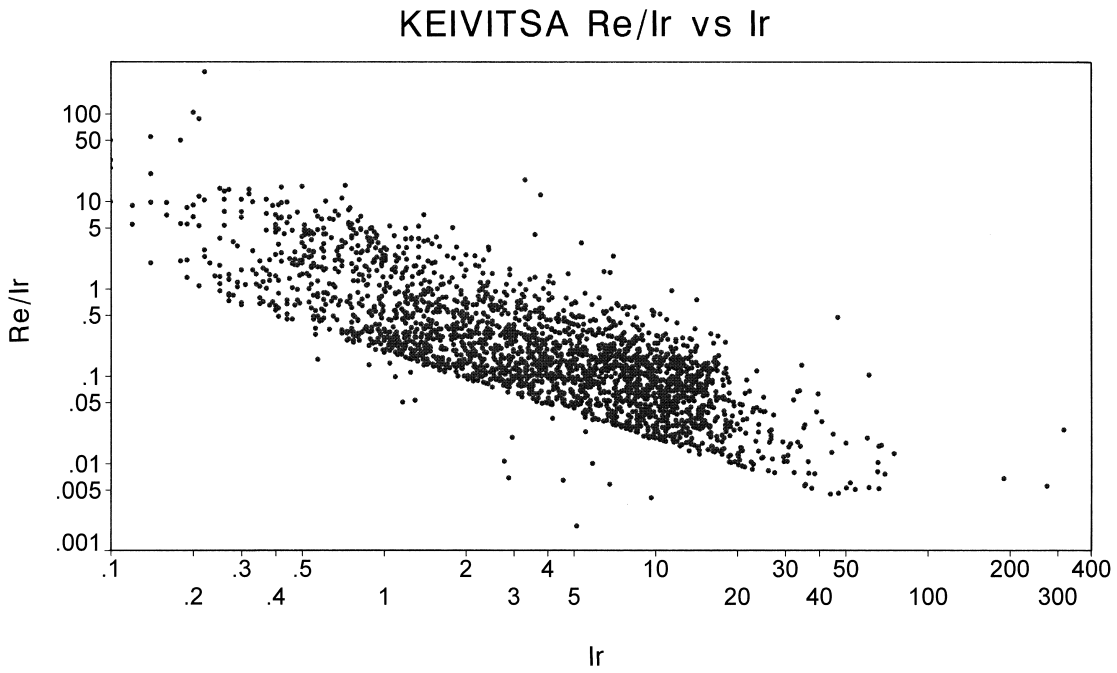

Fig. 69. Plot of Re/Ir vs Ir, Keivitsa.

and are characterized by a very low abundance of sulphides, high Ni/Cu (50–90) and Ni/Co (25–80), high Ni(100S) (40–60%), PGE(100S) (25–300 ppm) and low Au (max. 0.13 ppm). In general, the highest PGE contents are found in this type (Fig. 76). There is no correlation between PGE and S (Fig. 72) and only very weak correlation between Cu and S, particularly when compared with other ore types (Fig. 74). The sulphides are high in Ni (millerite, heazlewoodite, Ni-rich pentlandite). Because of the high Ni content in silicates (in olivine up to 1.74% NiO, in clinopyroxene up to 0.26% NiO), all calculated Ni(100S) values are far too high. Occasional high As values are characteristic.

Komatiitic xenoliths are very rare in host rocks of the transitional and Ni-PGE ore types.

Massive sulphide veins are common but volumetrically insignificant. They are simple or consist of branching stockworks or breccias. The contacts are sharp. Contact effects in fresh olivine peridotites (hydration, carbonate alteration) are conspicuously weak, although portions of metaperidotite usually contain networks of sulphide veins. Compositionally massive sulphides are of the false ore type, poor in Ni but occasionally rich in Cu. The PGE-Au is low (Figs 71–76). The record low is a massive sulphide vein with a mere 4 ppb Pt.

Ultramafic xenoliths within the ore contain fine-grained disseminated sulphides of the same composition as sulphides in the cumulate matrix. This suggests, as discussed above, that

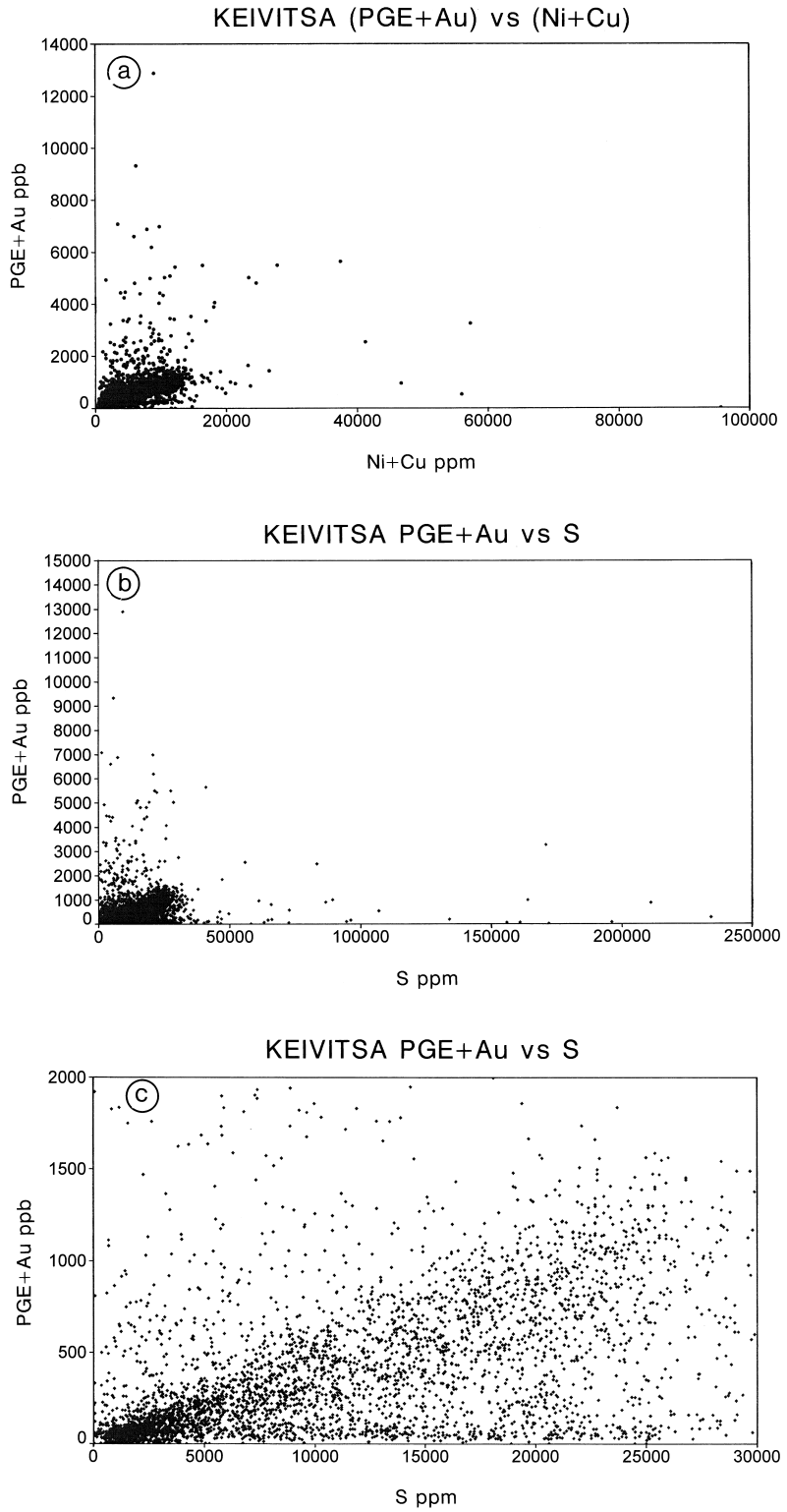

Fig. 70. Relationships between Au, sulphur and Ni+Cu, Keivitsa. a – plot of (PGE+Au) vs (Ni+Cu); b – plot of (PGE+Au) vs S, all samples; c – plot of (PGE+Au) vs S for samples with (PGE+Au) < 2000 ppb and S < 3%. Here false ores lie very near the horizontal axis.

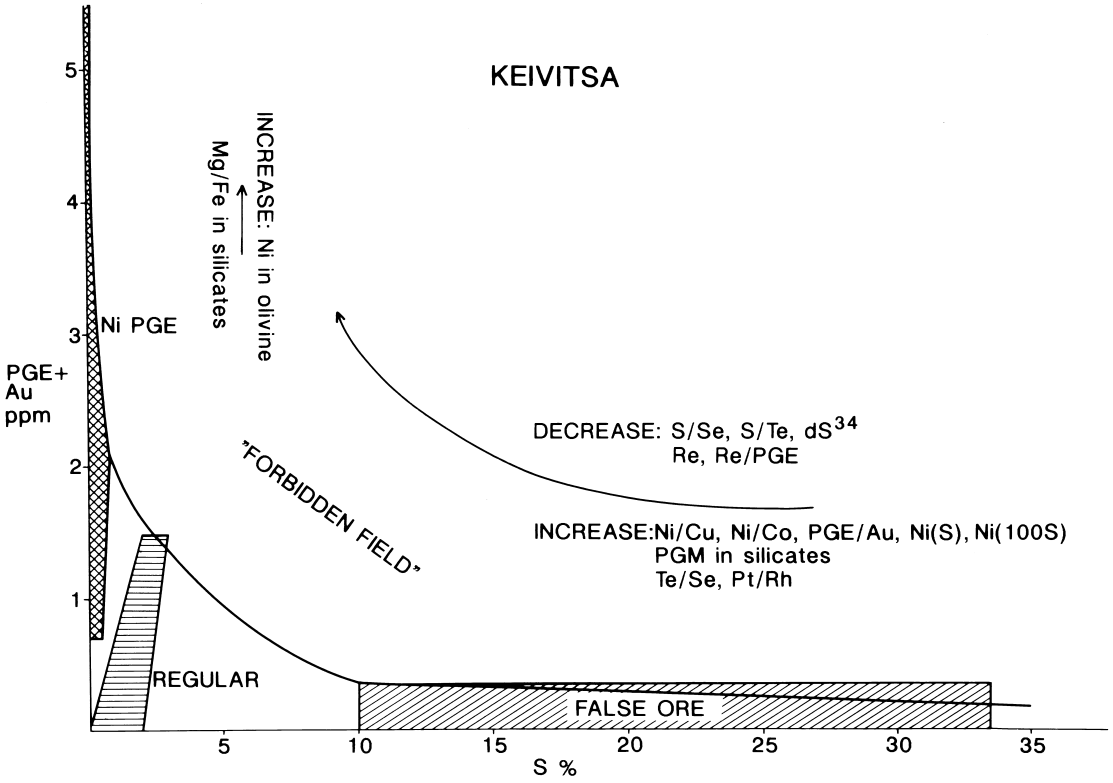

Fig. 71. Schematic diagram of the relationships between PGE+Au and S, and geochemical trends between ore types, Keivitsa intrusion.

sulphide liquid infiltrated into xenoliths from the surrounding matrix. The xenoliths, however, have lower total PGE, and their PGE(CN) diagrams are similar to those of the big serpentinite-peridotite xenolith (Fig. 76), suggesting that the PGE were not dissolved in the infiltrating sulphide liquid.

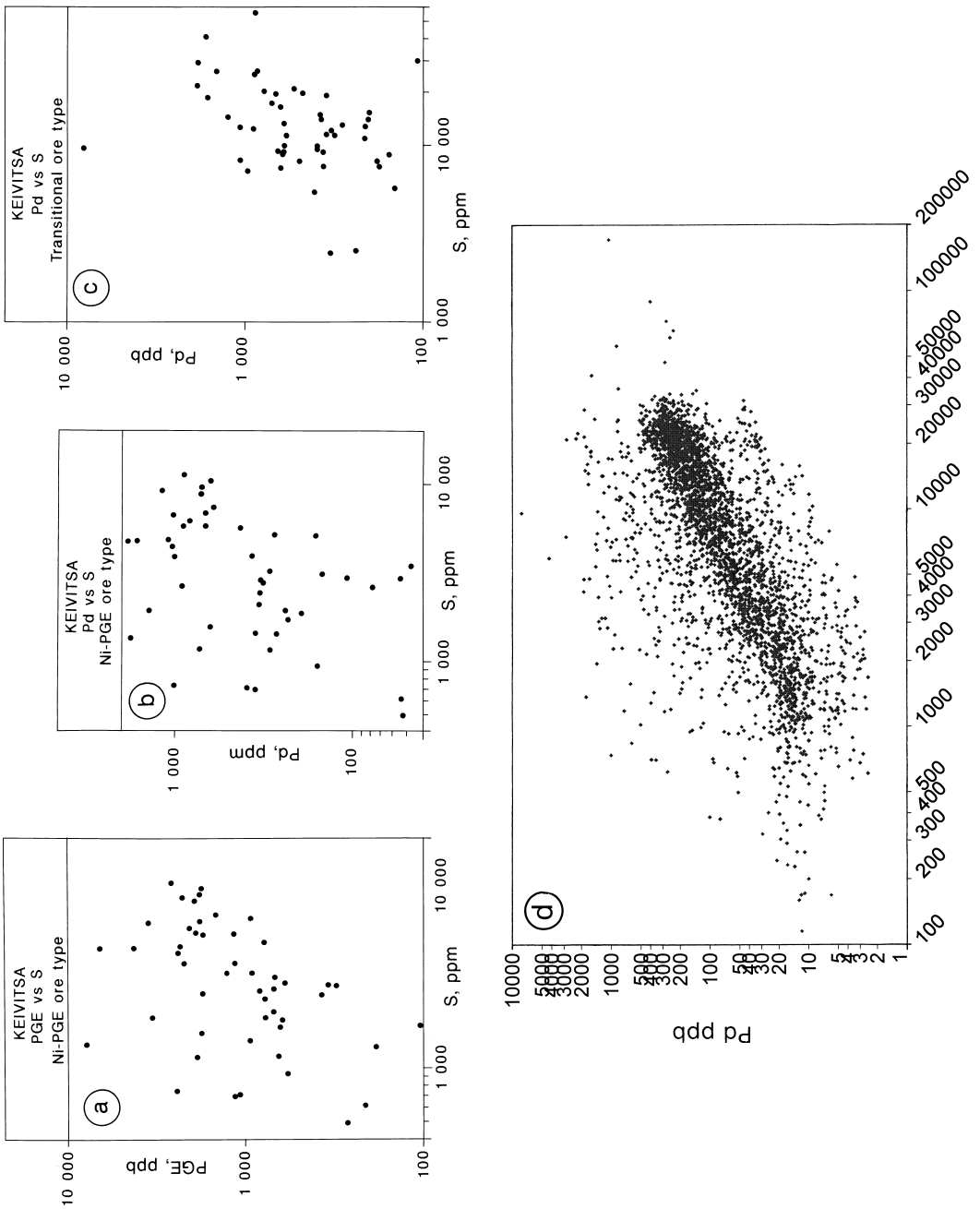

Fig. 72. Plot of PGE and Pd vs S, Keivitsa intrusion. a – PGE vs S, Ni-PGE ore type; b – Pd vs S, Ni-PGE ore type; c – Pd vs S, transitional ore type; d – Pd vs S, samples with Ni(100S) > 4%.

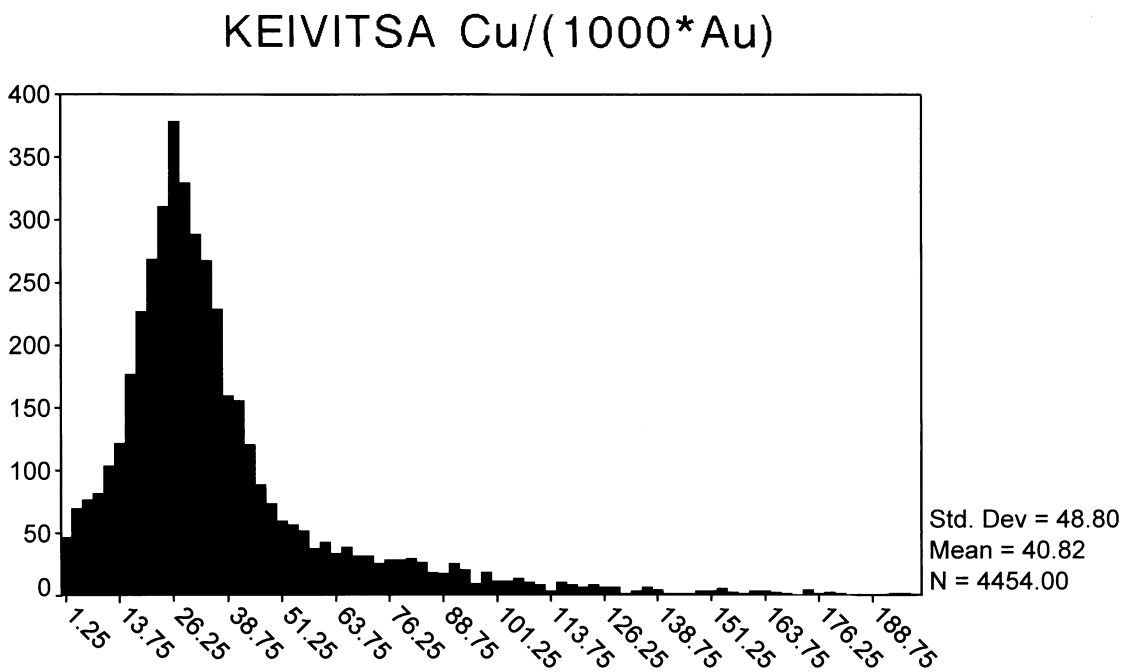

Fig. 73. Histogram of Cu/1000xAu ratios, Keivitsa.

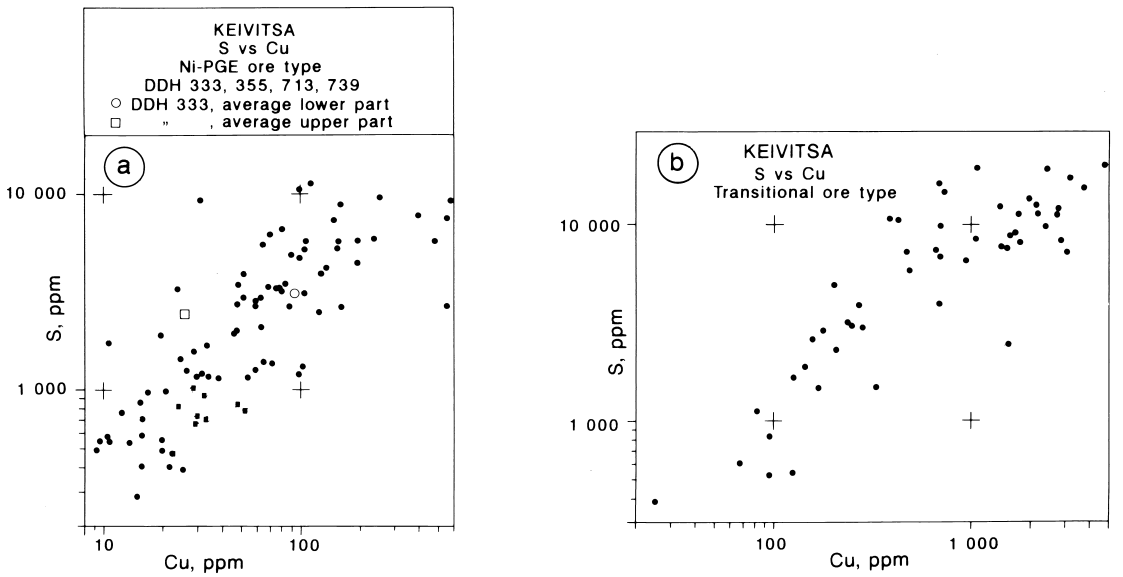

Fig. 74. Plots of S vs Cu, Keivitsa ore types. a – Ni-PGE type; b – transitional ore type; c – all samples; d – samples with S between 0.5 and 5 %, and Ni (100S) > 2 %.

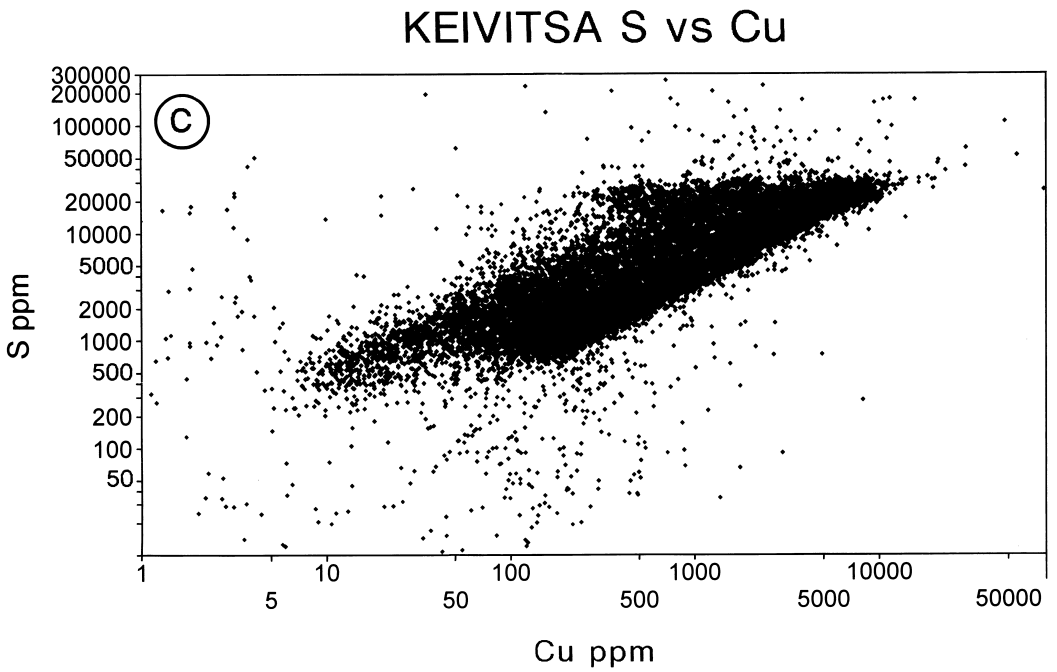
KEIVITSA S vs Cu
c
S ppm
300000
200000
100000
50000
20000
10000
5000
2000
1000
500
200
100
50
1
5
10
50
100
500
1000
5000
10000
50000
Cu ppm

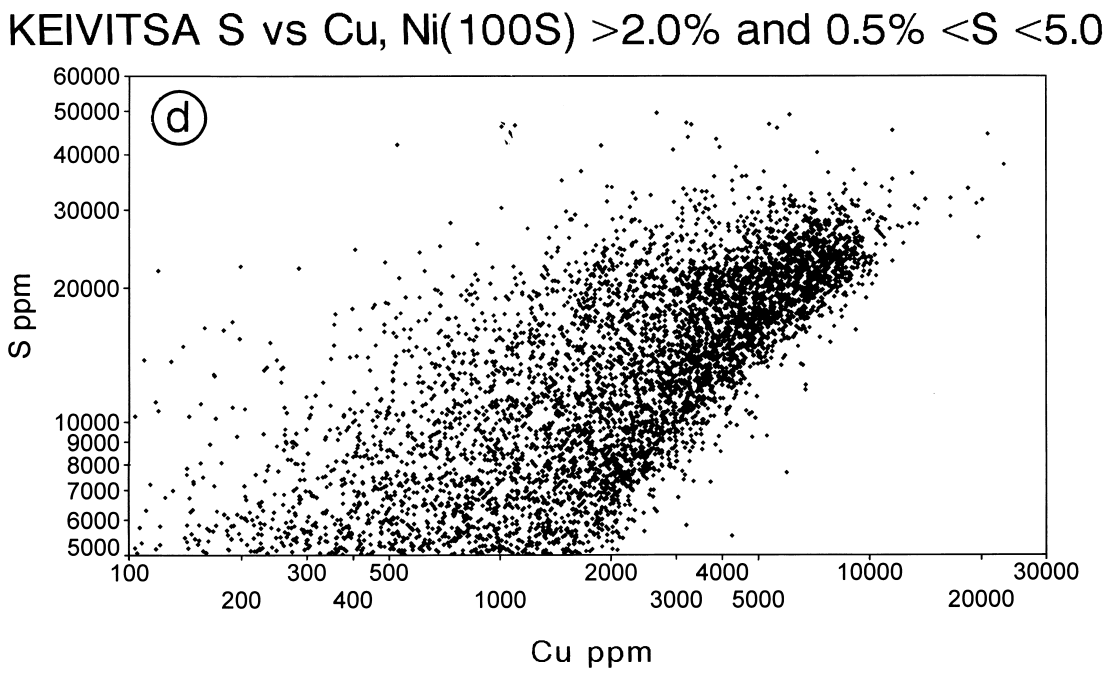
KEIVITSA S vs Cu, Ni(100S) >2.0% and 0.5% <S <5.0
d
S ppm
60000
50000
40000
30000
20000
10000
9000
8000
7000
6000
5000
100
200
300
400
500
1000
2000
3000
4000
5000
10000
20000
30000
Cu ppm

Fig. 74. c–d.

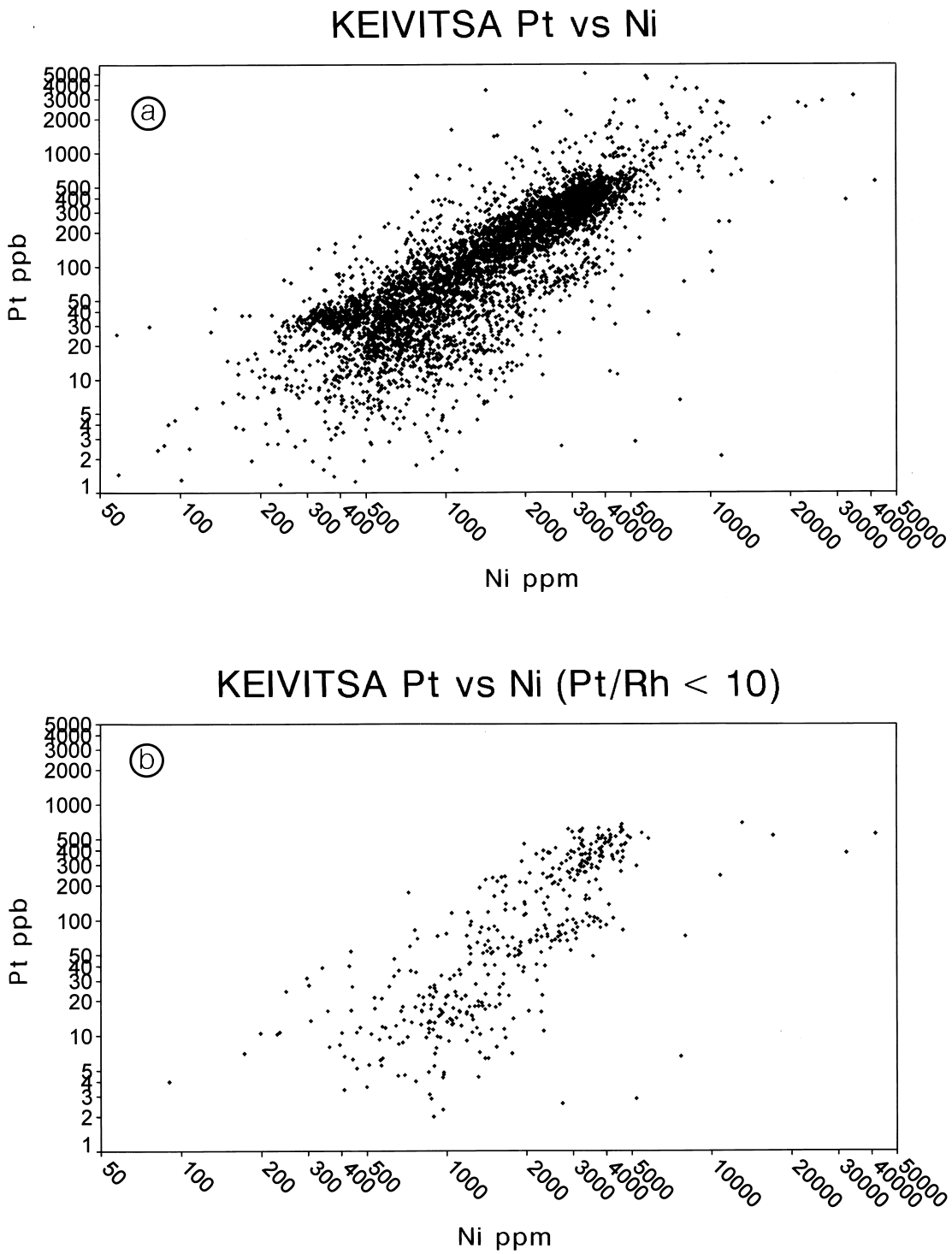

Fig. 75. Plots of Pt vs Ni, Keivitsa. a – all samples; b – samples with Pt/Rh < 10.

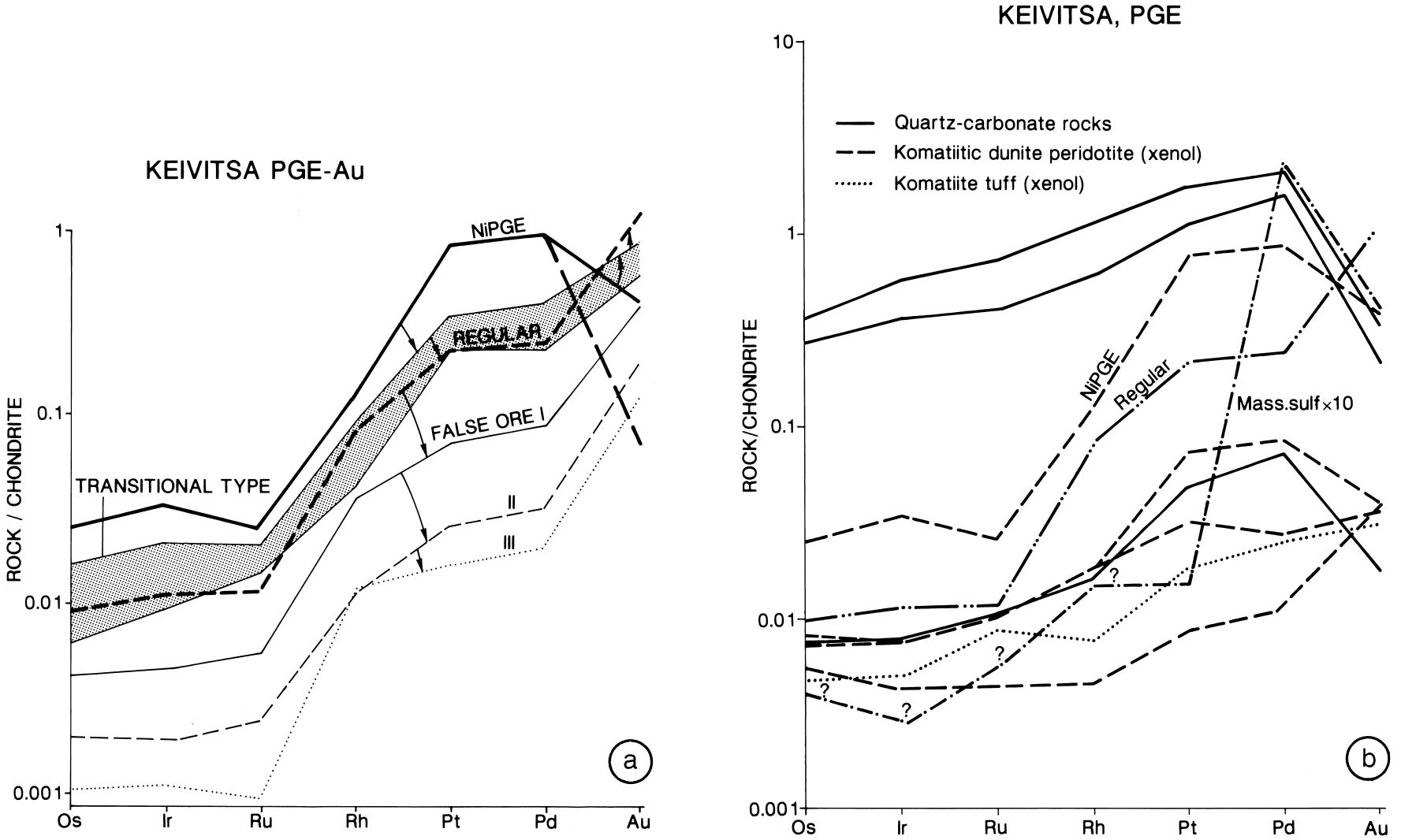

Fig. 76. Diagram of chondrite-normalized PGE-Au, Keivitsa. a – various ore types; b – komatiitic xenoliths and quartz-carbonate rocks.

Mineralogy of ore types

The petrographic description of the ultramafic rocks presented earlier applies in general to the host rocks of the ores, too, and so is not repeated. Here, only ore minerals and their textures are described.

In most of the ore types sulphides crystallized from the sulphide liquid and equilibrated to low temperatures. However, the present ore parageneses, which are characterized by the presence of troilite, talnakhite (Fig. 80) and graphite and the scarcity of primary and secondary magnetite, were predetermined by reducing magmatic conditions. Secondary magnetite, so common in sulphides in traditional Ni sulphide ores, is scantu in Keivitsa ores.

Rare findings of big sulphide beads (Figs 78a-d) allow a striking window into the secrets of phase separation in the Keivitsa intrusion. It is readily seen that olivine, clinopyroxene and plagioclase crystallized in equilibrium with two liquids, each with an identical composition (at a given time) in both liquids. Of course, because of the low solubility of silicates in sulphide liquid, silicates embedded in sulphide grew by diffusion through, not from, sulphide liquid. Postcumulus growth and reactions obscured these relationships in the surrounding silicate cumulate, but in sulphide beads they are clear – literally – as a mirror: the silicates crystallized in the order clinopyroxene -> olivine -> plagioclase (Fig. 78c-d). The decreasing ease of nucleation (Wager, 1959) is seen in the increase of grain sizes from olivine to clinopyroxene to plagioclase, which is also the order from simpler to more complicated compositions and lattices.

The sulphide droplets are additional evidence of settling of glomerophyric crystal packets. It can be seen that the surface of the sulphide droplet acted as a phase boundary collector for clinopyroxenes and olivines. This could also explain the mantled orthopyroxene euhedra (Fig. 77): sulphide liquid wetted the surfaces of orthopyroxene euhedra in magma suspension (phase boundary collector principle; Mutanen, 1992), prohibiting their growth.

The beads offer a clue to the cumulus silicate assemblages: clinopyroxene was the first primary silicate phase, then joined the olivine cotectic and both later joined the plagioclase cotectic. The nucleation of plagioclase was difficult in silicate liquid. Because of its oikocrystic growth in many cumulates plagioclase is judged too hastily as a postcumulus phase. The ghosts of euhedral plagioclase in postcumulus plagioclase in pyroxene cumulates of the Koitelainen and Akanvaara intrusions, the euhedral plagioclase included in orthopyroxene in Keivitsa intrusion (see above) and the tiny euhedral plagioclases in intercumulus spaces in the Porttivaara intrusion (Mäkelä, 1975) all suggest that plagioclase was often a cumulus mineral that failed to nucleate properly.

In false and regular ores the sulphide grain aggregates are mostly interstitial to silicates. These primary aggregates are joined by very thin “chicken wire” sulphide veins with a texture similar in appearance to nerve cells (Fig. 79). These mu-thin sulphide veins represent the fractal “ends” of the sulphide vein system. Secondary magnetite, associated with serpentinized olivine, also forms networks, but the sulphide veins do not follow them.

The sulphide/silicate grain boundaries are plain and smooth in unaltered rocks but irregular and serrated in metaperidotites, and an aureole of fine sulphide dust surrounds the primary sulphide grain aggregates.

The main sulphides are troilite, hexagonal pyrrhotite, chalcopyrite, pentlandite, talnakhite and cubanite; pyrite and monoclinic pyrrhotite are rare, and occur only in association with retrograde alteration, as in carbonate and albite-carbonate veins. Mackinawite and sphalerite occur regularly; molybdenite, ga-

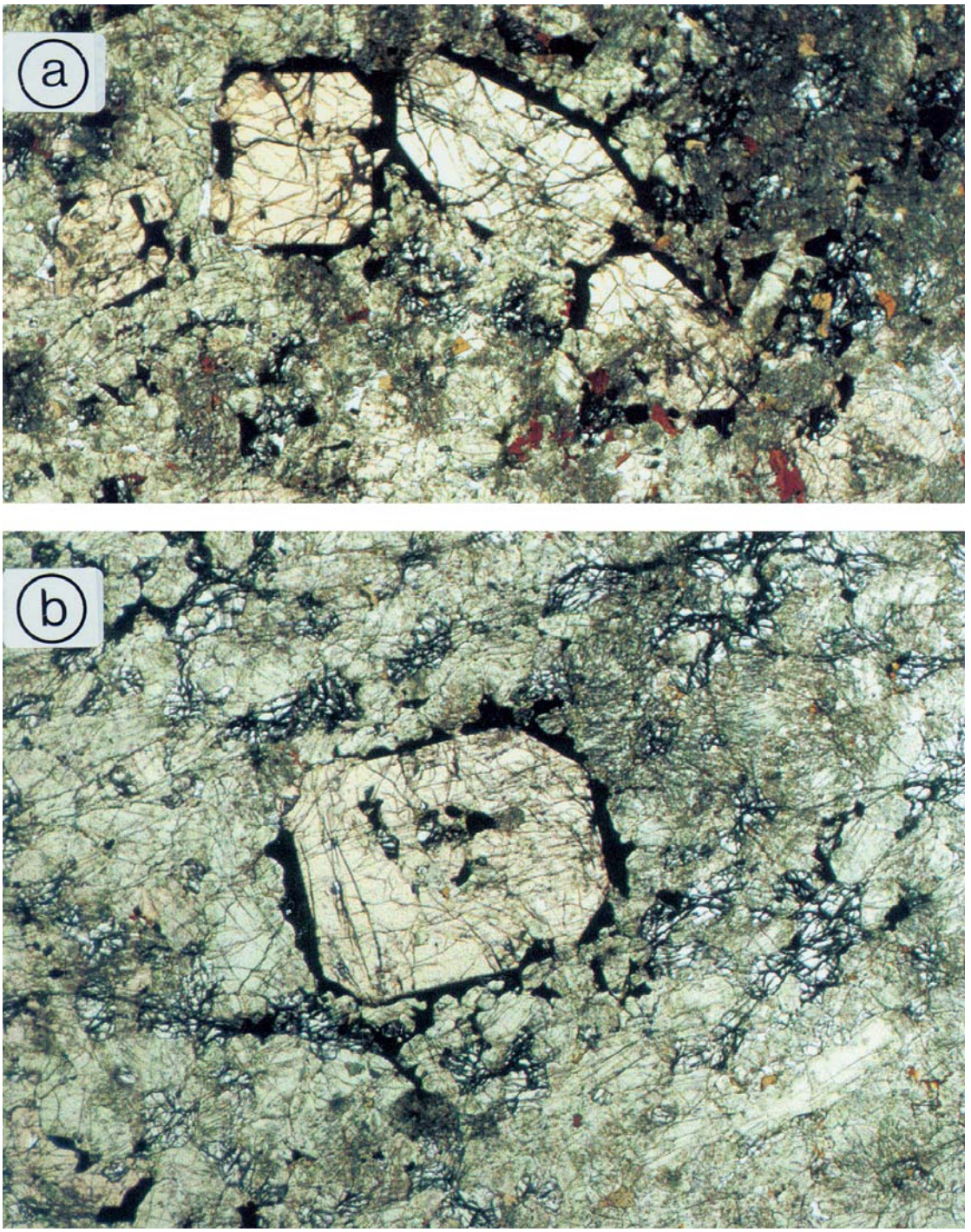

Fig. 77. Sulphide-mantled orthopyroxenes in olivine pyroxenites, Keivitsa. Diascanner photos by Reijo Lampela. a – discontinuous sulphide mantles around orthopyroxene with resorbed clinopyroxene inclusions. Non-mantled orthopyroxene oikocrysts (middle left and lower right corner) contain resorbed olivine and clinopyroxene. Primary intercumulus biotite-phlogopite (brown) is common. DDH672/6.35 m. Width of photo = 2.5 cm. b – mantled orthopyroxene (6 mm) with resorbed olivine and clinopyroxene. Most orthopyroxene grains are unmantled oikocrysts. DDH692/195.93 m.

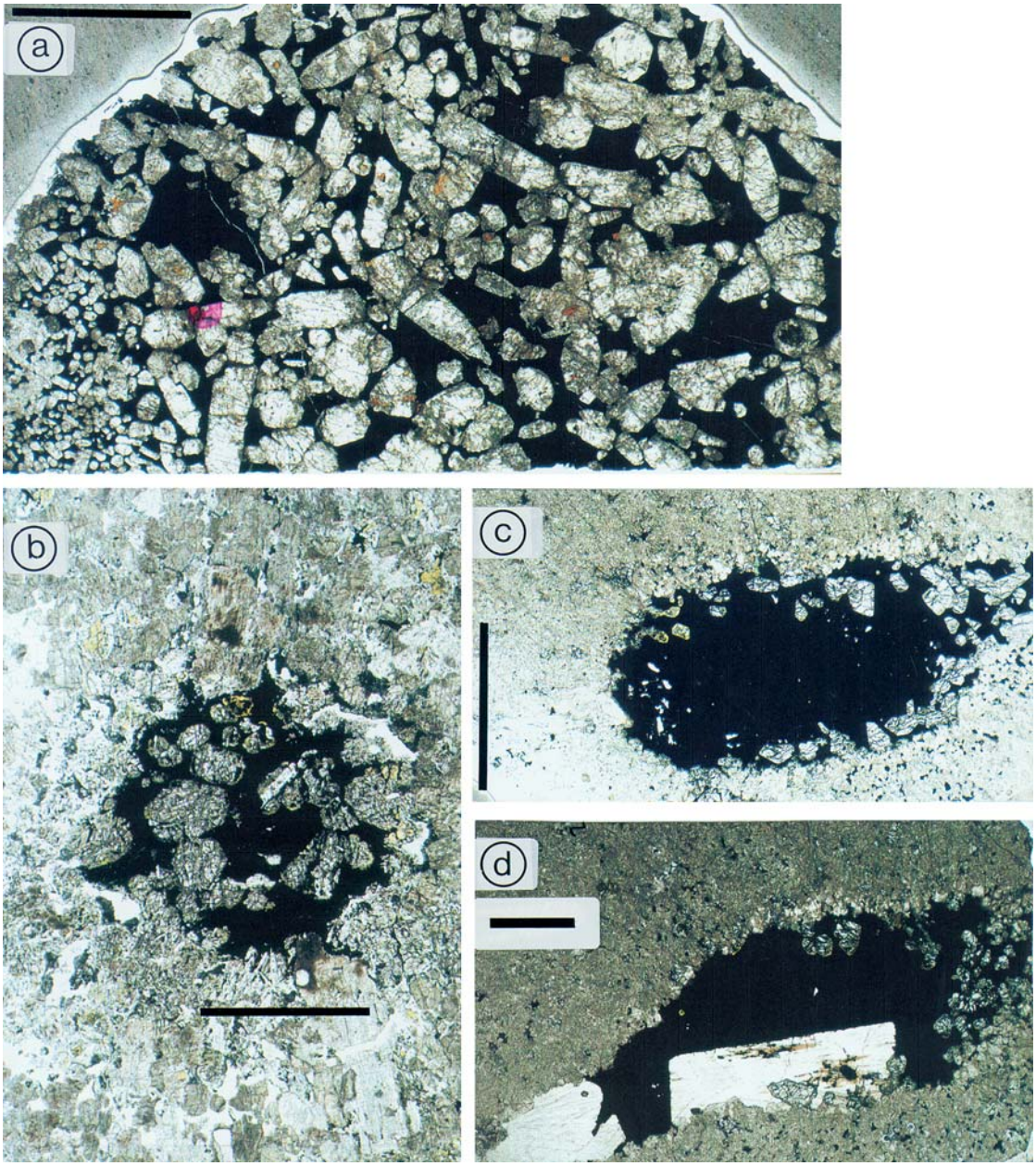

Fig. 78. Primary sulphides of the Keivitsa intrusion. Diascanner photos by Reijo Lampela. a – euhedral clinopyroxene crystals embedded in sulphides (mainly pyrrhotite, pentlandite and chalcopyrite), note small clinopyroxene crystals at left. Bar = 5 mm; b – sulphide droplet with euhedral olivine inclusions in olivine pyroxenite (with 13 vol% olivine, plus clinopyroxene, orthopyroxene, intercumulus plagioclase and primary biotite-phlogopite and hornblende). DDH688/473.60 m. Bar = 5 mm; c – a sulphide droplet with euhedral olivine in olivine pyroxenite (with 6 vol% olivine). Roundish inclusions of clinopyroxene occur in the cores of some olivines. DDH824/250.43A m. Bar = 1 cm; d – another section of the same droplet as in 78c. Euhedral olivine (top and right end of the droplet), euhedral plagioclase (white). Clinopyroxene is euhedral when in contact with the big plagioclase crystal. Bar = 5 mm.

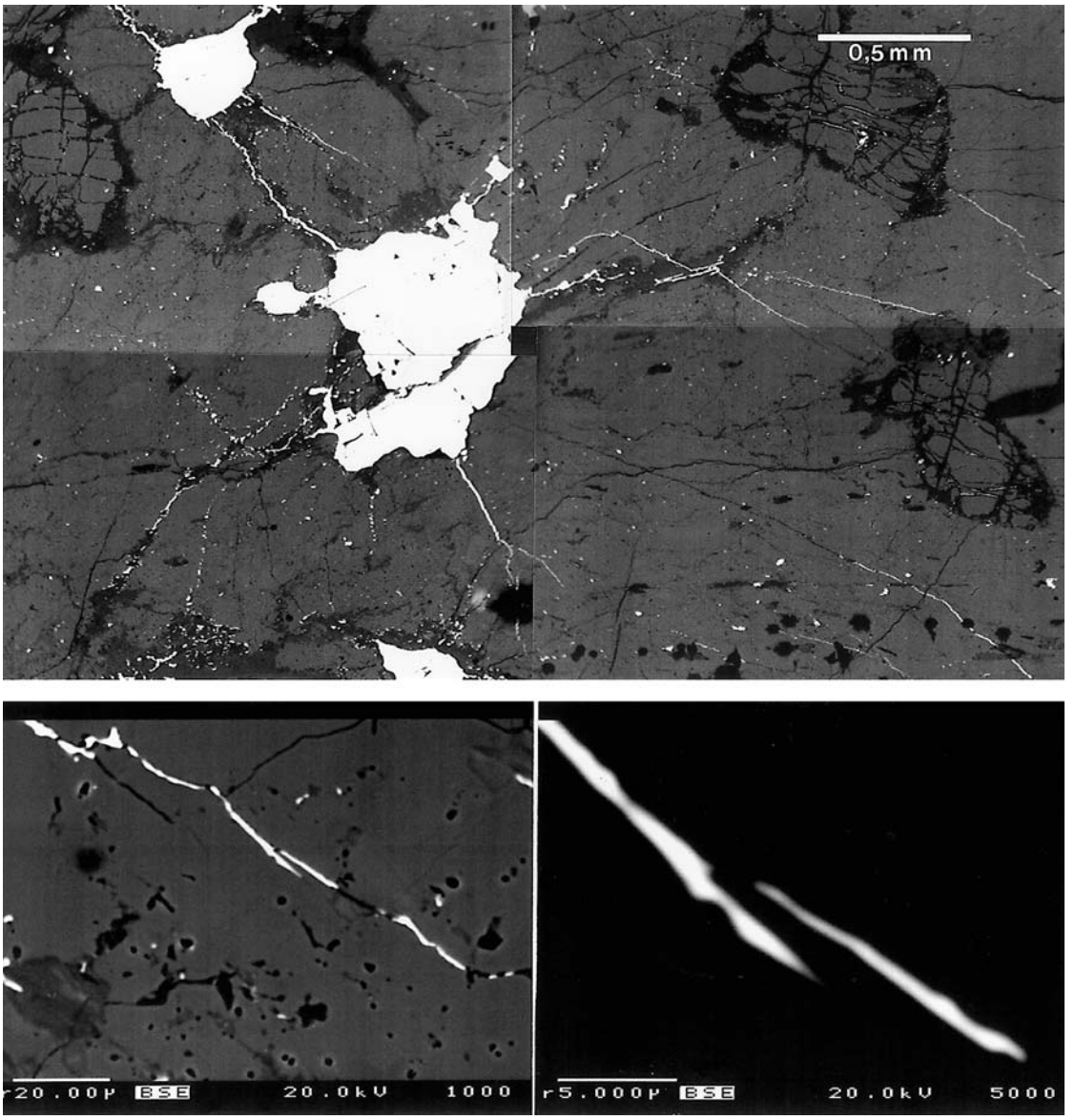

Fig. 79. "Chicken wire" sulphide network in olivine pyroxenite, Keivitsa. BE images by Lassi Pakkanen. a – chicken-wire texture of sulphide nuclei and "axons"; b and c – details of axons, with thicknesses of 0.5 mu and less. DDH713/38.90 m. See text.

lena and altaite occasionally. The ore minerals identified to date are listed in Table 10.

In the following description chalcopyrite denotes chalcopyrite proper, talnakhite and putoranite. Talnakhite and putoranite have been identified in XRD runs. Obviously, one or more of the compositionally similar and paragenetically related Cu-Fe sulphides (moo-

ihoekite, haycockite, Ni-putoranite) should occur in the ores, but no positive identifications have yet been made. Talnakhite has been identified from Karik I massif, eastern Pechenga area (Distler et al., 1988), and both talnakhite and putoranite from the Monchegorsk intrusion (Orsoev et al., 1994).

Pentlandite exsolved from high-T monosulphide solid solution (Mss) first by granule exsolution as equant grains; subsequent low-T exsolution produced lamellar and dendritic flake pentlandite. Flake pentlandite seems to be more common in false than in regular ores. Flake pentlandite also occurs in chalcopyrite. A thin seam of pentlandite is typically seen between pyrrhotite and chalcopyrite. Pentlandite in association with troilite and hexagonal pyrrhotite contains (in wt%) 27–36% Ni (average ca 32%); the pentlandite in the low-T paragenesis of the Ni-PGE type is very rich in Ni (40–42%).

One grain of copper pentlandite (with 3.2% Cu) has been analysed by electron microprobe. Several other "copper pentlandites" from partially oxidized trench samples have their stoichiometry (with S>Me) the wrong way. The mineral is probably a mixed violarite-carrollite thiospinel. Cu-pentlandite from Monchegorsk has a higher Cu (8.77%; Orsoev et al., 1994) than the Cu-pentlandite from Keivitsa.

Sulphides in the transitional ore type are rich in pentlandite; pyrrhotite is rare and sometimes absent; millerite occurs in pyrrhotite-free assemblages. Sulphides are interstitial to silicates, indicating that sulphide liquid was once present.

The ore paragenesis of the Ni-PGE ore type is quite different from that of other ore types. Graphite is ubiquitous and oxides are all but absent. The most unusual, and significant, feature is the low-T sulphide-arsenide-sulpharsenide paragenesis associated with a high-T silicate paragenesis (ol, cpx, pl). Pyrrhotite is absent, and the sulphides are not interstitial to silicates. The composite sulphide grain aggregates are roundish (hence the field name "pin-

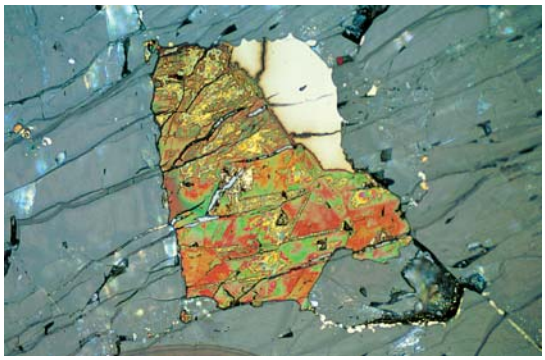

Fig. 80. Oxidized talnakhite in olivine pyroxenite. Creamy white mineral is pyrrhotite. Reflected light microphotograph by Jari Väätäinen. DDH679/148.80 m. Width of photo 0.7 mm.

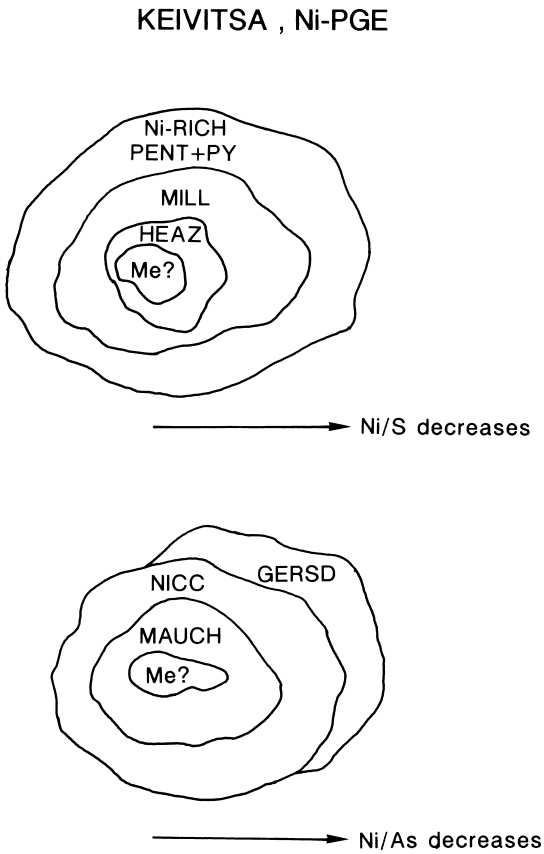

Fig. 81. Schematic drawing of the textures of the paragenetic sequences of the S and AsS minerals of the Ni-PGE ore type, Keivitsa.

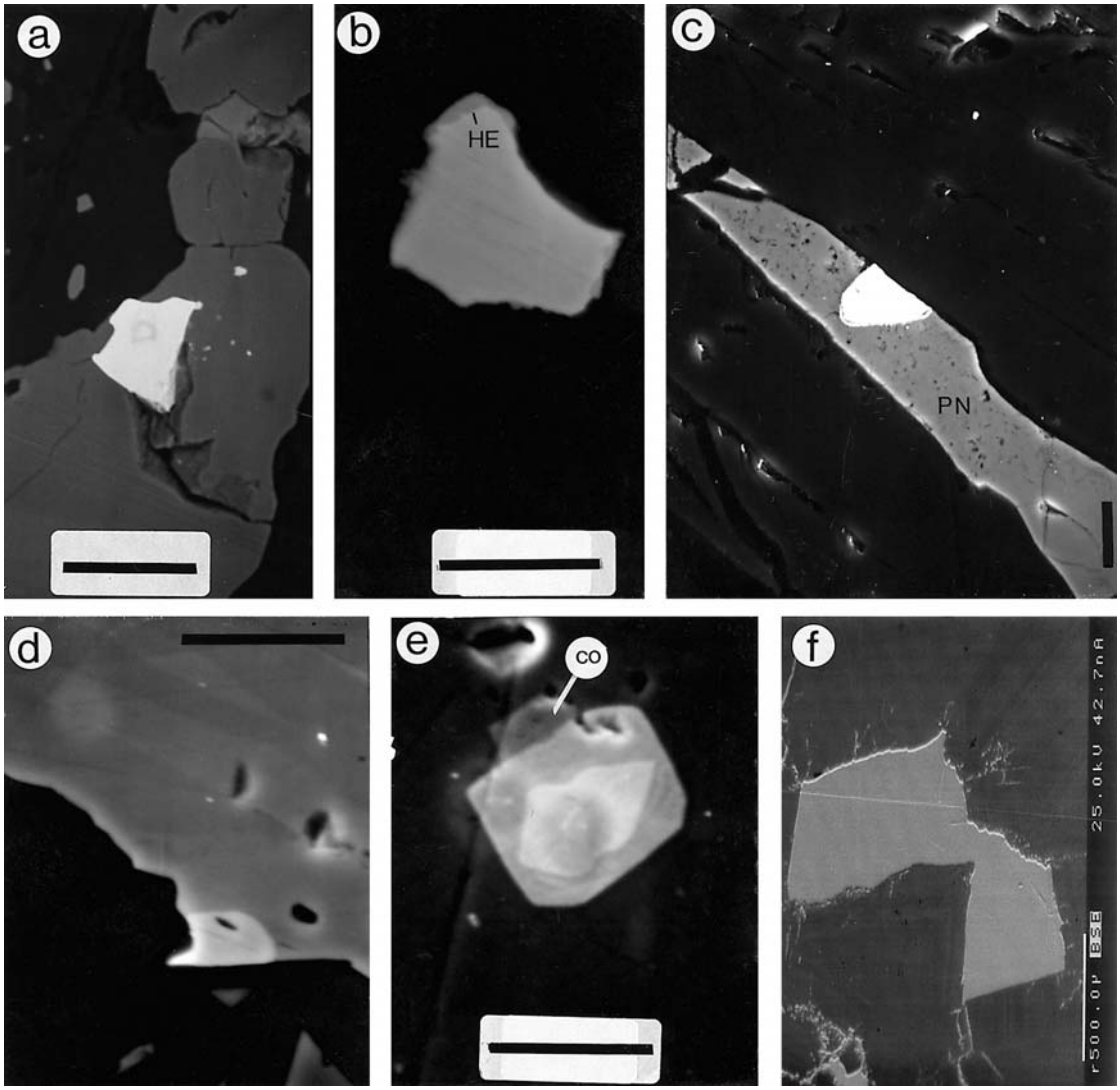

Fig. 82. PGM and tsumoite in Keivitsa-Satovaara. BE images (a,b,f) and SE images (c–e) by Lassi Pakkanen. a – sperrylite in magnetite. DDH330/106.35 m. Bar = 10 mu; b – Pt>Pd-Bi<Te phase (moncheite?), grey, with hessite (dark grey, HE) on rims. DDH336/54.15 m. Bar = 5 mu; c – moncheite (white) in pentlandite (grey). DDH333/109.30 m. Bar = 10 mu; d – Ni-Pd-Sb-Bi<Te phase (white) in contact with niccolite (grey). Satovaara DDH308/140.75 m. Bar = 5 mu; e – a zoned crystal of irarsite (core), hollingworthite (darker gray) and local cobaltite (CO). Satovaara DDH308/99.85 m. Bar = 5 mu; f – tsumoite, BiTe, Keivitsa DDH931/37.15 m. Bar = 500 mu.

heads"), and the sulphides in them are concentrically arranged, with the metal/sulphur ratio decreasing from the centre to the margin (see Fig. 81). The core of millerite (+heazlewoodite) is surrounded by Ni-rich pentlandite. The outermost zone is composed of pyrite and a very delicate symplectite of pyrite and pentlandite. The As(-S) paragenesis shows similar

grain forms and a similar concentric arrangement, with the metal/As ratio decreasing from the maucherite core to an intermediate zone of nickeline and to the gersdorffite rim. The rare Cu minerals (bornite, chalcocite, chalcopyrite) occur apart from the sulphide grain aggregates.

The low S content of the rocks and the high metal/S ratios of sulphides in this ore type indicate that the local magma system was very poor in sulphur. Paragenetic and mineralogical features suggest that a Ni alloy crystallized together with olivine and clinopyroxene in a reducing, low-sulphur magmatic environment. The concentric aggregates of sulphides and arsenides-sulpharsenides formed at low temperatures when errant S and As reacted with alloy particles (see Fig. 81).

Sulphide-associated secondary magnetite is more abundant in false and regular ores than in Ni-rich types. It is significant that, ample sediment contamination notwithstanding, all primary and secondary spinels are very poor in Zn. The maximum Zn content in primary cumulus magnetite is 0.37%, in chromite 0.34%, in secondary magnetite 0.08% and in sulphide-associated magnetite 0.06%.

PGE minerals (PGM in the following) mostly occur as small grains (< 10 mu) at the margins of sulphide grain-aggregates, in silicates or in secondary magnetite (Fig. 82). Most typical are Te-Bi compounds of Pt and Pd (moncheite, kotulskite, merenskyite, michenerite, maslovite) and sperrylite; sulphides (cooperite, braggite) and alloys (isoferroplatinum) are more rare. Zoned (Ir -> Rh -> Co) AsS grains, similar to those of Hitura (Häkli et al., 1976) occur in the Satovaara intrusion (Fig. 82e).

The Pt-Pd PGMs are either Pt-rich or Pd-rich; only 11% of the analyses fall to the range with the proportion of Pt (of the Pt+Pt sum) between 7 and 87 at%. Despite the polarized mineralogy, the average Pt/Pd ratio (wt%) of the analysed PGM is 1.82, the same as in ore-assays. The polarized distribution of Pd and Pt in different mineral phases seems to be a rule rather than an exception (see, e.g., Häkli et al., 1976; Piispanen & Tarkian, 1984; Volborth et al., 1986; Krivenko et al., 1989; Grokhovskaya et al., 1992). Generally this separation is explained by later redistribution of PGE by post-magmatic or metamorphic, generally Cl-rich fluids (Häkli et al., 1976; Vuorelainen et al., 1982; Orlova et al., 1987; see especially Springer, 1989; Li & Naldrett, 1993). Volborth and co-workers (1986) suggested that the Pt/Pd separation took place very early with the participation of chloride complexes.

Of the Pt-mineral grains 55.3% are included in silicates (even in pyroxene), 12.8% in sulphides and 31.9% are located at the silicate-sulphide contact; of Pd-minerals 25.0% are included in silicates, 29.5% in sulphides and 45.5% are at the silicate-sulphide contact. All this supports the idea that Pt and Pd parted into separate phases in the magmatic stage (see Mutanen et al., 1996).

Table 11 lists the PGM found so far in Keivitsa and KSC. Anomalous PGE and Au have been detected in several ore minerals; the most common PGE carrier is palladian melonite. The highest Pt contents are: 0.93% in mackinawite, 0.74% in pyrrhotite, 0.70% in maucherite, 0.61% in pentlandite and 0.23% in pyrite (in the Ni-PGE type). Rhodium has been detected in pentlandite (up to 0.1%), Pd in pyrite, pentlandite and gersdorffite (up to 0.10–0.11%), and Ir and Au in maucherite (0.46 and 0.43%, respectively; Kojonen et al., 1996). High Hg contents were analysed in several minerals, up to: 0.88% in pyrrhotite, 0.83% in chalcopyrite, 0.73% in maucherite, 0.48% in pentlandite and 0.43% in gersdorffite. Although the ore is relatively rich in Ag (1–4 ppm), sulphides are rather poor in Ag (max. 0.17% and 0.16% in chalcopyrite and pentlandite).

Ore petrology of the Keivitsa intrusion

The manifold ore types of the Keivitsansarvi deposit encompass an astounding range of element ratios (see e.g., Figs 62–63, 65–66, 76) probably greater than ever found within a single magmatic sulphide deposit (or, for that matter, in all such deposits combined). The variation, however, is not haphazard, nor caused or obscured by later events, but reflects original magmatic conditions and processes. These involved contamination by material from sulphide-rich, Mg-rich pelites, black schists and various komatiitic rocks. Due to carbonaceous contaminant material from black schists the magma became progressively reduced (Mutanen, 1994, 1996).

In diagrams of chalcophile and siderophile elements (e.g., Figs 63 and 65) all ore types are ordered neatly along an apparent mixing line from sedimentary sulphides to komatiitic dunite. Along this line Ni(100S) and Ni/Co increase and S/Se and S/Te decrease; there is also a regular decrease in Au/PGE, Rh/Pt, Re/PGE, and an increase in (Os+Ir+Ru)/(Pt+Pd+Rh), PGE(100S), PGE/Ni+Cu and total PGE (Figs 75–76, 83–84).

The mixing line most probably reflects true mixing of appropriate components of sedimentary and komatiitic end members. Recent S isotope data (see Hanski & al., 1996) explicitly affirm the important role of sedimentary sulphur in the deposit and support the idea that the ore types contain component mixtures of exotic end members.

The Pt/Pd ratio in all ore types is close to the chondritic ratio (Fig. 83), suggesting that all the ingredients (magma, komatiites and sediments) had this Pt/Pd ratio and that the processes of crystallization-fractionation did not disturb it. However, the sedimentary components may well have had a different Pt/Pd, but because of its supposedly low total PGE the sedimentary contribution was overwhelmed by other components richer in PGE. On the other hand, the effect of different PGE sources can be seen in the wide spread of the (Pt+Pd+Rh)/(Os+Ir+Ru) ratios (Fig. 84) and of the Pd/Ir ratios (Fig. 83). Note also the odd slope of the histogram, in Fig. 84.

The possibility of a significant sedimentary PGE component should be kept in mind, as the number of findings of PGE in sedimentary rocks is growing. It is interesting that the sedimentary PGE deposits contain high amounts of Sb, As and Se (e.g., Zoller et al., 1983; Delian et al., 1984; Coveney & al., 1992; Hulbert et al., 1992) which are not prominent in normal Ni ores.

The sedimentary rocks around the KSC are relatively rich in Se, their S/Se ratios being fairly close to mantle ratios (e.g., Hoatson et al., 1992). The relatively high Se and Te contents point to a restitic terrigeneous component in pelites; alternatively, they may be associated with pre-Keivitsa volcanism. Decrease of S/Se and S/Te ratios are known to be associated with subaerial degassing processes (Greenland & Aruscavage, 1980), where Se and Te are enriched in volcanic particulate matter (Zoller et al., 1983).

The very low S/Se and S/Te ratios (min. S/Se 21) of komatiitic dunites, the opposite end member, may be inherited from depleted mantle residue. As a result of Se contamination the S/Se ratios in ores are much lower than in ordinary magmatic sulphide deposits.

The Ni-PGE type rocks have higher mg#, Ni/Co, Ni/Cu, PGE, PGE/Au and As than other ore types. All these features are traceable to komatiite dunites. I suggest that these rocks contain material from disintegrated komatiite dunites, mainly refractory olivine debris. The debris sank through and interacted with contaminated roof magma enriched in Cl and float graphite. This contaminated part of the magma chamber was also enriched in total REE and still more in LREE (see Fig. 87). The REE(CN) pattern of the Ni-PGE type is quite different from that of the komatiitic xenoliths

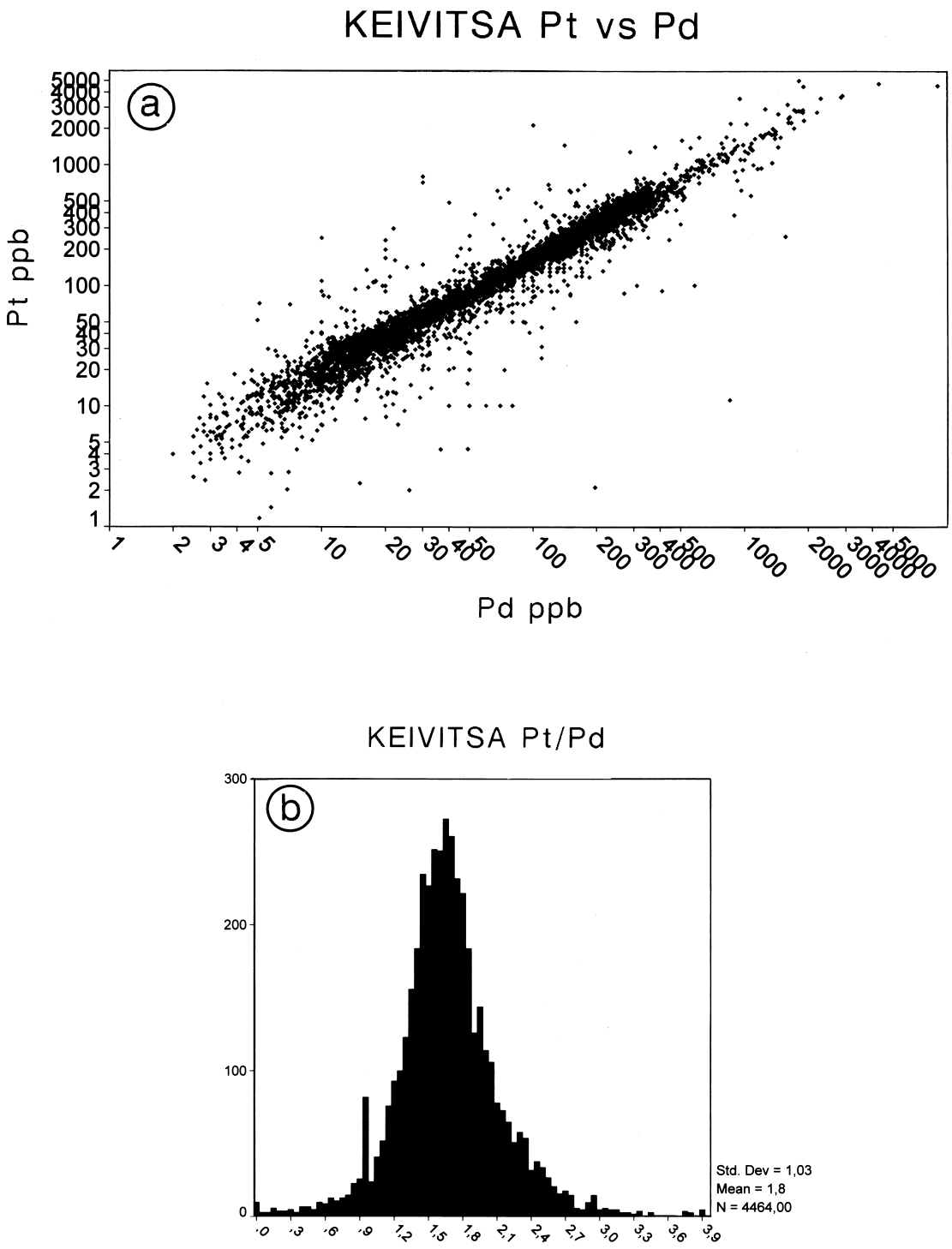

Fig. 83. Pt-Pd relationships, Keivitsa. a – Plot of Pt vs Pd, all samples; b – histogram of Pt/Pd ratios, all samples.

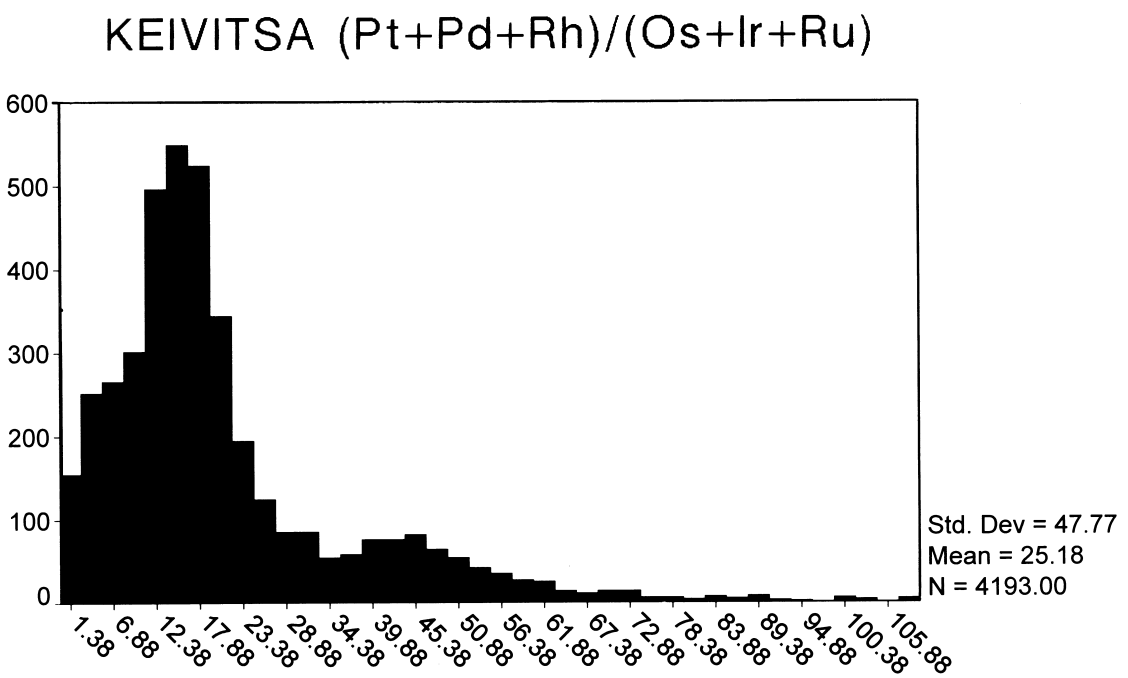

Fig. 84. Histogram of (Pt+Pd+Rh)/(Os+Ir+Ru) ratios, Keivitsa.

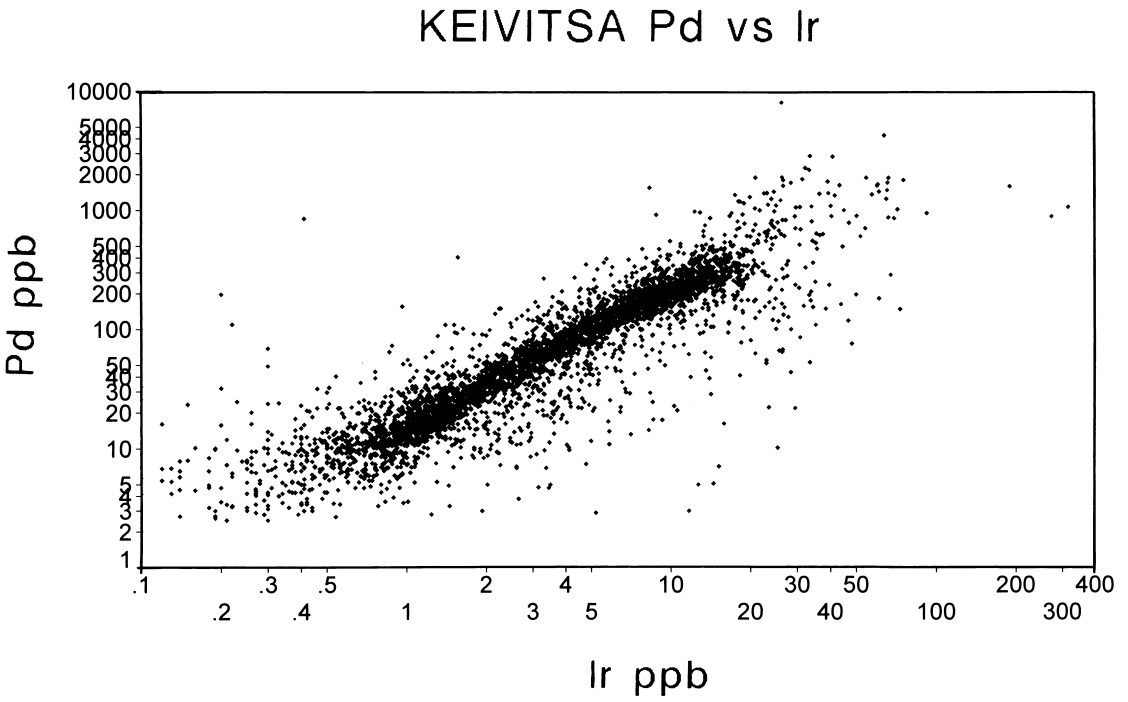

Fig. 85. Plot of Pd vs Ir, Keivitsa.

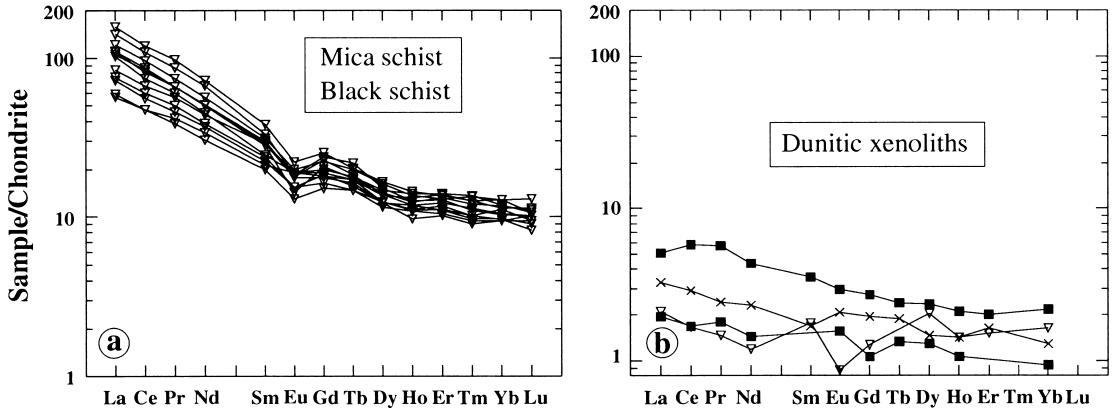

Fig. 86. Diagrams of chondrite-normalized REE for mica schist and black schist (left) and komatiitic dunite xenoliths (right), Keivitsa-Satovaara complex. Data and diagrams by Eero Hanski.

(Figs. 86–87); instead it resembles the pattern of sedimentary rocks, even showing the inherited negative Eu anomaly (Fig. 86). The metasomatic quartz-carbonate rocks may have contributed REE, as suggested earlier. The drooping leftward ends of the curves may be due to an exotic LREE-depleted component (komatiitic dunite). The contaminants (REE, Cl, H_2O) are such that they could have been conveyed from sediments to the roof magma by selective diffusion. The REE concentration in the local magma system seems to have been high enough for monazite to crystallize.

As suggested before, the low S in Ni-PGE magma system, combined with the high Ni and low oxygen pressure enabled crystallization of a Ni alloy from magma. The olivine that crystallized (or equilibrated) with the alloy became very rich in Ni, (Mutanen, 1994).

In the regular ore there is a good correlation between PGE and Ni+Cu, but in the deposit as a whole there is no correlation between PGE and sulphide (Fig. 71). The only regularities are that massive sulphides always have low total PGE, and the highest PGE are found in rocks which are very low in sulphides. In this respect Keivitsa is similar to the Ioko-Dovyren intrusion (Distler & Stepin, 1993).

There is no PGE-S correlation in Ni-PGE and transitional ore types (Fig. 72). This could mean that the original PGE phases crystallized directly from silicate liquid (Hiemstra, 1979; Augé, 1986; Distler & al., 1986). In regular ore, PGE correlate with Ni+Cu values. However, most of the PGM grains are not included in sulphides but occur at the sulphide-silicate boundary or in silicates, as is common in PGE deposits (see e.g., Bow et al., 1982; Viljoen et al., 1986a; Scoates et al., 1988; Harney & Merkle, 1990; Rudashevskii et al., 1991; Hoatson et al., 1992). My brief literature study showed that in PGE deposits 30–83% of the PGM grains occur outside sulphides.

With regard for the seemingly general acceptance of the idea that sulphide liquid is the universal solvent-collector of PGE it is surprising how often we must read about the lack of direct or any correlation between PGE and sulphides (e.g., Häkli et al., 1976; Alapieti & Lahtinen, 1986; Mutanen et al., 1987, 1988: Mutanen, 1989b; Dyuzhikov et al., 1988; Lee & Parry, 1988; Nielsen, 1989; Grokhovskaya

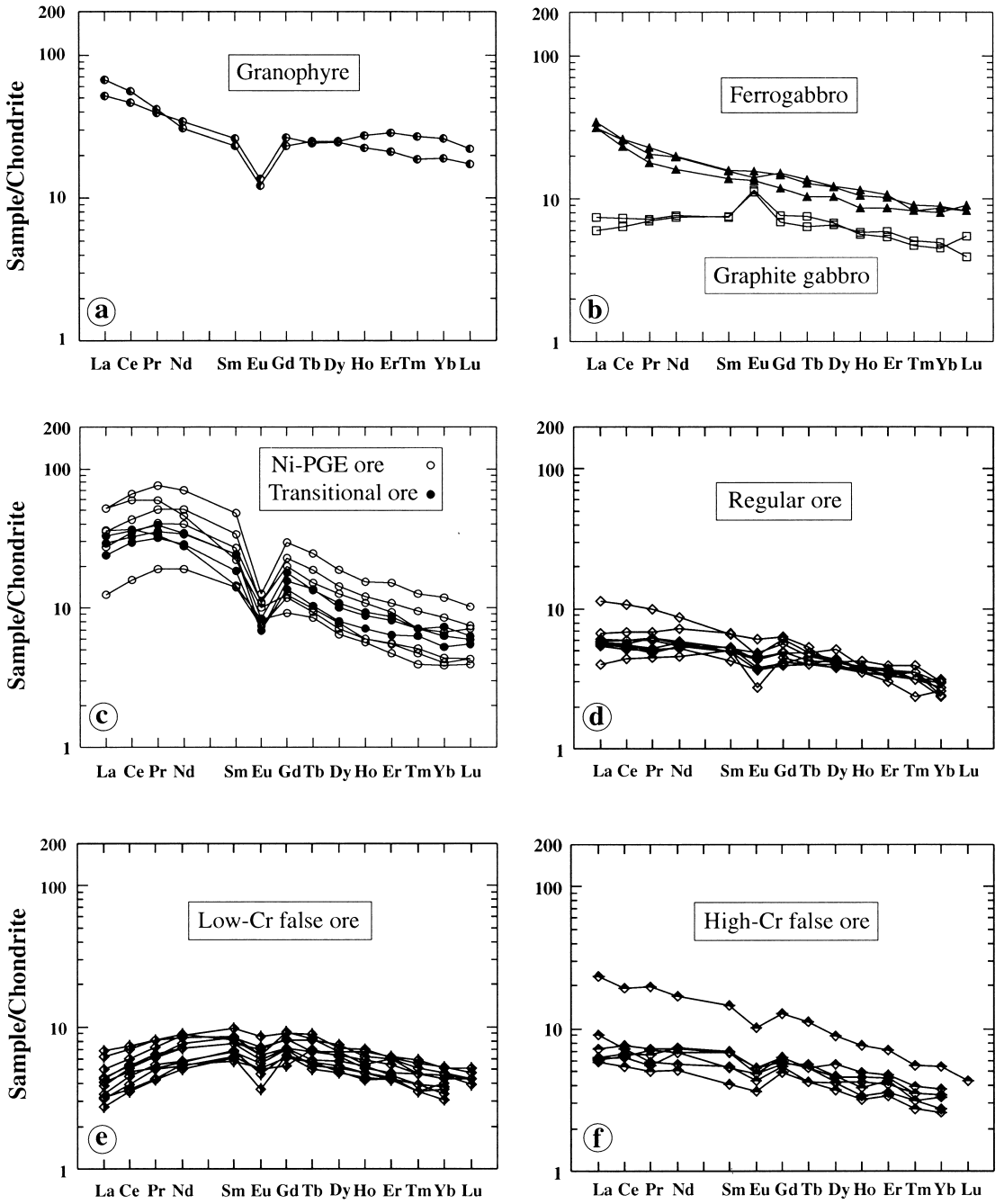

Fig. 87. Diagrams of chondrite-normalized REE for various ore types of the Keivitsa intrusion. Data and diagrams by Eero Hanski.

et al., 1989; Brügmann et al., 1990; Cowden et al., 1990; Halkoaho et al., 1990; Saini-Eidukat et al., 1990; Bird et al., 1991; Eales et al., 1993; Scoon & Teigler, 1994; Izoitko & Petrov, 1995; Reeves & Keays, 1995).

Sulphide Ni-Cu ores, epitomes of mantle magmas and mantle sulphides, are low in PGE in general, sometimes surprisingly so, as in the Bruvann ore in Norway (Boyd et al., 1987; Barnes, 1987). Whether sulphides are rich or poor in PGE, sulphide liquid is always found either as the cause of enrichment or culprit of impoverishment of the PGE (e.g., Barnes, 1987).

In some cases PGE seem to be chalcophobic more than chalcophile: Stone et al. (1991) describe a case where PGE-Au hike coincides with a drop of Ni, Cu and S. As in the Keivitsa intrusion, massive sulphides are sometimes depleted of PGE (Dillon-Leitch et al., 1986). The PGE often behave independently even in the presence of sulphide liquid (Mutanen, 1989b; Legendre & Augé, 1992).

It is too seldom noticed that PGE are, above all, siderophile elements (for rare exceptions, see Hiemstra, 1979; Tredoux et al., 1995). In general, it seems that too much is made of the chalcophile character of the PGE (as in the statement "Equilibration with sulfide is the only known mechanism that can effectively remove PGE from terrestrial magmas"; Naldrett & Duke, 1980).

A spatial connection of Cl minerals with PGE is commonly noted. We suggested earlier (Mutanen et al., 1987, 1988) that halogens acquired from sediments formed melt soluble complexes with PGE. These were able to enter the sulphide liquid only after breakdown of the complexes. Thus, the formation and breakdown of PGE complexes would govern the seemingly arbitrary, even irrational stratigraphic distribution of PGE, with little respect for sulphides. Others have also pleaded for the melt-soluble halogen complexes of PGE (Miller et al., 1988; Gorbachev et al., 1994b). Ringwood (1955) already accounted the enrichment of Cr and V in the upper part of the Skaergaard intrusion for melt-soluble complexes. The existence of haloid-metal autocomplexes in silicate liquids was suggested by Anfilogov and co-workers (1984).

The breakdown of PGE complexes could lead to the liberation of PGE and formation of metallic and other PGE compounds. In fact, direct crystallization of PGM from magmas is often observed or indicated (Distler & Laputina, 1981; Augé, 1986; Rosenblum et al., 1986; Distler et al., 1986; Lee & Tredoux, 1986; Lee & Parry, 1988; Nixon et al., 1990; Barkov et al., 1991; Legendre & Augé, 1992; Peck et al., 1992; Scoon & Teigler, 1994). The independent PGM particles would be available for other, non-solvent collectors.

That PGM grains are so often located at the sulphide/silicate grain boundaries makes one wonder whether the PGE-sulphide bind is mechanical rather than chemical. It is tempting to think that the sulphide liquid droplets acted as phase boundary collectors for tiny PGM particles that had already crystallized from silicate liquid (Mutanen, 1992; see and cf. Hiemstra, 1979). The particles should be real, stable minerals, not atomic-scale clusters collected by sulphide droplets (Tredoux et al., 1995). The process would thus be analogous to the old-time oil flotation.

Our experimental tests showed that the idea is feasible: skeletal crystals of a Cu-Pt alloy were found on sulphide beads (Fig. 88; see Mutanen et al., 1996; Mutanen, 1995). Further experiments should confirm whether the PGM (alloy particles in the experiment) nucleated on sulphide droplets (heterogeneous nucleation) or were mopped along by sinking sulphide droplets. In either case, the experiment indicated that the PGM alloy was a true liquidus phase. Remarkable was the absence of Pd phases on sulphide beads, suggesting that Pd behaved more like a chalcophile, while Pt was siderophile. The experiments on the distribution of Pt and Pd between silicate liquid, sulphide liquid and liquid metal, by Marakushev

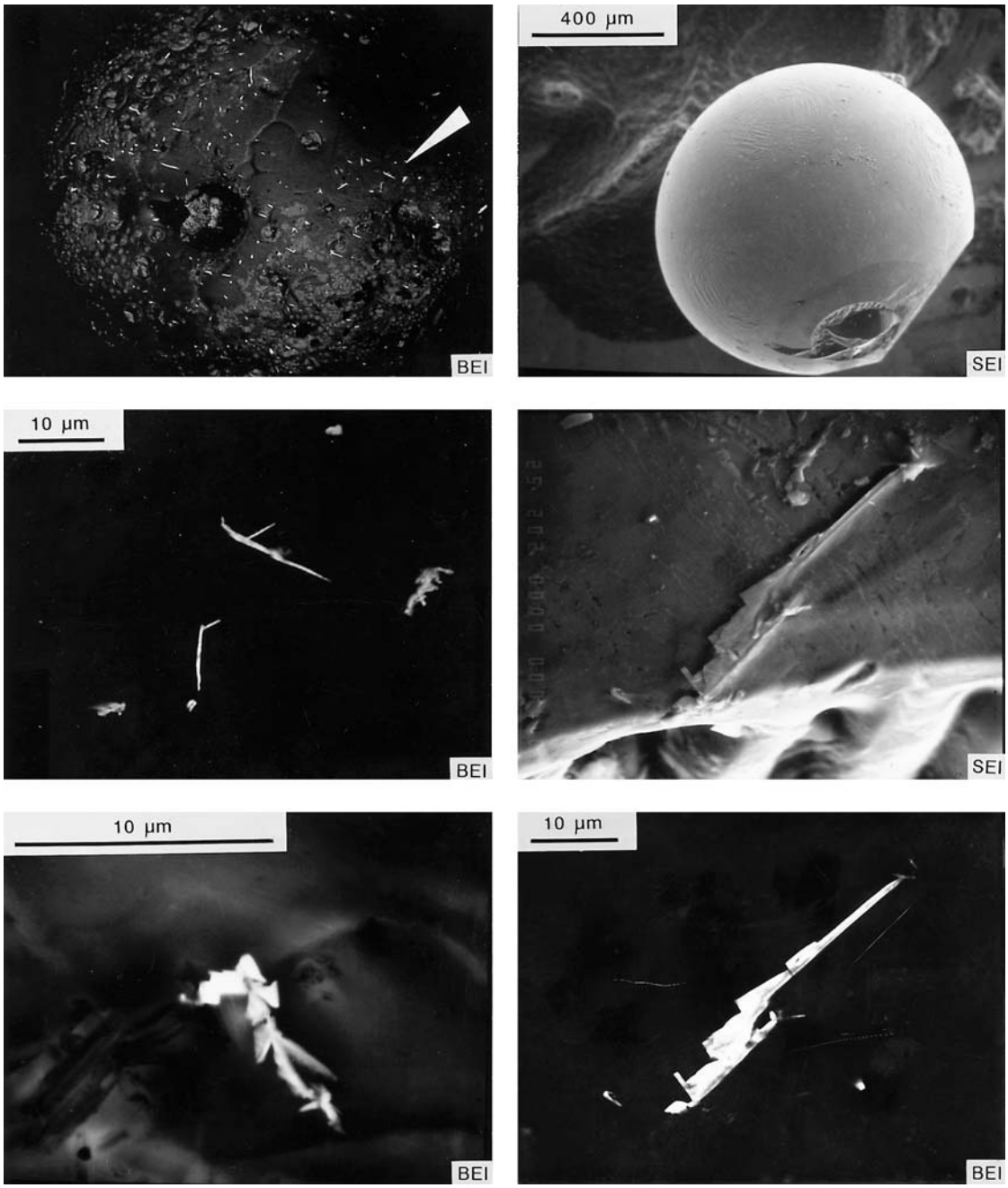

Fig. 88. Skeletal Pt-Cu alloy crystals on sulphide beads, BE and SE images by Bo Johanson. Top left – Pt-Cu crystals on a NiS bead; top right – NiS bead with a "crater"; middle left – detail of the arrow point area in top left image; middle right – detail of the crater rim in top right image, with a skeletal "harpoon" crystal of Pt-Cu; lower left – a feathery rosette of skeletal Pt-Cu crystals: lower right – BE image of the harpoon crystal in middle right image.

and Shapovalov (1996) confirmed our anticipation: calculated from their results the D-values between liquid phases were 350 for Pt(metal/sulph) and 1.8 for Pd(sulph/metal). The result also strongly suggests that the Pt-Pd separation, so common in PGE deposits (see above) may have its origin in the magmatic stage.

Our work has corollaries both practical and theoretical. I consider here only one. If metallic PGE particles can nucleate on sulphide, it may explain why the D-values of PGE (sulph/silic) calculated for natural systems are much lower than experimental values (Duke, 1990). I propose that the increase of D-values with decreasing oxidation of magma (Bezmen et al., 1991) is only apparent, and due to attached metallic particles of PGE on sulphide beads. The decrease of D values with increasing magma oxidation state (Crocket et al., 1992) is compatible with this interpretation and with our experimental results.

If PGM can nucleate on sulphide, they could preferentially nucleate on early spinels or even serve as sites of heterogeneous nucleation for them (Augé, 1986; Capobianco & Drake, 1990). We would then have a simple explanation for the association of PGE with oxide cumulates in the Koitelainen and Akanvaara intrusions.

ACKNOWLEDGEMENTS AND APOLOGIES

My early wilderness years in Koitelainen and Keivitsa-Satovaara were a time of lonely and quiet survival. In recent hectic years, however, cooperation in our Survey has increased, become welcome, and finally indispensable. I will not repeat the names of the seventy or so people who participated in the Keivitsa exploration project and helped me in many ways (Mutanen, 1994). If I were to compile a list of contributing fellow workers, supporters and critics, it would fall short. Anonymous though they may be I am grateful for their efforts.

The following are but a few of the many people who contributed to the preparation of this book: Seppo Aaltonen, Jukka Alakunnas, Eija Hyvönen, Hannu Kähkölä, Markku Lappalainen, Pertti Telkkälä, Markku Pänttäjä (computer matters). Anne Sandberg introduced and reintroduced me to the WP computer game, and handled the raw manuscripts and connections to the printing company. Soili Ahava, Viena Arvola, Ritva Kotiranta and Marjatta Kanste did the drawings. Kirsi Koskinen helped in checking the hyphenation of the first proofs. Reijo Lampela took many photos and made the diascan images. Anne Sandberg and Päivi Junttila (later Piittisjärvi) compiled tables, and Helena Murtovaara typed, ordered and standardized the long list of references. Pauli Vuojärvi was field assistant at Keivitsa and Akanvaara, Kari Sassali my field hand at Akanvaara. Pekka Tanskanen reported on diamond drilling at Akanvaara in 1996 and 1997.

I apologize to my fellow workers for my irritability and often irritating behaviour during the testing days in April, 1997.

Bo Johanson and Lassi Pakkanen (both GSF, Espoo) made most of the electron microprobe analyses referred to here; Bo Johanson provided the technical data of the microprobe analysis. Their skill and cooperation has been of the utmost value.

The discussions with Esko Kontas about chemical analyses, Hannu Huhma about isotope analyses, Juha Karhu about the stratigraphy and carbon isotope data of the pre-Keivitsa sediments, and Eero Hanski about the geochemical and isotopic data of the Keivitsa-

Satovaara complex helped me to clarify my thoughts and to sharpen and balance my argumentation. Eero Hanski also allowed me to use the REE analyses and prepared the REE diagrams (Figs 86 and 87). Pentti Kouri and Jorma Räsänen helped in checking and cross-checking the references; the errors that remain are mine. I thank all those mentioned above for their help. I also thank Dr Hanna-Leena Mutanen (née Vikman), Hannu Laitinen, Samuli Aikio, and Professor Anna-Leena Siikala for their help.

This work evolved out of a technical report compiled for the Ministry of Trade and Industry concerning the exploration of the Keivitsansarvi Cu-Ni-PGE-Au deposit (Mutanen, 1994) and the guidebook to the IGCP Field Conference (Mutanen, 1996). During the hectic preparation time I drew on the custody of my superiors Erkki Vanhanen and Ahti Silvennoinen, the latter as director of the GSF RONF. Ahti provided me with organizational and personal support, coached, used all kinds of legal and benign forms of motivation and coercion, and all this while showing remarkable patience both before and after deadlines.

I thank Erkki and Ahti for levelling my path. Professor Matti Saarnisto urged me to publish the excursion guidebook in the Bulletin series of the GSF, accepted the publication of the final form of the manuscript, encouraged me and otherwise did all in his power to get me over the finishing line.

Professor Ilmari Haapala, University of Helsinki was the official supervisor of my work. I thank him for his concern for my work.

Several people in the GSF's Information office helped me in my misery during the final months and weeks. Stiina Seppänen, Sini Autio and Jani Hurstinen – my thanks to you come from my heart.

I had the benefit and honour to have two eminent geologists, Professor Aulis Häkli and Docent Hannu Huhma, as official reviewers for this work. Their conscientious efforts improved the quality and somewhat modified the quantity of the manuscript. Gillian Häkli corrected the most part of the English of the manuscript. If there are any linguistic errors, queer words or expressions apparently too profound to understand, they are either due to my unintentional omissions of Gillian's advice, or unauthorized alterations of the corrected text. Aaron Hakso corrected the English of part of the manuscript. I also thank Petri Peltonen for his suggestions regarding an earlier version of the text.

During the long investigation very many chemists of the GSF have provided me with analyses and given their time and advice. First and foremost are Maija Hagel-Brunnström (XRF), Paula Lindström, Riitta Juvonen, Eeva Kallio and Mervi Wiik (the noble metal people) from the Espoo laboratory, Esko Kontas (Pd, Pd, Se, Te) and all the personnel of the Rovaniemi laboratory.

Finally, I thank my wife Leena, my children and grandchildren for their patience when the husband, father and grandpa was absent or absentminded.

REFERENCES

Abovyan, S. B. 1962. Gabbro-pegmatity ofiolitovoi formatsii Armyanskoi SSR. Izvestiya Akademii Nauk Arm. SSSR, geol. geogr. nauki 15 (5), 35–46.

Afanasev, A. P. 1968. Itogi i perspektivy izucheniya dolednikovoi kory vyvetrivaniya na Kolskom poluostrove. In: Ivanova, T. N. (ed.) Geologicheskie stroenie, razvitie i rudonosnost Kolskogo poluostrova. Apatity: Geol. inst. Kolskii filial Akademii Nauk SSSR, 207–213.

Afanasev, A. P. 1971. K voprosu o tipakh kor vyvetrivaniya Baltiiskogo shchita. Materialy po geologii i metallogenii Kolskogo poluostrova 2, 91–97.

Afanasev, A. P. 1977. Fanerozoiskie kory vyvetrivaniya Baltiiskogo shchita. Leningrad: Nauka. 244 p.

Akhmedov, A. M. & Golubev, A. I. 1995. Fonovye anomalii redkikh i blagorodnykh metallov kak istochniki vozniknoveniya mestorozhdenii kompleksnykh rud v chernykh slantsakh Baltiiskogo shchita. In: Rybakov, S. I. & Golubev, A. I. (eds.) Tezisy dokladov regionalnogo simpoziuma "Blagorodnye metally i almazy Severa Evropeiskoi chasti Rossii" i nauchno-prakticheskoi konferentsii "Problemy razvitiya mineralno-syrevoi bazy platinovykh metallov Rossii", 16–18.

Alapieti, T. 1982. The Koillismaa layered igneous complex, Finland – its structure, mineralogy and geochemistry, with emphasis on the distribution of chromium. Bulletin of the Geological Survey of Finland 319. 116 p.

Alapieti, T. 1996. Early Paleoproterozoic layered intrusions of the Fennoscandian Shield – a review. In: IGCP project 336 symposium in Rovaniemi, Finland, August 21–23, 1996 : program and abstracts. University of Turku. Division of geology and mineralogy. Publication 33, 1–2.

Alapieti, T. T., Filén, B. A., Lahtinen, J. J., Lavrov, M. M., Smolkin, V. F. & Voitsekhovsky, S. N. 1990. Early Proterozoic layered intrusions in the northeastern part of the Fennoscandian Shield. Mineralogy and Petrology 43, 1–22.

Alapieti, T. T., Kujanpää, J., Lahtinen, J .J .& Papunen, H. 1989. The Kemi stratiform chromitite [sic] deposit, northern Finland. Economic Geology 84, 1057–1077.

Alapieti, T. T. & Lahtinen, J. J. 1986. Stratigraphy, petrology, and platinum-group element mineralization of the early Proterozoic Penikat layered intrusion, northern Finland. Economic Geology 81, 1126–1136.

Alapieti, T. T. & Lahtinen, J. J. 1989. Early Proterozoic layered intrusions in the northeastern part of the Fennoscandian Shield. In: Alapieti, T. (ed.). 5th International Platinum Symposium. Guide to the post-symposium field trip, August 4–11, 1989. Geological Survey of Finland, Guide 29, 3–41.

Allard, G. D. 1986. Roof rock assimilation – a mechamism to explain the facies changes in the Dore Lake Complex, Chibougamau, Quebec. CAC, MAC, CGU Joint Annual Meeting, Carleton University, May 19–21, 1986. Program with Abstracts 11, p. 40.

Allègre, C. J., Treuil, M., Minster, J.-F., Minster, B. & Albarède, F. 1977. Systematic use of trace elements in igneous processes. Part I: Fractional crystallization processes in volcanic suites. Contributions to Mineralogy and Petrology 60, 57–75.

Al-Rawi, Y. & Carmichael, I. S. E. 1967. A note on the natural fusion of granite. American Mineralogist 52, 1806–1814.

Amelin, Yu. V., Heaman, L. M. & Semenov, V. S. 1995. U-Pb geochronology of layered mafic intrusions in the eastern Baltic Shield: implications for the timing and duration of Paleoproterozoic continental rifting. Precambrian Research 75, 31–46.

Amelin, Yu. V. & Neymark, L. A. 1995. Pb isotope geochemistry of Early Proterozoic layered intrusions in the eastern Baltic Shield. In: Proc. International Field Conference and Symposium, IGCP 336/ Petrology and Metallogeny of Volcanic and Intrusive Rocks of the Midcontinental Rift System, August 19 – September 1, 1995. Program and Abstracts. Duluth, Minnesota: University of Minnesota Duluth, 5–6.

Amelin, Yu. V. & Semenov, V. S. 1996. Nd and Sr isotopic geochemistry of mafic layered intrusion in the eastern Baltic Shield: implication for the evolution of Paleoproterozoic continental mafic magmas. Contributions to Mineralogy and Petrology 123, 255–272.

Anderson, A. T. 1967. Possible consequences of composition gradients in basalt glass adjacent to olivine phenocrysts. Transactions American Geophysical Union 48, 227–228.

Anderson, A. T. & Gottfried, D. 1971. Contrasting behavior of P, Ti, and Nb in a differentiated high-alumina olivine tholeiite and a calc-alkaline andesitic suite. Geological Society of America Bulletin 82, 1929–1942.

Andreeva, E. D. 1959. Gabbro-pegmatity v piroksenitakh gory Sinei na srednem Urale. Izvestiya Akademii Nauk SSSR 9, 40–53.

Anfilogov, V. N., Anfilogova, G. I., Bobylev, I. B. & Zyuzeva, N. A. 1984. Formy nakhozhdeniya ftora i khlora v silikatnykh rasplavakh. Geokhimiya 5,

751–756.

Anonymous 1995. Keivitsa bidders announced. Mining Journal 324, p. 158.

Aoki, K. 1967. Petrography and petrochemistry of latest Pliocene olivine tholeiites of Taos area, northern New Mexico, U.S.A. Contributions to Mineralogy and Petrology 14, 190–203.

Appleyard, E. C. 1974. Syn-orogenic igneous alkaline rocks of eastern Ontario and northern Norway. Lithos 7, 147–169.

Arculus, R. J. 1974. Solid solution characteristics of spinels: pleonaste-chromite-magnetite compositions in some island-arc basalts. Carnegie Institution of Washington, Year Book 73, 322–327.

Arculus, R. J. & Osborn, E. F. 1975. Phase relations in the system MgO – iron oxide – Cr_2O_3 – SiO_2. Carnegie Institution of Washington, Year Book 74, 507–512.

Arculus, R. J. & Powell, R. 1986. Source component mixing in the regions of arc magma generation. Journal of Geophysical Research 91 (B6), 5913–5926.

Arnason, J. G., Bird, D. K., Bernstein, S., Rose, N. M. & Manning, C. E. 1997. Petrology and geochemistry of the Kruuse Fjord Gabbro Complex, East Greenland. Geological Magazine 134 (1), 67–89.

Arutyunov, G. M. 1971. Novye dannye po geokhimii produktivnykh gneisov Chupino-Loukhskogo raiona (Severnaya Kareliya). In: Mineralogiya i geokhimiya dokembriya Karelii, vyp. 7, 48–53. Trudy Karelskii filial Akademii Nauk SSSR. Leningrad: Nauka. 200 p.

Ashworth, J. R. 1976. Petrogenesis of migmatites in the Huntly-Portsoy area, north-east Scotland. Mineralogical Magazine 40 (315), 661–682.

Atherton, M. P., Naggar, M. H. & Pitcher, W. S. 1975. Kyanite in some thermal aureoles. American Journal of Science 275, 432–443.

Augé, T. 1986. Platinum-group-mineral inclusions in chromitites from the Oman ophiolite. Bulletin de Minéralogie 109, 301–304.

Balashov, Yu. A. 1996. Paleoproterozoic geochronology of the Pechenga-Varzuga structure, Kola Peninsula. Petrology 4 (1), 1–22.

Balashov, Yu. A. & Torokhov, M. P. 1995. Vozrast, tektonicheskie polozhenie i genezis paleoproterozoiskikh EPG-soderzhashchikh bazitovykh rassloennykh intruzii Baltiiskogo shchita. In: Rybakov, S. I. & Golubev, A. I. (eds.) Tezisy dokladov regionalnogo simpoziuma "Blagorodnye metally i almazy Severa Evropeiskoi chasti Rossii" i nauchno-prakticheskoi konferentsii "Problemy razvitiya mineralno-syrevoi bazy platinovykh metallov Rossii", 18–19.

Baragar, W. R. A. 1967. Wakuach Lake map-area, Quebec-Labrador (230). Geological Survey of Canada, Memoir 344. 174 p.

Barkanov, I. V. 1976. Osnovnye cherty metallogenii shchitov i massivov drevnykh platform i oblastei ikh aktivizatsii: Vostochnaya chast Baltiiskogo shchita. In: Geologiya i metallogeniya shchitov drevnykh platform SSSR. Leningrad: Nedra, 263–275.

Barker, D. S. & Long, L. E. 1969. Feldspathoidal syenite in a quartz diabase sill, Brookville, New Jersey. Journal of Petrology 10, 202–221.

Barker, R. W. 1975. Metamorphic mass transfer and sulfide genesis, Stillwater Intrusion, Montana. Economic Geology 70, 275–298.

Barkov, A. Yu, Lednev, A. I., Trofimov, N. N. & Lavrov, M. M. 1991. Mineraly serii laurit-erlikmanit iz khromitovykh gorizontov rassloennykh intruzii Karelo-Kolskogo regiona. Doklady Akademii Nauk SSSR 319 (4), 962–965.

Barkov, A. Yu., Lednev, A. I. & Bakushkin, E. M. 1994a. Mineraly elementov gruppy platiny iz massiva gory Generalskoi, Kolskii poluostrov. Doklady Akademii Nauk 338 (6), 785–788.

Barkov, A. Yu., Pakhomovskii, Ya. A., Trofimov, N. N. & Lavrov, M. M. 1994b. Loveringite: A first occurrence in Russia, from the Burakovsky layered intrusion, Karelia. Neues Jahrbuch für Mineralogie Hefte 3, 101–111.

Barkov, A. Yu., Menshikov, Yu. P., Begizov, V. D. & Lednev, A. I. 1996a. Oulankaite, a new platinum-group mineral from the Lukkulaisvaara layered intrusion, northern Karelia, Russia. European Journal of Mineralogy 8, 311–316.

Barkov, A. Yu., Savchenko, Ye. E., Menshikov, Yu. P. & Barkova, L. P. 1996b. Loveringite from the Last-Yavr mafic-ultramafic intrusion, Kola Peninsula; a second occurrence in Russia. Norsk Geologisk Tidsskrift 76, 115–120.

Barkov, A. Yu., Savchenko, E. E. & Menshikov, Yu. P. 1993. Khlorapatit kak pokazatel flyudnoi mobilizatsii platinovykh elementov v intruzii Lukkulaisvaara, Severnaya Kareliya. Doklady Akademii Nauk 328 (1), 84–89.

Barley, M. E., Pickard, A. L. & Sylvester, P. J. 1997. Emplacement of a large igneous province as a possible cause of banded iron formation 2.45 billion years ago. Nature 385, 55–58.

Barnes, S. J. 1986. The effect of trapped liquid crystallization on cumulus mineral compositions in layered intrusions. Contributions to Mineralogy and Petrology 93, 524–531.

Barnes, S. J., McIntyre, J. R., Nisbet, B. W. & Williams, C. R. 1990. Platinum group element mineralization in the Munni Munni Complex, Western Australia. Mineralogy and Petrology 42, 141–164.

Barnes, S.-J. 1987. Unusual nickel and copper to no-

ble-metal ratios from the Råna Layered Intrusion, northern Norway. Norsk geologisk Tidsskrift 67, 215–231.

Barnes, S.-J., Naldrett, A. J. & Gorton, M. P. 1985. The origin of the fractionation of platinum-group elements in terrestrial magmas. Chemical Geology 53, 303–323.

Barth, T. F. W. 1969. Feldspars. London: John Wiley & Sons. 261 p.

Batashev, E. V., Begizov, V. D., Zaskind, E. S. & Kasyanov, A. V. 1976. Peridotit-gabbro-noritovyi massiv Lukkulaisvaara. In: Intruzivnye bazit-ultrabazitovye kompleksy dokembriya Karelii. Trudy Inst. geologii, Karelskii filial Akademii Nauk SSSR 32, 41–48.

Bateman, J. D. 1943. Bird River chromite deposit, Manitoba. Transactions of the Canadian Institute of Mining and Metallurgy 46, 154–183.

Bateman, J. D. 1945. Composition of the Bird River chromite, Manitoba. American Mineralogist 30, 596–600.

Batiza, R. 1978. Geology, petrology, and geochemistry of Isla Tortuga, a recently formed tholeiitic island in the Gulf of California. Geological Society of America Bulletin 89, 1309–1324.

Baumer, A., Caruba, R., Bizouard, H. & Peckett, A. 1983. Chlorapatite de synthèse: substitution et inclusions de Mn, Ce, U et Th en traces. The Canadian Mineralogist 21, 567–573.

Bayanova, T. B., Mitrofanov, F. P., Korchagin, A. U. & Pavlichenko, L. V. 1994. Vozrast gabbro-noritov nizhnego rassloennogo gorizonta (rifa) Fedorovo-Panskogo massiva (Kolskii poluostrov). Doklady Akademii Nauk 337 (1), 95–97.

Bayanova, T. B. & Smolkin, V. F. 1996. U-Pb isotopic study of the layered intrusions of the northern Pechenga area, Kola peninsula. In: IGCP project 336 symposium in Rovaniemi, Finland, August 21–23, 1996: program and abstracts. University of Turku. Division of geology and mineralogy. Publication 33, p. 49.

Belkov, I. V. 1963. Kianitovye slantsy svity Keiv. Moskva: Izdatelstvo Akademii Nauk SSSR. 320 p.

Betton, P. J. 1979. Isotopic evidence for crustal contamination in the Karroo rhyolites of Swaziland. Earth and Planetary Science Letters 45, 263–274.

Bezmen, N. I., Brugmann, G. E. & Naldrett, A. D. 1991. Mekhanizm kontsentratsii elementov platinovoi gruppy: raspredelenie mezhdu silikatnym i sulfidnym rasplavami. Geologiya Rudnykh Mestorozhdenii 5, 46–54.

Bhattacharji, S. & Smith, C. H. 1964. Flowage differentiation. Science 145 (3698), 150–153.

Bibikova, E, B. & Krylov, I. N. 1983. Izotopnyi vozrast kislykh vulkanitov Karelii. Doklady Akademii Nauk SSSR 268 (5), 1231–1234.

Bibikova, E. V., Vilyams, I. & Kompston, U. 1989. Geokhronologischeskoe issledovanie aktsessornykh tsirkonov iz drevneishikh porod SSSR na ionnom mikrozonde. Geokhimiya 5, 691–701.

Bichan, R. 1969. Origin of chromite seams in the Hartley Complex of the Great Dyke, Rhodesia. In: Wilson, H. D. B. (ed.) Magmatic ore deposits, a symposium. Economic Geology Monograph 4, 95–113.

Biggar, G. M. 1974. Phase equilibrium studies of the chilled margins of some layered intrusions. Contributions to Mineralogy and Petrology 46, 159–167.

Bird, D. K., Brooks, C. K., Gannicott, R. A. & Turner, P. A. 1991. A gold-bearing horizon in the Skaergaard intrusion, East Greenland. Economic Geology 86, 1083–1092.

Blake, D. H., Elwell, R. W. D., Gibson, I. L., Skelhorn, R. R. & Walker, G. P. L. 1965. Some relationships resulting from the intimate association of acid and basic magmas. Quaternary Journal of the Geological Society of London 121, 31–49.

Bogatikov, O. A. 1979. Anortozity. Moskva: Nauka. 231 p.

Boudreau, A. E. 1988. Investigations of the Stillwater Complex. IV. The role of volatiles in the petrogenesis of the J-M Reef, Minneapolis adit section. The Canadian Mineralogist 26, 193–208.

Boudreau, A. E. 1993. Chlorine as an exploration guide for the platinum-group elements in layered intrusions. Journal of Geochemical Exploration 48, 21–37.

Boudreau, A. E., Mathez, E. A. & McCallum, I. S. 1986. Halogen geochemistry of the Stillwater and Bushveld Complexes: evidence for transport of the platinum-group elements by Cl-rich fluids. Journal of Petrology 27, 967–986.

Boudreau, A. E. & McCallum, I. S. 1986. Investigations of the Stillwater Complex: III. The Picket Pin Pt/Pd deposit. Economic Geology 81, 1953–1975.

Boudreau, A. E. & McCallum, I. S. 1988. Degassing of large layered intrusions: A model for the apatite compositional trends in the Stillwater Complex, Montana. EOS 69 (44), 1469.

Bow, C. S., Turner, A. R., Barnes, S. J., Boudreau, A. & Wolfgram, D. 1981. The geology and petrogenesis of the Minneapolis platinum-group mineral deposit, Stillwater County, Montana, U.S.A. Third International Platinum Symposium. Geocongress '81, Pretoria, South Africa. Abstracts of papers, 6–7.

Bow, C., Wolfgram, D., Turner, A., Barnes, S., Evans, J., Zdepski, M. & Boudreau, A. 1982. Investigations of the Howland Reef of the Stillwater Complex, Minneapolis adit area: stratigraphy, structure, and mineralization. Economic Geology 77, 1481–1492.

Bowen, N. L. 1920. Deformation of crystallizing magma. The Journal of Geology 28, 265–267.

Bowen, N. L. 1928. The evolution of the igneous rocks. Princeton: Princeton University Press. 332 p.

Bowen, N. L. & Tuttle, O. F. 1949. The system MgO-SiO_2-H_2O. Geological Society of America Bulletin 60, 439–460.

Boyd, F. R., England, J. L. & Davis, B. T. C. 1964. Effects of pressure on the melting and polymorphism of enstatite, $MgSiO_3$. Journal of Geophysical Research 69, 2101–2109.

Boyd, R., McDade, J. M., Millard, H. T. & Page, N. J. 1987. Platinum metal geochemistry of the Bruvann nickel-copper deposit, Råna, North Norway. Norsk Geologisk Tidsskrift 67, 205–213.

Boyle, R. W. 1976. Mineralization processes in Archean greenstone and sedimentary belts. Geological Survey of Canada Paper 75–15. 45 p.

Boyle, R. W. 1979. The geochemistry of gold and its deposits. Geological Survey of Canada Bulletin 280. 584 p.

Brandeis, G. & Jaupart, C. 1986. On the interaction between convection and crystallization in cooling magma chambers. Earth and Planetary Science Letters 77, 345–361.

Bridgewater, D., Collerson, K.D. & Myers, J.S. 1978. The development of the Archaean Gneiss Complex of North Atlantic region. In: Tarling, D. H. (ed.) Evolution of the Earth's crust. London: Academic Press, 19–69.

Brügmann, G. E., Naldrett, A. J. & Duke, J. M. 1990. The platinum-group element distribution in the Dumont Sill, Quebec. Implications for the formation of Ni-sulfide mineralization. Mineralogy and Petrology 42, 97–119.

Buchanan, D. L. & Rouse, J. E. 1984. Role of contamination in the precipitation of sulphides in the Platreef of the Bushveld Complex. In: Buchanan, D. L. & Jones, M. J. (eds.) Sulphide deposits in mafic and ultramafic rocks. London: Institution of Mining and Metallurgy, 141–146.

Bunch T. E. & Keil, K. 1971. Contributions to mineral chemistry of Hawaiian rocks. I. Gabbroid pegmatoid dike segregations in the Waianae Range, Oahu, Hawaii. Contributions to Mineralogy and Petrology 31, 267–274.

Burnham, C. W. 1967. Hydrothermal fluids at the magmatic stage. In: Barnes, H. L. (ed.) Geochemistry of hydrothermal ore deposits. New York: Holt, Rinehart and Winston, Inc. 670 p.

Burnham, C. W. & Davis, N. F. 1971. The role of H_2O silicate melts I. P-V-T relations in the system $NaAlSi_3O_8$-H_2O to 10 kilobars and 1000°C. American Journal of Science 270, 54–79.

Butcher, A. R. 1985. Channelled metasomatism in Rhum layered cumulates – evidence from late-stage veins. Geological Magazine 122 (5), 503–518.

Byers, C. D., Christie, D. M., Muenow, D. W. & Sinton, J. M. 1984. Volatile contents and ferric-ferrous ratios of basalt, ferrobasalt, andesite and rhyodacite glasses from the Galapagos 95.5°W propagating rift. Geochimica et Cosmochimica Acta 48, 2239–2245.

Byers, C. D., Garcia, M. O. & Muenow, D. W. 1986. Volatiles in basaltic glasses from the East Pacific Rise at 21°N: implications for MORB sources and submarine lava flow morphology. Earth and Planetary Science Letters 79, 9–20.

Cajander, A. K. 1913. Studien über die Moore Finnlands. Acta Forestalia Fennica 2, 1–208.

Cameron, E. N. 1961. Origin of certain magnetite-bearing bodies in the eastern part of the Bushveld Complex. Economic Geology 56, p. 1495.

Cameron, E. N. 1969. Postcumulus changes in the Eastern Bushveld Complex. American Mineralogist 54, 754–779.

Cameron, E. N. 1970. Compositions of certain coexisting phases in the eastern part of the Bushveld Complex. In: Visser, D. J. L. & von Gruenevaldt, G. (eds.) Symposium on the Bushveld Igneous Complex and other layered intrusions. The Geological Society of South Africa, Special Publication 1, 46–58.

Cameron, E. N. 1978. The Lower Zone of the Eastern Bushveld Complex in the Olifants River Trough. Journal of Petrology 19, 437–462.

Cameron, E. N. 1980. Evolution of the Lower Critical Zone, Central sector, Eastern Bushveld Complex, and its chromite deposits. Economic Geology 75, 845–871.

Cameron, E. N. 1982. The upper critical zone of the eastern Bushveld Complex – precursor of the Merensky Reef. Economic Geology 77, 1307–1327.

Cameron, E. N. & Desborough, G. A. 1964. Origin of certain magnetite-bearing pegmatites in the Eastern part of the Bushveld Complex, South Africa. Economic Geology 59, 197–225.

Cameron, E. N. & Desborough, G. A. 1969. Occurrence and characteristics of chromite deposits – Eastern Bushveld Complex. In: Wilson, H. D. B. (ed.) Magmatic ore deposits, a symposium. Economic Geology Monograph 4, 23–40.

Cameron, E. N. & Emerson, M. E. 1959. The origin of certain chromite deposits of the eastern part of the Bushveld Complex. Economic Geology 54, 1151–1213.

Cameron, E. N. & Glover, E. D. 1973. Unusual titanian-chromian spinels from the Eastern Bushveld Complex. American Mineralogist 58, 172–188.

Cameron, W. E. 1985. Petrology and origin of primitive lavas from the Troodos ophiolite, Cyprus. Contributions to Mineralogy and Petrology 89, 239–

255.

Campbell, I. H. 1978. Some problems with the cumulus theory. Lithos 11, 311–323.

Campbell, I. H., Naldrett, A. J. & Roeder, P. L. 1979. Nickel activity in silicate liquids: some preliminary results. The Canadian Mineralogist 17, 495–505.

Campbell, I. H. & Turner, J. S. 1987. A laboratory investigation of assimilation at the top of a basaltic magma chamber. The Journal of Geology 95, 155–172.

Capobianco, C. J. & Drake, M. J. 1990. Partitioning of ruthenium, rhodium, and palladium between spinel and silicate melt and implications for platinum group element fractionation trends. Geochimica et Cosmochimica Acta 54, 869–874.

Carlson, R. W., Lugmair, G. W. & MacDougall, J. D. 1981. Columbia River volcanism: the question of mantle heterogeneity or crustal contamination. Geochimica et Cosmochimica Acta 45, 2483–3499.

Carmichael, I. S. E. & Nicholls, J. 1967. Iron-titanium oxides and oxygen fugacities in volcanic rocks. Journal of Geophysical Research 72, 4665–4687.

Carr, M. H. & Turekian, K. K. 1962. Chromium in granitic rocks. Geochimica et Cosmochimica Acta 26, 411–415.

Carroll, M. R. & Webster, J. D. 1994. Solubilities of sulfur, noble gases, nitrogen, chlorine, and fluorine in magmas. In: Carroll, M. R. & Holloway, J. R. (eds.) Volatiles in magmas, ch. 7. Washington, D.C.: Mineralogical Society of America, 231–279.

Cawthorn, R. G. 1994. Formation of chlor- and fluorapatite in layered intrusions. Mineralogical Magazine 58, 299–306.

Cawthorn, R. G. 1995a. A re-evaluation of magma compositions and processes in the upper Critical Zone of the Bushveld Complex. University of Witwatersrand Johannesburg, Economic Geology Research Unit, Information Circular 286, 22 p.

Cawthorn, R. G. 1995b. Incompatible trace-element abundances in plagioclase and pyroxenes in the Merensky Reef of the Bushveld Complex – evidence for metasomatism? University of Witwatersrand Johannesburg, Economic Geology Research Unit, Information Circular 287. 15 p.

Cawthorn, R. G. 1996. Re-evaluation of magma compositions and processes in the uppermost Critical Zone of the Bushveld Complex. Mineralogical Magazine 60, 131–148.

Chaumba, J. B. & Wilson, A. H. 1997. Au oxygen isotope study of the Lower Mafic Succession of the Darwendale Subchamber of the Great Dyke, Zimbabwe. Chemical Geology 135, 293–305.

Chelishchev, N. F. 1963. O pegmatoidnykh i zhilnykh gidrotermalnykh obrazovaniakh pervouralskogo mestorozhdeniya titanomagnetitov. Trudy IMGRE 16, 180–180.

Chen, C. F. & Turner, J. S. 1980. Crystallization in a double-diffusive system. Journal of Geophysical Research 85, 2573–2593.

Chorlton, L. B. & Martin, R. F. 1978. The effect of boron on the granite solidus. The Canadian Mineralogist 16, 239–244.

Coertze, F. J. 1974. The geology of the basic portion of the western Bushveld Igneous Complex. Geological Survey of South Africa, Memoir 66, 148 p.

Coertze, F. J., Burger, A. J., Walraven, F., Marlow, A. G. & MacCaskie, D. R. 1978. Field relations and age determination in the Bushveld Complex. Transactions of the Geological Society of South Africa 81 (1), 1–11.

Coish, R. A. & Church, W. R. 1979. Igneous geochemistry of mafic rocks in the Betts Cove ophiolite, Newfoundland. Contributions to Mineralogy and Petrology 70, 29–39.

Collerson, F. D., Jessau, C. W. & Bridgewater, D. 1976. Contrasting types of bladed olivine in ultramafic rocks from the Archean of Labrador. Canadian Journal of Earth Sciences 13, 442–450.

Compston, W., McDougall, I. & Heier, K. S. 1968. Geochemical composition of the Mesozoic basaltic rocks of Antarctica, South Africa, South America and Tasmania. Geochimica et Cosmochimica Acta 32, 129–149.

Condie, K. C. 1976. Trace-element geochemistry of Archean greenstone belts. Earth Science Reviews 12, 393–417.

Condie, K. C. & Crow, C. 1990. Early Precambrian within-plate basalts from the Kapvaal Craton in southern Africa: A case for crustally contaminated komatiites. The Journal of Geology 98 (1), 100–107.

Condie, K. C., Macke, J. E. & Reimer, T. O. 1970. Petrology and geochemistry of early Precambrian graywackes from the Fig Tree Group, South Africa. Geological Society of America Bulletin 81, 2759–2776.

Couturié, J.-P. 1973. Un nouveau gisement de granite orbiculaire dans le Massif Central français: le granite du Signal de Randon (Lozère). Contributions to Mineralogy and Petrology 42, 305–312.

Coveney, R. M., Jr., Murowchick, J. B., Grauch, R. I., Chen Nansheng & Glascock, M. D. 1992. Field relations, origins and resource implications for platiniferous molybdenum-nickel ores in black shales of South China. Exploration and Mining Geology 1 (1), 21–28.

Cowden, A., Ruddock, R., Reay, A., Nicolson, P., Waterman, P. & Banks, M. J. 1990. Platinum mineralisation potential of the Longwood Igneous Complex, New Zealand. Mineralogy and Petrology 42, 181–195.

Cox, K. G. 1985. Crystal setting is a major differentiation process. Terra cognita 5, 210–211.

Cox, K. G. & Mitchell, C. 1988. Importance of crystal settling in the differentiation of Deccan Trap basaltic magmas. Nature 333, 447–449.

Crawford, A. J., Falloon, T. J. & Green, D. H. 1989. Geochemistry and petrogeneis of Archaean and early Proterozoic siliceous high-magnesian basalts. In: Crawford, A. J. (ed.) Boninites. London: Unwin Hyman, 1–49.

Crocket, J. H., Fleet, M. E. & Stone, W. E. 1992. Experimental partitioning of osmium, iridium and gold between basalt melt and sulphide liquid at 1300°C. Australian Journal of Earth Sciences 39, 427–432.

Daly, R. A. 1914. Igneous rocks and their origin. New York: McGraw-Hill Book Company, Inc. 563 p.

Danchin, R. V. 1967. Chromium and nickel in the Fig Tree Shale from South Africa. Science 158, 261–262.

Dane, E. B., Jr. 1941. Densities of molten rocks and minerals. American Journal of Science 239, 809–818.

Davies, J. F. 1958. Chromite deposits of southeastern Manitoba. Canadian Mining Journal 79 (4), 112–114.

Davies, R. D., Allsopp, H. L., Erlank, A. J. & Mantun, W. I. 1970. Sr-isotopic studies on various layered mafic intrusions in southern Africa. In: Visser, D. J. L. & von Gruenewaldt, G. (eds.) Symposium on the Bushveld Igneous Complex and other layered intrusions. Geological Society of South Africa, Special Publication 1, 576–593.

Davis, B. T. C. 1968. Anorthositic and quartz syenitic series of the St. Regis Quadrangle, New York. In: Isachsen, Y. W. (ed.) Origin of anorthosites and related rocks. New York State Museum and Science Service, Memoir 18, 281–287.

De, A. 1974. Silicate liquid immiscibility in the Deccan Traps and its petrogenetic significance. Geological Society of America Bulletin 85, 471–474.

Delbov, F., Lebedev, E. B. & Malinin, S. D. 1986. Povedenie iona khlora i kationnyi obmen v sisteme magmaticheskii rasplav-flyuid. Geokhimiya 11, 1550–1558.

DePaolo, D. J. 1985. Isotopic studies of processes in mafic magma chambers: I. The Kiglapait intrusion, Labrador. Journal of Petrology 26, 925–951.

De Waard, D. 1968. Annotated bibliography of anorthosite petrogenesis. In: Isachsen, Y. W. (ed.) Origin of anorthosite and related rocks. New York State Museum and Science Service, Memoir 18, 1–11.

Dick, L. A. & Robinson, G. W. 1979. Chlorine-bearing hastingsite from a sphalerite skarn in southern Yukon. The Canadian Mineralogist 17, 25–26.

Dickin, A. P. 1981. Isotope geochemistry of tertiary igneous rocks from the Isle of Skye, N.W. Scotland. Journal of Petrology 22, 155–189.

Dillon-Leitch, H. C. H., Watkinson, D. H. & Coats, C. J. A. 1986. Distribution of platinum-group elements in the Donaldson West deposit, Cape Smith Belt, Quebec. Economic Geology 81, 1147–1158.

Distler, V. V., Grokhovskaya, T. L., Evstigneeva, T. L., Sluzhenikin, S. F., Filimonova, A. A., Dyuzhikov, O. A. & Laputina, I. P. 1988. Petrologiya sulfidnogo magmaticheskogo rudoobrazovaniya. Moskva: Nauka. 232 p.

Distler, V. V., Kryachko, V. V. & Laputina, I. P. 1986. Evolyutsiya paragenezisov platinovykh metallov v alpinotipnykh giperbazitakh. Geologiya Rudnykh Mestorozhdenii 5, 16–32.

Distler, V. V. & Laputina, I. P. 1981. Neobychnaya assotsiatsiya mineralov platinovykh metallov iz rassloennogo gabbro-norit-lertsolitovogo massiva na Kolskom poluostrove. Izvestiya Akademii Nauk SSSR, Ser. Geol. 2, 103–115.

Distler, V. V. & Stepin, A. G. 1993. Malosulfidnyi platinonosnyi gorizont Ioko-Dovyrenskogo rassloennogo giperbazit-bazitovogo intruziva (Severnoe Pribaikale). Doklady Akademii Nauk 328 (4), 498–501.

Dokuchaeva, V. S., Zhangurov, A. A. & Fedotov, Zh. A. 1982a. Imandrovskii lopolit – novyi krupnyi rassloennyi intruziv na Kolskom poluostrove. Doklady Akademii Nauk SSSR 275 (5), 1231–1234.

Dokuchaeva, V. S., Zhangurov, A. A., Radchenko, M. K. & Fedotov, Zh. A. 1982b. Rannekarelskie bazit-giberbazitovye intruzivnye obrazovaniya. In: Gorbunov, G. I. (ed.) Imandra-Varzugskaya zona Karelid (geologiya, geohkimiya, istoriya razvitiya). Leningrad: Nauka, 114–144.

Dokuchaeva, V. S., Zhangurov, A. A., Fedotov, Zh. A. & Sholokhnev, V. V. 1992. Geologiya i rudonosnost Imandrovskogo intruziva. Otechestvennaya Geologiya 10, 60–67.

Dolgov, Yu. A. 1963. Termodinamicheskie osobennosti genezisa kamernykh pegmatitov. Materialy po. geneticheskoi i eksperimentalnoi mineralogii 15 (1), 113–165.

Donaldsson, C. H. 1975. Ultramafic inclusions in anorthite megacrysts from the Isle of Skye. Earth and Planetary Science Letters 27, 251–256.

Duke, J. M. 1976. Distribution of the period four transition elements among olivine, calcic clinopyroxene and mafic silicate liquid: experimental results. Journal of Petrology 17, 499–521.

Duke, J. M. 1990. Mineral deposit models: nickel sulfide deposits of the Kambalda – type. The Canadian Mineralogist 28, 379–388.

Duncan, A. R. 1987. The Karoo igneous province – a problem area for inferring tectonic setting from ba-

salt geochemistry. Journal of Volcanology and Geothermal Research 32 (1–3), 13–34.

Dungan, M. A., Powell, B. N. & Weiblen, P. W. 1975. Petrology of some Apollo 16 felspathic basalts: KREEP melt rocks? Lunar Science VI, part I, Abstracts, 223–225.

Dungan, M. A. & Rhodes, J. M 1978. Residual glasses and melt inclusions in basalts from DSDP Legs 45 and 46: evidence for magma mixing. Contributions to Mineralogy and Petrology 67, 417–431.

Dyuzhikov, O. A., Distler, V. V., Strunin, B. M. Mkrtychyan, A. K., Sherman, M. L., Sluzhenikin, S. F. & Lure, A. M. 1988. Geologiya i rudonosnost Norilskogo raiona. Moskva: Nauka. 280 p.

Eales, H. V. 1959. The Khale dolerite sheet. Transactions of the Geological Society of South Africa 52, 81–109.

Eales, H. V. 1979. Anomalous Karroo spinels along the chromite-titanomagnetite join. South African Journal of Science 75, 24–29.

Eales, H. V. 1980. Contrasted trace-element variations in two Karroo cumulus complexes. Chemical Geology 29, 39–48.

Eales, H. V., Botha, W. J., Hattingh, P. J., de Klerk, W. J., Maier, W. D. & Odgers, A. T. R. 1993. The mafic rocks of the Bushveld Complex: a review of emplacement and crystallization history, and mineralization, in the light of recent data. Journal of African Earth Science 16 (1/2), 121–142.

Eales, H. V., de Klerk, W. J. & Butcher, A. R. 1990. The cyclic units beneath the UG1 chromitite (UG1FW-unit) at RPM Union Section Platinum Mine – Rosetta Stone of the Bushveld Upper Critical Zone. Mineralogical Magazine 54, 23–43.

Eales, H. V., Marsh, J. S., Mitchell, A. A., de Klerk, W. J., Kruger, F. J. & Field, M. 1986. Some geochemical constraints upon models for the crystallization of the upper critical zone – main zone interval, northwestern Bushveld Complex. Mineralogical Magazine 50, 567–582.

Eales, H. V. & Snowden, D. V. 1979. Chromiferous spinels of the Elephant's Head dike. Mineralium Deposita 14, 227–242.

Edwards, A. B. 1936. On the occurrence of almandine garnets in some Devonian rocks of Victoria. Proceedings of the Royal Society of Victoria 49 (1), 40–50.

Eichelberger, J. C. & Gooley, R. 1977. Evolution of silicic magma chambers and their relationship to basaltic volcanism. Geophysical Monograph (Washington) 20, 57–77.

Ein, A. S. 1984. Daiki bazitov Severo-Zapadnoi Karelii. In: Bogachev, A. I. (ed.) Intruzivnye bazity i giperbazity Karelii. Karelskii filial Akademii Nauk SSSR, Institut geologii, 30–41.

El Goresy, A. & Woermann, E. 1977. Opaque minerals as sensitive oxygen barometers and geothermometers in lunar basalts. In: Fraser, D. G. (ed.) Thermodynamics in geology. Dordrecht: D. Reidel Publishing Company, 249–277.

Elliott, W. C., Grandstaff, D. E., Ulmer, G. C. & Buntin, T. 1982. An intrinsic oxygen fugacity study of platinum-carbon associations in layered intrusions. Economic Geology 77, 1493–1510.

Elliott, W. C., Ulmer, G. C., Grandstaff, D. E. & Gold, D. P. 1981. A graphite-platinum association in layered intrusives? EOS 62, 421.

Elo, S. 1979. Penikan gabron oletetun syöttökanavan poikki mitattujen geofysikaalisten profiilien tarkastelu. Letter September 17, 1979.

Emmons, R. C. 1940. The contribution of differential pressure to magmatic differentiation. American Journal of Science 238, 1–21.

Ermakov, N. P. 1972. Geokhimicheskie sistemy vklyuchenii v mineralakh. Moskva: Nedra. 374 p.

Eugster, H. P. 1957. Stability of annite. Carnegie Institution of Washington, Year Book 56, 161–164.

Evans, B. W. 1964. Fractionation of elements in the pelitic hornfelses of the Cashel – Lough Wheelaun intrusion, Connemara, Eire. Geochimica et Cosmochimica Acta 28, 127–156.

Evans, B. W. & Moore, J. S. 1968. Mineralogy as a function of depth in the prehistoric Makaopuhi tholeiitic lava lake, Hawaii. Contributions to Mineralogy and Petrology 17, 85–115.

Evans, B. W. & Wright, T. L. 1972. Composition of liquidus chromite from the 1959 (Kilauea Iki) and 1965 (Makaopuhi) eruptions of Kilauea Volcano, Hawaii. American Mineralogist 57, 217–230.

Faggart, B. E., Jr., Basu, A. R. & Tatsumoto, M. 1985. Origin of the Sudbury Complex by meteorite impact: neodymium isotopic evidence. Science 230 (4724), 436–439.

Fan Delian, Yang Ruiying & Huang Zhongxiang 1985. The Lower Cambrian black shale series and the iridium anomaly in south China. In: Developments in Geoscience (Academia Sinica) Contribution to 27th International Geological Congress, 1984 Moscow. Beijing: Science Press, 215–224.

Feigin, Ya. M. 1971. O petrologicheskom znachenii ymensheniya obema magmaticheskikh rasplavov stratifitsirovannykh intruzii. In: Tugarinov, A. I. (ed.) Geokhimiya, petrologiya i mineralogiya shchelochnykh porod. Moskva: Nauka, 120–128.

Fenner, C. N. 1926. The Katmai magmatic province. The Journal of Geology 34, 673–772.

Fenner, C. N. 1937. A view of magmatic differentiation. The Journal of Geology 45, 158–168.

Fenogenov, A. N. & Emelyanenko, P. F. 1980. Pervichnye vklyucheniya v olivinakh rassloennykh bazit-giperbazitovykh trappovykh intruzivov severo-zapada Sibirskoi platformy. Doklady Akademii Nauk

SSSR 225 (6), 1467–1470.

Feoktistov, G. D. 1976. Trappovye silly bolshoi protyazhennosti na yuge Sibirskoi platformy. Sovetskaya Geologiya 12, 122–127.

Ferguson, J. 1969. Compositional variation in minerals from mafic rocks of the Bushveld Complex. Transactions of the Geological Society of South Africa 72 (III), 61–78.

Ferguson, J. & Botha, E. 1963. Some aspects of igneous layering in the basic zones of the Bushveld Complex. Transactions of the Geological Society of South Africa 66, 259–282.

Ferguson, J. & McCarthy, T. S. 1970. Origin of an ultramafic pegmatoid in the eastern part of the Bushveld Complex. In: Visser, D.J.L. & von Gruenewaldt, G. (eds.) Symposium of the Bushveld Igneous Complex and other layered intrusion. Geological Society of South Africa, Special Publication 1, 74–79.

Ferguson, J. & Wright, I. H. 1970. Compositional variation of plagioclases in the Critical Series, Bushveld Complex. In: Visser, D.J.L. & von Gruenewaldt, G. (eds.) Symposium of the Bushveld Igneous Complex and other layered intrusions. Geological Society of South Africa, Special Publication 1, 59–66.

Firsova, S. O. 1980. Grossulyaro-almandinovye granaty (redkii izomorfnyi ryad). Zapiski vsesoyuznogo mineralogicheskogo obshchestva 109 (2), 235–243.

Fleitout, L. & Froidevaux, C. 1980. Thermal and mechanical evolution of shear zones. Journal of Structural Geology 2, 159–164.

Fletcher, T. A. 1988. Nickel-copper and precious metal mineralisation in the Caledonian mafic and ultramafic intrusions of North-East Scotland. In: Prichard, H. M., Potts, P. J., Bowles, J.F. W. & Cribb, S. J. (eds.) Geo-Platinum 87. London and New York: Elsevier Applied Science, 163–164.

Fominykh, V. G. & Khostova, V. P. 1971. Osobennosti raspredeleniya metallov gruppy platiny v porodoobrazuyushchikh mineralakh Gusevogorskogo mestorozhdeniya. Doklady Akademii Nauk SSSR 200, 443–445.

Fountain, J. C., Hodge, D. S. & Hills, F. A. 1981. Geochemistry and petrogenesis of the Laramie anorthosite complex, Wyoming. Lithos 14, 113–132.

Francis, D. 1994. Chemical interaction between picritic magmas and upper crust along the margins of the Muskox intrusion, Northwest Territories. Geological Survey of Canada Paper 92–12. 94 p.

Freestone, I. C. 1978. Compositional dependence of liquid immiscibility. In: MacKenzie, W. S. (ed.) Progress in Experimental Petrology, 4th Report. NERC London, 7–10.

Friend, C. R. L. 1976. Field relationships and petrology of leucocratic schists from the Ravns Storø group near Fiskenæsset. Grønlands Geologiske undersøgelse Rapport 73, 81–85.

Frisch, T., Jackson, G. D., Glebovitsky, V. A., Yefimov, M. M., Bogdanova, M. N. & Parrish, R. R. 1995. U-Pb ages of zircon from the Kolvitsa gabbro-anorthosite complex, southern Kola Peninsula, Russia. Petrology 3 (3), 219–225.

Fröhlich, F. 1960. Beitrag zur Geochemie des Chroms. Geochimica et Cosmochimica Acta 20, 215–240.

Fryer, B. J., Kerrich, R., Hutchinson, R. W., Peirce, M. G. & Rogers, D. S. 1979. Archaean precious-metal hydrothermal systems, Dome Mine, Abitibi Greenstone Belt. I. Patterns of alteration and metal distribution. Canadian Journal of Earth Sciences 16, 421–439.

Furlong, K. P. & Myers, J. D. 1985. Thermal-mechanical modelling of the role of thermal stresses and stoping in magma contamination. In: Baker, B. H. & McBirney, A. R. (eds.) Processes in magma chambers. Journal of Volcanology and Geothermal Research 24, 179–191.

Furman, T. & Spera, F. J. 1985. Co-mingling of acid and basic magma with implications for the origin of mafic I-type xenoliths: field and petrochemical relations of an unusual dike complex at Eagle Lake, Sequoia National Park, California, U.S.A. In: Baker, B. H. & McBirney, A. R. (eds.) Processes in magma chambers. Journal of Volcanology and Geothermal Research 24, 151–178.

Gamble, J. A. 1979. The geochemistry and petrogenesis of dolerites and gabbros from the Tertiary Central Volcanic Complex of Slieve Gullion, North East Ireland. Contributions to Mineralogy and Petrology 69, 5–19.

Gelman, M. L. 1980. Granat v izverzhennykh porodakh (na primere Severo-Vostoka SSSR). Izvestiya Akademii Nauk SSSR, Ser. Geol. 8, 35–49.

Genkin, A. D., Distler, V. V. & Laputina, I. P. 1979. Khromitovaya mineralizatsiya differentsirovannykh trappovykh intruzii i usloviya ee obrazovaniya. In: Smirnov, V. I. (ed.) Usloviya obrazovaniya magmaticheskikh rudnykh mestorozhdenii. Moskva: Nauka, 105–126.

Ghiorso, M. S. & Carmichael, I. S. E. 1985. Chemical mass transfer in magmatic processes V. Applications in equilibrium crystallization, fractionation and assimilation. Contributions to Mineralogy and Petrology 90, 121–141.

Ghisler, M. 1976. The geology, mineralogy and geochemistry of the pre-orogenic Archaean stratiform chromite deposits at Fiskenaesset, West Greenland. Monograph Series on Mineral Deposits 14. 156 p.

Gibbs, A. K., Montgomery, C. W., O'Day, P. A. &

Erslev, E. A. 1986. The Archean – Proterozoic transition: Evidence from the geochemistry of metasedimentary rocks of Guyana and Montana. Geochimica et Cosmochimica Acta 50, 2125–2141.

Gibson, I. L. & Walker, G. P. L. 1964. Some composite rhyolite/basalt lavas and related composite dykes in eastern Iceland. Proceedings of the Geological Association, London 74 (3), 301–318.

Gilyarova, M. A. 1974. Stratigrafiya, struktury i magmatizm dokembriya vostochnoi chasti Baltiiskogo shchita. Leningrad: Nedra. 222 p.

Girnis, A. V., Ryabchikov, I. D., Saddebi, P., Kulikov, V. S. & Kulikova, V. V. 1990. Evolyutsiya dokembriiskoi mantin: interpretatsiya rezultatov izotopnogo Sm-Nd analiza komatiitov Vostochnoi Karelii. Geokhimiya 10, 1391–1399.

Glazunov, O. M. 1979. Kontaminatsiya i rudonosnost gabbroidnoi magmy v geokhimicheskom aspekte. In: Kontaktovye protsessy i orudenenie v gabbro-peridotitovykh intruziyakh. Moskva: Nauka, 108–124.

Glazunov, O. M., Afonin, V. P., Perfileva, L. A. & Frolova, A. P. 1973. Pervichnaya forma kontsentratsii K i Na v giperbazitakh. Geokhimiya 4, 622–625.

Glikson, A. Y. 1996. Mega-impacts and mantle-melting episodes: tests of possible correlations. AGSO Journal of Australian Geology and Geophysics 16 (4), 587–607.

Godlevskii, M. N. 1968. Magmaticheskie mestorozhdeniya. In: Smirnov, V. I. (ed.) Genezis endogennykh rudnykh mestorozhdenii. Moskva: Nedra, 7–83.

Golovenok, V. K. 1977. Vysokoglinozemistye formatsii dokembriya. Leningrad: Nedra. 268 p.

Golubev, A. I. & Filippov, N. B. 1995. Blagorodnometalnoe orudenenie titanomagnetitovykh mestorozhdenii Karelii. In: Rybakov, S. I. & Golubev, A. I. (eds.) Tezisy dokladov regionalnogo simpoziuma "Blagorodnye metally i almazy Severa Evropeiskoi chasti Rossii" i nauchno-prakticheskoi konferentsii "Problemy razvitiya mineralno-syrevoi bazy platinovykh metallov Rossii", 23–26.

Goodrich, C. A. & Bird, J. M. 1985. Formation of iron-carbon alloys in basaltic magma at Uivfaq, Disko Island: the role of carbon in mafic magmas. The Journal of Geology 93 (4), 475–492.

Goodwin, A. M. 1977. Archean basin-craton complexes and the growth of Precambrian shields. Canadian Journal of Earth Sciences 14, 2737–2759.

Gorbachev, N. S. 1989. Flyuidno-magmaticheskoe vzaimodeisvie v sulfidno-silikatnykh sistemakh. Moskva: Nauka. 127 p.

Gorbachev, N. S., Laitfut, P., Dokherti, V. & Naldrett, A. 1994a. Pervyie dannyie po eksperimentalnomu modelirovaniyu redkozemelnykh elementov i ittriya. Doklady Akademii Nauk 335 (1), 81–83.

Gorbachev, N. S., Naldrett, A., Brugmann, G., Khodorevskaya, L. I & Azif, M. 1994b. Eksperimentalnoe izuchenie raspredeleniya platinoidov i zolota mezhdu vodno-khloridnym flyudnom i bazaltovym rasplavom pri T = 1100–1350°C, P = 5 kbar. Doklady Akademii Nauk 335 (3), 356–358.

Gorbik, N. A. 1976. Bazitovye i ultrabazitovye kompleksy Gaikolskoi sinklinali. In: Intruzivnye bazit-ultrabazitovye kompleksy dokembriya Karelii. Trudy Institut geologii, Karelskii filial Akademii Nauk SSSR 32, 48–57.

Gordon, S. G. 1921. Desilicated granitic pegmatites. Proceedings of the Academy of natural sciences of Philadelphia 73, 169–172.

Gorman, B. E., Pearce, T. H. & Birkett, T. C. 1978. On the structure of Archean greenstone belts. Precambrian Research 6, 23–41.

Green, T. H. & Pearson, N. J. 1986. Ti-rich accessory phase saturation in hydrous mafic-felsic compositions at high P, T. Chemical Geology 54, 185–201.

Greenland, L. P. & Aruscavage, P. 1980. Volcanic emission of Se, Te, and As from Kilauea volcano, Hawaii. Journal of Volcanology and Geothermal Research 27, 195–201.

Gribble, C. D. & O'Hara, M. J. 1967. Interaction of basic magma with pelitic materials. Nature 24, 1198–1201.

Grinenko, L. N. 1967. Izotopnyi sostav sery sulfidov nekotorykh medno-nikelevykh mestorozhdenii i rudoproyavlenii Sibirskoi platformy. In: Urvantsev, N. N. (ed.) Petrologiya trappov Sibirskoi platformy. Leningrad: Nedra, 221–229.

Groeneveld, D. 1970. The structural features and the petrography of the Bushveld Complex in the vicinity of Stoffberg, Eastern Transvaal. In: Visser, D. J. L. & von Gruenewaldt, G. (eds.) Symposium on the Bushveld Igneous Complex and other layered intrusions. Geological Society of South Africa, Special Publication 1, 36–45.

Grokhovskaya, T. L., Distler, V. V., Klyunin, S. F., Zakharov, A. A. & Laputina, I. P. 1992. Malosulfidnaya platinovaya mineralizatsiya massiva Lukkulaisvaara (Severnaya Kareliya). Geologiya rudnykh mestorozhdenii 2, 32–50.

Grokhovskaja, T. L., Distler, V. V., Zakharov, A. A., Klyunin, S. F. & Laputina, I. P. 1989. Assotsiatsii mineralov platinovykh metallov v rassloennom intruzive Lukkulaisvaara, Severnaya Kareliya. Doklady Akademii Nauk SSSR 306 (2), 430–434.

Grokhovskaja, T. L., Laputina, I. P., Kuznetsov, G. S., Muravitskaya, G. N., Sokolov, S. V., Telnov, V. A. & Bolshakov, A. N. 1996. Platino-medno-nikelevoe orudenenie rassloennogo intruziva gory

Generalskoi (Pechengskii rudnyi raion, Kolskii poluostrov). Geologiya rudnykh mestorozhdenii 38 (3), 211–225.

Grove, T. L. & Bence, A. E. 1977. Experimental study of pyroxene- liquid interaction in quartz-normative basalt 15597. Proceedings of Lunar Science Conf. 8th, vol. 2. Geochimica et Cosmochimica Acta Supplement 8, 1549–1579.

GSF 1983. Kallioperäosaston toimintakertomus vuodelta 1982. Espoo. 74 p.

Gulyaeva, T. Ya., Gorelikova, N. V. & Karabtsov, S. A. 1986. High potassium-chlorine-bearing hastingsites in skarns from Primorye, Far East USSR. Mineralogical Magazine 50, 724–728.

Gunn, B. M., Coy-Yll, R., Watkins, N. D. Abranson, C. E. & Nougier, J. 1970. Geochemistry of an oceanite-ankaramite-basalt suite from East Island, Crozet Archipelago. Contributions to Mineralogy and Petrology 28, 319–339.

Gurulev, S. A. & Sambuev, K. S. 1968. Gabbroidizatsiya granitnykh pegmatitov v Chaiskom gabbroperidotitovom massive. Doklady Akademii Nauk SSSR 179 (1), 190–193.

Gustavsson, N., Noras, P., & Tanskanen, H. 1979. Seloste geokemiallisen kartoituksen tutkimusmenetelmistä. Summary: Report on geochemical mapping methods. Geological Survey of Finland, Report of Investigation 39. 20 p.

Häkli, T.A. 1971. Silicate nickel and its application to the exploration of nickel ores. Bulletin of the Geological Society of Finland 43, 247– 263.

Häkli, T. A., Hänninen, E., Vuorelainen, Y. & Papunen, H. 1976. Platinum-group minerals in the Hitura nickel deposit, Finland. Economic Geology 71, 1206–1213.

Halkoaho, T. A. A. 1994. The Sompujärvi and Ala-Penikka PGE Reefs in the Penikat Layered Intrusion, northern Finland: implications for PGE reef-forming processes. Acta Universitatis Ouluensis Series A, Scientiae Rerum Naturalium 249. 122 p.

Halkoaho, T. A. A., Alapieti, T. T. & Lahtinen, J. J. 1990. The Sompujärvi PGE Reef in the Penikat layered intrusion, northern Finland. Mineralogy and Petrology 42, 39–55.

Hall, A. L. & Nel, L.T. 1926. On an occurrence of corundum- sillimanite rock in the norite of the Bushveld Igneous Complex west of Lydenburg. Transactions of the Geological Society of South Africa 29, 1– 16.

Hamilton, J. 1977. Sr isotope and trace element studies of the Great Dyke and Bushveld Mafic Phase and their relation to early Proterozoic magma genesis in Southern Africa. Journal of Petrology 18, 24–52.

Hamlyn, P. R. & Keays, R. R. 1979. Origin of chromite compositional variation in the Panton Sill, Western Australia. Contributions to Mineralogy and Petrology 69, 75–82.

Hanski, E. J., Grinenko, L. N. & Mutanen, T. 1996. Sulfur isotopes in the Keivitsa Cu-Ni-bearing intrusion and its country rocks, northern Finland: evidence for crustal sulfur contamination. In: IGCP project 336 symposium in Rovaniemi, Finland, August 21–23, 1996: program and abstracts. University of Turku. Division of geology and mineralogy. Publication 33, 15–16.

Harmer, R. E., Auret, J. M. & Eglington, B. M. 1995. Lead isotope variations within the Bushveld Complex, Southern Africa: a reconnaissance study. Journal of African Earth Sciences 21 (4), 595–606.

Harney, D. M. W. & Merkle, R. K. W. 1990. Pt-Pd minerals from the upper zone of the eastern Bushveld Complex, South Africa. The Canadian Mineralogist 28, 619–628.

Hatton, C. J. 1989. Densities and liquidus temperatures of Bushveld parental magmas as constraints on the formation of the Merensky Reef in the Bushveld Complex, South Africa. In: Prendergast, M. D. & Jones, M. J. (eds.) Magmatic sulphides – The Zimbabwe volume. London: The Institution of Mining and Metallurgy, 87–93.

Heckroodt, R. O. 1959. The geology around the dunite pipe on Dreikop (Eastern Transvaal). Transactions of the Geological Society of South Africa 62, 59–73.

Hedlund, D. C., Moreira, J. F. de C., Pinto, A. C. F., da Silva, J. C. G. & Souza, G. V. V. 1974. Stratiform chromitite at Campo Formoso, Bahia, Brazil. Journal of research of the U.S. Geological Survey 2, 551–562.

Henderson, P. 1979. Irregularities in patterns of element partition. Mineralogical Magazine 43, 399–404.

Herd, R.K. 1973. Sapphirine and kornerupine occurrences within the Fiskenaesset complex. Grønlands geologiske Undersøgelse rapport 51, 64–71.

Hess, H. H. 1960. Stillwater Igneous Complex, Montana. A quantitative mineralogical study. Geological Society of America Memoir 80. 230 p.

Hess, P. C. & Rutherford, M. J. 1974. Elemental fractionation between immiscible melts (abstract). Lunar Science Institute, Houston. Lunar Science V, 328–330.

Hibbard, M. J. 1981. The magma mixing origin of mantled feldspars. Contributions to Mineralogy and Petrology 76, 158–170.

Hibbard, M. J. & Watters, R. J. 1985. Fracturing and diking in incompletely crystallized granitic plutons. Lithos 18, 1–12.

Hiemstra, S. A. 1979. The role of collectors in the formation of the platinum deposits in the Bushveld complex. The Canadian Mineralogist 17, 469–482.

Hills, E. S. 1936. Reverse and oscillatory zoning in plagioclase feldspars. Geological Magazine 73, 49–56.

Hiltunen, A. 1982. The Precambrian geology and skarn iron ores of the Rautuvaara, northern Finland. Geological Survey of Finland, Bulletin 318. 133 p.

Hirvas, H. & Tynni, R. 1976. Tertiääristä savea Savukoskella sekä havaintoja tertiäärisistä mikrofossiileista. Summary: Tertiary clay deposit at Savukoski, Finnish Lapland, and observations of Tertiary microfossils, preliminary report. Geologi 28 (3), 33–40.

Hoatson, D. M., Wallace, D. A., Sun, S.-S., Macias, L. F., Simpson, D. J. & Keays, R. R. 1992. Petrology and platinum-group-element geochemistry of Archaean layered mafic-ultramafic intrusions, west Pilbara Block, Western Australia. AGSO Bulletin 242. 319 p.

Hoefs, J. 1965. Ein Beitrag zur Geochemie des Kohlenstoffs in magmatischen und metamorphen Gesteinen. Geochimica et Cosmochimica Acta 29, 399–428.

Hoffer, A. 1966. Seismic control of layering in intrusives. Bulletin of Volcanology 29, 817–821.

Hoffman, R. D. 1931. Vlackfontein nickel deposits, Rustenburg area, Transvaal, South Africa. Economic Geology 26, 202–214.

Holtz, F. & Johannes, W. 1991. Effect of tourmaline on melt fraction and composition of first melts in quartzofeldspathic gneiss. European Journal of Mineralogy 3, 527–536.

Homma, F. 1932. Über das Ergebnis von Messungen an zonaren Plagioklasen aus Andesiten mit Hilfe des Universaldrehtisches. Schweizerische mineralogische und petrographische Mitteilungen 12, 345–352.

Hoover, J. D. 1989. The chilled marginal gabbro and other contact rocks of the Skaergaard intrusion. Journal of Petrology 30 (2), 441–476.

Hor, A. K., Hutt, D. K., Smith, J. V., Wakefield, J. & Windley, B. F. 1975. Petrochemistry and mineralogy of early Precambrian anorthositic rocks of the Limpopo belt, southern Africa. Lithos 8, 297–310.

Hotz, P. E. 1953. Petrology of granophyre in diabase near Dillsburg, Pennsylvania. Geological Society of America Bulletin 64, 675–704.

Hounslow, A. W. & Chao, G. Y. 1970. Monoclinic chlorapatite from Ontario. The Canadian Mineralogist 10, 252–259.

Huebner, J. S., Lipin, B. R. & Wiggins, L. B. 1976. Partitioning of chromium between silicate crystals and melts. Proceedings of the Lunar Science Conference, 7th, vol. 2. Geochimica et Cosmochimica Acta Supplement 7, 1195–1220.

Huhma, H., Cliff, R. A., Perttunen, V. & Sakko, M. 1990. Sm-Nd and Pb isotopic study of mafic rocks associated with early Proterozoic continental rifting: the Peräpohja schist belt in northern Finland. Contributions to Mineralogy and Petrology 104, 369–379.

Huhma, H., Hölttä, P. & Paavola, J. 1995a. Isotopic studies on the Archaean Varpaisjärvi granulites. In: Glebovitsky, V. A. & Kotov, A. B. (eds.) Precambrian of Europe: Stratigraphy, structure, evolution and mineralization. 9th Meeting of the Association of European Geological Societies (MAEGS), 4–15 September 1995, St. Petersburg, Russian Federation. Abstracts. St. Petersburg: Russian Academy of Sciences, 42–43.

Huhma, H., Mutanen, T., Hanski, E. & Walker, R. J. 1995b. Sm-Nd, U-Pb and Re-Os isotopic study of the Keivitsa Cu-Ni-bearing intrusion, northern Finland. In: The 22nd Nordic Geological Winter Meeting, Turku, Finland, January 8–11, 1996. Abstracts and oral poster presentations, p. 72.

Huhma, H., Mutanen, T., Hanski, E., Räsänen, J., Manninen, T., Lehtonen, M., Rastas, P., & Juopperi, H. 1996. Isotopic evidence for contrasting sources of the prolonged Palaeoproterozoic mafic-ultramafic magmatism in Central Finnish Lapland. In: IGCP project 336 symposium in Rovaniemi, Finland, August 21–23, 1996: program and abstracts. University of Turku. Division of geology and mineralogy. Publication 33, p. 17.

Huhtelin, T. A., Alapieti, T. T., Lahtinen, J. J. & Lerssi, J. 1989. Megacyclic units I, II and III in the Penikat layered intrusion. In: Alapieti, T. T. (ed.): Guide to the post-symposium field trip August 4–11, 1985. 5th International Platinum Symposium. Geological Survey of Finland, Guide 29, 59–69.

Hulbert, L. J., Grégoire, D. C., Paktunc, D. & Carne, R. C. 1992. Sedimentary nickel, zinc, and platinum-group-element mineralization in Devonian black shales at the Nick Property, Yukon, Canada: a new deposit type. Exploration and mining geology 1 (1), 39–62.

Hyppönen, V. 1983. Ontojoen, Hiisijärven ja Kuhmon kartta-alueiden kallioperä. Summary: Pre-Quaternary rocks of the Ontojoki, Hiisijärvi, and Kuhmo map-sheet areas. Geological Map of Finland 1 : 100 000. Explanation to the maps of pre-Quaternary rocks, Sheets 4411, 4412 and 4413. Geological Survey of Finland. 60 p.

Iljina, M. 1994. The Portimo Layered Igneous Complex: with emphasis on diverse sulphide and platinum-group element deposits. Acta Universitatis Ouluensis Series A, Scientiae Rerum Naturalium 258. 158 p.

Ireland, K. L. 1986. The Winterveld (TCL) Chrome Mine Limited, Eastern Bushveld Complex. In: Anhaeusser, C. R. & Maske, S. (eds.) Mineral deposits of Southern Africa, vol. II. Johannesburg: Geologi-

cal Society of South Africa, 1183–1188.

Irvine, T. N. 1967. Chromian spinel as a petrogenetic indicator. Part 2. Petrologic applications. Canadian Journal of Earth Sciences 4, 71–103.

Irvine, T. N. 1970a. Crystallization sequences in the Muskox intrusion and other layered intrusions. In: Visser, D. J. L. & von Gruenewaldt, G. (eds.) Symposium on the Bushveld Igneous Complex and other layered intrusions. Geological Society of South Africa, Special Publication 1, 441–476.

Irvine, T. N. 1970b. Heat transfer during solidification of layered intrusions. I. Sheets and sills. Canadian Journal of Earth Sciences 7, 1031–1061.

Irvine, T. N 1974. Chromitite layers in stratiform intrusions. Garnegie Institution of Washington, Year Book 73, 300–316.

Irvine, T. N. 1975a. Crystallization sequences in the Muskox intrusion and other layered intrusions – II. Origin of chromitite layers and similar deposits of other magmatic ores. Geochimica et Cosmochimica Acta 39, 991–1020.

Irvine, T. N. 1975b. Primary precipitation of concentrated deposits of magmatic ores. Geological Survey of Canada Paper 75–1B, 73–79.

Irvine, T. N. 1975c. The silica immiscibility effect in magmas. Carnegie Institution of Washington, Year Book 74, 484–492.

Irvine, T. N. 1975d. Olivine-pyroxene-plagioclase relations in the system Mg_2SiO_4-$CaAl_2Si_2O_8$-$KAlSi_3O_8$-SiO_2 and their bearing on the differentiation of stratiform intrusions. Carnegie Institution of Washington, Year Book 74, 492–500.

Irvine, T. N. 1976. Metastable liquid immiscibility and MgO-FeO-SiO_2 fractionation patterns in the system Mg_2SiO_4-Fe_2SiO_4-$CaAl_2Si_2O_8$-$KalSi_3O_8$-SiO_2. Carnegie Institution of Washington, Year Book 75, 597–611.

Irvine, T. N. 1977a. Origin of chromitite layers in the Muskox intrusion and other stratiform intrusion: A new interpretation. Geology 5 (5), 273–277.

Irvine, T. N. 1977b. Chromite crystallization in the join Mg_2SiO_4-$CaMgSi_2O_6$-$CaAl_2Si_2O_8$-$MgCr_2O_4$-SiO_2. Carnegie Institution of Washington, Year Book 76, 465–472.

Irvine, T. N. 1978a. Density current structure and magmatic sedimentation. Carnegie Institution of Washington, Year Book 77, 717–725.

Irvine, T. N. 1978b. Infiltration metasomatism, adcumulus growth and secondary differentiation in the Muskox intrusion. Carnegie Institution of Washington, Year Book 77, 743–751.

Irvine, T. N. 1979. Rocks whose composition is determined by crystal accumulation and sorting. In: Yoder, H. S., Jr. (ed.) The evolution of the igneous rocks. Fiftieth Anniversary perspectives. Princeton: Princeton University Press, 245–306.

Irvine, T. N., Keith, D. W. & Todd, S. G. 1982. Formation of the Stillwater J-M Reef by concurrent fractional crystallization and liquid mixing in a stratified magma body. Carnegie Institution of Washington, Year Book 81, 286–294.

Irvine, T. N. & Kushiro, I. 1976. Partitioning of Ni and Mg between olivine and silicate liquid. Carnegie Institution of Washington, Year Book 75, 668–678.

Irvine, T. N. & Smith, C. H. 1969. Primary oxide minerals in the layered series of the Muskox intrusion. In: Wilson, H. D. B. (ed.) Magmatic ore deposits, a symposium. Economic Geology Monograph 4, 76–94.

Irving, A. J. 1978. A review of experimental studies of crystal/liquid trace element partitioning. In: Drake, M. J. & Holloway, J. R. (eds.) Experimental trace element geochemistry. Geochimica et Cosmochimica Acta 6A, 743–770.

Isohanni, M. 1976. Porttivaaran ja Syötteen emäksisten kerrosintruusioiden sisäisestä sulfidimalmimuodostuksesta Koillismaalla. Unpublished licentiate's thesis, University of Oulu, Department of Geology. 121 p.

Ivanov, A. A. & Lizunov, N. V. 1944. Platinoidy v ultraosnovnykh porodakh Urala. Izvestiya Akademii Nauk SSSR, Ser. Geol. 5, 78–86.

Ivanov, O. K. 1977. Saranovskii massiv stratifitsirovannykh khromitonosnykh giperbazitov. In: Genezis ultrabazitov i svyazannogo s nimi orudeneniya. Sverdlovsk: Akademii Nauk SSSR, Uralskii nauchnyi tsentr. Trudy Instituta geologii i geokhimii 127, 51–62.

Izoitko, V. M. & Petrov, S. V. 1995. Veshchestvennyi sostav i tekhnologicheskie svoistva malosulfidnykh rud Fedorovo-Panskogo mestorozhdeniya. In: Rybakov, S. I. & Golubev, A. I. (eds.) Tezisy dokladov regionalnogo simpoziuma "Blagorodnye metally i almazy Severa Evropeiskoi chasti Rossii" i nauchno-prakticheskoi konferentsii "Problemy razvitiya mineralno-syrevoi bazy platinovykh metallov Rossii",52–53.

Jackson, E. D. 1961. Primary textures and mineral associations in the ultramafic zone of the Stillwater Complex, Montana. U.S. Geological Survey, Professional Paper 358. 106 p.

Jackson, E. D. 1963. Stratigraphic and lateral variation of chromite composition in the Stillwater Complex. Mineralogical Society of America, Special Paper 1, 46–54.

Jackson, E. D. 1967. Ultramafic cumulates in the Stillwater, Great Dyke, and Bushveld intrusions. In: Wyllie, P. J. (ed.) Ultramafic and related rocks. New York: John Wiley & Sons, Inc., 20–38.

Jackson, E. D. 1970. The cyclic unit in layered intrusions – a comparison of repetitive stratigraphy in

the ultramafic parts of the Stillwater, Muskox, Great Dyke, and Bushveld Complexes. In: Visser, D. J. L. & von Gruenewaldt, G. (eds.) Symposium on the Bushveld Igneous Complex and other layered intrusion. Geological Society of South Africa, Special Publication 1, 391–424.

Jacobson, S. S. 1975. Dashkesanite: high-chlorine amphibole from St. Paul's Rocks, Equatorial Atlantic, and Transcaucasia, U.S.S.R. Smithsonian Contributions to the Earth Sciences 14, 17–20.

Jahn, B. M., Vidal, P. & Kröner, A. 1984. Multichronometric ages and origin of Archaean tonalitic gneisses in Finnish Lapland: a case for long crustal residence time. Contributions to Mineralogy and Petrology 86, 398–408.

Janardhanan, A. S. & Leake, B. E. 1975. The origin of the meta-anorthositic gabbros and garnetiferous granulites of the Sittampundi Complex, Madras, India. Journal of the Geological Society of India 16 (4), 391–408.

Johnston, D. A. 1980. Volcanic contribution of chlorine to the stratosphere: more significant to ozone than previously estimated? Science 209, 491–493.

Jokinen, T., Valli, T. & Mutanen, T. 1994. SAMPO EM studies of Keivitsa nickel-copper deposit. In: European Association of Exploration Geophysicists 56th meeting and technical exhibition, Vienna, Austria, June 6–10, 1994. Extended abstracts, oral and poster presentations. Zeist: European Association of Exploration Geophysicists. 2 p.

Jolly, W. T. 1975. Subdivision of the Archean lavas of the Abitibi area, Canada, from Fe-Mg-Ni-Cr relations. Earth and Planetary Science Letters 27, 200–210.

Jolly, W. T. 1986. Geology and geochemistry of Huronian rhyolites and low-Ti continental tholeiites from the Thessalon region, central Ontario. Canadian Journal of Earth Sciences 24, 1360–1385.

Juopperi, A. 1977. The magnetite gabbro and related Mustavaara vanadium ore deposit in Porttivaara layered intrusion, northeastern Finland. Geological Survey of Finland, Bulletin 288. 68 p.

Juopperi, H. 1986. Savukoski. Geological Map of Finland 1 : 100 000, Pre-Quaternary Rocks, Sheet 3723 + 4711. Geological Survey of Finland.

Juvonen, R., Kallio, E. & Lakomaa, T. 1994. Determination of precious metals in rocks by inductively coupled plasma mass spectrometry using nickel sulfide concentration. Comparison with other pretreatment methods. Analyst 119, 617–621.

Kadik, A. A. 1970. Fizicheskie usloviya plavleniya na kontakte s intruzivnymi portsiami magm pri estestvennoi konvektsii rasplava. Geokhimiya 4, 460–474.

Kadik, A. A., Lebedev, E. B. & Khitarov, N. I. 1971. Voda v magmaticheskikh rasplavakh. Moskva: Nauka. 267 p.

Kalinin, S. K., Chakabaev, S. E., Kim, E. Kh. & Fain, E. E. 1985. O soderzhanii reniya v goryuchikh slantsakh Baikhozhinskogo mestorozhdeniya. Izvestiya Akademii Nauk Kazakhskoi SSR, Ser. Geol. 6, 35–59.

Kamineni, D. C., Bonardi, M. & Rao, A. T. 1982. Halogen-bearing minerals from Airport Hill, Visakhapatnam, India. American Mineralogist 67, 1001–1004.

Kapusta, Ya. S., Sumin, L. V., Shuleshko, I. K. & Berezhnaya, N. G. 1985. Zirkonometriya vulkanogennykh porod gimolskoi serii po izotopam ksenona i svintsa. Geokhimiya 3, 293–299.

Karhu, J. A. 1993. Paleoproterozoic evolution of the carbon isotope ratios of sedimentary carbonates in the Fennoscandian Shield. Geological Survey of Finland, Bulletin 371. 87 p., 2 app.

Karhu, J. A. & Holland, H. D. 1996. Carbon isotopes and the rise of atmospheric oxygen. Geology 24 (10), 867–870.

Karpinskii, A. P. 1926. O veroyatnom proiskhozhdenii korennykh mestorozhdenii platiny uralskogo tipa. Izvestiya Akademii Nauk SSSR 2, 123–170.

Karpov, R. V. 1959. Pegmatity osnovnykh porod Monchetundry i svyazannoe s nimi sulfidnoe orudenenie. Geologiya rudnykh mestorozhdenii 5, 74–90.

Kazimieras, K. 1996. Varena magnetite deposit in Lithuania (southern Baltic region) as the Honggetype layered magma chambers. 30th International Geological Congress. Abstracts, Vol. 2. Beijing, China, 8–14 August 1996. p. 659.

Kholmov, G. V. & Sholokhnev, V. V. 1974. Sravnitelnaya kharakteristika zhilnykh sulfidnykh medno-nikelevykh mestorozhdenii Monchegorskogo plutona (Kolskii poluostrov). Geologiya rudnykh mestorozhdenii 16 (1), 18–27.

Kobayashi, H. 1972. Some notes on orbicular rock. Journal of the Faculty of Science, Hokkaido University, Series IV 15 (1–2), 101–108.

Kojonen, K. 1981. Geology, geochemistry and mineralogy of two Archean nickel-copper deposits in Suomussalmi, eastern Finland. Geological Survey of Finland, Bulletin 315. 58 p.

Kojonen, K., Pakkanen, L. & Johanson, B. 1996. Tuloksia mikroanalysaattorilla tehdyistä automaattisista TURBO SCAN-hauista eräistä suomalaisista platinaryhmän metallien suhteen anomaalisista malmiaiheista. Geological Survey of Finland, unpublished report. M42.4/2343, 3112, 3142, 3714/–96/1. 5 p.

Kojonen, K., Johanson, B. & Pakkanen, L. 1997. Tuloksia mikroanalysaattorilla tehdyistä hivenaineanalyyseistä Keivitsan ja Kumisevan PGE-metallien suhteen anomaalista aiheista. Geological Survey of

Finland, unpublished report, M42.4/2343, 3714/–97/1. 4 p., 4 app. pages.

Kolbantsev, L. R. 1994. Maficheskie daikovye kompleksy riftogennykh sistem vostochnoi chasti Baltiiskogo shchita. Regionalnaya geologiya i metallogeniya 2, 13–25.

Konnikov, E. G., Epelbaum, M. B. & Chekhmir, A. S. 1981. Prichiny kontsentratsii kalia v endokontakte Chineiskogo gabbro-noritovogo plutona. Geokhimiya 2, 257–263.

Kontas, E., Niskavaara, H. & Virtasalo, J. 1990. Gold, palladium and tellurium in South African and Chinese and Japanese geological reference samples. Geostandards Newsletter 14 (3), 477– 478.

Kontinen, A. 1987. An early Proterozoic ophiolite – the Jormua mafic-ultramafic complex, northeastern Finland. Precambrian Research 35, 313–341.

Kornprobst, J., Pineau, F., Degiovanni, R. & Dautria, J. M. 1987. Primary igneous graphite in ultramafic xenoliths: I. Petrology of the cumulate suite in alkali basalt near Tissemt (Eggéré, Algerian Sahara). Journal of Petrology 28, 293–311.

Kouvo, O. 1976. Kallioperämme kronostratigrafiasta. In: Stratigrafia-symposio 8.9.1976. Geologiliitto r.y. Koulutusmoniste n:o 2, 1–13.

Kouvo, O. 1977. The use of mafic pegmatoids in geochronometry. ECOG V. Fifth European Colloquium of Geochronology, Cosmochronology and Isotope Geology, Pisa, September 5–10, 1977. Abstracts. 1 p.

Kovalenko, V. I., Naumov, V. B. & Solovova, I. P. 1992. Povedenie khlora pri differentsiatsii i izverzhenii magmaticheskikh rasplavov o. Pantelleriya. Geokhimiya 12, 1467–1471.

Koyaguchi, T., Hallworth, M. A., Huppert, H. E. & Sparks, R. S. J. 1990. Sedimentation of particles from a convecting fluid. Nature 343, 447–450.

Kozlov, E. K. 1973. Estestvennye ryady porod nikelenosnykh intruzii i ikh metallogeniya na primere Kolskogo poluostrova. Leningrad: Nauka. 287 p.

Kozlov, E. K., Yudin, B. A. & Dokuchaeva, V. S. 1967. Osnovnoi i ultraosnovnoi kompleksy [sic] Monche-Volchikh-Losevykh tundr. Leningrad: Nauka. 165 p.

Kozlov, M. T., Latyshev, L. N., Dokuchaeva, V. S., Bartenev, I. S., Shlyakhova, Kh. T., Kostin, S. M. & Pakhomovskii, Ya. A. 1975. Novyi tip khromitovogo orudeneniya v kvartsevykh gabbro-noritakh Monchegorskogo raiona. In: Osnovnye i ultraosnovnye porody Kolskogo poluostrova i ikh metallogeniya. Apatity: Kolskii filial Akademii Nauk SSSR, 108–125.

Krähenbühl, U., Morgan, J. W, Ganapathy, R. & Anders, E. 1973. Abundance of 17 trace elements in carbonaceous chondrites. Geochimica et Cosmochimica Acta 37, 1353–1370.

Kratts, K. O., Levchenkov, O. A., Ovchinnikova, G. V., Shuleshko, I. K., Yakovleva, S. Z., Makeev, A. F. & Komarov, A. N. 1976. Vozrastnye granitsy Yatuliiskogo kompleksa Karelii. Doklady Akademii Nauk SSSR 231 (5), 1191–1194.

Kratts, K. O., Sokolov, V. A., Gaskelberg, V. G., Zagorodnii, V. G., Negrutsa, T. F. & Shurkin, K. A. 1984. Novoe v izuchenii stratigrafii dokembriya sovetskoi chasti Baltiiskogo shchita. Sovetskaya Geologiya 7, 105–118.

Krivenko, A. P., Lavrentev, Yu. G., Maiorova, O. N. & Tolstykh, N. D. 1989. Telluridy platiny i palladiya v Panskom gabbro-noritovom massive na Kolskom poluostrove. Doklady Akademii Nauk SSSR 308 (4), 950–954.

Kröner, A. & Compston, W. 1990. Archaean tonalitic gneiss of Finnish Lapland revisited: zircon ion-microprobe ages. Contributions to Mineralogy and Petrology 104, 348–352.

Kröner, A., Puustinen, K. & Hickman, M. 1981. Geochronology of an Archean tonalite gneiss dome in northern Finland and its relation with an unusual overlying volcanic conglomerate and komatiitic greenstone. Contributions to Mineralogy and Petrology 76, 33–41.

Kruger, F. J. & Marsh, J. S. 1982. Significance of $^{87}Sr/^{86}Sr$ ratios in the Merensky cyclic unit of the Bushveld Complex. Nature 298, 53–55.

Krutov, G. A. 1936. Dashkesanit – novyi khlorsoderzhashchii amfibol gruppy gastingsita. Izvestiya Akademii Nauk SSSR, Otd. matem. i estestv. nauk 2–3, 341–373.

Krutov, G. A. & Vinogradova, R. A. 1966. Khlorgastingsity magnetitovogo mestorozhdeniya Odinochnoe v Vostochnom Sayane. Doklady Akademii Nauk SSSR 169 (1), 204–207.

Krutov, G. A., Vinogradova, R. A. & Kiseleva, I. A. 1970. Khlorsoderzhashchie mineraly i nekotorye voprosy genezisa metasomaticheskikh mestorozhdenii magnetita Mulga-Burlukskoi i Krasnokamenskoi grupp v Vostochnom Sayane. Vestnik Moskovskogo universiteta, Ser. Geol. 6, 31–42.

Kujanpää, J. 1964. Kemin Penikkain jakson rakenteesta ja kromiiteista. Unpublished licentiate's thesis, University of Helsinki, Department of Geology and Mineralogy. 118 p.

Kuno, H. 1950. Petrology of Hakone volcano and the adjacent areas, Japan. Geological Society of America Bulletin 61, 957–1020.

Kuno, H. 1965. Fractionation trends of basalt magmas in lava flows. Journal of Petrology 6 (2), 302–321.

Kuo, H. Y. & Crocket, J. H. 1979. Rare earth elements in the Sudbury Nickel Irruptive: Comparison with layered gabbros and implications for Nickel Irruptive petrogenesis. Economic Geology 74, 590–605.

Kuo, L-C. & Kirkpatrick, R. J. 1982. Pre-eruption history of phyric basalts from DSDP Legs 45 and 46: evidence from morphology and zoning patterns in plagioclase. Contributions to Mineralogy and Petrology 79, 13–27.

Kuschke, G. S. J. 1939. The critical zone of the Bushveld Igneous Complex, Lydenburg district. Transactions of the Geological Society of South Africa 42, 57–81.

Kushiro, I. 1973. Regularities in the shift of liquidus boundaries in silicate systems and their significance in magma genesis. Carnegie Institution of Washington, Year Book 72, 497–502.

Kushiro, I. 1974a. The system forsterite-anorthite-albite-silica-H_2O at 15 kbar and the genesis of andesitic magmas in the upper mantle. Carnegie Institution of Washington, Year Book 73, 244–248.

Kushiro, I. 1974b. Pressure effect on the changes of the forsterite-enstatite liquidus boundary with the addition of other cations and the genesis of magmas. Carnegie Institution of Washington, Year Book 73, 248–251.

Kushiro, I. 1974c. Electron microprobe analysis of glass. Carnegie Institution of Washington, Year Book 73, 603–605.

Lachenbruch, A. H. 1962. Mechanics of thermal contraction cracks and ice-wedge polygons in permafrost. Geological Society of America, Special Paper 70. 69 p.

Lacroix, A. 1928. Les pegmatitoïdes des roches volcaniques a facies basaltique. Comptes Rendus Acad. Sci., Août 8, 321–326.

Lambert, D. D., Morgan, J. W., Walker, R. J., Shirey, S. B., Carlson, R. W., Zientek, M. L. & Koski, M. S. 1989. Rhenium-osmium and samarium-neodymium isotopic systematics of the Stillwater Complex. Science 244, 1169–1174.

Lambert, D. D. & Simmons, E. C. 1983. Platinum-group element ore-forming process in mafic layered intrusions: Geochemical evidence from the Stillwater Complex, Montana. Mining Engineering 35 (9), 1291–1298.

Lambert, D. D. & Simmons, E. C. 1988. Magma evolution in the Stillwater Complex, Montana: II. Rare earth element evidence for the formation of the J-M reef. Economic Geology 83, 1109–1126.

Lambert, D. D., Unruh, D. M. & Simmons, E. C. 1985. Isotopic investigations of the Stillwater Complex: a review. In: Czamanske, G. K. & Zientek, M. L. (eds.) The Stillwater Complex, Montana: geology and guide. Montana Bureau of Mines, Special Publication 92, 46–54.

Lange, R. L. & Carmichael, I. S. E. 1990. Thermodynamic properties of silicate liquids with emphasis on density, thermal expansion and compressibility. In: Nicholls, J. & Russell, J. K. (eds.) Modern methods in igneous petrology: understanding magmatic processes. Washington: Mineralogical Society of America. Reviews in Mineralogy 24, 25–64.

Lapham, D. M. 1968. Triassic magnetite and diabase at Cornwall, Pensylvania. In: Ridge, J. D. (ed.) Ore Deposits in the United States, 1933–1967, Vol. I, 72–94.

Latysh, I. K 1959. Formy nakhozhdeniya platiny v rudakh Kachkanarskogo tipa na Urale. Trudy gornogeol. instituta Uralskoi filial Akademii Nauk SSSR 42, 3–15.

Lavrov, M. M. 1971. Geokhimiya differentsirovannykh gabbro-noritovykh intruzii Olangskaya gruppa intruzii. In: Geokhimiya giperbazitov Karelo-Kolskogo regiona. Trudy instituta geologii, Karelskii filial Akademii Nauk SSSR 9, 61–73.

Lavrov, M. M. 1979. Giperbazity i rassloennye peridotit-gabbro-noritovye intruzii dokembriya Severnoi Karelii. Leningrad: Nauka. 136 p.

Lavrov, M. M., Garbar, D. I., Bogachev, A. I., Chechel, E. K. & Mikhailyuk, E. M. 1978. Burakovskii peridotit-gabbro-noritovyi massiv. In: Intruzivnye bazit-ultrabazitovye kompleksy dokembriya Karelii. Trudy institut ageologii, Karelskii filial Akademii Nauk SSSR 32, 78–89.

Lavrov, M. M. & Pekki, A. 1987. Karelskaya metallogenicheskaya epokha, Girvasskii etap. In: Sokolov, V. A. (ed.) Geologiya Karelii. Leningrad: Nauka, 186–187.

Lavrov, M. M. & Trofimov, N. N. 1986. Stratiformnoe khromitovoe orudenenie v rassloennoi intruzii dokembriya Karelii. Doklady Akademii Nauk SSSR 289 (2), 449–452.

Lazarenkov, V. G., Balmasova, E. A., Glazov, A, I. & Onishchina, N. M. 1991. Raspredelenie elementov platinovoi gruppy v khromitakh Burakovsko-Aganozerskogo rassloennogo massiva (Prionezhe). Izvestiya Akademii Nauk, Ser. Geol. 9, 57–65.

Lazarenkov, V. G., Balmasova, E. A, Vaganov, P. A. & Onishchina, N. M. 1989. Raspredelenie blagorodnykh metallov i redkozemelnykh elementov v rudnom khromite Burakovsko-Aganozerskogo massiva. Vestnik Leningradskogo universita ser. 7, vyp. 4, 68–70.

Lazko, E. M., Sivoronov, A. A. & Bobrov, A. B. 1982. Problema tonalitovogo sloya v granitno-zelenokamennykh oblastyakh. Izvestiya Akademii Nauk SSSR, Ser. Geol. 9, 5–15.

Lea, S. D. 1996. The geology of the Upper Critical Zone, northeastern Bushveld Complex. South African Journal of Geology 99 (3), 263–283.

Lebedev, A. P. 1962a. Sootnosheniya magmatizma i rudoobrazovaniya v Chineiskom gabbro-anortozitovom plutone (Vostochnaya Sibir). In: Osnovnye porody i problemy ikh genezisa. Trudy Instituta geologii rudnykh mestorozhdenii, petrografii, miner-

alogii i geokhimii 77, 5–18.

Lebedev, A. P. 1962b. Chineiskii gabbro-anortozitovyi pluton (Vostochnaya Sibir). Trudy Instituta geologii rudnykh mestorozhedenii, petrografii, mineralogii i geokhimii 80. 100 p.

Lee, C. A. & Parry, S. J. 1988. Platinum-group element geochemistry of the lower and middle group chromitites of the eastern Bushveld Complex. Economic Geology 83, 1127–1139.

Lee, C. A. & Tredoux, M. 1986. Platinum-group element abundances in the lower and the lower critical zones of the eastern Bushveld Complex. Economic Geology 81, 1087–1095.

Leeman, W. P. & Dasch, E. J. 1978. Strontium, lead and oxygen isotopic investigation of the Skaergaard intrusion, East Greenland. Earth and Planetary Science Letters 41, 47–59.

Legendre, O. & Augé, T. 1992. Alluvial platinum-group minerals from the Manampotsy area, East Madagascar. Australian Journal of Earth Sciences 39, 389–404.

Levchenkov, O. A. & Zinger, T. F., Duk, V. L., Yakovleva, S. Z., Baikova, V. S., Shuleshko, I. K. & Matukov, D. I. 1996. U-Pb-vozrast tsirkonov giperstenovykh dioritov i granodioritov o. Pongon-Navolok (Baltiiskii shchit, Belomorskaya tektonicheskaya zona). Doklady Akademii Nauk 349 (1), 90–92.

Levin, E. M. 1970. Liquid immiscibility in oxide systems. In: Alper, A. M. (ed.) Phase diagrams, vol III, The use of phase diagrams in electronic materials and glass technology. New York: Academic Press, 143–236.

Lewis, S. F. 1964. Mineralogical and petrological studies of plutonic blocks from the Soufrière Volcano, St. Vincent, B. W. I. Unpublished D. Phil. thesis, University of Oxford.

Lewis, S. F. 1973. Mineralogy of the ejected plutonic blocs of the Sonfrière Volcano St. Vincent: olivine, pyroxene, amphibole and magnetite paragenesis. Contributions to Mineralogy and Petrology 38, 197–220.

Li, C. & Naldrett, A. J. 1993. Platinum-group minerals from the Deep Copper Zone of the Strathcona deposit, Sudbury, Ontario. The Canadian Mineralogist 31, 31–44.

Liebenberg, L. 1970. The sulphides in the layered sequence of the Bushveld Igneous Complex. In: Visser, D. J. L. & von Gruenewaldt, G. (eds.) Symposium on the Bushveld Igneous Complex and other layered intrusions. Geological Society of South Africa, Special Publication 1, 108–207.

Lightfoot, P. C., Naldrett, A. J. & Hawkesworth, C. J. 1984. The geology and geochemistry of the Waterfall Gorge section of the Insizwa Complex with particular reference to the origin of nickel sulfide deposits. Economic Geology 79, 1857–1879.

Likhachev, A. P. & Kukoev, V. A. 1973. O plavlenii i fazovykh otnosheniyakh v sulfidnykh, silikatnykh i sulfidno-silikatnykh sistemakh. Geologiya rudnykh mestorozhdenii 15 (5), 32–45.

Lindsley, D. H., Kesson, S. E., Hartzman, M. J. & Cushman, M. K. 1974. The stability of armalcolite: Experimental studies in the system Mg-Fe-Ti-O. Proceedings 5th Lunar Conference, Suppl. 5. Geochimica et Cosmochimica Acta 1, 521–534.

Lisitsyn, A. P. 1984. Osadochnoe telo okeana. In: Bogdanov, N. A. & Pushcharovskii, Yu. M. (eds.) Geologiya dna okeanov po dannym glubokovodnogo bureniya. Moskva: Nauka, 12–61.

Litvinovskii, B. A., Podladchikov, Yu. Yu., Zanvilevich, A. N. & Dunichev, V. M. 1990. Plavlenie kislikh vulkanitov v kontakte s bazitovoi magmoi na malykh glubinakh. Geokhimiya 6, 807–814.

Lobach-Zhuchenko, S. B., Sergeev, S. A., Guskova, E. G. & Krasnova, A. F. 1986. Pervye dannye ob izotopnom vozraste i paleomagnetizme bazitov i ultrabazitov Vodlozerskogo bloka Karelii. Doklady Akademii Nauk SSSR 290 (5), 1184–1187.

Loferski, P. J., Lipin, B. R. & Cooper, R. W. 1990. Petrology of chromite-bearing rocks from the lowermost cyclic units in the Stillwater Complex, Montana. U.S. Geological Survey Bulletin 1670. 28 p.

Lofgren, G. 1974a. An experimental study of plagioclase crystal morphology: isothermal crystallization. American Journal of Science 274, 243–273.

Lofgren, G. 1974b. Temperature induced zoning in synthetic plagioclase feldspar. In: MacKenzie, W. S. & Zussman, J. (eds.): The Feldspars: Proceedings of a NATO Advanced Study Institute Manchester, 11–21 July 1972. Manchester: Manchester University Press, 362–375.

Lofgren, G. & Donaldson, C. H. 1975. Curved branching crystals and differentiation in comb-layered rocks. Contributions to Mineralogy and Petrology 49, 309–319.

Lombaard, B. V. 1956. Chromite and dunite of the Bushveld Complex. Transactions of the Geological Society of South Africa 59, 59–76.

Lorand, J. P. & Ceuleneer, G. 1989. Silicate and base-metal sulfide inclusions in chromitites from the Maqsad area (Oman ophiolite, Gulf of Oman): A model for entrapment. Lithos 22, 173–190.

Lowe, D. R. 1987. Comparative sedimentology of the principal volcanic sequences of Archean greenstone belts in South Africa, Western Australia and Canada: implications for crustal evolution. Precambrian Research 17, 1–29.

Lu, F., Anderson, A. T. & Davis, A. M 1995. Diffusional gradients at the crystal/melt interface and their effect on the composition of melt inclusions. The Journal of Geology 103, 591–597.

Ludden, J. N. 1978. Fractionation trends defined by residual glasses in the lavas and xenoliths of Piton de la Fournaise, Reunion Island. The Canadian Mineralogist 16, 265–276.

Luhr, J. F. & Carmichael, I. S. E. 1980. The Colima volcanic complex, Mexico. I. Post-caldera andesites from Volcán Colima. Contributions to Mineralogy and Petrology 71, 343–372.

Luukkonen, E. 1988. The structure and stratigraphy of the northern part of the late Archaean Kuhmo greenstone belt, eastern Finland. In: Mattila, E. (ed.) Archaean geology of the Fennoscandian Shield, Finnish-Soviet Symposium in Finland July 28 – August 7, 1986. Geological Survey of Finland, Special Paper 4, 71–96.

Maaløe, S. 1976. The zoned plagioclase of the Skaergaard intrusion, East Greenland. Journal of Petrology 17 (3), 398–419.

MacDonald, R., Sparks, R. S. J., Sigurdsson, H., Mattey, D. P., McGarvie, D. W. & Smith, R. L. 1987. The 1875 eruption of Askja volcano, Iceland: combined fractional crystallization and selective contamination in the generation of rhyolitic magma. Mineralogical Magazine 51 (360), 183–202.

MacKenzie, W. S. 1972. The origin of trachytes and syenites. Progress in experimental petrology 2, 46–50.

Mainwaring, P. R. & Naldrett, A. J. 1977. Country-rock assimilation and the genesis of Cu-Ni sulfides in the Water Hen intrusion, Duluth Complex, Minnesota. Economic Geology 72, 1269–1284.

Makarov, V. N. 1972. K mineralogii pegmatitovykh i gidrotermalnykh zhil iz osnovnykh i ultraosnovnykh porod massiva Pilguyarvi. Mater. po mineralogii Kolskogo poluostrova 9, 160–169.

Mäkelä, T. 1975. Emäksisen magman kiteytyminen ja differentiaatio Porttivaaran alueella, Koillismaalla. Unpublished master's thesis, University of Oulu, Department of Geology. 103 p., 8 app. pages.

Manninen, T. 1981. Savukosken Akanvaaran alueen geologiasta. Unpublished master's thesis, University of Turku, Department of Geology. 98 p.

Manninen, T. 1991. Sallan alueen vulkaniitit. Lapin vulkaniittiprojektin raportti. Summary: Volcanic rocks in the Salla Area, northeastern Finland. A report of the Lapland Volcanite Project. Geological Survey of Finland, Report of Investigation 104. 97 p.

Manninen, T., Hyvönen, E., Johansson, P., Kontio, M., Pänttäjä, M. & Väisänen, U. 1995. The geology of the Keivitsa area, Central Finnish Lapland. In: The 22nd Nordic geological Winter Meeting, Turku, Finland, January 8–11, 1996. Abstracts and oral poster presentations.

Manninen, T., Hyvönen, E., Johansson, P., Kontio, M., Pänttäjä, M. & Väisänen, U. 1996. Keivitsan alueen geologiaa. Geological Survey of Finland, unpublished report K/21.42/96/1. 28 p., 27 app. pages.

Marakushev, A. A. 1980. O genezise khromitovykh rud i vmeshchayushchikh ikh giperbazitov. Geologiya Rudnykh Mestorozhdenii 22 (1), 3–23.

Marakushev, A. A. & Shapovalov, Yu., B. 1996. Eksperimentalnoe issledovanie fazovogo raspredeleniya platiny i palladiya pri zhelezo-sulfidno-silikatnom rasslaivanii rasplavom. Doklady Akademii Nauk 346 (2), 234–236.

Marsh, B. D. & Maxey, M. R. 1985. On the distribution and separation of crystals in convecting magma. Journal of Volcanology and Geothermal Research 24, 95–150.

Martin, C. E. 1989. Re-Os isotopic investigation of the Stillwater Complex, Montana. Earth and Planetary Science Letters 93, 336–344.

Martin, D. 1989. Fluid-dynamic study of crystal settling. 28th International Geological Congress, Washington, U.S.A. Abstracts, vol. 2, 376–377.

Martin, D. & Nokes, R. 1988. Crystal settling in a vigorously convecting magma chamber. Nature 332, 534–536.

Martin, D. & Nokes, R. 1989. A fluid-dynamical study of crystal settling in convecting magmas. Journal of Petrology 30 (6), 1471–1500.

Martinogle, J. 1974. Mechanism of differentiation in the Morin anorthosite complex. Contributions to Mineralogy and Petrology 46, 99–107.

Masaitis, V. L. & Yudina, V. V. 1976. Almandinsoderzhashchie porody v kontaktovykh oreolakh trappovykh sillov r. B. Patom. Geologiya i geofizika 10, 61–79.

Mathez, E. A. & Delaney, J. R. 1981. The nature and distribution of carbon in submarine basalts and peridotite nodules. Earth and Planetary Science Letters 56, 217–232.

Mathison, C. I. & Hamlyn, P. R. 1987. The McIntosh layered troctolite-olivine gabbro intrusion, East Kimberley, Western Australia. Journal of Petrology 28, 211–234.

Matrosov, I. I. 1979. Nekotorye osobennosti desilikatsii granitnykh pegmatitov (na primere Urala). Zapiski vsesoyuznogo mineralogicheskogo Obshchestva 108 (1), 29–37.

Maurel, C. & Maurel, P. 1982a. Étude expérimentale de la distribution de l'aluminium entre bain silicaté basique et spinelle chromifère. Implications pétrogénétiques: teneur en chrome des spinelles. Bulletin de Minéralogie 105, 197–202.

Maurel, C. & Maurel, P. 1982b. Etudé expérimentale de la solubilité du chrome dans les bains silicatés basiques et de sa distribution entre liquide et minéraux coexistants: conditions d'existence du spinelle chromifère. Bulletin de Minéralogie 105, 640–647.

Maurel, C. & Maurel, P. 1983. Influence du fer ferrique sur la distribution de l'aluminium entre bain silicaté basique et spinelle chromifère. Bulletin de Minéralogie 106, 623–624.

Maurel, C. & Maurel, P. 1984. Etudé expérimentale de la distribution fu fer ferreux et du magnésium entre spinelle chromifère et bain silicaté basique. Bulletin de Minéralogie 107, 767–776.

Maury, R. C. & Bizouard, H. 1974. Melting of acid xenoliths into a basanite: an approach to the possible mechanisms of crustal contamination. Contributions to Mineralogy and Petrology 48, 275–286.

McBirney, A. R. 1975. Differentiation of the Skaergaard intrusion. Nature 253, 691–694.

McBirney, A. R. 1980. Mixing and unmixing of magmas. Journal of Volcanology and Geothermal Research 7, 357–371.

McBirney, A. R. & Nakamura, Y. 1974. Immiscibility in late-stage magmas of the Skaergaard intrusion. Carnegie Institution of Washington, Year Book 73, 348–352.

McBirney, A. R. & Noyes, R. M. 1979. Crystallization and layering of the Skaergaard intrusion. Journal of Petrology 20 (3), 487–554.

McCallum, I. S., Raedeke, L. D. & Mathez, E. A. 1980. Investigations of the Stillwater Complex: Part I. Stratigraphy and structure of the Banded zone. American Journal of Science 280–A, 59–87.

McCarthy, T. S. & Cawthorn, R. G. 1983. The geochemistry of vanadiferous magnetite in the Bushveld Complex: implications for crystallization mechanisms in layered complexes. Mineralium Deposita 18, 505–518.

McCarthy, T. S., Lee, C. A., Fesq, H. W, Kable, E. J. D. & Erasmus, C. S. 1984. Sulphur saturation in the lower and critical zones of the Eastern Bushveld Complex. Geochimica et Cosmochimica Acta 48, 1005–1019.

McDonald, J. A. 1965. Liquid immiscibility as one factor in chromitite seam formation in the Bushveld Igneous Complex. Economic Geology 60, 1674–1685.

McDougall, I. 1962. Differentiation of the Tasmanian dolerites: Red Hill dolerite-granophyre association. Geological Society of America Bulletin 73, 279–316.

McLennan, S. M., Taylor, S. R. & Eriksson, K. A. 1983. Geochemistry of Archean shales from the Pilbara Supergroup, Western Australia. Geochimica et Cosmochimica Acta 47 (7), 1211–1222.

Mead, W. J. 1925. The geologic rôle of dilatancy. The Journal of Geology 33, 685–698.

Mekhonoshin, A. S. & Paradina, L. F. 1986. Baddeleit i khromshpinelid iz ilmenita ultraosnovnykh porod Vostochnogo Sayana. Doklady Akademii Nauk SSSR 287 (4), 967–969.

Metrich, N. 1990. Chlorine and fluorine in tholeiitic and alkaline lavas of Etna (Sicily). Journal of Volcanology and Geothermal Research 40, 133–148.

Mezger, K. & Krogstad, E. J. 1997. Interpretation of discordant U-Pb zircon ages: An evaluation. Journal of Metamorphic Geology 15, 127–140.

Michael, P. J. 1988. Chlorine in mid-ocean ridge basalts and FeTi basalts: Evidence for magma chamber contamination by a seawater-derived component? EOS 69 (44), 1469.

Michael, P. J. & Schilling, J.-G. 1989. Chlorine in mid-ocean ridge magmas: evidence for assimilation of seawater-influenced components. Geochimica et Cosmochimica Acta 53, 3131– 3143.

Mikhailov, N. P., Sharkov, E. V., Abramson, M. P. & Inyakhin, M. V. 1966. Zlatogorskii differentsirovannii massiv osnovnykh i ultraosnovnykh porod v Severnom Kazakhstane. Sovetskaya Geologiya 10, 92–101.

Mikkola, E. 1937. Sodankylä. General Geological Map of Finland 1 : 400 000, Pre-Quaternary rocks, Sheet C 7, Sodankylä. Geological Survey of Finland.

Mikkola, E. 1941. Kivilajikartan selitys. Explanation to the map of rocks. Map sheets B7 – C7 – D7, Muonio – Sodankylä – Tuntsajoki. General Geological Map of Finland 1 : 400 000. Geological Survey of Finland. 286 p.

Miller, T. L., Zoller, W. H., Crowe, B. M. & Finnegan, D. L. 1988. Variations in trace elements and halogens with eruptive activity at Kilauea Volcano. EOS 69 (44), 1469.

Mints, M. V., Sobotovich, E. V. & Tson, O. V. 1982. Svintsovo-izokhronnoe datirovanie gornykh porod Murmanskogo bloka i ego obramleniya (Kolskii poluostrov). Izvestiya Akademii Nauk SSSR, Ser. Geol. 10, 5–17.

Mints, M. V., Tson, O. V. & Shenkman, E. Ya. 1992. Izotopnye datirovanie tektonicheskoi evolyutsii Keivskoi struktury (Kolskoi poluostrov). Izvestiya Akademii Nauk, Ser. Geol. 10, 6–17.

Mitchell, A. A. 1990. The stratigraphy, petrography and mineralogy of the Main Zone of the northwestern Bushveld Complex. Journal of the Geological Society of South Africa 93 (5/6), 818–831.

Mitrofanov, F. P., Balabonin, N. L. & Korchagin, A. U. 1995a. Metallogeniya Kolskogo poyasa rassloennykh ultramafit-mafitovykh intruzii. Otechestvennaya Geologiya 6, 37–41.

Mitrofanov, F. P., Zhangurov, A. A., Fedotov, Zh. A., Torokhov, M. P., Bayanova, T. B., Karzhavin, V. K. & Galimzanova, R. M. 1995b. Perpektivy platinonosnosti Imandrovskogo rassloennogo intruziva. In: Platina Rossii. Problemy razvitiya mineralno-syrevoi bazy platinovykh metallov (Materialy tretego zasedaniya nauchno-meto-

dicheskogo soveta po programme "Platina Rossii"). Sbornik nauchnykh trudov, Tom II, Kniga 2, 26–42.

Mitrofanov, F. P., Balaganskii, V. V., Balashov, Yu. A., Gannibal, L. F., Dokuchaeva, V. S., Nerovich, L. I., Radchenko, M. K. & Ryungenen, G. I. 1993. U-Pb-vozrast gabbro-anortozitov Kolskogo poluostrova. Doklady Akademii Nauk 331 (1), 95–98.

Mitrofanov, F. P., Balashov, Yu. A. & Balagansky, V. V. 1991. New geochronological data on lower Precambrian complexes of the Kola Peninsula. In: Mitrofanov, F. P. & Balagansky, V. V. (eds.) Correlation of lower Precambrian formations of the Karelian-Kola region. U.S.S.R. and Finland, 12–16. Scientific and technical Co-operation between Finland and the U.S.S.R. in the field of geology, Theme 1.1. "Geological correlation". Apatity: The USSR Academy of Science, Kola Science Centre, Geological Institution, 13–34.

Molyneyx, T. G. 1974. A geological investigation of the Bushveld Complex in Sekhukhuneland and part of the Steelport Valley. Transactions of the Geological Society of South Africa 77, 329–338.

Moorbath, S. & Welke, H. 1969. Lead isotope studies on igneous rocks from the Isle of Skye, Northwest Scotland. Earth and Planetary Science Letters 5, 217–230.

Morse, S. A. 1969a. The Kiglapait layered intrusion. The Geological Society of America, Memoir 112. 204 p.

Morse, S. A. 1969b. Syenites. Carnegie Institution of Washington, Year Book 67, 112–120.

Morse, S. A. 1979a. Kiglapait geochemistry I: Systematics, sampling, and density. Journal of Petrology 20 (3), 555–590.

Morse, S. A. 1979b. Kiglapait geochemistry II: Petrography. Journal of Petrology 20 (3), 591–624.

Morse, S. A. 1985. Magmatic convection related to adcumulus growth. Terra Cognita 5, p. 210.

Morse, S. A. 1986. Motion of crystals, solute, and magma in layered intrusions. Joint Annual Meeting, May 19–21, 1986, Carleton University. Program with abstracts 11, p. 104.

Morse, S.A. 1988. Motion of crystals, solute, and heat in layered intrusions. The Canadian Mineralogist 26, 209–224.

Mudge, M. R. 1968. Depth control of some concordant intrusions. Geological Society of America Bulletin 79, 315–332.

Murase, T. & McBirney, A. R. 1973. Properties of some common igneous rocks and their melts at high temperatures. Geological Society of America Bulletin 84, 3563–3592.

Muraveva, N. S., Shevaleevskii, I. D. & Shcherbovskii, E. Ya. 1979. Kristallizatsiya khromshpinelidov v chetvertichnykh bazaltakh Islandii. Doklady Akademii Nauk SSSR 248, 452–456.

Mutanen, T. 1974. Petrography and protoclastic structures of the orbiculite boulders from Sääkslahti, Toivakka, Finland and the magmatic genesis of orbiculites. Bulletin of the Geological Society of Finland 46, 53–74.

Mutanen, T. 1975. Emäksiseen magmatismiin liittyvä sulfidimalmimuodostus. Abstract: Genesis of sulphide ores, associated with mafic magmatism. Geologi 27 (2), 9–16.

Mutanen, T. 1976a. Komatiites and komatiite provinces in Finland. Geologi 28 (4–5), 49–56.

Mutanen, T. 1976b. Koitelaisen malmitutkimukset 1975. Geological Survey of Finland, unpublished report, M19/3741/76/1/10. 45 p., 8 app. pages.

Mutanen, T. 1979a. Vanadiini- ja kromi-platinamalmitutkimukset Koitelaisenvosien alueella Sodankylässä vuosina 1973 – 1978. Geological Survey of Finland, unpublished report, M19/3741/–79/1/10. 130 p., 2 app. pages.

Mutanen, T. 1979b. Sääksjärvi on sittenkin astrobleemi. Summary: Lake Sääksjärvi – an astrobleme after all. Geologi 31 (9–10), 125–130.

Mutanen, T. 1981. A new type of platinum-bearing chromite ore in the Koitelainen mafic layered intrusion, northern Finland. In: 3rd International Platinum Symposium, Pretoria, South Africa, June 28-July 9, 1981. Abstracts of papers, 28–29.

Mutanen, T. 1989a. Koitelaisen malmitutkimukset vuosina 1979 – 1989. Geological Survey of Finland, unpublished report M19/37/–89/1/10. 81 p.

Mutanen, T. 1989b. Koitelainen intrusion and Keivitsa-Satovaara complex. 5th International Platinum Symposium. Geological Survey of Finland, Guide 28. 49 p.

Mutanen, T. 1992. Koitelaisen intruusion malmipetrologia. Unpublished licentiate's thesis, University of Oulu, Department of Geology. Unpaginated.

Mutanen, T. 1994. Keivitsansarven kupari-nikkelijalometalliesiintymä. Geological Survey of Finland, unpublished report M06/3714/–94/1/10. 61 p. (Classified).

Mutanen, T. 1995a. Keivitsan geologiasta. In: Kolmannet geokemian päivät, February 6–8, 1995. Extended abstracts. Espoo: Vuorimiesyhdistys, ser. B 57, 68–71.

Mutanen, T. 1995b. Mafic layered intrusions of Finnish Lapland. In: Proc. International Field Conference and Symposium, IGCP 336/Petrology and Metallogeny of Volcanic and Intrusive Rocks of the Midcontinent Rift System, August 19 – September 1, 1995. Program and abstracts. Duluth, Minnesota: University of Minnesota Duluth, 135–136.

Mutanen, T. 1996. The Akanvaara and Koitelainen intrusions and the Keivitsa-Satovaara complex: guide to the pre-symposium field trip in Finland,

August 20–21, 1996. IGCP Project 336. Field conference on layered mafic complexes and related ore deposits of northern Fennoscandia. Rovaniemi: Geological Survey of Finland. 113 p., 4 app. maps.

Mutanen, T., Kontas, E. & Johanson, B. 1996. Sulphide liquid droplets as phase boundary collectors for PGM liquidus crystals in mafic magmas. In: IGCP project 336 symposium in Rovaniemi, Finland, August 21–23, 1996: program and abstracts. University of Turku. Division of geology and mineralogy. Publication 33, 27–28.

Mutanen, T., Törnroos, R. & Johanson, B. 1987. The significance of cumulus chlorapatite and high-temperature dashkesanite to the genesis of PGE mineralizations in the Koitelainen and Keivitsa-Satovaara complexes, northern Finland. In: Geo-Platinum Symposium, The Open University, Milton Keynes, Buckinghamshire, U.K., April 23–24, 1987. Abstracts, Paper T9.

Mutanen, T., Törnroos, R. & Johanson, B. 1988. The significance of cumulus chlorapatite and high-temperature dashkesanite to the genesis of PGE mineralization in the Koitelainen and Keivitsa-Satovaara complexes, northern Finland. In: Prichard, H. M., Potts, P. J., Bowles, J. F. W. & Cribb, S. J. (eds.) Geo-Platinum 87. London and New York: Elsevier Applied Science, 159–160.

Myers, J. S. 1975. Igneous stratigraphy of Archaean anorthosite at Majorqap qâva, near Fiskenæsset, South-West Greenland. Grønlands Geologiske Undersøgelse, Rapport 74. 27 p.

Myers, J. S. 1985. Stratigraphy and structure of the Fiskenæsset Complex, southern West Greenland. Grønlands Geologiske Undersøgelse, Bulletin 150. 72 p.

Nagaitsev, Yu. V. & Galibin, V. A. 1977. Vtorostepennye i redkie elementy pri regionalnom metamorfizme i ultrametamorfizme. Vestnik Leningradskogo Universiteta 6, 24–34.

Naldrett, A. J. & Duke, J. M. 1980. Platinum metals in magmatic sulfide ores. Science 208 (4451), 1417–1424.

Naldrett, A. J., Greenman, L. & Hewins, R. H. 1972. The main Irruptive and the sub-layer at Sudbury, Ontario. Internation Geological Congress, 24th, Montreal 1972. Proceedings, Sec. 4, 206–214.

Naldrett, A. J. & Mason, G. D. 1968. Contrasting Archean ultramafic igneous bodies in Dundonald and Clergue Townships, Ontario. Canadian Journal of Earth Sciences 5, 111–143.

Naldrett, A. J., Rao, B. V. & Evensen, N. M. 1986. Contamination at Sudbury and its role in ore formation. In: Callagher, M. J., Ixer, R. A., Neary, C. R. & Prichard, H. M. (eds.) Metallogeny of basic and ultrabasic rocks. Proceedings of the Conference 'Metallogeny of basic and ultrabasic rocks'. Edinburgh, Scotland, 9–12, April, 1985, 75–91.

Naqvi, S. M. 1978. Geochemistry of Archaean metasediments; evidence for prominent anorthosite-norite-troctolite (ANT) in the Archaean basaltic primordial crust. In: Windley, B. F. & Naqvi, S. M. (eds.) Archaean geochemistry. Amsterdam: Elsevier, 343–360.

Nash, W. P. 1976. Fluorine, chlorine, and OH-bearing minerals in the Skaergaard intrusion. American Journal of Earth Sciences 276, 546–557.

Nash, W. P. 1984. Phosphate minerals in terrestrial igneous and metamorphic rocks. In: Nriagn, J-O. & Moore, P. B. (eds.) Phosphate minerals, chapter 6. Berlin: Springer Verlag, 215–241.

Naslund, H. R. 1984. Supersaturation and crystal growth in the roof-zone of the Skaergaard magma chamber. Contributions to Mineralogy and Petrology 86, 89–93.

Naslund, H. R. 1987. Lamellae of baddeleyite and Fe-Cr-spinel in ilmenite from the Basistoppen Sill, East Greenland. The Canadian Mineralogist 25, 91–96.

Naumov, V. B., Kovalenko, V. I. & Ivanitskii, O. M. 1996. Kontsentratsiya letuchikh komponentov (H_2O, Cl, S, CO_2) v magmaticheskikh rasplavakh po dannym izucheniya vklyuchenii v mineralakh. Doklady Akademii Nauk 347 (3), 391–393.

Němec, D. 1967. The miscibility of the pyralspite and grandite molecules in garnets. Mineralogical Magazine 36, 389–402.

Neradovskii, Yu. N. 1985. Nekotorye tipomorfnye svoistva khromshpinelidov v nikelenosnykh ultraosnovnykh porodakh Pechengi. Zapiski vsesoyuznogo mineralogicheskogo obshchestva 6, 698–702.

Neradovskii, Yu. N. & Smolkin, V. F. 1977. Neobichnye titan-khromovye shpineli v porodakh nikelenosnykh massivov Pechengi. In: Mineraly i paragenezisy mineralov osnovnykh i ultraosnovnykh porod Kolskogo poluostrova. Apatity: Kolskii filial Akademii Nauk SSSR, 125–135.

Neuvonen, K. J., Korsman, K., Kouvo, O. & Paavola, J. 1981. Paleomagnetism and age relations of the rocks in the Main Sulphide Ore Belt in Central Finland. Bulletin of the Geological Society of Finland 53 (2), 109–133.

Nickel, K. G. 1981. Magma mixing as the probable origin of some Permian volcanic rocks of the Saar-Nahe-Basin (SW-Germany). Geologische Rundschau 70 (3), 1164–1176.

Nielsen, R. L. & Dungan, M. A. 1985. The petrology and geochemistry of the Ocate volcanic field, north-central New Mexico. Geological Society of America Bulletin 96, 296–312.

Nielsen, T. F. D. 1989. Gold mineralization in the Skaergaard intrusion. Grønlands Geologiske Undersøgelse, Open file Series 89/7. 14 p.

Nikitichev, A. P. Sedykh, Yu. N., Veselovskii, N. N., Sviyazhennikov, F. I. & Polyakova, V. A. 1995. Novye dannye o platinonosnosti Fedorovo-Panskogo rassloennogo intruziva. In: Rybakov, S. I. & Golubev, A. I (eds.) Tezisy dokladov regionalnogo simpoziuma "Blagorodnye metally i almazy Severa Evropeiskoi chasti Rossii" i nauchno-prakticheskoi konferentsii "Problemy razvitiya mineralno-syrevoi bazy platinovykh metallov Rossii", 83–85.

Niskavaara, H. & Kontas, E. 1990. Reductive co-precipitation as a separation method for the determination of gold, palladium, platinum, rhodium, silver, selenium and tellurium in geological samples by graphite furnace atomic absorption spectrometry. Analytical Chimica Acta 231, 273–282.

Nixon, G. T., Cabri, L. J. & Laflamme, J. H. G. 1990. Platinum-group-element mineralization in lode and placer deposits associated with the Tulameen Alaskan-type complex, British Columbia. The Canadian Mineralogist 28, 503–535.

Nolan, J. 1966. Melting-relations in the system $NaAlSi_3O_8$ – $NaAlSiO_4$ – $NaFeSi_2O_6$ – $CaMgSi_2O_6$ – H_2O, and their bearing on the genesis of alkaline undersaturated rocks. Quarterly Journal of the Geological Society of London 122, 119–157.

Ohenoja, V. 1968. Porttivaaran-Kuusijärven alueen kallioperä. Unpublished master's thesis, University of Oulu, Department of Geology. 88 p.

Oliver, G. J. H. 1977. Feldspathic hornblende and garnet granulites and associated anorthosite pegmatites from Doubtful Sound, Fiordland, New Zealand. Contributions to Mineralogy and Petrology 65, 111–125.

Oliver, R. L. 1956. The origin of garnets in the Borrowdale Volcanic Series and associated rocks, English Lake District. Geological Magazine 93, 121–139.

Olmsted, J. F. 1979. Crystallization history and textures of the Rearing Pond gabbro, northwestern Wisconsin. American Mineralogist 64, 844–855.

Olshanskii, Ya. I. 1948. O bolshoi tekuchesti sulfidnykh rasplavov i vozmozhnom geologicheskom znachenii etogo yavleniya. Doklady Akademii Nauk SSSR 63, 187–190

Orlov, D. M. 1963. O mekhanizme formirovaniya postorogennykh intruzii v svyazi s yavleniem usadki pri kristallizatsii. Petrograficheskii sbornik 5, trudy VSEGEI, nov. ser. 98, 65–73.

Orlov, D. M. & Sokolova, V. N. 1982. O prostranstvenno-vremennykh sootnosheniyakh rudnykh zhil s porodami daikovoi i rassloennoi serii Monchegorskogo plutona. Sovetskaya Geologiya 3, 97–103.

Orlova, G. P., Ryabchikov, I. D., Distler, V. V. & Gladyshev, G. D. 1987. Flyudnaya migratsiya platiny pri magmaticheskom sulfidoobrazovanii. Geologiya rudnykh mestorozhdenii 19 (1), 106–108.

Orsoev, D. A., Konnikov, E. G. & Zaguzin, G. N. 1994. Orudenenie "peridotitovogo plasta" g. Sopcha v Monchegorskom plutone. Zapiski vsesoyuznogo mineralogicheskogo obshchestva 123 (3), 26–40.

Orsoev, D. A., Rezhenova, S. A. & Bogdanova, A. N. 1982. Sopcheit – $Ag_4Pd_3Te_4$ – novyi mineral iz medno-nikelevykh rud Monchegorskogo plutona. Zapiski vsesoyuznogo mineralogicheskogo obshchestva 111 (1), 114–117.

Osborne, F. F. 1928. Certain magmatic titaniferous iron ores and their origin. Part I. Economic Geology 23, 724–761.

Osipov, M. A. 1967. Usadochnye yavleniya v ostyvayushchikh magmakh kak prichina obrazovaniya kamernykh pegmatitov. Geologiya rudnykh mestorozhdenii 9 (6), 28–40.

Osipov, M. A. 1970. Priblizitelnaya otsenka termicheskogo sokrashcheniya obema intruzivov granitoidov malykh glubin. Zapiski vsesoyuznogo mineralogicheskogo obshchestva 99 (6), 726–730.

Osipov, M. A. 1982. Formirovanie rassloennykh plutonov s pozitsii termousadki. Moskva: Nauka. 100 p.

Paavola, J. 1986. A communication on the U-Pb and K-Ar age relations of the Archaean basement in the Lapinlahti-Varpaisjärvi area, Central Finland. In: Korsman, K. (ed.) Development of deformation, metamorphism and metamorphic blocks in eastern and southern Finland. Geological Survey of Finland, Bulletin 339, 7–15.

Page, N. J. 1977. Stillwater Complex, Montana: rock succession, metamorphism and structure of the complex and adjacent rocks. U.S. Geological Survey Professional Paper 999. 79 p.

Page, N. J. 1979. Stillwater Complex, Montana – Structure, mineralogy and petrology of the Basal zone with emphasis on the occurrence of sulfides. U.S. Geological Survey Professional Paper 1038. 69 p.

Palacz, Z. A. & Tait, S. R. 1985. Isotopic and geochemical investigation of unit 10 from the Eastern Layered Series of the Rhum inrusion, Northwest Scotland. Geological Magazine 122 (5), 485–490.

Pankhurst, R. J. 1969. Strontium isotope studies related to petrogenesis in the Caledonian basic igneous province of NE. Scotland. Journal of Petrology 10, 115–143.

Parry, S. J. 1984. Abundance and distribution of palladium, platinum, iridium and gold in some oxide minerals. Chemical Geology 43 (1–2), 115–125.

Patchett, P. J. 1980. Thermal effects of basalt on continental crust and crustal contamination of magmas. Nature 238, 559–561.

Patchett, J. & Kouvo, O. 1986. Origin of continental crust of 1.9–1.7 Ga age: Nd isotopes and U-Pb zir-

con ages in the Svecokarelian terrain of South Finland. Contributions to Mineralogy and Petrology 92, 1–12.

Paul, A. & Douglas, R. W. 1965. Ferrous-ferric equilibrium in binary alkali silicate glasses. Physics and Chemistry of Glasses 6, 207– 211.

Pavlov, A. L. & Dymkin, A. M. 1979. Termodinamika protsessov ferritizatsii v silikatnykh rasplavakh. Trudy Instituta geologii i geofiziki, vyp. 424. Novosibirsk: Nauka. 88 p.

Pavlov, D. I. 1968. Ob uchastii khlora v formirovanii Ampalyikskogo magnetitovogo mestorozhdeniya. Geologiya rudnykh mestorozhdenii 1, 108–110.

Pchelintseva, N. F. & Koptev-Dvornikov, E. V. 1993. Kontsentrirovanie blagorodnykh metallov v protsesse kristallizatsii Kivakkskogo rassloennogo intruziva (Severnaya Kareliya). Geokhimiya 1, 97–113.

Peck, D. C., Keays, R. R. & Ford, R. J. 1992. Direct crystallization of refractory platinum-group element alloys from boninitic magmas: Evidence from western Tasmania. Australian Journal of Earth Sciences 39, 373–387.

Peck, D. L., Wright, T. L. & Moore, J. G. 1966. Crystallization of tholeiitic basalt in Alae lava lake, Hawaii. Bulletin of Volcanology 29, 629–654.

Peltonen, P. T. 1986. Peurasuvannon vulkaaninen konglomeraatti Keski-Lapin liuskealueella. Unpublished master's thesis, University of Turku, Department of Geology and Mineralogy. 128 p.

Penttilä, S. 1961. Esimerkki murrosten kartoituksesta ilmakuvien avulla. Geologi 13 (3–4), 28–31.

Peredery, W. V. & Naldrett, A. J. 1975. Petrology of the upper irruptive rocks, Sudbury, Ontario. Economic Geology 70, 164–175.

Perring, R. J. & Vogt, J. H. 1989. The geology and PGE mineralization of the Wondinong Sequence, Windimurra Complex, Western Australia. 5th International Platinum Symposium Abstracts. Bulletin of the Geological Society of Finland 61 (2), 4–5.

Perttunen, V. 1971. Runkaus. Geological Map of Finland 1 : 100 000, Pre-Quaternary Rocks, Sheet 2544. Geological Survey of Finland.

Perttunen, V. 1991. Kemin, Karungin, Simon ja Runkauksen kartta-alueiden kallioperä. Summary: Pre-Quaternary rocks of the Kemi, Karunki, Simo and Runkaus map sheet areas. Geological Map of Finland 1 : 100 000, Explanation to the Maps of Pre-Quaternary rocks, Sheets 2541, 2542+2524, 2543 and 2544. Geological Survey of Finland. 80 p.

Philpotts, A. R. 1968. Parental magma of the anorthosite-mangerite suite. In: Isachsen, Y. W. (ed.) Origin of anorthosite and related rocks. New York State and Science Service, Memoir 18, 207–212.

Philpotts, A. R. & Carroll, M. 1996. Physical properties of partly melted tholeiitic basalt. Geology 24 (11), 1029–1032.

Pihlaja, P. & Manninen, T. 1988. The metavolcanic rocks of the Peurasuvanto area, northern Finland. In: Marttila, E. (ed.) Archaean geology of the Fennoscandian Shield. Proceedings of the Finnish-Soviet Symposium in Finland, July 28-August 7, 1986. Geological Survey of Finland, Special Paper 4, 201–213.

Piirainen, T., Alapieti, T., Hugg, R. & Kerkkonen, O. 1977. The marginal border group of the Porttivaara layered intrusion and related sulphide mineralization. Bulletin of the Geological Society of Finland 49, 125–142.

Piispanen, R. & Tarkian, M. 1984. Cu-Ni-PGE mineralization at Rometölväs, Koillismaa layered igneous complex, Finland. Mineralium Deposita 19, 105–111.

Poldervaart, A. & Taubeneck, W. H. 1959. Layered intrusion of Willow Lake type. Geological Society of America Bulletin 70, 1395–1397.

Polferov, D. V. 1966. O sootnosheniyakh sulfidov i silikatov medno-nikelevykh rud. Geologiya Rudnykh Mestorozhdenii 8, 49–62.

Popov, V. S., Boronikhin, V. A., Gmyra, V. G. & Semina, V. A. 1981. Granaty iz andezito-datsitov Kelskogo vulkanicheskogo nagorya. Zapiski vsesoyuznogo mineralogicheskogo obshchestva 1, 76–85.

Pouchou, J. L. & Pichoir, F. 1984. A new model for quantitative X-ray microanalysis. La Recherché Aerospatiale 3, 167–192.

Predovskii, A. A. & Zhangurov, A. A. 1968. Mikrokaverny v olivinovykh porodakh Pechengskogo raiona. Materialy po mineralogii Kolskogo poluostrova 6, 39–44.

Presnall, D. C. 1969. The geometrical analysis of partial fusion. American Journal of Science 267, 1178–1194.

Presnall, D. C. 1979. Fractional crystallization and partial fusion. In: Yoder, H. S. (ed.) The evolution of the igneous rocks. Fiftieth Anniversary Perspectives. Princeton, New Jersey: Princeton University Press, 59–75.

Prichard, H. M. & Cann, J. R. 1982. Petrology and mineralogy of dredged gabbro from Gettysburg Bank, eastern Atlantic. Contributions to Mineralogy and Petrology 79, 46–55.

Proskuryakov, V. V. 1967. Geologicheskie stroenie i osobennosti differentsiatsii osnovnoi intruzii Panskikh vyzot na Kolskom poluostrove. In: Ivanov, A. M. (ed.) Osnovnye i ultraosnovnye porody Kolskogo poluostrova. Leningrad: Nauka, 40–54.

Pukhtel, I. S., Shuravlev, D. Z., Kulikov, V. S. & Kulikova, V. V. 1991. Petrografiya i Sm-Nd vozrast differentsirovannogo potoka komatiitovykh

bazaltov Vetrenogo Poyasa (Baltiiskii Shchit). Geokhimiya 5, 625–634.

Purvis, A. C., Nesbitt, R. W. & Hallberg, J. A. 1972. The geology of part of the Carr Boyd Rocks Complex and its associated nickel mineralization, Western Australia. Economic Geology 67, 1093–1113.

Pushkarev, Yu. D., Kravchenko, E. V. & Shestakov, G. I. 1978. Geokhronometricheskie repery dokembriya Kolskogo poluostrova. Leningrad: Nauka. 136 p.

Raedeke, L. D. & McCallum, I. S. 1984. Investigations in the Stillwater Complex: Part II. Petrology and petrogenesis of the Ultramafic series. Journal of Petrology 25, 395–420.

Ramsay, C. R. & Davidson, L. R. 1970. The origin of scapolite in the regionally metamorphosed rocks of Mary Kathleen, Queensland, Australia. Contributions to Mineralogy and Petrology 25, 41–51.

Räsänen, J. 1983. Vuotostunturi. Geological Map of Finland 1 : 100 000, Pre-Quaternary Rocks, Sheet 3644. Geological Survey of Finland.

Razin, L. V. 1974. Mestorozhdeniya platinovykh metallov. In: Smirnov, V. I. (ed.) Rudnye mestorozhdeniya SSSR, Tom. 3. Moskva: Nedra, 96–116.

Razin, L. V. & Khomenko, G. A. 1969. Osobennosti nakopleniya osmiya, ruteniya i ostalnykh metallov gruppy platiny v khromshpinelidakh platinonosnykh dunitov. Geokhimiya 6, 659–672.

Reeves, S. J. & Keays, R. R. 1995. The platinum-group element geochemistry of the Buckhalla Layered Complex, central Queensland. Australian Journal of Earth Sciences 42, 187–201.

Reitan, P. H. 1968. Frictional heat during metamorphism. 2. Quantitative evaluation of concentration of heat generation in space. Lithos 1, 268–274.

Rice, A. R. & Eales, H. V. 1995. The densities of Bushveld melts: textural and hydrodynamic criteria. Mineralogy and Petrology 54, 45–53.

Richter, D. H. & Moore, J. G. 1966. Petrology of the Kilauea Iki lava lake, Hawaii. U.S. Geological Survey Professional Paper 537–B. 26 p.

Ridley, W. I. 1977. The crystallization trends of spinels in tertiary basalts from Rhum and Muck and their petrogenetic significance. Contributions to Mineralogy and Petrology 64, 243–255.

Ringwood, A. E. 1955. The principles governing trace-element behaviour during magmatic crystallization. Part II. The role of complex formation. Geochimica et Cosmochimica Acta 7 (5–6), 242–254.

Ripley, E. M. 1978. Sulfur isotopic studies of the Dunka Road Cu-Ni deposit, Duluth Complex, Minnesota. Economic Geology 73 (7), 1396–1397.

Roedder, E. 1951. Low temperature liquid immiscibility in the system K_2O-FeO-Al_2O_3-SiO_2. American Mineralogist 36, 282–286.

Roedder, E. 1979. Origin and significance of magmatic inclusions. Bulletin de Minéralogie 102, 487–510.

Roedder, E. 1984. Fluid inclusions. Mineralogical Society of America, Reviews in mineralogy 12. 644 p.

Roedder, E. & Weiblen, P. W. 1970. Lunar petrology of silicate melt inclusions, Apollo 11 rocks. Proceedings of Apollo 11 Lunar Science Conference. Geochimica et Cosmochimica Acta, Supplement 1, vol. 1, 801–837.

Roedder, E. & Weiblen, P. W. 1971. Petrology of silicate melt inclusions, Apollo 11 and Apollo 12 and terrestrial equivalents. Proceedings of the 2nd Lunar Science Conference. Geochimica et Cosmochimica Acta Supplement 2, vol. 1, 507–528.

Roedder, E. & Weiblen, P. W. 1972. Petrographic features and petrologic significance of melt inclusions in Apollo 14 and 15 rocks. Proceedings of the 3rd Lunar Science Conference. Geochimica et Cosmochimica Acta Supplement 3, vol. 1, 251–279.

Roeder, P. L. & Emslie, R. F. 1970. Olivine-liquid equilibrium. Contributions to Mineralogy and Petrology 29, 275–289.

Roeder, P. & Hill, R. 1974. The crystallization of spinel from basaltic liquid as a function of oxygen fugacity. The Journal of Geology 82, 709–729.

Roobol, M. J. 1974. The geology of the Vesturhorn Intrusion, SE Iceland. Geological Magazine 111 (4), 273–286.

Rose, W. I. 1996. Volcanic geology of Isle Royale, Michigan. In: Miller, J. D., Jr. (ed.) Field trip quide book for the geology and ore deposits of the Midcontinent Rift in the Lake Superior Region, 1995. IGCP Project 336 Field Conference and symposium Petrology and Metallogeny of Volcanic and Intrusive Rocks of the Midcontinent Rift System, Duluth, Minnesota August 19 – September 1, 1996. Minnesota Geological Survey University of Minnesota, Guidebook 20, 23–72.

Rosenblum, S., Carlson, R. R., Nishi, J. M. & Overstreet, W. C. 1986. Platinum-group elements in magnetic concentrates from the Goodnews Bay district, Alaska. U.S. Geological Survey, Bulletin 1660. 38 p.

Rosenbusch, H. 1887. Mineralien und Gesteine. II. Massige Gesteine. Zweite gänzlich umgearbeitete Auflage. Stuttgart: E. Schweizerbart'sche Verlagshandlung.

Rozhkov, I. S., Kitsul, V. I, Razin, L. V. & Borishanskaya, S. S. 1962. Platina Aldanskogo shchita. Moskva: Izvestiya Akademii Nauk SSSR. 119 p.

Rozova, E. B., Frantsesson, E. V., Pleshakov, A. P., Botova, M. M. & Filippova, A. P. 1979. Geikiloilmenit [sic] i titanovyi khromit iz kimberlitovoi trubki "Zimnyaya" (Zapadnaya Yakutiya). Doklady Akademii Nauk SSSR 248 (3), 721–726.

Rudashevskii, N. S., Yakovleva, O. A, Semenov, V.

S. & Koptev-Dvornikov, E. V. 1991. K modeli formirovaniya Pt-Pd-rud malosulfidnogo tipa v rassloennykh ultrabazit-bazitovykh massivakh (na primere rud massiva Lukkulaisvaara, Severnaya Kareliya). Doklady Akademii Nauk SSSR 319 (2), 479–482.

Rundkvist, D. V. & Sokolova, V. N. 1978. Zonalnost orudeneniya Monchegorskogo medno-nikelevogo mestorozhdeniya. Zapiski vsesoyuznogo mineralogicheskogo obshchestva 107 (6), 633–649.

Rutherford, M. J. & Hess, P. C. 1974. Origin of lunar granites as immiscible liquids. Houston: Lunar Science Institute. Lunar Science V, 696–698.

Rutland, R. W. R. 1965. Tectonic overpressures. In: Pitcher, W. S. & Flinn, G. W. (eds.) Controls of metamorphism. Edinburgh: Oliver & Boyd, 119–139.

Ryabov, V. V., Tsimbalist, V. G. & Yakobi, N. Ya. 1982. O kontsentratsii khroma i platinoidov v krovle rassloennykh intruzii Norilskogo tipa. Doklady Akademii Nauk SSSR 266 (2), 466–469.

Ryerson, F. J. & Hess, P. C. 1978. Implications of liquid-liquid distribution coefficients to mineral-liquid partititioning. In: Drake, M. J. & Holloway, J. R. (eds.) Experimental trace element geochemistry. Geochimica et Cosmochimica Acta 6A, 921–932.

Sack, R. O., Carmichael, I. S. E. & Ghiorso, M. S. 1980. Ferric-ferrous equilibria in natural silicate liquids at 1 bar. Contributions to Mineralogy and Petrology 75, 369–376.

Sahama, T. G. 1945. Spurenelemente der Gesteine im südlichen Finnisch-Lappland. Bulletin de la Commission géologique de Finlande 135. 86 p.

Saini-Eidukat, B., Weiblen, P. W., Bitsianes, G. & Glascock, M. D. 1990. Contrasts between platinum group element contents and biotite compositions of Duluth Complex troctolitic and anorthositic series rocks. Mineralogy and Petrology 42, 212– 240.

Sakuyama, M. 1981. Petrological study of the Myoko and Kurohime volcanoes, Japan: crystallization sequence and evidence for magma mixing. Journal of Petrology 22, 553–583.

Sampson, E. 1932. Magmatic chromite deposits in southern Africa. Economic Geology 27, 113–144.

Sampson, E. 1969. Discussion: Stillwater, Montana chromite deposits. In: Wilson, H. D. B. (ed.) Magmatic ore deposits. Economic Geology Monograph 4, 72–75.

Sasaki, A. & Smith, D. 1979. Sulfur isotopic evidence of diabase-granophyre-sedimentary rocks interaction, Sierra Ancha, central Arizona. Geochemical Journal 13, 227–229.

Schiffries, C. M. 1982. The petrogenesis of a platiniferous dunite pipe in the Bushveld Complex: infiltration metasomatism by a chloride solution. Economic Geology 77, 1439–1453.

Schiffries, C. M. & Rye, D. M. 1989. Stable isotopic systematics of the Bushveld Complex: I. Constraints of magmatic processes in layered intrusions. American Journal of Science 289, 841–873.

Schmidt, E. R. 1952. The structure and composition of the Merensky Reef and associated rocks on the Rustenburg platinum mine. Transactions of the Geological Society of South Africa 55, 233–279.

Schnetzler, C. C. & Philpotts, J. A. 1970. Partition coefficients of rare-earth elements between igneous matrix material and rock-forming mineral phenocrysts – II. Geochimica et Cosmochimica Acta 34, 331–340.

Schreiber, H. D. & Haskin, L. A. 1976. Chromium in basalts: experimental determination of redox states and partitioning among synthetic silicate phases. Proceedings of the 7th Lunar Science Conference. Geochimica et Cosmochimica Acta Supplement 7, vol. 2, 1221–1259.

Schwellnus, C. M. 1935. The nickel-copper occurrence in the Bushveld igneous complex west of the Pilandsbergen. Geological Survey of South Africa, Bulletin 5. 36 p.

Schwellnus, J. S. I. 1970. Andalusite-staurolite relationships in the north-eastern metamorphic aureole of the Bushveld Complex. In: Visser, D.J.L. & von Gruenewaldt, G. (eds.) Symposium on the Bushveld Igneous Complex and other layered intrusions. Geological Society of South Africa Special Publication 1, 326–335.

Scoates, R. F. J., Eckstrand, O. R. & Cabri, L. J. 1988. Interelement correlation, stratigraphic variation and distribution of PGE in the ultramafic series of the Bird River Sill, Canada. In: Prichard, H. M., Potts, P. J. Bowles, J. F. W. & Cribb, S. J. (eds.) Geo-Platinum 87. London and New York: Elsevier Applied Science, 239–249.

Scoon, R. N. & Teigler, B. 1994. Platinum-group element mineralization in the Critical Zone of the western Bushveld Complex: I. Sulfide poor-chromitites [sic] below the UG-2. Economic Geology 89, 1094–1121.

Serdyuchenko, D. P. 1975. Some Precambrian scapolite-bearing rocks evolved from evaporites. Lithos 8, 1–7.

Sergeev, S. A., Bibikova, E. V., Levchenkov, O. A., Lobach-Zhuchenko, S. B., Yakovleva, S. Z., Ovchinnikova, G. V., Neimark, L. A., Komarov, A. N. & Gorokhovskii, B. M. 1990. Izotopnaya geokhronologiya Vodlozerskogo gneisovogo kompleksa. Geokhimiya 1, 73–83.

Sergeev, S. A., Levchenkov, O. A., Lobach-Zhuchenko, S. B. & Yakovleva, S. Z. 1989. 3.5 mlrd. let – drevneishii vozrast, ustanovlennyi dlya dokembriya Baltiiskogo shchita. Doklady Akademii

Nauk SSSR 308 (4), 942–945.

Seward, T. P. III 1970. Metastable phase diagrams and their application to glass-forming ceramic systems. In: Alper, A. M. (ed.) Phase diagrams, vol. I. New York: Academic Press, 295–338.

Shannon, E. V. 1924. The mineralogy and petrology of intrusive triassic diabase at Goose Creek, London County, Virginia. Proceedings of the U.S. National Museum 66, art. 2, 1–86.

Sharkov, E. V. 1980. Petrologiya rassloennykh intruzii. Leningrad: Nauka. 184 p.

Sharkov, E. V. & Sidorenko, V. V. 1980. Gabbro-anortozitovaya formatsiya: Keivskii kompleks. In: Mitrofanov, F. P. & Shurkin, K. A. (eds.) Magmaticheskie formatsii rannego dokembriya territorii SSSR, kniga 2. Moskva: Nedra, 172–178.

Sharma, R. S. 1981. Mineralogy of a scapolite-bearing rock from Rajasthan, northwest peninsular India. Lithos 14, 165–172.

Sharpe, M. R. 1981. The chronology of magma influxes to the eastern compartment of the Bushveld Complex as exemplified by its marginal border groups. Journal of the Geological Society of London 138, 307–326.

Shatskii, G. V. & Zaitsevskaya, Yu. V. 1994. Izotopiya sery fonovoi sulfidnoi mineralizatsii chernoslantsevykh porod yugo-vostochnoi chasti Baltiiskogo shchita v svyazi s problemoi drevneishikh evaporitov. Doklady Akademii Nauk 334 (5), 629–631.

Shaw, C. S. J. & Penczak, R. S. 1996. Barium- and titanium-rich biotite and phlogopite from the Western and Eastern Gabbro, Coldwell alkaline complex, northwestern Ontario. The Canadian Mineralogist 34, 967–975.

Shcheka, S. A. 1969. Petrologiya i rudonosnost nikelenosnykh dunito-troktolitovykh intruzii Stanovogo khrebta. Moskva: Nauka. 135 p.

Shemyakin, V. M. 1980. Charnokitoidnaya formatisya glubinnykh razlomov: Topozerskii kompleks. In: Mitrofanov, F. P. & Shurkin, K. A. (eds.) Magmaticheskie formatsii rannego dokembriya territorii SSSR, kniga 2. Moskva: Nedra, 193–198.

Sheraton, J. W. 1980. Geochemistry of Precambrian metapelites from East Antarctica: secular and metamorphic variations. BRM Journal of Australian Geology and Geophysics 5, 279–288.

Shipulin, F. K. 1971. K geokhimii magmaticheckikh protsessov. Izvestiya Akademii Nauk SSSR, Ser. Geol. 3, 5–12.

Shiraki, K. 1966. Some aspects of the geochemistry of chromium. Journal of Earth Sciences, Nagoya University 14 (1), 10–55.

Shurkin, K. A., Dobrokhotov, M. N., Zagorodnyi, V. G., Negrutsa, V. Z., Sokolov, V. A., Stenar, M. M. & Shcherbak, N. P. 1979. Rannii dokembrii Vostochno-Evropeiskoi platformy (stratigrafiya, korrelyatsiya). In: Shurkin, K. A. & Sokolov, V. A. (eds.) Stratigrafiya arkheya i nizhnego proterozoya SSSR. Leningrad: Nauka, 5–23.

Sibson, R. H. 1975. Generation of pseudotachylyte by ancient seismic faulting. The Geophysical Journal of the Royal Astronomical Society 43, 775–794.

Sibson, R. H. 1977. Fault rocks and fault mechanisms. Journal of the Geological Society of London 133, 191–213.

Sidorenko, V. V. Fizhenko, V. V. & Shurkin, K. A. 1974. Kompleks differentsirovannykh peridotit-gabbro-noritovykh intruzii i svyazannykh s nimi palingennykh granofirovykh granitoidov. In: Shurkin, K. A. (ed.) Geologiya i magmatizm oblasti sochleneniya Belomorid i Karelid. Leningrad: Nauka, 127–134.

Sidorenko, V. V. & Shemyakin, V. M. 1974. Daikovye kompleksy porod osnovnogo sostava. In: Shurkin, K. A. (ed.) Geologiya i magmatizm oblasti sochleneniya Belomorid i Karelid. Leningrad: Nauka, 138–143.

Sigurdsson, H. & Sparks, R. S. J. 1981. Petrology of rhyolitic and mixed magma ejecta from the 1875 eruption of Askja, Iceland. Journal of Petrology 22, 41–84.

Silver, L. T. 1968. A geochronologic investigations of the anorthosite complex, Adirondack Mountains, New York. In: Isachsen, Y. W. (ed.) Origin of anorthosites and related rocks. New York State Museum and Science Service, Memoir 18, 233–251.

Sivell, W. J., Foden, J. D. & Lawrence, R. W. 1985. The Entire anorthositic gneiss, eastern Arunta Inlier, Central Australia: geochemistry and petrogenesis. Australian Journal of Earth Sciences 32, 449–465.

Skinner, B. J. 1966. Thermal expansion. In: Clark, S.-P., Jr. (ed.) Handbook of physical constants. Geological Society of America, Memoir 97, 75–96.

Slobodskoi, R. M. 1981. Elementoorganicheskie soedineniya v magmatogennykh i rudoobrazuyushchikh protsessakh. Novosibirsk: Nauka. 133 p.

Smirnova, T. A., Loginov, V. N. & Ganin, V. A. 1996. Chromite horizons of the Burakovsky layered intruzion [sic], eastern part of the Baltic Shield, Russia. In: IGCP project 336 symposium in Rovaniemi, Finland, August 19–30, 1996: program and abstracts. University of Turku. Division of geology and mineralogy. Publication 33, p. 33.

Smith, D. & Silver, L. T. 1975. Potassic granophyre associated with Precambrian diabase, Sierra Ancha, Central Arizona. Geological Society of America Bulletin 86, 503–513.

Smith, D. G. W. 1969. Pyrometamorphism of phyllites by a dolerite plug. Journal of Petrology 10, 20–55.

Smolkin, V. F. 1995. The early Proterozoic (2.5–1.7) midcontinent rift system of the northeastern Baltic Shield. In: Proc. International Field Conference and Symposium, IGCP 336/Petrology and Metallogeny of Volcanic and Intrusive Rocks of the Midcontinent Rift System, August 19 – September 1, 1995. Proceedings and Abstracts, Duluth, Minnesota: University of Minnesota Duluth, p. 177.

Smolkin, V. F. & Pakhomovskii, Ya. A. 1985. Paragenezis olivin-khromshpinelid v ultramafitakh Pechengi i ego petrogeneticheskoe znachenie. Izvestiya Akademii Nauk SSSR, Ser. Geol. 4, 57–73.

Söhnge, P. G. 1963. Genetic problems of pipe deposits in South Africa. Proceedings of the Geological Society of South Africa 66, xix–lxxii.

Soininen, H. T., Jokinen, T. J. & Oksama, M. K. 1995. Electromagnetic studies of the Keivitsa nickel-copper deposit. In: SEG International Exposition and 65th Annual Meeting, October 8–13, 1995, Houston: expanded abstracts with biographies, 1995, technical program. Tulsa: Society of Exploration Geophysicists, 807–810.

Sokolov, V. A. 1980. Jatulian formations of the Karelian ASSR. In: Silvennoinen, A. (ed.) Jatulian geology in the eastern part of the Baltic Shield. Proceedings of a Finnish-Soviet Symposium held in Finland, 21st–26th August, 1979. Rovaniemi: The Committee for Scientific and Technical Co-operation between Finland and Soviet Union, 163–220.

Sokolova, V. N. 1976. Novye dannye o geologicheskom stroenii intruzivnogo kompleksa Monche-Chuna-Volchikh tundr (Kolskii p-ov). Sovetskaya Geologiya 6, 100–111.

Sørensen, H. & Larsen, L. M. 1987. Layering in the Ilimaussaq alkaline intrusion, South Greenland. In: Parsons, I. (ed.) Origins of igneous layering. Dordrecht: D. Reidel Publishing Co., 1–28.

Sparks, R. S. J., Huppert, H. E., Kerr, R. C., McKenzie, D. P. & Tait, S. R. 1985. Postcumulus processes in layered intrusions. Geological Magazine 122 (5), 555–568.

Springer, G. 1989. Chlorine-bearing and other uncommon minerals in the Strathcona Deep Copper Zone, Sudbury district, Ontario. The Canadian Mineralogist 27, 311–313.

Stepanov, V. S. 1984. Vozrastnye vzaimootnosheniya i petrokhimicheskie osobennosti osnovnykh magmatitov Pyaozera. In: Bogachev, A. I. (ed.) Intruzivnye bazity i giperbazity Karelii. Karelskii filial Akademii Nauk SSSR, Inst. geol., 41–52.

Stevenson, J. S. & Colgrove, G. L. 1968. The Sudbury Irruptive: some petrogenetic concepts based on recent field work. XXIII International Geological Congress, Praque, Part 3–4, 27–35.

Stewart, B. W. & DePaolo, D. J. 1989. Mafic magma chamber geometrics and processes: Nd and Sr isotope evidence and constrains. 28th International Geological Congress, Washington D.C., U.S.A. July 9–19, 1989. Abstracts, Vol. 3, p. 181.

Stewart, B. W. & DePaolo, D. J. 1992. Diffusive isotopic contamination of mafic magma by coexisting silicic liquid in the Muskox Intrusion. Science 255, 708–711.

Stewart, D. B., Walker, G. W., Wright, T. L. & Fahey, J. J. 1966. Physical properties of calcic labradorite from Lake County, Oregon. American Mineralogist 51, 177–197.

Stone, W., Crocket, J. H. & Fleet, M. E. 1991. Platinum-group element mineralization in the Boston Creek flow Fe-rich basaltic komatiite, Abitibi Belt, Ontario. Geological Association of Canada & Mineralogical Association of Canada, Joint Annual Meeting with the Society of Economic Geologists, May 27–29, 1991. Program with abstracts 16, p. 119.

Sun, S.-S., Nesbitt, R. W. & McCulloch, M. T. 1989. Geochemistry and petrogenesis of Archaean and early Proterozoic siliceous high-magnesian basalts. In: Crawford, J. J. (ed.) Boninites. London: Unwin Hyman, 148–173.

Suwa, K., Enami, M. & Horiuchi, T. 1987. Chlorine-rich potassium hastingsite from West Ongul Island, Lützow-Holm Bay, East Antarctica. Mineralogical Magazine 51, 709–714.

Suwa, K. & Suzuki, K 1977. Chromian phlogopite in the Bushveld anorthosite, South Africa. Association for African Studies: Preliminary Report of African Studies, Nagoya University 2, 133–138.

Symonds, R. B., Rose, W. I., Briggs, P. & Gerlach, T. M. 1988. The speciation and fluxes of gases at Augustine volcano, Alaska: the degassing of a Cl-rich volcanic system. EOS 69 (44), p. 1469.

Symonds, R. B., Rose, W. I., Gerlach, T. M., Briggs, P. H. & Harmon, R. S. 1990. Evaluation of gases, condensates, and SO_2 emissions from Augustine volcano, Alaska: the degassing of a Cl-rich volcanic system. Bulletin of Volcanology 52, 355–374.

Taborszky, F. K. 1972. Das Problem der Cl-Apatite. Lithos 5, 315–324.

Tait, S. R., Huppert, H. E. & Sparks, R. S. J. 1984. The role of compositional convection in the formation of adcumulate rocks. Lithos 17, 139–146.

Takahashi, T. & Sasaki, A. 1983. Isotopic composition of sulfur in the Oshirabetsu gabbroic complex and the associated nickeliferous pyrrhotite ore – Magmatic sulfide mineralization and the external source of sulfur. Mining Geology 33 (6), 399–409.

Talkington, R. W., Watkinson, D. H., Whittaker, P. J. & Jones, P. C. 1984. Platinum-group minerals and other solid inclusions in chromite of ophiolite complexes: occurrence and petrological significance. Tschermaks mineralogische und petrogra-

phische Mitteilungen 32, 285–301.

Talvitie, J. & Paarma, H. 1980. Precambrian basic magmatism and the Ti-Fe ore formation in Central and Northern Finland. In: Siivola, J. (ed.) Metallogeny of the Baltic Shield. Geological Survey of Finland, Bulletin 307, 98–107.

Tarkian, M. & Mutanen, T. 1987. Loveringite from the Koitelainen layered intrusion, northern Finland. Mineralogy and Petrology 37, 37–50.

Taubeneck, W. H. & Poldervaart, A. 1960. Geology of the Elkhorn mountains, Northeastern Oregon: Part 2. Willow Lake intrusion. Geological Society of America Bulletin 71, 1295–1322.

Taylor, S. R. & McLennan, S. M. 1985. The continental crust: its composition and evolution. Oxford: Blackwell Scientific Publications. 312 p.

Tegtmeyer, K. J. & Farmer, G. L. 1990. Nd isotopic gradients in upper crustal magma chambers: Evidence for in situ magma – wall-rock interaction. Geology 18, 5–9.

Thayer, T. P. 1973. Chromium. U.S. Geological Survey, Professional Paper 820, 111–121.

Thompson, J. F. H. & Naldrett, A. J. 1984. Sulphide-silicate reactions as a guide to Ni-Cu-Co mineralization in Central Maine, U.S.A. In: Buchanan, D.L. & Jones, M.J. (eds.) Sulphide deposits in mafic and ultramafic rocks, 103–113. Proc. IGCP Projects 161 and 91, Third Nickel Sulphide Field Conference, Perth, Western Australia, May 23–25, 1982. London: The Institution of Mining and Metallurgy. 164 p.

Thompson, R. N. 1973. Titanian chromite and chromian titanomagnetite from a Snake River Plain basalt, a terrestrial analogue to lunar spinels. American Mineralogist 58, 826–836.

Thompson, R. N. 1975. The 1-atmosphere liquidus oxygen fugacities of some tholeiitic intermediate, alkalic and ultra-alkalic lavas. American Journal of Science 275, 1049–1072.

Thompson, R. N. 1982. Magmatism of the British Tertiary Volcanic Province. Scottish Journal of Geology 18, 49–107.

Thompson, R. N., Dickin, A, P., Gibson, I. L. & Morrison, M. A. 1982. Elemental fingerprints of isotopic contamination of Hebridean Palaeocene mantle-derived magmas by Archaean sial. Contributions to Mineralogy and Petrology 79, 159–168.

Thornber, C. R., Roeder, P. L. & Foster, J. R. 1980. The effect of composition on ferric-ferrous ratio in basaltic liquids at atmospheric pressures. Geochimica et Cosmochimica Acta 44, 525–532.

Todd, S. G., Keith, D. W., Leroy, L. W., Schissel, D. J., Mann, E. L. & Irvine, T. N. 1982. The J-M platinum-palladium reef of the Stillwater Complex, Montana: I. Stratigraphy and petrology. Economic Geology 77, 1454–1480.

Touysinhthiphonexay, Y., Gold, D. P., Deines, P., Ulmer, G. C. & Korn, R. 1984. Some properties of graphite from the Stillwater Complex, Montana, and the Bushveld Igneous Complex, South Africa. Geological Society of America, Abstracts with programs 16, p. 677.

Tredoux, M., de Wit, M. J., Hart, R. J., Lindsay, N. M., Verhagen, B. & Sellschop, J. P. T. 1989. Chemostratigraphy across the Cretaceous-Tertiary boundary and a critical assessment of the iridium anomaly. The Journal of Geology 97, 585–605.

Tredoux, M., Lindsay, N. M., Davies, G. & McDonald, I. 1995. The fractionation of platinum-group elements in magmatic systems, with the suggestion of a new causal mechanism. South African Journal of Geology 98 (2), 157–167.

Trofimov, N. N. 1995. Mekhanizm formirovaniya stratiformnogo zoloto-platino-palladievogo i titanomagnetitovogo orudeneniya v gabbro-doleritov ykh intruziyakh nizhnego proterozoya Karelii. In: Rybakov, S. I. & Golubev, A. I. (eds.) Tezisy dokladov regionalnogo simpoziuma "Blagorodnye metally i almazy Severa Evropeiskoi chasti Rossii" i nauchno-prakticheskoi konferentsii "Problemy razvitiya mineralno-syrevoi bazy platinovykh metallov Rossii", 97–98.

Trofimov, N. N., Lavrov, M. M. & Barkov, A. Yu. 1995. Mineraly platinovoi gruppy v Burakovskom rassloennom massive. In: Rybakov, S. I. & Golubev, A. I. (eds.) Tezisy dokladov regionalnogo simpoziuma "Blagorodnye metally i almazy Severa Evropeiskoi chasti Rossii" i nauchno-prakticheskoi konferentsii "Problemy razvitiya mineralno-syrevoi bazy platinovykh metallov Rossii", 98–100.

Tsuchiyama, A. 1985. Dissolution kinetics of plagioclase in the melt of the system diopside-albite-anorthite, and origin of dusty plagioclase in andesites. Contributions to Mineralogy and Petrology 89, 1–16.

Tuganova, E. V. & Malich, K. N. 1990. K voprosu o platinonosnosti intruzii Norilskogo tipa. Doklady Akademii Nauk SSSR 313 (1), 178–183.

Tyrväinen, A. 1980. Sattanen. Geological Map of Finland 1 : 100 000, Pre-Quaternary rocks, Sheet 3714. Geological Survey of Finland.

Tyrväinen, A. 1983. Sodankylän ja Sattasen karttaalueiden kallioperä. Summary: Pre-Quaternary rocks of the Sodankylä and Sattanen map-sheet areas. Geological Map of Finland 1 : 100 000, Explanation to the Maps of Pre-Quaternary Rocks, Sheets 3713 and 3714. Geological Survey of Finland. 59 p.

Tyson, R. M. & Chang, L. L. Y. 1978. The petrology of the Partridge River Troctolite and its importance to sulfide mineralization. Economic Geology 73 (7), p. 1399.

Ulff-Møller, F. 1990. Formation of native iron in sedi-

ment-contaminated magma: I. A case study of the Hanekammen Complex on Disko Island, West Greenland. Geochimica et Cosmochimica Acta 54, 57–70.

Ulmer, G. C. 1983. Increasing evidence for graphite as a primary phase in many large mafic plutons. In: 96th Annual Meeting of the Geological Society of America, Indianapolis, Indiana. Abstracts with programs 15, 709.

Umeji, A. C. 1975. Gravity stratification in the Freetown basic igneous layered complex, Sierra Leone, West Africa. Geological Journal 10 (2), 107–130.

Vakar, V. A. 1967. Rol assimilyatsii v protsessakh differentsiatsii trappovoi magmy. In: Urvantsev, N. N. (ed.) Petrologiya trappov Sibirskoi platformy. Leningrad: Nedra, 124–126.

Van Biljon, S. 1963. Structures in the Basic Belt of the Bushveld Complex. Transactions of the Geological Society of South Africa 66, 11–31 and 41–47.

Vanhala, H. & Soininen, H. 1994. Spectral-induced polarization method at the Keivitsa Ni-Cu deposit, northern Finland. In: SEG International Exposition & 64th Annual Meeting, October 23–28, 1994, Los Angeles: expanded abstracts with author's biographies 1994 technical program. Los Angeles: Society of Exploration Geophysicists, 516–519.

Vanko, D.A. 1986. High-chlorine amphiboles from oceanic rocks: product of highly-saline hydrothermal fluids? American Mineralogist 71, 51–59.

Van Rensburg, W. C. J. 1965. The mineralogy of the titaniferous magnetite and associated sulphides on Kennedy's Vale 361 KT, Lydenburg District, Transvaal. Annals of the Geological Survey, Republic of South Africa 4, 113–127.

Van Zyl, J. S. 1950. Aspects of the geology of the northern Soutpansberg area. Annale Universiteit van Stellenbosch, Sect. A 26 (3–11), 1–95.

Vartiainen, H. & Woolley, A.R. 1974. The petrography, mineralogy and chemistry of the fenites of the Sokli carbonatite intrusion, Finland. Bulletin of the Geological Society of Finland 46, 81–91.

Vasiljev, Yu. R. & Zolotukhin, V. V. 1975. Ultraosnovnye pegmatoidy nekotorykh olivinovykh intruzii severa Sibirskoi platformy. In: Sobolev, V. S. (ed.) Materialy po geneticheskoi i eksperimentalnoi mineralogii 8, 237–263.

Veltheim, V. 1962. On the geology of the chromite deposit at Kemi, North Finland. In: Kahma, A., Siikarla, T., Veltheim, V., Vaasjoki, O. & Heikkinen, A. On the prospecting and geology of the Kemi chromite deposit, Finland. Bulletin de la Commission géologique de Finlande 194, 31–66.

Venkov, D. A., Dolgopolov, V. F. & Kiselev, L. I. 1978. Boksito-rudnye formatsii. In: Rudnye formatsii mestorozhdeniya rud khroma, vanadiya, silikatnogo nikelya i kobalta boksitov. Alma-Ata: Nauka, 155–218.

Vermaak, C. F. 1976. The nickel pipes of Vlakfontein and vicinity, Western Transvaal. Economic Geology 71, 261–286.

Vermaak, C. F. & Hendriks, L. P. 1976. A review of the mineralogy of the Merensky Reef, with specific reference to new data on the precious metal mineralogy. Economic Geology 71, 1244–1269.

Vielzeuf, D. & Holloway, J. R. 1988. Experimental determination of the fluid-absent melting relations in the pelitic system. Consequences for crustal differentiation. Contributions to Mineralogy and Petrology 98, 257–276.

Viljoen, M. J., de Klerk, W. J., Coetzer, P. M., Hatch, N. P., Kinloch, E. & Peyerl, W. 1986a. The Union Section of the Rustenburg Platinum Mines Limited with reference to the Merensky Reef. In: Anhaeusser, C. R. & Maske, S. (eds.) Mineral deposits of Southern Africa, vol. II. Johannesburg: Geological Society of South Africa, 1061–1090.

Viljoen, M. J., Theron, J., Underwood, B., Walters, B. M., Weaver, J. & Peyerl, W. 1986b. The Amandelbult Section of the Rustenburg Platinum Mines Limited, with reference to the Merensky Reef. In: Anhaeusser, C.R. & Maske, S. (eds.) Mineral Deposits of Southern Africa, vol. II. Johannesburg: Geological Society of South Africa, 1041–1060.

Viljoen, M. J. & Scoon, R. N. 1985. The distribution and main geologic features of discordant bodies of iron-rich ultramafic pegmatite in the Bushveld Complex. Economic Geology 80, 1109–1128.

Viljoen, M. J. & Viljoen, R. P. 1969. The geology and geochemistry of the Onverwacht Group and a proposed new class of igneous rocks. In: Upper Mantle Project. Geological Society of South Africa Special Publication 2, 55–85.

Viljoen, R. P. & Viljoen, M. J. 1971. The geological and geochemical evolution of the Onverwacht volcanic group of the Barberton Mountain Land, South Africa. Geological Society of Australia Special Publication 3, 133–149.

Vinogradov, A. P., Tarasov, L. S. & Zykov, S. I. 1959. Izotopnyi sostav rudnykh svintsov Baltiiskogo shchita. Geokhimiya 7, 571–607.

Vogel, T. A. & Wilband, J. T. 1978. Coexisting acidic and basic melts: geochemistry of a composite dike. The Journal of Geology 86, 353–371.

Vogt, J. H. L. 1924. The physical chemistry of the magmatic differentiation of igneous rocks. Videnskapsselskapets Skrifter I. Matematisk-naturvitenskapelig Klasse 15. 132 p.

Volborth, A. & Housley, R. M. 1984. A preliminary description of complex graphite, sulphide, arsenide and platinum group element mineralization in a pegmatoid pyroxenite of the Stillwater Complex,

Montana, U.S.A. Tschermaks Mineralogische und Petrographische Mitteilungen 33, 213–230.

Volborth, A., Tarkian, M., Stumpfl, E. F. & Housley, R. M. 1986. A survey of the Pd-Pt mineralization along the 35-km strike of the J-M Reef, Stillwater Complex, Montana. The Canadian Mineralogist 24, 329–346.

Volfinger, M., Robert, J.-L., Vielzeuf, D. & Neiva, A. M. R. 1985. Structural control of the chlorine content of OH-bearing silicates (micas and amphiboles). Geochimica et Cosmochimica Acta 49, 37–48.

Von Gruenewaldt, G. 1973. The Main and Upper Zones of the Bushveld Complex in the Roossenekal area, Eastern Transvaal. Transactions of the Geological Society of South Africa 76, 207–227.

Von Gruenewaldt, G. 1979. A review of some recent concepts of the Bushveld Complex, with particular reference to sulfide mineralization. The Canadian Mineralogist 17, 233–256.

Vuollo, J. Huhma, H., Kamo, S. & Stepanov, V. 1996. Geochemistry and U-Pb and Sm-Nd isotope studies of a 2.45 Ga dyke swarm: identification of parental magma composition to Fennoscandian layered intrusions? In: IGCP project 336 symposium in Rovaniemi, Finland, August 21–23, 1996: program and abstracts. University of Turku. Division of geology and mineralogy. Publication 33, p. 45.

Vuollo, J., Piirainen, T. & Huhma, H. 1992. Two Early Proterozoic tholeiitic diabase dyke swarms in the Koli-Kaltimo area, eastern Finland – their geological significance. Geological Survey of Finland, Bulletin 363, 1– 32.

Vuorelainen, Y., Häkli, T. A., Hänninen, E., Papunen, H., Reino, J. & Törnroos, R. 1982. Isomertieite and other platinum-group minerals from the Konttijärvi layered mafic intrusion, northern Finland. Economic Geology 77 (6), 1511–1518.

Wadsworth, W. J. 1973. Magmatic sediments. Minerals Science and Engineering 5 (1), 25–35.

Wadsworth, W. J. 1986. Silicate mineralogy in the later fractionation stages of the Insch intrusion, NE Scotland. Mineralogical Magazine 50, 583–595.

Wadsworth, W. J. 1988. Silicate mineralogy of the Middle Zone cumulates and associated gabbroic rocks from the Insch intrusion, NE Scotland. Mineralogical Magazine 52, 309–322.

Wager, L. R. 1959. Differing powers of crystal nucleation as a factor producing diversity in layered igneous intrusions. Geological Magazine 96, 76–80.

Wager, L. R. & Brown, G. M. 1968. Layered igneous rocks. Edinburgh and London: Oliver & Boyd. 588 p.

Wager, L. R. & Mitchell, R. L. 1951. The distribution of trace elements during strong fractionation of basic magma – a further study of the Skaergaard intrusion, East Greenland. Geochimica et Cosmochimica Acta 1, 129–208.

Wagner, P. A. 1929. The platinum deposits and mines of South Africa. Edinburgh: Oliver and Boyd. 326 p.

Walker, F. 1930. The geology of the Shiant Isles (Hebrides). Quarterly Journal of the Geological Society of London 86, 355–398.

Walker, F. 1940. Differentiation of the Palisade diabase, New Jersey. Geological Society of America Bulletin 51, 1059–1106.

Walker, F. 1953. The pegmatitic differentiates of basic sheets. American Journal of Science 251, 41–60.

Walker, F. & Poldervaart, A. 1949. Karroo dolerites of the Union of South Africa. Geological Society of America Bulletin 60, 591–706.

Walker, J. A. 1984. Volcanic rocks from the Nejapa and Granada cinder cone alignments, Nicaragua, Central America. Journal of Petrology 25, 299–342.

Walker, K. R. 1969. The Palisades sill, New Jersey, a reinvestigation. Geological Society of America, Special Paper 111. 178 p.

Walraven, F., Armstrong, R. A. & Kruger, F. J. 1990. A chronostratigraphic framework for the north-central Kaapvaal craton, the Bushveld Complex and the Vredefort structure. Tectonophysics 171, 23–48.

Walraven, F. & Hattingh, E. 1993. Geochronology of the Nebo Granite, Bushveld Complex. South African Journal of Geology 96, 31–41.

Watson, E. B. 1976. Two-liquid partition coefficients: experimental data and geochemical implications. Contributions to Mineralogy and Petrology 56, 119–139.

Watson, E. B. 1982. Basalt contamination by continental crust: some experiments and models. Contributions to Mineralogy and Petrology 80, 73–87.

Weaver, B. L. & Tarney, J. 1981. The Scourie dyke suite: petrogenesis and geochemical nature of the Proterozoic sub-continental mantle. Contributions to Mineralogy and Petrology 78, 175–188.

Wiebe, R. A. 1979. Fractionation and liquid immiscibility in an anorthosite pluton of the Nain Complex, Labrador. Journal of Petrology 20, 239–269.

Wiebe, R. A. 1984. Commingling of magmas in the Bjerkrem-Sogndal lopolith (southwest Norway): evidence for the compositions of residual liquids. Lithos 17, 171–188.

Wiebe, R. A. 1990. Dioritic rocks in the Nain complex, Labrador. Schweizerische Mineralische und Petrographische Mitteilungen 70, 199–208.

Willemse, J. 1969a. The geology of the Bushveld Igneous Complex, the largest Repository of magmatic ore deposits in the world. In: Wilson, H. D. B. (ed.) Magmatic ore deposits. Economic Geology Monograph 4, 1–22.

Willemse, J. 1969b. The vanadiferous magnetic iron ore of the Bushveld Igneous Complex. In: Wilson, H. D. B. (ed.) Magmatic ore deposits. Economic Geology Monograph 4, 187–208.

Willemse, J. & Viljoen, E. A. 1970. The fate of argillaceous material in the gabbroic magma of the Bushveld Complex. In: Visser, D. J. L. & von Gruenewaldt, G. (eds.) Symposium on the Bushveld Igneous Complex and other layered intrusions. Geological Society of South Africa Special Publication 1, 336–366.

Williams, C. T. 1978. Uranium-enriched minerals in mesostasis areas of the Rhum layered pluton. Contributions to Mineralogy and Petrology 66, 29–39.

Williams, H. & McBirney, A. R. 1979. Volcanology. San Francisco: Freeman, Cooper & Co. 397 p.

Windley, B. F., Herd, R. K. & Bowden, A. A. 1973. The Fiskenaesset Complex, West Greenland. Part 1. Grønlands Geologiske Undersøgelse, Bulletin 106. 80 p.

Windley, B. F. & Smith, J. V. 1974. The Fiskenaesset Complex, Western Greenland. Grønlands Geologiske Undersøgelse, Bulletin 108. 54 p.

Wones, D. R. 1980. Contributions of crystallography, mineralogy, and petrology to the geology of the Lucerne pluton, Hancock County, Maine. American Mineralogist 65, 411–437.

Wones, D. R. & Eugster, H. P. 1965. Stability of biotite: experiment, theory and application. American Mineralogist 50, 1228–1272.

Wooden, J. L., Czamanske, G. K. & Zientek, M. L. 1991. A lead isotopic study of the Stillwater Complex, Montana: constraints on crustal contamination and source regions. Contributions to Mineralogy and Petrology 107, 80–93.

Worst, B. G. 1960. The Great Dyke of Southern Rhodesia. Southern Rhodesia Geological Survey Bulletin 47. 234 p.

Wright, T. L. & Okamura, R. T. 1977. Cooling and crystallization of tholeiitic basalt, 1965 Makaopuhi Lava Lake, Hawaii. U.S. Geological Survey, Professional Paper 1004. 78 p.

Wronkiewicz, D. J. & Condie, K. C. 1987. Geochemistry of Archean shales from the Witwatersrand Supergroup, South Africa: Source-area weathering and provenance. Geochimica et Cosmochimica Acta 51, 2401–2416.

Wronkiewicz, D. J. & Condie, K. C. 1990. Geochemistry and mineralogy of sediments from the Ventersdorp and Transvaal Supergroups, South Africa: Cratonic evolution during the early Proterozoic. Geochimica et Cosmochimica Acta 54, 343–354.

Wyllie, P. J. 1960. The system CaO-MgO-FeO-SiO_2 and its bearing on the origin of ultrabasic and basic rocks. Mineralogical Magazine 32, 459–470.

Wyllie, P. J. & Tuttle, O. F. 1961. Hydrothermal melting of shales, Geological Magazine 98, 56–66.

Yagi, K. 1953. Petrochemical studies on the alkali rocks of the Morotu district, Sakhalin. Geological Society of America Bulletin 64, 769–810.

Yakovlev, Yu. N., Distler, V. V., Mitrofanov, F. P., Pazhev, S. A., Grokhovskaya, T. L. & Veselovsky, N. N. 1991. Mineralogy of PGE in the mafic-ultramafic massifs of the Kola region. Mineralogy and Petrology 43, 181–192.

Yoder, H. S., Jr. 1952. Change of melting point of diopside with pressure. The Journal of Geology 60, 364–374.

Yoder, H. S., Jr. 1965. Diopside-anorthite-water at five and ten kilobars and its bearing on explosive volcanism. Carnegie Institution of Washington, Year Book 64, 82–89.

Yoder, H. S., Jr. 1971. Contemporaneous rhyolite and basalt. Carnegie Institution of Washington, Year Book 69, 141–145.

Yoder, H. S., Jr. & Tilley, C. E. 1962. Origin of basalt magmas: An experimental study of natural and synthetic rock systems. Journal of Petrology 3, 342–532.

Young, R. A., Sudarsanan, K. & Mackie, P. E. 1968. Structural origin of some physical property differences among three apatites. Bulletin de la Society Chimique de France NS, 1760–1763.

Yusupov, S. Sh. 1972. Otritsatelnye anomalii ftora v granitakh vokrug kamernykh pegmatitov. Geologiya i geofizika 3, 59–68.

Zavaritskii, A. N. 1937. O fuzivnykh magmaticheskikh mestorozhdeniyakh. Izvestiya Akademii Nauk SSSR, Ser. Geol. 4, 765–788.

Zhangurov, A. A., Sholokhnev, V. V., Fedotov, Zh. A., Torokhov, M. P. & Bayanova, T. B. 1994. Imandra layered intrusion. In: Mitrofanov, F. & Torokhov, M. (eds.) Kola Belt of layered intrusions. Guide to the pre-symposium field trip. 7th International Platinum Symposium, July 27–31, 1994. Geological Institute KSC RAS, 42–70.

Zoller, W. H., Parrington, J. R. & Kotra, J. M. P. 1983. Iridium enrichment in airborne particles from Kilauea volcano: January 1983. Science 222, 1118–1121.

Zolotukhin, V. V., Ryabov, V. V., Vasilev, Yu. R. & Shatkov, V. A. 1975. Petrologiya Talnakhskoi rudonosnoi differentsirovannoi trappovoi intruzii. Novosibirsk: Nauka. 436 p.

D: Supper in brotherly harmony

Tätä julkaisua myy

GEOLOGIAN TUTKIMUSKESKUS (GTK)
Julkaisumyynti
PL 96
02151 Espoo
☎ 0205 50 11
Telekopio: 0205 50 12

GTK, Väli-Suomen aluetoimisto
Kirjasto
PL 1237
70211 Kuopio
☎ 0205 50 11
Telekopio: 0205 50 13

GTK, Pohjois-Suomen aluetoimisto
Kirjasto
PL 77
96101 Rovaniemi
☎ 0205 50 11
Telekopio: 0205 50 14

Denna publikation säljes av

GEOLOGISKA FORSKNINGSCENTRALEN (GFC)
Publikationsförsäljning
PB 96
02151 Esbo
☎ 0205 50 11
Telefax: 0205 50 12

GFC, Distriktsbyrån för Mellersta Finland
Biblioteket
PB 1237
70211 Kuopio
☎ 0205 50 11
Telefax: 0205 50 13

GFC, Distriktsbyrån för Norra Finland
Biblioteket
PB 77
96101 Rovaniemi
☎ 0205 50 11
Telefax: 0205 50 14

This publication can be obtained from
GEOLOGICAL SURVEY OF FINLAND (GSF)
Publication sales
P.O. Box 96
FIN-02151 Espoo, Finland
☎ +358 205 50 11
Telefax: +358 205 50 12

GSF, Regional office for Mid-Finland
Library
P.O. Box 1237
FIN-70211 Kuopio, Finland
☎ +358 205 50 11
Telefax: +358 205 50 13

GSF, Regional office for Northern Finland
Library
P.O. Box 77
FIN-96101 Rovaniemi, Finland
☎ +358 205 50 11
Telefax: +358 205 50 14

E-mail: info@gsf.fi
WWW-address: http://www.gsf.fi

ISBN 951-690-652-4
ISSN 0367-522X

9 789516 906525

Appendix 1

AKANVAARA LAYERED INTRUSION

Faults, shear zones (with blastomylonites and metapseudotachylytes)

Post-intrusion rocks of the Ritaselkä formation (quartzites, fuchsite quartzites, blastomylonites

Mafic dykes

AKANVAARA INTRUSION

Granophyre

Ferrogabbro, ferrodiorite (A=cumulus apatite), interlayers of mottled anorthosite and ultramafic cumulates

Magnetite gabbro

Gabbro (upper zone, main zone, lower zone) Several anorthosite layers in the main zone, pyroxene cumulate layers in the lower part

Anorthosite (mottled anorthosite and other plagioclase-rich cumulates

UC chromitite and associated anorthosites

Olivine-pyroxene (-chromite) cumulate and ULC chromitite

Pyroxene cumulates (with cumulus chromite and intercumulus plagioclase); LC-chromitite layers

Lower marginal chill (microgabbro, "crescumulate" microgabbro), with chromitite layers and chromitite autoliths in the upper part

Pre-intrusion rocks: acid volcanic rocks, blastomylonites

Metahornfelses from acid volcanic rocks

Igneous layering

D Detail map area (Appendix 2)

AKANVAARA INTRUSION (MAP AREA SHADED)

2 km

0 1 km

Compiled by Tapani Mutanen 1997

Printed by Kartatekniikka Oy, Helsinki, Finland 1997

Appendix 2

AKANVAARA LAYERED INTRUSION

Tuorelehto

Upper Chromitite outcrop

5 m

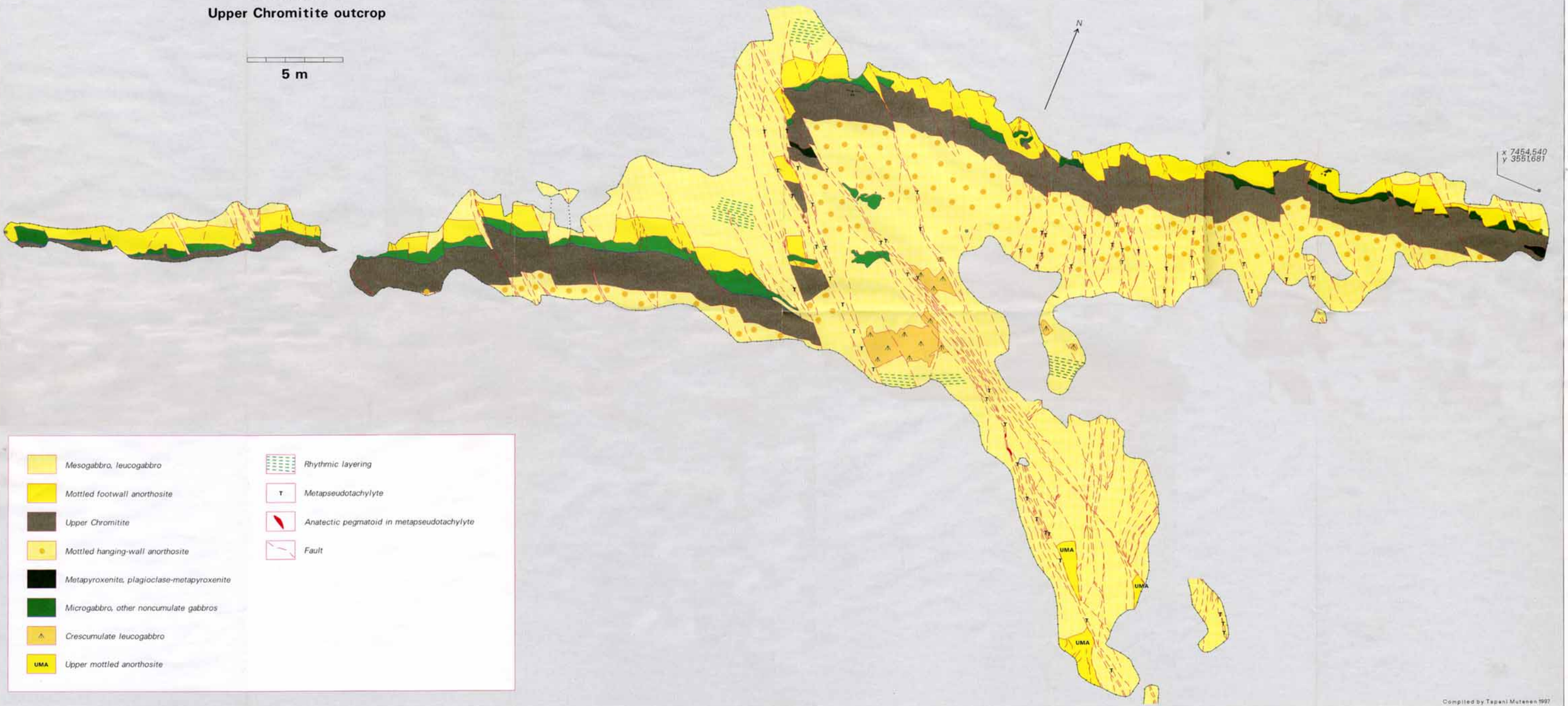

Compiled by Tapani Mutanen 1997
Printed by Karttakeskus Oy, Helsinki, Finland 1997

KOITELAINEN LAYERED INTRUSION

Mafic and ultramafic dykes / Pegmatoids

Granophyre / Monzonite diapirs

Magnetite gabbro

Anorthosite and Upper Chromitite

Gabbroic cumulates / Pigeonite

Lower chromitite layers

Pyroxene / olivine (+-pyroxene) cumulates

Lower marginal chill
incl. pre-Koitelainen mafic sill

Metavolcanic rocks: komatiites, low-Ti basalts, acid volcanic rocks+conglomerates; mafic-ultramafic sills

Metasedimentary rocks: high-Al pelite, high-Mg pelite, subarkose and black schist

Basement gneiss complex / granite

Fault

K = Keivitsa intrusion
S = Satovaara intrusion

0 1 2 3 4 5 km

Compiled by Tapani Mutanen 1997

Printed by Karttakeskus Oy, Helsinki, Finland 1997

Appendix 4

Keivitsa-Satovaara Complex

Geological map

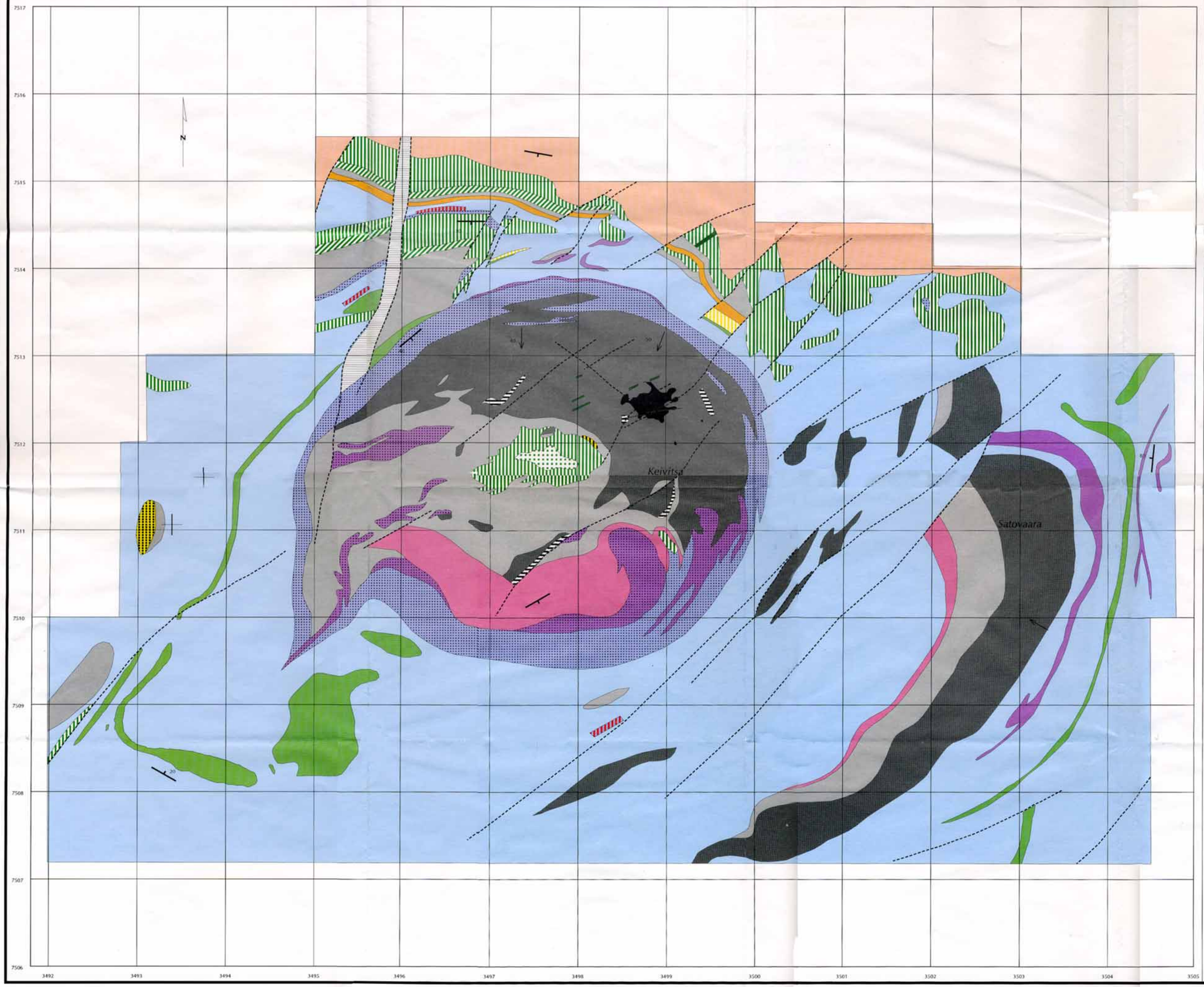

Shear zone

Fault

Dip of intrusion basal contact

Layering

Dykes

Diabase, olivine gabbro-diabase

Keivitsa intrusion, Keivitsa-Satovaara complex

PGE-Cr-V deposit

False ore sulphides

Cu-Ni-PGE-Au ore

Granophyre

Gabbro

Olivine pyroxenite (Satovaara: peridotite)

Puilettilampi hydrothermal pipe

Albite-carbonate (-magnetite-pyrite) rock

Gabbro

Komatiite peridotites and komatiitic sills

Gabbro

Pyroxenite

Peridotite

Serpentinite

Sedimentary and volcanic rocks

Chlorite-amphibole rocks (low-Ti basalts and basaltic komatiites)

Pelitic hornfels and metahornfels, sulphide-poor

Pelitic and black schist hornfels, sulphide-rich

Black schist

Mica schists and other pelitic rocks (including graphite- and sulphide-bearing interlayers, acid volcanic material; also magnesian pelites)

Arkosic quartzite, subarkose

Calcareous metasedimentary rocks

Micaceous arkose

Koitelainen intrusion

Granophyre

Scale 1:20000

0 200 400 600 800 1000 m

Geological Survey of Finland
Regional Office for Northern Finland
Tapani Mutanen, Seppo Aaltonen, Markku Pänttäjä
1994, revised 1997

Keivitsa

Keivitsansarvi

Cu-Ni-PGE-Au deposit

Ore types

Profile x = 7512.250

Regular ore

- High grade
- Low grade

Other ore types

- Transitional ore type (between regular and Ni-PGE type)
- Ni-PGE type
- False ore, Ni(100S) 2-4%
- False ore, Ni(100S) < 2%

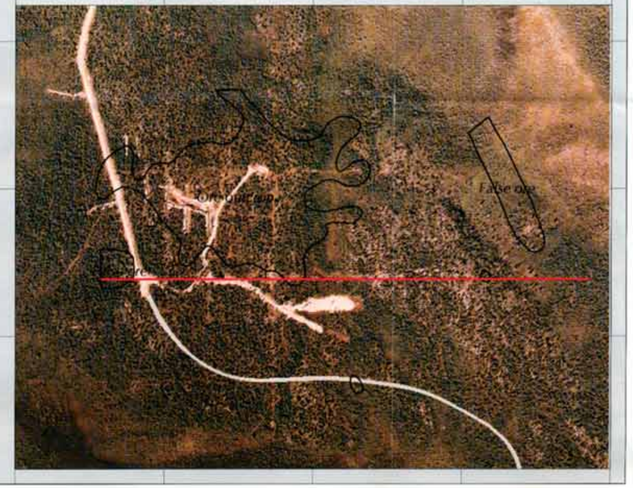

Scale 1:2000

0 20 40 60 80 100 m

Geological Survey of Finland
Regional Office for Northern Finland
Tapani Mutanen, Seppo Aaltonen, Markku Pänttäjä

1994, revised 1997